INVESTIGATION INTO SOLAR POWERED ADSORPTION COOLING SYSTEMS

- ADSORPTION TECHNOLOGY AND SYSTEM ANALYSIS -

Uwe Schürger

A thesis submitted in partial fulfilment
of the requirements of De Montfort University
for the degree of Doctor of Philosophy (PhD)

March 2007

Institute of Energy and Sustainable Development
De Montfort University Leicester

Faculty of Civil Engineering, Building Physics and Economics
Stuttgart University of Applied Sciences

ABSTRACT

Due to the fact that the worldwide energy consumption caused by cooling devices in buildings has been increasing steadily and also the fact that the pressure has been rising to provide this cooling energy with environmentally friendly technology, solar powered DEC-systems (Desiccative and Evaporative Cooling) have begun capturing increasing interest over the past few years.

However, up to now little experience has been gained in the operation of these systems and thus currently little information is available about the performance, the efficiency, the control strategy and the best component choice. This lack of knowledge has resulted in a low rate of acceptance of this technology so far. The studies presented in this thesis serve as a contribution to the advancement of DEC technology by providing fundamental knowledge about the operation and attainable performance of these systems.

A comprehensive study of desiccant wheels was undertaken which provides detailed information about the operation and the achievable dehumidification performance of this component. A detailed simulation model for desiccant wheels was developed and verified with measured data from a desiccant wheel test plant.

Additionally, two commercially used DEC-systems (one in a public library in Spain and the other in a plastics processing factory building in Germany) were monitored for the purposes of evaluating the performance of these systems and resolving existing problems in their operation and control strategies. In spite of the generally positive validation of the planned and expected cooling performances in both cases, the monitoring also showed that there are considerable possibilities for improvement, especially with the regulation of the system.

The knowledge gained in this study was used to create principal design guidelines for solar powered DEC-systems with the goal of aiding planning engineers with their future projects and increasing the acceptance of this technology.

ACKNOLEDGEMENTS

This research was carried out at the Institute of Energy and Sustainable Development at De Montfort University Leicester in collaboration with the Faculty of Civil Engineering, Building Physics and Economics at the University of Applied Sciences Stuttgart.

I would like to thank Prof. Dr. Ursula Eicker, Prof. Dr. Victor Hanby and Dr. Malcolm Cook for their support and supervision and for their revision of this thesis. Furthermore, I am grateful to my colleagues at the Faculty of Civil Engineering, Building Physics and Economics at the University of Applied Sciences Stuttgart for their assistance, especially to Andres Trinkle and Martin Huber.

I declare that the content of this submission is my own work. The contents of the work have not been submitted for any academic or professional award. I acknowledge that this thesis is submitted according to the conditions laid down in the regulations. Furthermore, I declare that the work was carried out as a part of the course for which I was registered. I draw attention to any relevant considerations of rights of third parties.

CONTENT

LIST OF FIGURES

VERIFICATION OF DESICCANT WHEEL MODEL WITH MEASURED DATA

OPTIMISATION POSSIBILITIES IN CONTROL STRATEGY AND DESIGN

DESIGN GUIDELINES

SUMMARY

LIST OF TABLES

NOMENCLATURE

LATIN LETTERS

A	[m²]	surface, area
c_p	[J/kg K]	specific heat capacity (at constant pressure)
d	[m]	diameter
h	[m]	height
h	[J/kg]	specific enthalpy
h_{ad}	[J/kg]	specific adsorption enthalpy (in this study always $h_{ad} \hat{=} h_{ad,H_2O}$)
h_b	[J/kg]	specific binding enthalpy (in this study always $h_b \hat{=} h_{b,H_2O}$)
h_e	[J/kg]	specific evaporation enthalpy (in this study always $h_e \hat{=} h_{e,H_2O}$)
l	[m]	lenght
l'	[m]	characteristic length (for Nu, Sh and Re)
m	[kg]	mass
$\dot{m}$	[kg/s]	mass flow
M	[kg/mol]	specific molar mass
Nu	[-]	Nusselt-number (heat transmission)
p	[Pa]	(total) pressure
Pr	[-]	Prandtl-number (heat transmission)
p_{sat}	[Pa]	saturation vapour pressure (in this study always $p_{sat} \hat{=} p_{sat,H_2O}$)
p_v	[Pa]	partial vapour pressure (in this study always $p_v \hat{=} p_{v,H_2O}$)
Q	[J]	thermal energy / heat
$\dot{Q}$	[W]	heat flow
R	[$J/kg\ K$]	specific gas constant
Re	[-]	Reynolds-number (flow: laminar, turbulent)

R_m	$[J/mol\ K]$	general/molar gas constant (8.3145 J/mol K)
Sc	[-]	Schmidt-number (mass transmission)
Sh	[-]	Sherwood-number (mass transmission)
T	$[K]$	absolute temperature (273.15 K = 0 °C)
t	$[s]$	time
U	$[m]$	circumference
V	$[m^3]$	volume
v	$[m/s]$	flow velocity
X	$[kg/kg]$	load (in this study always $X \triangleq X_{H_2O}$)
$\dot{X}$	$[kg/kg\ s]$	mass flow because of load
x	$[kg/kg]$	absolute humidity of air
$\dot{x}$	$[kg/kg\ s]$	mass flow because of absolute humidity of air

GREEK LETTERS

α	$[W/m^2\ K]$	heat transmission coefficient
β	$[m/s]$	mass transmission coefficient
$\Delta...$	[-]	Difference
δ_{eff}	$[m^2/s]$	effective diffusion coefficient (gas diffusion in porous solid material)
δ_N	$[m^2/s]$	normal gas diffusion coefficient (gas in gas)
η	$[Pa\ s]$/[-]	dynamic viscosity / efficiency
φ	[-]	relative humidity of air
λ	$[W/m\ K]$	heat conductivity
μ_p	[-]	gas diffusion resistance coefficient of porous solid materials
ν	$[m^2/s]$	kinetic viscosity
θ	$[°C]$	temperature
ρ	$[kg/m^3]$	density
ψ_p	[-]	porosity of solid material

INDICES

H_2O	water
i / N	index (0,1,2...) / number
in	inlet
out	outlet
con	convective
ads	adsorption
dehum	dehumidification
reg	regeneration
amb	ambient
max	maximal / maximum
min	minimal / minimum

ABBREVEATIONS

COP	**C**oefficient **O**f **P**erformance
DEC	**D**esiccative and **E**vaporative **C**ooling
RPH	**R**evolution **P**er **H**our
RSHI	**R**egeneration **S**pecific **H**eat **I**nput

CHAPTER 01

INTRODUCTION

The worldwide energy consumption of cooling devices in buildings is increasing steadily. The main reasons for this are, for one the increasing amount of electrical devices in modern workplaces such as computers, lights etc., which cause high internal gains, and for another, the increased desire for comfortable conditions at the work place.

In addition, the cooling and air conditioning industry around the world is under increased pressure to replace the Chloro-Fluoro-Carbon (CFC) based systems in order to meet environmental requirements. The discussion of global warming, the CO_2-problem and the rapid depletion of known sources of energy is causing the scientific world to consider the utilisation of renewable energy sources.

In recent years, applied researchers have become increasingly interested in solar powered cooling systems. In this context, the open cycle adsorption cooling system called DEC (Desiccative and Evaporative Cooling), which is the subject matter of this dissertation, clearly offers an alternative to conventional cooling technologies. This system has a very important advantage in that it needs only low grade thermal energy instead of high grade electricity. Added attractions are both the fact that it can work with low temperature solar thermal energy sources and the fact that the cooling load is almost in phase with available solar energy. Furthermore, it also doesn't use an environmentally harmful refrigerant.

A large part of the research and development for this system was carried out using pilot plants. However, up to now there has only been little experience gained in the operation of commercial solar powered adsorption cooling systems, particularly in combination with solar air collectors. Thus there is

currently little knowledge available about the performance, the efficiency, the control strategy and the best component choice for different boundary conditions. Lack of experience in operation and high costs have caused a low acceptance of this cooling technology so far.

For the DEC-system, the most important influence on the performance is the dehumidification capacity and the energy efficiency of the desiccant wheel. In current literature however, there is no published report that directly addresses the influence of different operation parameters or gives detailed information about the performance for the whole operation range of desiccant wheels.

This thesis should serve as a contribution to help DEC technology push forward by providing fundamental knowledge about this technology's attainable efficiency and by supporting planning engineers by demonstrating the potential but also the problems with the first commercially used DEC-systems that use solar air collectors. Additional principal design guidelines and suggestions for control strategies are also given.

In this thesis, the fundamental principles of DEC technology and the physical foundations of the "adsorption from gas phase" will be shown. Furthermore, a physically based dynamic simulation model for desiccant wheels, which is verified by measurements on a test plant for desiccant wheels, will be introduced. A further part of this work will be the evaluation of measurements from two commercially used, solar powered adsorption cooling systems with solar air collectors in Spain and in Germany. The measurements are mainly used to investigate the achieved efficiencies and to discover operation problems that can occur with such systems. With the evaluated data from the DEC-system in Germany, a closer look will be taken at the control strategy and the component choice. Possible improvements will be explored using a simulation model for the DEC-system. The knowledge gained in this study will then be summarized in design guidelines for solar powered DEC-systems.

CHAPTER 02

DESICCANT COOLING TECHNOLOGY

2.1 TECHNOLOGY DESCRIPTION

The DEC-system (**D**esiccative and **E**vaporative **C**ooling) is based on the principle of adiabatic evaporative cooling in which water evaporates and draws the necessary thermal energy from the air. Thereby the water content of the air increases. The extent to which the supply air can be cooled through humidification is usually limited by the maximally allowed water content of the building's air. The cooling capacity increases with a lower water content of the air at the beginning of the process. The air is dehumidified by adsorption: through this, the air gets warmer and must be pre-cooled with the exhaust air using a heat exchanger. For a continuous dehumidification of the process air, the water adsorbed on the desiccant material has to be removed, which is done by allowing hot air to flow through the desiccant material (regeneration).

Earlier dehumidifiers, which were commonly used in the 70's, were composed of packed beds of desiccant materials. Such packed beds had the disadvantage of causing very high pressure drops which in turn demanded high fan power (SLAYZAK et. al., 1999).

Today, rotating wheels with a desiccant laden matrix are used. The so-called desiccant wheels have the advantage of causing less of a pressure drop while still having a very large surface area for the desiccation by adsorption.

The construction of a standard desiccant cooling system is shown in Fig. 2.1. The air handling process of the air flows is shown in Fig. 2.2 in a Mollier diagram. The numbers shown in Fig. 2.1 correspond to the those in Fig. 2.2.

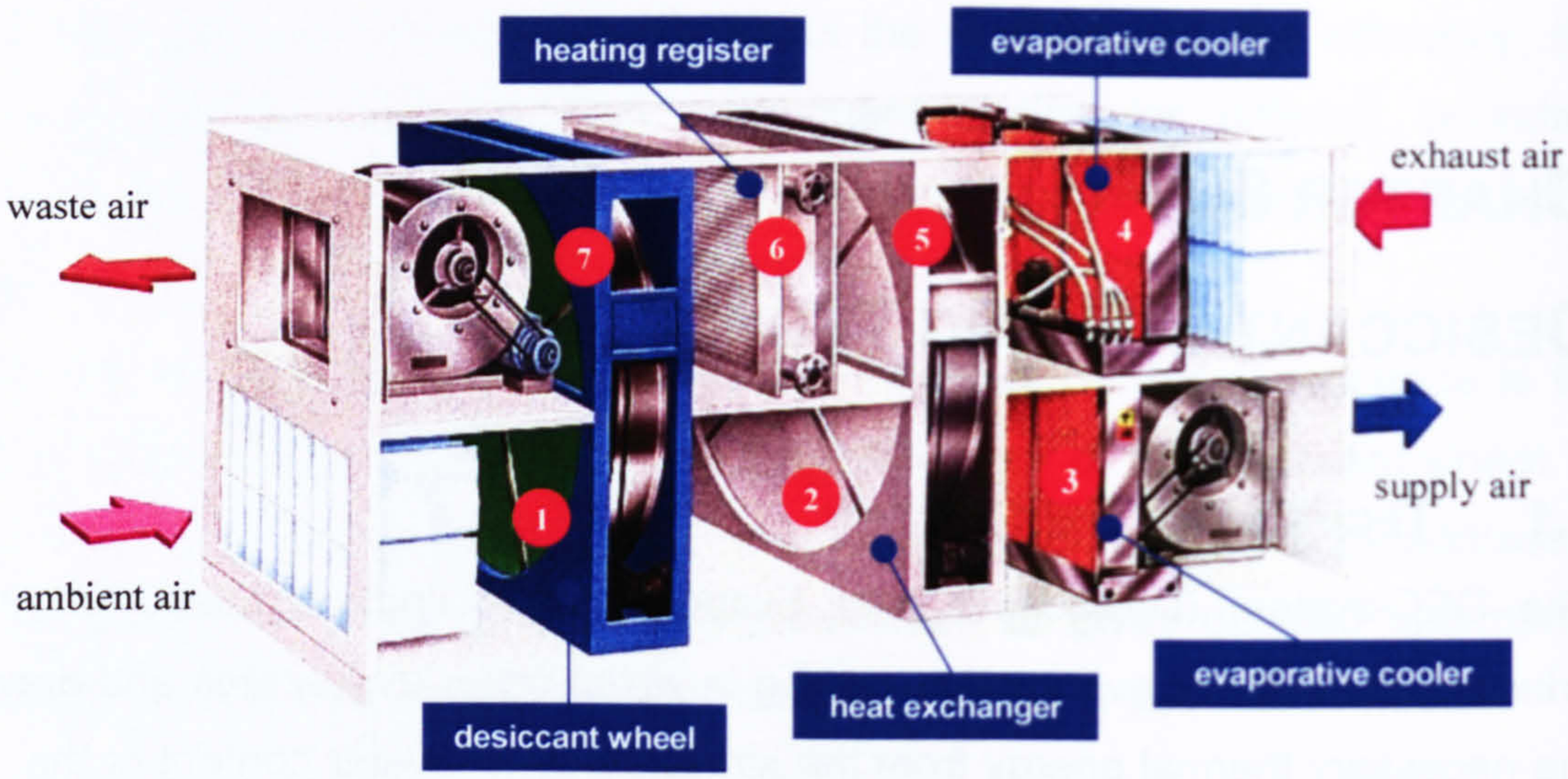

Fig. 2.1: *Standard DEC-system (reference: MUNTERS product information)*

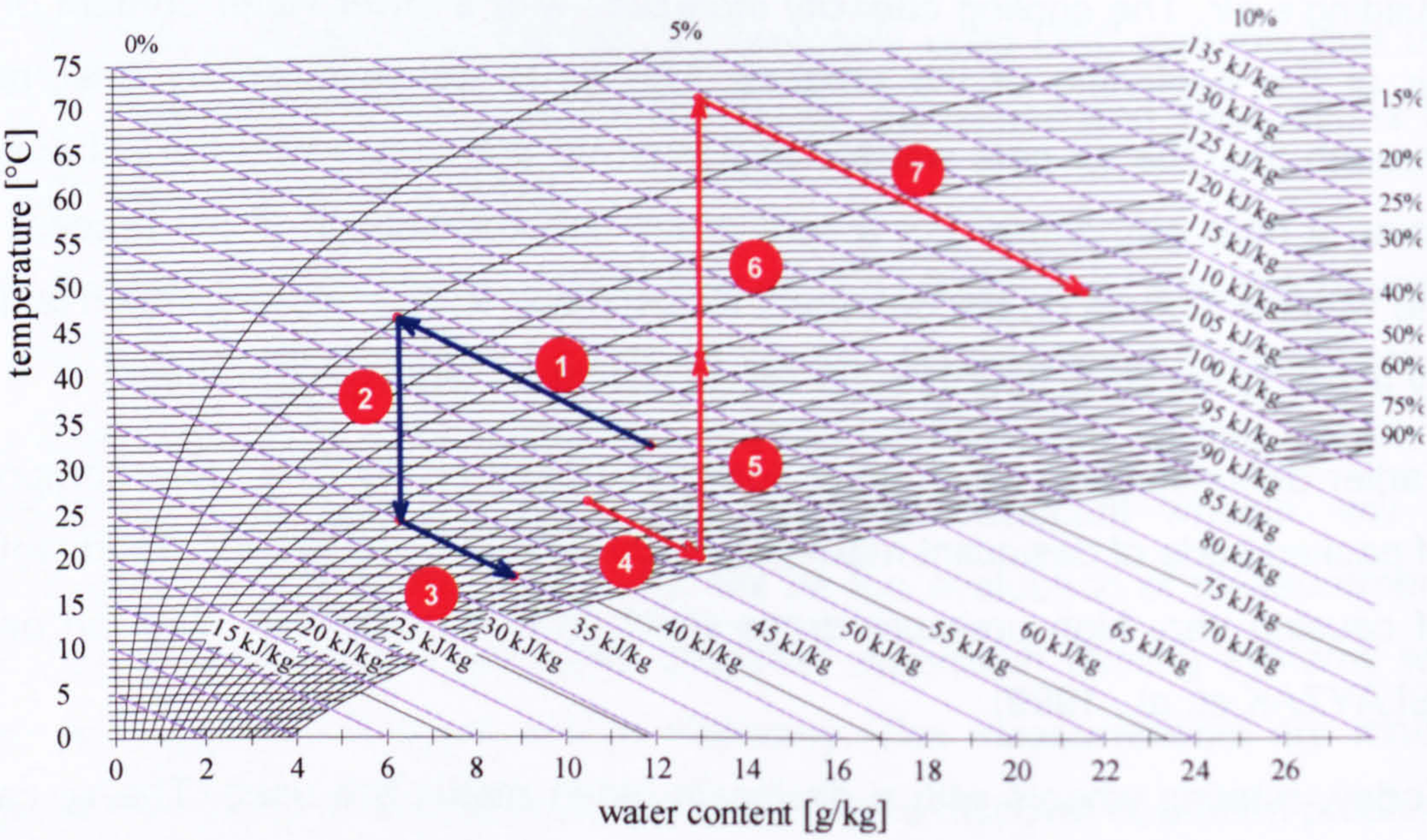

Fig. 2.2: *Standard DEC-process in a Mollier diagram, numbers like in Fig. 2.1*

The ambient air (in Fig. 2.1 at the bottom) is dehumidified in a desiccant wheel (1). Since the adsorption process is exothermic, the air is heated as it dehumidifies. Next, the air is pre-cooled by the exhaust air in the rotary heat exchanger (2) and then is cooled down to the necessary supply air temperature with an evaporative cooler (3). The exhaust air (in Fig. 2.1 at the top) flows in

the reverse direction. The air is cooled down with an evaporative cooler (4) by humidification up to the point of near saturation and is then preheated by the supply air with a rotary heat exchanger (5). With the input of thermal energy by a heating register (6), the exhaust air is heated up to regeneration temperature and is used to dehumidify the desiccant wheel (7).

Beside this standard system design, which is called "closed cycle system", there are some other designs varying mainly in airflow conduction or by using additional cooling devices instead of humidifiers. An overview of the mostly used designs of DEC-systems is given in chapter 10.3.3 showing the pros and cons of each design.

The control of a DEC-systems works in principle in three steps with a rising cooling demand as follows:

1. switch on supply air humidifier
2. switch on exhaust air humidifier and rotary heat exchanger
3. switch on desiccant wheel and supply regeneration heat

Because almost every system works under special boundary conditions using different sources of regeneration energy etc., in most cases this control strategy must be modified more or less.

2.2 DESICCANT WHEELS

2.2.1 WHEEL CONSTRUCTION

The matrix of a desiccant wheel is made from a honeycomb-shaped material. The honeycomb structure is lightweight, durable and exposes a large surface to the air. Well-made desiccant wheels offer an internal surface of about 3000 m^2 / m^3 and the pressure drop caused by the wheel is very low which minimises the power consumption of the fans.

Most manufacturers use a construction that is based on the design of the first enthalpy exchanger introduced by the Munters company in 1958. In these

wheels a stack of alternating flat and corrugated sheets is sealed together with a ceramic binder. The stack is then machine-worked into the shape of a wheel.

Other manufacturers, such as the Engelhard HexCore LP company use a hexagonal structure. The production of these wheels starts with a block of flat sheets with narrow strips of adhesive between them. While exposed to steam and hot air, the block is slowly stretched by being pulled apart at both ends. The sheets are made from a mixture of glass and ceramic fibres or from high-temperature plastic.

The desiccant can be inserted into the matrix in several ways. Often, a mixture of desiccant powder and adhesive is coated on the surface after the matrix is formed. In another method, the matrix is soaked in a solution of a liquid desiccant and then dried. The dried liquid crystallises, forming a thin layer of water-soluble desiccant throughout the honeycomb. (GAS RESEARCH INSTITUTE. 2001; HEINRICH and FRANZKE, 1997).

2.2.2 DESICCANT MATERIALS

SILICA GEL

The synthetically-produced silica gel is a fine pored solid silicic acid which consists of 99 % of silicon dioxide. It can hold up to 40% of its dry weight in water when in equilibrium with air at saturation. Thereby, the water is attracted and held to the walls of the fine pores within the material (adsorption), but there is no chemical reaction between the silica gel and the water molecules. Silica gel can withstand temperatures up to 400 °C and is a solid, insoluble desiccant. No special precautions are required when it is exposed to air at 100 % relative humidity. It is also possible to wash a wheel in water if dust or other particulate block the air passageways. Silica gel does not undergo any chemical or physical change during the adsorption process. It is inert, non-toxic, stable and resistant to most chemicals. (GUTERMUTH, 1980; HEINRICH and FRANZKE, 1997; KAST, 1988; MUNTERS, 2001).

LITHIUM CHLORIDE

Lithium chloride has a high working capacity. It can attract and hold over ten times its weight in water and is one of the most hygroscopic compounds that exist. Its ability to attract and hold water is caused by the ability to absorb water through a chemical reaction (absorption). As a result the salt and the water molecules build up a homogeneous phase. As lithium chloride is water soluble, precautions are required to protect the wheel from high relative humidity. Lithium chloride prevents the growth of bacteria on the wheel surface. It can also significantly reduce the number of organisms which may be carried in the air stream. Test results show there is typically a 25% to 50% reduction in the bacteria content of the air as it passes through the wheel. Lithium chloride is unaffected by most air stream pollutants, and resistant to many contaminants such as petroleum vapour, solvents, etc. (GUTERMUTH, 1980; HEINRICH and FRANZKE, 1997; MUNTERS, 2001).

MOLECULAR SIEVE

A molecular sieve is a crystalline material of aluminium silicate which is capable of separating molecules of different sizes by sorption. Therefore, small molecules, such as water molecules for example, are adsorbed while large molecules pass through the wheel. Due to the fact that water molecules are polar and the molecular sieve has a high surface energy, water molecules are effectively adsorbed, even at low water vapour pressures. As a result, molecular sieve materials are suitable for specialty applications that call for the dehumidification of air to a very low level of humidity and extremely low dew points of about -40°C to -60°C. For the same reason, the molecular sieve has a better sorption capacity at higher temperatures than other sorbents. Chemically and thermally-speaking, a molecular sieve is highly stable. The properties of molecular sieves do not change under normal conditions. (HEINRICH and FRANZKE, 1997; KAST, 1988; MUNTERS, 2001).

There are a few other types of wheels available with different adsorbents such as activated alumina, synthetic polymers etc. but they are relatively unimportant in terms of their use with desiccant cooling systems.

2.3 HEAT EXCHANGERS

Heat exchangers can be divided into two main groups: regenerators and recuperators.

With **recuperators,** the heat is transferred from one fluid to another through very thin solid materials shaped like channels or tubes. The heat is thus transferred continuously through the separating material. An advantage of these systems is that they prevent any mixing of the two fluids. The disadvantages of these systems are a lower efficiency (compared with regenerators) and the fact that they often cause high pressure drops. In DEC-systems, recuperators are usually used to heat the regeneration air using thermal energy from waste heat, solar thermal collectors etc., where the energy must be transferred from a liquid to air.

With **regenerators,** the heat is transferred first from one fluid to an intermediate "material" (fluid or solid) and later from that material to the second fluid and so on. The rotating heat exchanger is a special kind of regenerator which is constructed similarly to desiccant wheels, only without a sorption material built in. With rotating heat exchangers, usually aluminium is used for the matrix. The advantages of these regenerators are relatively high efficiencies, which are given at about 0.7 to 0.8 by RECKNAGEL et. al., 1997, and low pressure drops. The disadvantage is that the air flows are not completely separated from each other, so that a mixing of flows can not be completely avoided. Rotating heat exchangers have dominated on DEC-systems because of their high efficiencies and because in most cases a little admixture of one airflow to the other is not critical or can be controlled by commissioning the pressure drops in the system.

2.4 HUMIDIFIERS

Humidifiers are responsible for the actual cooling process in the DEC-system. The supply air and/or the exhaust air are cooled down by humidification. This cooling principle (evaporative cooling) has been well-known for a very long time and is based on the evaporative process of water. The evaporation of water is an endothermal process which takes the necessary thermal energy from the surrounding air. The air that leaves the humidifier is therefore humidified and cooled simultaneously without the use of any external energy supply for the evaporation process. For the DEC-system, usually all kinds of evaporative humidifiers are suitable that operate with liquid water (but not steam).

Evaporative humidifiers for DEC-systems are usually spray humidifiers or so-called contact or trickle humidifiers which can be described as follows:

Spray humidifiers produce extremely small water drops, so-called aerosols, which float in the air and change phase after a short period of time. Depending on the sprayer, a certain distance in air flow direction is necessary to ensure the complete evaporation of the aerosols. To prevent the following components from direct contact with liquid water, usually the installation of mist collectors is necessary.

With **Contact humidifiers** (see Fig. 2.3), the air flows through a porous body which is trickled with water. The advantage of these humidifiers is that almost no aerosols are generated and so the depth of the humidifier is very small and no mixing distance or mist collectors are necessary. To prevent water consumption that is too high, these humidifiers could operate with a circulation pump. It would however then be necessary to prevent salt deposits on the surfaces using an appropriate rate of fresh water.

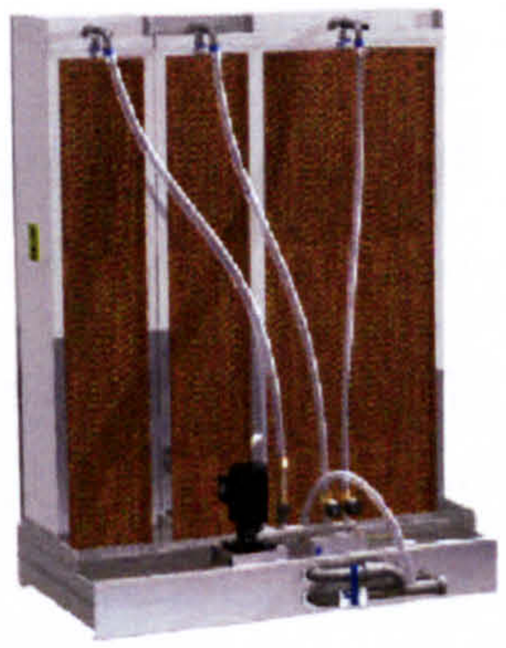

Fig. 2.3: *Contact humidifier (reference: MUNTERS product information)*

2.5 PROS AND CONS OF DEC-SYSTEMS

Just like every other cooling technology, the DEC-system has advantages and disadvantages determine the feasibility or otherwise of the use of this system. Most of the pros and cons of the DEC-system result from the air- based principle of the system, where the cooling energy is supplied by the cooled air flow, whereas most other systems supply cooled liquids.

PROS

- For operation, the DEC-system needs only low grade thermal energy instead of high grade electricity (e.g. as is required by compression-type cooling devices) or high grade thermal energy (e.g. for absorption cooling devices).
- Because low temperatures are sufficient for DEC-system operation, regenerative energy can easily be used, e.g. solar energy from solar thermal collectors or solar air collectors. Other available waste heat sources, e.g. from production processes can also be used easily.
- If solar energy is used for operation, the cooling load is in most cases in phase with the current available solar energy (seasonally and daily), so that the expenditure for energy storage devices can be avoided, at least in some cases.
- Because the refrigerant medium in DEC-systems is water, there is no need for environmentally harmful refrigerants.
- The DEC-system can be used for cooling but also for ventilation and every other kind of air conditioning such as dehumidification, heating, heat or enthalpy recovery in winter. Most other technologies require additional devices in order to work as complete air conditioning systems.

CONS

- High cooling loads require a high air flow volume because of the low specific heat capacity of air. High air flow volumes cause high energy consumption from the fans.

- For some applications high volume flows cause problems, for example in situations with large cooling demands but almost no need of ventilation, or a situation with a great demand on comfort when, for instance, no noticeable air velocities are allowed in the building.
- The DEC-system requires a large floor space for the system itself and also for the air tubes/channels.
- As a matter of principle, with DEC-systems it is normally not possible to produce lower temperatures than about 16-17 °C under design conditions.

CHAPTER 03

THEORETICAL ANALYSIS OF THE ADSORPTION PROCESS

3.1 PRINCIPLES OF ADSORPTION

Adsorption is the binding of molecules from a fluid phase (gas or liquid) onto a surface or interphase. The reverse process, the donation of molecules to the fluid phase is called desorption.

To describe the adsorption process, it is useful to introduce the "load" X. The load is the ratio between the mass of the adsorbed adsorbate ($m_{adsorbate}$) and the mass of the unloaded adsorption material ($m_{adsorption\ material}$).

$$X = \frac{m_{adsorbate}}{m_{adsorption\ material}} \qquad \text{(Eq. 3.1)}$$

To reach high loads the specific surface of the adsorption material should be as large as possible. Therefore, most solid adsorption materials have a high porosity.

The binding of molecules onto a surface is caused by physical or chemical forces. During chemical absorption there is a chemical reaction between the sorption material and the sorbate, therefore the binding energy of chemical absorption is usually higher than that of physical adsorption. The transition region between chemical absorption and physical adsorption is often not very clear. The subject matter of this study is the physical adsorption process.

Due to the forces involved, there is an energy change during adsorption. The energy released by the adsorption of a molecule from a liquid phase to a surface is called “binding-energy”. If a molecule is adsorbed from a gas phase there is additional energy released called “evaporation energy”.

The energy released during the adsorption process from the liquid phase (binding energy) is dependent on the temperature and on the load of the adsorption material. There, the influence of the load is much higher than the influence of the temperature. As the loads increase, the forces at the surface that cause the binding of the molecules get smaller and thus the energy released by the binding decreases.

For adsorption from the gas phase, the specific adsorption enthalpy (h_{ad}) can be calculated as the sum of the load- and temperature-dependent specific binding enthalpy (h_b) and the specific evaporation enthalpy (h_e).

$$h_{ad}(X,T) = h_b(X,T) + h_e(T) \qquad \text{(Eq. 3.2)}$$

3.2 ADSORPTION EQUILIBRIUM

The adsorption equilibrium between the adsorption material and the adsorbate is fundamental for the description of the adsorption process. If a dry sorption material is exposed to an air flow with a constant temperature and a constant vapour pressure from the adsorbate, the load of the adsorption material increases until the adsorption equilibrium is reached.

The adsorption equilibrium and the load (X) of the adsorption material are dependent on the partial vapour pressure (p_v) of the adsorbate in the fluid phase and the temperature (T) of the adsorption material.

$$X = f(p_v, T) \qquad \text{(Eq. 3.3)}$$

This function is usually shown in a diagram with the load plotted on the ordinate and the partial vapour pressure plotted on the abscissa. Sometimes the ratio between the partial vapour pressure and saturation vapour pressure is used instead of the partial vapour pressure, e.g. the relative humidity for water as adsorbate. This display is called the sorption isotherm. Different temperatures are shown as different curves. In Fig. 3.1, the sorption isotherms of silica gel WS and water are shown.

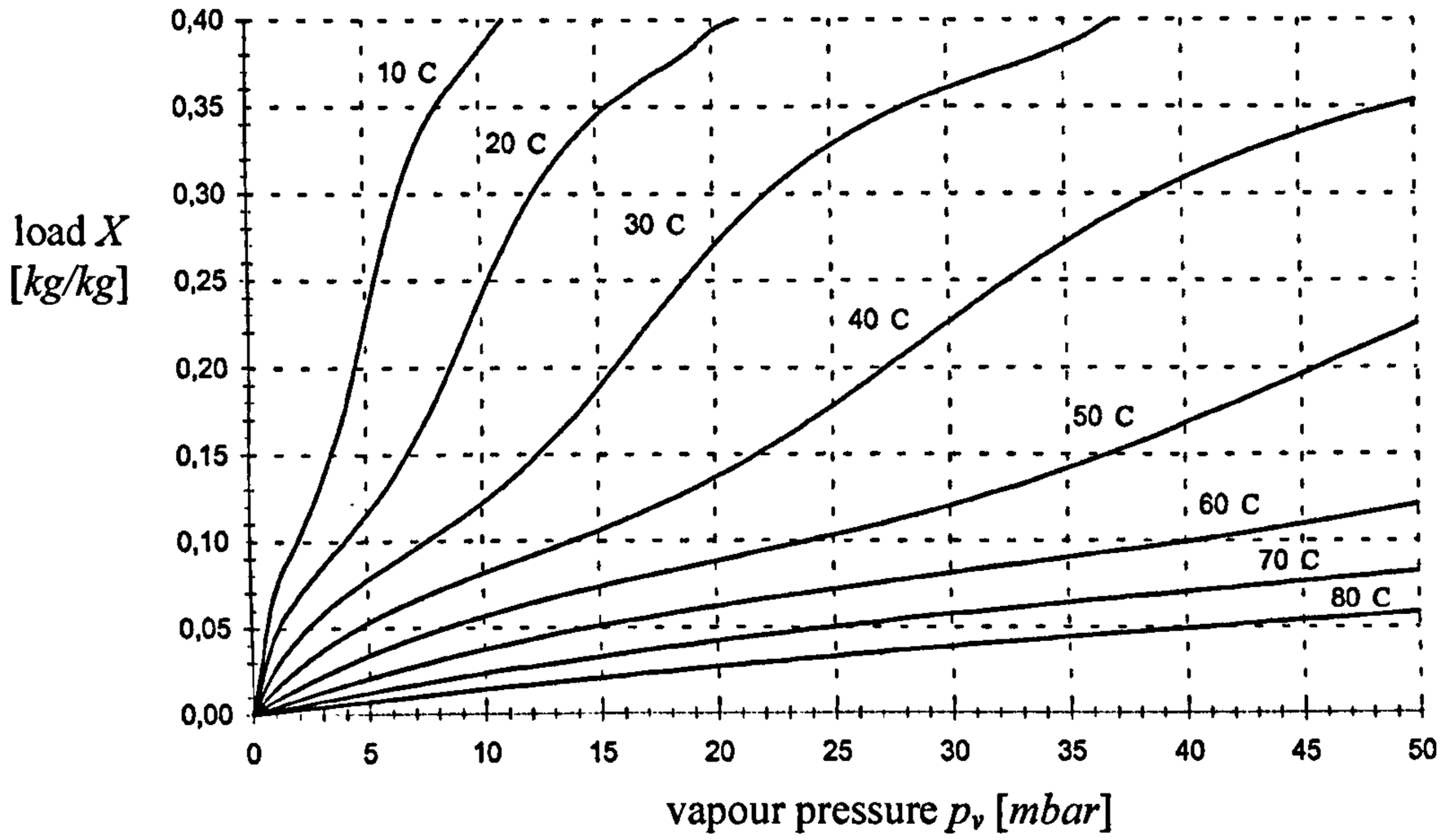

Fig. 3.1: *Sorption isotherms of silica gel WS and water (BAUER, 1998)*

The sorption isotherms are normally measured in an experimental laboratory. The measured data often show an effect that is called hysteresis whereby, the outcomes of measurements obtained by an experimental run with increasing vapour pressure are different from measurements with decreasing vapour pressure, in that measurements with decreasing vapour pressure produce higher loads. An explanation of this effect is the so called "bottleneck" effect. During adsorption, the smaller pores in the adsorption material are filled first followed by the larger ones. During desorption, the larger pores are drained first. However, if the draining of the larger pores is prevented by some of the smaller ones which are still filled with water, the big pores cannot be drained before the smaller ones. Therefore, the load can be influenced by large pores locked in between smaller ones.

For the mathematical description of the sorption isotherms there are several semi-empirical theories.

The first physical model for the calculation of sorption isotherms was developed by Langmuir (LANGMUIR, 1918). His model describes the adsorption of

molecules in a mono molecular layer on the surface of the adsorption material. In 1938 the model of Langmuir was extended by Brunauer, Emmet and Teller (BRUNAUER et. al., 1938) to a multi molecular layer model. They introduced an equation which is still one of the most widely used equations used to calculate sorption isotherms today. This equation needs experimental data to determine some of the parameters necessary for calculation.

Another theory used to describe the adsorption process was developed by Polanyi (POLANYI, 1914) and Dubinin (DUBININ, 1960). They describe adsorption by introducing an adsorption potential. The model was developed because for micro porous adsorption materials, e.g. activated carbon, the pores are not much bigger than the molecules of the adsorbate. In this case the multi molecular layer BET-theory (Brunauer, Emmet, Teller) is not applicable.

3.3 HEAT AND MASS TRANSPORT

The adsorption process is coupled with heat and mass transport. Each process influences the other, thus a separate consideration of each process is not possible.

In the adsorption process, the adsorbate is transported from the fluid to the surface by convection. From the outer surface to the interior surface there are several possible transport mechanisms such as flow, diffusion and molecular movement.

The heat is also transported form the fluid to the surface by convection. The transport into the adsorption material structure is carried out through conduction. Additionally the energy released by the adsorption process must be taken into consideration.

3.4 ADSORPTION KINETICS

Adsorption kinetics describe the time behaviour of the adsorption process. Mathematically, there are two ways to describe adsorption kinetics.

One way is the so-called diffusion model. With this model, the transport mechanisms in the sorption material are described as physical models. There are models for the gas diffusion, the flow, the molecular movements etc., but the calculation is very complex. Additional accurate data about the pore sizes, pore distribution etc. is necessary.

The other way is the so-called kinetic model. With this model all the internal transport mechanisms are replaced by an overall mass transfer coefficient which includes the external mass transfer (convection). In order to derive this coefficient, experimental investigations are necessary, hence this model is an empirical one.

In most cases, the governing factor for the time behaviour of the mass transport is the internal transport mechanism in the sorption material because the mass transport by convection from the fluid phase to the surface is normally much higher than the mass transport from the surface into the adsorption material. (KAST, 1988)

3.5 CALCULATION OF THE ADSORPTION PROCESS

3.5.1 GENERAL EQUATIONS

For the calculation of the adsorption process of water out of air it is necessary to have equations that describe the functional connection between the absolute humidity (x), the relative humidity (φ), the temperature (T) and the pressure (p).

The water content or the absolute humidity (x) of air describes the ratio between the mass of the water (m_{H_2O}) and the mass of the dry air ($m_{dry\,air}$):

$$x = \frac{m_{H_2O}}{m_{dry\,air}} \qquad \text{(Eq. 3.4)}$$

The relative humidity (φ) is defined as the ratio of the partial vapour pressure (p_v) and the saturation vapour pressure (p_{sat}):

$$\varphi = \frac{p_v}{p_{sat}} \qquad \text{(Eq. 3.5)}$$

The absolute humidity of air (x) can be calculated with the following, common, approximate equation:

$$x = 0.622 \frac{p_v}{p - p_v} = 0.622 \frac{\varphi \cdot p_{sat}}{p - \varphi \cdot p_{sat}} \qquad \text{(Eq. 3.6)}$$

where:

x	=	absolute humidity of air	$[kg/kg]$
p_v	=	partial vapour pressure	$[Pa]$
p	=	total pressure	$[Pa]$
p_{sat}	=	saturation vapour pressure	$[Pa]$
φ	=	relative humidity	[-]

After resolving, the relative humidity becomes:

$$\varphi = \frac{x}{x + 0.622} \frac{p}{p_{sat}} \qquad \text{(Eq. 3.7)}$$

The saturation vapour pressure is dependent on the temperature ($p_{sat} = f(T)$). This function describes the equilibrium between the liquid phase and gas phase and can be calculated using a "Carnot Cycle" with evaporating and sublimating gas with the supply or removal of the evaporation enthalpy. From this consideration follows the equation of Clausius-Clapeyron (Eq. 3.8), (HERING et. al., 1997):

$$\frac{dp_{sat}}{dT} = \frac{h_e \cdot m}{\left(V_{gas} - V_{liquid}\right) \cdot T} \qquad \text{(Eq. 3.8)}$$

where:

p_{sat}	=	saturation vapour pressure
h_e	=	specific evaporation enthalpy
m	=	mass of the gas
$V_{gas/liquid}$	=	volume of the gas / liquid
T	=	temperature

With the simplification $V_{gas} >> V_{liquid}$ and the assumption of an ideal gas (Eq. 3.9)

$$V_{gas} = \frac{m \cdot R \cdot T}{p_{sat}} \qquad \text{(Eq. 3.9)}$$

where: R = specific gas constant

follows:

$$\frac{dp_{sat}}{p_{sat}} = \frac{h_e}{R \cdot T^2} dT \qquad \text{(Eq. 3.10)}$$

The specific evaporation enthalpy (h_e) of water is the difference between the specific enthalpy of the water vapour/steam (h_{steam}) and the specific enthalpy of the liquid water (h_{water}):

$$h_e = h_{steam} - h_{water} \qquad \text{(Eq. 3.11)}$$

The specific enthalpy of steam (h_{steam}) and the specific enthalpy of liquid water (h_{water}) can be calculated with the following approximate equations depending on the temperature (GLUECK, 1991):

$$h_{steam} = 2501.482 + 1.789736 \cdot \theta + 8.957546 \cdot 10^{-4} \cdot \theta^2 - 1.300254 \cdot 10^{-5} \cdot \theta^3 \qquad \text{(Eq. 3.12)}$$

$$h_{water} = -2.25 \cdot 10^{-2} + 4.2063437 \cdot \theta - 6.014696 \cdot 10^{-4} \cdot \theta^2 + 4.381537 \cdot 10^{-6} \cdot \theta^3 \qquad \text{(Eq. 3.13)}$$

where: h_{steam} = specific enthalpy of steam in $[kJ/kg]$

h_{water} = specific enthalpy of liquid water in $[kJ/kg]$

θ = temperature in $[°C]$

The error using these approximate equations is less than 0.04% in the range of temperature between 10°C < θ < 200°C.

With the equations (Eq. 3.10) - (Eq. 3.13) follows for the saturation vapour pressure (p_{sat}) of water:

$$p_{sat} = 611 \exp\begin{pmatrix} -1.91275 \cdot 10^{-4} + 7.258 \cdot 10^{-2} \cdot \theta - 2.939 \cdot 10^{-4} \cdot \theta^2 ... \\ ... + 9.841 \cdot 10^{-7} \cdot \theta^3 - 1.92 \cdot 10^{-9} \cdot \theta^4 \end{pmatrix} \qquad \text{(Eq. 3.14)}$$

where: p_{sat} = saturation vapour pressure in $[Pa]$

θ = Temperature in $[°C]$

The error with this equation is less than 0.02% in the range of temperature between 0°C < θ < 100°C (GLUECK, 1991).

The density of humid air (ρ_{air}) is dependent on the total pressure (p), the partial water vapour pressure (p_v) and the temperature (T) and can be calculated with the following approximate equation:

$$\rho_{air} = 10^{-4} \cdot \left(34.8 \cdot \frac{p}{T} - 13.2 \cdot \frac{p_v}{T} \right) \qquad \text{(Eq. 3.15)}$$

where: ρ_{air} = density of humid air in [kg/m^3]
p = total pressure in [Pa]
p_v = partial vapour pressure in [Pa]
T = Temperature in [K]

The specific enthalpy of humid air (h_{air}) is composed of the specific enthalpy of the dry air ($h_{dry\ air}$), the specific enthalpy of the water vapour ($x \cdot h_{steam}$) and the specific evaporation enthalpy of the water ($x \cdot h_e$) (HERING et. al., 1997):

$$h_{air} = h_{dry\,air} + x \cdot h_{steam} + x \cdot h_e = c_{p,dry\,air} \cdot \theta + x \cdot c_{p,steam} \cdot \theta + x \cdot h_e \qquad \text{(Eq. 3.16)}$$

where: h_{air} = specific enthalpy of humid air
$h_{dry\,air}$ = specific enthalpy of dry air
x = water content
h_{steam} = specific enthalpy of water vapour
h_e = specific evaporation enthalpy of water
$c_{p,\,dry\,air}$ = heat capacity of dry air
$c_{p,steam}$ = heat capacity of water vapour
θ = temperature [°C]

The specific heat capacity of dry air $c_{p,dry\,air}$, steam $c_{p,steam}$ and water $c_{p,water}$ is temperature-dependent and can be approximately calculated using the following equations by GLUECK, 1991:

$$c_{p,dry\,air} = 1.0065 + 5.309587 \cdot 10^{-6} \cdot \theta + 4.758596 \cdot 10^{-7} \cdot \theta^2 - \ldots$$
$$\ldots 1.136145 \cdot 10^{-10} \cdot \theta^3 \quad [kJ/kg \cdot K] \qquad \text{(Eq. 3.17)}$$

with an accuracy of ± 0.05% in a range of -20°C < h < 200°C

$$c_{p,steam} = 1.863 + 2.680862 \cdot 10^{-4} \cdot \theta + 6.794704 \cdot 10^{-7} \cdot \theta^2 - ... \\ ...2.641422 \cdot 10^{-10} \cdot \theta^3 \quad [kJ/kg \cdot K] \qquad \text{(Eq. 3.18)}$$

with an accuracy of ± 0.04% in a range of 25°C < h < 400°C

$$c_{p,water} = 4.177375 - 2.144614 \cdot 10^{-6} \cdot \theta - 3.165823 \cdot 10^{-7} \cdot \theta^2 + ... \\ ...4.134309 \cdot 10^{-8} \cdot \theta^3 \quad [kJ/kg \cdot K] \qquad \text{(Eq. 3.19)}$$

with an accuracy of ± 0.02% in a range of 10°C < h < 200°C

3.5.2 ADSORPTION EQUILIBRIUM

For the description of the adsorption equilibrium, the extended theory by Brunauer, Emmett and Teller (BRUNAUER et. al, 1938) is used. The equation for the adsorption isotherm is:

$$\frac{X}{C_m} = \frac{\varphi}{1-\varphi} + \frac{2(b-1)\varphi + 2(b-1)^2\varphi^2 + \left(Nb^2 + Nh - N^2b^2\right)\varphi^N ...}{2\left(1 + 2(b-1)\varphi + (b-1)^2\varphi^2 + \left(b^2 + h - 2b - Nb^2\right)\varphi^N ...\right.} \\ \frac{...+\left(2b + N^2b^2 + 2Nb - 2b^2 - Nb^2 - 2h - 2Nh\right)\varphi^{N+1} + (Nh + 2h)\varphi^{N+2}}{...+\left(Nb^2 + 2b - 2b^2 - 2h\right)\varphi^{N+1} + h\varphi^{N+2}\Big)} \qquad \text{(Eq. 3.20)}$$

where: X = load in $[kg/kg]$

φ = relative humidity in [-]

C_m, b, N, h = parameters dependent on adsorption material, adsorbate and temperature in [-]

The equation gives the load (X) of the sorption material that is dependent on the relative humidity (φ) for a constant temperature:

$$X|_{T=const.} = f(\varphi) \qquad \text{(Eq. 3.21)}$$

For the case that silica gel is used as the adsorption material, water is used as the adsorbate and at a temperature of 40°C, the following parameters apply (KAST, 1988):

$$C_m = 0.11 \;/\; b = 11 \;/\; N = 7.2 \;/\; h = 19000$$

The equation is valid for a load of up to about 0.4 kg/kg.

In order to calculate the load (X) with the above mentioned equation (Eq. 3.20) at a given relative humidity (φ) and a given different temperature ($\theta \neq 40°C$), the following implicit equation can be used as an approximation. As the specific binding enthalpy is dependent on the load ($h_b = f(X)$), and the load is dependent on the relative humidity ($X = f(\varphi)$), the equation has to be solved iteratively as follows (EICKER, 2001; BAUER, 1998):

$$X(\varphi,\theta) = X|_{\theta=40°C}(\varphi_i) \qquad \text{(Eq. 3.22)}$$

with:

$$\varphi_{i+1} = \varphi_i \cdot \left(\frac{p_{sat}(40°C)}{p_{sat}(\theta)} \right)^{\frac{h_b\left(X|_{\theta=40°C}(\varphi_i)\right)}{h_e}} \quad \text{iteration until: } \varphi_{i+1} = \varphi_i \qquad \text{(Eq. 3.23)}$$

where:
- X = load in [kg/kg]
- φ = given relative humidity in [-]
- θ = given Temperature [$°C$]
- $\varphi_{i/i+1}$ = new calculated relative humidity in [-] (Eq. 3.23)
- p_{sat} = saturation vapour pressure in [Pa]
- h_b = specific binding enthalpy in [kJ/kg]
- h_e = specific evaporation enthalpy [kJ/kg]

The specific adsorption enthalpy (h_{ad}) is composed of the load-dependent specific binding enthalpy ($h_b(X)$) and the temperature-dependent specific evaporation enthalpy ($h_e(T)$). The influence of the temperature on the binding enthalpy can be ignored for most considerations, thus for the adsorption enthalpy follows:

$$h_{ad}(X,T) = h_b(X) + h_e(T) \qquad \text{(Eq. 3.24)}$$

An approximate equation for the specific binding enthalpy ($h_b(X)$) is given by Otten (OTTEN, 1989):

$$h_b(X) = h_{ad}(X,T) - h_e(T) = h_0 \cdot \left(1 + a \cdot X + b \cdot X^2\right) - h_e(T) \qquad \text{(Eq. 3.25)}$$

where: h_0, a, b = parameters dependent on adsorption material, adsorbate and temperature, h_0 in [kJ/kg], a and b in [-]

X = load in [kg/kg]

h_e = evaporation enthalpy in [kJ/kg]

The parameters for silica gel acting as adsorption material, water as adsorbate and a temperature of 20°C are:

$$a = -2.34 \quad / \quad b = 6.05 \quad / \quad h_0 = 3172\ [kJ/kg]$$

The evaporation enthalpy of water at this temperature is $h_e\ (20°C) = 2454\ [kJ/kg]$. With a load of $X = 0.1934\ [kg/kg]$, the above equation gives $h_b = 0$, thus for higher loads the binding enthalpy equals 0.

Another approximate equation for the binding enthalpy dependent on the load (X) is given by Gassel (GASSEL, 1998):

$$h_b(X) = 1000\left[\frac{kJ}{kg}\right] - X\left[\frac{kg}{kg}\right] \cdot 4000\left[\frac{kJ}{kg}\right] \qquad \text{(Eq. 3.26)}$$

This equation delivers much higher binding enthalpies than equation (Eq. 3.25).

3.5.3 HEAT AND MASS TRANSPORT

The overall heat and mass transport is dependent on the type of transport mechanism that governs the process.

For the heat transfer from the fluid to the adsorption material, the heat transmission resistance is the determining transport mechanism (KAST, 1988).

The mass transport however is governed in most cases by the internal transport mechanism in the adsorption material and not by the mass transmission resistance (KAST, 1988). Assuming that the interior transport is mainly responsible for the adsorption kinetics and that the controlling transport mechanism is the gas diffusion, the effective coefficient of diffusion (δ_{eff}) in the adsorption material can be calculated as follows:

$$\delta_{eff} = \frac{\psi_p \cdot \delta_N}{\mu_p} \qquad \text{(Eq. 3.27)}$$

where: ψ_p = porosity of solid material

δ_N = normal gas diffusion coefficient (gas in gas)

μ_p = gas diffusion resistance coefficient of porous solid material

Contrary to fixed bed adsorbers however, the construction of a desiccant wheel offers only a very thin layer of adsorption material and provides a very large surface. The thickness of the adsorption material layer in commonly-used desiccant wheels is only about 0.1 mm. According to Mertins (MERTINS, 2000), in such thin layers of silica gel, the ratio between mass transmission resistance and interior mass transport resistance is about 5. Thus the governing transport mechanism for mass transport from the gas to the desiccant wheel is the mass transmission resistance and not the internal transport mechanisms as is the case with fixed bed adsorbers.

In order to describe the coupled heat and mass transport between a gas and a surface, transmission coefficients are defined.

The thermal energy (Q) transferred by transmission can be calculated with the following equation:

$$Q = A \cdot \alpha \cdot \left(T_{gas} - T_{surface}\right) \cdot t \qquad \text{(Eq. 3.28)}$$

where: Q = amount of heat transferred by transmission

A = heat transferring area

α = heat transmission coefficient

$T_{gas/surface}$ = temperature

t = time

The mass (m) transferred by transmission can be calculated with:

$$m = A \cdot \frac{\beta \cdot M}{R_m \cdot T} \cdot \left(p_{v,gas} - p_{v,surface}\right) \cdot t \qquad \text{(Eq. 3.29)}$$

where:

m	=	mass transferred by transmission
A	=	mass transferring area
β	=	mass transmission coefficient
M	=	specific molar mass
R_m	=	molar gas constant
T	=	temperature
$p_{v,gas/surface}$	=	partial vapour pressure
t	=	time

The transmission coefficients (α, β) can be calculated from dimensionless characteristic numbers. For heat transmission, it is the Nusselt-number (Nu) and for mass transfer it is the Sherwood-number (Sh).These numbers can be expressed in terms of other dimensionless numbers: the Reynolds-number (Re) which describes the kind of flow (laminar, turbulent), the Prandtl-number (Pr), which is a characteristic number for the heat transmission of the fluid and the Schmidt-number (Sc), a dimensionless number characterising mass transmission.

$$Nu = f\left(Re, Pr\right) = \frac{\alpha \cdot l'}{\lambda} \qquad \text{(Eq. 3.30)}$$

$$Sh = f\left(Re, Sc\right) = \frac{\beta \cdot l'}{\delta_N} \qquad \text{(Eq. 3.31)}$$

$$Re = \frac{v \cdot l'}{\nu} \qquad \text{(Eq. 3.32)}$$

$$Pr = \frac{\nu \cdot \rho \cdot c_p}{\lambda} \qquad \text{(Eq. 3.33)}$$

$$Sc = \frac{\nu}{\delta_N} \qquad \text{(Eq. 3.34)}$$

where:

α	=	heat transmission coefficient
l'	=	characteristic length
λ	=	heat conductivity of the fluid

β	=	mass transmission coefficient
δ_N	=	normal gas diffusion coefficient
v	=	flow velocity
ν	=	kinetic viscosity of the fluid
ρ	=	density of the fluid
c_p	=	specific heat capacity of the fluid

The dimensionless numbers Nu and Sh are dependent on flow conditions and the geometry of the surface. This dependence can usually be described by the following equations:

$$Nu = C \cdot Re^m \cdot Pr^n \cdot \left(\frac{l_1}{l'}\right)^q \cdot \left(\frac{l_2}{l'}\right)^p \qquad \text{(Eq. 3.35)}$$

$$Sh = C \cdot \mathrm{Re}^m \cdot Sc^n \cdot \left(\frac{l_1}{l'}\right)^q \cdot \left(\frac{l_2}{l'}\right)^p \qquad \text{(Eq. 3.36)}$$

where:

l'	=	characteristic length
l_1, l_2	=	parameters (geometry of surface)
C, m, n, q, p	=	parameters (flow terms) in [-]

For the same flow terms and the same geometry, the exponents of equations (Eq. 3.35) and (Eq. 3.36) are the same. Therefore, the ratio between the heat transmission coefficient and the mass transmission coefficient can be calculated as follows:

$$\frac{\alpha}{\beta} = c_p \cdot \rho \cdot \left(\frac{\lambda}{\delta_N}\right)^{1-n} \qquad \text{(Eq. 3.37)}$$

where:

α	=	heat transmission coefficient
β	=	mass transmission coefficient
c_p	=	specific heat capacity of the fluid
ρ	=	density of the fluid
λ	=	heat conductivity of the fluid
δ_N	=	normal gas diffusion coefficient
$1-n$	=	flow parameter

For laminar flow, the exponent (1-n) assumes the value of $^2/_3$, for turbulent flow 0.58 (KAST, 1988).

For the normal gas diffusion coefficient (δ_N) of water vapour in air, the following equation is valid for a temperature range of 20°C and 90°C (KRISCHER et. al, 1978):

$$\delta_N = \frac{22.6 \cdot 10^{-6}}{p} \cdot \left(\frac{T}{273}\right)^{1.81} \qquad \text{(Eq. 3.38)}$$

where: δ_N = normal gas diff. coefficient (water vapour in air) in [m^2/s]
T = temperature in [K]
p = total pressure in [bar]

The following Tab. 3.1 shows empirical equations for the heat transmission coefficient:

No:	geometry	flow	Nusselt-correlation	characteristic length
1	gap	laminar (Re<2300)	$Nu = \left[7.541^3 + 1.841 \cdot \sqrt[3]{\mathrm{Re} \cdot \mathrm{Pr} \cdot \frac{l'}{l}} + \left(\frac{2}{1+22 \cdot \mathrm{Pr}}\right)^{1/6} \cdot \left(\mathrm{Re} \cdot \mathrm{Pr} \cdot \frac{l'}{l}\right)^{0.5}\right]^{1/3}$	$l' = 2 \cdot h$
2		turbulent (Re>8000)	$Nu = 0.116 \cdot \left(Re^{2/3} - 125\right) \cdot Pr^{1/3} \left[1 + \left(\frac{l'}{l}\right)^{2/3}\right]$	$l' = \frac{4 \cdot A}{U}$
3	tube	laminar (Re<2320)	$Nu = \left(49.0 + 4.17 \cdot Re \cdot Pr \cdot \frac{l'}{l}\right)^{1/3}$	$l' = d_i$
4		turbulent (Re>2320)	$Nu = 0.116 \cdot \left(Re^{2/3} - 125\right) \cdot Pr^{1/3} \left[1 + \left(\frac{l'}{l}\right)^{2/3}\right]$	$l' = d_i$

h	distance of surfaces in [m]	A	free cross sectional area of gap or tube in [m^2]
l'	characteristic length in [m]	U	circumference in [m]
l	length of gap or tube in [m]	d_i	internal diameter in [m]

No.1: AL-AMOURI, 1994; No.2: GREGORIG, 1959; No.3: HERING et. al., 1997; No.4: GREGORIG, 1959.

***Tab. 3.1**: Nusselt-correlations*

03 Theoretical Analysis Of The Adsorption Process

CHAPTER 04

DYNAMIC SIMULATION MODEL

FOR DESICCANT WHEELS

4.1 INTRODUCTION

Within the DEC-system the desiccant wheel is probably the most important component. It is however, also a very complex component to simulate. For this reason, in most existing simulation programs only simple calculation models are used. An example of a simple model is the type that uses a fixed "dehumidification efficiency". Other simple models that are often delivered by manufacturers are models based on equations obtained through curve fits of measured values or the measured values are given as design-graphs. These simple models are often sufficient for the simulation of desiccant wheels under design conditions, but they quickly reach their limits when other operation conditions are to be investigated (rotation velocity, volume flow and volume flow ratio, regeneration temperature etc.). Thus the simple models are normally not sufficient for detailed investigations with different operating conditions or investigations of control strategies and component selection.

Other models are based on detailed physical foundations and lead to complex equation systems which are very complicated to solve and thus need to be solved iteratively, e.g. with the use of mathematical equation solvers. These models are normally not suitable for long time simulations because of the necessary calculation time and expenditure of calculation.

Therefore, a physical model has been developed which is based on a numerical solution of the coupled heat and mass transport between the airflow and the desiccant wheel. Due to the physical basis, all important operation parameters

can be taken into account and because of the finite element-based numerical solution, the complexity of the calculation is quite acceptable.

4.2 DEFINITIONS OF TERMS

For a better understanding of the calculation model, some terms have been introduced which are defined as follows:

- wheel	rotating solid body of the desiccant wheel with a honeycomb structure (see Fig. 4.1). The wheel consists of the matrix material and the adsorption material
- process airflow:	airflow that is dried within the desiccant wheel (see Fig. 4.1)
- regeneration airflow:	heated airflow used for the regeneration (drying) of the desiccant wheel (see Fig. 4.1)
- adsorption phase	phase when a finite mass element of the wheel stays in the process airflow and dries the airflow through adsorption
- regeneration phase	phase when a finite mass element of the wheel stays in the regeneration airflow and is dried by the airflow (desorption)
- internal surface	surface of the matrix structure that is in contact with the airflow. This area is about 2000 to 3000 m^2/m^3 in "standard" desiccant wheels
- cross-sectional area	see Fig. 4.1
- hypothetical surface	assumed surface that has no physical properties

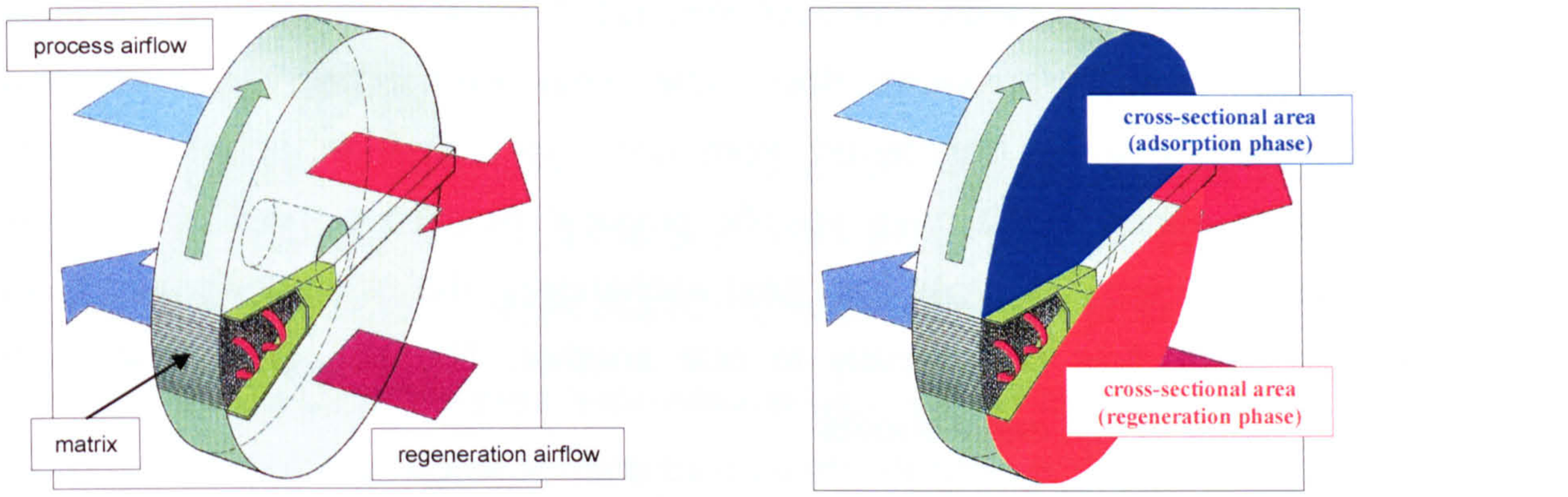

Fig. 4.1: *Definitions of terms used to describe the simulation model*

4.3 MODEL DEVELOPMENT

4.3.1 SUBSTITUTE MODEL

For the modelling of the desiccant wheel, the coupled heat and mass transport between the wheel and the airflow has to be calculated for both the adsorption and the regeneration phases.

When infinitesimally small mass elements of the wheel are considered, it can be seen that they always move alternating through the process and regeneration air flows at the same intervals, independent of their real position on the wheel. There the length of time the mass elements stay in the airflows (the "dwell time") only depends on the rotation velocity and the ratio of the cross-sectional areas of the wheel that are exposed to the blown-in air.

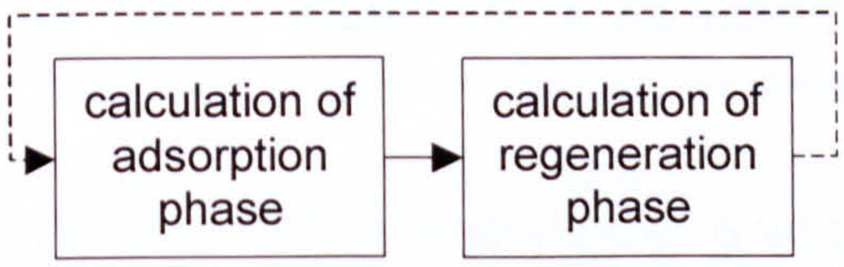

Fig. 4.2: *Schema of the calculation divided into two phases*

The dwell time is not dependent on the position of the mass element in the wheel. Thus the calculation of the desiccant wheel can be divided into two alternating phases (adsorption-/regeneration-phase) (Fig. 4.2). To calculate one of the phases, where heat and mass (water in our case) is transferred from the airflow to the wheel or

reverse, a substitute model has been introduced which is based on a numerical calculation model for cross flow plate heat exchangers. In such heat exchangers, heat is transferred from one mass flow to another through separating plates which have specific physical properties (heat conductivity, heat capacity etc.). In cross flow heat exchangers, the mass flows, which are always fluids, flow orthogonally to one another. The separating plates are usually made of thin metal sheets.

Thus in a plate heat exchanger the mass flows consist of two fluids, contrary to the desiccant wheel where the mass flows consist of one fluid (air flow) and one solid mass (rotating wheel). Furthermore, in a plate heat exchanger the mass flows are separated by plates, whereas the mass flows by the desiccant wheel have direct contact to one another (Fig. 4.3).

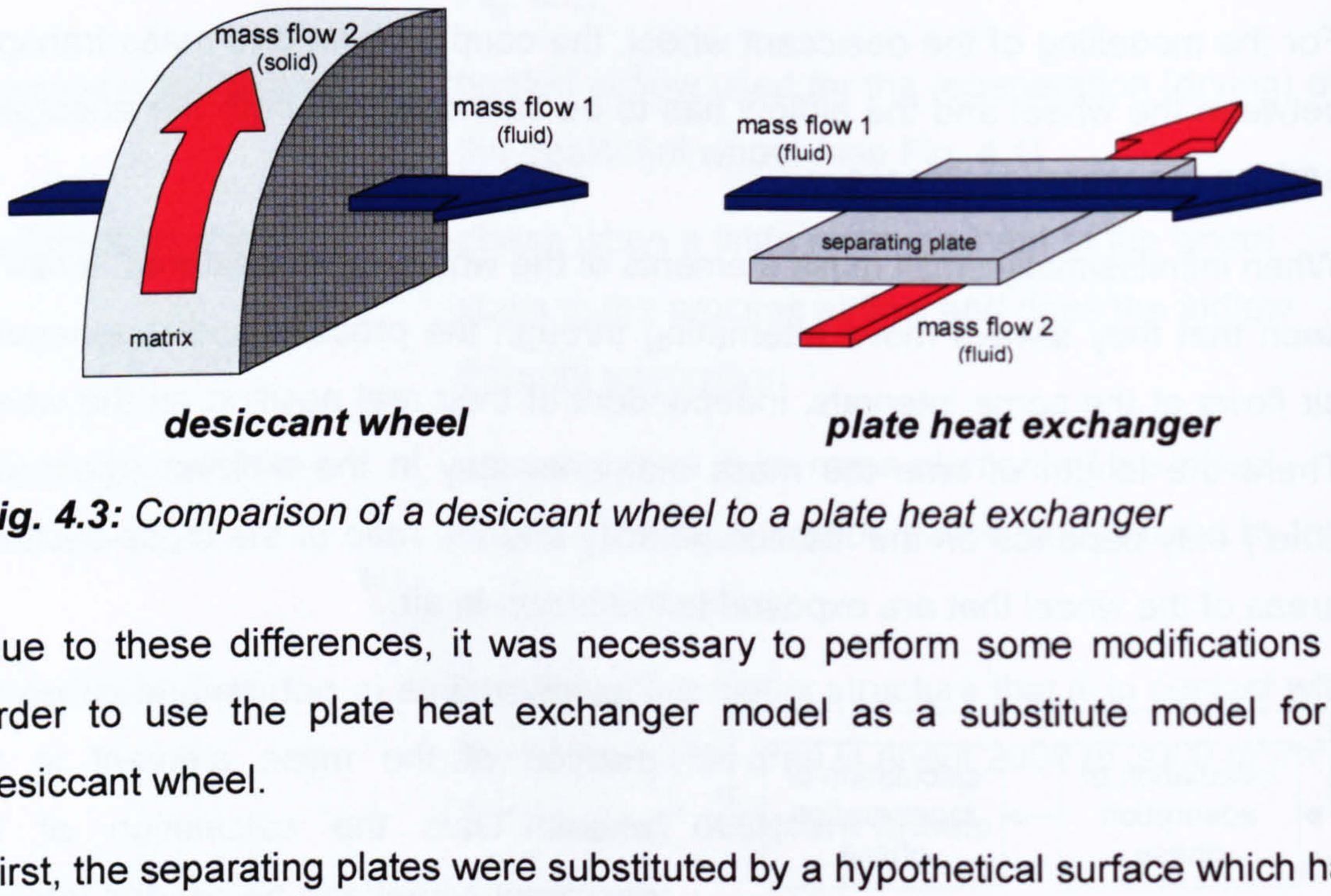

Fig. 4.3: *Comparison of a desiccant wheel to a plate heat exchanger*

Due to these differences, it was necessary to perform some modifications in order to use the plate heat exchanger model as a substitute model for a desiccant wheel.

First, the separating plates were substituted by a hypothetical surface which has no physical properties at all. Thereby the direct contact of the mass flows in the desiccant wheel is considered in the substitute model. In comparison to a "typical" model of a plate heat exchanger, the introduction of the hypothetical surface leads to a simplification of the heat transfer calculation because no heat storage and conductivity of the separating plates have to be considered. As a

result of this, the calculation of the heat transfer between the mass flows can now be calculated using only a single heat transmission coefficient.

A further benefit of the hypothetical surface is the possibility of implementing the mass (water) transfer analogues to the heat transfer because the hypothetical surface need not be considered due to the missing physical properties.

In a further step, the complex 3-dimensinal geometry of the desiccant wheel is reduced to a 2-dimensional surface by a careful division of the wheel into single segments (Fig. 4.4).

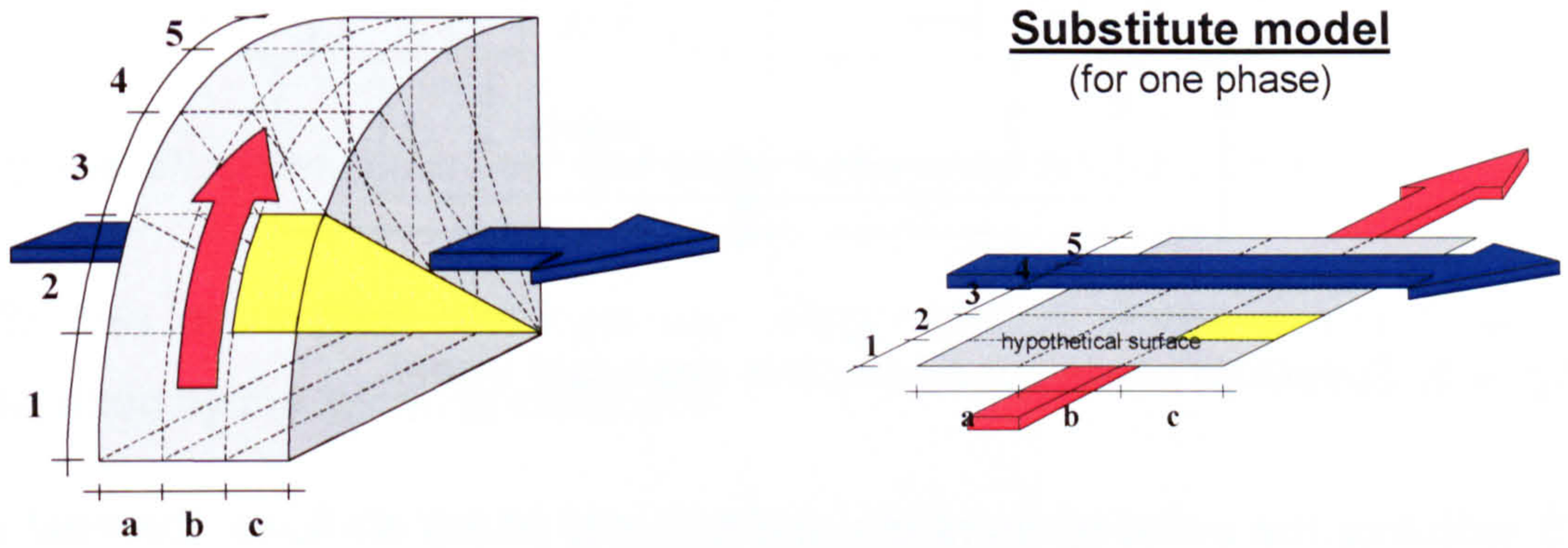

Fig. 4.4: *Simplification of geometry and substitute model for one phase*

Hereby, the area of a 2-dimensional segment corresponds to the real heat and mass transferring internal surface of a 3-dimensional segment of the matrix. The heat and mass transfer coefficients used for the calculation also result from the real geometry of the desiccant wheel.

With these model ideas and modifications the desiccant wheel can be described by a substitute model consisting of two “modified” plate heat exchangers linked by a closed circuit of one of the mass flows which serves as the rotating mass of the matrix. In Fig. 4.5, a diagram of the substitute model for a desiccant wheel with different cross-sectional areas for process and regeneration airflow is shown.

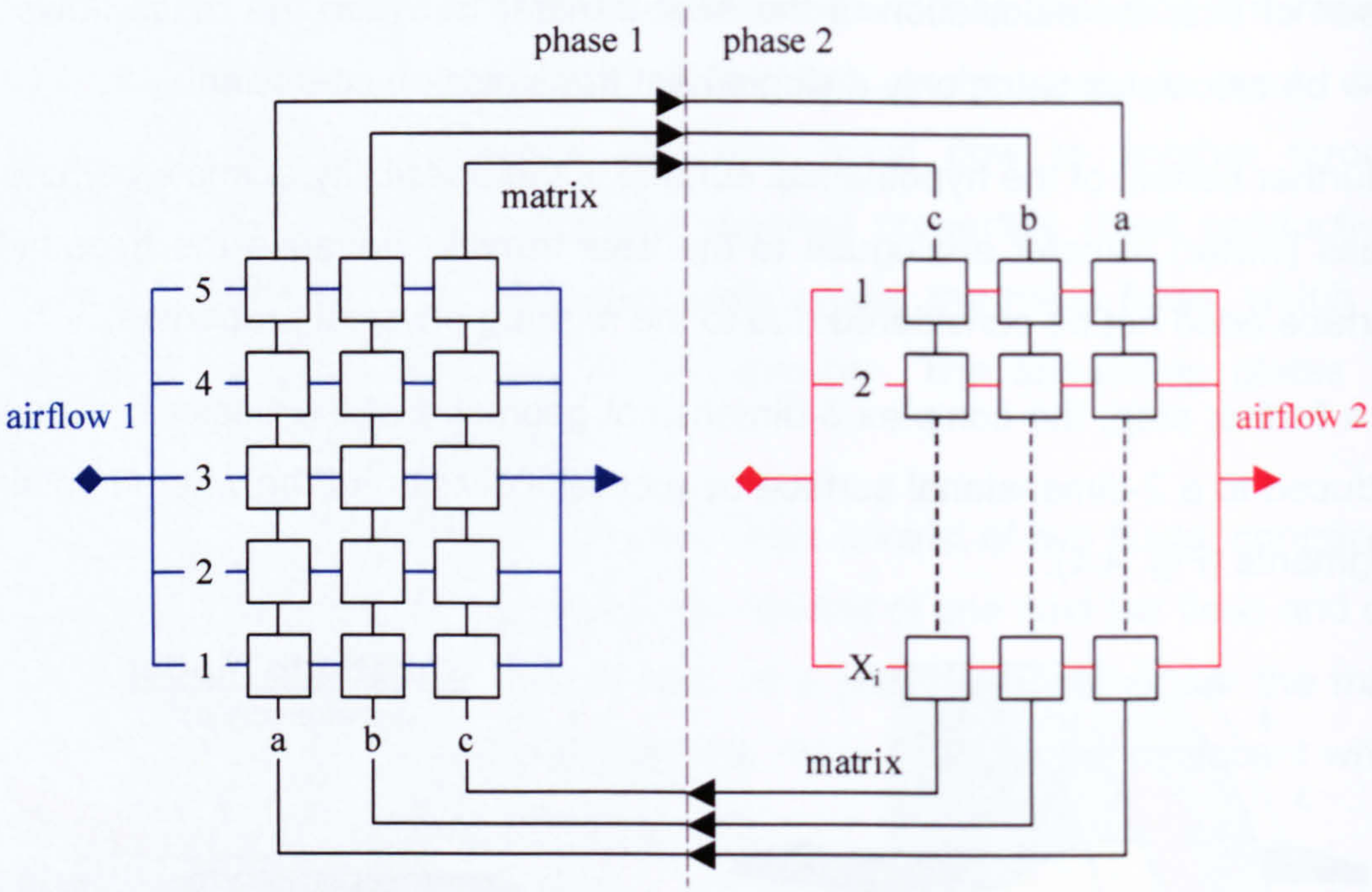

Fig. 4.5: *Substitute model for a complete desiccant wheel*

To calculate the outlet temperature and humidity of the air flows, the heat and mass transfer for each segment of the hypothetical surface has to be calculated. For the calculation of phase 1 (see Fig. 4.5) e.g., the calculation must start with segment 1-a. The inlet temperature and load of the wheel must be estimated for the first step, whereas the inlet temperature of the air is known. The outlet temperature and humidity of the airflow of segment 1-a is then used as the inlet temperature and humidity of the airflow for segment 1-b and so on.

The second phase can then be calculated similarly to phase one. For this calculation, the outlet temperature and load of the wheel in phase one is used as the inlet temperature and load in phase two and so on.

4.3.2 HEAT AND MASS BALANCE OF ONE SEGMENT

For the simulation of the desiccant wheel, the heat and mass balance of each segment must be calculated. With the assumption that the energy (heat) released by the adsorption process is transferred completely to the wheel, the

heat and mass balance of one segment can be described by the following diagram (Fig. 4.6).

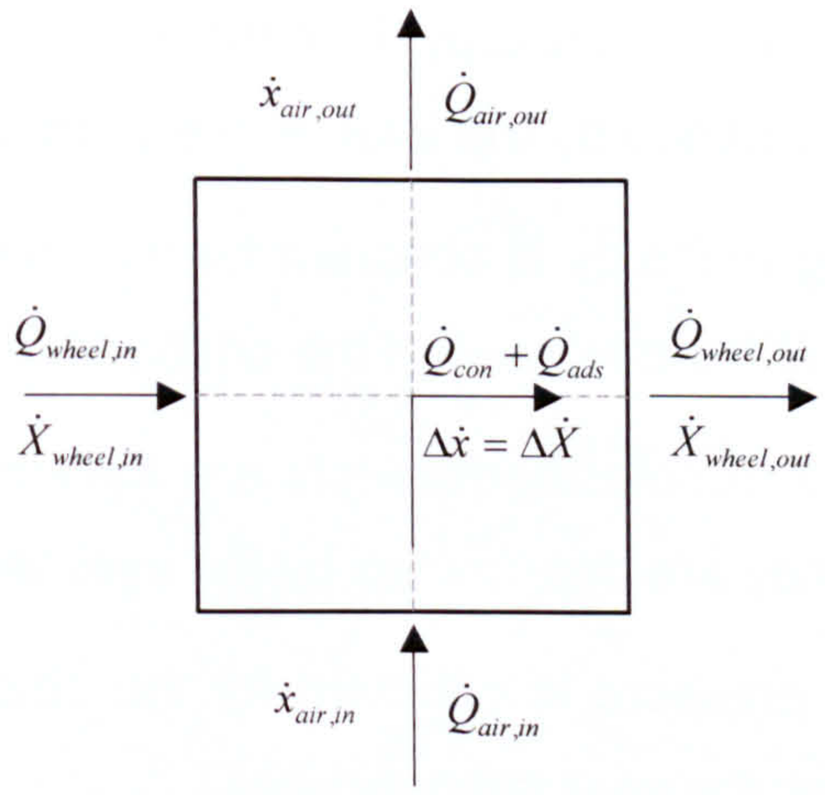

Fig. 4.6: *Diagram of the heat and mass balance for one segment*

With this assumption, the heat and mass balance of one segment can be described by the following equations:

$$\Delta\dot{Q} = \dot{Q}_{air,in} - \dot{Q}_{air,out} = \dot{Q}_{wheel,out} - \dot{Q}_{wheel,in} \qquad \text{(Eq. 4.1)}$$

$$\Delta\dot{Q} = \dot{Q}_{con} + \dot{Q}_{ads} \qquad \text{(Eq. 4.2)}$$

$$\Delta\dot{X} = \Delta\dot{x} = \dot{x}_{air,in} - \dot{x}_{air,out} = \dot{X}_{wheel,out} - \dot{X}_{wheel,in} \qquad \text{(Eq. 4.3)}$$

where:

$\dot{Q}_{air}$	=	heat flow because of caloric content of the air
$\dot{Q}_{wheel}$	=	heat flow because of caloric content of the wheel
$\dot{Q}_{con}$	=	heat flow transferred by convection
$\dot{Q}_{ads}$	=	heat flow transferred by adsorption
$\dot{x}_{air}$	=	mass flow because of the water content of the air
$\dot{X}_{wheel}$	=	mass flow because of the load of the wheel

In order to reduce the complexity of the calculation, the following simplifications have been introduced, which will not influence the outcomes significantly if the number of segments is high enough:

a) The specific heat capacities are constant for the calculation of one segment and they are determined by the inlet temperatures.

b) The specific evaporation enthalpy is constant for the calculation of one segment and is determined by the inlet temperature of the air.

c) The specific binding enthalpy is constant for the calculation of one segment and is determined by the inlet load of the adsorption material.

d) The heat and mass transfer coefficients are constant for the calculation of one segment and they are determined by the inlet temperature of the airflow.

e) The partial vapour pressure is constant for the calculation of one segment and is determined by the inlet temperatures.

With these simplifications the heat and mass flows for one segment can be calculated using the following equations:

$$\dot{Q}_{air,in} = \dot{m}_{air} \cdot c_{p,air} \cdot \theta_{air,in} + \dot{x}_{air,in} \cdot c_{p,steam} \cdot \theta_{air,in} + \dot{x}_{air,in} \cdot h_e \qquad \text{(Eq. 4.4)}$$

$$\dot{Q}_{air,out} = \dot{m}_{air} \cdot c_{p,air} \cdot \theta_{air,out} + \left(\dot{x}_{air,in} - \Delta\dot{X}_{ads}\right) \cdot c_{p,steam} \cdot \theta_{air,out} + \left(\dot{x}_{air,in} - \Delta\dot{X}_{ads}\right) \cdot h_e \qquad \text{(Eq. 4.5)}$$

$$\dot{Q}_{wheel,in} = \left(\dot{m}_{matrix} \cdot c_{p,matrix} + \dot{m}_{silica} \cdot c_{p,silica}\right) \cdot \theta_{wheel,in} + \dot{X}_{wheel,in} \cdot c_{p,water} \cdot \theta_{wheel,in} \cdots \\ \cdots + \dot{X}_{wheel,in} \cdot h_b \qquad \text{(Eq. 4.6)}$$

$$\dot{Q}_{wheel,out} = \left(\dot{m}_{matrix} \cdot c_{p,matrix} + \dot{m}_{silica} \cdot c_{p,silica}\right) \cdot \theta_{wheel,out} + \left(\dot{X}_{wheel,in} + \Delta\dot{X}_{ads}\right) \cdots \\ \cdots \cdot c_{p,water} \cdot \theta_{wheel,out} + \left(\dot{X}_{wheel,in} + \Delta\dot{X}_{ads}\right) \cdot h_b \qquad \text{(Eq. 4.7)}$$

$$\dot{Q}_{con} = \alpha \cdot A \cdot \left(\frac{\theta_{air,in} + \theta_{air,out}}{2} - \frac{\theta_{wheel,in} + \theta_{wheel,out}}{2} \right) \qquad \text{(Eq. 4.8)}$$

$$\dot{Q}_{ads} = \Delta\dot{X}_{ads} \cdot h_{ads} = \beta \cdot A \cdot \frac{M}{R_m(\theta + 273{,}15)} \cdot \left(p_{v,air,in} - p_{v,wheel,in}\right) \cdot \left(h_b + h_e\right) \qquad \text{(Eq. 4.9)}$$

In (Eq. 4.4) to (Eq. 4.8), there are only two unknown parameters: the outlet temperature of the airflow ($\theta_{air,out}$) and the outlet temperature of the wheel ($\theta_{wheel,out}$). Thus for the calculation only two independent equations are necessary. From (Eq. 4.1) follows:

$$\dot{Q}_{air,in} + \dot{Q}_{wheel,in} = \dot{Q}_{air,out} + \dot{Q}_{wheel,out} \qquad \text{(Eq. 4.10)}$$

and from (Eq. 4.1) and (Eq. 4.2) follows:

$$\dot{Q}_{air,out} = \dot{Q}_{air,in} - \dot{Q}_{con} - \dot{Q}_{ads} \qquad \text{(Eq. 4.11)}$$

The mass transport is also considered in these equations because the heat flow by adsorption ($\dot{Q}_{ads}$) is dependent on the mass of water adsorbed from the air.

By solving these equations, the outlet temperatures of the air flow and the wheel can be calculated for each segment. The load of the wheel and the humidity of the air flow can then be derived from (Eq. 4.3).

The equations were solved and simplified with the use of the program MATHEMATICA 4.2 (2002), which is a powerful equation solving tool. For the outlet temperature of one segment follows:

$$\begin{aligned}
\theta_{wheel,out} = {} & (2 \cdot c_{p,air} \cdot \dot{m}_{air} \cdot (-\Delta\dot{X}_{ads} \cdot h_b + \dot{Q}_{ads} + \theta_{wheel,in} \cdot (c_{p,matrix} \cdot \dot{m}_{matrix} + \ldots \\
& \ldots c_{p,silica} \cdot m_{silica} + c_{p,water} \cdot \dot{X}_{wheel,in})) + A \cdot \alpha \cdot (\Delta\dot{X}_{ads} \cdot (-h_b + h_e) + c_{p,air} \cdot \ldots \\
& \ldots \dot{m}_{air} \cdot (2 \cdot \theta_{air,in} - \theta_{wheel,in}) + \theta_{wheel,in} \cdot (c_{p,matrix} \cdot \dot{m}_{matrix} + c_{p,silica} \cdot \dot{m}_{silica} + \ldots \\
& \ldots c_{p,water} \cdot \dot{X}_{wheel,in})) + c_{p,silica} \cdot (2 \cdot \Delta\dot{X}_{ads}^2 \cdot h_b + x_{air,in} \cdot (2 \cdot \dot{Q}_{ads} + A \cdot \alpha \cdot \ldots \\
& \ldots (2 \cdot \theta_{air,in} - \theta_{wheel,in}) + 2 \cdot \theta_{wheel,in} \cdot (c_{p,matrix} \cdot \dot{m}_{matrix} + c_{p,silica} \cdot \dot{m}_{silica} + c_{p,water} \cdot \ldots \\
& \ldots \dot{X}_{wheel,in})) - \Delta\dot{X}_{ads} \cdot (2 \cdot \dot{Q}_{ads} + A \cdot \alpha \cdot (\theta_{air,in} - \theta_{wheel,in}) + 2 \cdot (c_{p,matrix} \cdot \dot{m}_{matrix} \cdot \ldots \\
& \ldots \theta_{matrix,in} + c_{p,silica} \cdot \dot{m}_{silica} \cdot \theta_{wheel,in} + h_b \cdot \dot{x}_{air,in} + c_{p,water} \cdot \theta_{wheel,in} \cdot \dot{X}_{wheel,in})))) / \ldots \\
& \ldots (2 \cdot c_{p,air} \cdot \dot{m}_{air} \cdot (c_{p,matrix} \cdot \dot{m}_{matrix} + c_{p,silica} \cdot \dot{m}_{silica} + c_{p,water} \cdot (\Delta\dot{X}_{ads} + \ldots \\
& \ldots \dot{X}_{wheel,in})) + A \cdot \alpha \cdot (c_{p,air} \cdot \dot{m}_{air} + c_{p,matrix} \cdot \dot{m}_{matrix} + c_{p,silica} \cdot \dot{m}_{silica} + c_{p,water} \cdot \ldots \\
& \ldots (\Delta\dot{X}_{ads} + \dot{X}_{wheel,in})) - c_{p,silica} \cdot (\Delta\dot{X}_{ads} - \dot{x}_{air,in}) \cdot (A \cdot \alpha + 2 \cdot c_{p,matrix} \cdot \dot{m}_{matrix} + \ldots \\
& \ldots 2 \cdot (c_{p,silica} \cdot \dot{m}_{silica} + 2 \cdot c_{p,water} \cdot (\Delta\dot{X}_{ads} + \dot{X}_{wheel,in})))
\end{aligned} \qquad \text{(Eq. 4.12)}$$

For the outlet temperature of the air flow of one segment follows:

$$\begin{aligned}
\theta_{air,out} = {} & \frac{1}{-c_{p,steam} \cdot \Delta\dot{X}_{ads} + c_{p,air} \cdot \dot{m}_{air} + c_{p,steam} \cdot \dot{x}_{air,in}} \cdot ((h_e - h_b) \cdot \Delta\dot{X}_{ads} + \ldots \\
& \ldots (c_{p,air} \cdot \dot{m}_{air} + c_{p,steam} \cdot \dot{x}_{air,in}) \cdot \theta_{air,in} + (c_{p,matrix} \cdot \dot{m}_{matrix} + c_{p,silica} \cdot \dot{m}_{silica} + \ldots \\
& \ldots c_{p,water} \cdot \dot{X}_{wheel,in}) \cdot \theta_{wheel,in} - (c_{p,water} \cdot \Delta\dot{X}_{ads} + c_{p,matrix} \cdot \dot{m}_{matrix} + c_{p,silica} \cdot \dot{m}_{silica} \ldots \\
& \ldots + c_{p,water} \cdot \dot{X}_{wheel,in}) \cdot \theta_{wheel,out})
\end{aligned} \qquad \text{(Eq. 4.13)}$$

04 Dynamic Simulation Model For Desiccant Wheels

CHAPTER 05

EXPERIMENTAL INVESTIGATIONS ON A TEST PLANT

5.1 DESCRIPTION OF THE TEST PLANT

5.1.1 DESIGN

The test plant at the University of Applied Sciences in Stuttgart was designed to measure characteristic figures of merit of different commercial desiccant wheels under changing operating conditions, so that comparative advantages and disadvantages of different wheels could be determined.

In the test plant, all operation parameters such as temperature, humidity, flow rates and the rotation velocity of the wheel could be set to different values as required. The limits of the air flows were 0 - 2500 m^3/h for both the process and regeneration air flows. The approximate limits for possible temperature and relative humidity values for the ambient air were 10°C, 50% to 40°C, 70% and for regeneration air 20°C, 50% up to 100°C, 3%.

An assortment of vacuum tube collectors and two electrical heaters (18 kW and 24 kW) were used for heating the regeneration air and a 16kW electrical heater was used for heating the process air. The air was drawn using a 1.5 kW electric fan on both the process and regeneration sides. The relative humidity in both air flows was set using steam humidifiers. The setup of the test plant is shown in Fig. 5.1.

The test wheels were supplied in cassettes by manufacturers. Plenums fabricated from sheet metal and flexible ducting were used to connect the process and the regeneration air flow to these cassettes. This approach made short interchange times possible for different cassettes and the plenums

ensured a uniform air flow distribution and helped to avoid the so-called "blow through" effect, by which the air is introduced through small ducts too closely to the wheel or at a bad angle. The "blow through" effect would deprive some parts of the wheel of air and would raise the flow velocity in others thereby worsening the performance.

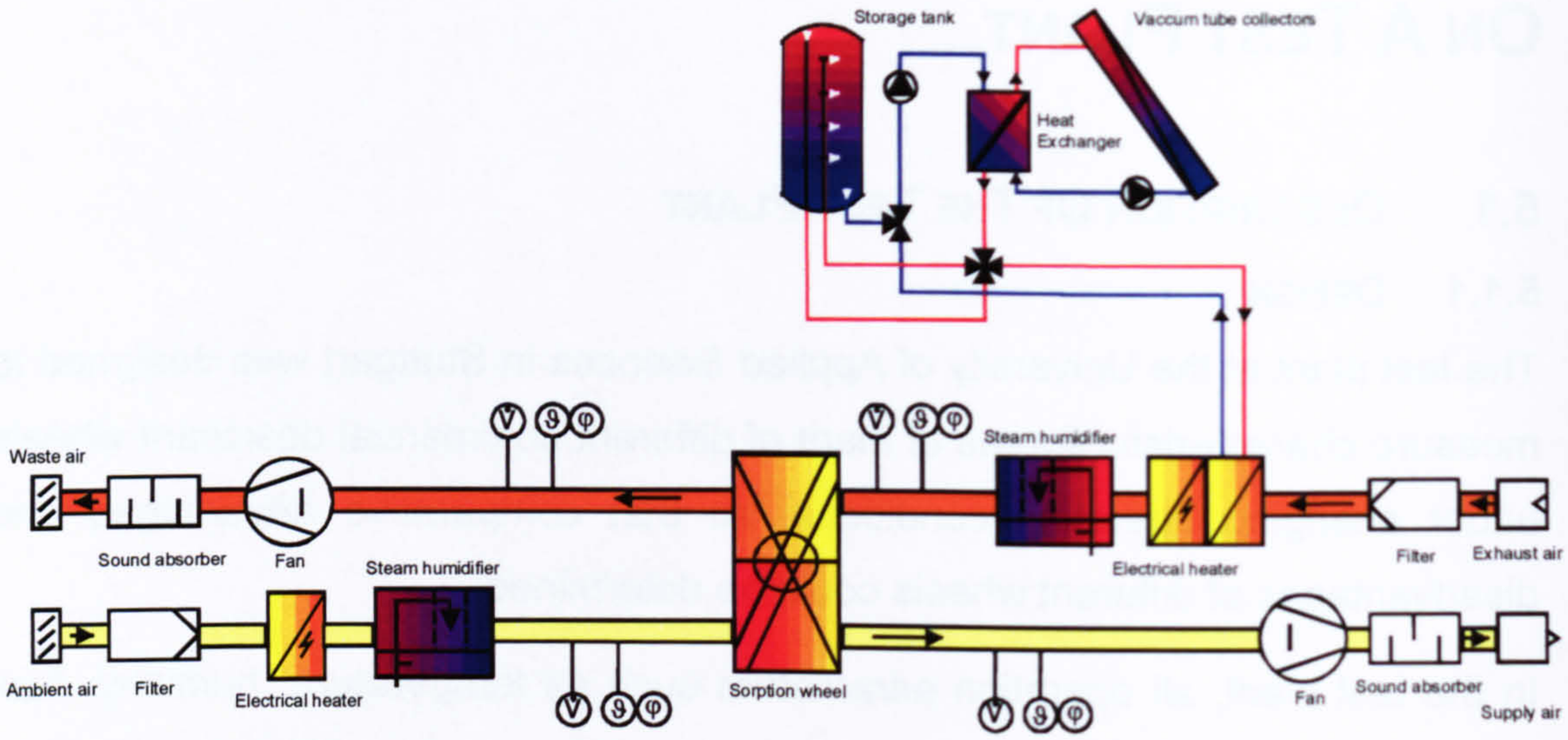

Fig. 5.1: *Setup of test plant at the University of Applied Sciences, Stuttgart*

Long straight tubes were installed in as many places as possible at the test plant in order to get measuring points with an uniform airflow as a non uniform airflow would falsify the measurements.

Essentially the goal was to design a test plant that meets the requirements of the test facilities described in the "Desiccant Dehumidification Wheel Test Guide" (SLAYZAK et. al, 2000). In order to meet these requirements however, much more capital expenditure and space would have been necessary than was at disposal for this project.

The "Desiccant Dehumidification Wheel Test Guide" e.g. recommends the use of four fans to prevent air leakage between the airflows caused by pressure drops or to "simulate" different pressure drop conditions. If four fans are not available, the Test Guide suggests minimizing pressure drops opposite from the fans in order to minimize the pressure differences between the regeneration air

and the process air. With two fans, the process air should be blown through the wheel and the regeneration air should be drawn through it. This normally leads to pressure conditions in which no regeneration air can force its way into the process side of the cassette, an occurrence that can seriously worsen the performance of the wheel.

For the test plant, only two fans were available and both fans could only be situated behind the wheel, meaning that both of them drew the air through the desiccant wheel. Naturally, with this design air leakage from the regeneration air to the process side of the wheel could not be prevented. On the other hand, it should be taken into consideration, that while a test plant that meets the requirements of the Test Guide is surely suitable for determining the maximum performance of wheels under optimal conditions, the design of commercial plants is usually far from optimal. In both commercial plants monitored in this study for example (see chapters 07 and 08), the fans are situated behind the desiccant wheels and only two fans are used. Furthermore, the tubing and the connection of the desiccant wheel to the other components in commercial plants do not usually even remotely meet the requirements of the Test Guide for test facilities.

Overall the design of the test plant did not meet all the requirements specified by the Wheel Test Guide, but the design was much more compliant with the typical built-in situation of desiccant wheels in complete DEC-systems. Thus the outcome of the experiments probably does not show the maximum possible performance of the wheel, but most likely provides better insight into the performance that can be expected of DEC-systems.

5.1.2 MEASURING DEVICES

The temperature, relative humidity and flow rates were measured near the sorption wheel on both the inlet and outlet of the process and regeneration air flows. The measurement data was collected using a Hewlett Packard HP 34970 A data acquisition system. The temperature and humidity measurements were

taken using *Micatrone* sensors (type: Micaflex MF-HTT). These sensors measure the temperature with a resistance thermometer. With this kind of thermometer, the electrical resistance either increases or decreases as the temperature changes. In order to obtain the measurement, a constant voltage is supplied to the sensor head and the voltage drop on the sensor head is monitored for changes in ohmic resistance. In this case a PTC-resistor (Positive Temperature Coefficient) made of platinum was used (Pt1000). The accuracy of this type of temperature sensor is given as ± 0.5 °C by the manufacturer. The measurement of the relative humidity was taken with capacitive humidity sensors, with which the relative humidity is determined from the change of the electrical capacity of a hygroscopic capacitor. The accuracy of the humidity sensors is given as ± 2 % of relative humidity by the manufacturer.

The air flows were measured using flow meter *Micatrone* sensors (type: Micaflex MF-FD), with which the flow velocity or volume flow was determined by measuring the pressure difference. The measuring principle is shown in Fig. 5.2.

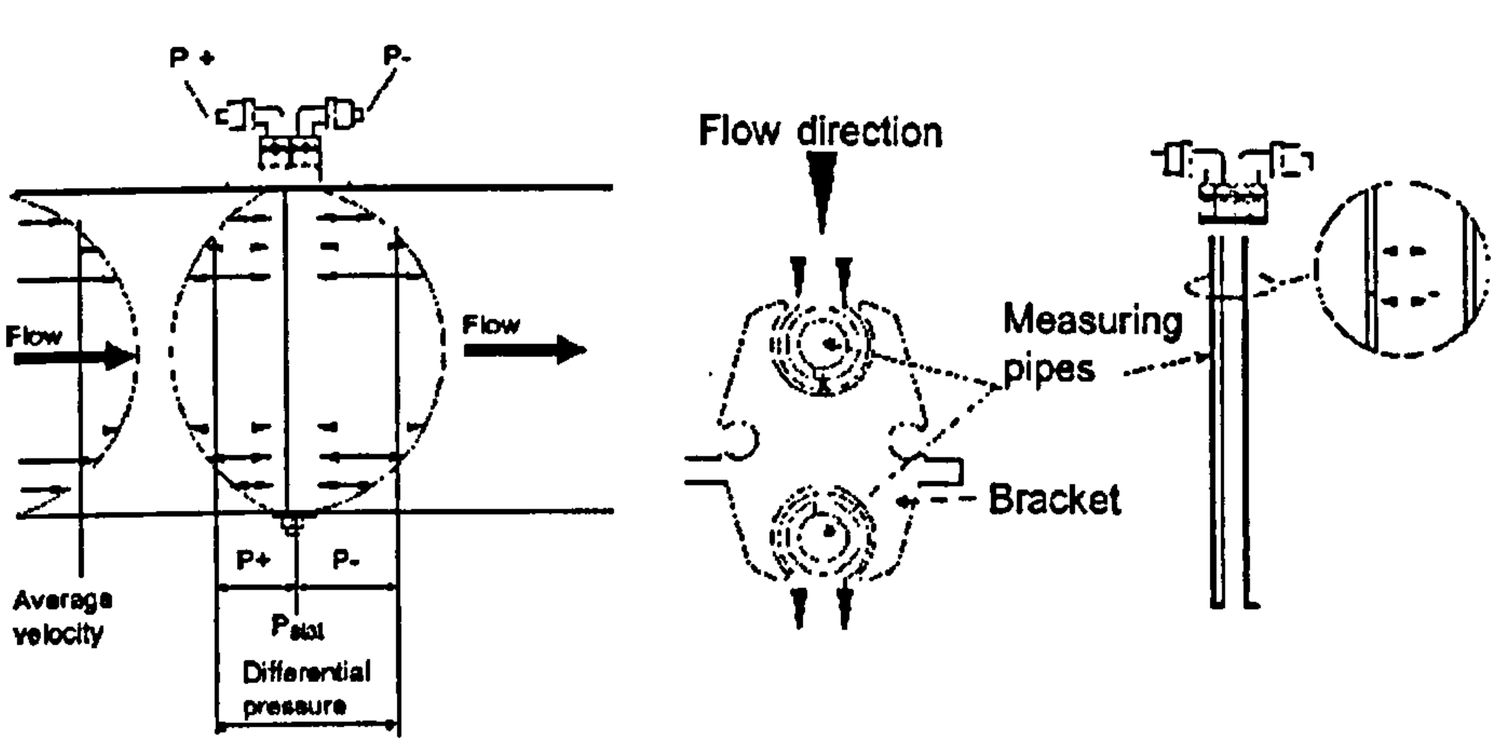

Fig. 5.2: *Measuring principle of flow meter sensors (reference: Micatrone product information)*

The empirical function for the connection between the measured pressure difference and the flow velocity is given by the manufacturer. With the sensors that were used, the flow velocity is proportional to the root of the pressure

difference ($v \sim \sqrt{\Delta p}$). The measuring range of the sensors was from 0 Pa to 200 Pa, what corresponds to a volume flow up to about 3000 m³/h or a flow velocity of up to about 12 m/s at the test plant. The accuracy of the sensors is given as ± 3 % of the measured pressure difference.

5.2 MEASUREMENTS / EXPERIMENTS

5.2.1 INVESTIGATED WHEELS

At the University of Applied Sciences in Stuttgart three different desiccant wheels were available for comprehensive experiments. For this study primarily a desiccant wheel from the Engelhard Hexcore, LP company and a wheel from the Klingenburg company (see Tab. 5.1) were tested because the third wheel from the Munters company had already been tested as part of a study by HOEFKER, 2001.

Manufacturer:	**Engelhard HexCore, LP DES-H-Hexcore-DC15/N**	**Klingenburg SECO 1000**	Munters MCC-1-870-Si
Wheel specfications:			
Matrix material	Hexcore Nomex™	Cellulose	ceramic bonded mineral fibre
Desiccant type	Hexcore ETS™ (titanium silicate)	lithium chloride	silica gel
Matrix structure	honeycomb	sinusoidal structure	sinusoidal structure
Wheel depth	140 mm	250 mm	200 mm
Wheel diameter	870 mm	895 mm	850 mm
revolutions per hour	15-100 (dehumidification)	20 (dehumidification) up to 600 (heat recovery)	-
face velocity	2 – 2.6 m/s	1.5 – 2 m/s	-
Reg. temp.	55°C to 85°C (max. 120°C)	40°C up to 70°C	95 °C

Tab. 5.1: *Desiccant wheels tested at the University of Applied Sciences, Stuttgart*

5.2.2 FIGURES OF MERIT

The characteristic properties of the desiccant wheels are described in this study mainly by the following figures of merit:

- dehumidification capacity (Δx) as a type of "performance" figure
- Regeneration Specific Heat Input (*RSHI*) as an "energy efficiency" figure
- dehumidification efficiency (η_{dehum}) as a type of "quality" figure
- enthalpy change of process air (Δh) as a type of "thermal quality" figure

The dehumidification capacity (Δx) is defined as the amount of moisture removed from the process airflow. The *RSHI* is the thermal energy flux supplied to the device for regeneration in relation to the dehumidification capacity flux (Eq. 5.1):

$$RSHI = \frac{\Delta \dot{Q}_{reg-amb}}{\Delta x \cdot \dot{m}_{process}} \left[\frac{kJ}{g}\right] \qquad \text{(Eq. 5.1)}$$

The thermal energy supplied for regeneration in this study is always linked to the ambient air temperature (Eq. 5.2).

$$\Delta \dot{Q}_{reg-amb} = c_{p,air} \cdot \dot{m}_{reg} \cdot \left(\theta_{reg} - \theta_{amb}\right) \qquad \text{(Eq. 5.2)}$$

For the calculation of the *RSHI*, the specific heat capacity of the air is set at a constant 1.007 [*kJ/kg K*].

The dehumidification efficiency η_{dehum} is defined as the ratio of the actually-reached dehumidification capacity by the desiccant wheel Δx, to the maximum (theoretically) possible dehumidification Δx_{max}.

$$\eta_{dehum} = \frac{\Delta x}{\Delta x_{\max}} [-] \qquad \text{(Eq. 5.3)}$$

The calculation of the dehumidification efficiency was performed using a simplified calculation model which is also used e.g. by the Klingenburg company to describe their desiccant wheels. Hereby the maximum

dehumidification capacity is obtained by examining the sorption isotherm of the adsorption material. The sorption isotherm describes the functional connection between the load X of the adsorption material and the relative humidity φ and temperature θ of the surrounding air ($X = \text{funct.}(\varphi, \theta)$). The sorption isotherms for different temperatures usually show only slight deviations from one another, thus the temperature influence is ignored. With the application of these simplifications, the sorption behaviour can be described by one sorption isotherm whereby the load is solely a function of the relative humidity ($X = \text{funct.}(\varphi)$). Additionally, it is assumed that during the adsorption process a phase change takes place from gas (steam in the humid air) to liquid (water adsorbed on the adsorption material) and that the evaporation enthalpy of the adsorbed water is set free warming the air, which leads to an isenthalpic change of the state of the process air as it dries.

With these simplifications it follows that the maximum possible dehumidification capacity is reached when the process airflow with the relative humidity φ_0 and the absolute humidity x_0 reaches the relative humidity of the regeneration airflow φ_{reg}. The dehumidification process follows an isenthalpic curve. One real advantage of this calculation model is that the function of the sorption isotherm must not be known because the "end" point of the drying process is determined only by the enthalpy of the process air and the relative humidity of the regeneration air.

Although both the relative humidity and the enthalpy are dependent on the temperature and the absolute humidity, the equations can not be solved analytically, and therefore must be done so iteratively.

Due to the fact that the relative humidity is a continuous, monotonic function of the absolute humidity (at a constant temperature), the ratio of corresponding differential values can be set equal to each other.

$$\frac{\varphi_0 - \varphi_i}{x_0 - x_i} = \frac{\varphi_0 - \varphi_{reg}}{x_0 - x_{min}} \qquad \text{(Eq. 5.4)}$$

Solving this equation for x_{min} yields:

$$x_{\min} = x_0 - (\varphi_0 - \varphi_{reg}) \cdot \frac{x_0 - x_i}{\varphi_0 - \varphi_i} \qquad \text{(Eq. 5.5)}$$

For the calculation a new absolute humidity x_i must first be presumed and the corresponding relative humidity φ_i must be determined using the constant enthalpy of the process air h_0. With these values, the new absolute humidity x_{min} can then be calculated. The new x_{min} and the relative humidity φ_{reg} yield the enthalpy, which can be compared to h_0. If the enthalpies are not identical it is necessary to repeat the procedure with a new presumption of x_{min}. The dehumidification efficiency is then calculated as follows (Eq. 5.6):

$$\eta_{dehum} = \frac{x_0 - x_{real}}{x_0 - x_{\min}} [-] \qquad \text{(Eq. 5.6)}$$

When comparing different desiccant wheels, the dehumidification efficiency alone is not always sufficient to rate the quality of the wheel. Thus, for example, if the dehumidification capacity of two wheels is the same but one shows a higher temperature rise in the process air (e.g. caused by heat transfer from the regeneration air, a higher binding enthalpy during adsorption or an exothermal chemical reaction during absorption) the dehumidification efficiency is also identical. However, the wheel with the lower temperature rise is surely better for DEC-systems. Therefore, in addition to the dehumidification efficiency, the enthalpy change (Δh) of the process air during dehumidification must also be considered in the quality rating.

The figures of merit determined for the two desiccant wheels in the test plant are shown in paragraph 5.3. They are dependent on the rotation velocity, the volume flow ratio between regeneration and process air and the conditions and different volume flows of the regeneration and ambient air. An overview and detailed description of the results of the measurement series are shown in Appendix A.

5.2.3 INFLUENCE OF MEASUREMENT ACCURACY

The sensors used for the measurements were of high quality and for the design of the plant as well, the systematic errors were reduced to the greatest extent possible considering the available devices. Furthermore a great amount of time was spent optimising the measuring points by testing different sensors at different positions under different conditions. Despite this effort however, there remains an inaccuracy in the measuring devices themselves that is not negligible.

For the calculation of the dehumidification capacity, the absolute humidity of the process air in front of and behind the desiccant wheel had to be determined. As the sensors that were used could only measure the relative humidity and the temperature, the absolute humidity had to be calculated using these two values. Therefore, both the accuracy of the relative humidity measurement and the accuracy of the temperature measurement influence the absolute humidity.

The maximum error that can be caused by the inaccuracies of the measurement devices can be estimated with an error propagation calculation.

If the sought-for value y is a function of a faulty input value $x+\Delta x$, the influence of Δx on the outcome can be estimated with a Taylor series (LEUPOLD, 1991):

$$y = y(x) \Rightarrow y(x+\Delta x) = y(x) + \frac{1}{1!}\cdot\frac{\partial y}{\partial x}\cdot\Delta x + \frac{1}{2!}\cdot\frac{\partial^2 y}{\partial x^2}\cdot(\Delta x)^2 + \ldots \qquad \text{(Eq. 5.7)}$$

If the error of the input value is small, the Taylor series can be stopped after the linear term which delivers the following approximate solution for the error of the desired value:

$$y(x+\Delta x) - y(x) = \Delta y = \frac{\partial y}{\partial x}\cdot\Delta x \qquad \text{(Eq. 5.8)}$$

If the sought-after value is a function of different, faulty input values $x_i+\Delta x_i$, the error of the searched value can be calculated as follows:

$$\Delta y = \sum_{i=1}^{N}\frac{\partial y}{\partial x_i}\cdot\Delta x_i \qquad \text{(Eq. 5.9)}$$

If only the error limits of the input values ($\pm\Delta x_i$) are known but not the error itself, the same mathematical formulas can be used to calculate the error limit of the sought-after value. To this end, the error limits of the input values must be entered as positive values (e.g. $\pm 2 => 2$) and the differential term must also be entered as a positive value:

$$\Delta y = \sum_{i=1}^{N} \left| \frac{\partial y}{\partial x_i} \right| \cdot \Delta x_i \qquad \text{(Eq. 5.10)}$$

The thus determined error limit for the desired value represents the "worst case" scenario as it results in the largest possible error.

The calculation of the absolute humidity from the measured values can be performed using the following equation (see Chapter 3, Eq. 3.6):

$$x = x(\varphi, p_{sat}) = 0.622 \frac{\varphi \cdot p_{sat}}{p - \varphi \cdot p_{sat}}$$

Thus it follows for the error limits of the absolute humidity with (Eq. 5.10), that:

$$\Delta x = 0.622 \cdot \left(\begin{array}{l} \left| \frac{p_{sat} \cdot (p - \varphi \cdot p_{sat}) + \varphi \cdot p_{sat}^2}{(p - \varphi \cdot p_{sat})^2} \right| \cdot \Delta\varphi + \ldots \\ \ldots \left| \frac{\varphi \cdot (p - \varphi \cdot p_{sat}) + \varphi^2 \cdot p_{sat}}{(p - \varphi \cdot p_{sat})^2} \right| \cdot \Delta p_{sat} \end{array} \right) \qquad \text{(Eq. 5.11)}$$

The error propagation is shown by the example of an isenthalpic dehumidification process from air with 32°C and 40 % relative humidity to that with 46.2°C and a relative humidity of 10 %. In the first step, the error determining the absolute humidity of air with 32°C and 40 % relative humidity must be calculated with (Eq. 5.11). Using the accuracies given by the manufactures (temperature: ± 0.5°C / relative humidity: ± 2 % r.h.), a total pressure p of 100000 [Pa] and the use of equation 3.14 (see Chapter 3) for the saturation vapour pressure, for the absolute humidity follows:

$$x_{32°C/40\%} = 12.1\,[g/kg] \pm 1.0\,[g/kg]$$

For air with 46.2°C and a relative humidity of 10 % follows:

$$x_{46.2°C/10\%} = 6.4\,[g/kg] \pm 1.5\,[g/kg]$$

Additionally, with (Eq. 5.10) the following calculation laws for the determination of error limits can be determined:

- For the summation/subtraction of two measured values the **absolute** errors were added.
- For products/ratios of two measured values the **relative** errors were added.

Thus for the error limits of the dehumidification capacity in the above-mentioned example follows:

$$\Delta x = x_{32°C/40\%} - x_{46.2°C/10\%} = 5.7\,[g/kg] \pm 2.5\,[g/kg]$$

This example is also shown in Fig. 5.3 in a Mollier diagram.

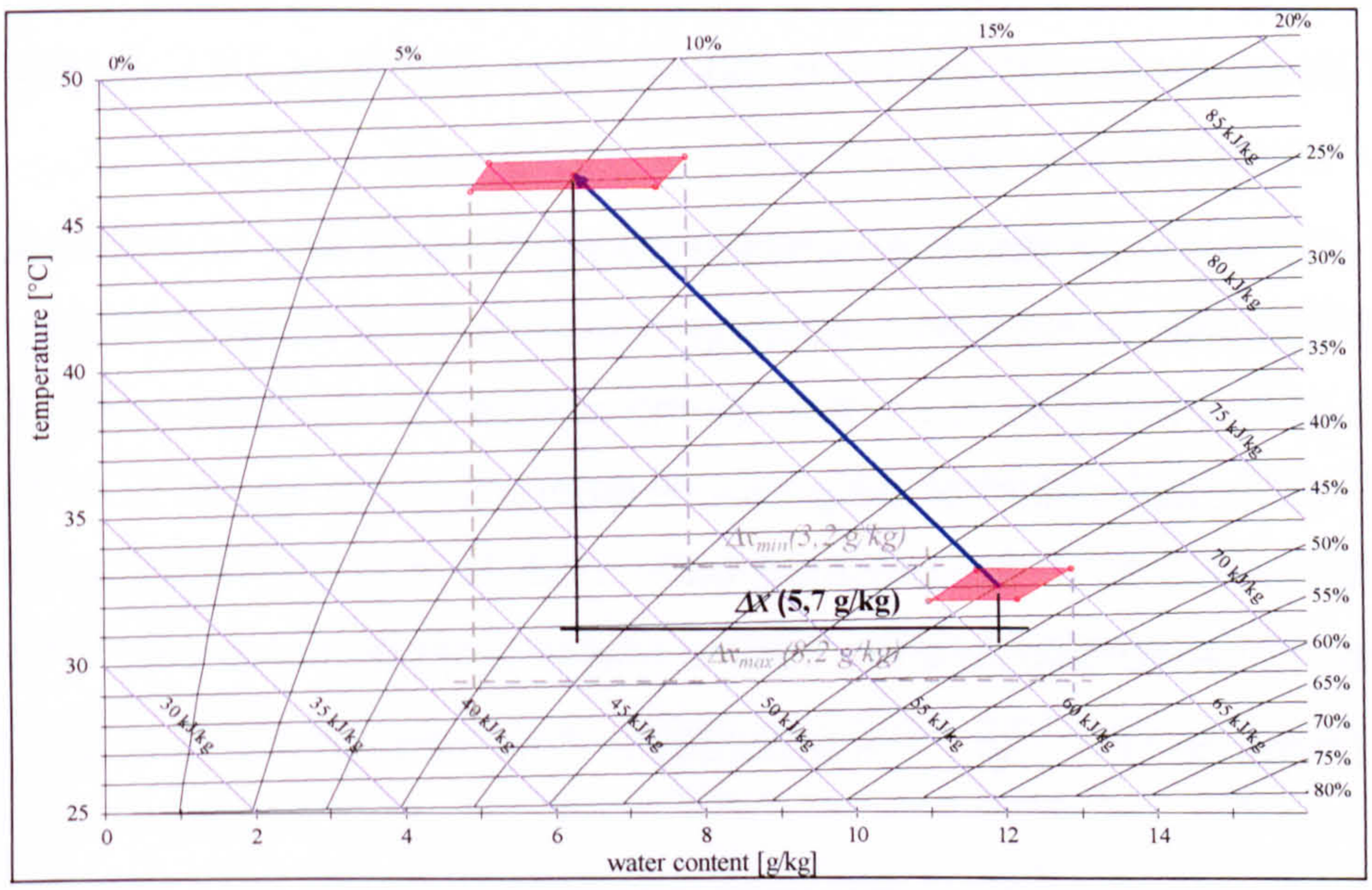

Fig. 5.3: *Isenthalpic dehumidification process in a Mollier diagram with displayed areas of measurement inaccuracy (red)*

The isenthalpic dehumidification process of air from 32°C and 40 % relative humidity to a relative humidity of 10 % is shown by the blue line. Around the

"end"-points of the process, the sensor accuracies given by the manufacturers are depicted by the red areas. With regard to these areas, the maximum deviations are depicted by the grey lines; the "real" value is shown by the black line.

Furthermore, it can be seen that the inaccuracy of the relative humidity measurement can cause increasing deviations in the absolute humidity as the temperatures rise. For example, at a temperature of 32°C and a relative humidity of 40 %, the absolute humidity is about 12.1 g/kg. With an accuracy of ± 2 % r.h., this corresponds to a relative humidity of between 38 % and 42 %; the absolute humidity reaches values between 11.5 g/kg and 12.7 g/kg, which represent an absolute deviation of ± 0.6 g/kg. With the same absolute humidity (12.1 g/kg) but at a higher temperature of e.g. 70°C (the corresponding relative humidity for this condition is 6.1 %), the accuracy of ± 2 % r.h. results in values that lie between 8.1 g/kg und 16.1 g/kg, which corresponds to an absolute deviation of ± 4.0 g/kg. Thus the deviation of the absolute humidity caused by measurement inaccuracies can be more than 6 times higher at 70°C than at 32°C.

Aside from the temperature and the humidity measurements, the volume flow measurements can also cause errors resulting from sensor inaccuracy. With the above-mentioned flow meter sensors, the volume or mass flow can be indirectly determined by the measurement of the pressure difference. The accuracy of the sensors is given at ± 3 % of the pressure difference. Due to the fact that the empirical function used to calculate the volume flow is proportional to the root of the pressure difference ($\dot{V} \sim \sqrt{\Delta p}$), the accuracy of flow measurements is about ± 1.7 %.

The maximum error of the *RSHI* caused by the inaccuracy of the flow meter sensors can be estimated again with an error propagation calculation. The assumption that only the inaccuracies of the flow measurements cause the error of the *RSHI* (which is obviously incorrect but nevertheless provides a closer look at the influence of the volume flow measurements), leads to a proportional

relationship between the *RSHI* and the quotient of the mass flows ((Eq. 5.12) and (Eq. 5.13)):

$$RSHI = \frac{\Delta \dot{Q}_{reg}}{\Delta x \cdot \dot{m}_{process}} = \frac{c_{p,air} \cdot \left(\theta_{reg} - \theta_{amb}\right)}{\Delta x} \cdot \frac{\dot{m}_{reg}}{\dot{m}_{process}} \qquad \text{(Eq. 5.12)}$$

$$RSHI \approx \frac{\dot{m}_{reg}}{\dot{m}_{process}} \qquad \text{(Eq. 5.13)}$$

Using the calculation laws to determine the resulting error limits (for ratios of two measured values, the relative errors were added) in combination with the given relative accuracy of ± 1.7 % for the flow measurements, a maximum error limit of 3.4 % is obtained for the *RSHI* as a result of the volume flow measurements. Compared with the errors that occurs with the humidity measurements this error can most likely be ignored.

A look at these significant errors makes a sensible evaluation of the measured data seem almost impossible. The real errors are however, much smaller than these calculated maximum values, especially if the measured values are "far away" from the measuring limits. For the determination of the figures of merit, mainly the process air conditions are of interest. The value for the relative humidity of the regeneration air is only required for the determination of the dehumidification efficiency. The normal values of the process airflow lie within the "best" measuring range of the used sensors, thus the real inaccuracies should usually be much less than the given maximum inaccuracies. The measurements of the relative humidity of the regeneration air however must be considered critically. With relative humidities under 10 %, the absolute humidity can most likely not be determined with an accuracy that is sufficient for our needs. Due to this, in the test plant the humidity of the regeneration air has been measured before heating. With this determined absolute humidity the corresponding relative humidity at regeneration air temperature must then be calculated. With this procedure, overly large inaccuracies in the determination of the dehumidification efficiency could be avoided.

Overall the measuring accuracy of the humidity sensors has the main influence on the possible error in determining the figures of merit, especially at high temperatures. Fortunately, in our case, the usual temperatures of the process air flow lie within a very accurate measuring range of the sensors. The biggest problem with measurement accuracy (the determination of the relative humidity of the regeneration air) could be avoided by measuring the humidity of the "cold" regeneration air.

The results of the measurements also indicate that the errors caused by measuring inaccuracies are not as big as the error propagation calculation could lead one to expect as they always show that the affinities of the influence of the different operation parameters are sensible and explainable. Only the measurements in which the regeneration air was humidified (and therefore the humidity could not be determined by measuring the cold regeneration air) resulted in partly untrustworthy figures of merit.

The following evaluations in chapter 5.3 show therefore the tendentious influence of the investigated operation parameters on the figures of merit. The outcomes are indisputably suitable for use in comparing the different measurements: however, unrealistically high demands on the absolute values of the determined figures of merit should not be made.

Hereby it should also be considered that the figures of merit of air handling systems are often published in the literature without mention of the boundary conditions of their determination. In many such cases it must be supposed that the determination of the figures of merit was done under less advantageous conditions than those in our test plant. Thus the published values can also contain very large inaccuracies!

5.2.4 MEASURING PROCEDURES

Due to the fact that the wheel matrix is generally not perfectly uniform, the air flow resistance varies with the position of the wheel and as a result of this the

volume flow rates varies synchronised with the rotation frequency of the wheel. Furthermore, the conditioning of the airflows by heating and humidifying (steam humidifiers) also causes fluctuations in the measured values because of the control strategies of these devices, especially with the steam humidifiers. For the purpose of eliminating these fluctuations, the values were monitored every 2 to 4 seconds over a time of at least 5 minutes, or, if longer, over the time of more than 3 complete revolutions of the wheel, e.g. 9 min at a rotation velocity of 20 RPH (**R**evolutions **P**er **H**our). The measuring period was not started before steady state conditions had been achieved. The check on steady state conditions was done by observing the gradients of the measured values. If no more significant changes took place, steady state conditions were assumed and the measurements were started.

The measured values shown in Appendix A are the averaged values of the monitored times. The given range (±) is the standard deviation of the measured values.

Most of the measurements were done with a process mass flow of about 2400 kg/h (corresponding to 2000 m³/h at 20°C / 50 %) and a ratio of 0.75 between the regeneration and process air flow.

5.3 RESULTS

5.3.1 INERTIA OF TEST PLANT

The first item that was examined was the time required to regain steady state conditions after a change had been made to the operation conditions in order to get a better feeling of the inertia of the test plant.

In Fig. 5.4, the time behaviour curves of the measured values are shown for a change in regeneration air temperature. The determined time period needed to regain steady state conditions in this example was about 15 min. Thus the measurements were started at the earliest, 15 to 20 minutes after a change had been made in the operation conditions and only if the observed monitored

values clearly showed steady state conditions. Normally, the measurements were started 30 to 45 min after the change was made in the operating conditions.

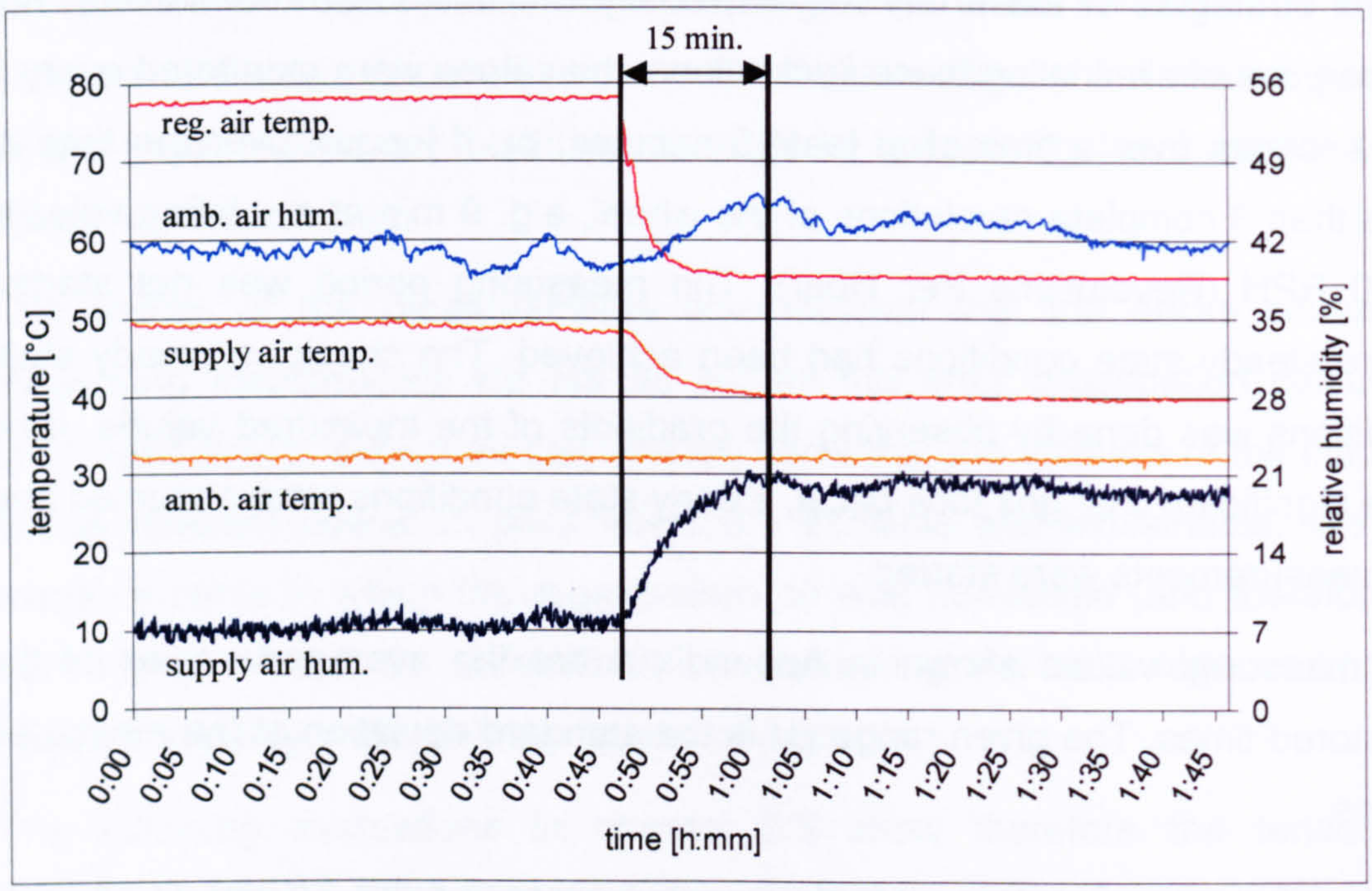

Fig. 5.4: *Time before steady state condition after a change of regeneration air temperature*

5.3.2 INFLUENCE OF ROTATION VELOCITY

Compared to rotating heat exchangers, desiccant wheels operate at much lower rotation velocities. Rotating heat exchangers normally operate at 600 RPH. Desiccant wheels in dehumidification operation run at between 15 and 100 RPH. Of course, at higher rotation velocities the desiccant wheels can also be used for heat recovery operation, but due to the lower specific heat capacity of the matrix material they are not as efficient as pure heat exchangers.

In the following paragraphs the influence of the different operation parameters is evaluated for a wide range of rotation velocities. Thus, at the end, the influence of the different operation conditions can be judged as a factor of the rotation velocity.

When comparing the results of the two tested wheels it should be considered that the influence of the rotation velocity is different for each wheel. With the Hexcore wheel for example, the dehumidification capacity usually increases as rotation velocities rise up to 85 - 100 RPH. The Klingenburg wheel however shows a decrease in the dehumidification capacity as rotation velocities rise above about 25 RPH. This different behaviour is most likely caused by the different sorption mechanisms of the used sorption materials. For the Hexcore wheel, the sorption material used is silica gel and the sorption mechanism is the adsorption process (see Chapter 2.2.2), for the Klingenburg wheel, the sorption material is lithium chloride and the sorption process is most likely the absorption process. Thus the different behaviour could be caused by the different dynamics of these processes. The results lead one to assume that the absorption process is quite a bit slower than the adsorption process. This can also be the reason for why with the measurements of the Klingenburg wheel, especially at higher rotation velocities, sometimes the dehumidification process becomes a humidification process (negative dehumidification capacity). In addition, the kind of matrix material, which is also different for the two wheels studied, can certainly influence the sorption dynamics.

5.3.3 INFLUENCE OF VOLUME FLOWS

In this and the following paragraphs the outcomes of the measurements are shown in diagrams. In these diagrams the measurement series are named with the letter "H" for measurements of the Hexcore wheel, "K" for measurements of the "Klingenburg" wheel and an ongoing number for the single measurement series. A complete overview and detailed information about the boundary and operation conditions for every measurement series is shown in Appendix A. The boundary and operation conditions of the displayed measurement series in the single paragraphs are also shown at the beginning of the corresponding paragraph.

Desiccant wheel:	Engelhard HexCore, LP / DES-H-Hexcore-DC15/N						
No:	process airflow (set values)			reg. airflow (set values)			Volume flow ratio
	θ [°C]	φ [%]	V [m³/h]	θ [°C]	φ [%]	V [m³/h]	$V_{reg}/V_{process}$ [-]
H1	32	40	2000	75	-	2000	1.0
H5	32	40	2000	75	-	1500	0.75
H6	32	40	2000	75	-	1000	0.5
Desiccant wheel:	**Klingenburg, SECO 1000**						
K2	32	40	2000	60	10	2000	1.0
K3	32	40	2000	60	10	1000	0.5
K9	32	40	2000	60	10	1500	0.75

Tab. 5. 2: *Boundary and operation conditions of the measurement series used for investigations of the influence of volume flows*

DES-H-HEXCORE-DC15/N

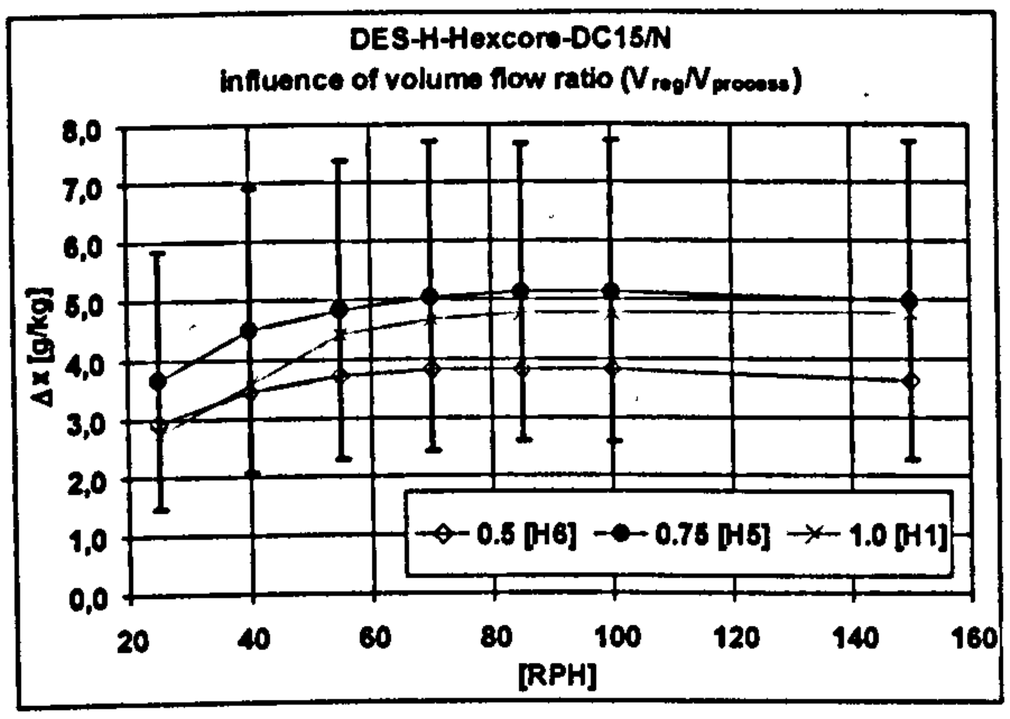

Fig. 5.5: *Dehumidification capacity, measurement series H1 / H5 / H6. Error bars shown for measurement series H5*

Fig. 5.5 shows the influence that the rotation velocity and the volume flow ratio between the process and the regeneration air flows have on the dehumidification capacity. As an example for the maximum possible errors which could be caused by measurement inaccuracy (see paragraph 5.2.3), the error bars for the measurement series H5 are shown.

The dehumidification capacity rises to about 85 - 100 RPH as the rotation velocity increases. At higher rotation velocities the dehumidification capacity decreases slightly. It is evident that the dehumidification capacity is higher at a volume flow ratio of 0.75 than at a ratio of 1. Normally, it would be expected that the dehumidification capacity should rise even more with higher volume flows because the matrix can be dried more due to the higher transfer coefficients caused by higher flow velocities. An explanation for this behaviour could be the so called "heat inhibition" effect by which the wheel matrix becomes too warm

during regeneration and has to be cooled down first in the dehumidification phase before it can effectively dehumidify the air.

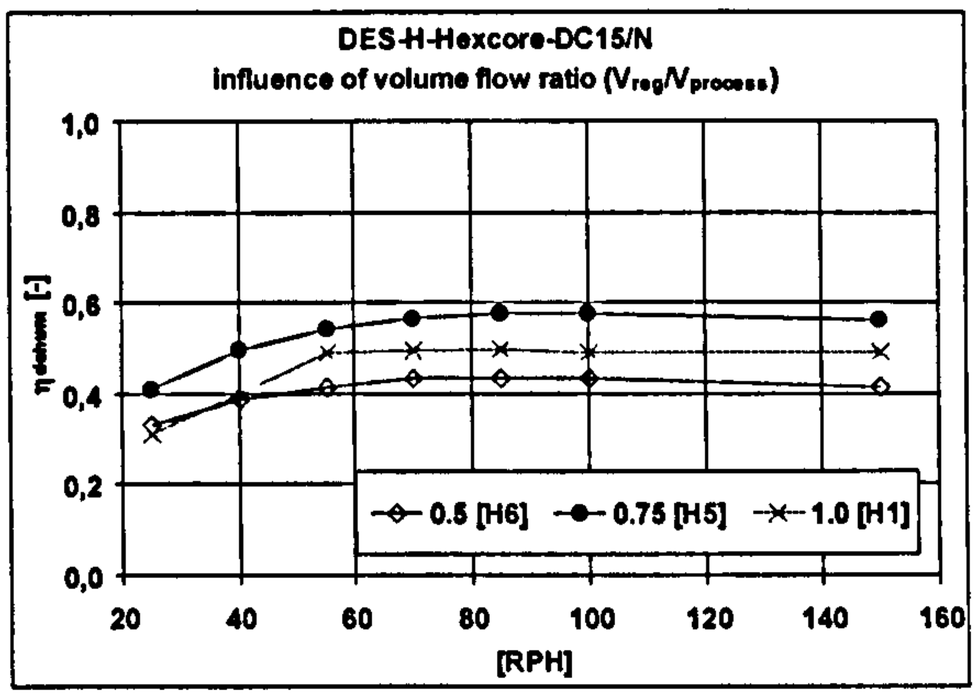

Fig. 5.6: *Dehumidification efficiency, measurement series H1 / H5 / H6*

In Fig. 5.6, the dehumidification efficiency for the same measurement series is shown. Similar to the dehumidification capacity, the dehumidification efficiency is highest at a volume flow ratio of 0.75. This is also caused by the heat inhibition effect for high volume flows of the regeneration air.

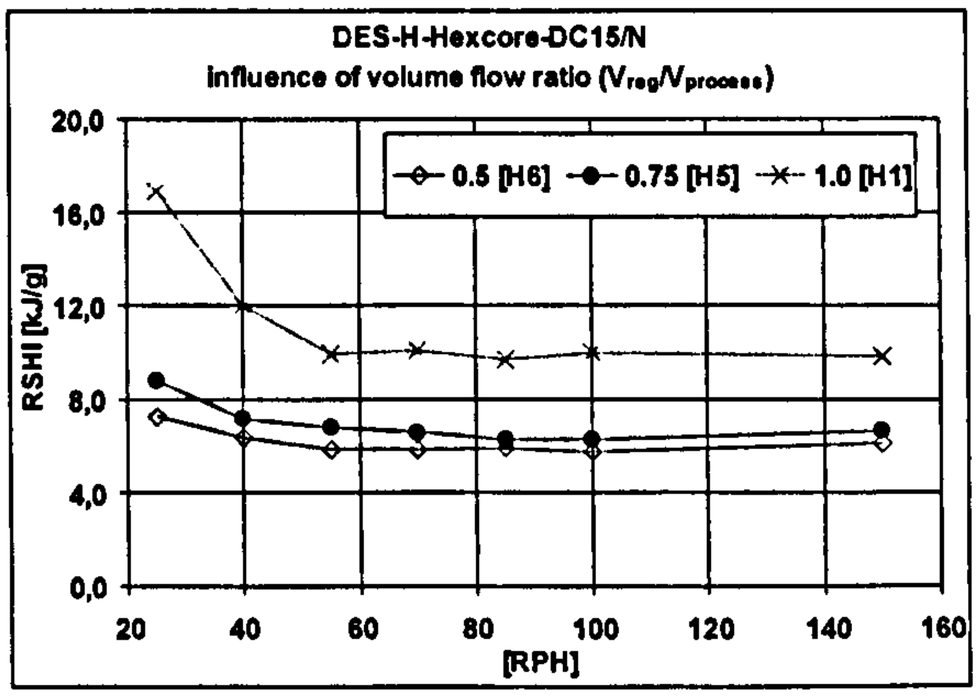

Fig. 5.7: *RSHI, measurement series H1 / H5 / H6*

A look at the RSHI (see Fig. 5.7) shows, that the energy efficiency is a little bit better at a volume flow ratio of 0.5 than it is at 0.75, especially at low rotation velocities. The relatively high RSHI at a volume flow ratio of 1.0 is again caused by the heat inhibition effect.

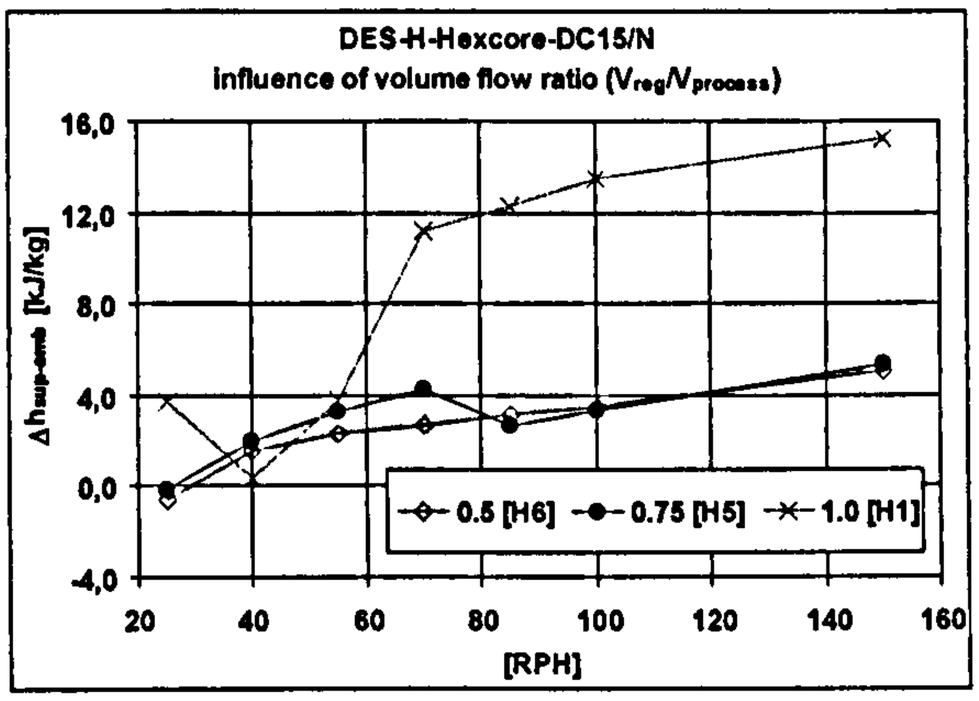

Fig. 5.8: *Enthalpy change, measurement series H1 / H5 / H6*

The curves of the enthalpy change (see Fig. 5.8) for the measurement series H5 and H1 are not actually steady. This is caused by an inadequacy in the volume flow control at the test plant. The decreasing values at 40 and 55 RPH for the measurement series H1 and 85 and 100 RPH for measurement

series H5 were caused by a decreasing regeneration air volume flow (see detailed measurement data in Appendix A). Nevertheless, the trend of the enthalpy change behaviour seems clear. The enthalpy increase at a volume flow ratio of 1.0 is clearly higher than it is at a volume flow ratio of 0.75 or 0.5. This points to a high heat transfer rate from the regeneration air to the supply air and is also partly caused by the heat inhibition effect. The enthalpy change at the volume flow ratios of 0.5 and 0.75 doesn't deviate much, but it tends to be a bit higher at a ratio of 0.75.

As a matter of principle the enthalpy change curves, as shown e.g. in Fig. 5.8, must theoretically start at the zero point (RPH = 0 / Δh = 0) and should then rise steadily up to a maximum which can be at a point that is far above the drawn rotation velocities in the diagrams shown. With the assumption of an isenthalpic dehumidification process by adsorption and when ignoring the binding enthalpy, the enthalpy change can be caused only by heat transfer (heat capacity flow of the wheel or air leakages). Thereby the enthalpy change at the slowest measured rotation velocities should normally not deviate too much. So for the shown enthalpy change diagrams, the sometimes very different levels in the enthalpy change curves were probably caused by measurement errors due to unavoidable inaccuracies of the measuring devices. Thus, for example, at a temperature of 50°C and a relative humidity of 20%, the given error limits of the relative humidity measurement of ± 2 % r.h. can cause deviations of about 8.4 kJ/kg in calculated enthalpy.

KLINGENBURG SECO 1000

The influence of the volume flows was also studied using the Klingenburg wheel. Please note: The results may not be compared directly with the results shown above from the Hexcore wheel because the relative humidity of the regeneration air is very different in both series of experiments. Detailed information about the boundary conditions is shown in Appendix A for each measurement series.

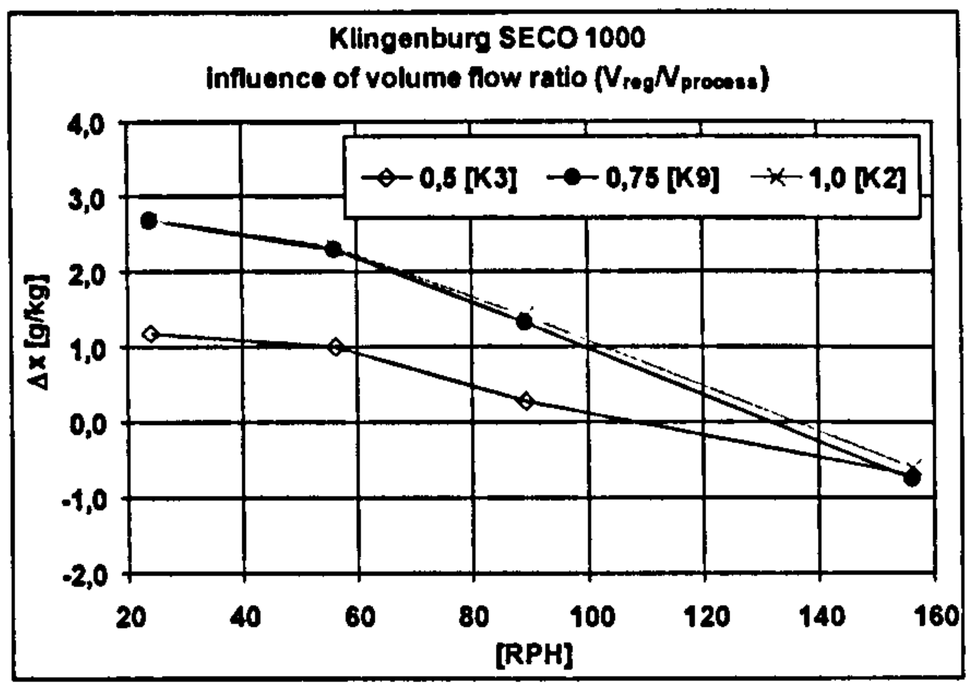

Fig. 5.9: *Dehumidification capacity, measurement series K3 / K2 / K9*

In contrast to the measurements of the Hexcore wheel, the dehumidification capacity of the Klingenburg wheel decreases as the rotation velocities increase (see explanation in paragraph 5.3.2). Considering the different volume flows, the dehumidification capacity does not increase when the volume flow rate is increased from 0.75 to 1.0, but a clear heat inhibition effect, as was observed with the Hexcore wheel, can not be found. The reason for this could also be a result of the lower regeneration air temperature of 60°C in this measurement series. At a volume flow ratio of 0.5 the dehumidification capacity is very low.

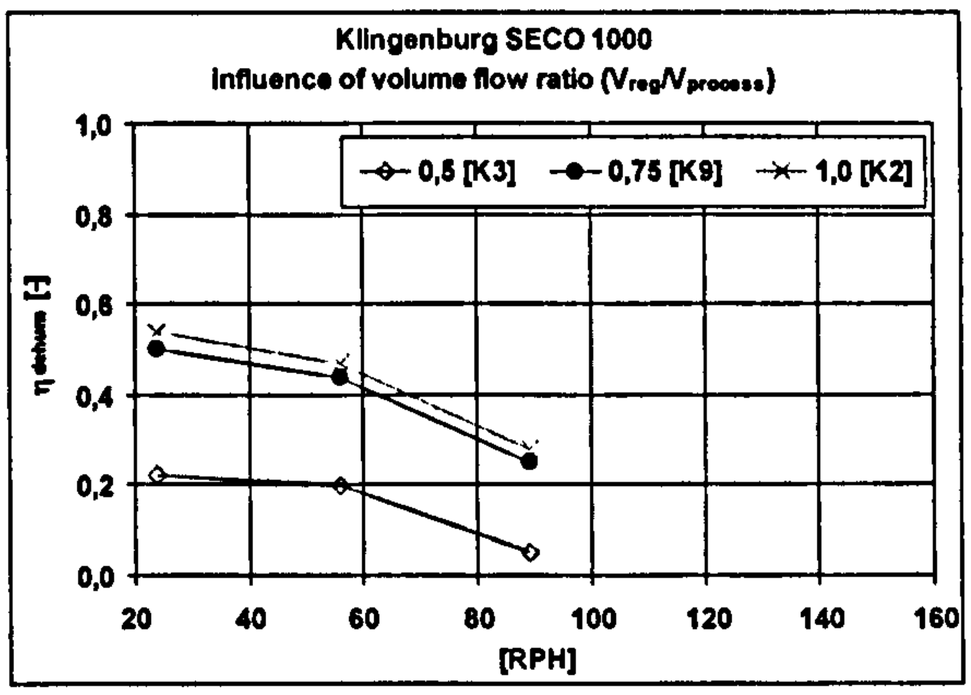

Fig. 5.10: *Dehumidification efficiency, measurement series K3 / K9 / K2*

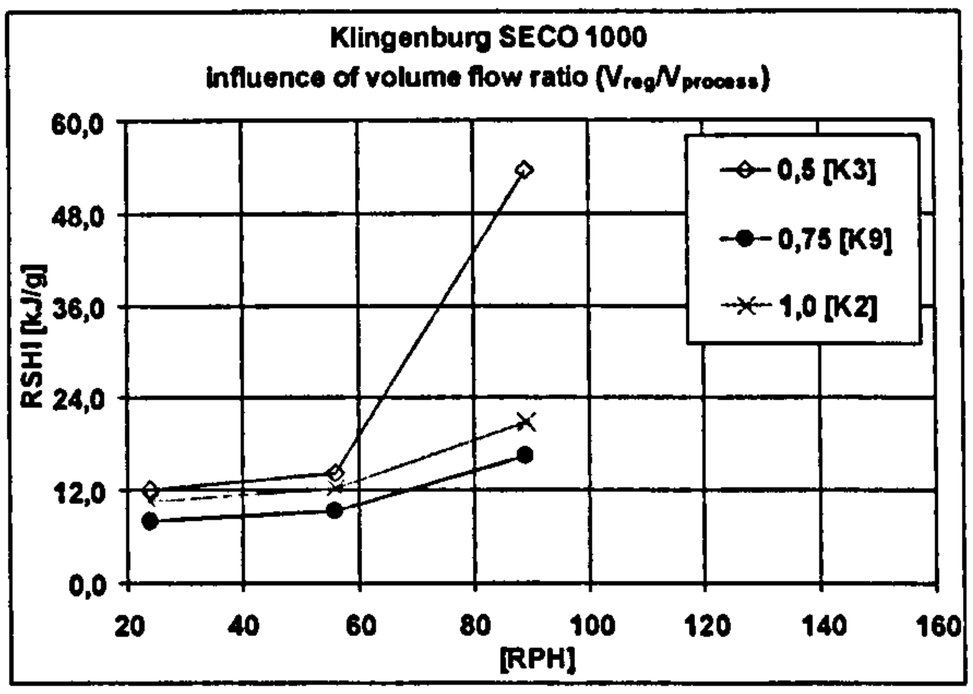

Fig. 5.11: *RSHI, measurement series K3 / K9 / K2*

A look at the dehumidification efficiency (Fig. 5.10) and at the RSHI (Fig. 5.11) does not show anything unexpected. The dehumidification efficiency at a volume flow ratio of 0.5 must be considered to be a very poor one.

The overall relatively low levels of the dehumidification capacities, especially at higher rotation velocities, where the values even change into negative ones, are partly caused by the high humidity of the regeneration air (10 %) in this measurement series, but this effect can also be observed in continuing

measurement series with lower relative humidities of the regeneration air. This tendential behaviour of the Klingenburg wheel is further explained in paragraph 5.3.7.

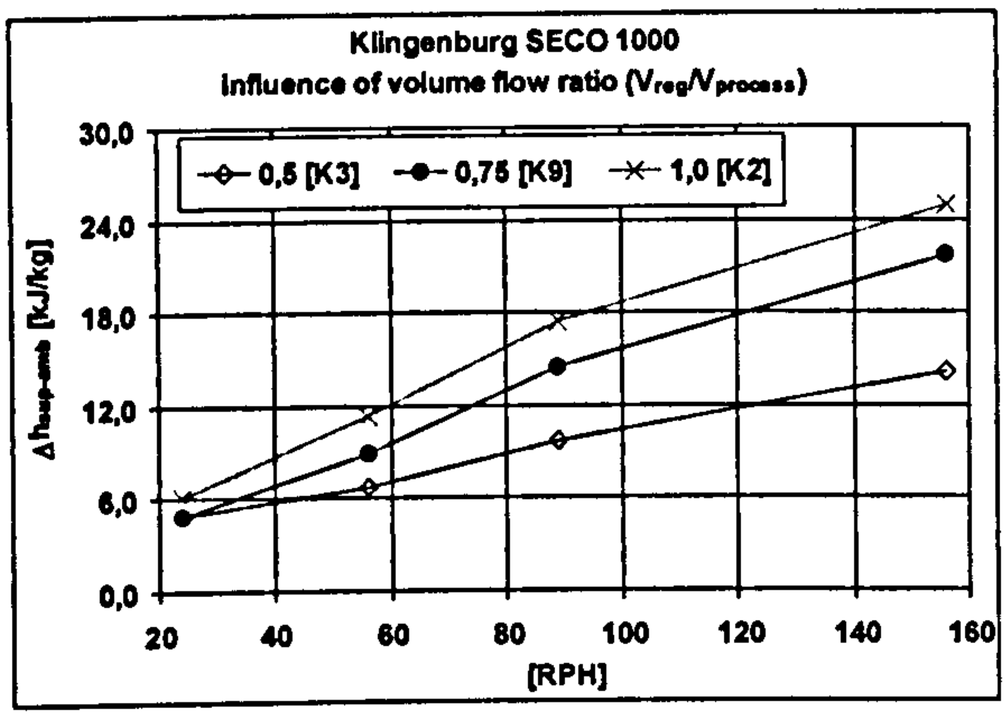

Fig. 5.12: *Enthalpy change, measurement series K3 / K9 / K2*

A look at the enthalpy change (see Fig. 5.12) shows almost equal values at low rotation velocities. With rising rotation velocities and rising volume flow ratios, the enthalpy change increases as is to be expected because of the increasing heat transfer from the regeneration air.

5.3.4 INFLUENCE OF REGENERATION AIR TEMPERATURE

Desiccant wheel: **Engelhard HexCore, LP / DES-H-Hexcore-DC15/N**

No:	process airflow (set values)			reg. airflow (set values)			Volume flow ratio
	θ [°C]	φ [%]	V [m³/h]	θ [°C]	φ [%]	V [m³/h]	$V_{reg}/V_{process}$ [-]
H4	32	40	2000	60	-	1500	0.75
H5	32	40	2000	75	-	1500	0.75
H9	32	40	2000	90	-	1500	0.75
Desiccant wheel:	**Klingenburg, SECO 1000**						
K6	32	40	2000	70	10	1500	0.75
K8	32	40	2000	45	10	1500	0.75
K9	32	40	2000	60	10	1500	0.75

Tab. 5.3: *Boundary and operation conditions of the measurement series used for investigations of the influence of regeneration air temperatures*

DES-H-HEXCORE-DC15/N

Fig. 5.13 shows the influence of different regeneration air temperatures and the rotation velocity on the dehumidification capacity. The dehumidification capacity rises both as the temperature increases and also as the rotation velocity increases up to about 100 RPH. At higher rotation velocities the dehumidification capacity decreases slightly. A look at the dehumidification

efficiency (Fig. 5.14) shows almost equal values for each measurement series. By following the curve of the dehumidification capacity, it can be seen that the dehumidification efficiency rises until it reaches rotation velocities of about 100 RPH.

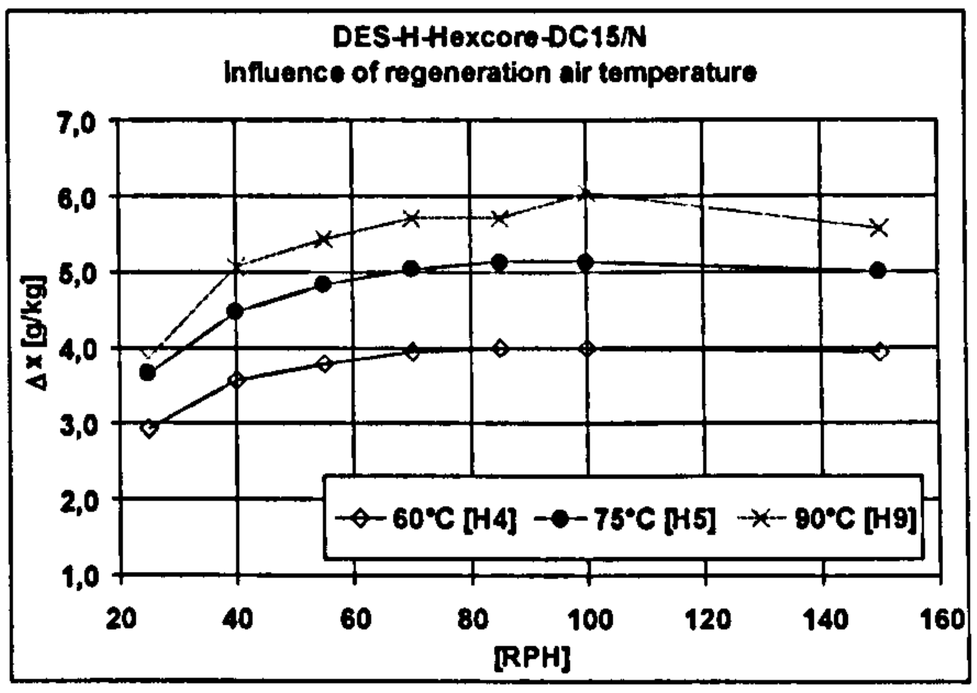

Fig. 5.13: *Dehumidification capacity, measurement series H4 / H5 / H9*

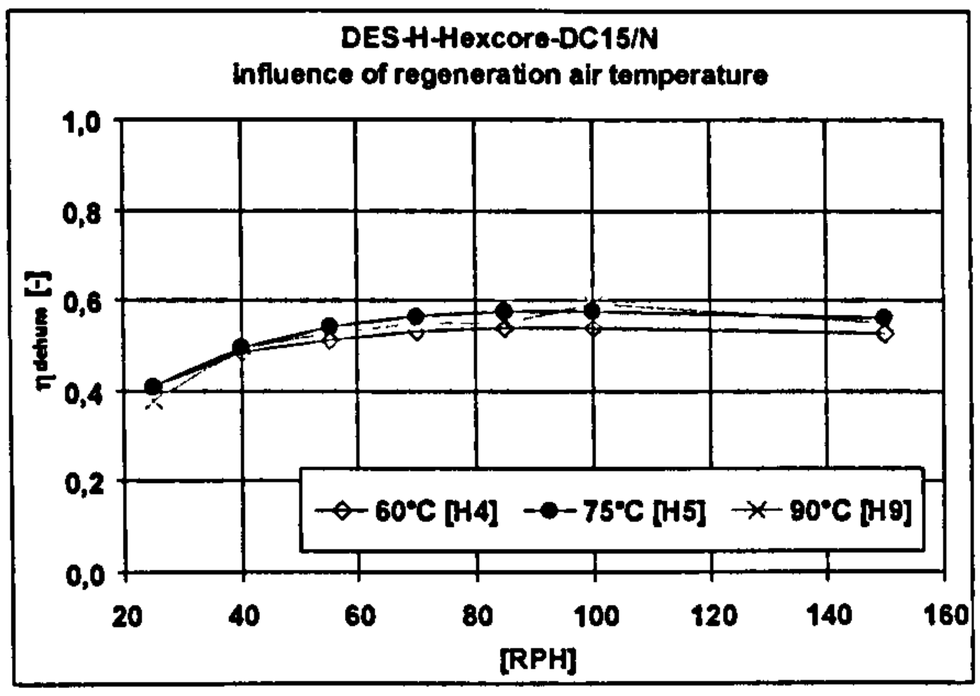

Fig. 5.14: *Dehumidification efficiency, measurement series H4 / H5 / H9*

The RSHI (Fig. 5.15) shows the expected tendency: the RSHI rises as the regeneration temperature increases. The difference however, is not very great. The enthalpy change of the process air tends to (Fig. 5.16) show the expected behaviour and rises as the regeneration air temperature and the rotation velocity increase.

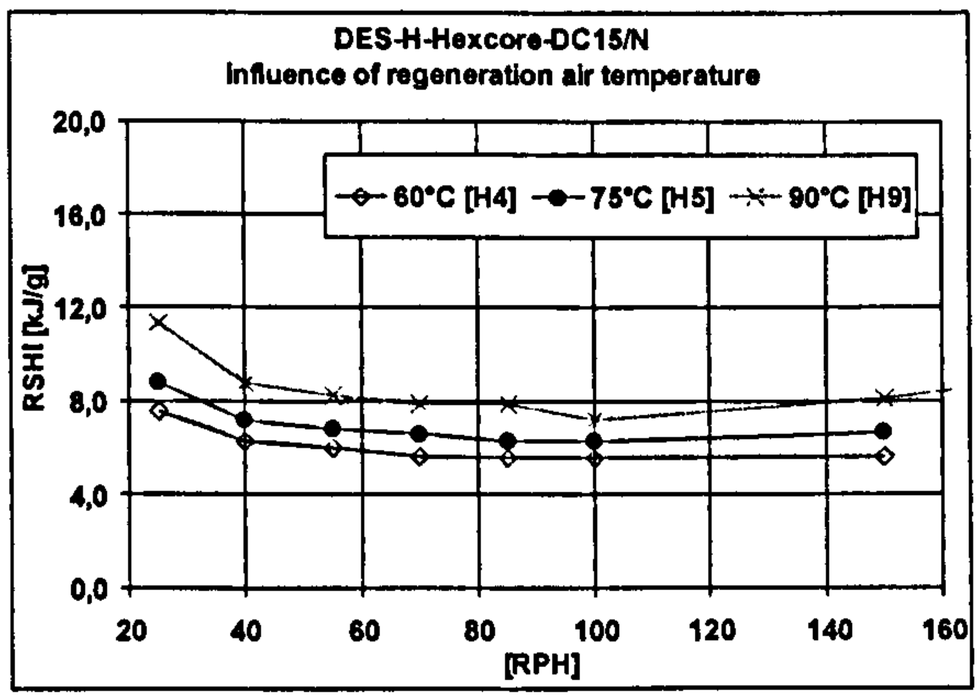

Fig. 5.15: *RSHI, measurement series H4 / H5 / H9*

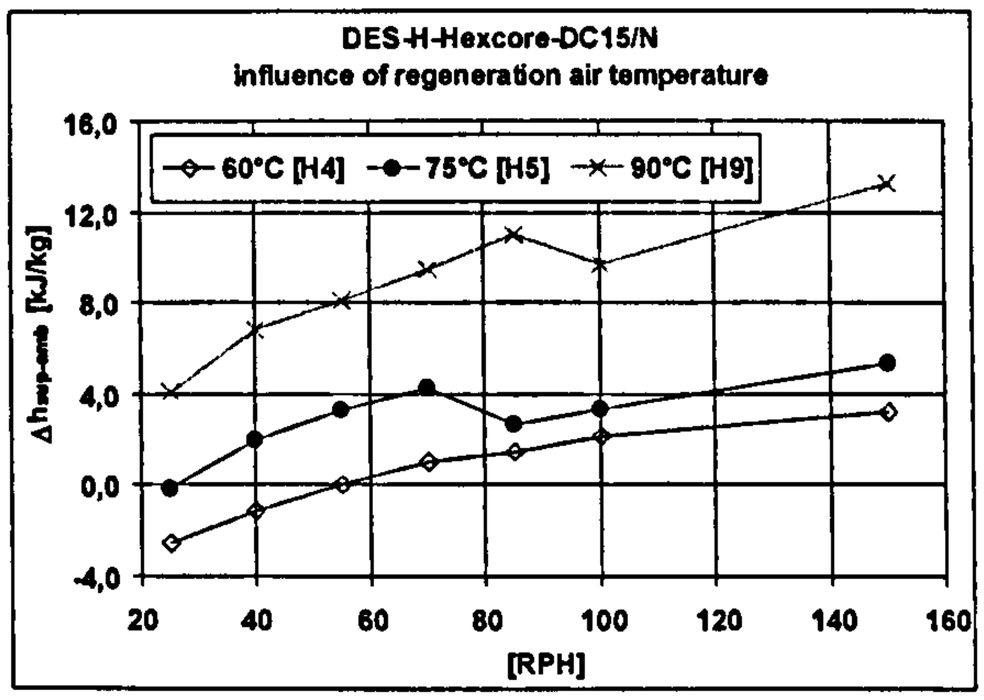

Fig. 5.16: *Enthalpy change, measurement series H4 / H5 / H9*

The slightly unsteady curves from the measurement series H5 and H9 are again caused by the inadequacy of the volume flow control at the test plant.

KLINGENBURG SECO 1000

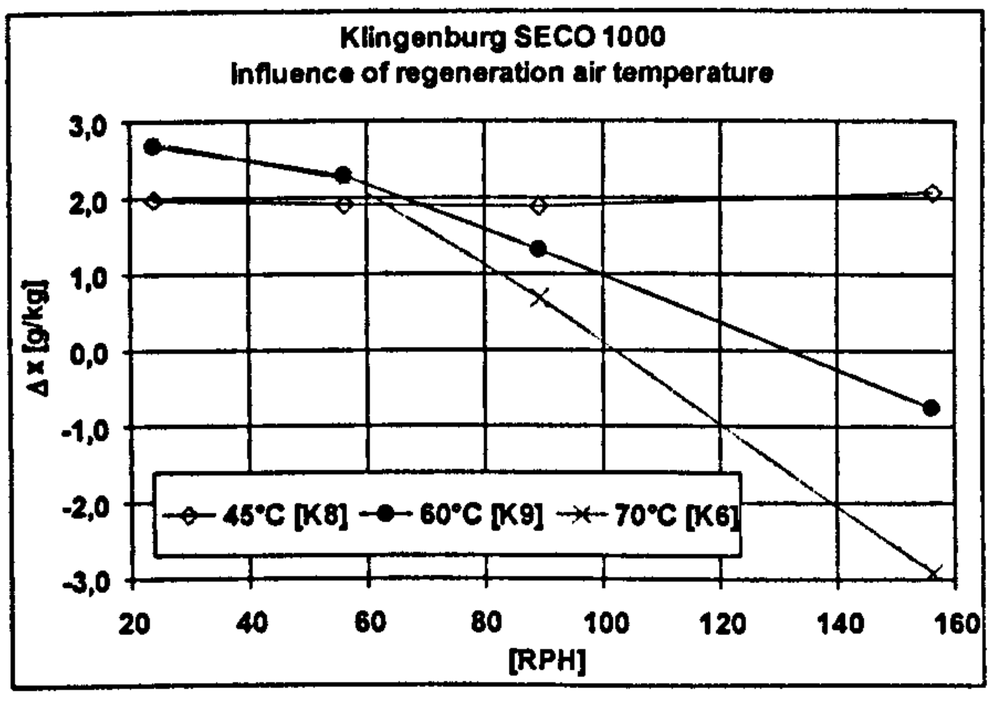

Fig. 5.17: *Dehumidification capacity, measurement series K8 / K9 / K6*

Fig. 5.17 shows the influence of the regeneration air temperature on the dehumidification capacity for the Klingenburg wheel. The dehumidification capacity decreases again along with the rotation velocity. Only at the very low regeneration air temperature of 45°C does this effect not exist. Furthermore, it is worth noting that raising the regeneration temperature from 60°C to 70°C does not lead to an improvement in the dehumidification capacity, on the contrary it leads to a change for the worse at higher rotation velocities. This behaviour can be explained by the "slow" absorption process (chemical reaction) and the constant relative humidity of the regeneration air (about 10%) in this measurement series.

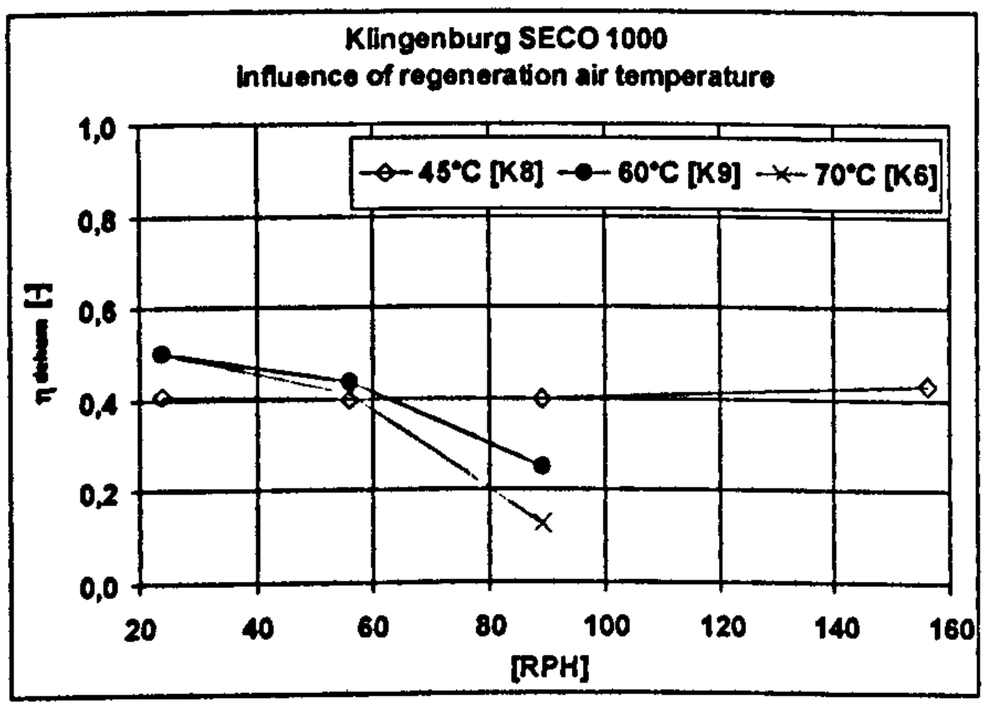

Fig. 5.18: *Dehumidification efficiency, measurement series K8 / K9 / K6*

The water content of the regeneration air at 70°C was 20 g/kg, at 60°C 13 g/kg and only 7 g/kg at 45°C. For measurements with constant absolute humidities, the dehumidification capacity would most certainly be greater at higher regeneration air temperatures.

Looking at the dehumidification efficiency in Fig. 5.18, this shows an almost equal performance of the higher regeneration air temperatures, at least

at low rotation velocities. The dehumidification efficiency at a regeneration air temperature of only 45°C is nearly constant along with rising rotation velocities.

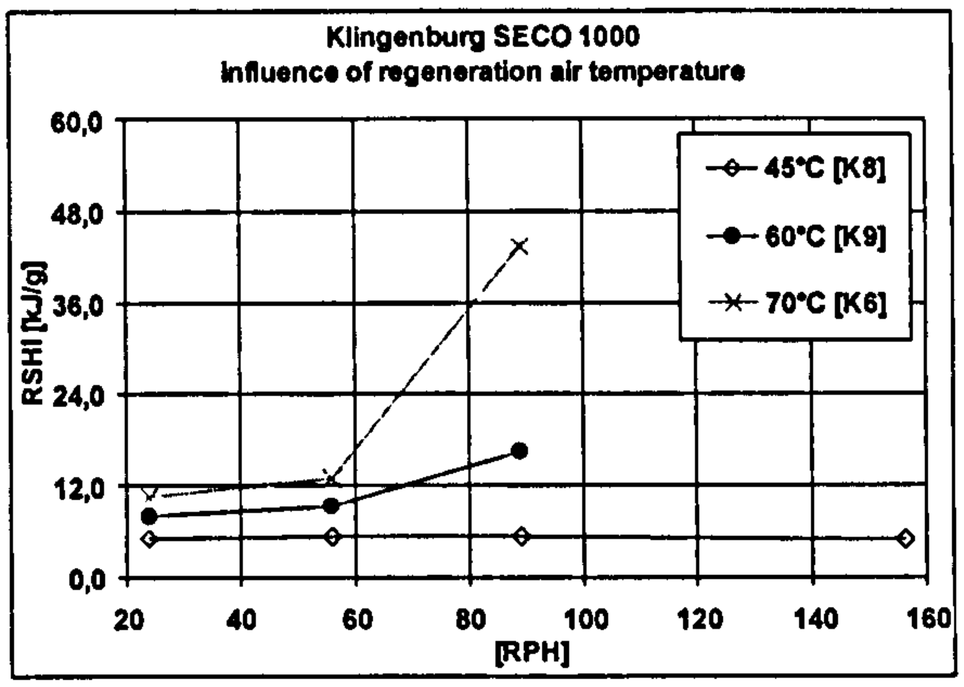

Fig. 5.19: *RSHI, measurement series K8 / K9 / K6*

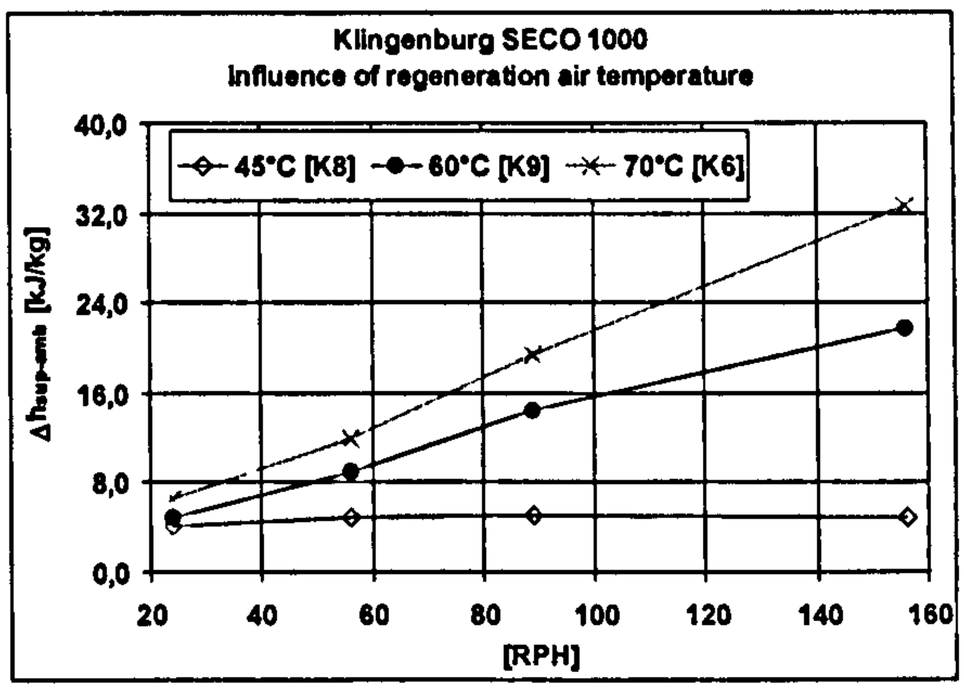

Fig. 5.20: *Enthalpy change, measurement series K8 / K9 / K6*

The RSHI (Fig. 5.19) rises along with the regeneration air temperature as expected. The differences here are slightly larger than those from the measurements of the Hexcore wheel, which again can be explained by the constant relative humidity of the regeneration air in this measurements series.

A look at the enthalpy change (see Fig. 5.20) shows once more the expected behaviour of a rising enthalpy change with rising rotation velocities and rising regeneration air temperatures.

5.3.5 INFLUENCE OF REGENERATION AIR WATER CONTENT

Desiccant wheel: **Klingenburg, SECO 1000**

No:	process airflow (set values)			reg. airflow (set values)			Volume flow ratio
	θ [°C]	φ [%]	V [m³/h]	θ [°C]	φ [%]	V [m³/h]	$V_{reg}/V_{process}$ [-]
K1	32	40	2000	60	-	1500	0.75
K9	32	40	2000	60	10	1500	0.75
K10	32	40	2000	60	20	1500	0.75

Tab. 5.4: *Boundary and operation conditions of the measurement series used for investigations of the influence of regeneration air water content*

The influence of the water content of the regeneration air was studied by taking measurements with the Klingenburg wheel.

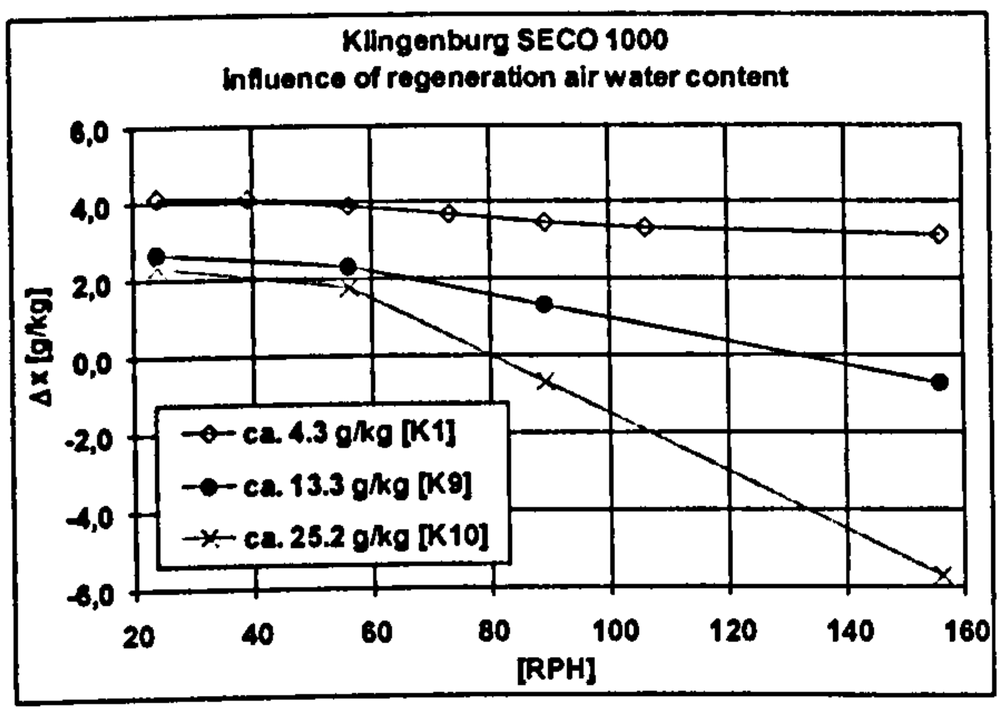

Fig. 5.21: *Dehumidification capacity, measurement series K1 / K9 / K10*

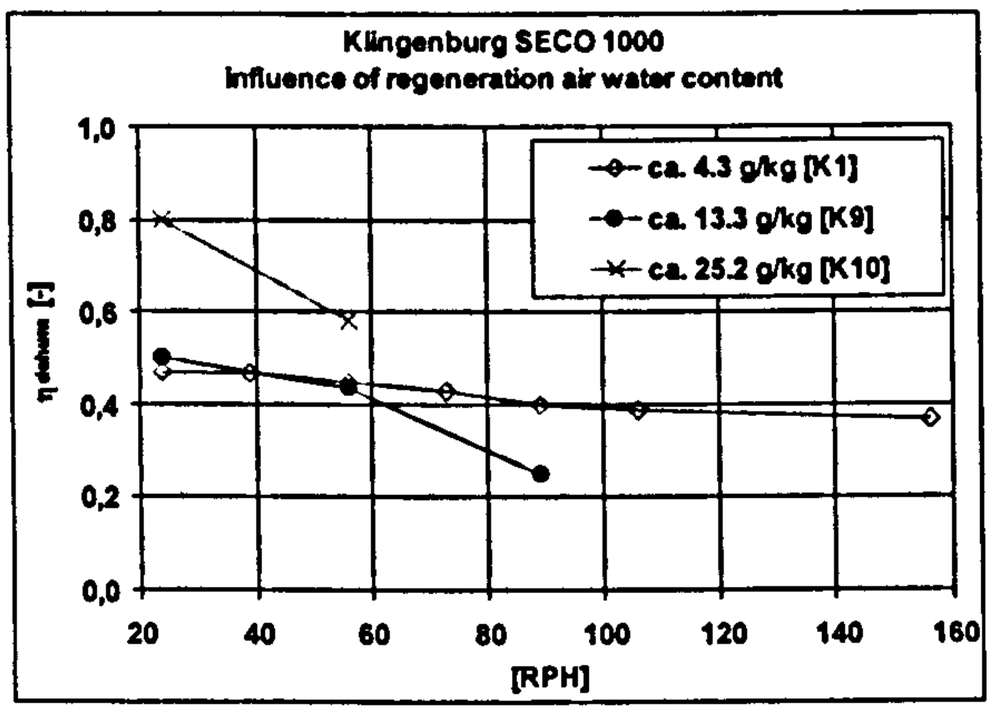

Fig. 5.22: *Dehumidification efficiency, measurement series K1 / K9 / K10*

The dehumidification capacity (Fig. 5.21) was found to decrease along with the rotation velocity and becomes negative at higher rotation velocities especially when the water content of the regeneration air is high. With low water content in the regeneration air, the influence of the rotation velocity is clearly smaller. The dehumidification capacity tends to fall when the water content of the regeneration air rises. The dehumidification efficiency (Fig. 5.22) at 24 RPH increases along with the increasing water content of the regeneration air despite the opposing tendency of the dehumidification capacity. Thus with high water content in the regeneration air, the efficiency appears to be quite good, but the capacity is poor.

Due to the fact that the RSHI (Fig. 5.23) per definition is calculated from the dehumidification capacity and the necessary amount of heat for regeneration, which is not dependent on the regeneration air water content, the curves of the RSHI cannot show an unexpected behaviour.

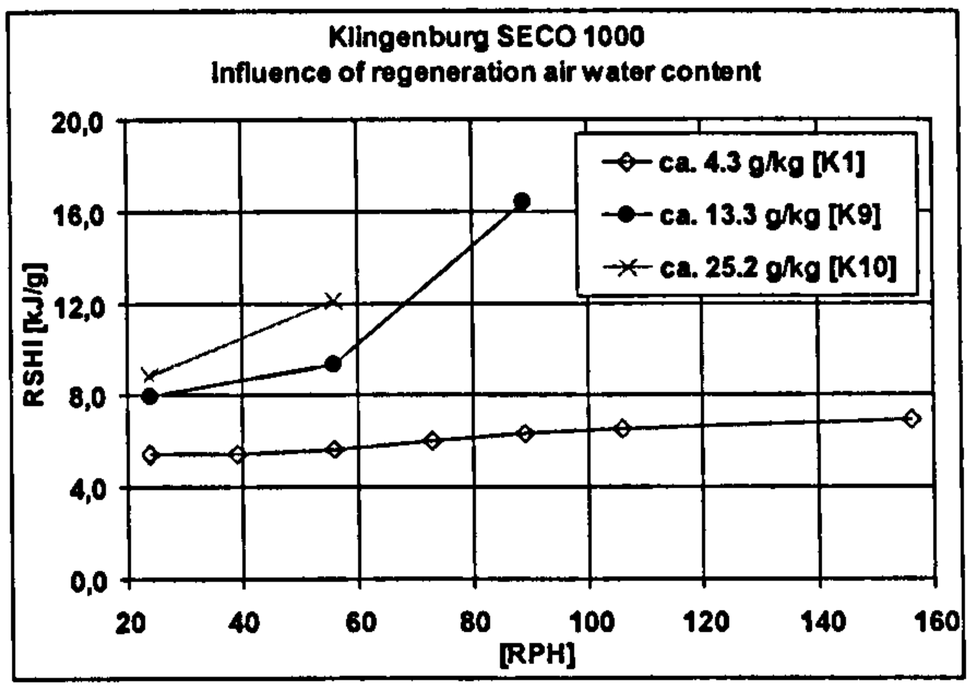

Fig. 5.23: *RSHI, measurement series K1 / K9 / K10*

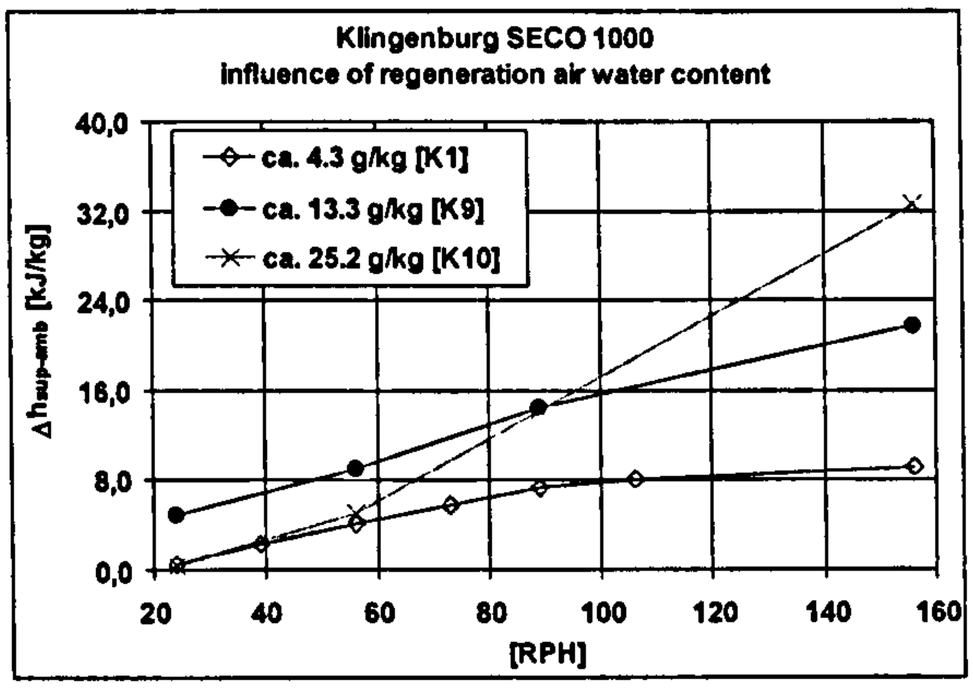

Fig. 5.24: *Enthalpy change, measurement series K1 / K9 / K10*

The enthalpy change (Fig. 5.24) shows a tendency to rise along with the rotation velocity. Furthermore the kink in the curve K10 at 55 RPH can be explained by the change of the dehumidification process into a humidification process. The very different level of the curve K9 even at low rotation velocities can only be explained by measurement errors due to inaccuracies of the used measuring devices as mentioned before.

5.3.6 INFLUENCE OF AMBIENT AIR WATER CONTENT

Desiccant wheel: **Engelhard HexCore, LP / DES-H-Hexcore-DC15/N**

No:	process airflow (set values)			reg. airflow (set values)			Volume flow ratio
	θ [°C]	φ [%]	V [m³/h]	θ [°C]	φ [%]	V [m³/h]	$V_{reg}/V_{process}$ [-]
H3	36	60	2000	75	-	1500	0.75
H5	32	40	2000	75	-	1500	0.75
H8	28	40	2000	75	-	1500	0.75

Tab. 5.5: *Boundary and operation conditions of the measurement series used for investigations of the influence of ambient air water content*

Fig. 5.25 shows the influence of the rotation velocity and the water content of the ambient air on the dehumidification capacity. The trend is: the higher the water content of the ambient air, the higher the dehumidification capacity as well. A look at the dehumidification efficiency (Fig. 5.26) shows almost equal efficiencies for measurement series H8 and H9. Only at very high water contents (H3) is the dehumidification efficiency lower.

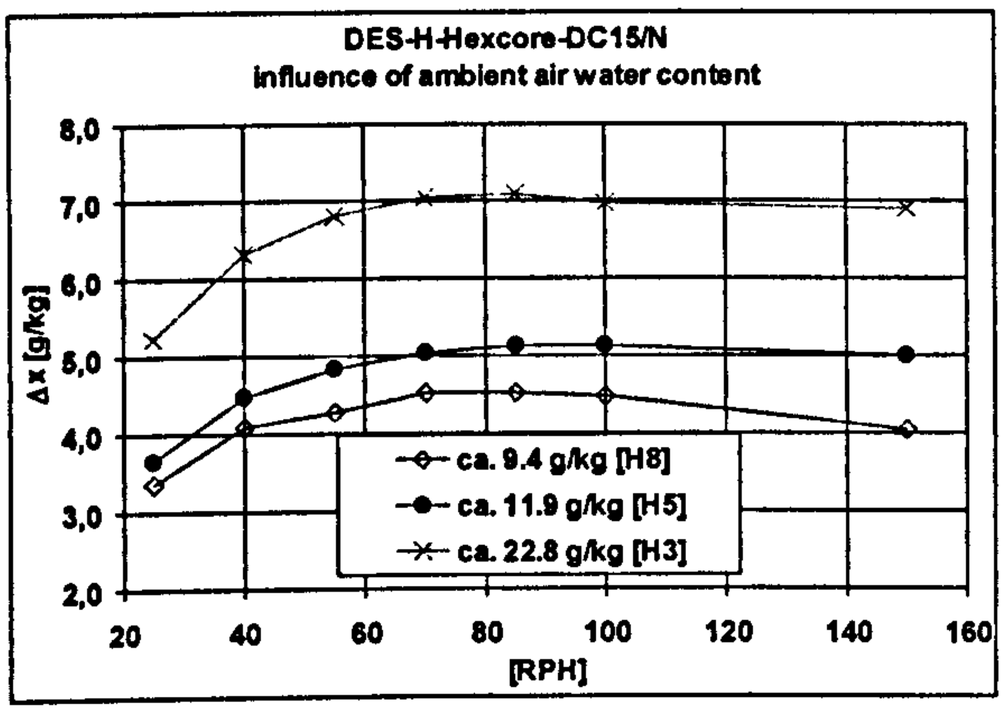

Fig. 5.25: *Dehumidification capacity, measurement series H8 / H5 / H3*

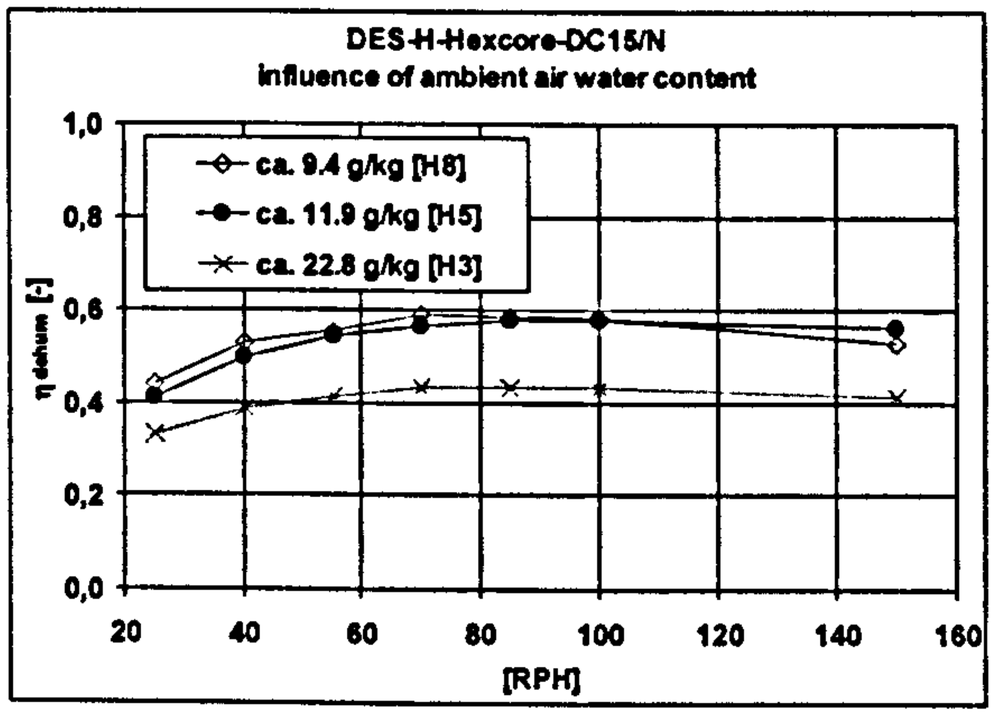

Fig. 5.26: *Dehumidification efficiency, measurement series H8 / H5 / H3*

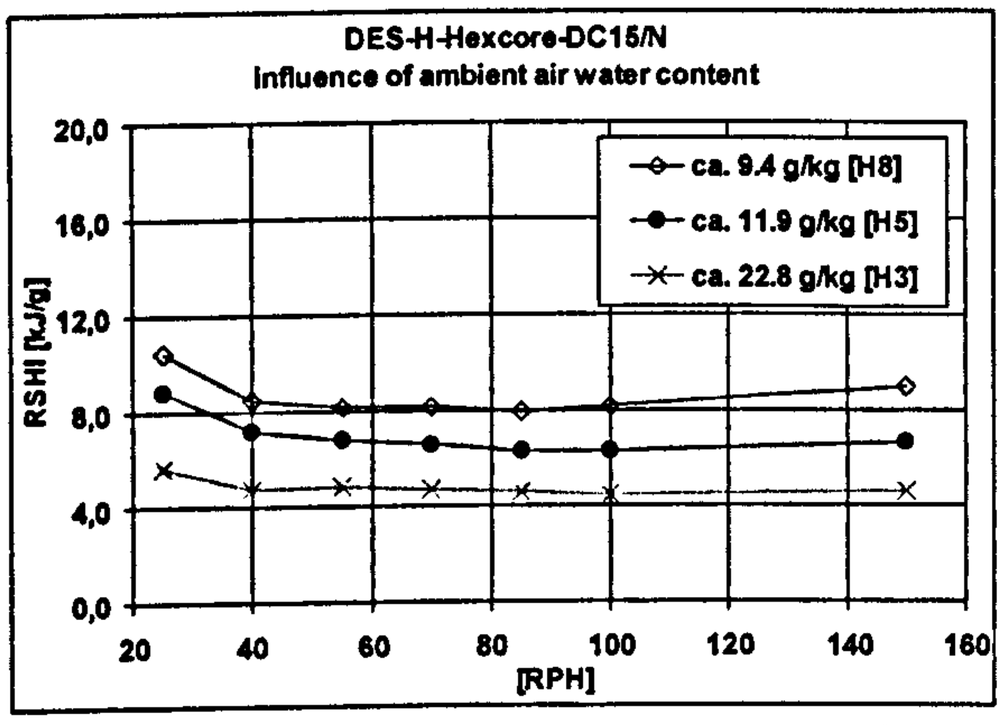

Fig. 5.27: *RSHI, measurement series H8 / H5 / H3*

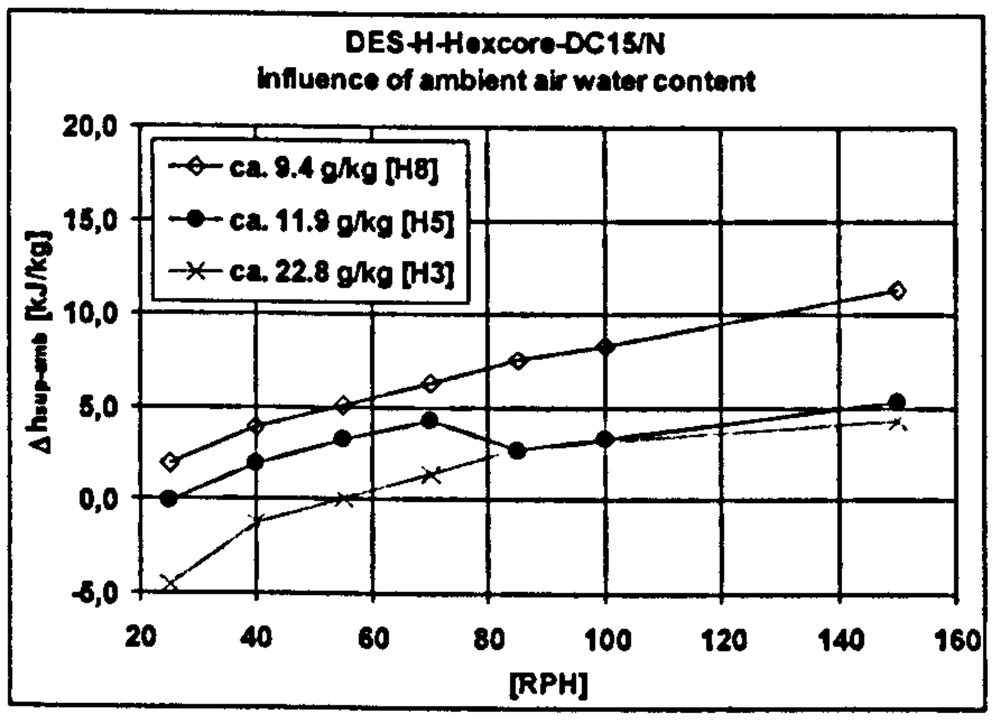

Fig. 5.28: *Enthalpy change, measurement series H8 / H5 / H3*

The curves of the RSHI (Fig. 5.27) show the expected behaviour. The RSHI falls as the water content of the ambient air rises. The enthalpy change curves (Fig. 5.28) show the expected behaviour of a rising enthalpy change with the rotation velocity. The kink in curve H5 is caused by an inadequacy in the

volume flow control and the very different levels at low rotation velocities point again to measurement errors.

5.3.7 COMPARISON OF THE HEXCORE AND KLINGENBURG WHEEL

Desiccant wheel: **Engelhard HexCore, LP / DES-H-Hexcore-DC15/N**

No:	process airflow (set values)			reg. airflow (set values)			Volume flow ratio
	θ [°C]	φ [%]	V [m³/h]	θ [°C]	φ [%]	V [m³/h]	$V_{reg}/V_{process}$ [-]
H4	32	40	2000	60	-	1500	0.75
H5	32	40	2000	75	-	1500	0.75

Desiccant wheel: **Klingenburg, SECO 1000**

K1	32	40	2000	60	-	1500	0.75

Tab. 5.6: *Boundary and operation conditions of the measurement series used for comparison of the Hexcore and Klingenburg wheel*

The comparison between the silica gel wheel from Engelhard HexCore LP (Type: DES-H-Hexcore-DC15/N) and the lithium chloride wheel from Klingenburg (Type: SECO 1000) was performed once under almost identical conditions and once under design conditions with the recommended operation parameters as specified by the manufacturers.

The first comparison was carried out under the following conditions for both wheels: 32°C / 40% for the ambient air, 60°C / 3.3% [K1] and 5.4% [H4] for the regeneration air, a process air volume flow of 2000 m³/h and a volume flow ratio between the process air and the regeneration air of 0.75.

Fig. 5.29 shows the comparison of the dehumidification capacities. Again the different behaviour along with rising rotation velocities is evident. Whereas the Klingenburg wheel reaches its maximum dehumidification capacity between 20 and 30 RPH, the Hexcore wheel does the same at about 100 RPH. The absolute maximum values however do not deviate much. Considering that the water content of the regeneration air was slightly lower with the Klingenburg measurements than it was with the Hexcore measurements, the difference under absolute similar conditions would probably be even smaller.

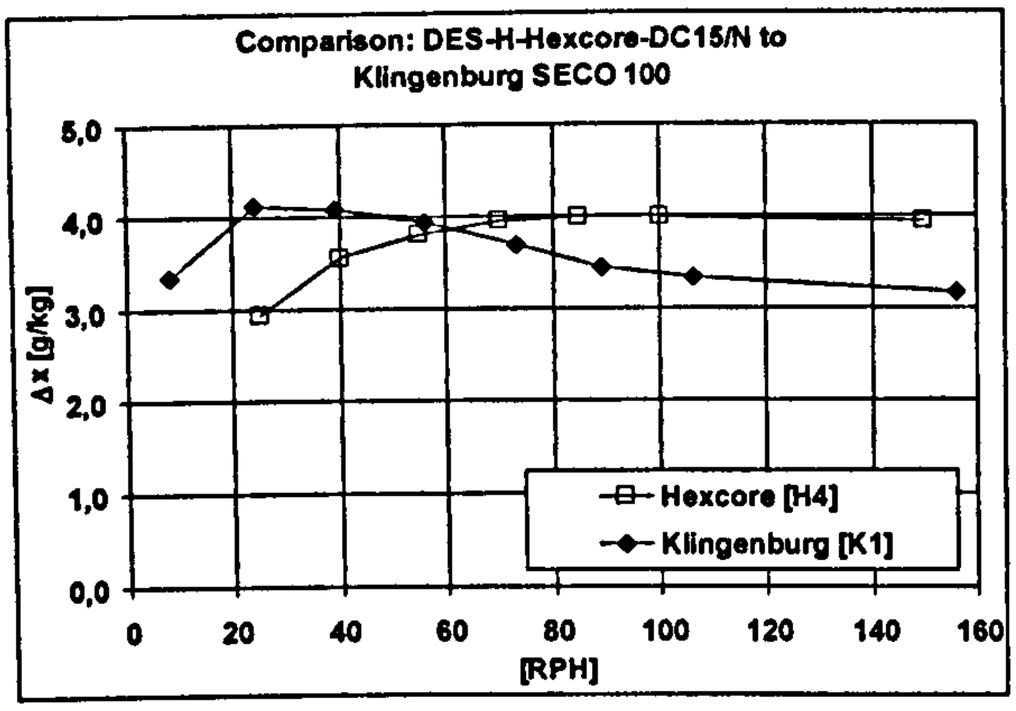

Fig. 5.29: *Comparison of the dehumidification capacity, measurement series K1 / H4*

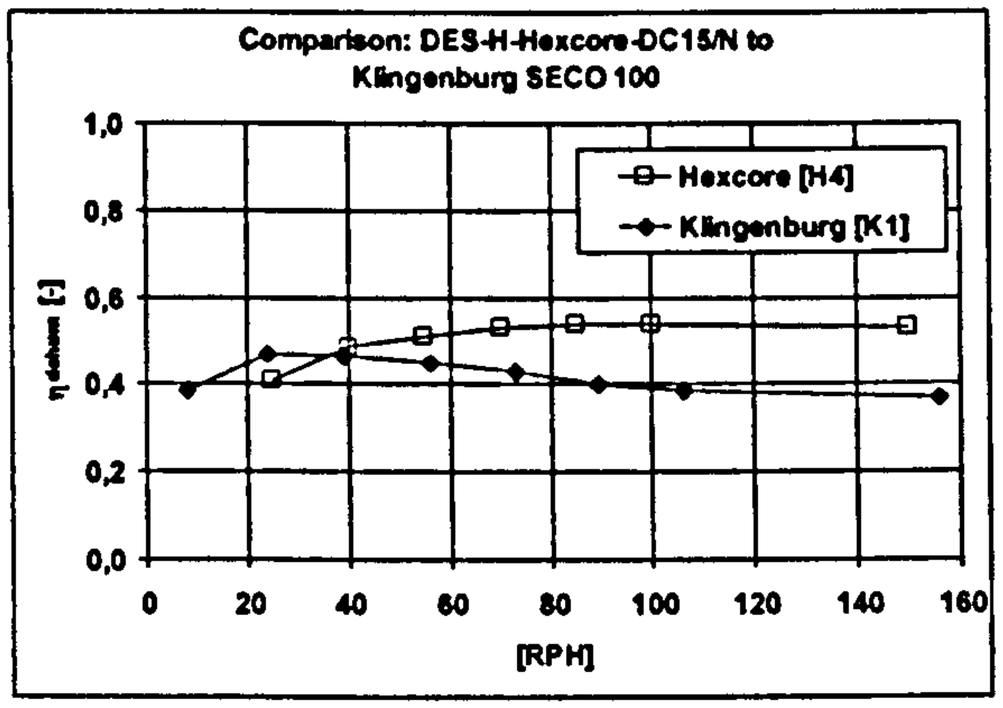

Fig. 5.30: *Comparison of the dehumidification efficiency, measurement series K1 / H4*

Fig. 5.30 shows the comparison of the dehumidification efficiency. As for the dehumidification capacity, the maximum values of the dehumidification efficiency were reached at different rotation velocities. The maximum values of the Hexcore wheel are a little bit higher than the maximum values of the Klingenburg wheel. This vice versa relationship between the maximum dehumidification capacity and the maximum dehumidification efficiency can only be explained by the slightly different water contents of the regeneration air within the measurement series.

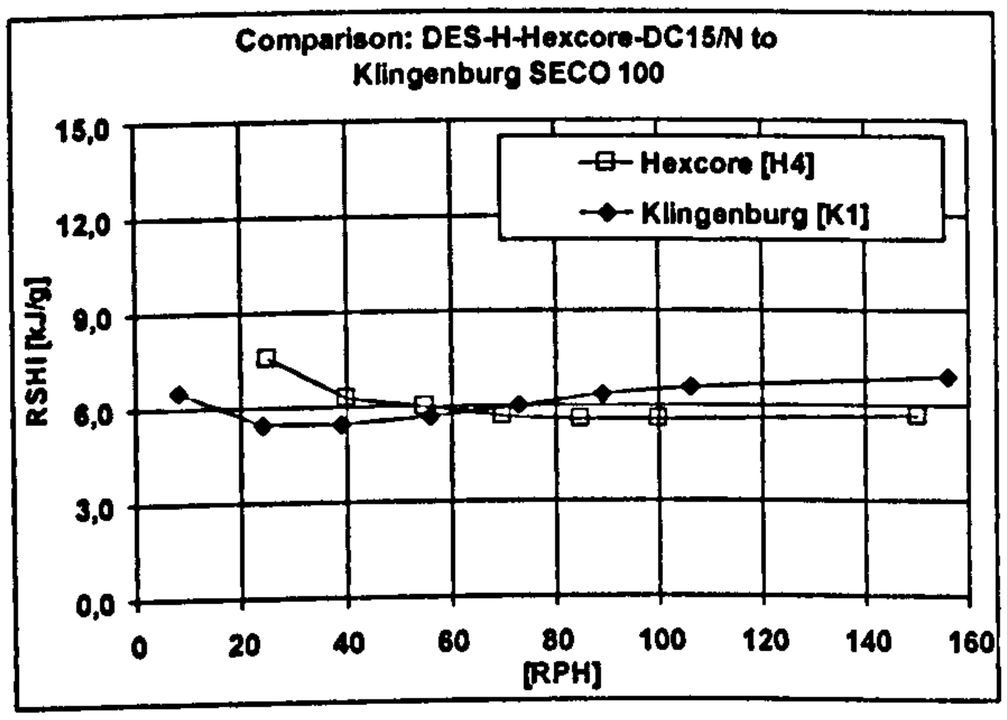

Fig. 5.31: *Comparison of the RSHI, measurement series K1 / H4*

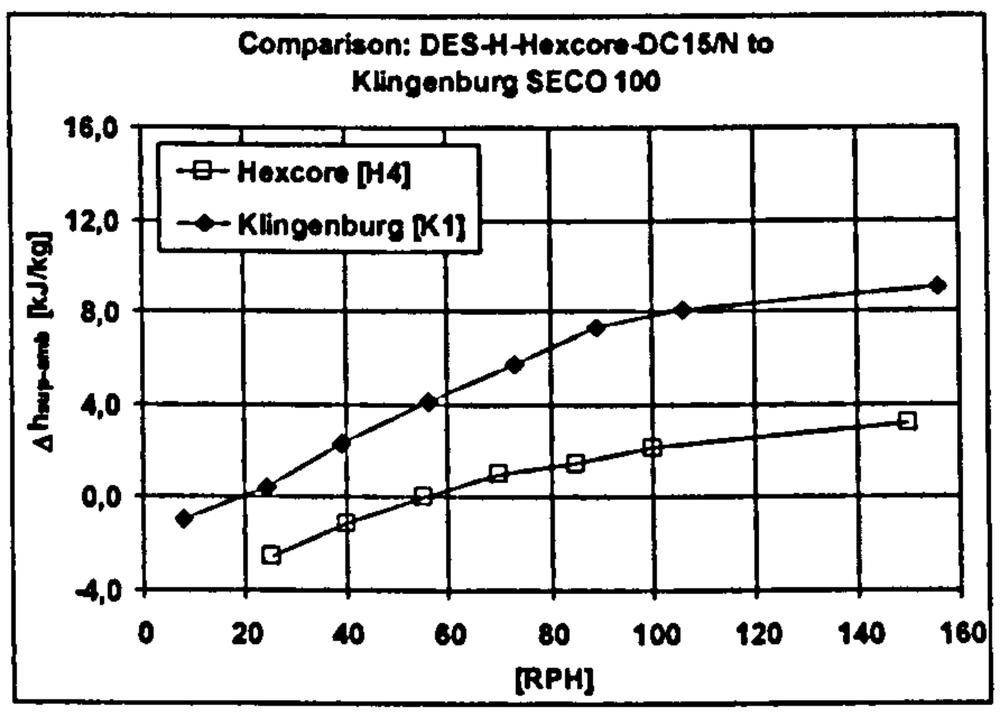

Fig. 5.32: *Comparison of enthalpy change, measurement series K1 / H4*

Due to the above mentioned, almost equal dehumidification capacities and the almost equal regeneration air conditions in this measurement series, the

minimum RSHI values (Fig. 5.31) must also be equal to one another, naturally at different rotation velocities. The enthalpy change curves (Fig. 5.32) show again the expected behaviour which is a rising enthalpy change along with rising rotation velocities. Again the different levels of the two curves must be caused by the mentioned deficiencies of the test plant. Considering only the gradients of the curves, the enthalpy rise with the Hexcore wheel is a little bit slower than that of the Klingenburg wheel. When examining the rotation velocity with the best dehumidification capacity however, the enthalpy rise seems to be more advantageous (smaller) with the Klingenburg wheel than it is with the Hexcore wheel.

The second comparison was done for design conditions with the operation parameters recommended by the manufactures, which were the same as in the first comparison for the Klingenburg wheel, but with a higher regeneration air temperature for the Hexcore wheel. Thus the conditions were: 32°C / 40% for the ambient air at a volume flow of 2000 m³/h and a volume flow ratio between the process and regeneration air of 0.75. The settings for the regeneration air were as follows: 60°C / 3.3 % [K1] for the Klingenburg wheel and 75°C / 3.0 % [H5] for the Hexcore wheel.

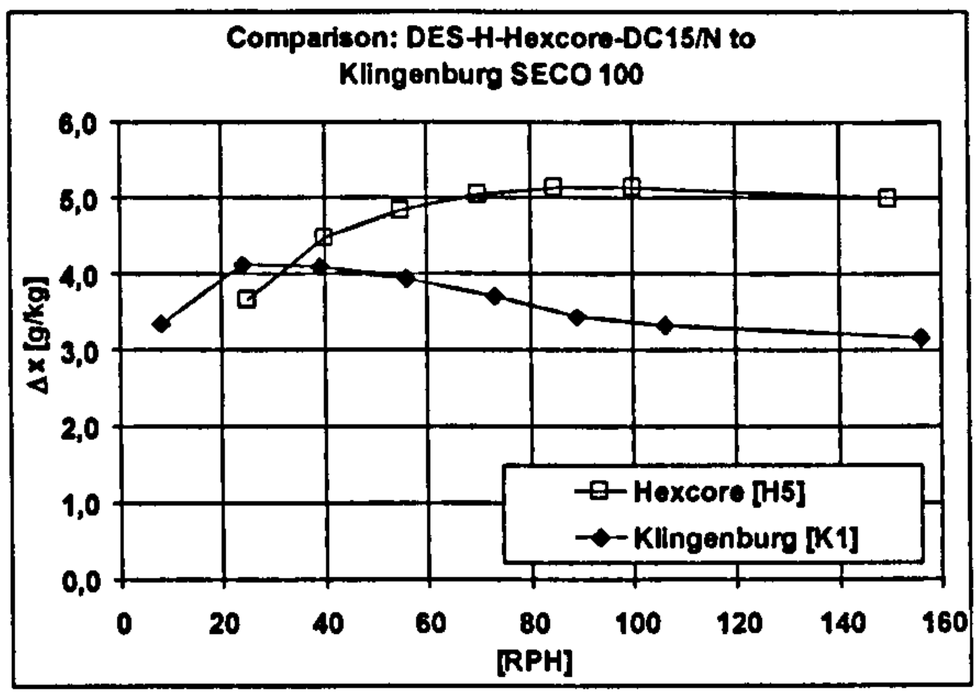

Fig. 5.33: Comparison of the dehumidification capacity, measurement series K1 / H5

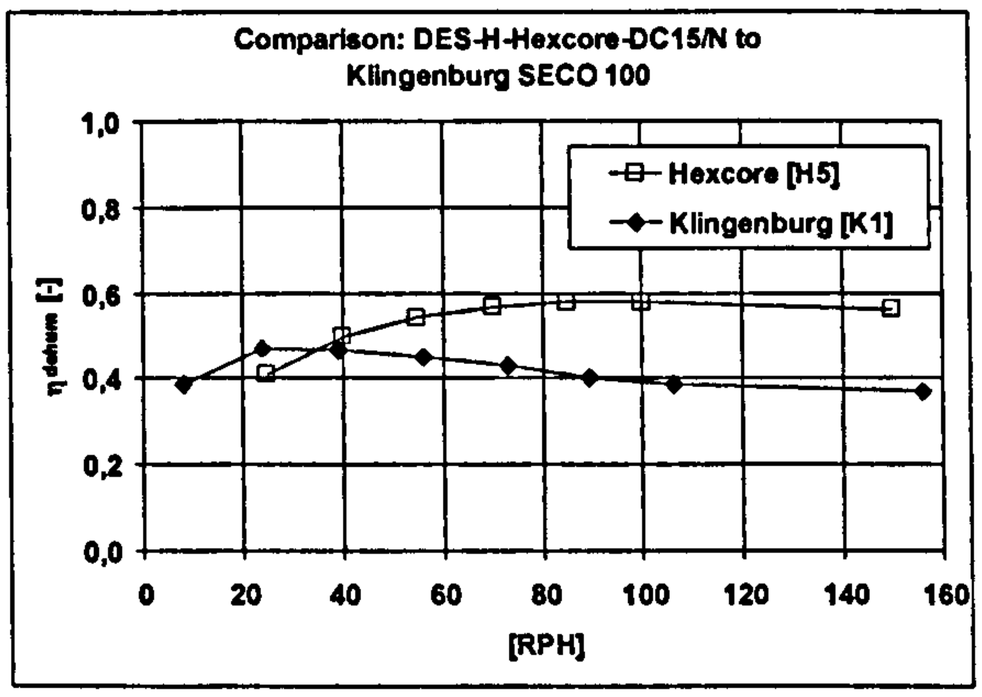

Fig. 5.34: Comparison of the dehumidification efficiency, measurement series K1 / H5

Fig. 5.33 shows again the comparison of the dehumidification capacity. This time the maximum value is clearly higher with the Hexcore wheel. The

behaviour along with rising rotation velocities is the same as it was before. The dehumidification efficiency (Fig. 5.34) is now also higher with the Hexcore wheel, but the rise is not very large (from 0.54 to 0.58). However, as a consequence of the higher regeneration air temperature, the RSHI (Fig. 5.35) of the Hexcore wheel also became higher than it was before, meaning that it worsened.

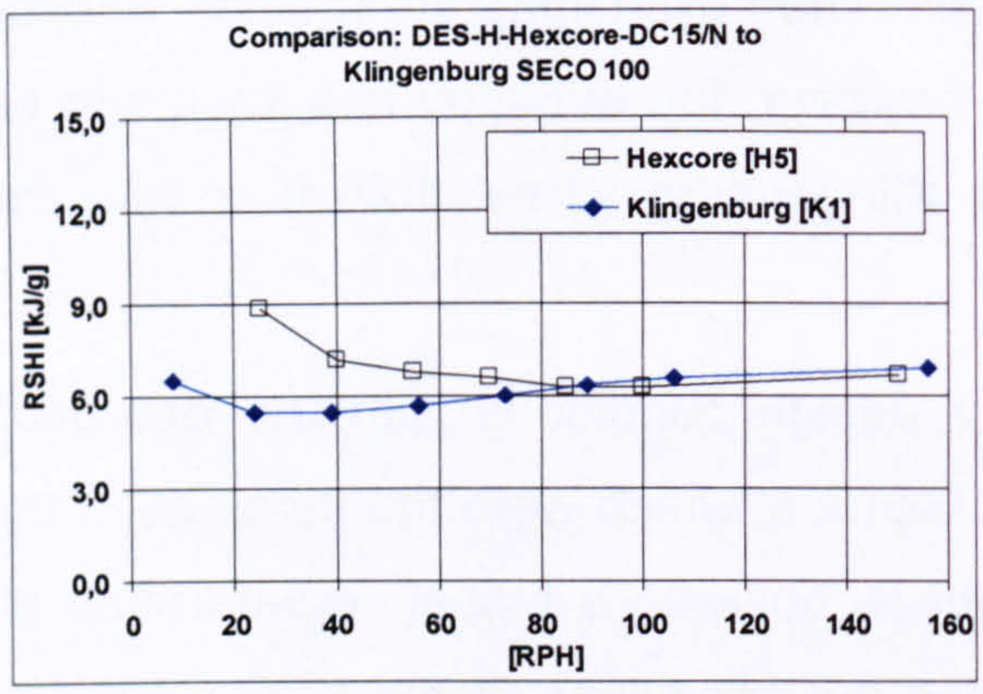

Fig. 5.35: *Comparison of the RSHI, measurement series K1 / H5*

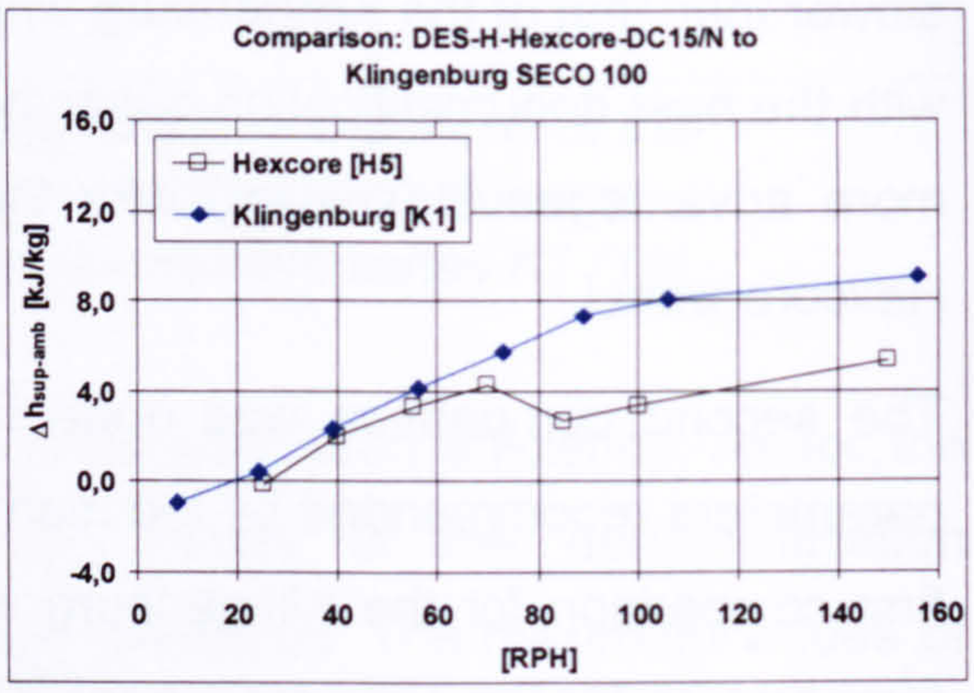

Fig. 5.36: *Comparison of enthalpy change, measurement series K1 / H5*

The enthalpy change curves (Fig. 5.36) show in principle the same thing as before. The kink on the curve H5 is caused by an inadequacy in the volume flow control. The levels of both curves are too low, but in relation to one another the gradients of the curves seem trustworthy and show once more a slower rise of the Hexcore curve as the rotation velocity increases. When considering the rotation velocity with the best dehumidification capacity, it can be seen that the enthalpy rise is more advantageous (smaller) with the Klingenburg wheel than with the Hexcore wheel.

5.4 CONSIDERATION OF BEST OPERATION PARAMETERS

5.4.1 ROTATION VELOCITY

In terms of the best rotation velocity, the results shown above indicate that there are different values for the two wheels. For the Hexcore wheel, the best performance was determined to take place at about 85 to 100 RPH for all of the

experiments, whereas for the Klingenburg wheel, the best performance for all of the experiments was measured at about 20 to 30 RPH. This fundamental difference is probably mainly caused by the different sorption and matrix materials that are used for the two wheels. It is notable, that the best rotation velocity almost does not vary as a result of the other operation parameters such as the volume flow ratio or the regeneration / ambient air conditions. Thus the best rotation velocity of the wheels can regarded as independent of the other parameters.

Naturally the rotation velocity could be used for the control of a DEC-system, e.g. if the maximum dehumidification capacity is not necessary, however in most cases it would be much more energy efficient to change other operation parameters such as the volume flow or the regeneration air temperature.

5.4.2 VOLUME FLOWS

The dehumidification process for the different volume flow ratios is shown in Fig. 5.37 in a Mollier diagram:

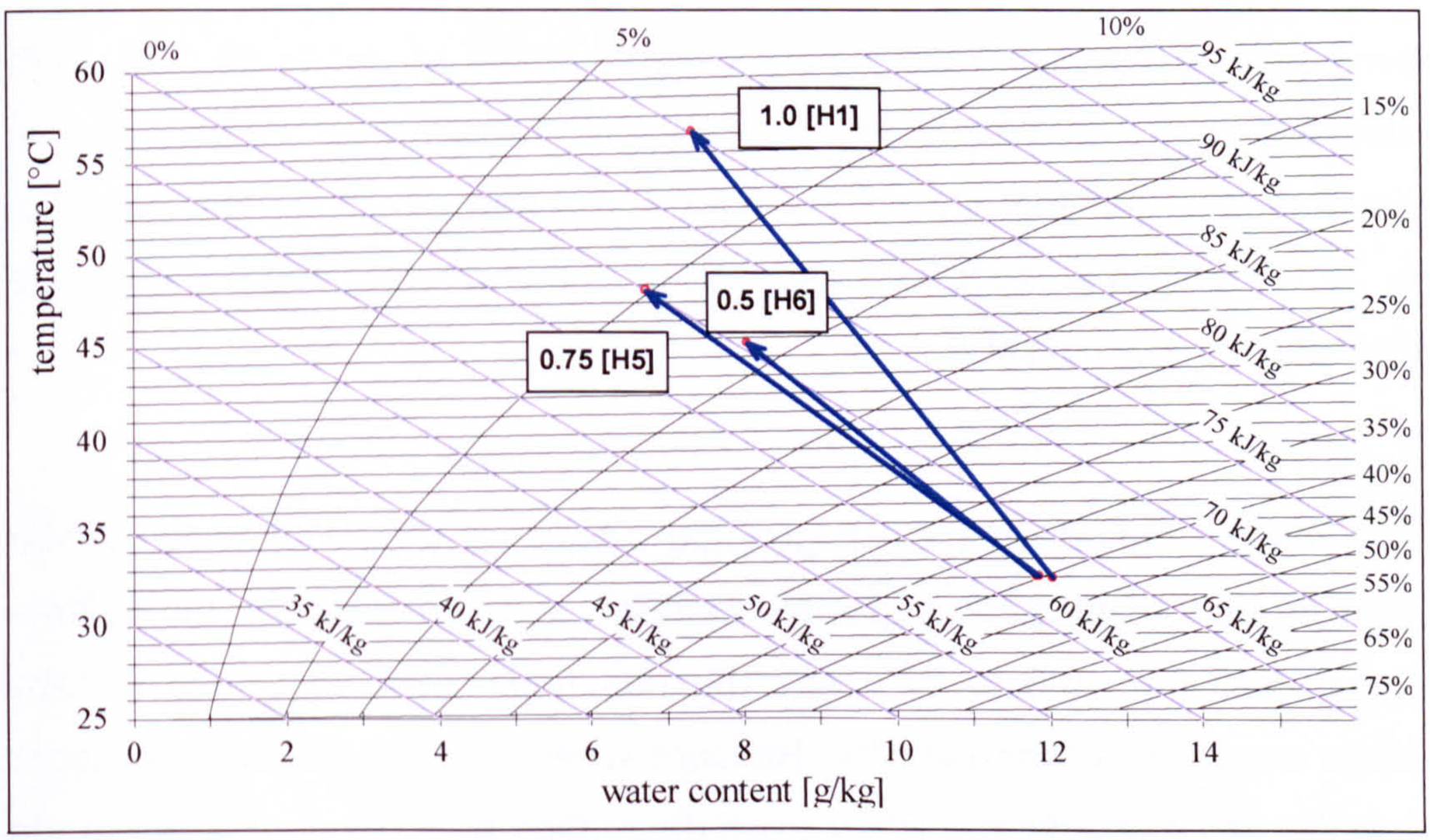

Fig. 5.37: *Hexcore: Dehumidification of process air dependent on volume flow ratio in a Mollier diagram [H1 / H5 / H6]. 85 RPH*

The studies of the influence of the volume flow ratio for the Hexcore wheel show a significant increase in the dehumidification capacity when the volume flow ratio is increased from 0.5 to 0.75 with a simultaneous higher dehumidification efficiency (at 85 RPH). Despite the greater energy demand of higher regeneration airflow, the RSHI increases only little. A further increase of the volume flow ratio to 1.0 does not lead to a further improvement of the dehumidification capacity; on the contrary the heat inhibition effect even decreases the dehumidification capacity. Subsequently, the RSHI is substantially higher with a volume flow ratio of 1.0.

A consideration of the dehumidification process as described in the Mollier diagram further shows that the curve for the dehumidification process has almost the same gradient up to a volume flow ratio of 0.75, whereas the dehumidification capacity increases from a volume flow ratio of 0.5 to 0.75. With a volume flow ratio over 0.75, the heat transfer then increases markedly and therefore the enthalpy of the supply air grows, which is usually not advantageous for the cooling function of DEC-systems, especially if there is no further improvement in dehumidification capacity.

Thus the best volume flow ratio for the Hexcore wheel seems to be 0.75. With less demand on the dehumidification capacity, the regeneration air volume flow can be reduced even further, which would save energy twofold; first, less fan power is needed and secondly because the energy required to heat the regeneration air is diminished.

The studies performed on the Klingenburg wheel (at 24 RPH) show similar results. The dehumidification capacity increases significantly when the volume flow ratio rises from 0.5 to 0.75 and the dehumidification efficiency thereby increases even more than with the Hexcore wheel. Due to the clearly higher dehumidification capacity, the RSHI even decreases as a result of a rise in the volume flow ratio. A further increase of the volume flow ratio to 1.0 does not

result in a further improvement of the dehumidification capacity, but the RSHI is clearly higher.

A look at the dehumidification process using a Mollier diagram (Fig. 5.38) shows, that with the Klingenburg wheel, the influence of the volume flow ratio on the change in enthalpy does not seem to be very significant. This can be explained by the low rotation velocity (no significant heat transfer because of a very low heat capacity flow by the rotating matrix) and probably by the low regeneration air temperatures (60 °C).

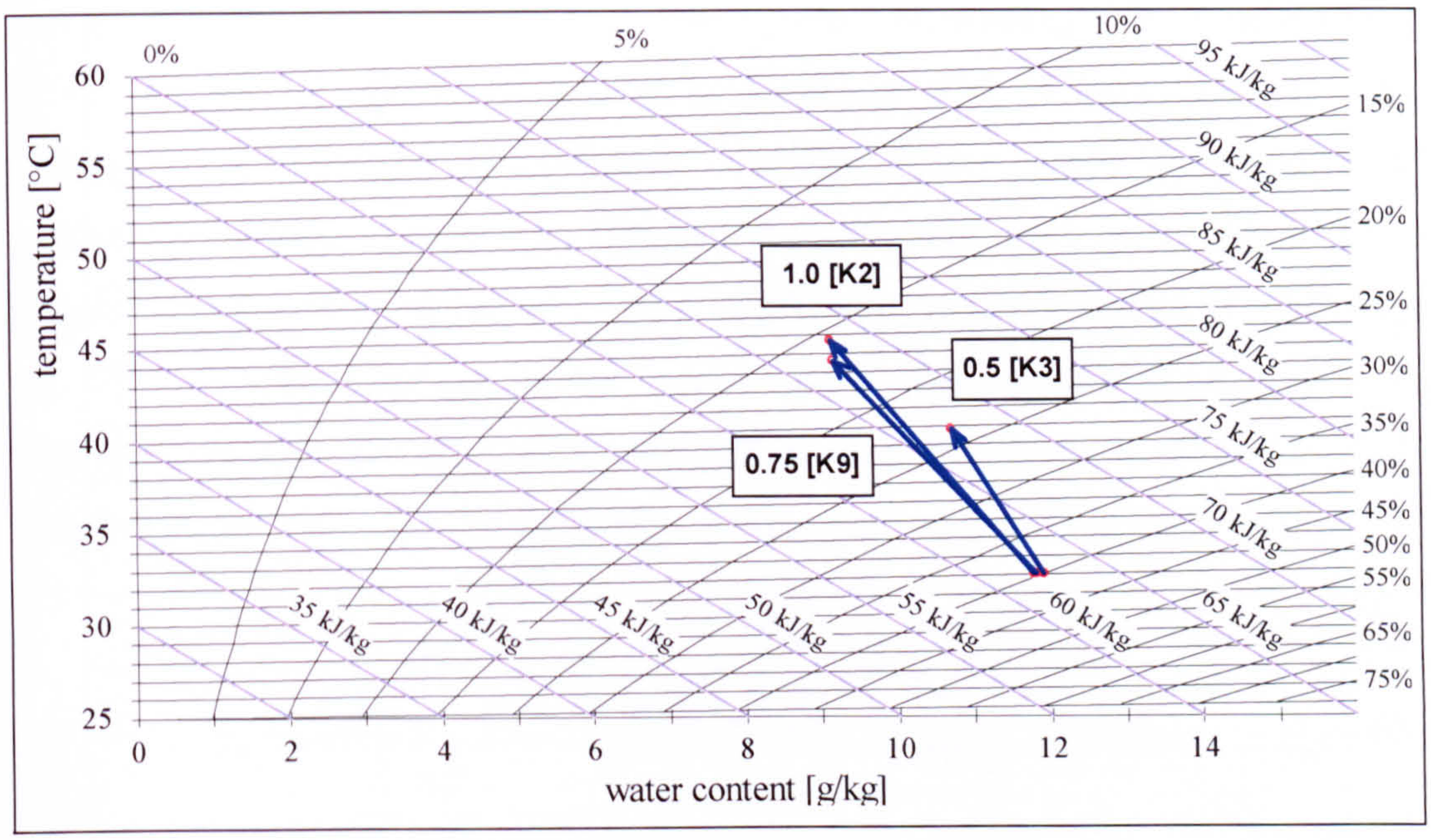

Fig. 5.38: *Klingenburg: Dehumidification of process air dependent on volume flow ratio in a Mollier diagram [K2 / K3 / K9]. 24 RPH*

For the Klingenburg wheel, the best volume flow ratio also seems to be 0.75 with the same possibility of energy saving with less demand on the dehumidification capacity by reducing the volume flow ratio.

5.4.3 REG. TEMPERATURE

For the Hexcore wheel, the measurements show that with rising regeneration air temperatures, the dehumidification capacity also clearly increases while at

the same time the dehumidification efficiency stays almost constant. As expected, the RSHI also increases slightly as the regeneration air temperature rises, but the absolute rise in dehumidification capacity is higher for the increase from 60°C to 75°C than from 75°C to 90°C.

These results seem to suggest that it is best to obtain the highest regeneration air temperatures possible. It should be considered however, that with higher regeneration air temperatures, the heat transfer and thereby the enthalpy of the supply air clearly rises.

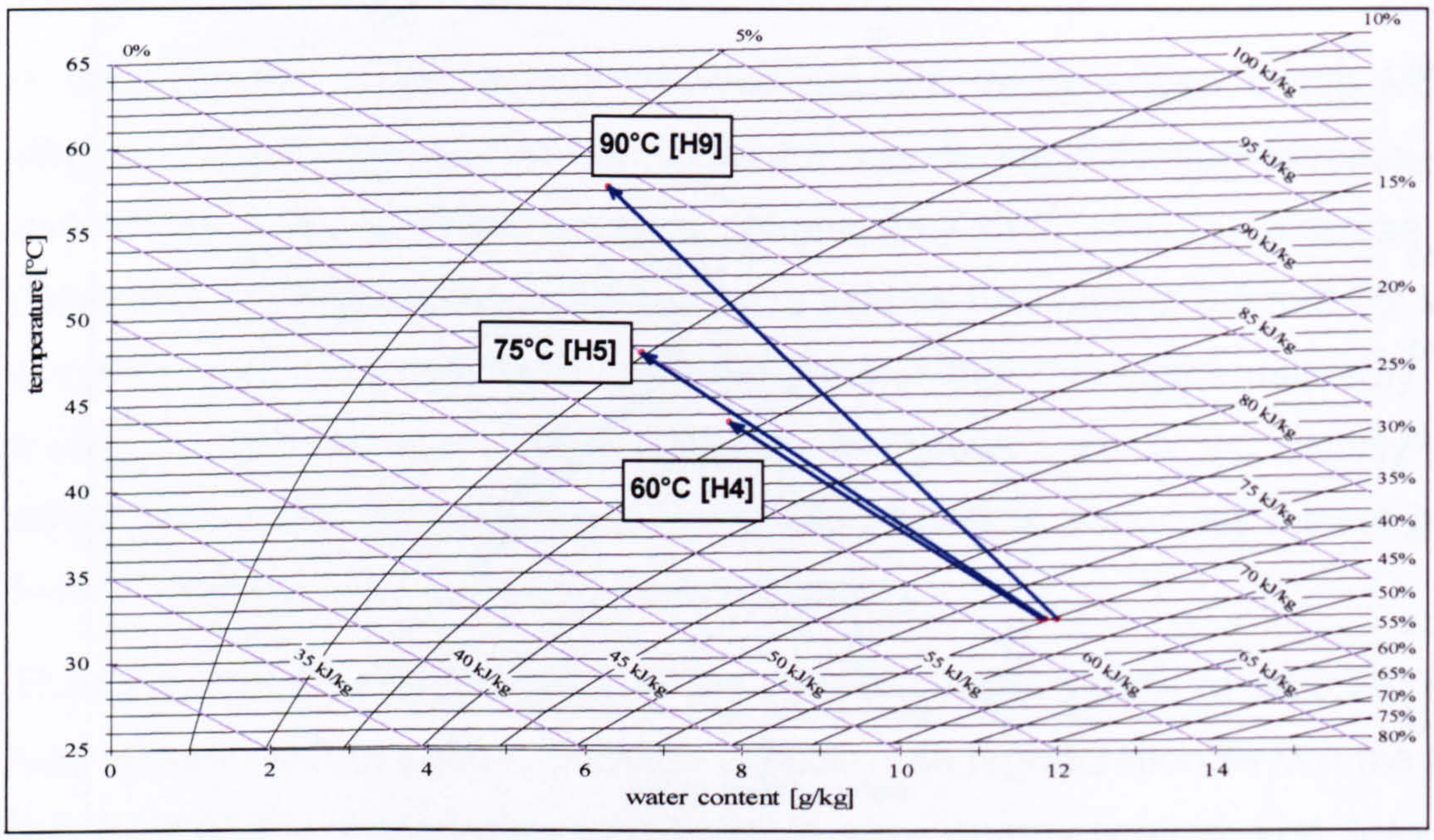

Fig. 5.39: *<u>Hexcore:</u> Dehumidification of process air dependent on regeneration air temp. in a Mollier diagram [H4 / H5 / H9]. 85 RPH*

Fig. 5.39 shows the dehumidification process at different regeneration air temperatures in a Mollier diagram. The increase of the regeneration air temperature from 60°C to 75°C causes a higher dehumidification without significantly increasing the enthalpy. An increase from 75°C to 90°C however, does not have much influence on the dehumidification capacity but it increases the enthalpy of the supply air. This rise of the enthalpy can only be explained by a rising part of heat transfer which is not something that is desirable for cooling operation. Thus the best regeneration air temperature seems to be about 75°C.

If the dehumidification process has main priority (before cooling process), it is possible to increase the dehumidification capacity by increasing the regeneration air temperature, but then a higher enthalpy of the supply air must be accepted. In order to reach very low supply air dew point temperatures, the regeneration air temperature can be increased up to 120°C (manufacturer data).

The outcomes for the Klingenburg wheel show, that the dehumidification capacity clearly rises when the regeneration air temperature is increased from 45°C to 60°C (at 24 RPH), but that further increasing this temperature from 60°C to 70 °C does not serve to increase the dehumidification capacity. However, it must be considered, that the experiments were done with a constant relative humidity of the regeneration air, and as a result the water content was clearly higher at a regeneration air temperature of 70°C than it was at 60°C. With constant water contents in the regeneration air, a higher dehumidification capacity and also higher dehumidification efficiency could be expected, as was observed by the experiments with the Hexcore wheel.

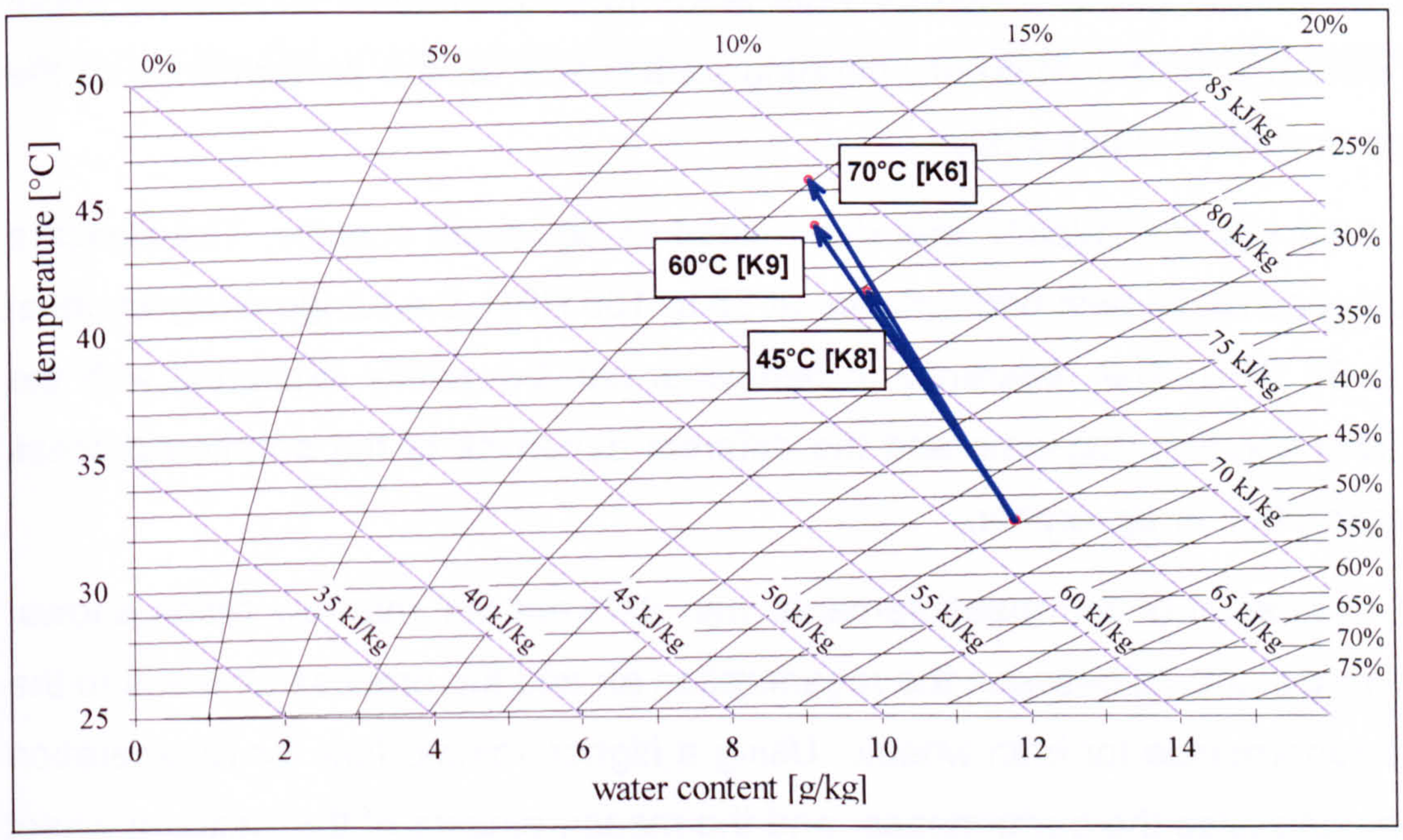

Fig. 5.40: *Klingenburg: Dehumidification of process air dependent on regeneration air temp. in a Mollier diagram [K6 / K8 / K9]. 24 RPH*

Fig. 5.40 shows the dehumidification process at different regeneration air temperatures for the Klingenburg wheel. The increase in the regeneration air temperature from 45°C to 60°C causes a higher dehumidification capacity without significantly increasing the enthalpy. A further rise however from 60°C to 70°C does not lead to an improvement in dehumidification but also does not increase the enthalpy of the process air as was observed with the Hexcore wheel.

The best regeneration air temperature for the Klingenburg wheel seems to be 60°C, however with a constant water content in the regeneration air (and not a constant relative humidity) a further improvement of the dehumidification capacity could be expected up to 70°C. Higher temperatures may not be used as this could damage the wheel. Therefore, the best regeneration temperature will lie between 60°C and 70°C for the Klingenburg wheel.

5.5 CONCLUSIONS

The evaluation of the measurements leads to new, detailed knowledge about the influence of the different operating parameters on the performance of the sorption wheels in this study.

The best rotation velocity was determined to be wheel specific. The Hexcore wheel reaches its best performance at 85 to 100 RPH, the Klingenburg wheel at 20 to 30 RPH. This difference in behaviour can be mainly explained with the different sorption materials and the different dynamics of the sorption process by adsorption or absorption.

The evaluation of the measurements with different volume flow ratios shows, that a ratio of 0.75 between the regeneration air and the process air leads to the best performance for both wheels. Using a higher volume flow for regeneration cannot increase the performance, and the measurements of the Hexcore wheel even show a decrease in the performance with a higher volume flow ratio, which can be explained by the so-called "heat inhibition effect". For the most

part lower volume flow ratios resulted in lower performance, whereby the performance of the Klingenburg wheel decreased more than the performance of the Hexcore wheel.

Additionally, the experiments showed that a higher regeneration air temperature leads principally to higher dehumidification potentials at almost equal dehumidification efficiencies. The energy efficiency (RSHI) worsened slightly as the regeneration temperatures rose. It is however to be considered, that along with the regeneration air temperature, the enthalpy of the process air also rises due to the heat transferred by the matrix material.

The influence of the regeneration air humidity was also notable. The reduction of the relative humidity within one series of experiments from 20% to 6% caused a rise of almost 100% in the dehumidification capacity. Due to this, the regeneration air should be also as dry as possible in order to achieve good performance.

Finally, the measurements show as a further matter of principle, that rising water content in the ambient air causes the dehumidification capacity to rise, whereby the dehumidification efficiency falls as a result of rising water content.

05 Experimental Investigations On A Test Plant

CHAPTER 06

VERIFICATION OF DESICCANT WHEEL MODEL WITH MEASURED DATA

6.1 INTRODUCTION

In this chapter the simulation model for desiccant wheels that was described in Chapter 04 is verified using measured data from the test plant for the Hexcore wheel (DES-Hexcore-DC15/N). For the application of the calculation model, the necessary input data was determined using the product data given by the manufacturer, as far as this was possible. Missing data was determined as accurately as possible by estimation. Next a comprehensive parameter variation was carried out in order to determine the influence of the single parameters and to investigate the influence of single physical properties on the results (such as heat transmission coefficients, heat capacity of the wheel etc.). Additionally, the best values for the grid (number of segments) were determined by looking for sufficient accuracy and the quickest calculation, which led to the implementation of a termination criterion for when steady state conditions are reached.

6.2 APPLICATION OF THE SIMULATION MODEL ON THE DES-HEXCORE-DC15/N

6.2.1 MATERIAL PROPERTIES OF THE DESICCANT WHEEL

In order to use the simulation model for a commercial desiccant wheel, the basic material properties and the basic geometries of the wheel must be known. Most of the data is usually given by the manufacturer. The few properties not given can normally be found in literature. The properties of the fluids (in this

case, air) are well known and can be calculated using the equations shown in Chapter 03.

In Tab. 6.1, the material properties for the desiccant wheel that must be known are listed. The data not given by the manufacturer is in *italic* letters.

material property	**symbol**	**value [unit] / equation**
mass of rotating matrix material	m_{matrix}	7.9 [kg]
specific heat capacity of the matrix material	$c_{p,matrix}$	1440 [J/kgK]
mass of adsorption material (silica gel)	m_{silica}	6.9 [kg]
specific heat capacity of the adsorption material (silica gel)	$c_{p,silica}$	*960 [J/kgK]* (1)
sorption isotherm of silica gel	$X_{silica}(\theta,\varphi)$	*(Eq. 3.17)*
binding enthalpy of water on silica gel	h_b	*(Eq. 3.22 /3.23)*

(1) KAST, 1988

Tab. 6.1: *Material properties of the DES-H-Hexcore-DC15/N*

6.2.2 GEOMETRY OF THE DESICCANT WHEEL

In Tab. 6.2, the geometry data that must be known is listed. Most of the values are given by the manufacturer. The data not given by the manufacturer again is in *italic* letters.

wheel geometry	**symbol**	**value [unit]**
internal heat and mass transferring surface of the matrix	A_{tot}	2300 [m²/m³] => *191 [m²]*(1)
free cross sectional area of the matrix (dependent on thickness of the material used for honeycomb structure)	A_{free}	0.497 [m²]
average diameter of a single tube/channel in the matrix	d_{tube}	*1.1 [mm]*(2)
depth of desiccant wheel	l_{wheel}	140 [mm]
effective diameter of the desiccant wheel	$d_{eff,wheel}$	870 [mm]

(1) calculated from given values
(2) measured on wheel

Tab. 6.2: *Geometry data of the DES-H-Hexcore-DC15/N*

6.2.3 PHYSICAL PROPERTIES OF HUMID AIR

The physical properties that must be known from the air flows can be calculated using the equations listed in Chapter 3 (see Tab. 6.3).

physical properties of humid air	symbol	equations
specific heat capacity of dry air	$c_{p,air}$	(Eq. 3.17)
specific heat capacity of steam	$c_{p,steam}$	(Eq. 3.18)
specific heat capacity of water	$c_{p,water}$	(Eq. 3.19)
evaporation enthalpy of water	h_e	(Eq. 3.11)

Tab. 6.3: *Physical properties of humid air*

6.2.4 OPERATION PARAMETERS

In addition to the physical properties of the materials, the operation parameters must be defined for the calculation(Tab. 6.4).

operation parameters	symbols
mass flow, temperature and humidity of process and regeneration air	$\dot{m}_{tot,air}, \theta_{air}, \varphi \; or \; x$
rotation velocity	RPH
ratio of cross-sectional area for regeneration air flow to process air flow	$A_{reg.} / A_{process}$

Tab. 6.4: *Operation parameters*

6.2.5 GRID / NUMBER OF SEGMENTS

The grid (or more specifically, the number of single segments that are to be calculated) must be determined. This is dependent on the size of the desiccant wheel.

Grid	symbols
Number of segments in direction of airflow (see Fig. 4.4)	N_{air}
Number of segments in direction of the rotating matrix (see. Fig 4.4)	N_{wheel}

Tab. 6.5: *Symbols to describe the grid*

The number of segments influences the speed of the calculation process significantly, therefore a grid should be chosen that is as wide as possible, but narrow enough to insure sufficient calculation accuracy. A study of the best grid size is described later in this chapter.

6.2.6 HEAT AND MASS TRANSMISSION

The heat and mass transmission coefficients are determined by Nusselt-/Sherwood-correlations (see Eq. 3.30 to 3.31), where the mass transmission coefficient is obtained through a similarity consideration of the heat transmission coefficient (Eq. 3.37). The driving force for the mass (water) transmission is the difference in partial vapour pressure between the surface of the adsorption material and the air. The calculation of the partial vapour pressure of the air can be done using Eq. 3.5, 3.6 and 3.14. The relative humidity over the adsorption material must be determined iteratively with the equations Eq. 3.20 and 3.23. The partial vapour pressure can then be calculated using Eq. 3.5.

6.2.7 DERIVED VALUES FOR THE CALCULATION OF ONE SEGMENT

In order to use the calculation model, the given properties and parameters must be adapted to the calculation of one single segment. The calculation procedure of this adaptation is shown in Tab. 6.6 (for the values for which it is required).

derived values	calculation
mass flow of air through one segment	$\dot{m}_{air} = \frac{\dot{m}_{tot,air}}{N_{wheel}}$
mass flow of matrix material through one segment	$\dot{m}_{matrix} = \frac{m_{matrix} \cdot RPH}{N_{air}}$
mass flow of silica gel through one segment	$\dot{m}_{silica} = \frac{m_{silica} \cdot RPH}{N_{air}}$
heat transferring area of one segment	$A = \frac{A_{tot}}{N_{air} \cdot N_{wheel}}$

Tab. 6.6: *Calculation procedure for adaptation of the given values to single segments*

6.3 CALIBRATION OF MODEL WITH MEASURED DATA

6.3.1 FIRST OUTCOMES OF THE CALCULATION

For the calibration of the calculation model to the Hexcore wheel, the data from paragraph 6.2 was first used to recalculate the results of the measurements evaluated in Chapter 05. The grid for these first calculations was set to 100 segments in the direction of the air flow and to 200 segments in the direction of the mass flow for each phase, which means 100 x (200+200) = 4000 segments altogether.

The comparison of the results is shown below in which the three measurement series H5, H8 and H9 are used as examples (Fig. 6.1 to Fig. 6.3).

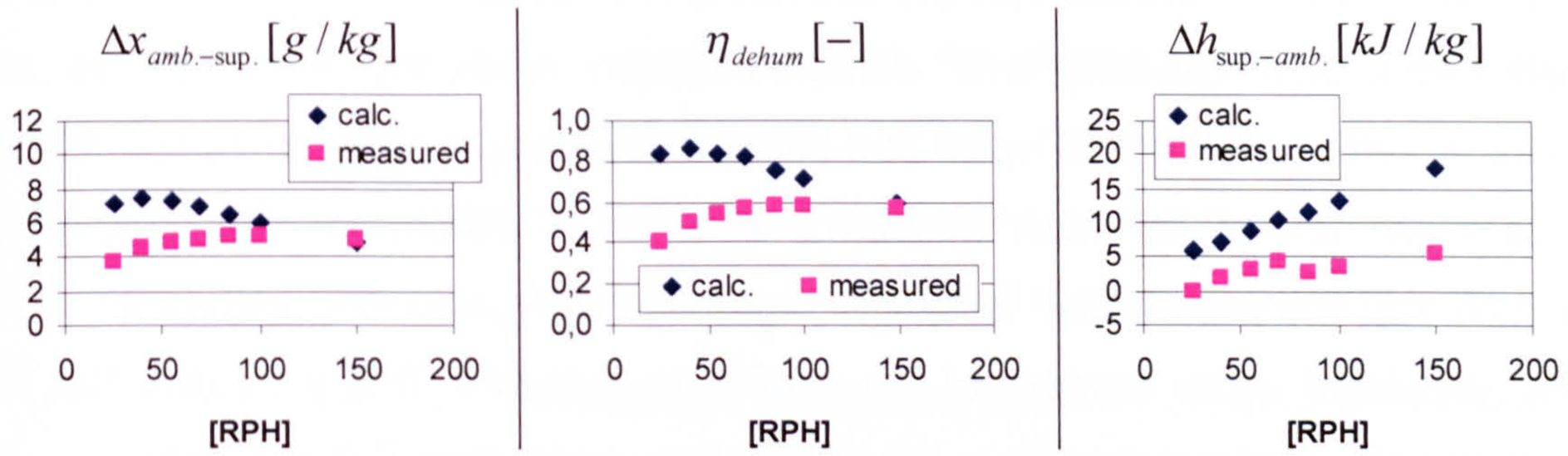

Fig. 6.1: *Comparison of calculation and measurement, dehumidification capacity / efficiency and change in enthalpy of process air (measurement series H5)*

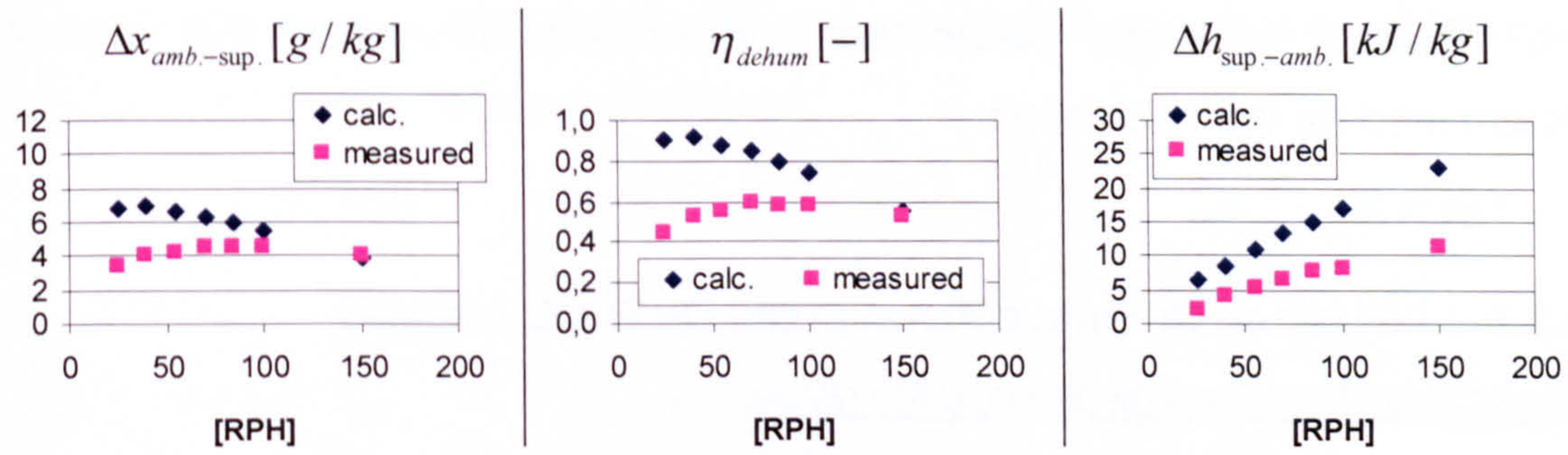

Fig. 6.2: *Comparison of calculation and measurement, dehumidification capacity / efficiency and change in enthalpy of process air (measurement series H8)*

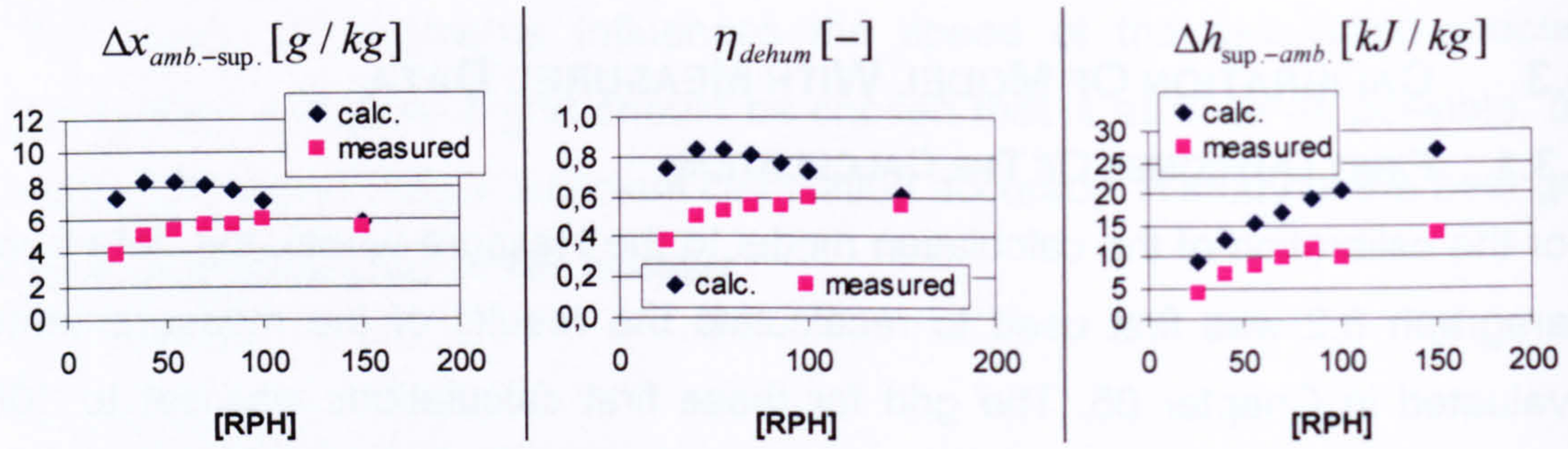

Fig. 6.3: *Comparison of calculation and measurement, dehumidification capacity / efficiency and change in enthalpy of process air (measurement series H9)*

When the calculated and the measured values are compared, it can be seen that in principle, both the absolute values and also the behaviour that is dependent on the rotation velocity are not similar at all. Whereas the measured dehumidification capacity and dehumidification efficiency both rise as the rotation velocity increases up to 100 RPH, a calculation of these values results in a maximum at as soon as about 40 RPH. Furthermore, the change in enthalpy of the process air is clearly higher for the calculated values although the calculated water content of the supply air is lower. This indicates that the heat transfer is clearly higher in the calculation model than it is in reality.

Altogether, the outcome of these calculations is unsatisfactory. In order to determine the reason for the deviations, the calculation model was examined for the influence of single parameters and physical properties that must be determined for the calculation.

6.3.2 INFLUENCE OF SINGLE PARAMETERS ON THE OUTCOMES

EFFECTIVE MASS OF ADSORPTION MATERIAL

The deviations between the measurements and the calculations must result from a significant difference between the calculation model and the real sorption wheel. In order to find these differences, numerous parameters and physical properties were varied for many simulations of all the measurement series of the Hexcore wheel listed in Appendix A. In varying the parameters and

properties, only a change of the "effective mass" of the adsorption material (here silica gel) led to a significant improvement in the dehumidification of both the absolute values and also the behaviour that is dependent on the rotation velocity. As the simulations were being performed, the question also arose as to whether or not the assumption is correct that, because of the very thin adsorption material layers, the decisive mass transport mechanism is the mass transmission resistance and not the internal transport mechanisms in the adsorption material (see paragraph 3.5.3). However, if this assumption were incorrect, the agreement between the calculation and measurement of the dehumidification capacity should be better at low rotation velocities and deviate more at higher ones, which was not observed to be the case. Thus it must be assumed that for the "real" desiccant wheel, the effective or operating mass of silica gel is much smaller than the mass given by the manufacturer. This could be caused for example, by the production process, in which some of the pores of the silica gel could be closed or inactivated by the adhesives used.

Any other change of the parameters and properties did not serve to improve the outcome of the dehumidification process in a significant manner. The following Fig. 6.4 to Fig. 6.6 show the results of the change of the silica gel mass from 6.9 kg (as given by the manufacturer) to 2.5 kg. It was determined that the best agreement between the measured and calculated values was obtained by reducing the mass of silica gel bit by bit.

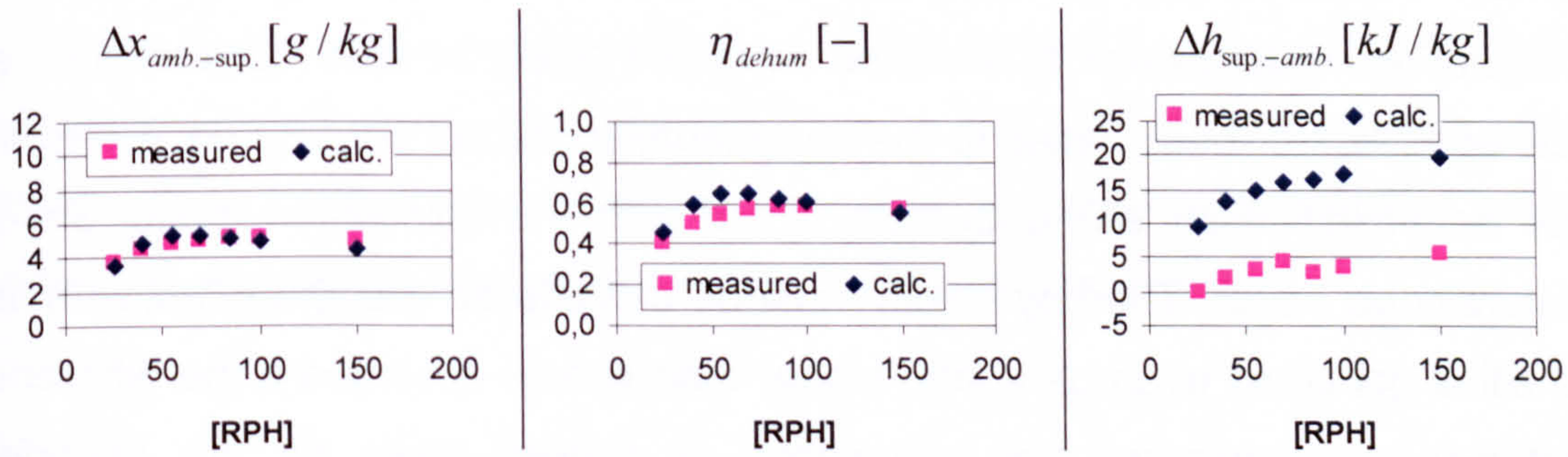

Fig. 6.4: *Comparison of calculation and measurement, dehumidification capacity / efficiency and change in enthalpy of process air (measurement series H5). Modification of model: mass of silica gel = 2.5 kg*

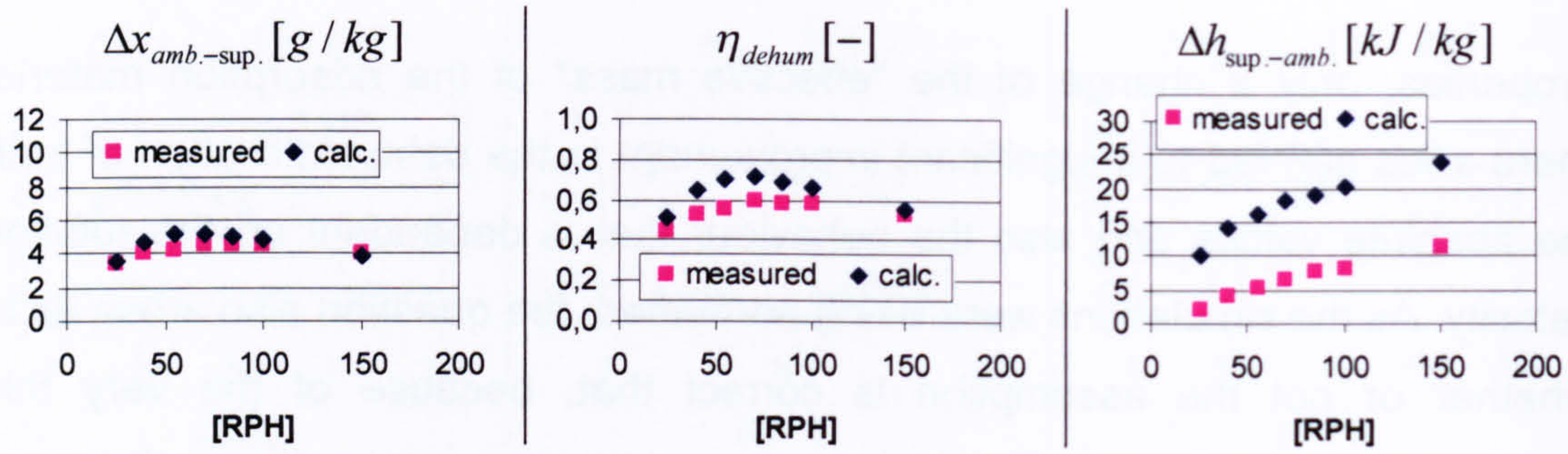

Fig. 6.5: *Comparison of calculation and measurement, dehumidification capacity / efficiency and change in enthalpy of process air (measurement series H8). Modification of model: mass of silica gel = 2.5 kg*

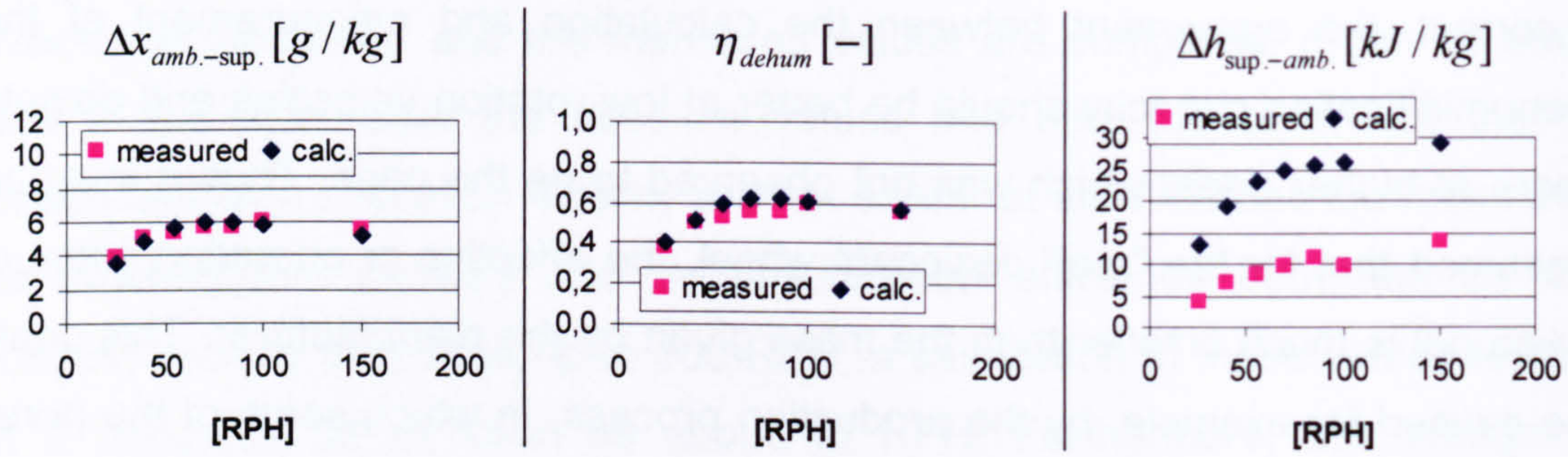

Fig. 6.6: *Comparison of calculation and measurement, dehumidification capacity / efficiency and change in enthalpy of process air (measurement series H9). Modification of model: mass of silica gel = 2.5 kg*

With this modification, the absolute measured and calculated values of the dehumidification capacity correspond quite well and also the dehumidification efficiencies correspond very well for the series H5 and H9. Only for the series H8 does the dehumidification efficiency not correspond as well as the other series. However, for the evaluation, it should not be forgotten that the calculation model describes an ideal desiccant wheel in which for example, air leakage rates or heat losses to the surroundings are not considered. Therefore the dehumidification efficiency determined with the calculation model should naturally be better. Thereby it also must be considered that the effective mass of silica gel could even be a little higher than is now assumed if the difference between measurement and calculation is caused more by the imperfect operation conditions of the real wheel (e.g. air leakage etc.).

Thus, in general, the agreement of the dehumidification capacity and efficiency must now be determined to be quite good. Only the agreement with the change of enthalpy of the process air is not satisfactory.

Therefore, with the "new effective mass" of silica gel (2.5 kg), all the parameters and physical properties that could have an influence on the heat transfer were varied again with the goal of examining especially the enthalpy change of the process air.

INTERNAL HEAT AND MASS TRANSFERRING SURFACE

First the heat and mass transferring surface was varied by about ± 20%. The results are shown in Fig. 6.7 using the measurement series H5 as an example.

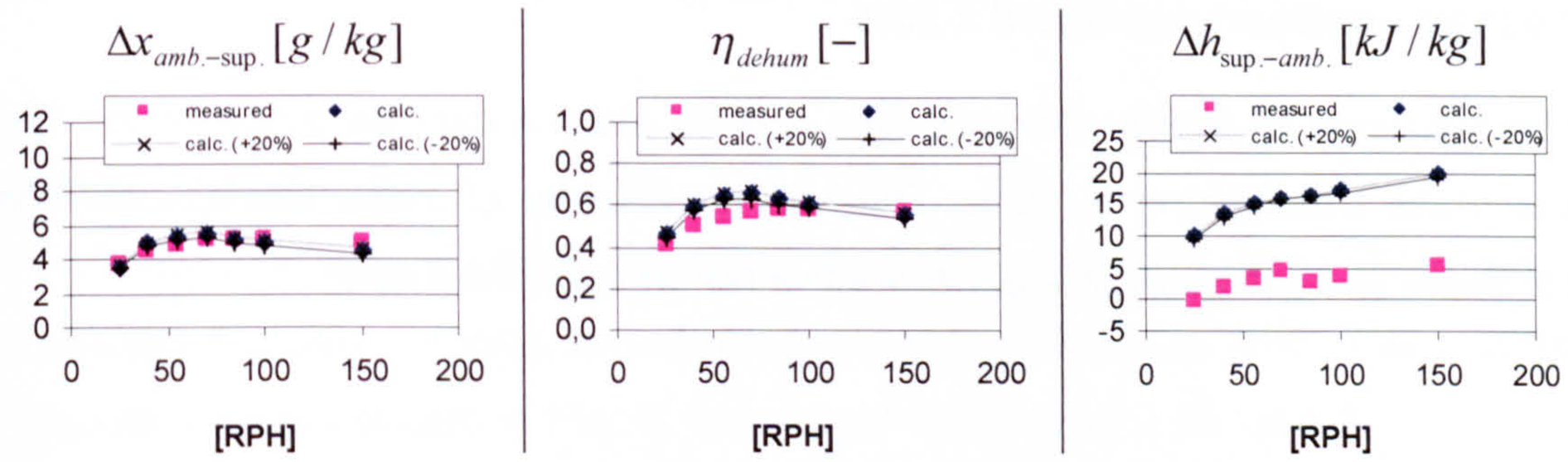

Fig. 6.7: *Comparison of calculation and measurement, dehumidification capacity / efficiency and change in enthalpy of process air (measurement series H5). Modification of model: 1. mass of silica gel = 2.5 kg / 2. heat and mass transferring surface ± 20%*

The results show only a minor influence of this variation on the dehumidification capacity and efficiency. Also, the influence on the change of enthalpy is almost nonexistent. Thus an uncertainty in the real heat and mass transferring surface does not seem to be responsible for the remaining deviations.

06 Verification Of Desiccant Wheel Model With Measured Data

Heat And Mass Transmission Coefficients

The next parameters investigated were the heat and mass transmission coefficients. These values were varied also by about ± 20%. The results are shown in Fig. 6.8 again using the measurement series H5 as an example.

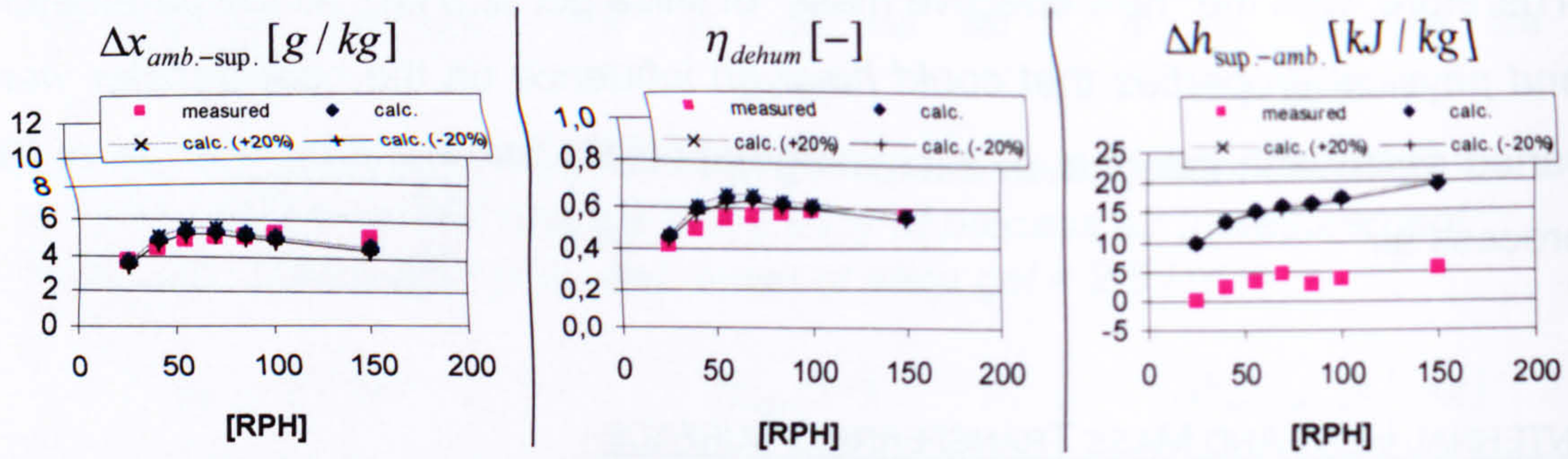

Fig. 6.8: *Comparison of calculation and measurement, dehumidification capacity / efficiency and change in enthalpy of process air (measurement series H5). Modification of model: 1. mass of silica gel = 2.5 kg / 2. heat and mass transmission coefficient ± 20%*

The influence of these changes was just as insignificant as those of the heat and mass transferring surface. Thus an uncertainty of these coefficients does not seem to be responsible either for the remaining deviations.

Specific Heat Capacities Of Materials

Another property that could influence the heat transfer between the air flows and the desiccant wheel is the specific heat capacity of the wheel (varied about ± 20 %). The results of the variation of this property are shown in Fig. 6.9 for the measurement series H5.

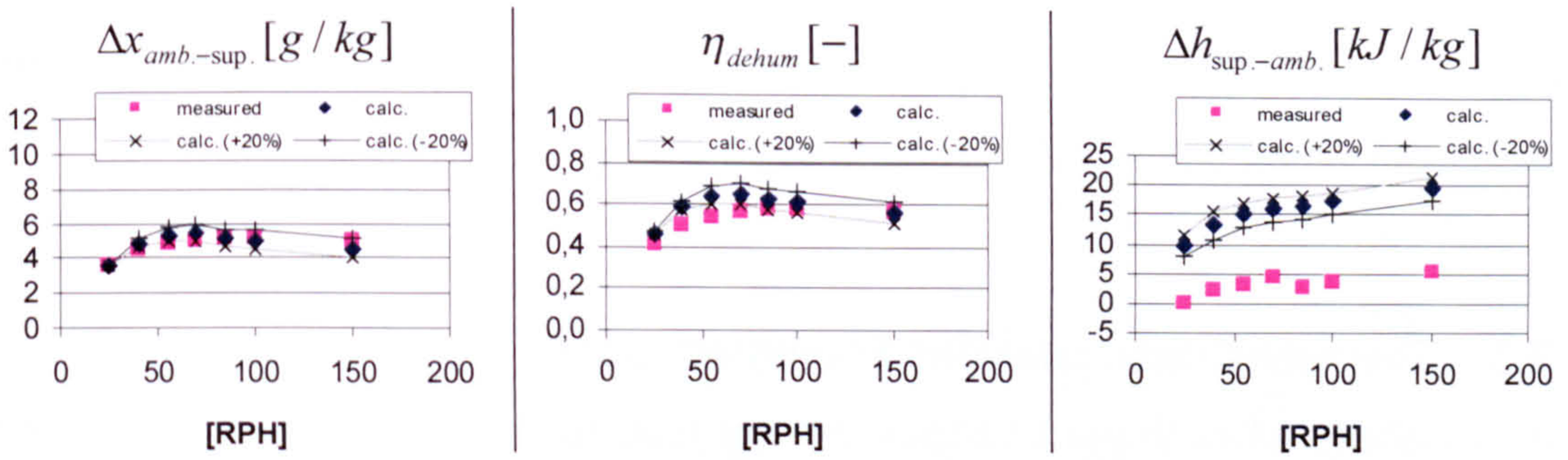

Fig. 6.9: *Comparison of calculation and measurement, dehumidification capacity / efficiency and change in enthalpy of process air (measurement series H5). Modification of model: 1. mass of silica gel = 2.5 kg / 2. specific heat capacity ± 20%*

The heat capacity influences the results a little bit more than the heat and mass transferring surface or the transmission coefficients, but this change is not sufficient enough to reduce the deviations to an acceptable level.

BINDING ENTHALPY

The last variation performed was an investigation of the influence of the binding enthalpy. For this purpose, the binding enthalpy was set to zero. The results of this variation are shown in Fig. 6.10 for the measurement series H5.

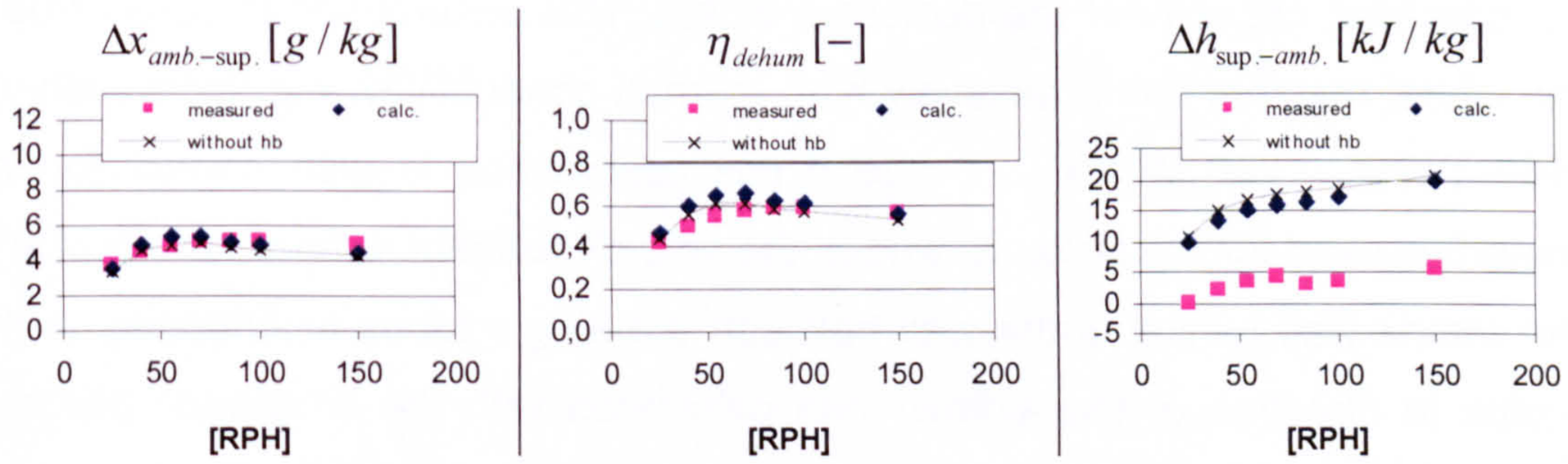

Fig. 6.10: *Comparison of calculation and measurement, dehumidification capacity / efficiency and change in enthalpy of process air (measurement series H5). Modification of model: 1. mass of silica gel = 2.5 kg / 2. without binding enthalpy*

When no binding enthalpy is considered, the dehumidification capacity only decreases slightly as does the efficiency. The effect of this variation on the change of enthalpy makes the results even worse.

6.3.3 FURTHER CONSIDERATIONS FOR IMPROVEMENT

On the whole all of these changes did not lead to sufficient results concerning the change in enthalpy of the process air. Therefore there must be a further difference between the real wheel and the assumptions made for the calculation model. Due to the fact that the dehumidification itself is already calculated sufficiently, the deviations are most probably rooted in the heat transfer process. Up to now, it has been supposed that the heat transfer between the air and the wheel is governed by the heat transmission coefficient as described e.g. by KAST, 1988. In addition, for the calculation model, it was assumed that the heat transferred from the air to the wheel results in a temperature profile in the wheel material with no significant temperature gradients. This assumption was made mainly because the layers of both the matrix material and the silica gel are very thin (altogether about 0.2 mm). The surface temperature of the wheel could then be calculated for the next step considering the complete specific heat capacity of the desiccant wheel. This assumption is surely true if the wheel material has a relatively high thermal conductivity, e.g. for aluminium (160 W/mK - 220 W/mK). To see if this assumption is also correct for the materials used for the Hexcore wheel, the time dependent temperature profile in the matrix wall (which is the wall between the single tubes or channels in the matrix in direction of the airflow) was calculated with the simulation program FEMLAB/COMSOL (finite-element based program for simulating multi-physics applications) for a temperature jump of the surrounding air from 30°C to 75°C. Such a temperature jump always happens if the matrix rotates from process airflow (30°C) into the regeneration airflow (75°C). For this calculation the heat transfer coefficient was set to 20 W/m²K, what is an usual value for the present geometry and airflow velocity (tube-diameter of 1 - 2 mm, airflow velocity 1 - 2

m/s). The physical properties of the matrix material, a kind of plastic called Hexcore Nomex™, silica gel and aluminium are listed in Tab. 6.7.

physical property	Nomex™	silica gel	Aluminium
thermal conductivity λ [W/mK]	0.12	0.025(*)	160 - 220
specific heat capacity c_p [J/kgK]	1440	960	900
density ρ [kg/m³]	600	650	2700

Tab. 6.7: *Physical properties of Hexcore Nomex™, silica gel and aluminium.*
(*) (WEBER, 2001)

Using the given data, the thickness of the matrix material can be estimated to be 0.1 mm as the thickness of the silica gel layer on each side must be about 0.05 mm. The real time corresponding to one calculation step in the desiccant wheel model can be about 0.1 s (see paragraph 6.3.4), thus the calculation with FEMLAB/COMSOL was done in time steps of 10 ms for a time period of 0.1 s.

The outcome of the FEMLAB/COMSOL calculation is shown in Fig. 6.11 for the desiccant wheel and also (for comparison) for aluminium.

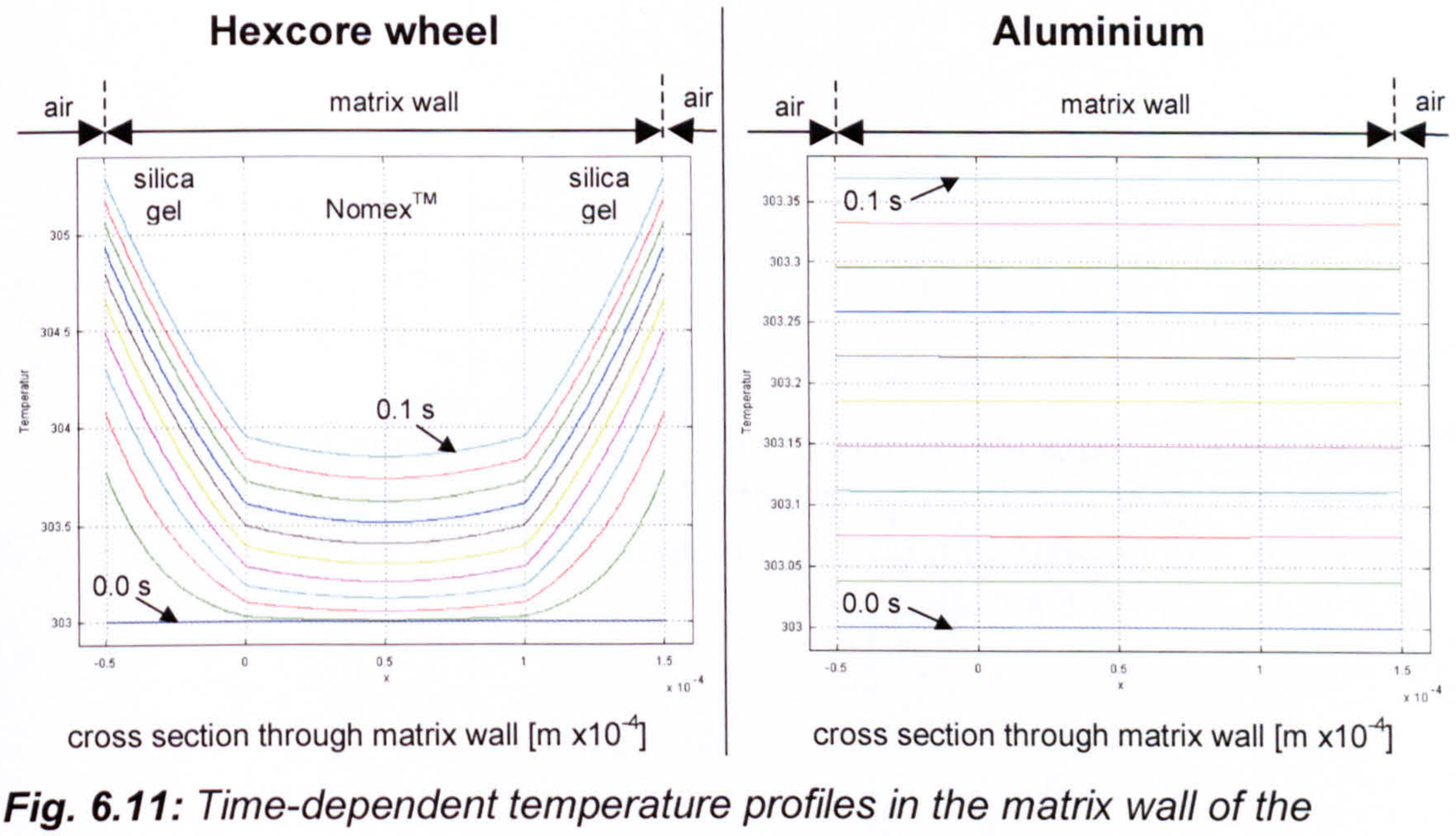

Fig. 6.11: *Time-dependent temperature profiles in the matrix wall of the Hexcore wheel and in aluminium. Boundary conditions: temperature jump from 30°C (303 K) to 75°C of the surrounding air, heat transfer coefficient 20 W/m²K, time step for the single profiles: 10 ms, plotted time 0 s - 0.1 s*

The results clearly show that the assumptions are adequate when aluminium is used as the matrix material but not for the Hexcore wheel. Despite the very thin layers, a steep temperature gradient occurs in the Hexcore wheel material during heat capture. This behaviour influences both the transferred energy from the air to the surface (due to the increasing surface temperature and therefore smaller temperature difference between surface and air) and also the useable thermal storage mass.

As this physical behaviour could not be used directly in the developed simulation model, it was approximated by a reduction of the heat transmission coefficient, which is calculated with the equation (Eq. 3.30) using the empirical Nusselt-correlations for tubes shown in Tab. 3.1., and the specific heat capacity of the wheel to "effective values". In Fig. 6.12 to Fig. 6.14, the results are shown for an effective heat transmission coefficient of 20% from the value determined with Eq. 3.30 ff. and an "effective specific heat capacity" of 50 % of the values given by the manufacturer. These effective values were determined to bring about the best results.

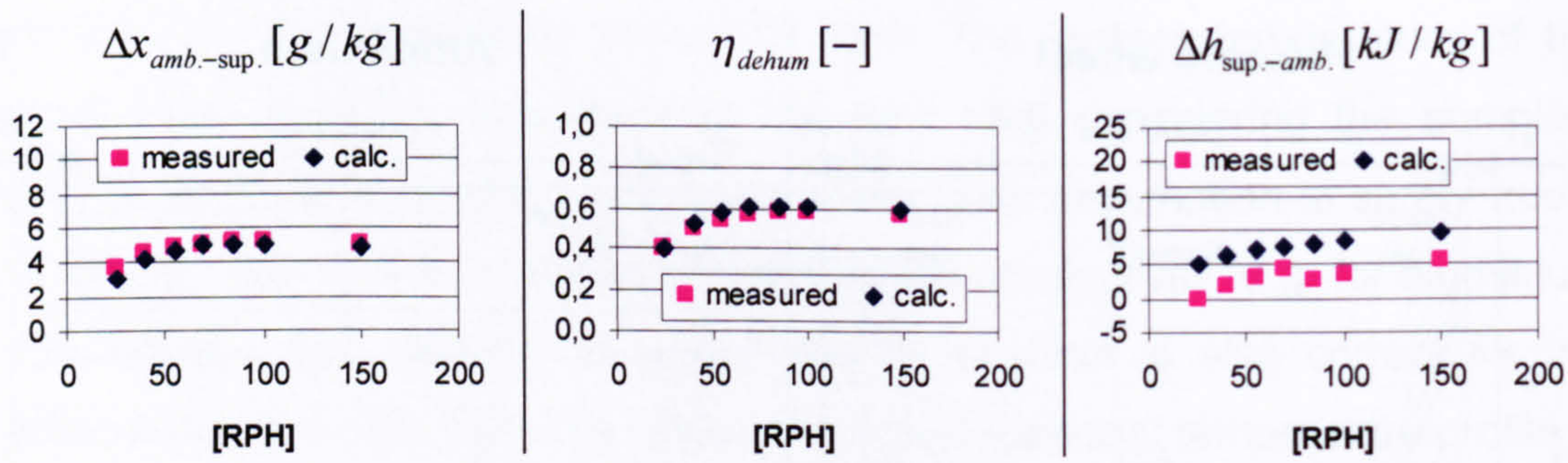

Fig. 6.12: *Comparison of calculation and measurement, dehumidification capacity / efficiency and change in enthalpy of process air (measurement series H5). Modification of model: 1. mass of silica gel = 2.5 kg / 2.* $\alpha_{new} = 0.2 \times \alpha$ */ 3.* $c_{p,wheel,new} = 0.5 \times c_{p,wheel}$

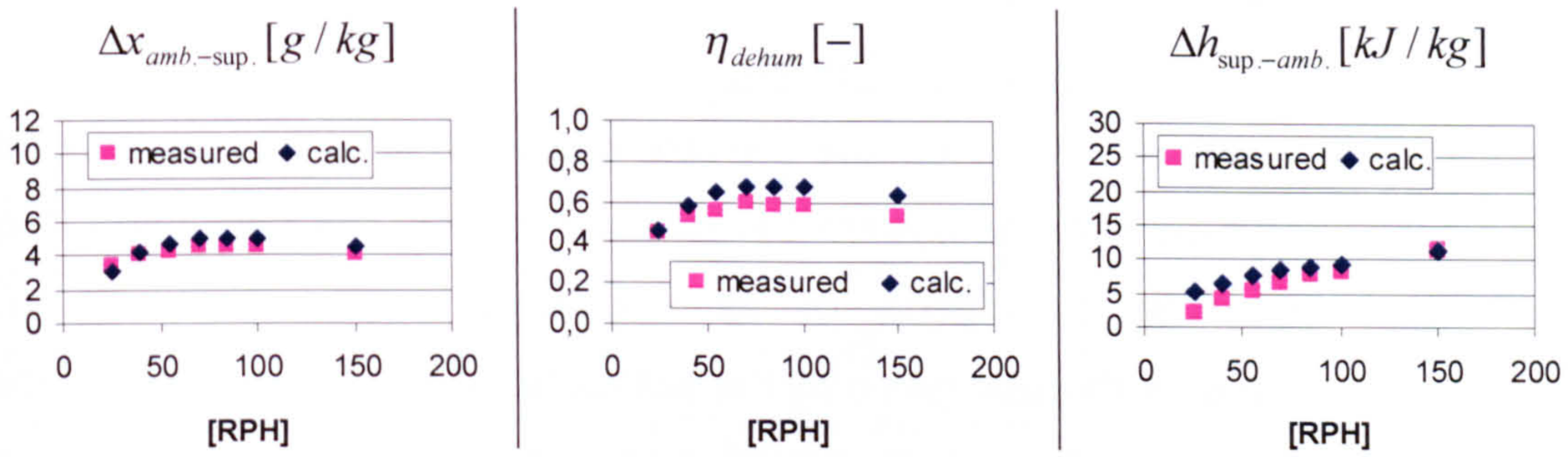

Fig. 6.13: *Comparison of calculation and measurement, dehumidification capacity / efficiency and change in enthalpy of process air (measurement series H8). Modification of model: 1. mass of silica gel = 2.5 kg / 2.* α_{new} *= 0.2 x* α */ 3.* $c_{p,wheel,new}$ *= 0.5 x* $c_{p,wheel}$

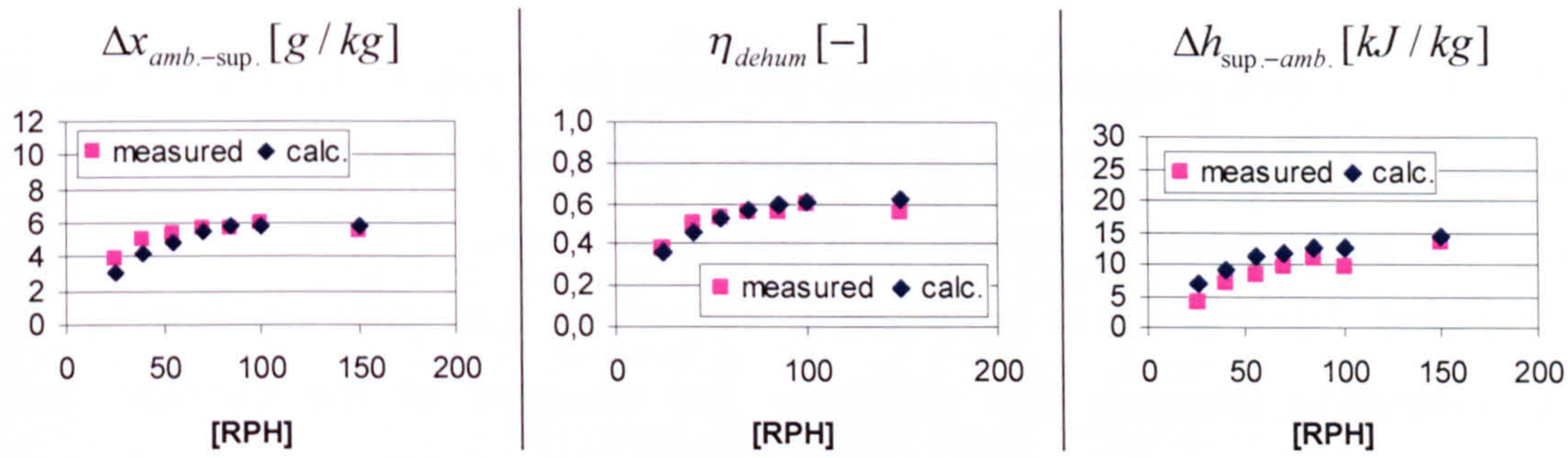

Fig. 6.14: *Comparison of calculation and measurement, dehumidification capacity / efficiency and change in enthalpy of process air (measurement series H9). Modification of model: 1. mass of silica gel = 2.5 kg / 2.* α_{new} *= 0.2 x* α */ 3.* $c_{p,wheel,new}$ *= 0.5 x* $c_{p,wheel}$

These results suggest that this is most probably the reason for the deviations. Now the agreement between the measured and the calculated values is quite good and considering the fact that here an "ideal" model is used to recalculate a "real" desiccant wheel, the results are better than expected. The range of the remaining deviations can easily be explained by measurement inaccuracy, air leakage rates, heat losses and so on.

In Appendix B the comparison of the calculations and measurements of all of the Hexcore measurement series from Chapter 03 is shown.

6.3.4 IMPROVEMENT OF CALCULATION SPEED

IMPLEMENTATION OF A TERMINATION CRITERIA

In principal, it is possible to determine the real operation time that corresponds to the calculated time with the dynamic simulation model. The calculated "time step" (one complete calculation of all segments in the process- and regeneration phase) is thereby given by the set rotation velocity and the number of segments in the direction of the wheel mass flow. The "time step" can be calculated as follows:

$$\Delta t = \frac{3600}{RPH \cdot N_{wheel}} [s]$$

When the boundary conditions remain constant for a long time period, there are sometimes no further changes in the outlet values and the wheel has reached a "steady state" operating condition. If this is the case, the calculation can be terminated. For a check of termination, a controller has been implemented into the simulation program that observes the changes of the average outlet temperatures and outlet water contents of the airflows. After many tests it was determined that steady state conditions are achieved with the following criteria:

$$\Delta \bar{\theta}_{air,out} < \pm 0.01 [K] \qquad \& \qquad \Delta \bar{x}_{air,out} < \pm 0.00001 [kg/kg]$$

With these criteria, the calculation is normally halted under constant boundary conditions at the latest after the calculation of about 30 time steps. At low rotation velocities, the calculation of just 4 to 8 time steps is usually sufficient.

DECREASING ACCURACY IN CALCULATION OF SORPTION ISOTHERM

In addition to the iterative calculation of the two phases in the model, the partial vapour pressure over the adsorption material must also be calculated iteratively for each segment because the equation of the sorption isotherm (see Eq. 3.20) can not be solved analytically for the relative humidity. Therefore the influence of the termination criterion of that iteration on the speed of the calculation of the complete model was investigated.

In order to determine the relative humidity over the wheel surface from the load and the temperature of the adsorption material, the relative humidity has to be changed iteratively until the calculated load of the matrix is equal to the given load. To this end, the first set criterion was that the calculated load must not deviate more than 0.00001 [kg/kg] from the given load. Many tests showed that without a significant change in the results, the calculation time could be reduced by about 20% by reducing the criterion by a tenth power to 0.0001 [kg/kg].

DETERMINATION OF BEST GRID

Searching for the best grid entails finding out how many elements are necessary for a sufficient level of accuracy for the results and a stable calculation process. Furthermore, the grid should contain as few elements as possible for the best calculation speed. The first calculations were done with a grid of altogether 40000 segments ($N_{air,100}$ x ($N_{matrix,reg,200}$ + $N_{matrix,process,200}$). In order to investigate the influence of the grid many other simulations with up to 200000 segments were performed. The results with this "high definition grid" were used as reference values and the elements were then enlarged.

In Tab. 6.8 the results of the study are listed for process air of 32°C / 40% / 2000 m³/h and regeneration air of 60°C / 3% / 1500 m³/h and a rotation velocity of 25 RPH.

N_{air} x N_{wheel}: Grid	100 x 2000 200000	300 x 600 180000	50 x 1000 50000	140 x280 39200	100 x 200 20000	50*300 15000	25 x 500 12500	25 x 300 7500	15 x 300 4500
$A_{segment}$ [m²]	0,0010	0,0011	0,0038	0,0049	0,0096	0,0127	0,0153	0,0255	0,0424
outcomes	reference	values							
$\theta_{process, out}$	50,206	50,185	50,243	50,202	50,214	50,247	50,315	50,319	50,411
$\varphi_{process, out}$	7,775	7,798	7,736	7,778	7,763	7,729	7,657	7,653	7,554
$\theta_{reg, out}$	33,644	33,67	33,6	33,648	33,632	33,594	33,513	33,509	33,401
$\varphi_{reg, out}$	37,444	37,34	37,623	37,43	37,497	37,652	37,982	37,997	38,451
	reference	deviation							
$\theta_{process, out}$	50,206	-0,04%	0,07%	-0,01%	0,02%	0,08%	0,22%	0,23%	0,41%
$\varphi_{process, out}$	7,775	0,30%	-0,50%	0,04%	-0,15%	-0,59%	-1,52%	-1,57%	-2,84%
$\theta_{reg, out}$	33,644	0,08%	-0,13%	0,01%	-0,04%	-0,15%	-0,39%	-0,40%	-0,72%
$\varphi_{reg, out}$	37,444	-0,28%	0,48%	-0,04%	0,14%	0,56%	1,44%	1,48%	2,69%
estimated time saving		6%	74%	81%	88%	92%	93%	96%	97%

Tab. 6.8: *Search for best grid. Absolute outcomes and deviations to reference grid*

For evaluation of the accuracy, deviations of less than 0.5 % from the reference values were declared to be sufficient. With this evaluation criterion the best grids seem to be those with 20000 to 40000 segments, and which result in almost the same outcomes as the reference grid, but take less than 20% of the time to calculate. These grids have segments with a heat and mass transferring surface that is between 0.005 m² and 0.01 m² in our case. Further enlarging the segments not only create greater inaccuracies, but also the stability of the calculation process becomes progressively worse. Thus grids with less than 20000 segments result sometimes in untrustworthy results, especially at low rotation velocities, and should therefore not be used. This behaviour can be explained by the simplifications that were introduced into the calculation model, whereby e.g. the heat and mass transfer is calculated by the inlet conditions of each single segment. If the surface of the segments is too big, these simplifications are no longer suitable.

Therefore the best grid seems to be one where the single segments have an internal heat and mass transferring surface that is not bigger than 0.01 m². Furthermore, an equal segment size for the regeneration and process phase is recommended, which results in different values of N_{wheel} for the calculation of each phase if the cross-sectional areas are not identical.

INVESTIGATION OF DIFFERENT START-CONDITIONS

Finally, the influences of different starting temperatures and loads on the wheel were tested. For this purpose, fixed and averaged values that are dependent on the air flow conditions were tested. The results of these tests were not significant, and even with the use of earlier calculated outlet conditions, the calculation time could not be significantly decreased. Thus, the starting conditions have no decisive influence on the calculation speed.

FURTHER POSSIBILITIES

A further possibility for the improvement of the calculation speed is to use constant values for some of the properties. This does not influence the outcome much, e.g. for the specific heat capacities of water, steam and dry air or the heat conductivity of air. Another possibility would be the implementation of a simplified function for the sorption isotherm, ideally an analytically resolvable function, so that an iterative solution is not necessary. This would result in a significant improvement of the calculation time.

6.4 CONSIDERATIONS ON THE USE OF THE DETAILED MODEL

With the above mentioned adjustments and improvements for the calculation speed, the calculation takes about 1 to 5 seconds on a computer with a 1.7 Ghz processor until steady state conditions are reached. In this time, the calculation of the two phases (corresponding to one time step) were usually performed 4 to 25 times depending on the rotation velocity.

Annual energy simulations or simulations over the cooling period of complete DEC-systems are usually done using at least hourly data for the boundary conditions. Due to the time demand of the desiccant wheel calculation model alone, such an annual simulation would last up to 12 hours, which is quite long. On the other hand however, it is often unnecessary for annual simulations with hourly data to use such a detailed simulation model. For this it is more suitable to simulate short time periods, e.g. one day, with 5-minute values and then to determine an average dehumidification efficiency which can be used for a simplified model (dehumidification efficiency model) for the annual simulation.

The detailed model can be used for final improvements on the control strategy of desiccant cooling plants. For this defined and/or expected operation situations can be simulated and the best operation parameters can then be determined using the simulation model.

Additionally, the detailed model is very good for the development or improvement of the design of desiccant wheels because all important physical properties (specific heat capacity, different adsorption materials etc.) and geometries (depth of wheel, internal surface, tube geometries, cross sectional area rates etc.) are considered in the model, and thus the influence of all of these can be evaluated precisely.

6.5 CONCLUSIONS

After the calibration of the desiccant wheel model was made using the studied Hexcore wheel, the results of the calculations were in good agreement with the measured values for all of the measurement series (H1 to H9, see Appendix B). The remaining small deviations in the results can be explained by processes that were not considered in the model, e.g. air leakage rates or heat losses/gains to/from the surroundings. Furthermore, the deviations could also be caused by measuring inaccuracies of the used devices.

For the calibration of the model, mainly two modifications were necessary. First, the mass of adsorption material given by the manufacturer had to be reduced from 6.9 kg to an "effective or operating" mass of about 2.5 kg, which can be explained probably by the construction process. The second modification was the adjustment of the heat transfer from the air to the matrix material, which can in this case not be described by the heat transmission resistance alone, but is determined also by the internal heat transport in the wheel material (thermal conductivity).

In principle, the detailed calculation model is better suited for the simulation of shorter time periods with accurate input data than for annual simulations. Furthermore, it is suitable for working out final improvements in desiccant wheel control strategies.

Development of the desiccant wheel or improvement of the design is also possible with the simulation model, as it takes all important physical properties and geometries into consideration.

06 Verification Of Desiccant Wheel Model With Measured Data

CHAPTER 07

MONITORING OF A DEC-SYSTEM

IN A PUBLIC LIBRARY

7.1 INTRODUCTION

In a public library in Mataró/Spain (near Barcelona), a cost-effective desiccant cooling system was to be designed, built and integrated into the existing conventional cooling system. The DEC-system was planned for the purpose of replacing one of the four air-conditioning units supplied with cooling energy from a central electrical compressor chiller. The desiccant system was to be coupled with a PV-solar air heating system.

In order to obtain information about the operation parameters and control strategy, desiccant wheels were also tested under laboratory conditions. The tests were carried out on an existing small-sized solar air heated DEC-system pilot plant installed at the University of Applied Sciences in Stuttgart. For this purpose, the existing pilot plant was turned into a desiccant wheel test plant (see chapter 05) which delivered detailed performance characteristics for a wide range of flow and air temperature/humidity conditions. Using the test and simulation results, the control strategy for the system was developed and implemented in the existing building management system in Mataró (EICKER, 2002).

Aside from laboratory testing at the University of Applied Sciences in Stuttgart, the DEC-system could also be monitored and ultimately evaluated in operation in the Mataró library building.

7.2 DESIGN OF PLANT

The public library building in Mataró/Spain was built in 1994 and has a total air-conditioned floor space of 3500 m². The building was originally equipped with four conventional air conditioning units, for which cooling energy was provided by heat exchangers from a central electrical compressor chiller. One of the air conditioning units for the children's reading and multimedia room, which has an area of 510 m², has been replaced by the desiccant cooling unit which provides this room with an air volume flow of up to 12000 m³/h via 15 ceiling air outlets.

The building has a ventilated photovoltaic south facade (244 m²) and south-oriented shed roofs (330 m²) with a total electrical power of 55 kW_p. The thermal heat produced by the photovoltaic modules is transferred into a 14 cm wide air gap, which is exhausted by the desiccant cooling regeneration fan. Two additional air collector fields in top of the facade (50 m²) and on the roof (105m² at a 34° tilt angle, south-oriented) can then increase the temperature level to the required regeneration air temperature. The common regeneration fan is volume flow controlled to provide a regeneration air temperature that lies between 50°C and 70°C.

With a yearly irradiance of about 1440 kWh/m²a on the horizontal surface (corresponding to 1020 kWh/m²a on the vertical south facade and 1570 kWh/m²a on the shed roofs), the combined solar thermal energy system is designed to produce nearly 70000 kWh of useful thermal energy from April to October. This covers over 90% of the approx. 40000 kWh cooling demand.

The thermal efficiency of the ventilated photovoltaic system is rather low (12% - 15%), due to the fact that the flow velocities in the numerous parallel large air gaps reach only 0.3 m/s and the maximum temperature level increase is between 10-15 K. The complete volume flow through the ventilated PV system of 3000-9000 m³/h passes three parallel air collector fields so that flow velocities in the 9.5 cm air channels are between 3 and 9 m/s and the efficiencies are considerably higher (about 50%). A schema of the desiccant cooling system is shown in Fig. 7.1.

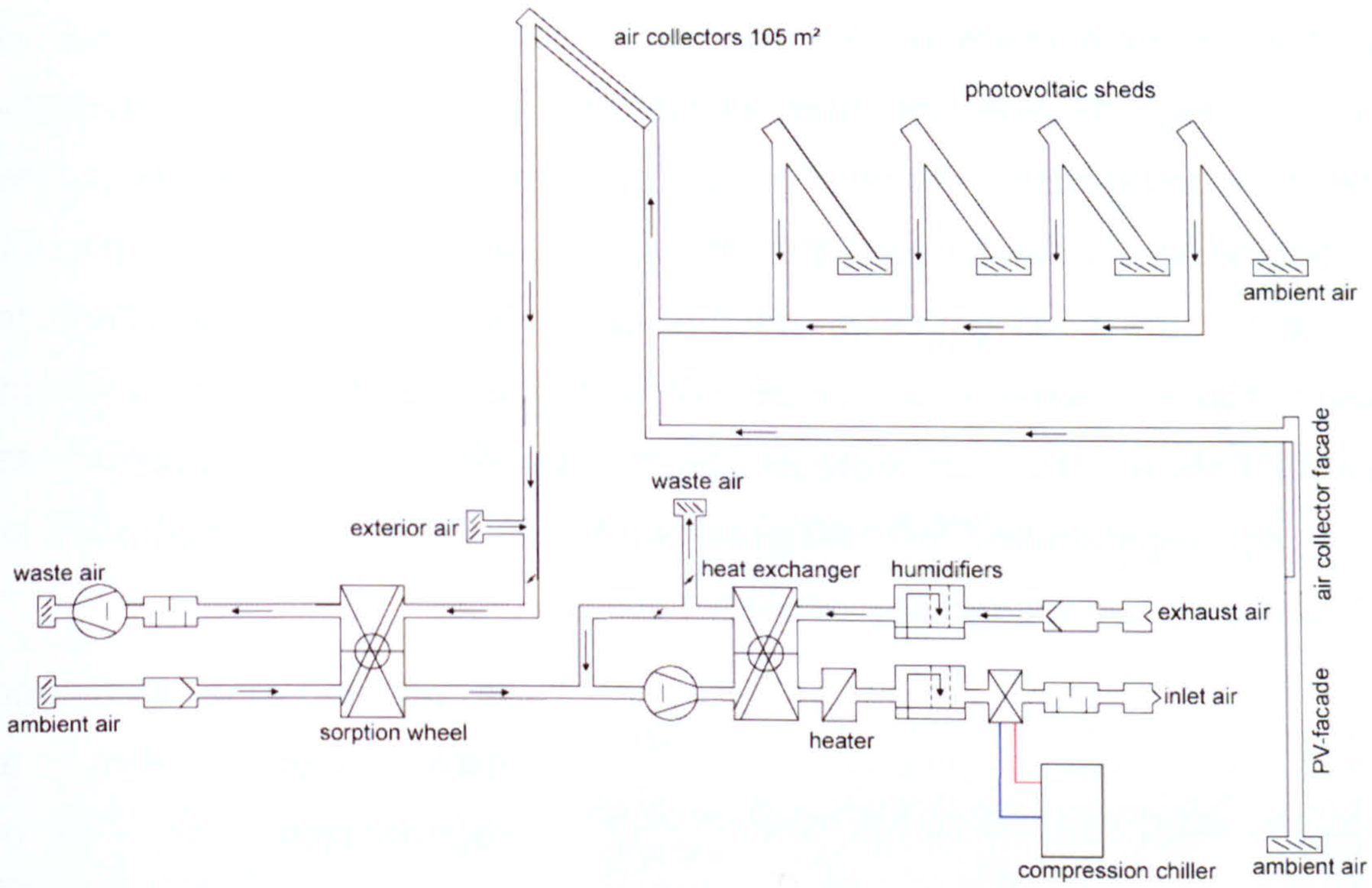

Fig. 7.1: *Schema of the desiccant cooling system in the public library in Mataró/Spain*

7.3 SHORT TIME MEASUREMENTS

Short time measurements were taken in June 2002. With this data, the correct operation of the whole desiccant cooling unit could be confirmed in principle. Measurements for the full desiccant cooling operation on the 17th of June 2002 are shown as an example (see Fig. 7.2 and Fig. 7.3).

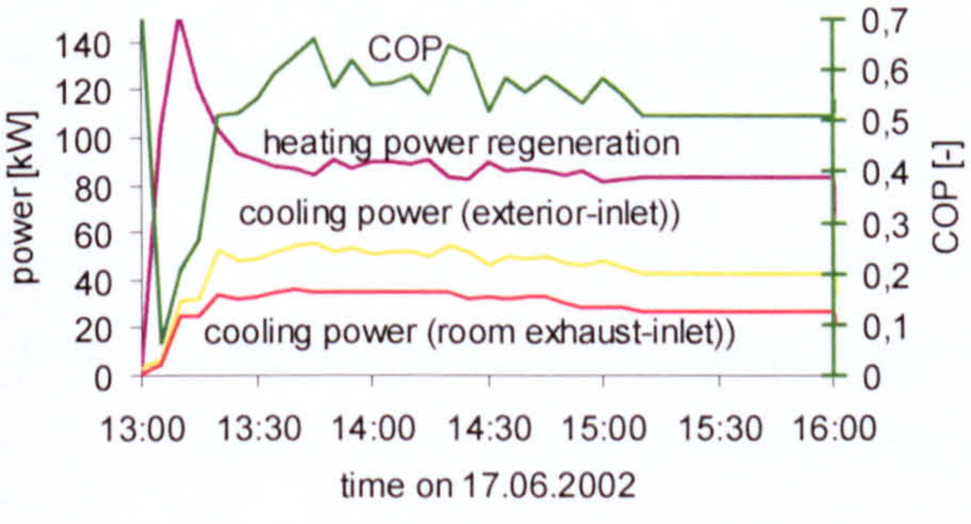

Fig. 7.2: *Heating and cooling power during full desiccant cooling operation*

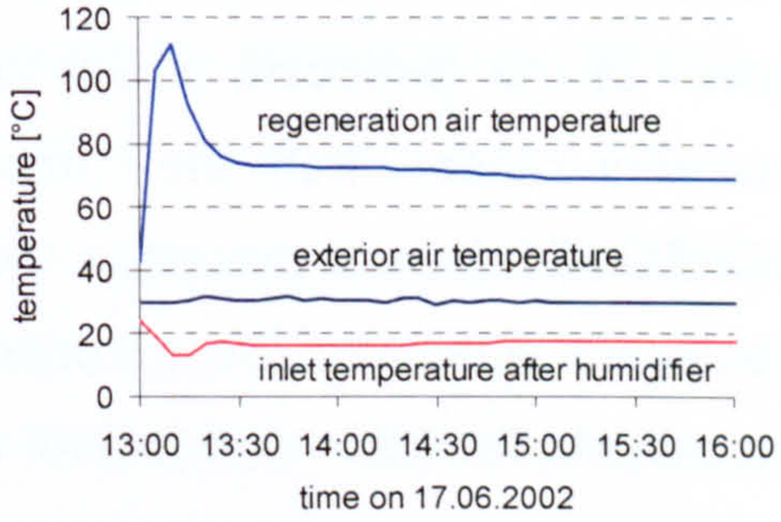

Fig. 7.3: *Temperature levels during full desiccant cooling operation*

When the machine starts up for afternoon operation, the heating power is initially very high because the solar air collector field had been at a standstill temperature beforehand. The coefficient of performance is correspondingly low at the beginning of operation and then stabilises to around 0.5 to 0.6. During full regeneration, the cooling power reaches up to 55 kW (enthalpy difference between inlet and exterior air) or 35 kW when calculated from the enthalpy difference between the room exhaust and inlet air. At exterior air temperatures of 31°C and regeneration temperatures around 70°C, an inlet temperature of 16-17°C is obtained without any auxiliary cooling.

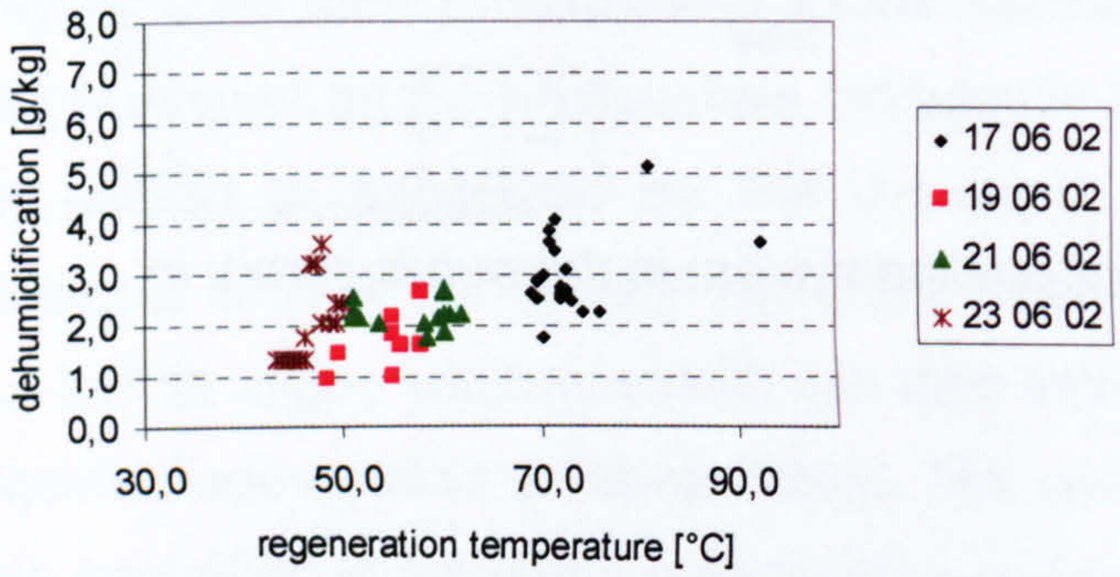

Fig. 7.4: *Measured dehumidification capacity of the silica gel desiccant wheel with regard to the regeneration temperature*

In addition, the measured data shows, that at regeneration air temperatures of between 50°C and 70°C, the dehumidification capacity of the installed desiccant wheel was between 2 and 4 g/kg (Fig. 7.4).

Due to the fact that the building management system measured strong fluctuations in the dehumidification capacity, more detailed measurements were taken at the desiccant wheel in September of 2002. Four temperature and humidity sensors from the company Ebro Electronik GmbH & Co. KG (Type: EBI-2TH-611) were placed in the process air flow behind the 2.1 m diameter desiccant wheel for the purpose of measuring representative values and to investigate the inhomogeneity of the airflow leaving the desiccant wheel.

More measurements were also taken in the process airflow in front of the desiccant wheel in order to evaluate the single point temperature sensor from the building management system.

A comparison of the measured temperature values is shown in Fig. 7.5 for the time period between 10:00 and 13:00 on the 19th of September 2002.

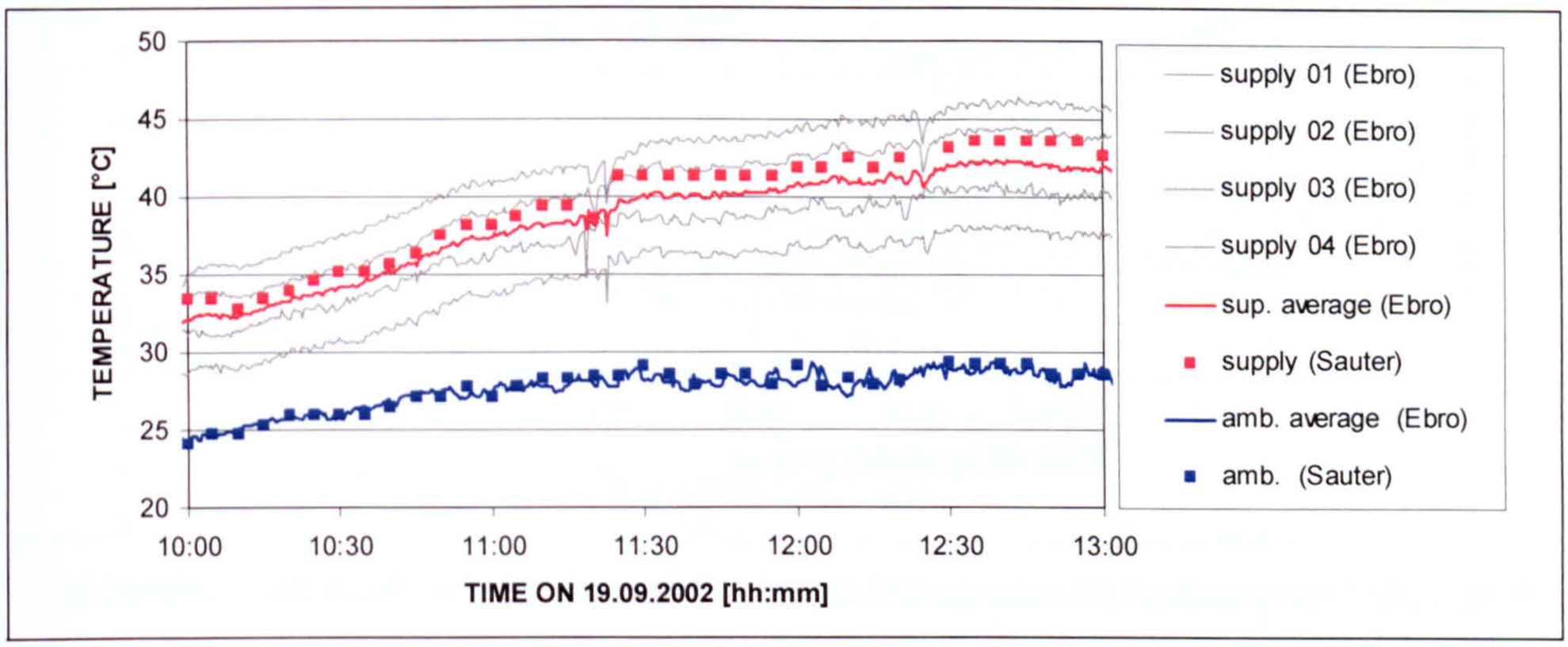

Fig. 7.5: *Comparison of measured temperature levels at the desiccant wheel by different sensors.*

The measurements show that the air temperature behind the desiccant wheel was the highest at the position where the dried desiccant wheel matrix enters the process air flow after regeneration. The average temperature, which is measured by the Ebro sensors behind the desiccant wheel, deviates only about 1 to 2 K from the single point measurement with the Sauter sensors, however the deviations of the single values given by the different Ebro sensors are quite significant (up to 8 K). Within the measurement period, the temperature of the solar heated regeneration air steadily increased from 51°C at 10:00 to 62°C at 13:00. It is obvious that the rising regeneration temperature causes the difference between the measured values to rise.

A comparison of the measured temperature values in the process airflow in front of the desiccant wheel shows that at this position the single point temperature measurement of the building management system corresponds very well to the measurements taken by the Ebro sensors.

Aside from the temperature measurements, the measurements of the relative humidity were also verified. A comparison of the Ebro and the Sauter sensors is shown in Fig. 7.6.

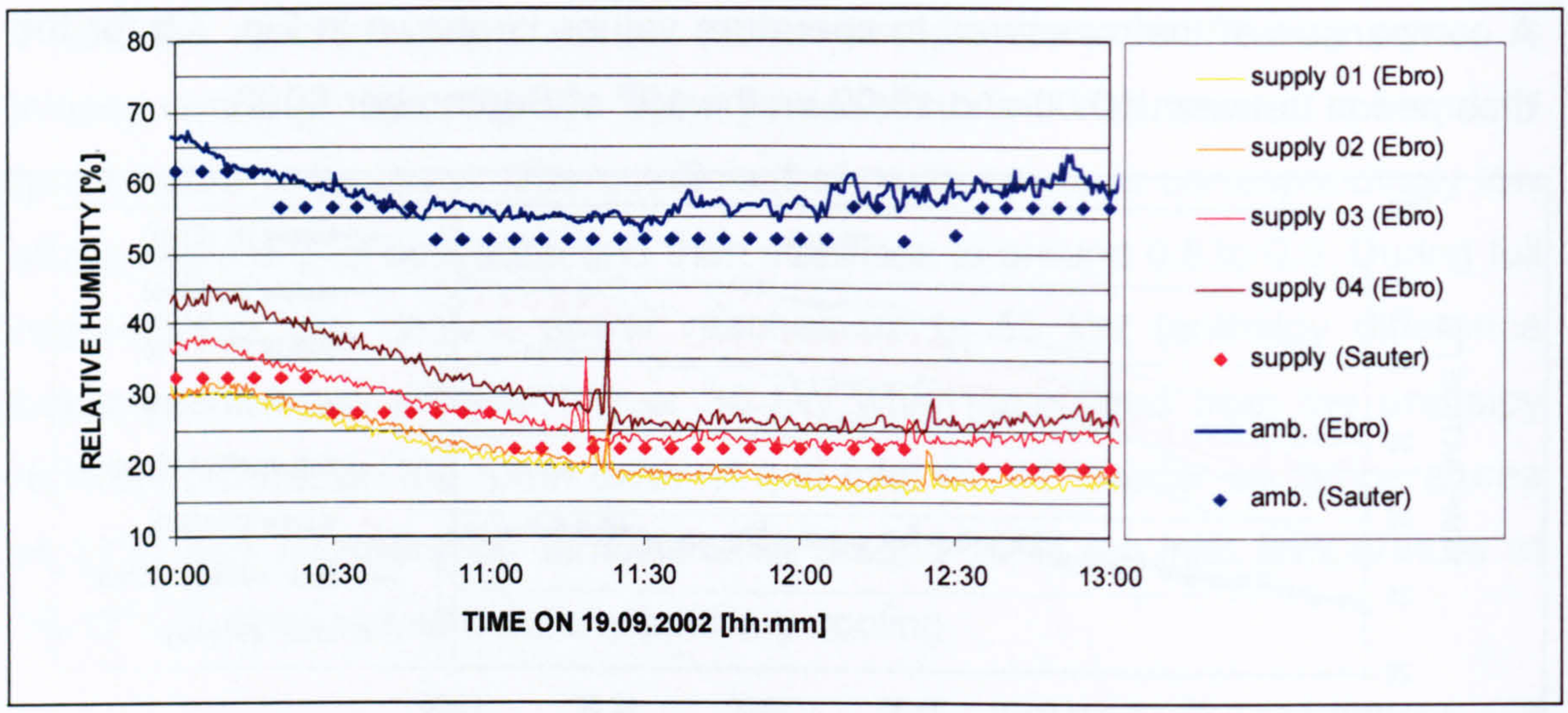

Fig. 7.6: *Comparison of measured relative humidity at the desiccant wheel by different sensors.*

The relative humidity measurements as recorded by the Sauter sensors show an incremental change for every 5% change in humidity. This is purely due to the implemented recording strategy of the building management system, because for the control of the system no accurate data about the relative humidity is necessary. But if the data should be used also for the evaluation of operation, this recording strategy must be adjusted to get more detailed results. As the used capacitive humidity sensors are surely suited right to deliver more detailed values, it is not clear why this recording strategy is implemented into the building control system.

The values of the ambient air measurements are slightly lower when taken with the Sauter sensors. For the supply air measurements, the Sauter values are within the same range as the Ebro values. To evaluate the humidity measurements directly from the relative humidity by averaging the single values is not possible; the evaluation can only be done with values of the absolute humidity that are calculated using both temperature and relative humidity (Fig. 7.7). The comparison of the absolute humidity values shows that the deviations in temperature and relative humidity measurements lead to strong deviations in absolute humidity of up to more than 1.0 g/kg. The fact that in general the

Sauter sensors provide lower values for the ambient air humidity, but higher values for the supply air is significant. It must also be mentioned, that the fluctuation of the Sauter values is greater.

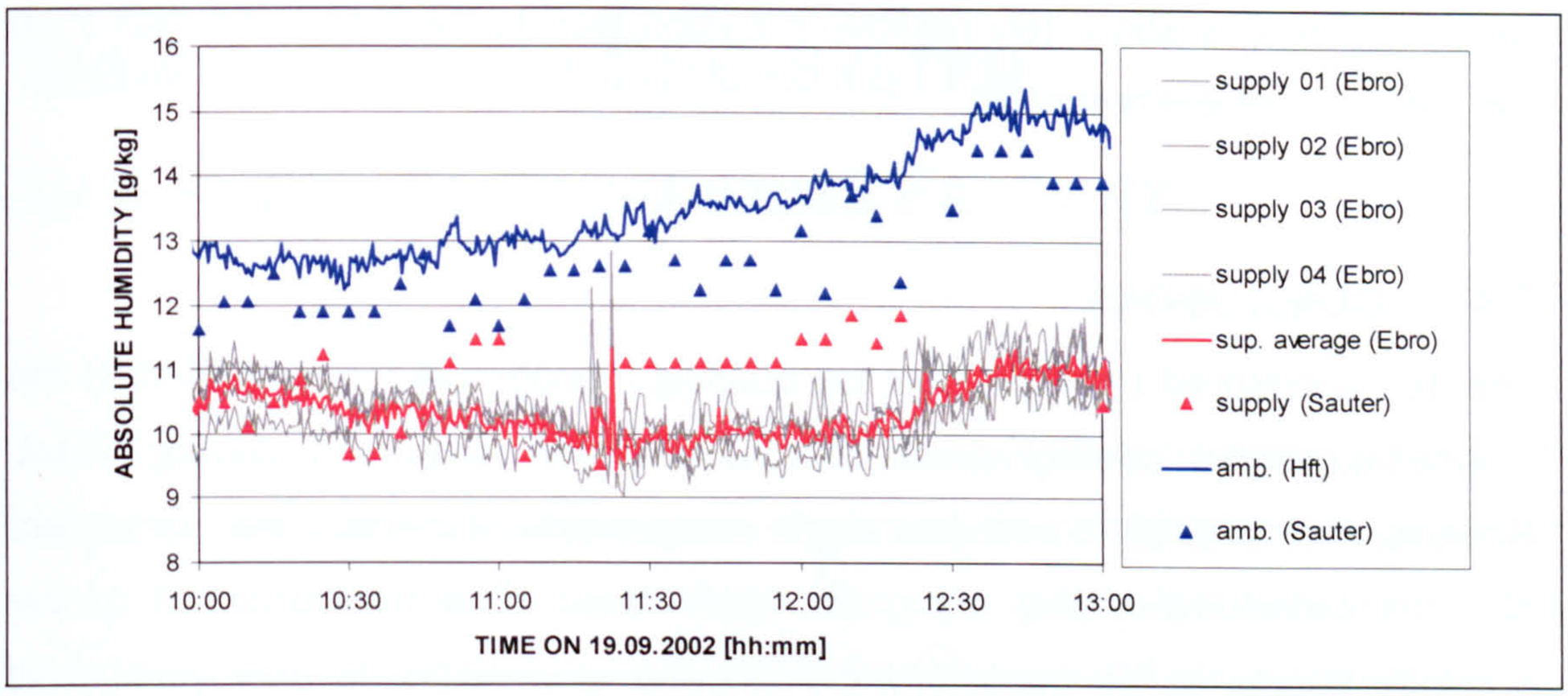

Fig. 7.7: *Comparison of absolute humidity at the desiccant wheel by different sensors*

If the difference between the absolute humidities of the ambient air and supply air (dehumidification capacity) is now calculated, it can be seen that the values obtained with the building management system are not really useful (see Fig. 7.8).

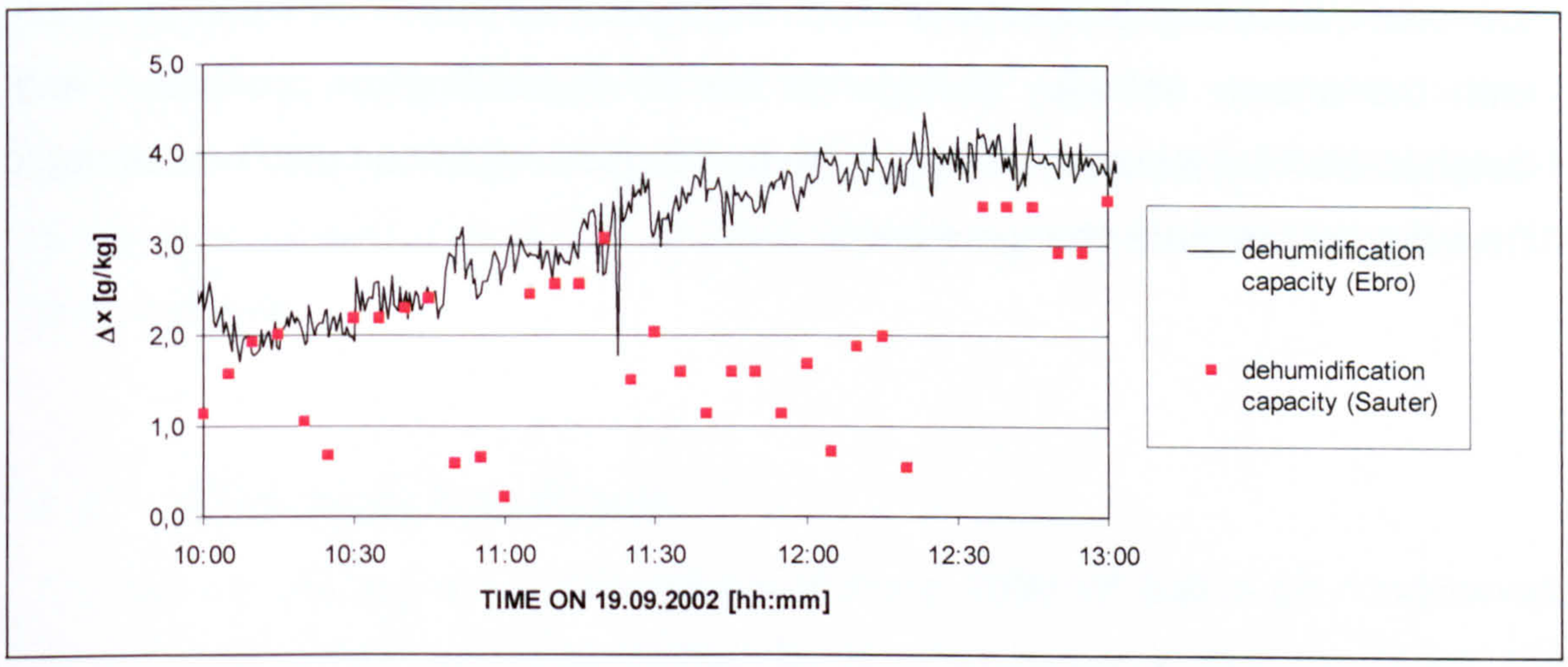

Fig. 7.8: *Comparison of dehumidification capacity obtained with different sensors*

These measurements were taken on a sunny day. The ambient air temperature during measurement was about 28°C, the relative humidity about 55%. The regeneration air temperature was about 60 °C. The measured dehumidification capacity (Ebro) is absolutely reliable in comparison to the measured data from the desiccant wheel test plant.

7.4 CONCLUSIONS

The data monitored by sensors of the building management system confirm the planned/expected cooling power of the installed desiccant cooling plant. However, the attempt to evaluate single components (especially the humidifiers and the desiccant wheel) using this data failed. The measurement of the humidity seems to be especially difficult and susceptible to error, similar to experiences with the test plant for desiccant wheels in Stuttgart (see chapter 05). If humidity measurements are to be used for evaluation, a large amount of technical expenditure is necessary, especially for commercial systems, where usually only very little space is available (there is almost no space to install measuring devices between the single components).

As the temperature measurement is much more accurate and there are also low-cost measuring devices with which multi-point measurements can be taken, with the known enthalpy change of the de-/humidification processes (e.g. established from laboratory testing) the de-/humidification can also be estimated from the temperature change alone.

CHAPTER 08

MONITORING OF A DEC-SYSTEM

IN A PLASTICS PROCESSING FACTORY

8.1 INTRODUCTION

Until now there has been almost no experience gained in the operation of solar powered adsorption cooling systems, especially in combination with solar air collectors. There is also no knowledge about the achievable performance, the efficiency and the best component choice for solar operation in commercial use. Due to this fact, such systems must be inevitably designed to be larger than necessary in order to guarantee the performance level wanted by the user, which of course increases the costs. Due to the high costs, lack of experience in operation and vague information about actual performance, this cooling technology has so far only been rarely accepted by potential users.

In order to gain more experience with this technology, a pilot plant for a factory building in Althengstett, Germany, which is the first commercial solar powered adsorption cooling system in Europe with 100 m² of solar air collectors, was monitored. The monitored data was used to obtain fundamental data about the achievable performance and to discover operation problems that can occur with such systems.

8.2 DESIGN OF THE PLANT

The factory building has a floor space of about 1600 m² that is air-conditioned. Due to unavoidable air contamination by the plastics processing machines, the building also needed a high fresh air rate, something for which the air based desiccant cooling system is very well suited.

The desiccant wheel that was installed was made by the manufacturer Klingenburg and uses lithium chloride as the sorption material. The process air flow is about 18000 m³/h and the regeneration air flow is about 11000 m³/h. Both air flows are set to a constant rate and a reduction of the air flows at partial cooling load operation is not part of the control strategy. As the room exhaust air is contaminated, it is not used for regeneration, mainly to avoid a damage/pollution of the desiccant wheel.

Heating energy for regeneration is provided by the rather small solar air collector field and the waste heat recovered from the plastics processing machine coolers. The air collector field consists of two parallel strings each with a collector surface of 50 m². The single collectors on each string are connected in series. The air collector type is the same as the collectors used for the public library in Mataró/Spain and has 9.5 cm high flow channels. The heat recovered from production is intended to deliver a maximum of about 45 kW and is used for preheating the regeneration air before it goes to the solar air collectors. This order is necessary because of the low temperature level of the waste heat from production. Thus the disadvantage of a lower efficiency of the solar air collectors caused by the higher inlet air temperatures was not avoidable. In order to limit the specific volume flow through the collectors, the regeneration air flow is only partially heated by the air collectors with a maximum volume flow of about 6000 m³/h.

If both solar energy and waste heat cannot sufficiently provide the required regeneration air temperature, auxiliary energy is provided by an already existing oil-based heating system.

The main cooling loads in the factory building are internal loads from the processing machines, thus the DEC-system is mainly in operation when the production is running.

If there is no cooling demand for the production hall, the solar energy and the waste heat can be used to provide warm air for an air heating system that

supplies an assembly hall (first upper floor) and/or an older, badly insulated storage hall. A schema of the desiccant cooling system is shown in Fig. 8.1.

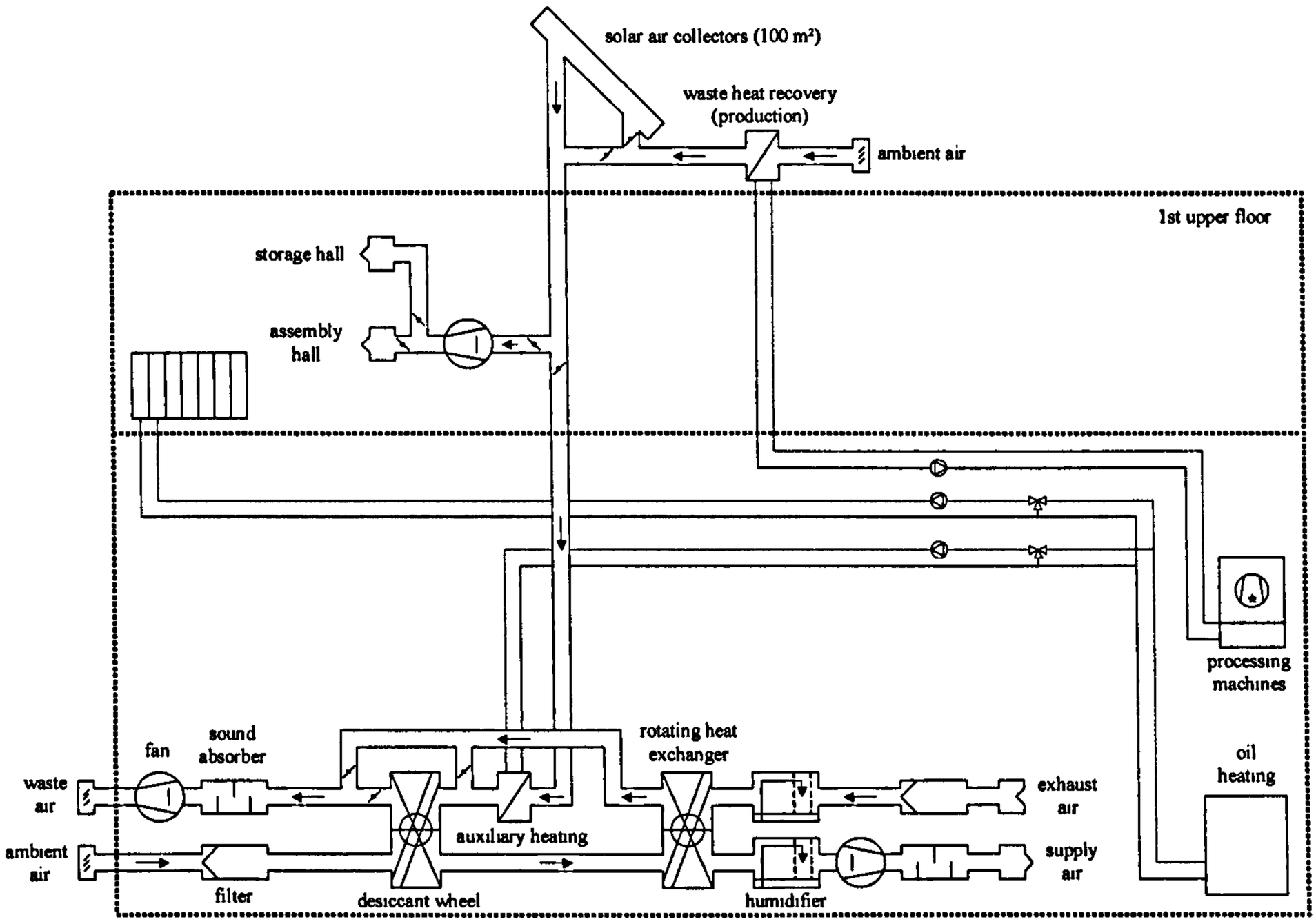

Fig. 8.1: *Schema of the DEC-system in the factory building in Althengstett, Germany*

The design and dimensioning of the plant was done with the following principal considerations and assumptions. The necessary maximum cooling power (exhaust air to supply air) of the plant was decided by simulations to be 60 kW. With a minimum room inlet temperature of 17°C and an assumed room exhaust air temperature of about 28°C, the necessary process air volume flow comes to 18000 m³/h. To cool 18000 m³/h of ambient air from 32°C to 17°C, a cooling power of about 90 kW is required. Assuming a COP of 0.9 for desiccant cooling operation, about 100 kW of heating power is required. This heating power should be supplied by the waste heat from the production (assumed with 45 kW) and from the solar air collectors (assumed with 60 kW at a maximum). With this heating power and a regeneration air flow of about 11000 m³/h, the

temperature rise will be about 30 K, thus regeneration temperatures of about 60°C should be reached.

8.3 COMMISSIONING

For the development of the control strategy, the integration of the waste heat use from the processing machine coolers was especially difficult, as trouble free operation of the processing machines requires a continuous dissipation of the waste heat. In addition to the heat exchanger in the regeneration air flow, the processing machine coolers can also dissipate the waste heat via fans directly into the air in the rooms, but this would lead to a higher cooling load for the building and should be principally avoided. In order to obtain a satisfactory solution for this problem, many attempts and optimisations were necessary.

Another problem was the durability of the lithium chloride desiccant wheel that was used. Due to malfunctions or mistakes in the control strategy, the wheel was sometimes at a standstill even though air was being blown through it. As a result, the wheel absorbed so much water that its own weight caused damage (cracks) to the wheel matrix.

Due to these problems (and many other smaller ones) during installation and test operation in the years 2000 and 2001, the solar powered DEC-system did not work satisfactorily until the year 2002. Thus for the further improvement of the control strategy and in order to investigate the real performance of the system, comprehensive measurements were taken again from January to October of 2002. This measured data is presented in the following paragraphs in detail.

Despite the previous improvements in the control strategy, an evaluation of the measured data shows some more operation conditions which must be reconsidered. Furthermore, malfunction of components and errors in the control strategy again caused avoidable energy losses and thereby a considerable reduction of the efficiency/performance during the monitored time period.

8.4 MONITORING

8.4.1 PRINCIPAL CONSIDERATIONS

Measurements on commercially used, air based air conditioning plants are usually accompanied by measuring complications. Measurements of temperature, relative humidity and volume flow that are taken in sufficiently long tubes or channels have an accuracy that in most cases is good enough, therefore single point measurements are often sufficient for the determination of representative values. In commercial plants however, there is rarely space between the single components to install measuring sensors. Thus single point measurements can deliver values which deviate significantly from the representative values, especially near rotating components such as rotary heat exchangers or desiccant wheels. Even multi point measurements (available at least for temperature and volume flow measurements) are sometimes not really sufficient for determining representative values if there are difficult flow conditions. Thus in general a scientific evaluation of single components by free field measurements can be problematic.

Although for the measurements the installed sensors were periodically confirmed by manually-taken measurements, the values measured inside the DEC-System near the single components must be considered with caution. For the determination of the tendency behaviour however, or to track down malfunctions in operation, these measured values are essential.

For an energy evaluation of the complete system, the measured values are usually sufficiently accurate because the measuring points are situated outside the plant and far away from components in the channel system.

8.4.2 INSTALLED MEASURING DEVICES

Data from two different monitoring systems was used for the evaluation. The first monitoring system (*Saia-Burgess Electronics GmbH & Co. KG*) was installed by the manufacturer of the system and is used for control. As comprehensive data logging is not offered by this system, the data was

monitored with a data logging system installed by the Stuttgart University of Applied Sciences. The second monitoring system was also installed by the Stuttgart University of Applied Sciences for the purpose of obtaining data from positions which are not measured by the control system but are necessary for a detailed evaluation. The data from these sensors is also monitored with the installed data logging system.

The sensors in the control system are called **"Saia"**-sensors (after the name of the manufacturer of the control system) and the sensors installed by the University of Applied Sciences are called **"HfT"**-sensors (HfT is an abbreviation of the German name for the University of Applied Sciences which is 'Hochschule für Technik'). An overview of the measurement points is given in Appendix C.

The measuring sensors and the monitoring system installed by the HfT are the same as those used at the desiccant wheel test plant (chapter 05). The Saia-sensors are from the company *Thermokon Sensortechnik GmbH*. The measuring range and the accuracy of the sensors, as given by the manufacturers, are shown in Tab. 8.1:

manufacturer	measuring range		accuracy	
	temperature	rel. humidity	temperature	rel. humidity
Micatrone (HfT)	-30...80°C	0...100%	± 0.5°C	± 2% (r.h.)
Thermokon (Saia)	-20...80°C	5...95%	± 0.3°C	± 2% (r.h.) between 35...75%

Tab. 8.1: *Measuring range / accuracy of the different sensors (as given by the manufactures)*

Due to the fact that there are two installed measuring systems, there are some points that are measured by two different sensors. Naturally these sensors should record equal values. To check this, five temperature-values were compared that were measured by both the Saia- and the HfT-sensors. The comparison shows that there are much greater deviations between these values than one would expect from the measurement accuracy of the sensors

(according to SCHELLER, 2003, the expected inaccuracy is about 1 to 2 K for the complete measuring arrangement). The discovered deviations were up to about 3 K in the monthly averaged values and single 5-minutes-values even show deviations of up to 10 K.

The large deviations of the single 5-minute-values can partly be explained by the different inertia of the sensors, but this cannot explain the deviations in the monthly average values. These deviations must be caused by the positioning of the sensors in the tubes or by a bad calibration.

As the monitored plant is a commercially-used system, naturally no comprehensive precautions were taken to improve the accuracy of the monitoring sensors, such as with the installation of diffusers, damping tubes etc. The dimensions of the plant and the pressure losses rather were taken into account in order to reduce the space demand and energy consumption of the system. As a result, most of the sensors had to be installed very close to components, which is something that could have a considerable influence on the measured values due to heat radiation or by causing them to only be representative for parts of the volume flow for example.

Above and beyond the possible influence of the positioning, it is noticeable that the measured values by the Saia-sensors are always lower (1 to 3K on average) than the values measured by the HfT-sensors. This indicates an additional systematic error or a bad calibration between the Saia- and the HfT-sensors.

Due to the occurrence of these deviations, for the following evaluation of single components, only values from the same measuring system were used (where possible). If values of both systems were available, the values from the HfT-system were used because comprehensive experience has been gained over the course of previous projects with these sensors. Furthermore, these sensors were installed with the concrete goal of obtaining representative values and not only for controlling the system.

8.5 DATA PROCESSING / EVALUATION

8.5.1 EVALUATION PROCEDURES

For the evaluation of the monitored data a comprehensive plausibility check was necessary for each value, because sometimes values were recorded that could not be explained with reference to other measured data. Sometimes there were also a few values missing from the monitored data because of a malfunction in the monitoring system or the sensors.

Other problems that arose were, that sometimes the monitored data showed operation conditions which were confirmed by all the monitored values but which made no sense with reference to the boundary conditions. This must have been due to a malfunction in the control system or the control strategy must still have had substantial errors.

The monitored data consists of about 60 monitored values measured every five minutes, which amounts to about 17000 monitored values each day and more over 4000000 values over the course of the monitoring from January to October in 2002. In order to handle this huge amount of data it was necessary to develop evaluation procedures to determine the operation status of the plant and the components automatically by simultaneously eliminating the times for which no evaluation was possible.

A main problem for evaluation was that the monitored values of the building control system were not reliable over long periods of time (e.g. the control signal of the desiccant wheel). Another problem was the time delay between the control signal and the effect on the operation. Each component has specific time delays between the control signal (release) and the appearance of the effect on the operation. The humidifiers e.g. need about 5 to 10 minutes after release to reduce the air temperature at the outlet significantly and the cooling effect does not stop before 45 minutes after being switched off. Thus if the control signals were to be used for the evaluation of the humidifiers, in each period of operation, about 40 minutes of the real cooling operation would not be taken into consideration. Therefore, the evaluation was done mainly with the

use of the temperature differences at the single components. The difference of the two evaluation procedures is shown in Fig. 8.2 with an example of the exhaust air humidifier on July 10th.

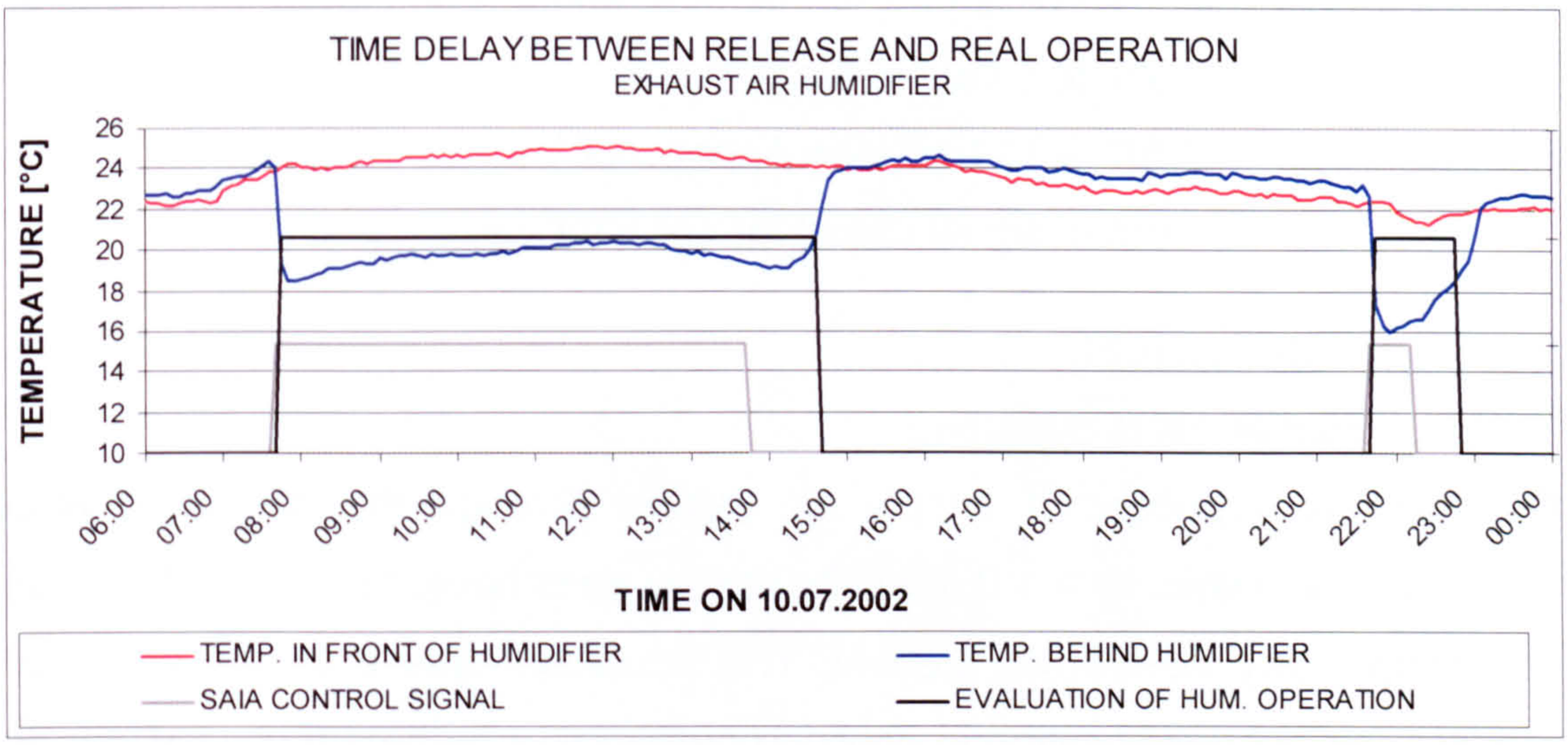

Fig. 8.2: *Time delay between release by control signal and the appearance of the effect on the operation*

In Fig. 8.2, the temperatures in front of and behind the humidifier, the control signal of the Saia-system (release of humidifier) and the evaluation of operation by temperature differences are shown.

For the evaluation of the monitored data limiting values were defined (temperature differences) by which the operation mode of the single components was evaluated (on/off). Using the operation modes of the single components, the operation mode of the complete system could be determined (cooling, heating, free ventilation, etc.). The evaluation procedures that were used are as follows:

[1] DEC-SYSTEM (GROUND FLOOR)

Ventilation is running in the production hall.

Operation is supposed if a volume flow of the supply air and the exhaust air is measured (measured flow velocity > 1 m/s) and no contradictory values are present.

Sensors used: V2/3 & V4/5 (see Appendix C)

[2] AIR COLLECTORS

The collectors are operating.

Operation is supposed if the collectors have airflow (measured flow velocity > 0.5 m/s and collector valve is open), the input and the output temperatures are known and no contradictory values are present.

Sensors used: V6/7 & T14/18 (see Appendix C)
control signal (Saia) for collector valve > 0

[3] DESICCANT WHEEL

The desiccant wheel is operating.

Operation is supposed if supply air passes through the desiccant wheel (measured flow velocity > 1.0 m/s), the supply air is heated up ($\Delta T > 3.0$ K) and no contradictory values are present. This could be caused by the adsorption process (air dehumidification in cooling operation) or by heat recovery from the regeneration or exhaust air.

Sensors used: V2/3 & $\Delta T1/2$ (see Appendix C)

[4] SUPPLY AIR HUMIDIFIER

The supply air humidifier is operating.

Operation is supposed if supply air passes through the humidifier (measured flow velocity > 1.0 m/s), the supply air is cooled down ($\Delta T > 3.0$ K) and no contradictory values are present.

Sensors used: V2/3 & $\Delta T5/7$ (see Appendix C)

[5] EXHAUST AIR HUMIDIFIER

The exhaust air humidifier is operating.

Operation is supposed if exhaust air passes through the humidifier (measured flow velocity > 1.0 m/s), the exhaust air is cooled down ($\Delta T > 3.0$ K) and no contradictory values are present.

Sensors used: V4/5 & $\Delta T9/11$ (see Appendix C)

[6] ROTATING HEAT EXCHANGER

The rotating heat exchanger is operating.

Operation is supposed if exhaust air passes through the rotating heat exchanger (measured flow velocity > 1.0 m/s), the exhaust air is cooled down or heated up (ΔT > 3.0 K) and no contradictory values are present.

Sensors used: V4/5 & ΔT10/12 (see Appendix C)

[7] REGENERATION

Regeneration air, heated by waste heat from the processing machines, solar air collector gain or auxiliary heat, is used to air-condition the ground floor with the DEC-System. This means, the regeneration airflow passes through the desiccant wheel, which can be for cooling operation (full desiccant cooling) or heating (heat recovery).

Operation is supposed if the DEC-system [1] is operating, the measured flow velocity of the regeneration air is > 0.5 m/s, the desiccant wheel bypass is inactive (control signal bypass Saia = 0) and no contradictory values are present.

Sensors used: V9 & sensors used for [1] (see Appendix C)
control signal (Saia) for Desiccant wheel bypass = 0

[8] AIR HEATING SYSTEM

The assembly hall in the first upper floor and/or the old storage hall of the company is heated by the air heating system (powered by waste heat from processing machines and/or solar air collector gain).

Operation is supposed if the measured flow velocity of the regeneration air is > 0.5 m/s but no REGENERATION [7] takes place, the air heating system is enabled by the Saia control system (control signal = 1) and no contradictory values are present.

Sensors used: V9 & sensors used for [7] (see Appendix C)
control signal (Saia) for air heating system = 1

[9] HEAT RECOVERY FROM PRODUCTION

Waste heat from the processing machines is used to heat the regeneration air.

Operation is supposed if a regeneration air flow is present (measured flow velocity > 0.5 m/s), the regeneration air is heated up ($\Delta T > 3.0$ K) by the waste heat exchanger (on the roof) and no contradictory values are present.

Sensors used: V9 & $\Delta T13/14$ (see Appendix C)

[10] AUXILIARY HEATING

Auxiliary heat from the existing oil-based heating system is used to heat the regeneration air.

Operation is supposed if regeneration air passes through the auxiliary heat exchanger (measured flow velocity > 0.5 m/s), the regeneration air is heated up ($\Delta T > 5.0$ K) and no contradictory values are present. The higher temperature difference criterion in this case is necessary because of the large distance between the single sensors.

Sensors used: V9 & $\Delta T18/22$ (see Appendix C)

In some cases, there are different possibilities for the evaluation of several components, so e.g. for the collectors there are three different combinations of sensors which can be used to determine the operation mode and the collector gain. For theses cases, the above listed procedures have been determined using comprehensive investigations to be the most suitable ones. The criteria (temperature differences) have also been counter checked manually in order to obtain the correct operation mode with the evaluation procedures.

8.5.2 PERIODS OF EVALUATION

Using the above listed evaluation procedures, the total time that a detailed evaluation of the operation mode is possible during the time period of the monitoring was determined. The monitored values start on January 1st, 2002 and end on October 8th, 2002. Thus the heating operation can be studied during a winter period and the cooling operation during a summer period. About 60

different values (temperature, relative humidity, volume flow, control signals) were monitored every 5 minutes during operation, but due to malfunctions in the monitoring systems and break down of single sensors, the evaluation is obviously not possible the entire time. The percentile of time per month that a detailed evaluation is possible is listed in Tab. 8.2.

Month	Percentile of evaluated time	Month	percentile of evaluated time
January	58,2 %	June	64,1 %
February	78,7 % (holidays: 15.02 to 28.02)	July	82,6 %
March	67,3 %	August	84,9 % (holidays: 03.08 to 25.08)
April	58,2 %	September	41,5 %
May	79,2 %	October	40,2 % (up to 8.10.2002)

Tab. 8.2: *Percentile of time when detailed evaluation of operation is possible (including regular shut off times)*

For the whole period from the 1st of January to the 8th of October the percentile of time when a detailed evaluation is possible is about 66 %.

Of all the months, July seems to be best for a comprehensive evaluation of the cooling performance. Furthermore, from June 26th on, an exhaust air humidifier malfunction was finally solved, making July the first month in the monitored period in which no significant malfunctions of single components took place.

8.5.3 INFLUENCE OF EVALUATION PROCEDURES AND USED SENSORS

For the determination of the cooling performance for example, the evaluation procedure and the choice of sensors influence the outcomes vitally. This influence is shown below with a comparison of the evaluations done with the above mentioned evaluation procedures and an evaluation that was done for the final project report in November of 2002 (EICKER and HUBER and MAIER, 2002).

The comparison was done for the cooling performance in the month of July in 2002. The evaluations done within the framework of this thesis (subsequently

called: "current evaluation") are based on determined operation modes that consider the “real” operation of the single components. In this way for example, cooling operation is determined by the operation of at least one humidifier, desiccant cooling is determined if at least one humidifier and the sorption wheel is operating etc. In contrast, the evaluation for the 2002 final project report (EICKER and HUBER and MAIER, 2002) was done by determining a temperature decrease between the ambient air and the supply air for cooling operation, full regeneration was determined only by the control signal of the sorption wheel bypass flap. Due to these different evaluation procedures alone, which seem very straight forward, there are great deviations in the determined cooling energy and operation times.

Thus the total cooling energy obtained in the current evaluation in July is about 4144 kWh in contrast to the value of 10754 kWh, which was obtained in the evaluation for the 2002 project report. This means that the cooling energy determined in the current evaluation is only 39% of the cooling energy determined in the 2002 project report. The operation times also deviate enormously. The determined overall cooling time in the current evaluation is about 173 h in contrast to 309 h in the evaluation for the 2002 project report. These results are shown in Fig. 8.3 and Fig. 8.4.

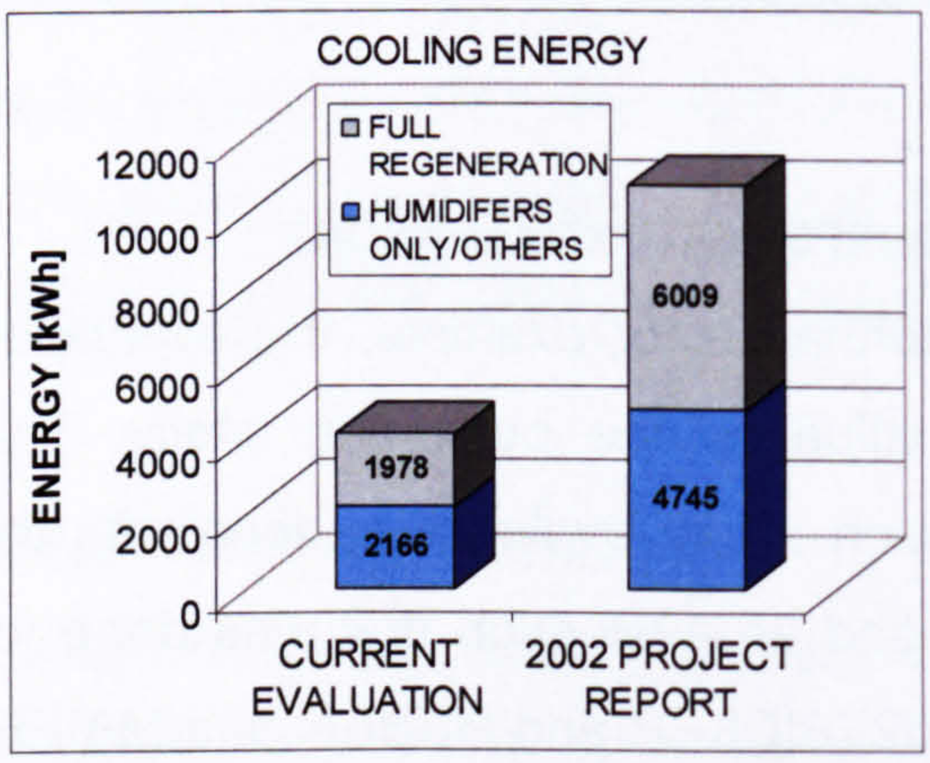

Fig. 8.3: *Comparison of cooling energy determined with different evaluation procedures*

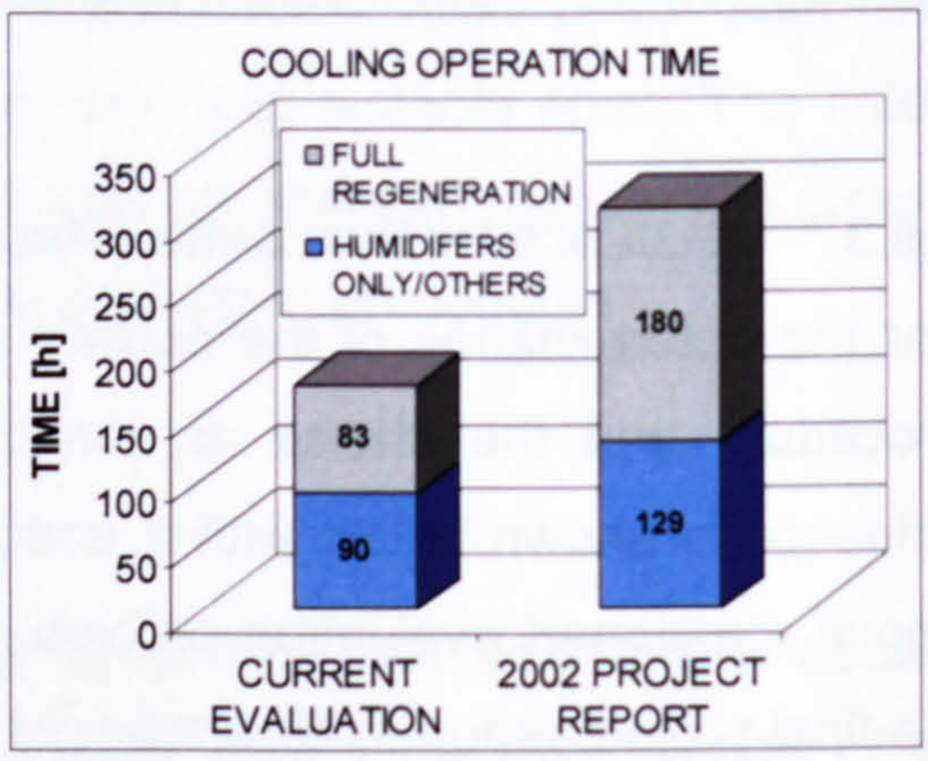

Fig. 8.4: *Comparison of cooling operation time determined with different evaluation procedures*

In order to find out why the outcomes were so different, a closer look at the measured data was necessary. The main problem seemed to be that different values for the ambient air temperature were used. For the current evaluation, the ambient air temperature was measured using a Saia-sensor. The sensor is placed in the process air flow directly in front of the sorption wheel (T1, see Appendix C). For the evaluation in the project report the ambient air temperature was measured by the HfT sensor on the roof of the building (T13, see Appendix C). This sensor is placed in front of the heat exchanger which is supplied by waste heat from the processing machines.

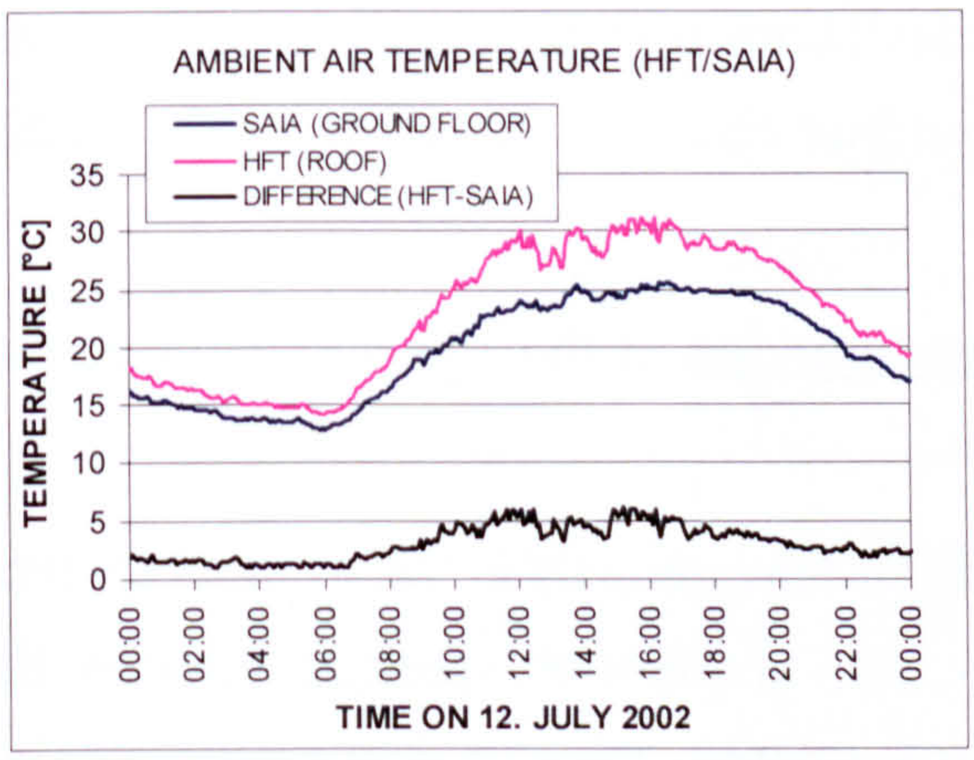

Fig. 8.5: *Deviations in measured ambient air temperatures at different positions*

A comparison of the temperature curves shows that the deviation between the monitored values of the two sensors is sometimes up to 6 K. Thus it seems obvious that the results must be different. The deviation of the two sensors is shown in Fig. 8.5 using the 12th of July, 2002 as an example. Between 12:00 and 18:00 the supply air temperature is at about 18°C. The monitored ambient air temperatures are approximately 29°C on the roof (HfT) and 24°C on the ground floor (Saia). With a volume flow of about 18000 m³/h, the calculated cooling power then is 61 KW with the HfT values and 33 kW with the Saia values.

These deviations can be caused in principle by the following possible factors:

- random errors (measuring)
- systematic errors (measuring)
- different actual temperatures at the measurement points.

Random errors can be eliminated by repeating the measurement and building an average value. In this case, independent of the averaged time period, the deviations could not be eliminated. Thus the deviations can not be caused by random errors only.

Systematic errors occur because of less than perfect measuring techniques, e.g. bad calibration, bad measuring position etc. In principle, systematic errors can be calculated and corrected. For the purpose of checking the measured data for systematic errors, the temperature profiles were investigated extensively for the months of May and July. An attempt was made to find both relative and absolute regularities in the deviations that would point to systematic errors, but all in all no errors were found that could be completely responsible for the deviations.

Thus there must be in fact different temperatures at the measurement points, perhaps combined with systematic errors.

The Saia sensor is placed in the process air flow, directly in front of the sorption wheel. Before it reaches this position, the ambient air passes through the production hall in a tube that is not heat insulated. Thus it must be considered that there could be a kind of pre-conditioning of the ambient air that is dependent on the indoor temperature of the production hall.

The HfT-sensor is placed on the roof in a tube in front of a heat exchanger. In this position no pre-conditioning of the ambient air is expected. The problem with this sensor is that the roof of the production hall and also the surrounding air is heated by solar irradiation, necessitating the consideration of an influence due to solar irradiation.

In order to determine the influence of the indoor temperature on the deviation of the monitored ambient air temperatures, the monitored values in May and July were plotted (shown in Fig. 8.6 and Fig. 8.7) for the temperature difference of the ambient and indoor air during periods with no significant solar irradiation (10 to 50 W/m²).

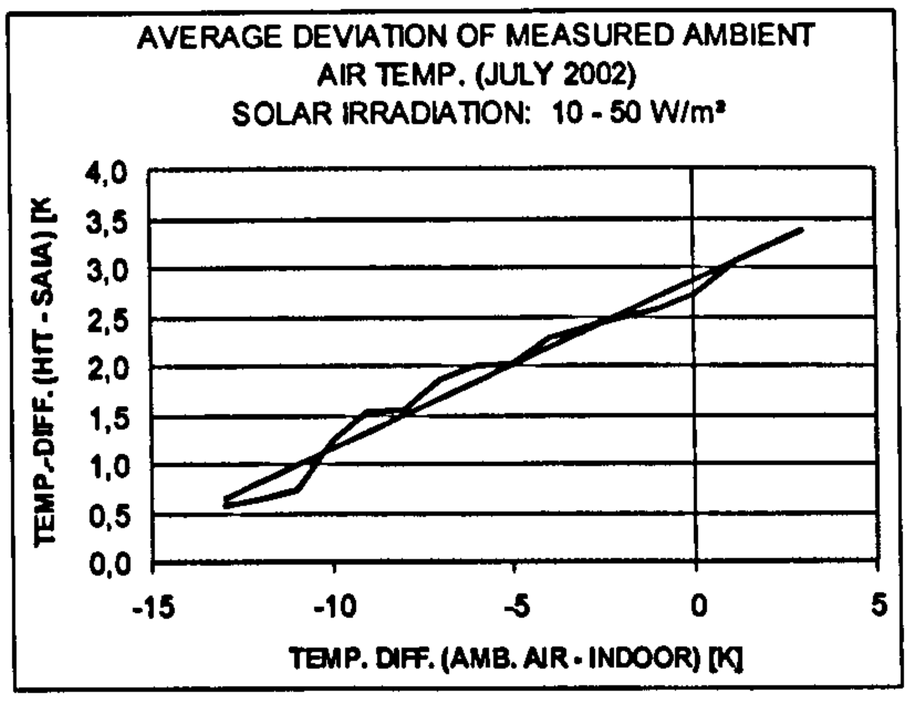

Fig. 8.6: *Influence of indoor temp. on the deviation of the monitored ambient temperatures (July 2002)*

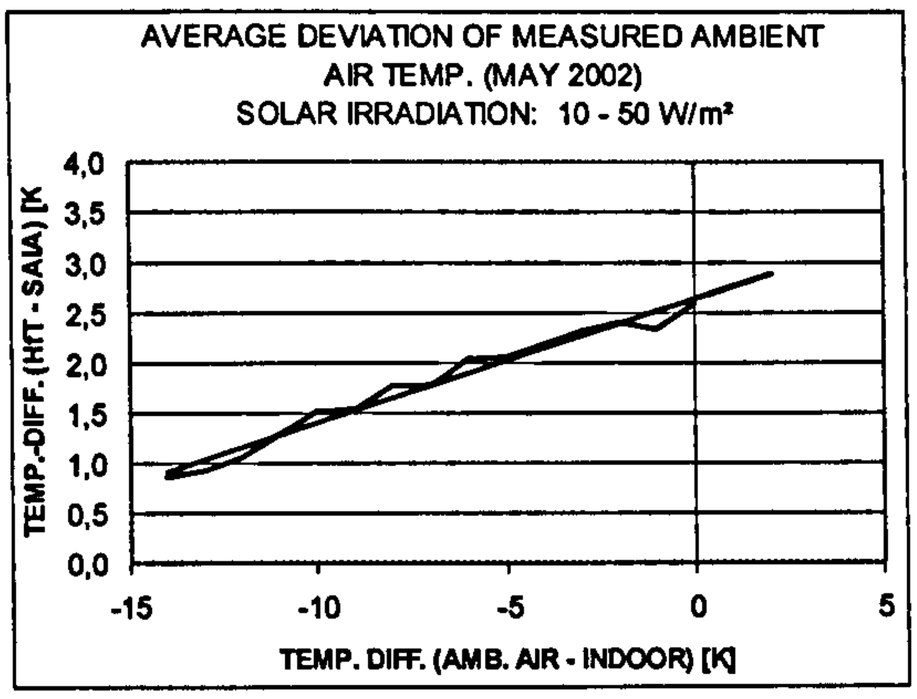

Fig. 8.7: *Influence of indoor temp. on the deviation of the monitored ambient temperatures (May 2002)*

The results show that the temperature difference between the ambient air and the indoor air has a remarkable influence on the deviation of the two measured ambient air temperatures. It is also significant however, that without a temperature difference between ambient and indoor air, i.e. when pre-conditioning can be ruled out, a deviation of about 3 K remains which therefore must be due to a calibration error.

To determine the influence of the solar irradiation on the deviation of the monitored ambient air temperatures, the monitored values in May and July during periods with no significant temperature difference between the ambient and indoor air (difference < 2 K) were plotted with respect to the solar irradiation (see Fig. 8.8 and Fig. 8.9).

These results also show that solar irradiation has a remarkable influence on the deviation between the two values, and in addition an expected deviation of about 3 K remains (calibration error), even when no solar irradiation is monitored.

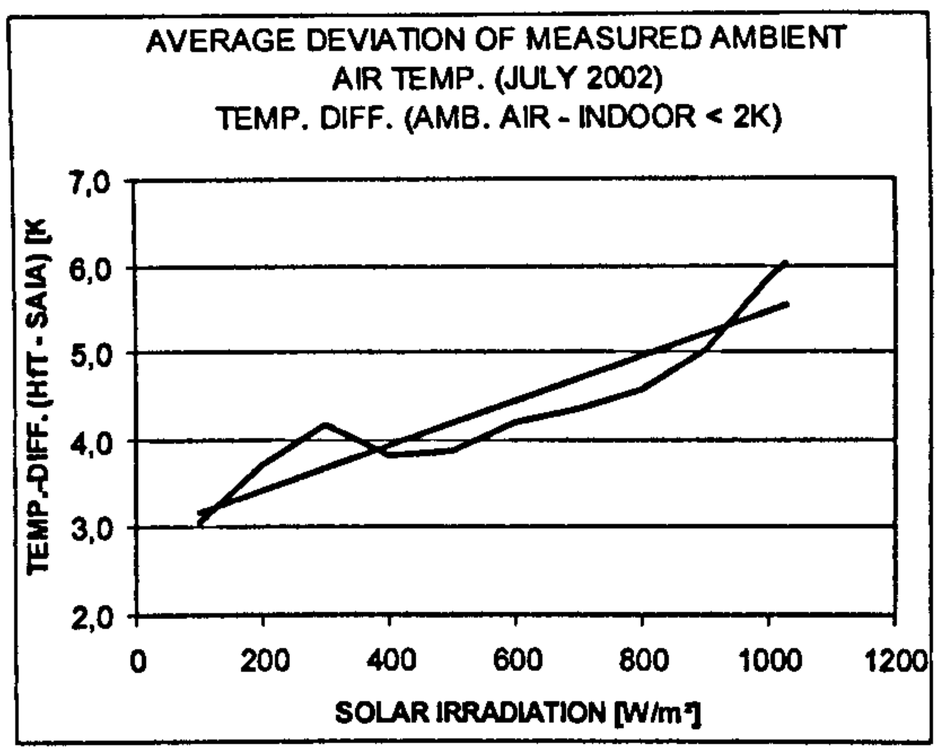

Fig. 8.8: *Influence of solar irradiation on the deviation of the monitored ambient temperatures (July 2002)*

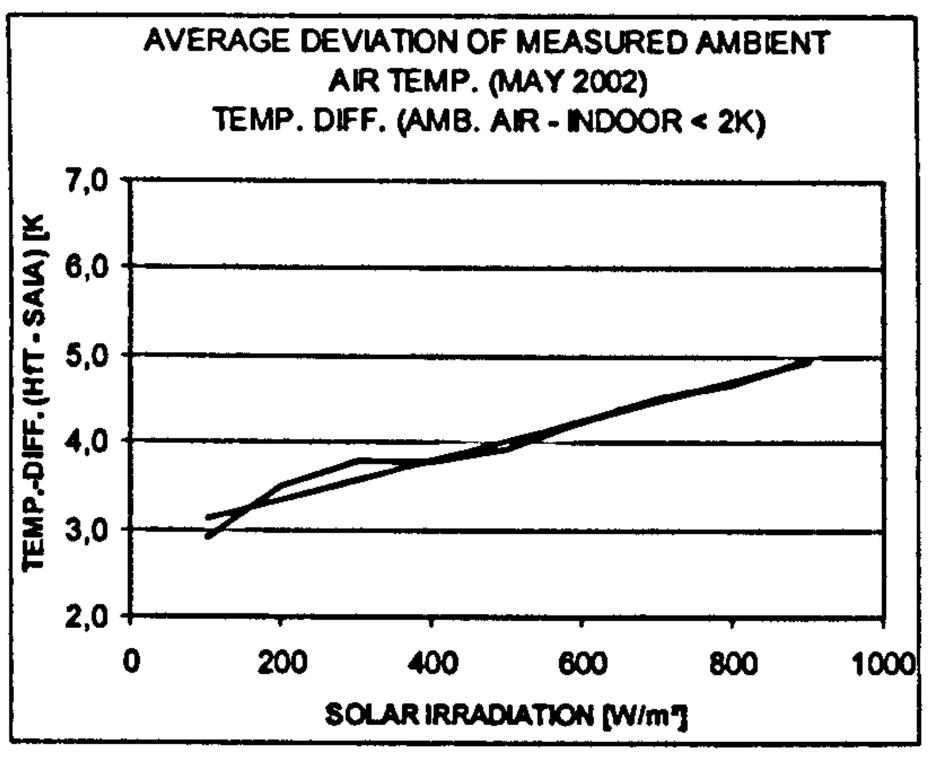

Fig. 8.9: *Influence of solar irradiation on the deviation of the monitored ambient temperatures (May 2002)*

Altogether the indoor temperature and the solar irradiation have a strong influence on the measured ambient air temperatures. In addition, a systematic error (bad calibration of one or both sensors) which causes a deviation between the measured temperatures of about 3 K must exist.

The question now arises as to which temperature is right or at least better for the evaluation. First of all, none of the measured temperatures show the outdoor temperature exactly. The temperature measured by the Saia-sensor is pre-conditioned by the indoor temperature of the production hall and the temperature measured by the HfT-sensor is indirectly influenced by solar irradiation. For the evaluation of the cooling performance of the DEC-system itself, the real temperature at the inlet of the plant should be used, no matter what happens to the air beforehand. Thus the Saia value seems to be better suited for the evaluation than the HfT value in this case. The supply air temperature to the production hall is measured by both a Saia-sensor and a HfT-sensor. Supposing that the calibration between sensors from the same system is better than from different systems, the above-determined systematic error should also be smaller. This was also counter checked during the operation mode "free ventilation" in the month of July when the inlet air temperature was almost the same as the supply air temperature. This counter

check showed an average deviation of about 1.3 K over the course of 178 hours of free ventilation operation, which is very acceptable considering all of the possible influences on the measurements.

For the purposes of comparing the evaluation procedures of the current evaluation and the evaluation for the 2002 project report, the evaluation for the 2002 project report was repeated using the Saia values instead of the HfT values. The results from this showed much less deviation in the cooling energy and operation time. The total cooling energy now determined for the modified evaluation for the 2002 project report is about 5382 kWh. The earlier value was 10754 kWh. Thus the cooling energy determined in the current evaluation (4144 kWh) is only 33 % less than the cooling energy determined in the modified 2002 project report. The operation times also correspond much better. The overall cooling time for the modified evaluation for the 2002 project report is now about 228 h. The value in the current evaluation is 173 h (see Fig. 8.10 and Fig. 8.11).

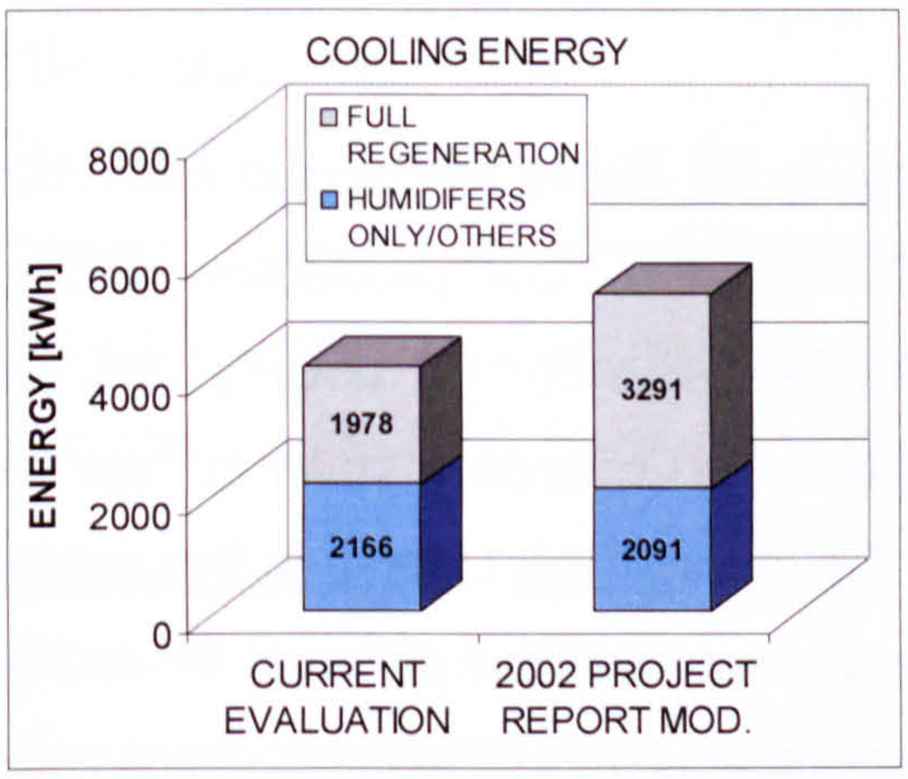

Fig. 8.10: *Comparison of cooling energy determined by different evaluation procedures after modifications of evaluation procedures*

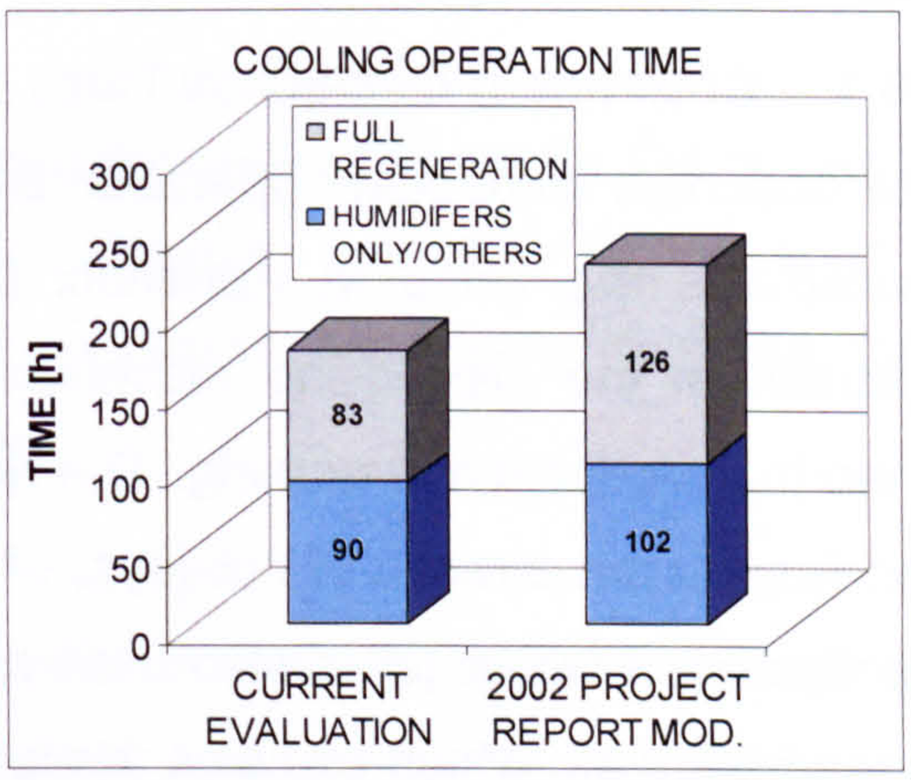

Fig. 8.11: *Comparison of cooling operation times determined by different evaluation procedures after modifications of evaluation procedures*

The deviations that now remain can be explained by the different evaluation procedure methods. For the current evaluation, much more data is necessary for the evaluation compared to the method used for the 2002 project report. Sometimes single measurement values are not available and thus the

corresponding component can not be evaluated. For the method in the current evaluation this means that no evaluation is possible in this case, but that the method for the 2002 project report can still be used. Thus there are times when one method achieves results and the other does not. For example, in July, 528 hours can be evaluated using the method for the 2002 project report compared to only 413 hours with the current evaluation method. Standardized on operation times, the results are nearly equal. The average cooling power determined with the method of the evaluation for the 2002 project report is about 23.6 kW and with the current evaluation method it is about 24.0 kW.

This investigation shows in an impressive way, how sensibly measured and published energy performance figures should be handled and that it is always important to verify the way the figures have been ascertained.

8.6 EVALUATION

8.6.1 COMPONENT OPERATION TIMES

The observed component operation times with the above mentioned evaluation procedures are listed in Appendix D. Due to the heat production and air pollution of the processing machines, the DEC-System [1] usually operates when the production is running. The relatively short operation times in February and August are a result of holidays, when the factory was closed. In this system the desiccant wheel [3] is also used for heat recovery from exhaust air or from regeneration air, which explains the long operation times of the desiccant wheel in the winter. Active cooling (with humidifiers [4] and/or [5]) started in March and lasted until the end of the monitored time period in October of 2002. It is notable, that the exhaust air humidifier [5] first started operating in June due to a malfunction of the water pump, which was not repaired before the 21st of June, 2002. The rotating heat exchanger [6] is only used to pre-cool the supply air with the exhaust air in active cooling operation. This heat exchanger was not used for heat recovery (heating) in winter. Regeneration [7] starts like the active cooling by humidifiers already in March. The air heating system [8] operates

mainly in winter, but it also operates in summer (exclusively in August). A closer look at the air heating system follows below. The operation times of the heat recovery from the production [9] are very long, which is caused by the need for continuous heat dissipation, even when no energy for regeneration or the air heating system is required. The auxiliary heating [10] starts already in March and ends in August, when the auxiliary heating was deactivated on the 27th of August by the user because of the high oil consumption during summer. Remarkably, despite the auxiliary heating being disabled, the user was still satisfied with the cooling power of the system. This outcome will also be investigated in chapter 09.

8.6.2 OPERATION MODES OF THE DEC-SYSTEM

The evaluated times for when the DEC-System operates in different "modes" are listed in Appendix E. These "modes" are defined as follows:

[1] AIR HEATING SYSTEM

The first upper floor and/or the old storage hall is/are heated by the air heating system (powered by waste heat from processing machines and/or solar air collector gain). The air heating system operates separately from the DEC-System, but the DEC-System has priority.

[2] HEAT RECOVERY REG. AIR

The heat from the regeneration air is used to preheat the supply air (heating of new production hall) with the desiccant wheel.

[3] HEAT RECOVERY EXHAUST AIR

The heat from the room exhaust air is used to preheat the supply air (heating of new production hall) with the desiccant wheel.

[4] FREE VENTILATION

The DEC-system supplies the production hall with fresh air, but no air-conditioning (heating, cooling, de-/humidification) takes place.

[5] COOLING BY HUMIDIFIERS

The supply air is cooled by humidification of the supply air and/or the exhaust air (via rotating heat exchanger).

[6] COOLING BY REGENERATION

Cooling by regeneration means full desiccant cooling operation. The supply air is dried by the desiccant wheel, pre-cooled by the humidified exhaust air (via rotating heat exchanger) and humidified by the supply air humidifier (if possible).

[7] NOT DEFINED

This mode is set if no other mode from [2] to [6] can be detected. This happens usually if the operation mode had changed and the inertia of single components results in contradictory values.

The air heating system [1] operates independent of the DEC-System. The sum of the times of the different operation modes [2] to [7] equals the total operation time of the DEC-System (see Appendix D). The operation mode [2] "HEAT RECOVERY REG. AIR" is not used for heating the supply air in winter, but is used to raise the supply air temperature if it is getting too low during cooling operation. This operation mode usually occurs after full desiccant cooling at moderate ambient air temperatures (in the monitored period, this takes place mainly in June). Heat recovery from the exhaust air [3] however is used to heat the supply air until it exceeds the limit of 17°C at low ambient air temperatures. This operation mode is mainly used up until May, but also sometimes during the summer months (June to August/September). In the summer months, this operation mode is observed mainly in the mornings and at night. Free ventilation [4] is used if the ambient air temperature is not too low (higher than 17°C) and no active cooling is required, which is usually the case in the colder months around midday and in the warmer months in the mornings and in the evenings/nights. Cooling time from the humidifiers only starts in March and tends to increase until May. In June, the portion of the cooling process covered by regeneration [6] begins to increase.

8.6.3 AIR HEATING SYSTEM

The air heating system can be evaluated for an operation time of 1943 h in the time period from January to October. For the evaluated time period, the supplied heating energy was about 58950 kWh, whereby only 9540 kWh were supplied by the air collectors and 49410 kWh by the waste heat recovery from the processing machines. However, when evaluating these absolute values it must be considered, that the monitored data could be evaluated in detail only about 66% of the time, thus the real supplied heating energy was probably higher. The average heating power during monitored operation of the air heating system was about 30 KW. The maximum power (determined from 5 minute values) that was supplied to the air heating system from the collectors in May was 96.3 kW and the maximum power supplied from the waste heat exchanger in February was 102.2 kW.

In Fig. 8.12 and Fig. 8.13, the monthly operation time of the air heating system and the supplied energy are shown respectively.

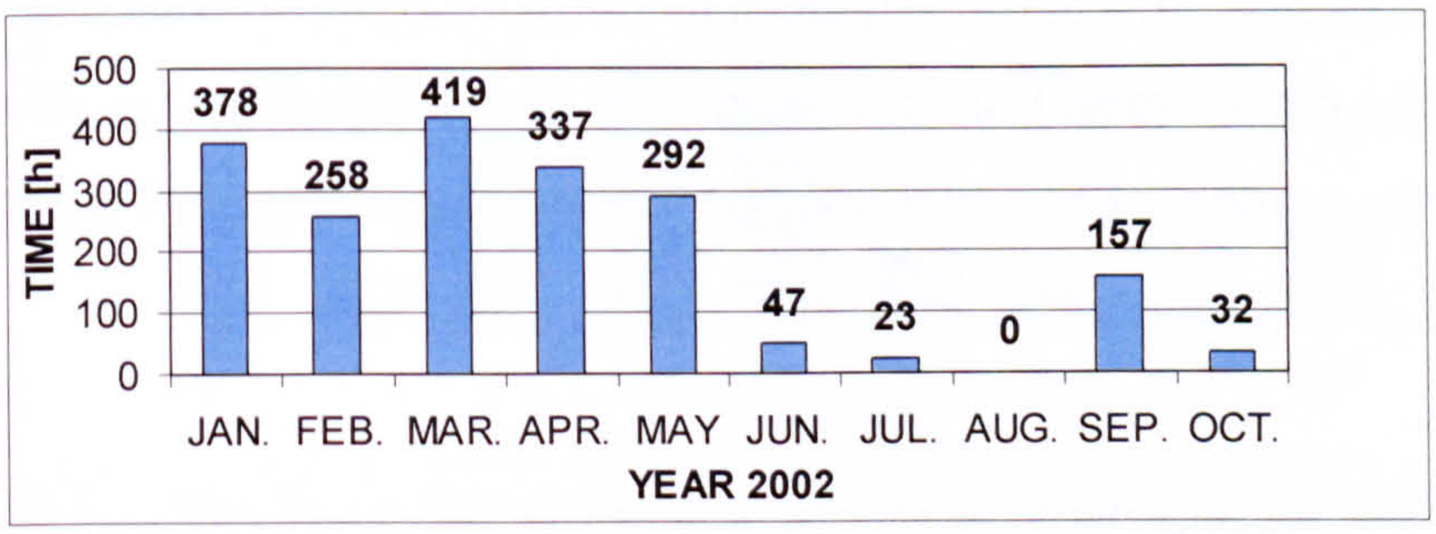

Fig. 8.12: *Monthly operation times of air heating system*

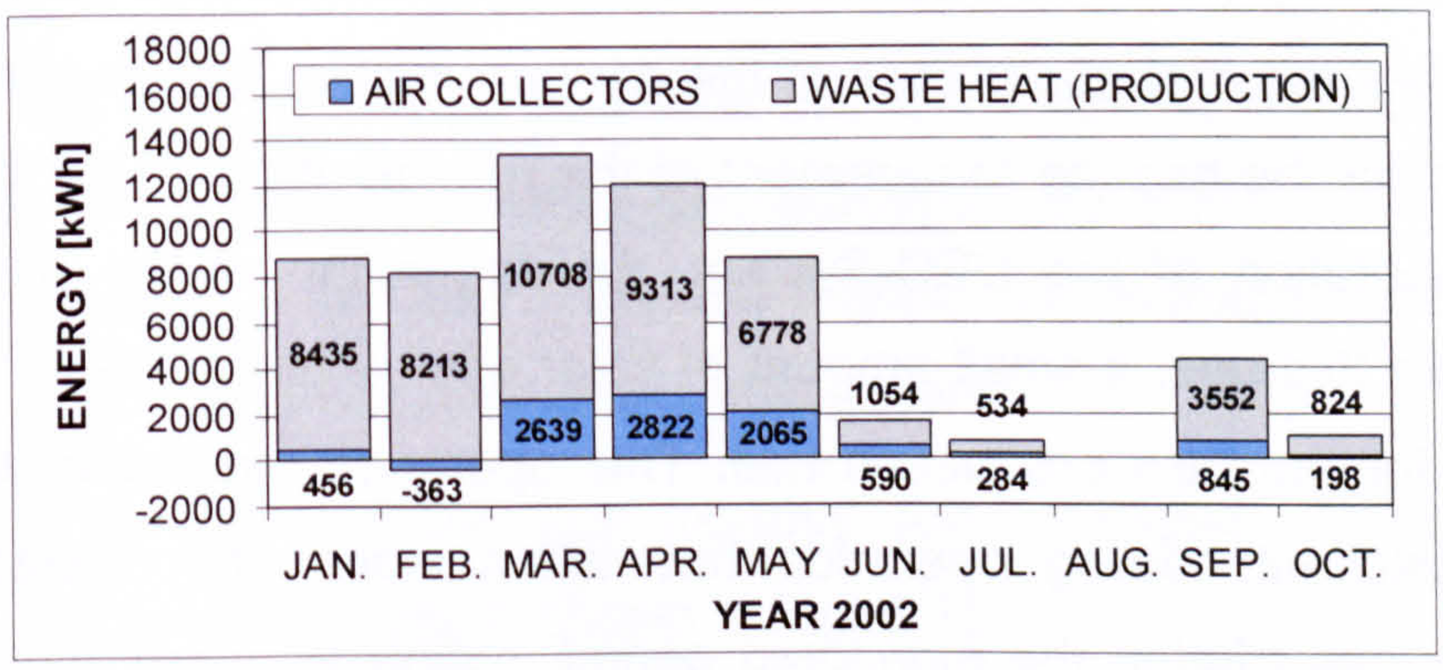

Fig. 8.13: *Supplied energy for the air heating system*

It can be seen that the collector gain was very low in the winter. In February, the collector gain was even negative. Negative collector gain means that the inlet air temperature at the collectors must had been higher than the outlet temperature, thus heat was actually dissipated by the collectors. This can most likely be explained by a malfunction in the control system or a non-suitable control strategy for the collector operation. A detailed analysis of the collector operation is given in the next paragraph.

In addition, it can be seen that the air heating system was also operating during the summer months (except August), during which time usually no heating operation is to be expected. Double-checking the monitored room temperatures, it was determined that the required temperature level on the first upper floor was reasonable for the air heating operation in the summer. The control strategy for the air heating system requires a temperature on the upper floor of between 22°C and 24°C. The monitored data shows that the room temperature even in the summer months remained at the lower limit of 22°C, usually in the early mornings, which caused the control system to demand heat. In contrast to the first upper floor, the old storage hall is heated only to a temperature level of 12°C to 15°C. For this portion of the building, no heating was required during the summer.

8.6.4 SOLAR AIR COLLECTORS

The energy gained by the solar air collectors is mainly used for the air heating system (which supplies the first upper floor of the new production hall and the old storage hall) and for the heating requirement of the regeneration air for the desiccant cooling operation of the DEC-System. An evaluation of the data shows that aside from this use, a small amount of solar energy is also used to heat the supply air for the new production hall. This operation mode usually occurs after full desiccant cooling operation has taken place at moderate ambient air temperatures (during the monitored period, mainly in June), when the supply air temperature went under the lower limit of 17°C. Furthermore, a

significant amount of energy was supplied by the collectors, even when no heat was needed by the system at all. This operation mode usually occurred when there was a change in the operation mode from regeneration to cooling with humidifiers only or to free ventilation. Thus in the months from May to August the collector was often flown for long time periods and the energy that was obtained was not used. However, considering that there is no possibility for energy storage with the solar air collectors, this operation is not really disadvantageous. Moreover, considering the lower pressure drop in the regeneration channel when the air collectors have airflow (if the collector bypass flap is also open), this could even be advantageous for the energy consumption of the fan. The operation time of the collectors during the different operation modes is shown in Fig. 8.14.

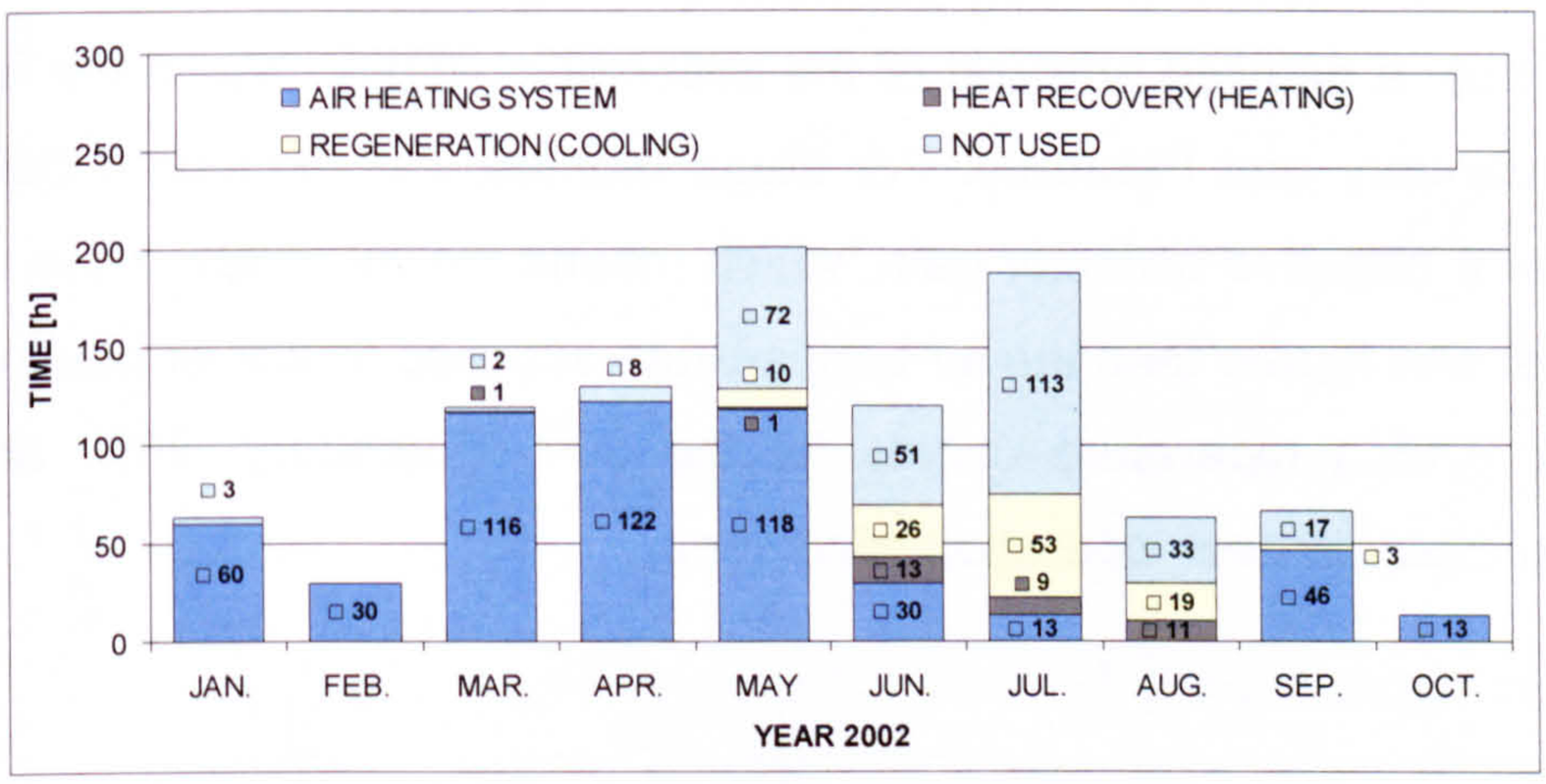

Fig. 8.14: *Operation times for use of collector gain for different operation modes*

The monthly energy from solar irradiation (on the horizontal and on the collector surface) and the collector gain during the different operation modes is shown in Appendix F for each separate month. The average collector efficiency for the different operation modes is also shown.

An overview of the total monthly solar irradiation, the collector gain and the collector efficiency is shown in Fig. 8.15.

08 Monitoring Of A DEC-System In A Plastics Processing Factory

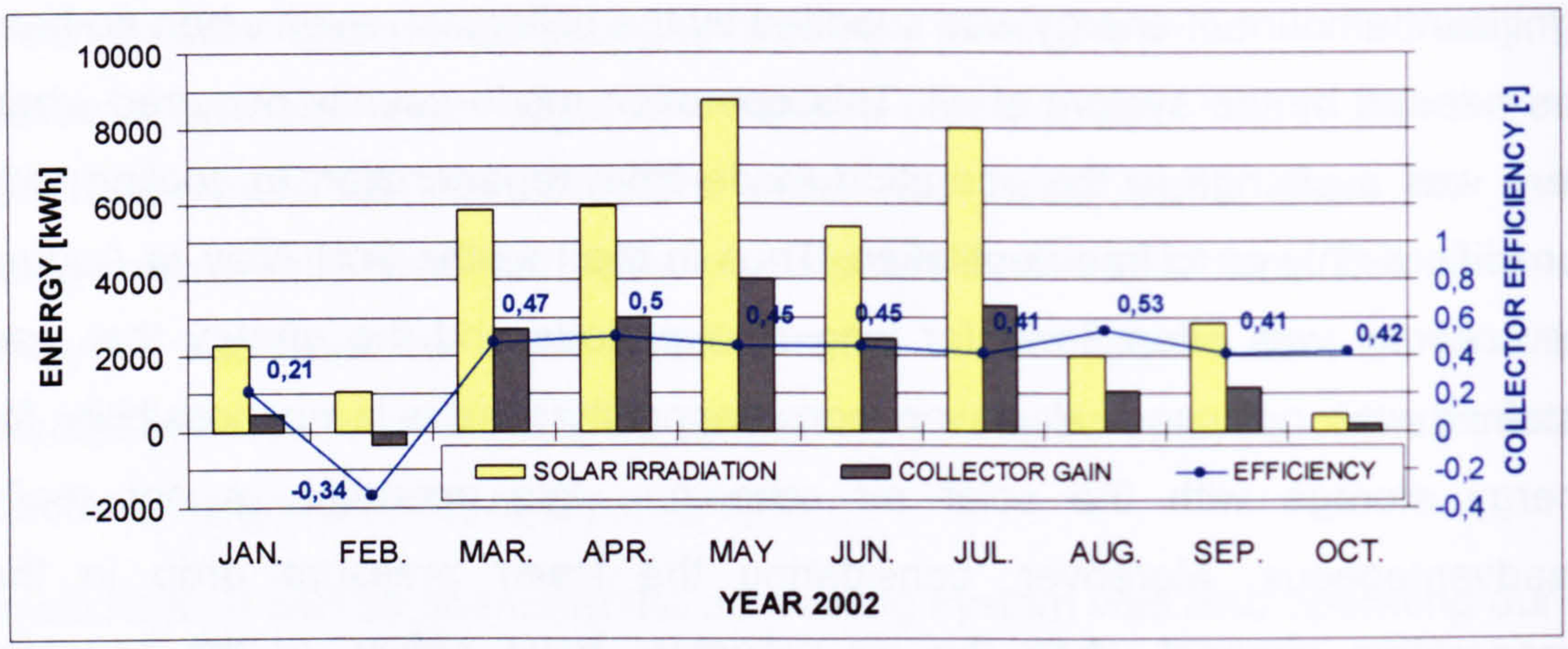

Fig. 8.15: *Solar irradiation on the collector surface (100 m²), collector gain and collector efficiency during collector operation*

It can be seen, that the collector efficiency in January, at a value of only 0.21, was very low. In February, the efficiency assumed a negative value. To find an explanation for this, a detailed analysis of the collector operation was done for the months of January and February. For these months, the monitored data sometimes show a negative collector gain, which means the air temperature at the collector inlet was higher than the air temperature supplied to the air heating system. In Fig. 8.16, temperature curves for the 30th of January, 2002 are shown as an example of these operation conditions.

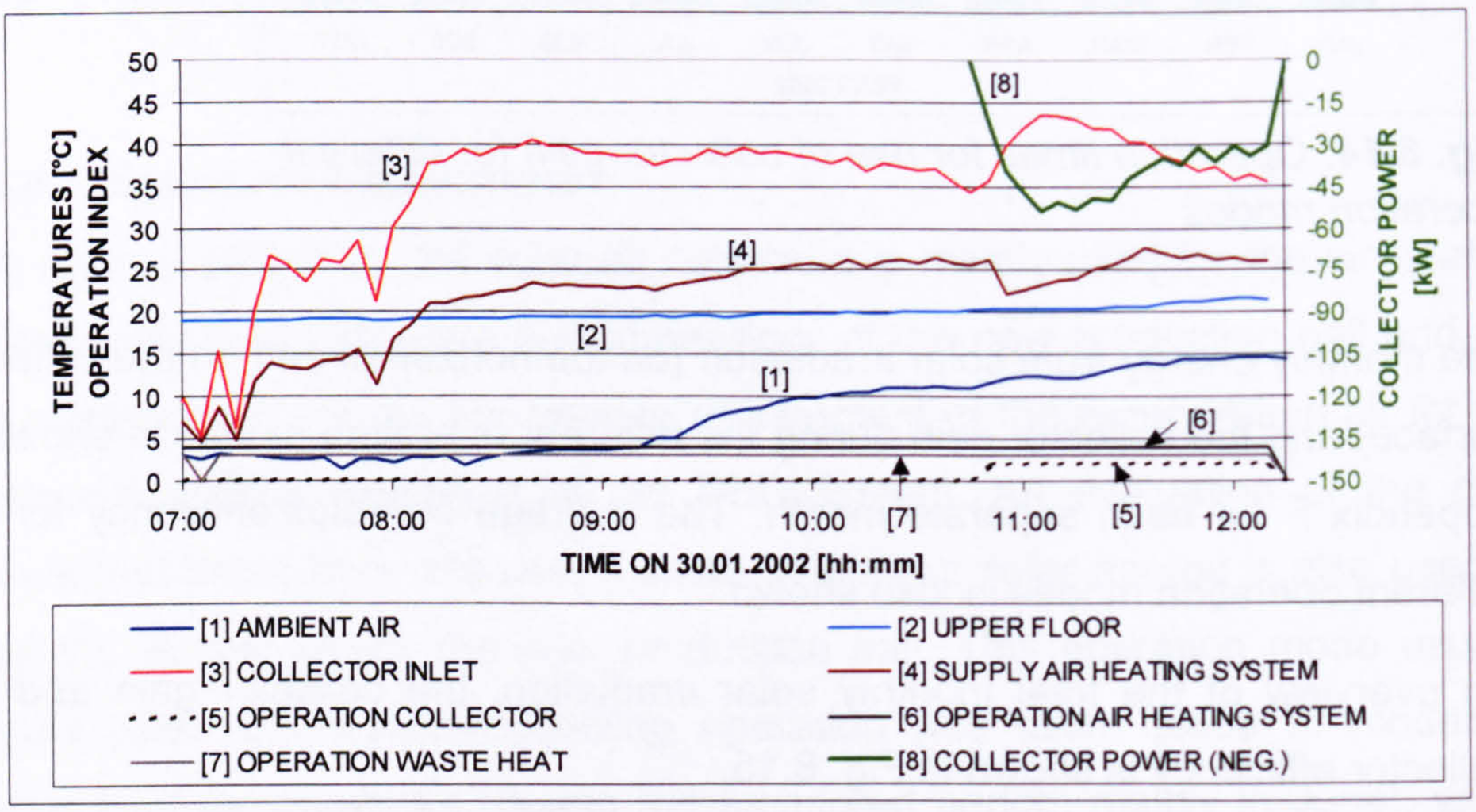

Fig. 8.16: *Temperature curves and (neg.) collector gain on 30th of January 2002*

Curve [6] shows that the air heating system was working for the whole recorded time, the waste heat recovery from the processing machines operated continuously from 7:15 a.m. on (curve [7]) and the collectors started operation at about 10:45 a.m. [curve 5].

First of all, the deviation between the temperature curves of the collector inlet [3] (corresponding to the air temperature after waste heat recovery) and the provided supply air temperature for the air heating system [4] is significant. Before 10:45 a.m., when the collectors were not yet operating, these values should have been almost equal. As the deviations are too big to be explained by heat loss to the surroundings or by a measuring inaccuracy of the installed sensors, a closer look was taken at the collector operation. In Fig. 8.17, the collector volume flows for each collector field are shown with the corresponding outlet temperatures.

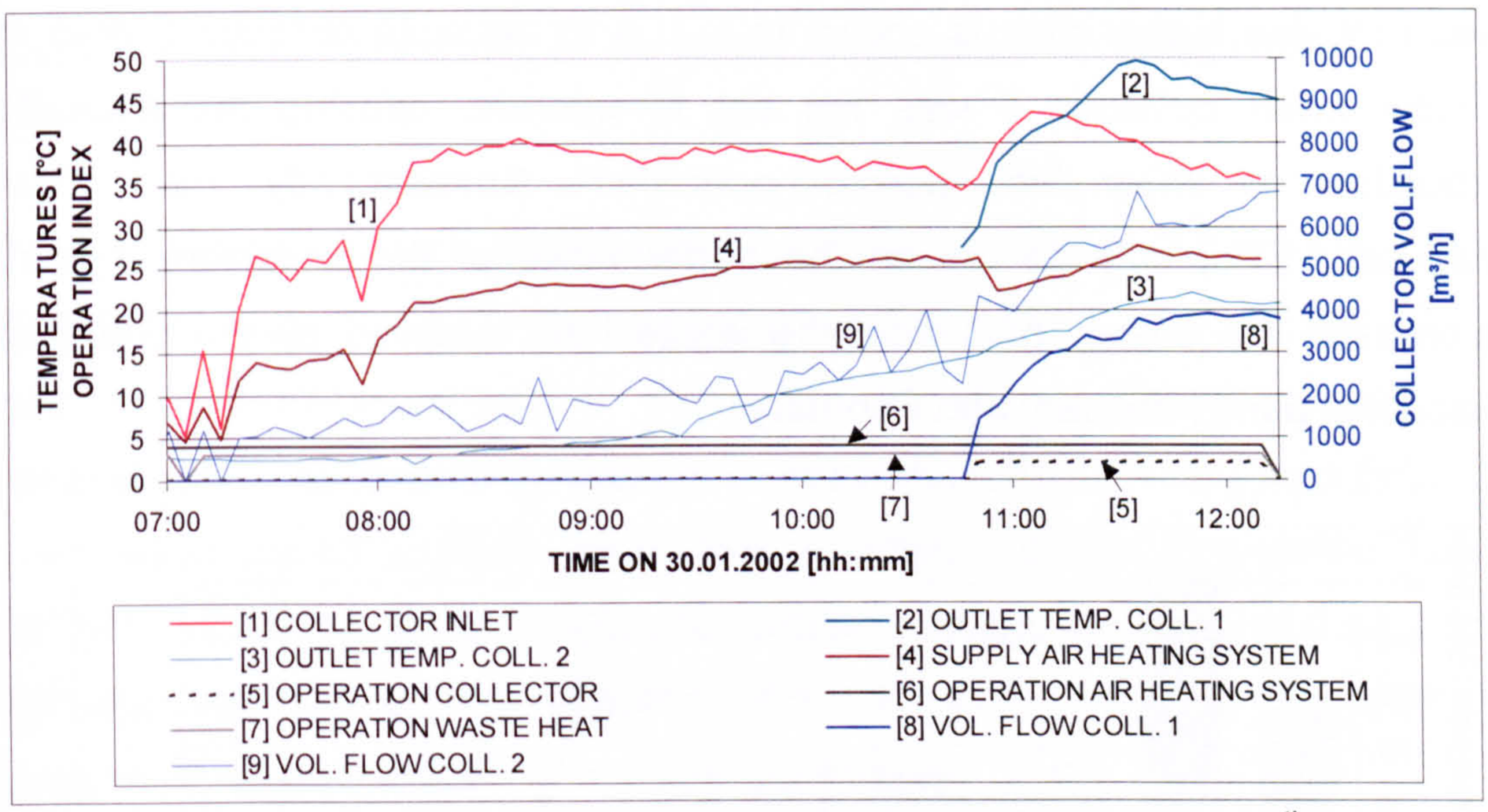

Fig. 8.17: *Collector volume flows and in-/outlet temperatures on 30th of January 2002*

For collector 1, the surface temperature of which is used for the control strategy, the operation started as expected at 10:45 a.m. and then provided reasonable outlet temperatures to the air heating system. An examination of the other collector field however shows that a malfunction occurred (probably with a

collector flap), which obviously caused the monitored negative collector gains. This collector field had airflow continuously starting at 7:15 a.m., a time at which surely no solar irradiation was actually present. This malfunction explains why the displayed temperature curves of the collector inlet and the provided supply air temperature for the air heating system deviate so much, even if the control strategy did not require collector operation. In addition, during collector operation (which started at 10:45 a.m.) the volume flow through collector 2 was much higher than that of collector 1, which resulted in significantly lower temperatures at the outlet of collector 2.

The malfunction "disappeared" during the holidays in February, and from March on, the collectors operated well.

In Fig. 8.18, the observed energy loss during collector operation is shown. Here it must also be considered that the real energy loss caused by the malfunction was probably higher than is shown in Fig. 8.18 because collector 2 also had airflow when collector 1 was not set to operate, causing the evaluation procedure to show "no collector operation". Consequently, the collector malfunction not only decreased the performance of the collectors, but also decreased the energy gain from the waste heat supplied by the processing machines during January and February.

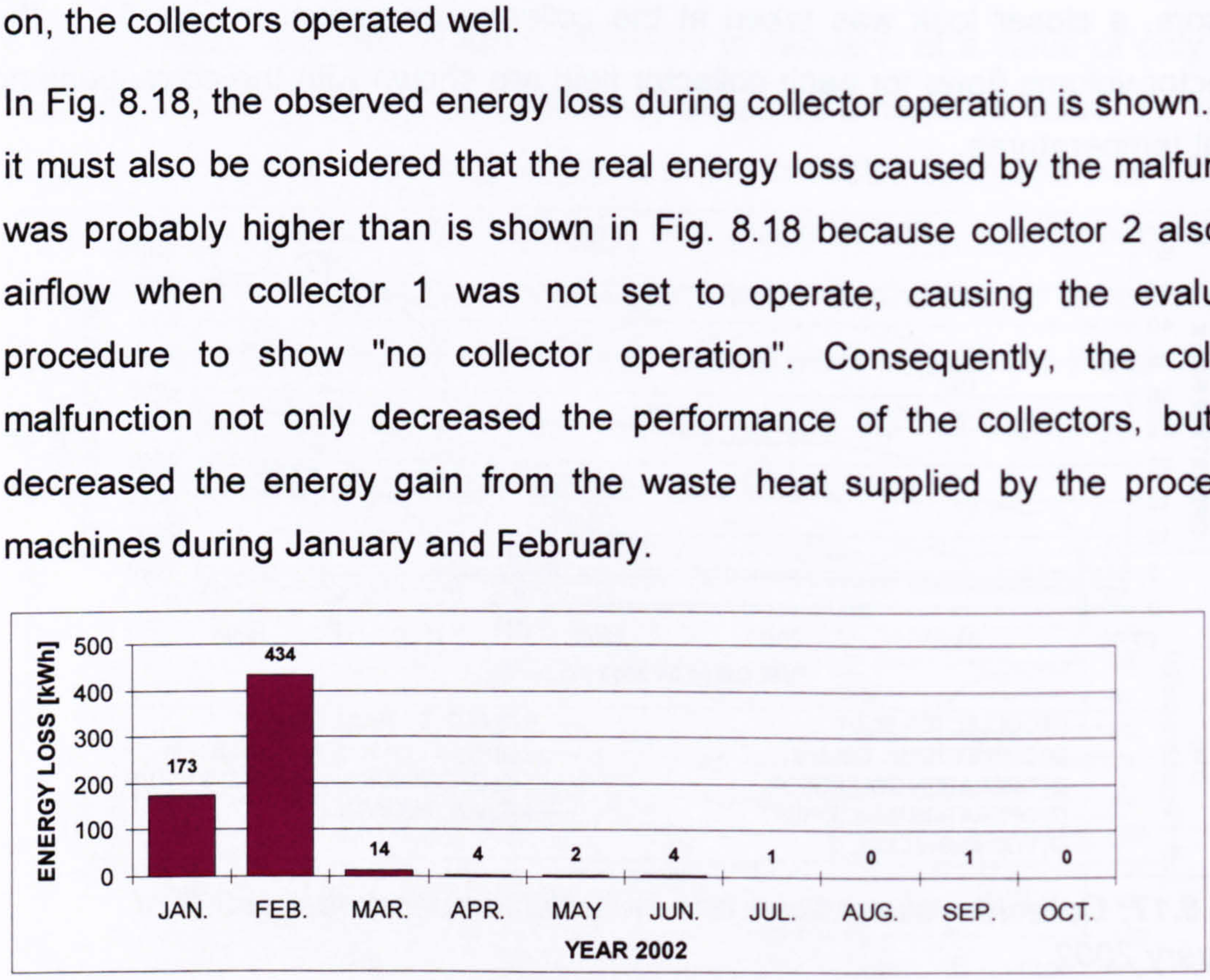

Fig. 8.18: *Observed "energy losses" during collector operation*

Thus, without the collector malfunction, the already large share of waste heat use for the air heating system would have been higher once again in January and February. The small energy losses from March to October were caused by

short operation conditions that occurred due to changes in the operation modes and are not significant to the energy evaluation (as the losses are smaller than 0.5% of the gains).

In Fig. 8.19, the collector gain and efficiency are shown for the individual operation modes for the monitored time period.

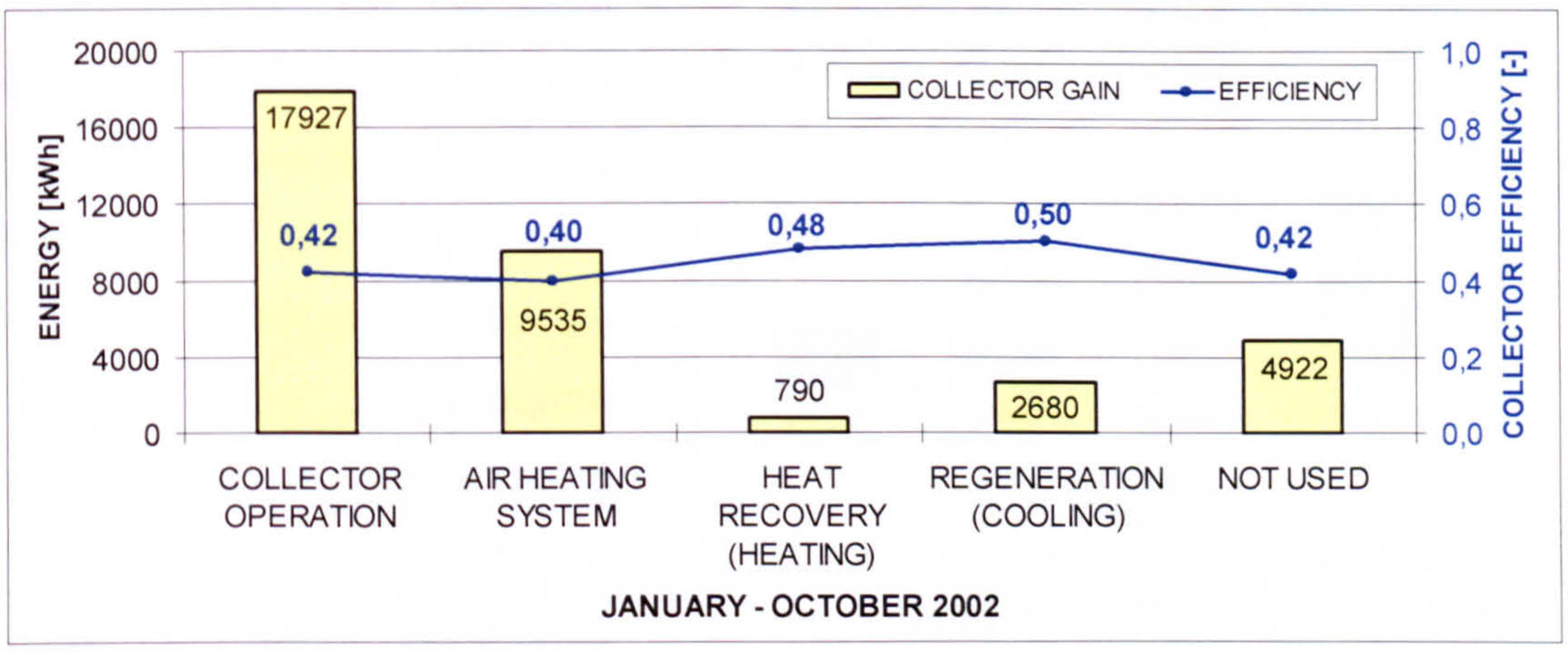

Fig. 8.19: *Overall collector gain for different operation modes, collector efficiency*

Altogether the observed collector gain for the monitored period from January to October was about 18000 kWh with an average efficiency of about 0.42. The relatively low efficiency of 0.40 during the air heating system operation was caused mainly by the malfunction of collector field 2 in January and February. The "actually used" collector gain (without collector gain during period marked as "NOT USED") is about 13000 kWh with an average efficiency of 0.42. During full desiccant cooling (regeneration), only 2680 kWh of energy was produced, however the average COP of 0.5 was satisfactory.

8.6.5 DEC-SYSTEM

OPERATION MODE

A detailed monthly analysis of the component operation times and the single operation modes of the DEC-system have already been shown in paragraph 8.6.2 and Appendix E. The overall operation time of the DEC-system for the air-

conditioning of the new production hall during the evaluated time period from January to October 2002 is shown in Fig. 8.20.

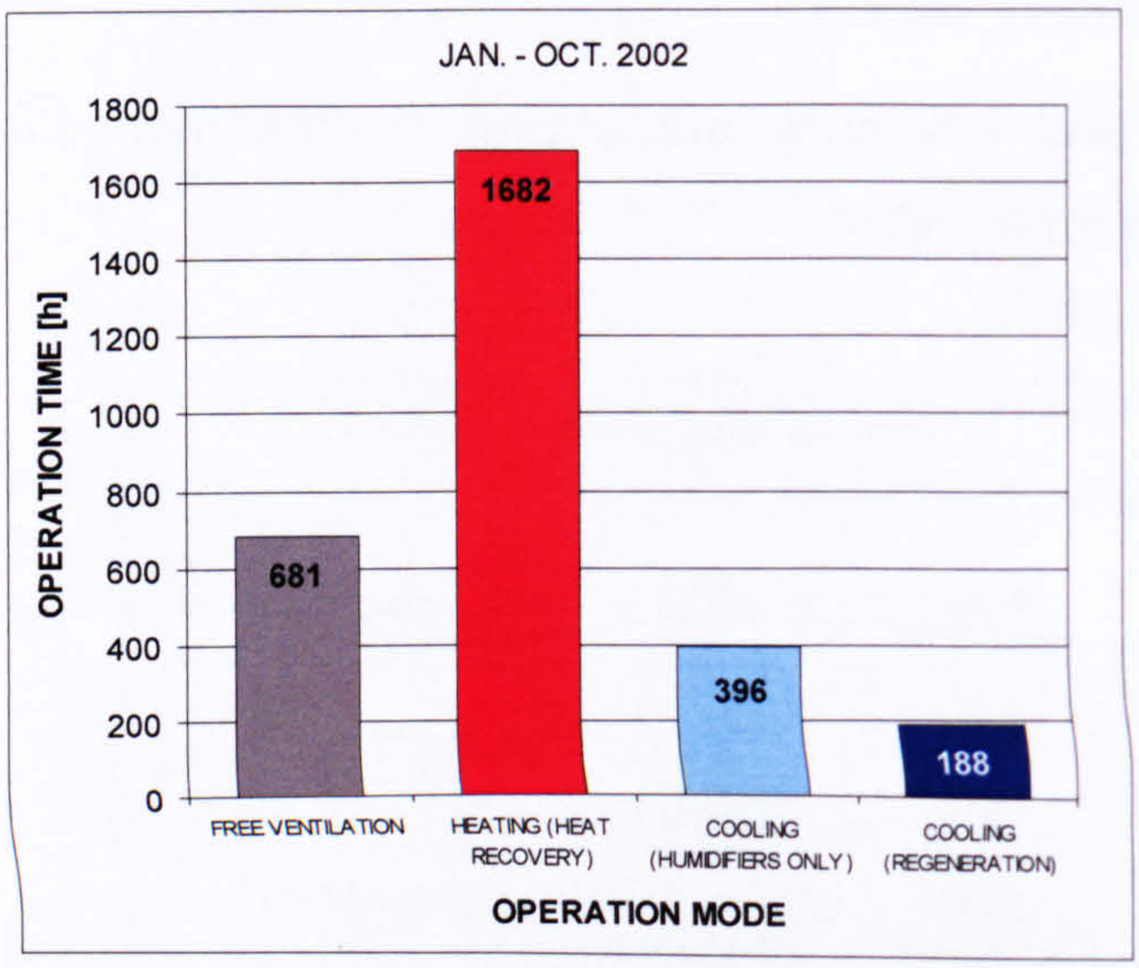

Fig. 8.20: *Overall operation time of the DEC-system for different operation modes*

Altogether about 2947 hours of the DEC-system operation was monitored and can be evaluated. Of this time, clearly more than half was taken up by heating operation by heat recovery from the room exhaust air at low ambient air temperatures. Additionally, for a significant amount of time the system was in the free ventilation mode, as active heating or cooling was not necessary at this time. For only 584 hours, which is about 20 % of time, active cooling (operation of humidifiers) was necessary.

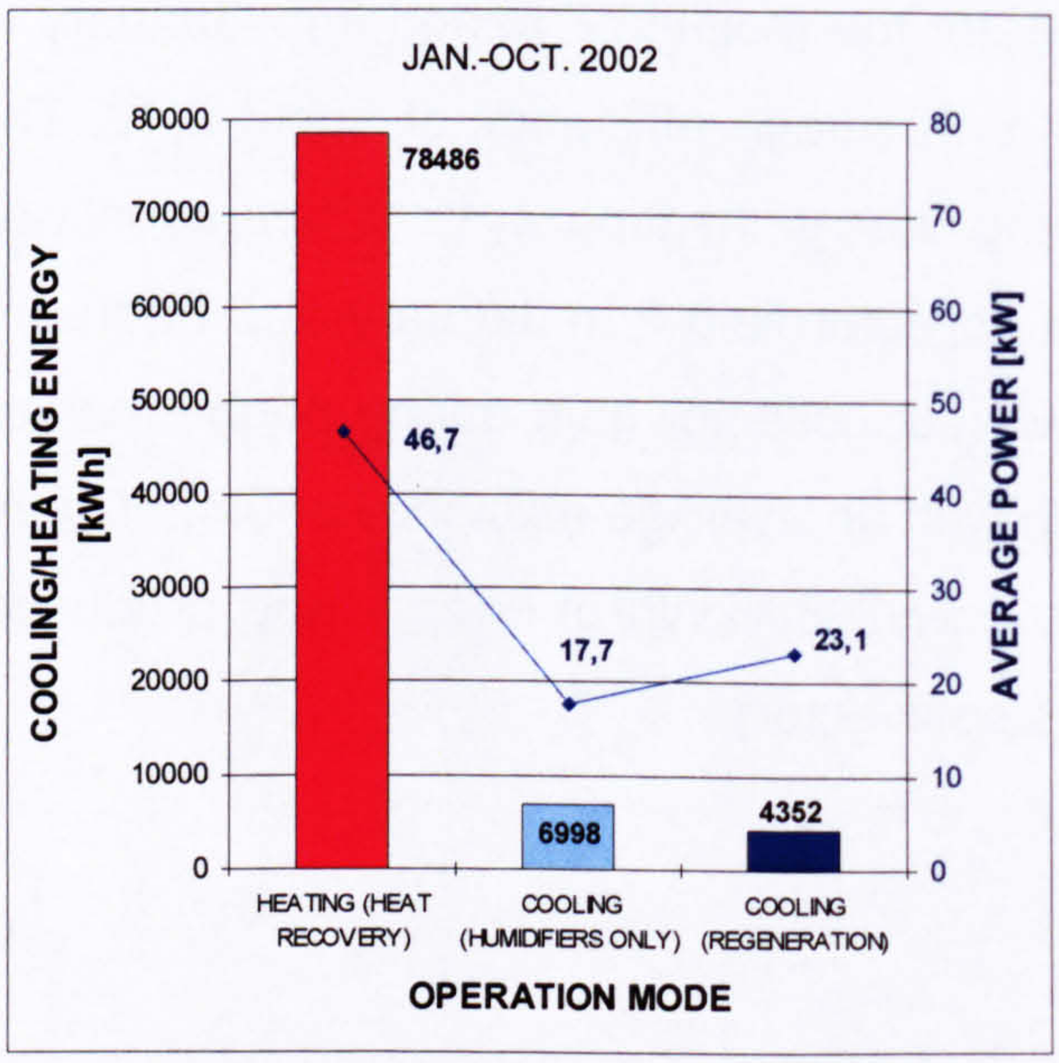

Fig. 8.21: *Heating/cooling energy supplied by the DEC-system. Averaged heating/cooling power*

The heating and cooling energy supplied by the DEC-system during the evaluated time period as well as the average heating/cooling power is shown in Fig. 8.21.

The depicted amounts of energy are calculated taking only sensible cooling into consideration (inlet - outlet air temperature difference), as the determination of the enthalpy is too unreliable (humidity measurements). Altogether 78486

kWh of heat were recovered from the exhaust air for heating operation with an average heating power of 46.7 kW. The supplied cooling energy was only 11350 kWh, of which 6988 kWh were supplied by the humidifiers alone and 4352 kWh by full desiccant cooling operation (regeneration). The average cooling power was 17.7 kW for cooling with the humidifiers only and 23.1 kW for full desiccant cooling operation. The ratio between the heating and cooling shows that despite the internal loads in the production hall, the heating demand was much higher than the cooling demand, which was required only during 20% of time in the year.

COOLING PERFORMANCE

The monthly relationship between the cooling energy supplied by the humidifiers only and by full desiccant cooling operation is shown in Fig. 8.22.

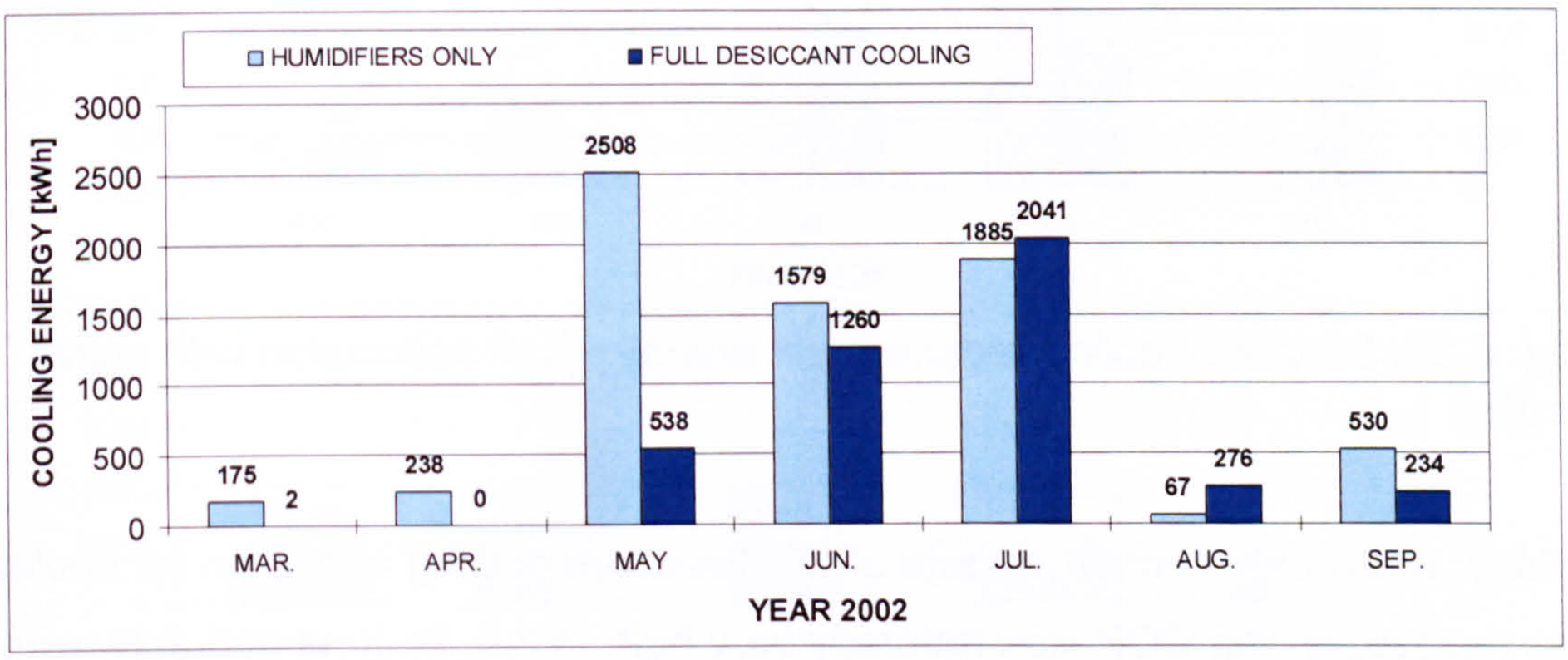

Fig. 8.22: *Relationship between the cooling energy supplied only by the humidifiers and the full desiccant cooling operation (regeneration)*

In March and April the cooling demand was relatively low and could be supplied almost completely by the humidifiers alone. In May the cooling demand was much higher, but could also be supplied mainly by the humidifiers alone. In June and July almost half of the cooling energy was produced by the humidifiers alone and half was supplied through full desiccant cooling operation. In August the supplied amount of cooling energy was very low because of the

holidays (only short operation times) and the cooling energy was supplied mainly by full desiccant cooling operation. In September, the cooling demand was relatively low and up to 70% of this demand was supplied by the humidifiers alone.

Thus active cooling was first monitored in March 2002, but significant cooling operation, which is meaningful for the evaluation, occurred from May to September. The monthly supplied cooling energy and the thus required regeneration energy is shown in Fig. 8.23. The COP (associated with active cooling) is also shown.

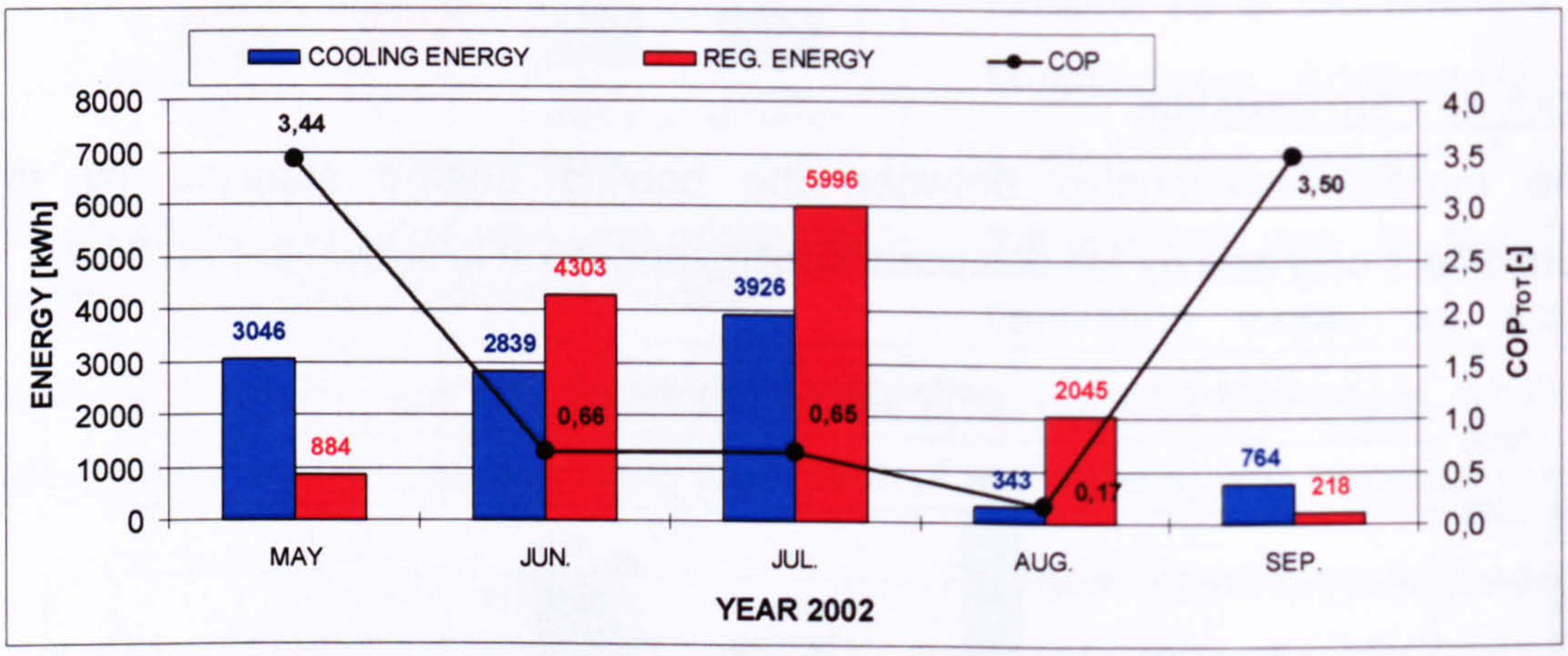

Fig. 8.23: *Supplied cooling/regeneration energy. COP associated with active cooling*

In May, when only a small amount of full desiccant cooling operation for cooling was necessary, the COP was naturally very high at 3.4. In June and July, when the cooling energy was almost half supplied by full desiccant cooling operation, the COP decreased to about 0.7. In August, when the cooling energy was supplied mainly by full desiccant cooling operation, the COP was very low at 0.2. Finally, in September the COP was once more very high at 3.5. It is notable that in September, when about 30 % of the cooling energy was supplied by full desiccant cooling operation, the COP was higher than in May, at which time only 18 % of the cooling energy was supplied by full desiccant cooling operation. This can be explained by the behaviour of the user, who disabled the

auxiliary heating in September because the oil consumption was too high during the summer.

The average COP from May until September was 0.81 with a supplied cooling energy of 10918 kWh and a required regeneration energy of 13446 kWh. A main feature of the desiccant cooling process is that heating energy is only required for full desiccant cooling operation and that cooling with humidification only does not require additional energy. Thus the COP approaches infinity if the humidifiers provide sufficient cooling power.

When considering the relationship between the regeneration energy and the cooling energy supplied during full desiccant cooling operation only, it can be seen that the COP is naturally lower than the value shown above. The monthly supplied cooling energy from full desiccant cooling operation, the regeneration energy and the COP associated with full desiccant cooling operation is shown in Fig. 8.24.

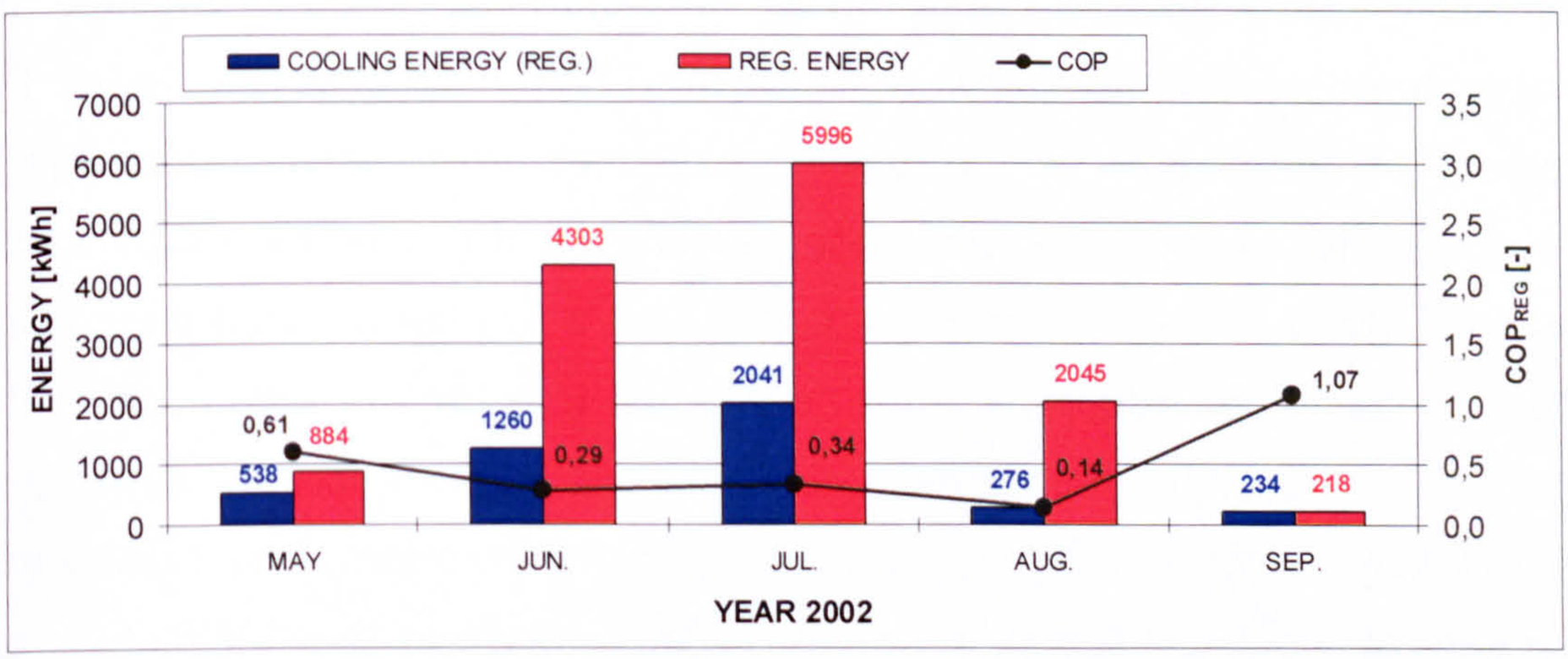

Fig. 8.24: *Supplied cooling energy (during regeneration)/regeneration energy. COP associated with regeneration cooling only*

In May the COP associated with full desiccant cooling operation was 0.61. The average ambient air temperature during regeneration was 23.3°C and the average supply air temperature was 16.6°C. For this cooling power (average temperature decrease of 6.7 K) an average regeneration air temperature of only 46.8°C was sufficient. This relatively good performance was surely contributed

by the relatively low absolute humidity of the ambient air and thus only a little dehumidification was needed during the full desiccant cooling operation.

In June the COP associated with regeneration operation was very low at 0.29. The average ambient air temperature during regeneration was 24.9°C and the attained average supply air temperature was only 21.0°C. Thus the temperature decrease that was reached was only 3.9 K. The reason for this poor efficiency was a malfunction of the exhaust air humidifier which began operating on the 21st of June. Due to this malfunction, the regeneration air was heated to a maximum temperature (average regeneration air temperature in June was 55.7°C) and thus consumed a large amount of auxiliary heating energy. Without this malfunction, the COP in May and June would surely have been higher.

In July, although the malfunction of the exhaust air humidifier was removed, the COP was quite low at 0.34. This can be explained by the relatively low ambient air temperatures (22.1°C in average) during the full desiccant cooling operation. Principally, DEC-systems work more efficiently at higher ambient air temperatures (design temperature is usually 32°C) because the lower the ambient air temperature is, the lower the reachable temperature decrease is with the same use of regeneration energy. This is not caused by a significantly lower efficiency of the dehumidification process, but rather a worse pre-cooling effect by the room exhaust air due to a small temperature difference in the rotary heat exchanger. Additionally, the absolute humidity in July was higher than in May, which is also disadvantageous for the performance (associated with sensible cooling). The supply air temperature that was reached in July was 18.0°C on average. The average regeneration air temperature was 48.8°C.

In August the COP associated with full desiccant cooling operation was very poor at 0.14. Again this was caused by the very low ambient air temperatures and the high humidity. The average ambient air temperature was only 21°C during desiccant cooling operation and was thus once again lower than it was in July. The temperature decrease of the supply air that was attained was only about 1.5 K on average. The average regeneration air temperature was 47.2°C.

The COP associated with full desiccant cooling operation in September was 1.07, which is very good, especially with the low average ambient air temperature of 21.7°C during desiccant cooling. This high COP is mainly caused by the behaviour of the user who deactivated the auxiliary heating in September because of the high oil consumption during summer operation. With the resulting low average regeneration air temperature of only 33.6°C, the dehumidification capacity was very low, but because of the low humidity of the ambient air, it was sufficient for an effectively working supply air humidifier.

The average COP for full desiccant cooling operation from May untill September was only 0.32 with a supplied cooling energy of 4349 kWh and a required heating energy of 13446 kWh. This low COP was caused for one by a malfunction of the exhaust air humidifier, but mainly by full desiccant operation at relatively low ambient air temperatures.

REGENERATION ENERGY

In Fig. 8.25, the monthly operation times of regeneration and the time of operation of each heating device is shown.

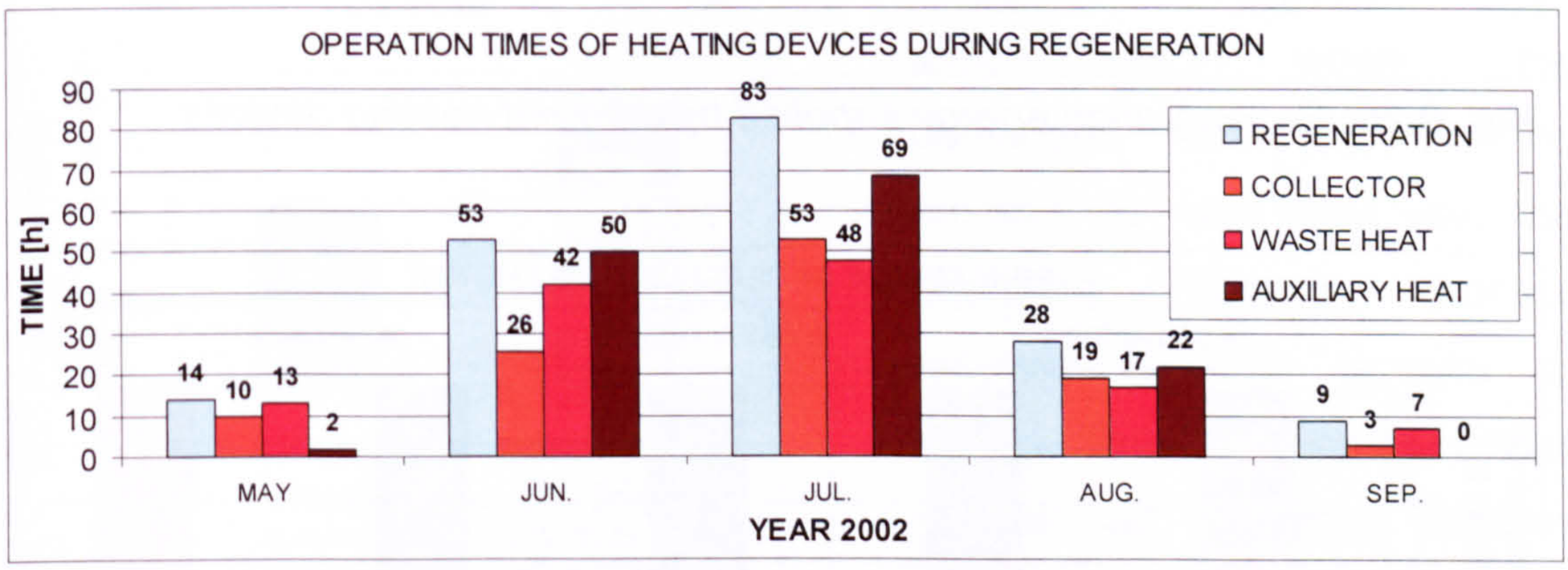

Fig. 8.25: *Monthly operation times of regeneration and the time of operation of each heating device*

The regeneration energy is supplied by solar air collectors, waste heat use from processing machines and, if required, by an oil burner (auxiliary heater). The auxiliary heater was planned for use only if the required temperature level of the

regeneration air is not reached by the solar air collectors and the waste heat use.

In May the regeneration time was only 14 hours. Most of this time the collector gain and the waste heat use was sufficient and auxiliary heating was only necessary for two hours. In June the regeneration time was much longer. It is notable that auxiliary heating was used almost the whole regeneration time, which is caused by the malfunction of the exhaust air humidifier (see above). In July and August as well, the time period in which the auxiliary heater ran was very long. In September auxiliary heating was deactivated by the user.

In Fig. 8.26 and Fig. 8.27, the amount of supplied regeneration energy and the percentage of each heating device is shown respectively.

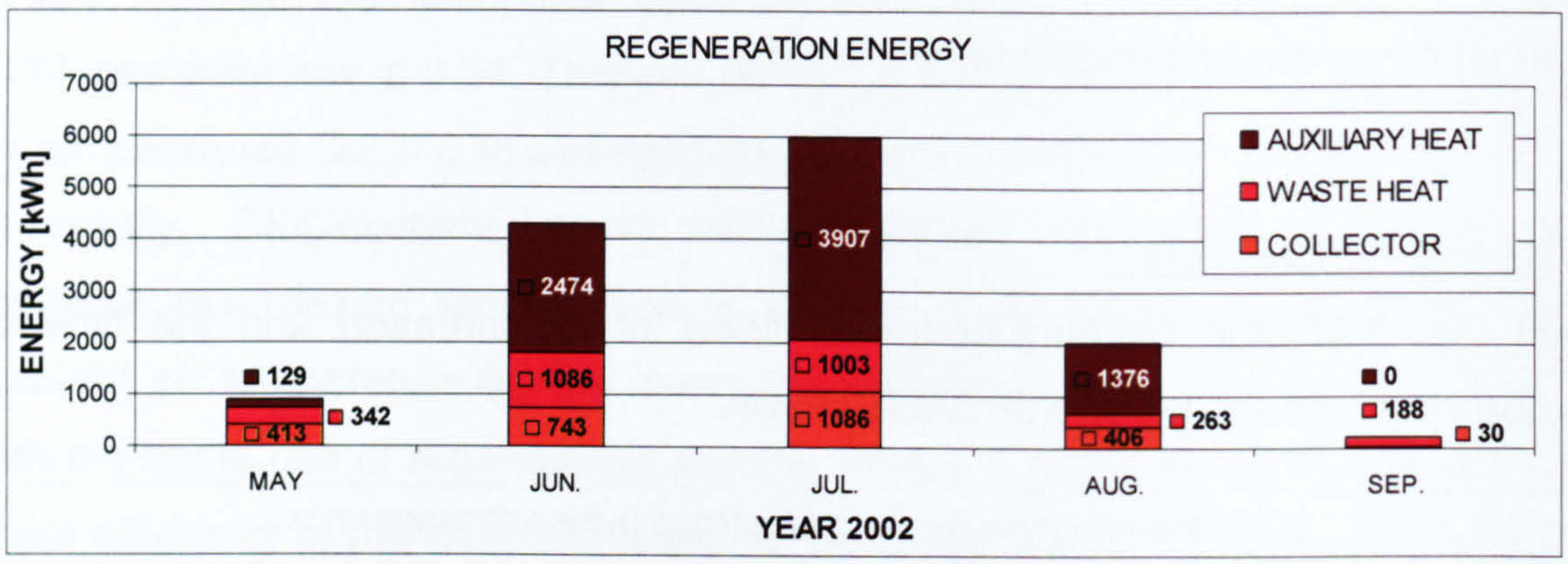

Fig. 8.26: *Regeneration energy supplied by different heating devices*

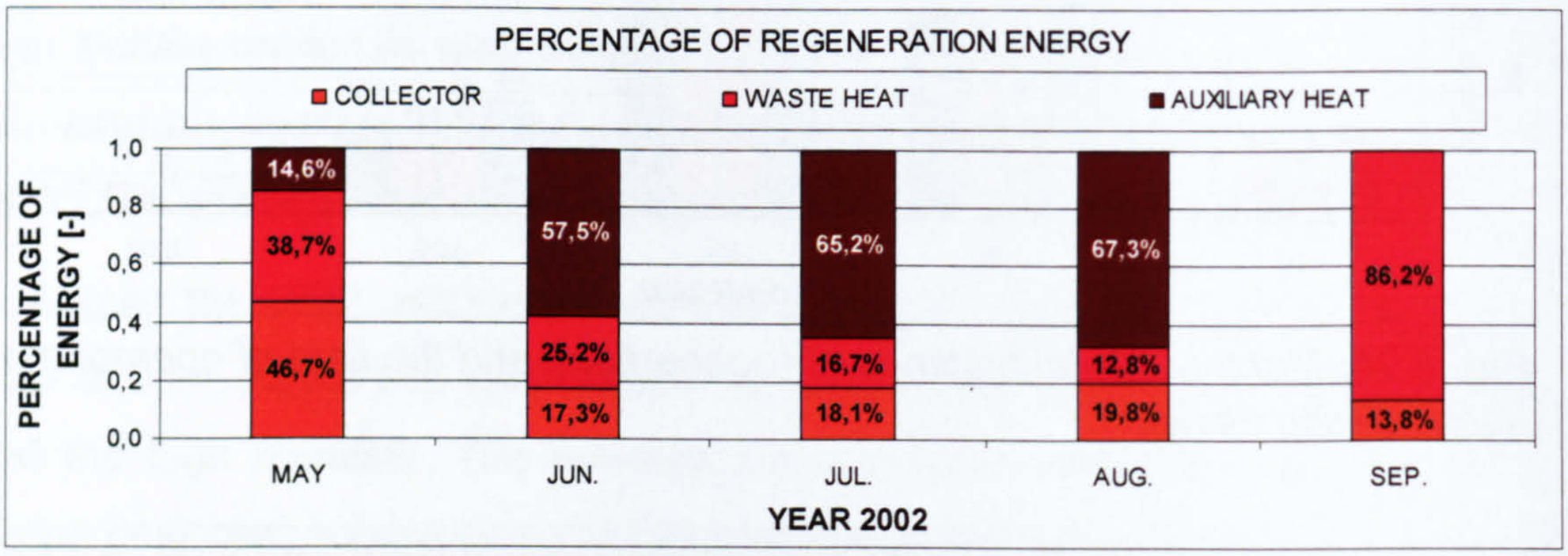

Fig. 8.27: *Percentage of energy from the different heating devices*

It can be seen that from June to August, when solar irradiance should be expected to be the highest, the collector contributed less than 20 % to the regeneration energy. Additionally, the large portion of auxiliary heating energy shows that the oil burner is not really used as a backup system for rarely occurring boundary conditions but seems vital for full desiccant cooling in the summer at relatively low ambient air temperatures. But note: additional investigations in chapter 09 will show that the high amount of auxiliary energy would not have been necessary for satisfactory system performance. This is also demonstrated by the system operation in September, as auxiliary heating was disabled by the user.

An interesting fact is that much of the auxiliary heating energy was consumed when outside temperatures were rather low. Thus for example, in July (see Fig. 8.28) 3906 kWh of regeneration energy was supplied by auxiliary heating, and clearly more than half of this energy was supplied when the ambient air temperature was less than 20°C. 888 kWh were supplied at ambient air temperatures between 20°C and 25°C and only 838 kWh were supplied at ambient air temperatures over 25°C.

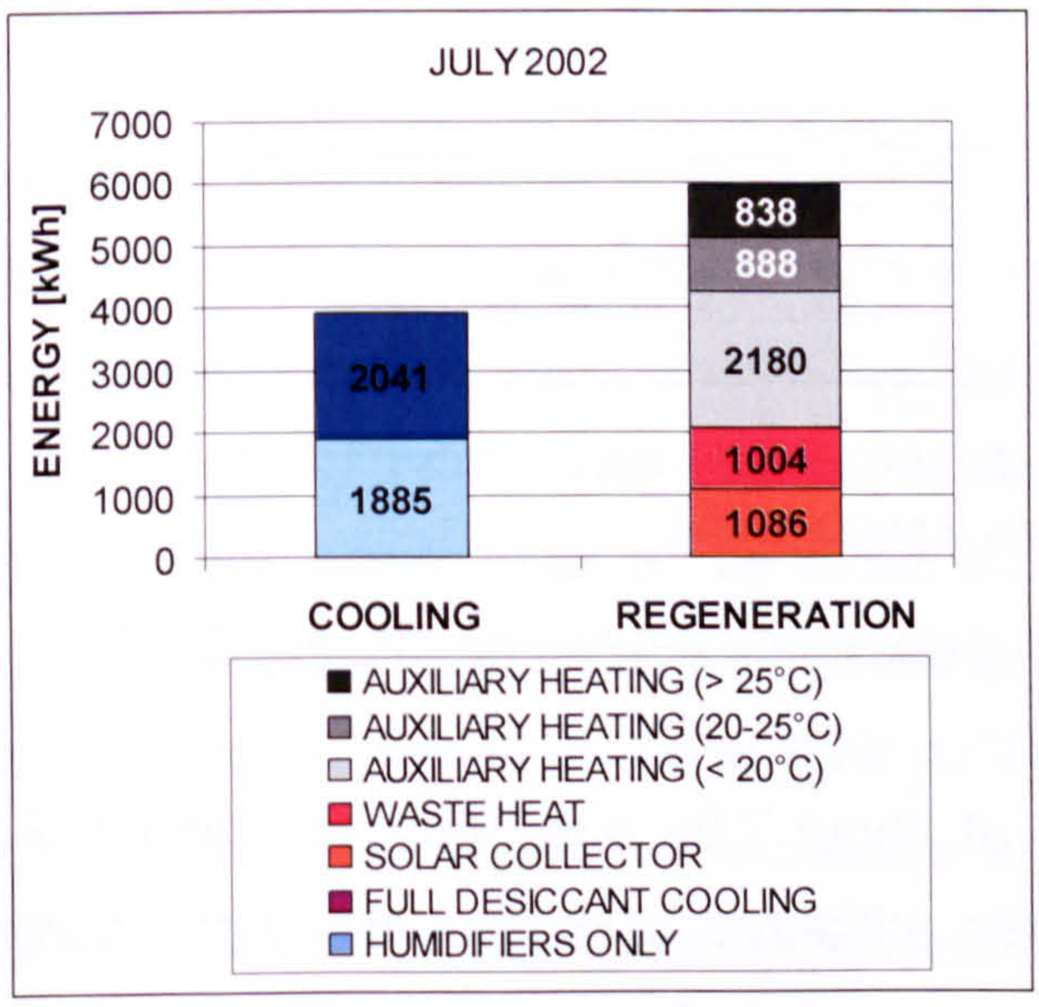

Fig. 8.28: *Regeneration energy supplied by different heating devices in July 2002*

Thus, at low ambient air temperatures, when the demanded reduction of the process air was only low, the desiccant cooling process required a large amount of energy. Thus for such conditions (partial load operation) auxiliary cooling would possibly be preferable instead of full desiccant cooling operation with a high energy demand. Altogether the supplied

regeneration energy from May to September was 13446 kWh with 2677 kWh (19.9%) coming from the collectors, 2882 kWh (21.4%) from waste heat use and 7887 kWh (58.7%) from auxiliary heating.

OPERATION UNDER DESIGN CONDITIONS

So far, mostly the monthly average values of the DEC-system have been evaluated, but not the operation under design conditions. For this purpose, a search was performed for a day in the monitored time period in which the boundary conditions came close to the design conditions (see. paragraph 8.2). Altogether there were only a few days with ambient air temperatures that were over 30°C and full desiccant cooling demand. Of these days, the 8th of July is the one that came closest to the design conditions and it is also the only day with continuous desiccant cooling operation of about 9 hours (from 8:25 a.m. to 17:30). The corresponding temperature curves are shown in Fig. 8.29.

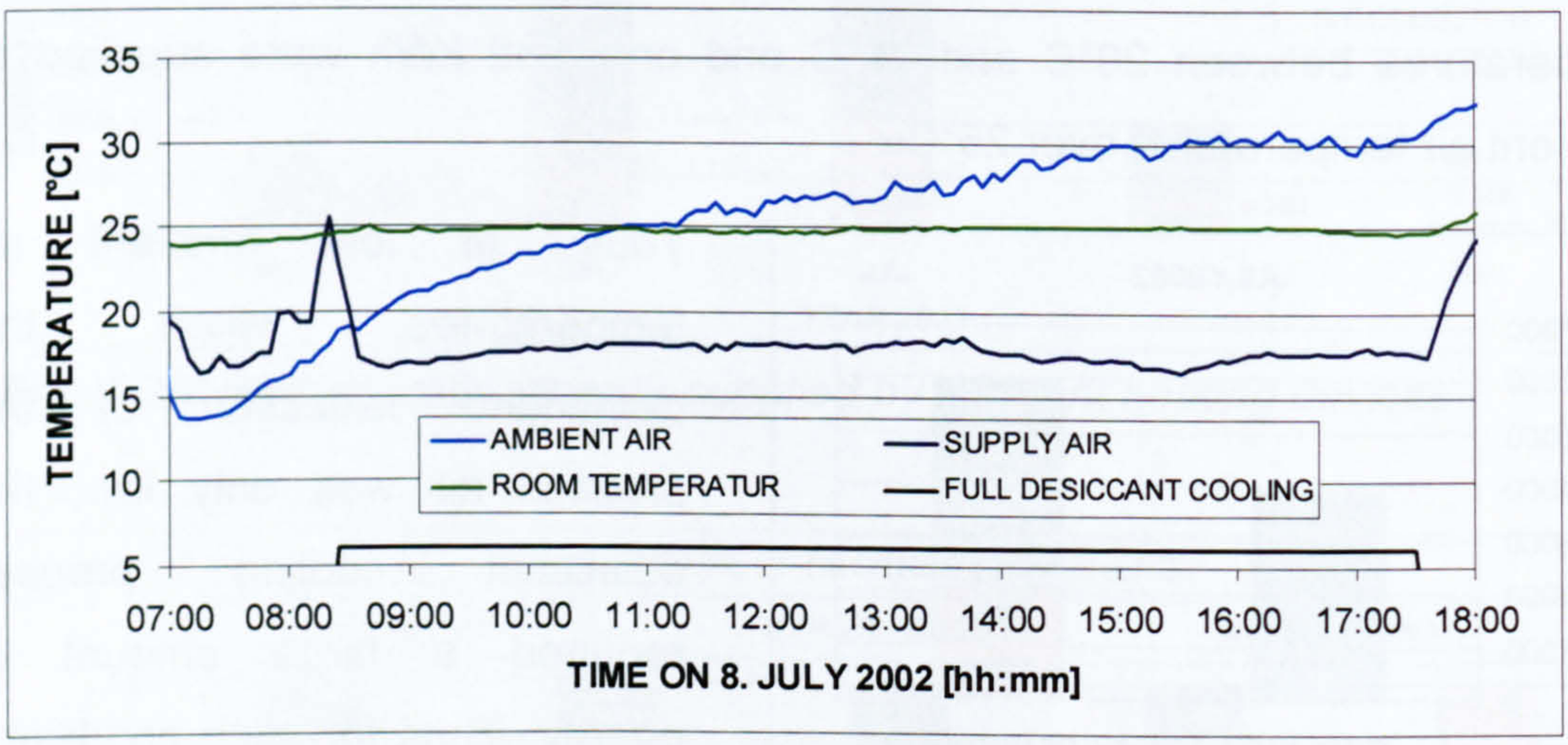

Fig. 8.29: *Related temperatures to full desiccant cooling on 08. July 2002*

The DEC-system started operation at about 7:00 a.m. (free ventilation). Full desiccant cooling operation was then initialized at 8:15 a.m. by the control system and took effect at 8:30 a.m.. A closer look on the initialization process and why the supply air temperature is increased at the beginning by this process follows in the next chapter. At 17:30, the DEC-system was completely

shut off. During the day the ambient air temperature rose up to a maximum of about 30°C at 15:00. The achieved supply air temperature was between 16.5°C and 18.6°C during full desiccant cooling. The room temperature could be kept at less than 25°C. Thus the desired supply air temperature was achieved for the whole time on this day, also when the temperatures outside exceeded 30°C. In Fig. 8.30, the achieved cooling power and the expended regeneration power is shown.

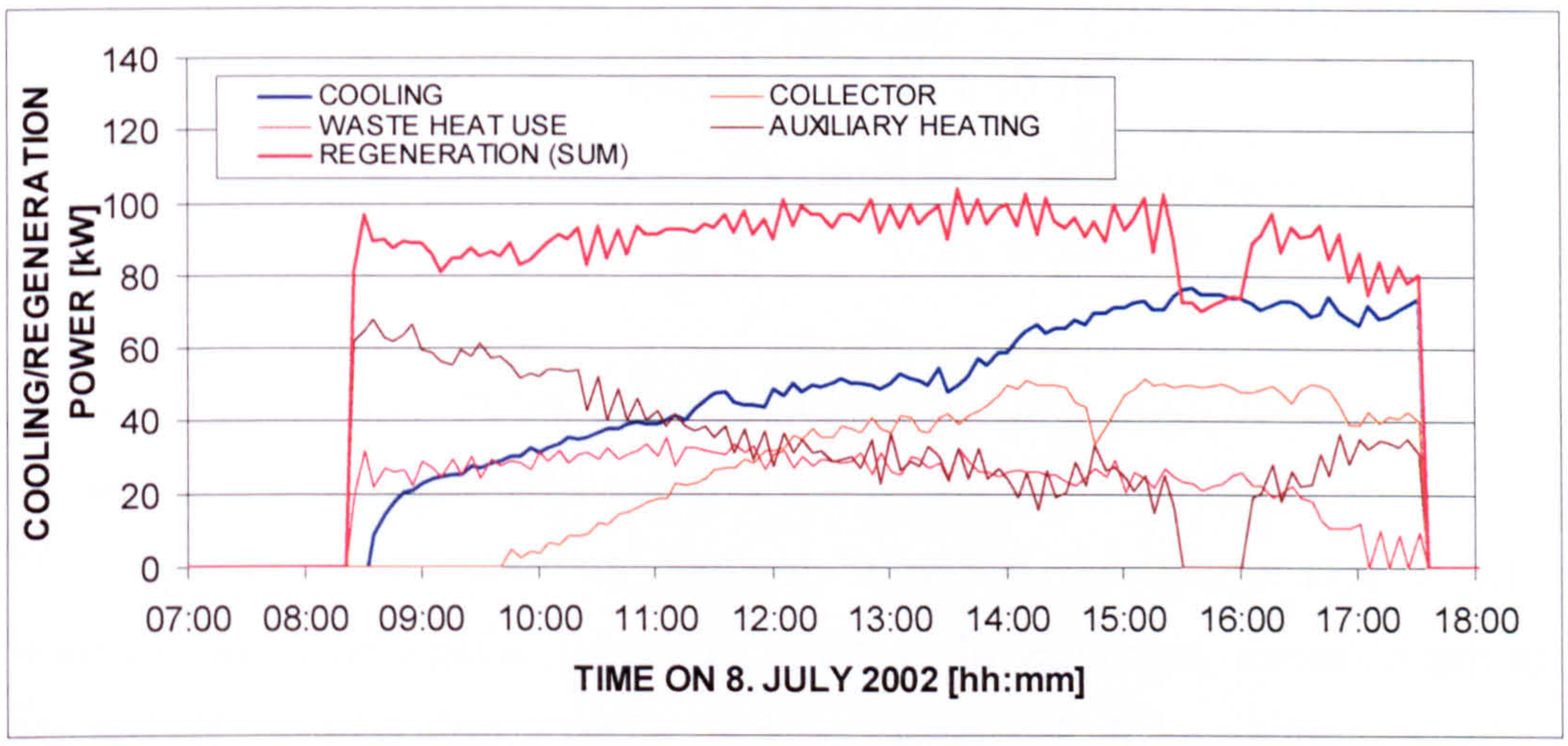

Fig. 8.30: *Cooling/regeneration power during full desiccant cooling on 8th of July 2002*

It can be seen that independent of the ambient air temperature (see. Fig. 8.29), the regeneration power used is almost constant (90 to 100 kW) during operation. The short decrease in the regeneration power at 15:30 is caused by the shut off of the auxiliary heating as the supply air temperature became a bit to low. The power obtained by waste heat use remained relatively constant at values between 20 to 30 kW as long as the processing machines worked continuously (until 16:00). The solar collector operation for regeneration started at 9:45 a.m. and the yield increased to a maximum power of about 50 kW starting at 14:00. In contrast to the used regeneration power, the cooling power increased until 15:30 to about 75 kW. In Fig. 8.31, the solar irradiation on the collector surface, the collector efficiency and the COP of the DEC-system associated with full desiccant cooling is shown.

08 MONITORING OF A DEC-SYSTEM IN A PLASTICS PROCESSING FACTORY

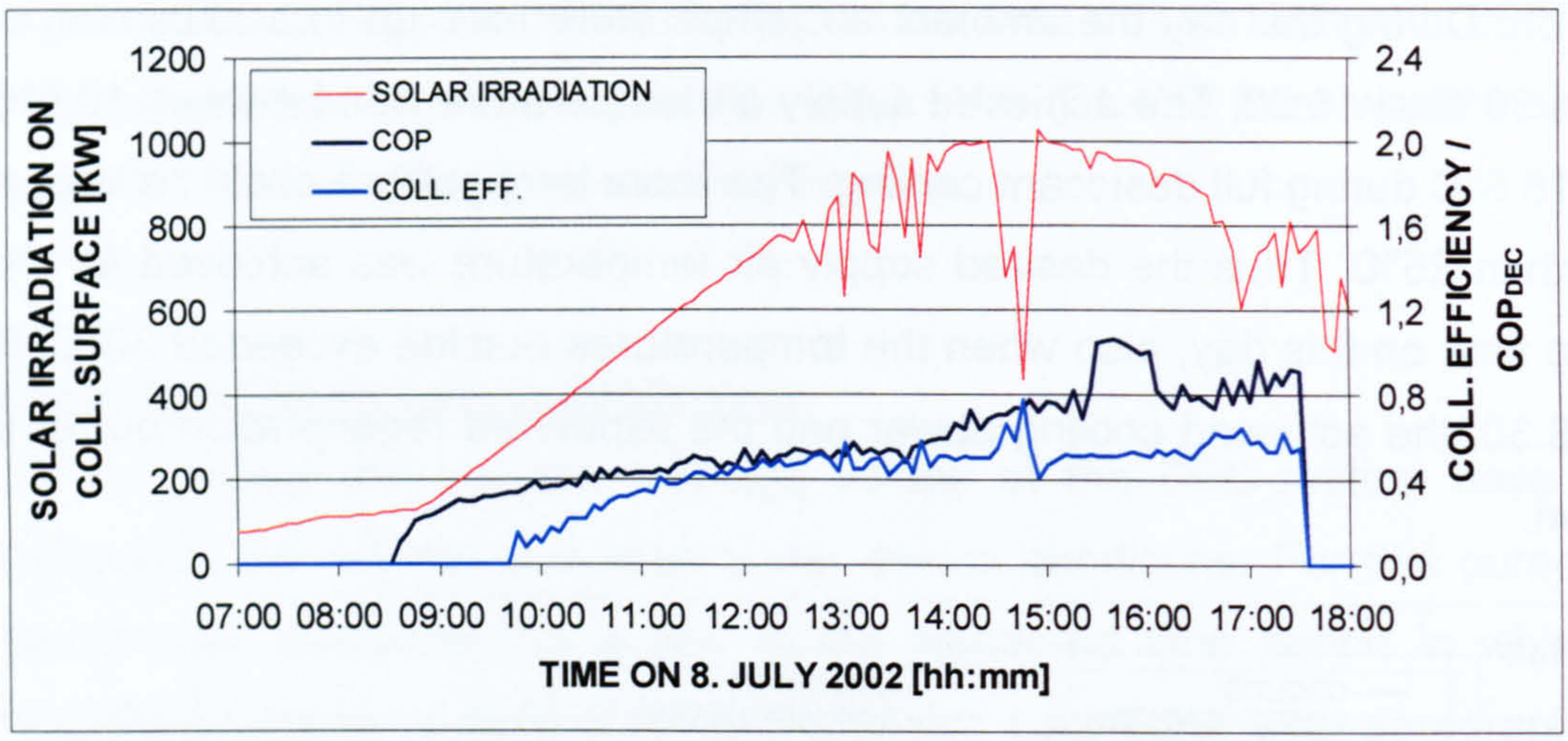

Fig. 8.31: *Solar irradiation, collector efficiency and COP during full desiccant cooling on 8th of July 2002*

The solar irradiation was only slightly influenced by clouds on this day and reached about 1000 W/m² at 14:00. The collector efficiency increased until about 12:00 p.m. and then remained relatively constant at about 50 %. The peak of the collector efficiency at 14:45 to about 80 % was only caused by the inertia (heat capacity) of the collector field. The COP of the DEC-system reached values of up to 1.1 when auxiliary heating was shut off. In addition it can be seen that the shut off of the auxiliary heating did not influence the cooling power critically (see. Fig. 8.30), but improved the COP a great deal.

When comparing the monitored performance to the expected design values, the plant works quite well under these conditions. The achieved cooling power was about 75 kW with a COP of about 0.8 to 1.1 at ambient air temperatures of about 30°C. Assuming the same COP also with ambient air temperatures that are a little bit higher (design temperature is 32°C), the design cooling power of 90 kW seems achievable. The heating power for regeneration was not achieved however. The power supplied by waste heat use was only about 25 kW on average instead of 45 kW. The collectors supplied a maximum of about 50 kW with an efficiency of about 0.5 to 0.6, which is close to the assumed 60 kW. This power was however, not achieved before 14:00. Thus, in the morning 60 kW of the heating power had to be supplied by auxiliary heating and even after

midday, when waste heat use and collector gain reached their maximum, about 25 kW of auxiliary heating power was provided to achieve the demanded regeneration air temperature of at least 60°C. On a side note: in chapter 09 it will be shown that auxiliary heating would not have been necessary at all on the 8th of July 2002.

8.7 CONCLUSIONS

After a relatively long time period during which the control strategy was adapted to fit the special requirements of this pilot plant and after the removal of many small and large problems, the pilot plant was able to function properly from January 2002 onward.

For the evaluation of the comprehensive monitored data, it was mainly the inadequacy of the measuring devices that led to big problems. Thus the shown evaluations could only be done by evaluating temperature and volume flow measurements because the humidity measurements were too unreliable to be used. Furthermore, the failure times of the measuring system or of single sensors reduced the time that could be evaluated in detail to only 66 % of the whole time period.

A comparison of the two different evaluation procedures showed, in an impressive way, how different the outcomes can depend on the choice of sensors and evaluation criteria. Thus, the determined values must always be judged in relation to the evaluation procedures used.

The energy evaluation of the air heating system showed that about 59000 kWh of heating energy were supplied for heating demand of the first upper floor of the production hall and an older storage hall. 16 % of that energy was produced by collector operation and 84 % by waste heat use.

The gain from the solar air collectors was mainly used for the air heating system as the time with full desiccant cooling operation was short. The average efficiency of the air collectors was 0.4 during the time that it was used for the air

heating system and 0.5 when it was used for full desiccant cooling operation. However, with these efficiencies a malfunction of the collectors in January and February must be considered which decreased the collector efficiency strongly during the air heating operation. A further disadvantage is caused by fact that the air that flows through the collectors is pre-heated by waste heat from the processing machines, which decreases the performance of the collectors, especially at lower temperatures.

For the operation of the DEC-System, the evaluation shows that altogether 78500 kWh of heat were supplied through heat recovery from the exhaust air to heat the new production hall at low ambient air temperatures (caution: not be be confused with the air heating system). For cooling, only 11350 kWh were supplied. Thus despite the high thermal loads from production, the DEC-system acted more often as a heat recovery system (heating) than a cooling system.

The average COP (May until September 2002) associated with active cooling was 0.81, and associated with full desiccant cooling, it was only 0.32. While operating under design conditions however, such as on the 8th of July, the COP associated with full desiccant cooling reached values of between 0.8 and 1.1 as was assumed during planning. The low average COP was caused by full desiccant cooling operation at relative low ambient air temperatures, when high amounts of regeneration energy were used and only small temperature decreases could be achieved.

In contrast to the yields that were predicted during the planning phase, both the collectors and the waste heat use did not completely achieve the expected energy. On the 8th of July (under almost design conditions), the collectors obtained instead of the planned 60 kW, only about 50 kW at a solar irradiation of 1000 W/m² and only 36 kW on average over a time span of 9 hours of full desiccant cooling operation. The waste heat gain, which assumed to be 45 kW on average, was only about 25 kW. Thus the missing energy was supplied by auxiliary heating which made up about 59% of the whole regeneration energy.

Furthermore, it was interesting to learn that the largest amount of auxiliary energy was consumed at ambient air temperatures that were less than 20°C.

In summary the DEC-technology can be rated in principle as a forward looking, environmental friendly and also economically operating cooling system, if the cooling demand is in phase with available thermal energy (solar energy, waste heat etc.). There the system works much better in hot and dry climates than in climates with moderate temperatures and a high relative humidity.

In cases where the standard design conditions (usually: 32°C / 40 % r.h.) are rarely reached (e.g. in moderate climate), the suitability of a DEC-system has to be checked in detail, because the manufacturer given cooling power or COP is only guilty for design conditions and with lower ambient air temperatures the cooling power and the efficiency strongly decreases.

08 MONITORING OF A DEC-SYSTEM IN A PLASTICS PROCESSING FACTORY

CHAPTER 09

OPTIMISATION POSSIBILITIES IN CONTROL STRATEGY AND DESIGN

9.1 INTRODUCTION

In this chapter, an analysis of the influence of the control strategy and of the design on the performance of the DEC-system in Althengstett will be presented. The study was carried out with the detailed monitored and analysed data shown in Chapter 08. In order to evaluate the influence of the obtained improvements in control strategy and design, the DEC-system was simulated. The simulated results using the possible improvements were compared to the actual obtained performance that was measured in July of 2002.

9.2 SIMULATION MODEL FOR THE DEC-SYSTEM

The simulations of the complete DEC-system were done with the use of the modular simulation environment INSEL (**IN**tegrated **S**imulation **E**nvironment **L**anguage).

The simulation of the complete DEC-system has been done using static simulation models (efficiency models) for the humidifiers, the rotary heat exchanger and for the desiccant wheel. Only the solar air collectors were simulated with a physically based dynamic model considering the inertia of the collectors, as the results were not satisfactory with an efficiency model.

The suitability of the simulation models was verified by the measured data from the pilot plant in Althengstett. For this, the single components were simulated alone with measured data used as the input. The simulated outlet air conditions were then compared with the measured values. This was done for several

different time periods and the input parameters of the models were varied in order to find out which settings best apply for the monitored DEC-system.

9.2.1 DESICCANT WHEEL MODEL

The model that was used for the calculation of the desiccant wheel is a model that uses a dehumidification efficiency only. The calculation procedure for this model has already been explained in detail in Chapter 05, paragraph 5.2.2, where the dehumidification efficiency is introduced.

Of course, instead of this simple model, the detailed model developed in this study (Chapters 05 and 06) could also have been used for the simulation. However, as the experiments with the desiccant wheel test plant (see Chapter 05) showed, there is a specific rotation velocity for every wheel at which the best dehumidification performance is achieved. Thus, to control the DEC-system usually no change in rotation velocity is needed. In addition, with the DEC-system in Althengstett, the volume flows are constant and also the other parameters (temperatures, humidities) do not vary much. Under these operation conditions the experiments in Chapter 05 showed a nearly constant dehumidification efficiency and therefore the use of the simple efficiency model is sufficient for the purpose of simulating the DEC-system in Althengstett.

Because the humidity measurements are often not trustworthy, the verification of the simulation model for the desiccant wheel was done using only the temperature curves. With the knowledge that the enthalpy change is almost proportional to the dehumidification capacity over a wide range of operation parameters (what is clearly proved by the measurements taken at the test plant for desiccant wheels for the Klingenburg wheel, see Chapter 05), the temperature change can also be used for judging the dehumidification. For this, the dehumidification efficiency model, which basically assumes that the dehumidification process is isenthalpic, was extended by the empirically determined enthalpy change of the process air (about 2 kJ/kg for a dehumidification capacity of 1 g/kg) for this kind of wheel. In Fig. 9.1 the

verification of the desiccant wheel model is shown using measured data for two days in July 2002 with long times of full desiccant cooling operation as examples.

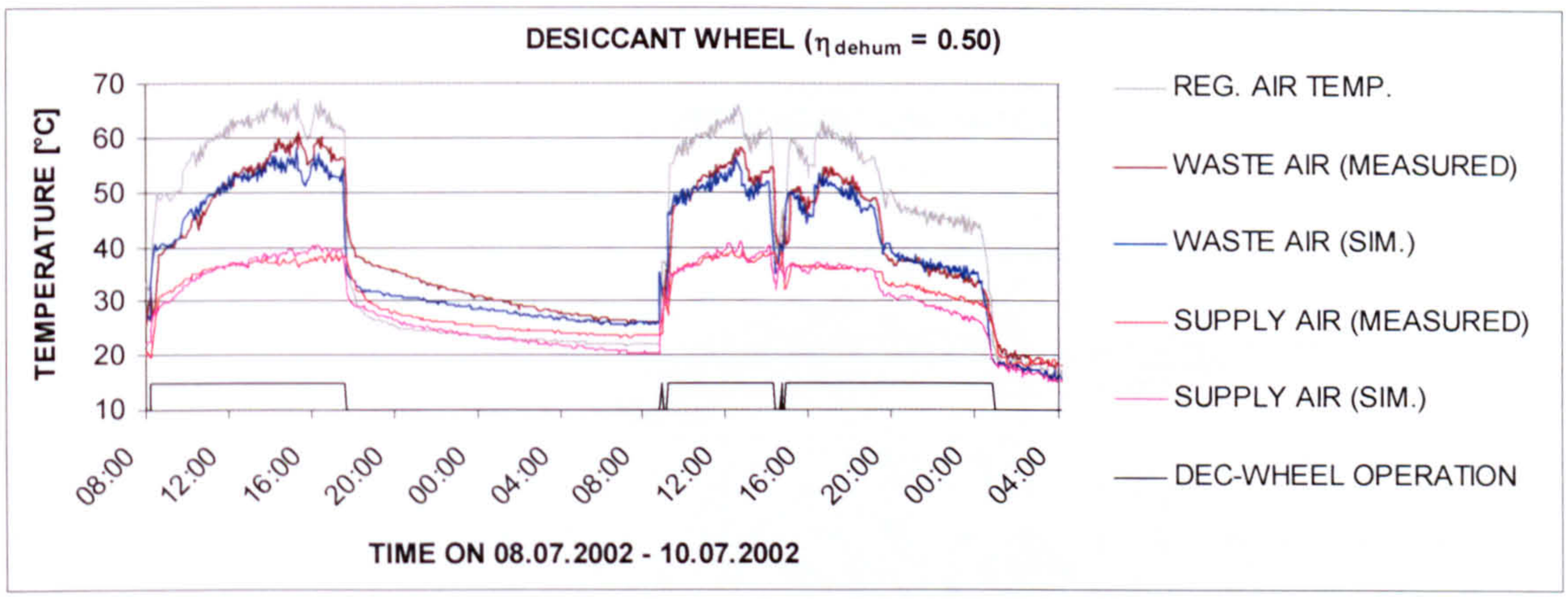

Fig. 9.1: *Verification of desiccant wheel model using measured data*

By varying the dehumidification efficiency, which is the only parameter for the simple desiccant wheel model, the best accordance between simulation and measurement was determined for a dehumidification efficiency of about 0.5. This dehumidification efficiency is proved also by the measurements at the test facility for the same kind of desiccant wheel (Klingenburg SECO).

Note: With the assumption of isenthalpic dehumidification (without considering the empirically determined enthalpy change) the best accordance between simulation and measurement would have been at a dehumidification efficiency of about 0.7.

9.2.2 ROTARY HEAT EXCHANGER

The model used for the rotary heat exchanger is also a simple "efficiency model" that only considers heat recovery efficiency.

By varying the heat recovery efficiency, which is the only parameter for this heat exchanger model, the best accordance between simulation and measurement was determined for an efficiency of about 0.7, which corresponds well to the efficiency given by the manufacturer for these operating conditions which is also

about 0.7. The verification using measured data is shown in Fig. 9.2 using the measured data from the same days in July 2002 as was used for the verification of the desiccant wheel as an example. For the verification, the supply air flow was given priority.

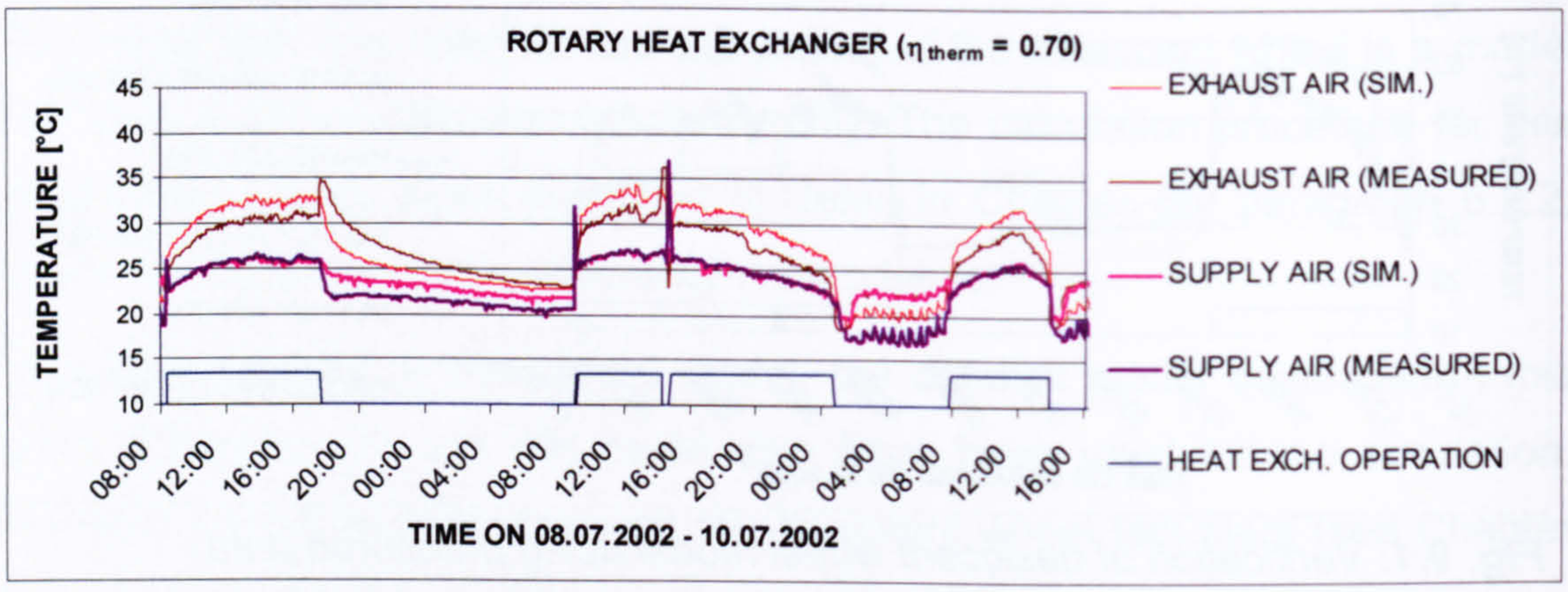

Fig. 9.2: *Verification of heat exchanger model using measured data, with the process airflow having priority*

It can be seen in this case that the simulated supply air outlet temperature corresponds very well to the measured one, but that the simulated exhaust outlet temperature deviates strongly. This can be explained however by the measuring sensors, as the verification of the supply air flow could be done with data from HfT-sensors only. For the measurement of the outlet temperature of the exhaust air however, data from a Saia-sensor must be used because no HfT-sensor is available at that location. Considering the calibration errors between the two sensor systems that have already been mentioned many times, these deviations are explainable.

9.2.3 HUMIDIFIERS

The model uses a humidification efficiency for the humidifiers that is defined as follows:

$$\eta_{hum} = \frac{x_2 - x_1}{x_{\max} - x_1} [-]$$

Here, x_1 is the water content of the air humidifier inlet, x_2 is the water content at humidifier outlet and x_{max} is the maximum achievable water content by a humidification along the "fog-isotherm line". Compared to the isenthalpic humidification, the humidification along the "fog-isotherm line" considers the enthalpy/temperature of the evaporated water; however this difference is quite small at low temperatures.

Verification using measured data is shown in Fig. 9.3 for the supply air humidifier and in Fig. 9.4 for the exhaust air humidifier.

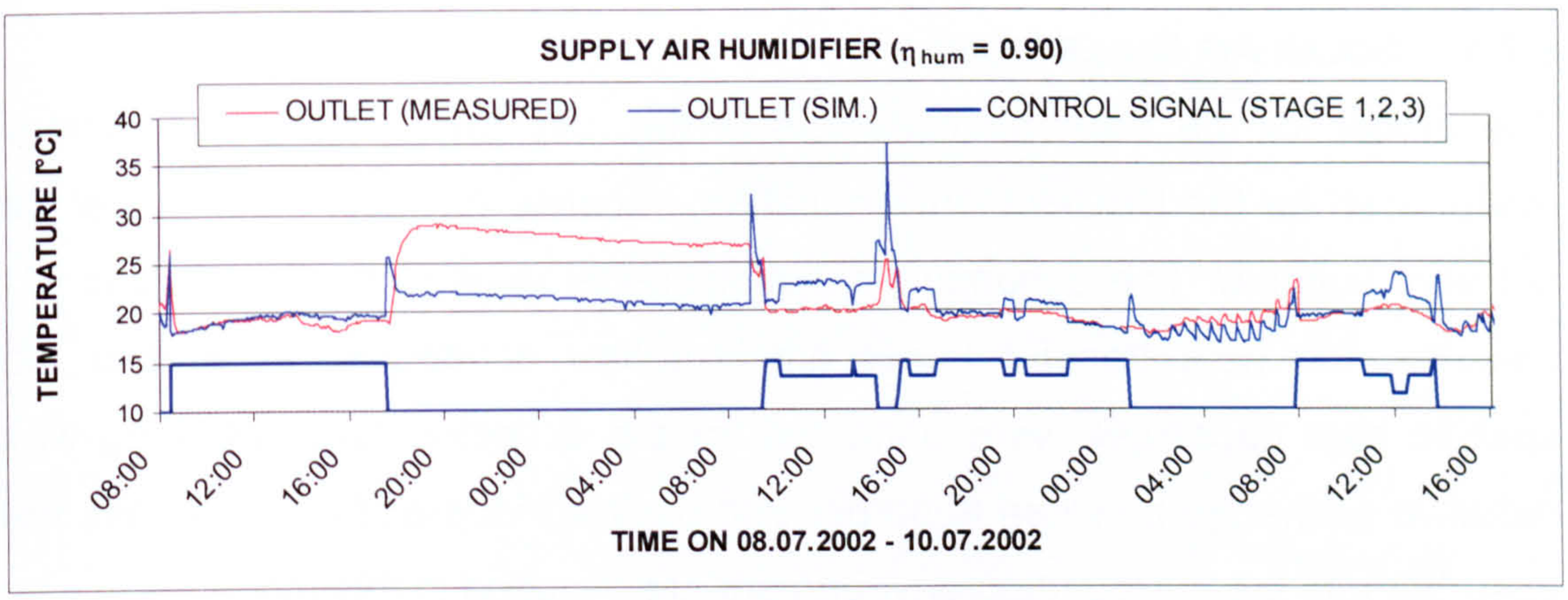

Fig. 9.3: *Verification of supply air humidifier model by measured data*

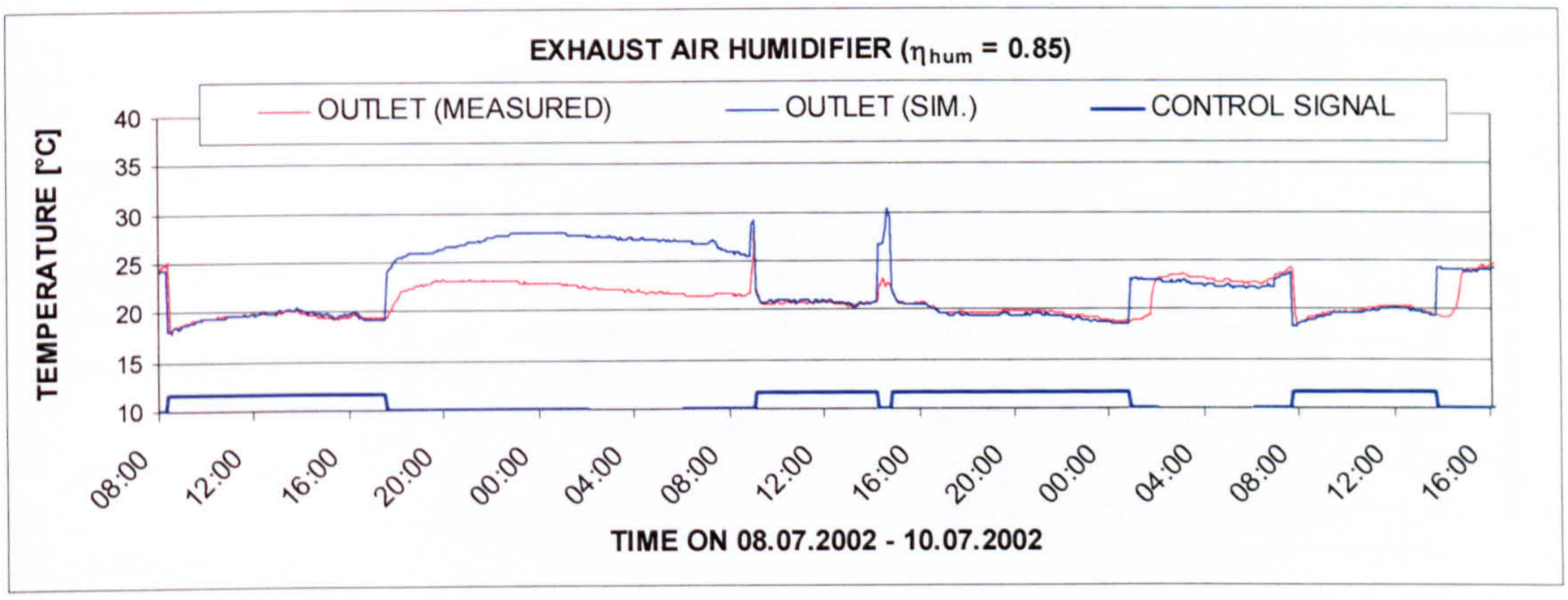

Fig. 9.4: *Verification of exhaust air humidifier model using measured data*

By varying the humidification efficiency, an efficiency of about 0.90 for the 3-stage supply air humidifier and 0.85 for the 1-stage exhaust air humidifier was found to result in the best match between the simulation and the measurement.

These values also correspond well with the efficiency given by the manufacturer of about 0.93 at design conditions for the DEC-system in Althengstett.

As the humidity measurements are not trustworthy, the verification was done again with the temperature change only. For both humidifiers, the inertia of the real humidifiers could be seen, especially at switch off. This behaviour is not considered in the simulation model used. However at longer operation times, the correspondence between the measured and simulated values is quite good.

9.2.4 SOLAR AIR COLLECTORS

The model for the solar air collectors is the only physically based dynamic model used for the DEC-system simulation, because a simple static model was not very suitable. The dynamic simulation model uses Nusselt correlations to calculate the heat transfer under different flow conditions. In addition, the specific heat capacities were attributed for the collector materials, long wave radiative exchange between absorber and back surface and the heat loss from absorber into the surrounding environment are included in this model.

A comparison of the static and the dynamic model and the verification with measured data is shown in Fig. 9.5.

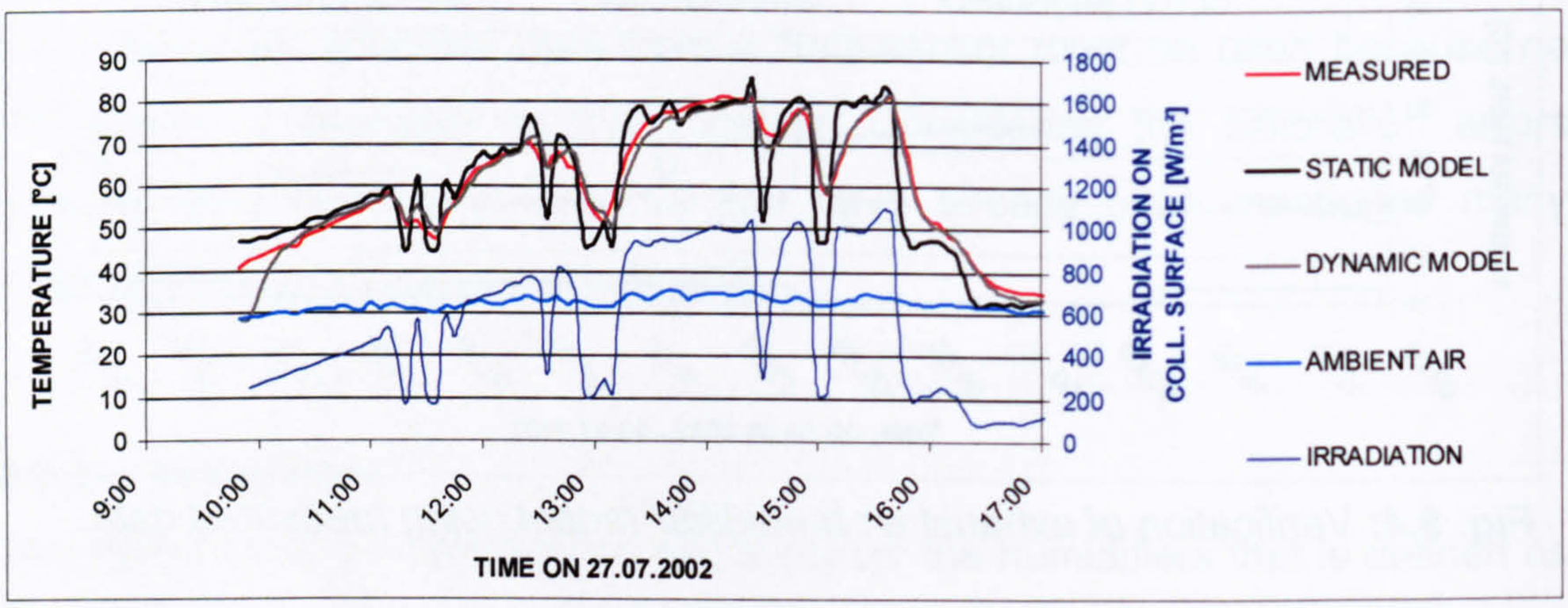

Fig. 9.5: *Comparison of static and dynamic model for solar air collectors and verification with measured data*

On a sunny day with fast moving clouds, the accuracy of the dynamic model can be demonstrated. The collector volume flow was about 3000 m³/h. Temperature levels of 80°C or a 47 K temperature increase was reached at maximum irradiance of 1000 W/m². Whereas the static model results in very high temperature gradients at changing irradiance conditions, the dynamic model is capable of very precise simulation of the dynamic collector response. The time constant for the temperature change is approximately 15 minutes.

9.2.5 CONTROLLER

For the regulation of the single components, an implemented "control module" from INSEL is used which was originally developed for the DEC-system in Mataró. To use the control module for the DEC-system in Althengstett, several modifications had to be made as there were mainly the implementation of the pre-heating of the collector inlet airflow by waste heat use and the only partial heating of the regeneration airflow by the solar air collectors (the complete regeneration airflow is constant at 11000 m³/h, the maximal collector air flow is 6000 m³/h). The waste heat use was set constant to the average value determined by measured data, which was 20 kW for July of 2002.

The control strategy used for the simulations was the same as the control strategy which is implemented in the real plant in Althengstett. This control strategy operates on a step-by-step basis for an increasing cooling demand as follows:

1. supply air humidifier (stage 1 to 3)
2. exhaust air humidifier and rotary heat exchanger
3. full desiccant cooling operation with use of waste heat from production and collector gain for regeneration
4. variable auxiliary heating energy supply.

Furthermore, for the simulations also the limits and set-points from Althengstett, which are listed in paragraph 9.3, were used.

9.2.6 COOLING LOAD FILE

For the simulation, the cooling demand of the building must be defined as a "cooling load file". Usually such cooling load files are gained from building simulations. But these simulations are only as good as the input data is. As a result the cooling load files created with building simulations often delivers a good tendency of the real behaviour of the building, but not a very detailed course of the time depending cooling demand. This is caused by the deviations between reality and the assumptions made for simulation (internal loads, boundary conditions, operation times etc.).

To get a cooling load file which is very close to reality for the plant in Althengstett, I determined the cooling energy provided by the real plant out of the measured "five minute" values (supply and exhaust air temperature, volume flow) and used this cooling energy as the cooling demand for the cooling load file. With this approach no detailed knowledge about the building was necessary, as the building response on provided cooling energy under corresponding boundary conditions is contained in the measured values. Thus a real close comparison of simulation and measurement is possible.

Because the provided cooling energy of the real plant includes fluctuations caused by malfunctions in operation and control of the real plant, this created cooling load file can be rated as a "worst case" cooling load file. In reality the demanded cooling energy would be more even. Additional the controller in the simulation model rates the given cooling demand as a minimum demand. Due to the stepwise rising of the provided cooling energy, the supplied cooling energy is usually a bit higher than the demand, which also leads to a "worst case" consideration. The outcomes of the simulations are therefore on the "safe side".

9.3 CONTROL STRATEGY ALTHENGSTETT

The DEC-system in Althengstett operates with a constant process air volume flow of about 18000 m^3/h. The cooling demand is controlled by the indoor

temperature in the new production hall, which should be held at 20°C preferably. But due to the dimensioning and construction of the plant, the preferred indoor temperature of 20°C can not be reached under all boundary conditions. Decisive for dimensioning of the plant was, that the indoor temperature should never exceed 26°C.

To take into consideration the thermal comfort of the working people, the lowest allowed supply air temperature has been set to 17°C.

If the indoor temperature exceeds 20°C, the control demands cooling. First the supply air humidifier is enabled, however supply air humidification is only activated if the indoor air humidity is lower than 11.7 g/kg. This limit is set once for thermal comfort of the working people but is also decisive for the production processes. If supply air humidification is not sufficient, the exhaust air humidifier and the rotary heat exchanger are switched on. If active cooling with the humidifiers is not sufficient for the cooling demand, full desiccant cooling operation is started. For this the desiccant wheel starts operation and waste heat from production and solar gains, if available, are used to heat the regeneration air. The collector begins to operate if the collector temperature is more than 6 K higher than the air temperature at the collector inlet. The maximum air flow through the collectors is limited to 6000 m³/h with a constant regeneration air flow of altogether 11000 m³/h. If the energy from waste heat use and from the collectors is not sufficient, auxiliary heating is used. For the required auxiliary heating the target regeneration air temperature is at least 60°C. The maximum regeneration air temperature is limited to 72°C (as advised by the manufacturer) as higher temperatures could damage the desiccant wheel.

9.4 DETERMINED OPTIMISATION POTENTIAL

9.4.1 REQUIRED TIMES FOR FULL DESICCANT COOLING OPERATION

The full desiccant cooling operation mode is often initiated even though active cooling with the humidifiers alone is sufficient. In addition to this, the dynamic

and somewhat slow response of the single components, especially of the humidifiers, is not adequately considered in the control strategy of the plant, as mentioned before in Chapter 08, paragraph 8.5.

A typical effect of the dynamics of the single components not being considered and a somewhat inadequate control strategy is a strong fluctuation of the supply air temperature during cooling operation. This effect is shown in Fig. 9.6 which uses the 11th of July 2002 as an example.

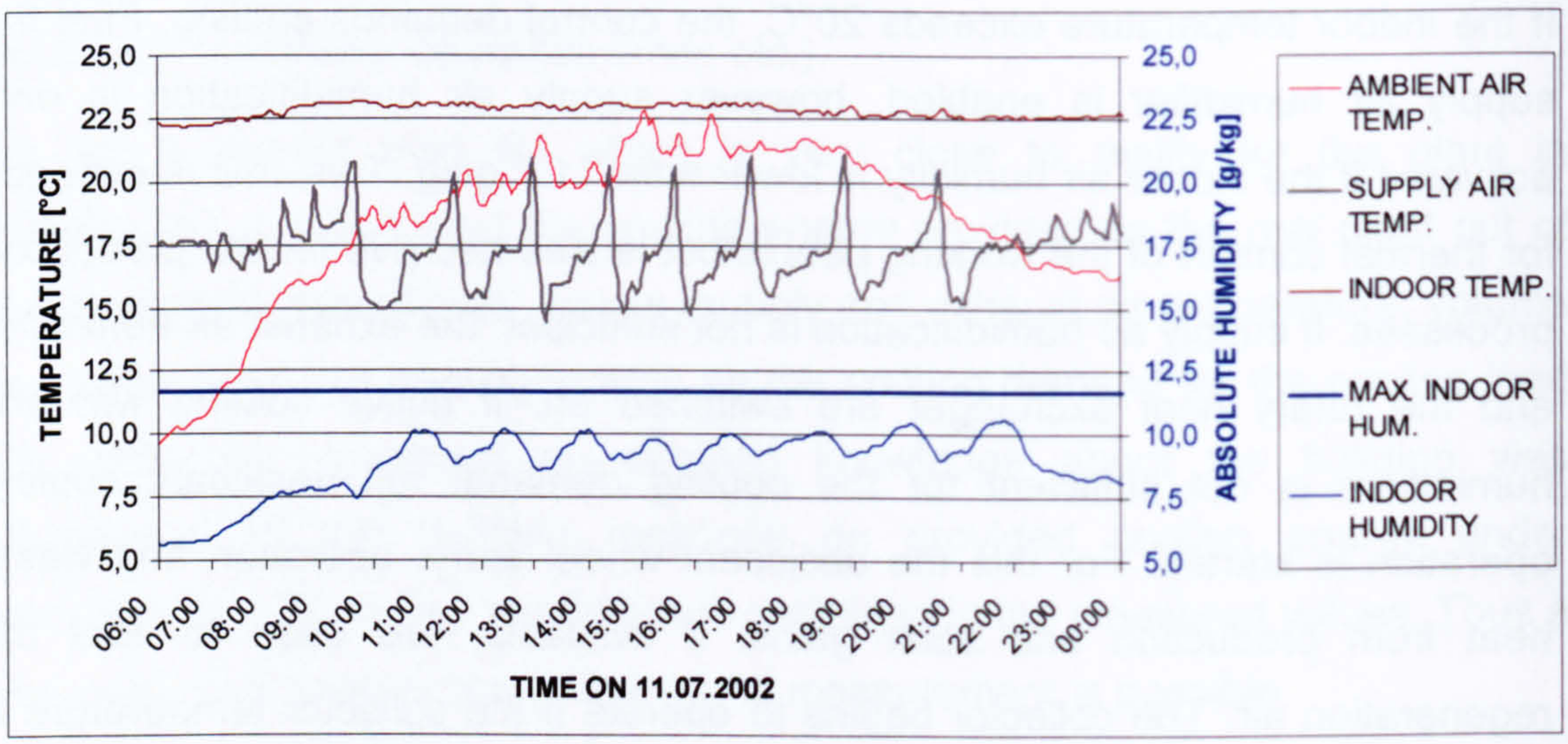

Fig. 9.6: *Fluctuations in the supply air temperature as the result of an inadequate control strategy on 11th of July 2002*

In the morning, when the ambient air temperature was still low, the DEC-system was in heat recovery mode (desiccant wheel operation) in order to obtain supply air temperatures of over 17°C (until 7:45 a.m.). When the ambient air temperature then further increased, the control strategy changed to free ventilation (until 9:30 a.m.). The fluctuations of the supply air temperature during this time periods were caused by slightly unsteady volume flows. So far, so good, but when the supply air temperature exceeded 20°C for the first time (at 9:30 a.m.), the control strategy changed immediately to full desiccant cooling operation, this time even with auxiliary heating demand. This behaviour must be rated as a malfunction in the system control, as it doesn't follows the implemented control strategy listed in chapter 9.2.5.

The full desiccant cooling operation then led to a decrease of the supply air temperature to below the set-point of 17°C in less than 15 minutes. Consequently, the humidifiers were then switched off and a few minutes later the rotation velocity of the desiccant wheel was increased in order to raise the temperature level in the heat recovery mode. Thus the measured supply air temperature fluctuated by more than 6 K, when active cooling and heat recovery strategies operated in short intervals after one another. Looking at the absolute humidity in the production hall (indoor humidity), at least for the early times of the day with cooling demand, one can see that supply air humidification should have been sufficient, meaning that full desiccant cooling operation should not have been started at all. A closer look at the control signals on 11th of July 2002 is shown in Fig. 9.7.

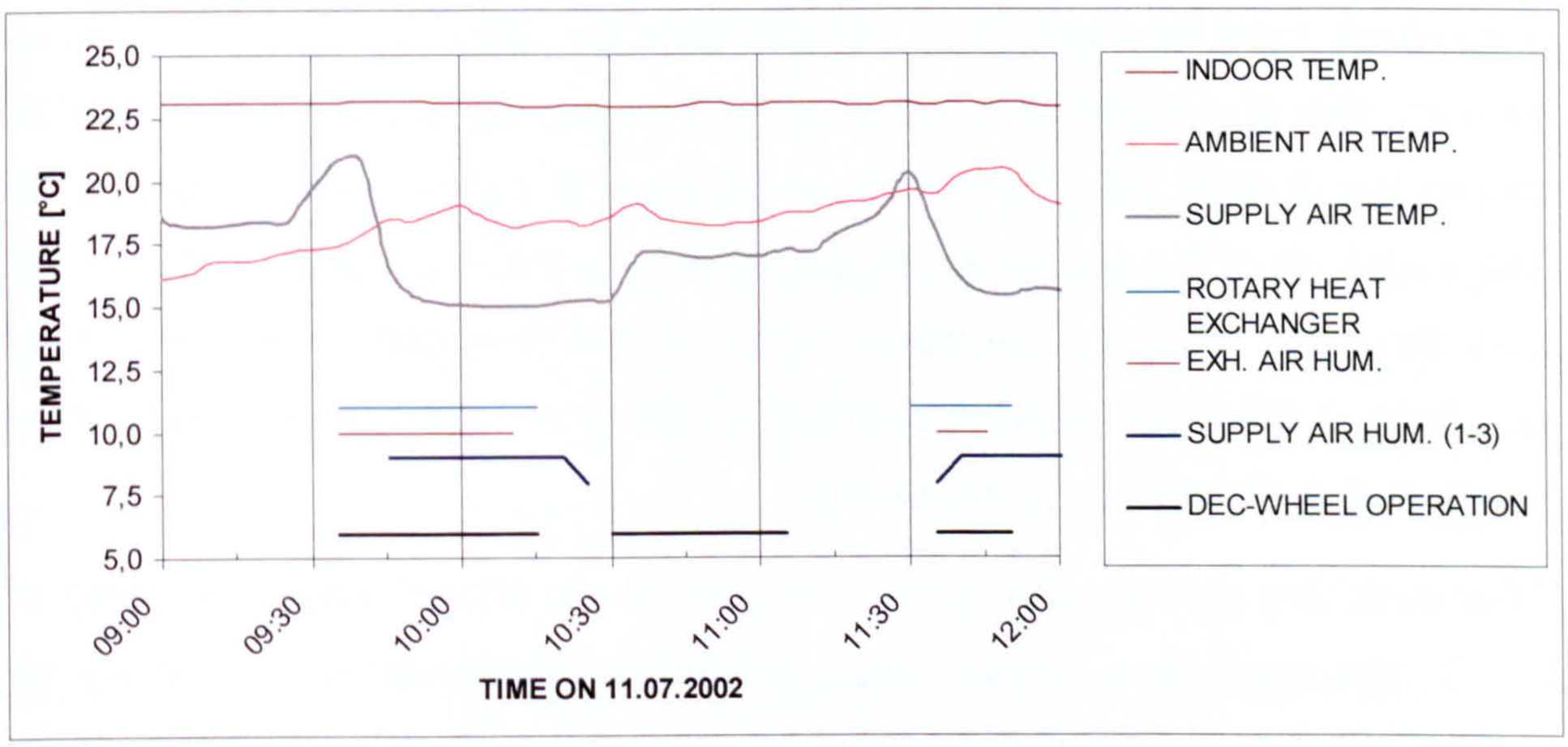

Fig. 9.7: *Control strategy / signals on 11th of July 2002*

At 9:35 a.m. the control strategy required full desiccant cooling operation and in the first 20 minutes, even auxiliary heating was required. For the full desiccant cooling operation the desiccant wheel, the exhaust air humidifier and the rotary heat exchanger were switched on at the same time at 9:35 a.m. As the exhaust air humidifier needs about 5 to 10 minutes after being switch on before taking effect, the supply air was heated at this point of time by both the rotary heat exchanger and by the desiccant wheel up to 21°C (at an ambient air

temperature of 18°C!). The supply air humidifier was not switched on before 9:45 a.m. and thus took effect at the earliest starting at about 9:50 a.m. As the supply air temperature was getting too low at 10:10 a.m., the exhaust air humidifier, the rotary heat exchanger (at 10:15 a.m.) and the desiccant wheel were switched off. At 10:20 a.m. the third stage of the supply air humidifier and at 10:25 a.m. the complete supply air humidifier was switched off. As the supply air temperature rises only very slowly (supply air humidifier took effect until 11:10 a.m.) at 10:30 a.m. the desiccant wheel was started for heat recovery until 11:10 a.m. As the supply air temperature again exceeded 20°C at 11:30 a.m., the control strategy requested full desiccant cooling operation again.

To avoid such control problems, a step-by-step regulation that considers the individual response times of the different components, especially for the humidifiers, must be used. Thus, for example, the different stages of the supply air humidifier should be switched on only after waiting at least 5 to 10 minutes so that the change can take effect before the next control step is implemented. The switch off of the supply air humidifier usually takes about 30 to 45 minutes, thus the heat recovery operation mode of the desiccant wheel is a useful possibility if there are sudden changes in the cooling demand. In most cases however this should not be necessary.

After switching on the exhaust air humidifier, there should also be a pause of 5 to 10 minutes before further steps are taken. In particular, the rotary heat exchanger must not be switched on before the exhaust air humidifier has taken noticeable effect in order to avoid an unwanted heat recovery from the exhaust air, as was observed for example, at 11:30 a.m. in Fig. 9.7. The switch off of the exhaust air humidifier however is no problem as the cooling effect stops immediately after the rotary heat exchanger has ceased to operate.

In order to study the influence of the partially inadequate control strategy on the system performance, the measured cooling energy was used to create a "cooling load file" for the production hall in Althengstett. Although "cooling load files" were available from the planning phase, these files were less suitable for

this purpose as these files were created with general, averaged climatic boundary conditions from a "test reference year" and in addition, the internal loads were also only estimated.

In order to compare the measurement with the simulation, one must take into account the fact that the used cooling load file naturally contains the fluctuations in the cooling demand which were caused alone by the inadequacies of the real control system, especially by the strong supply air temperature fluctuations, as mentioned above. If these fluctuations did not exist, the cooling demand course would also be more uniform and the necessary changes in operation mode would clearly be fewer. However, despite the (not considered) inertia of the single components in the simulation model, the thereby resulting changes in the operation mode are not vital to the average energetic outcomes.

The monitored data shows that in July, the time period with full desiccant cooling operation was about 83 hours. The simulation however, shows that only 33 hours would have been necessary. During the other 50 hours active cooling with the humidifiers alone would have been sufficient. For the auxiliary heating demand, the monitored data shows a total of 69 hours of auxiliary heating operation, whereas the simulation only shows 6 hours. The times with full desiccant cooling operation, as determined by measurement and simulation are shown in Fig. 9.8.

Aside from the influence of the times required with full desiccant cooling operation, the influence of a fixed regeneration air temperature during operation with auxiliary heating was also studied. For this, the additional auxiliary heating energy was calculated that would occur, if during times with an auxiliary heating demand the regeneration air temperature should reach at least 60°C, regardless of whether or not it is necessary for providing the required cooling demand. This strategy is implemented in the "real" control system in Althengstett. The maximal available auxiliary heating power was set to 80 kW, which is determined to be the maximal auxiliary heating power recorded in the monitored data.

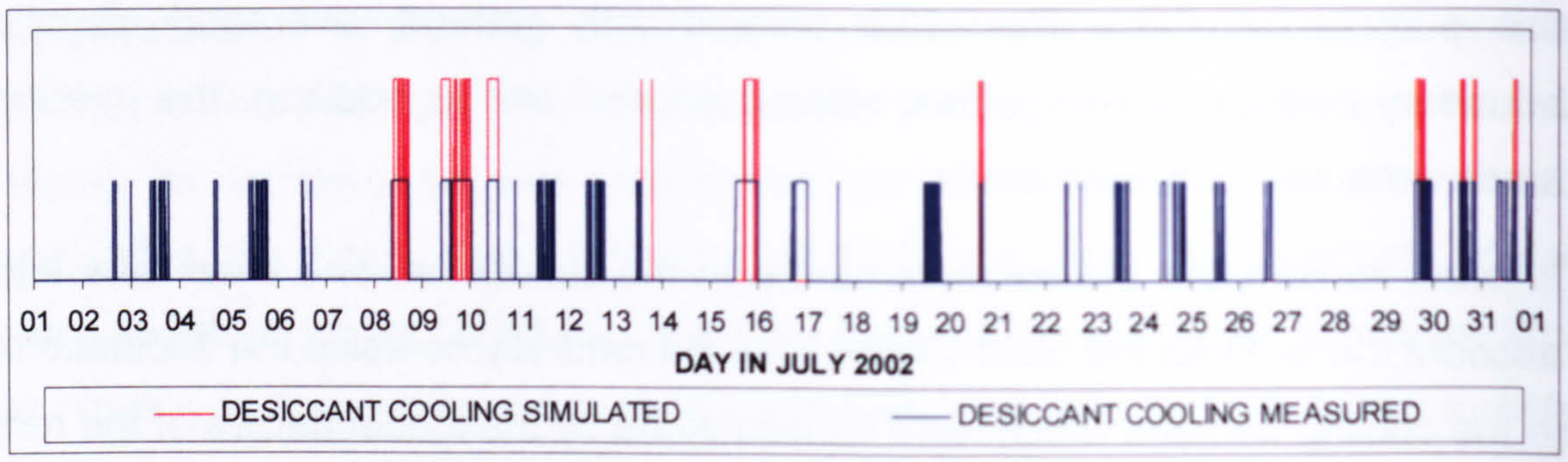

Fig. 9.8: *Times with full desiccant cooling operation in July, determined by measurements and simulation*

A comparison of the simulated energies (only full desiccant cooling operation) with the measured ones is shown in Fig. 9.9.

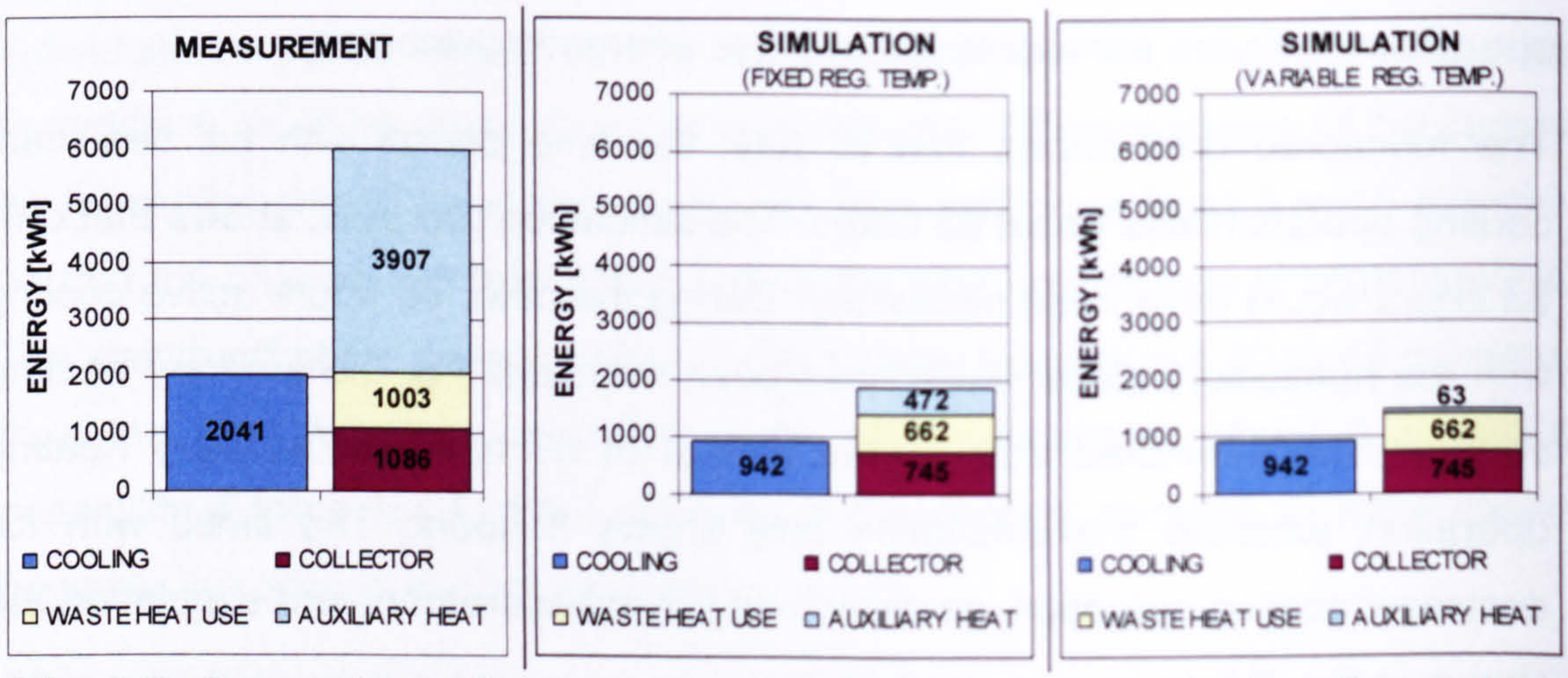

Fig. 9.9: *Comparison of measurement and simulation, supplied cooling and required regeneration energy for full desiccant cooling operation*

The simulation results show that with the "right" control strategy, only 942 kWh of the required cooling energy would have had to have been supplied by full desiccant cooling operation instead of the measured 2041 kWh of cooling energy during full desiccant cooling operation of the "real" plant. The difference of 1099 kWh of cooling energy could have been supplied by cooling operation of the humidifiers only. Thereby the required regeneration energy would have been clearly lower at 1879 kWh instead of 5996 kWh. Thus the COP for full

desiccant cooling operation would have been about 0.50 instead of the measured 0.34.

If in addition, the regeneration air temperature would not have been set to a fixed level (60°C) when auxiliary heat was required, the auxiliary heat demand could have been decreased once more to only 63 kWh. Thereby the COP would have increased to 0.64, which is a value that is quite good for desiccant cooling operation. When the COP is associated with active cooling (altogether 3926 kWh of active cooling energy), the examined improvements could have raised the COP from the measured 0.65 to 2.1 with a fixed regeneration air temperature during auxiliary heating and even 2.67 with a variable regeneration air temperature.

9.4.2 LOW COLLECTOR FRACTION

As a conclusion of the monitoring of the DEC-system in Althengstett, the solar contribution for heating the regeneration air was lower than expected. Altogether the solar energy used for regeneration during summer was only about 2680 kWh with a total amount of 13450 kWh of regeneration energy. The solar contribution was thus less than 20 %.

In July of 2002, from a total of 413 operation hours, 83 hours needed the full desiccant cooling mode, whereas for 90 of the total hours active cooling with humidifiers alone was sufficient. The dominant operation mode even in July was free ventilation with a total of 178 operating hours. From the 83 hours of required regeneration, the collector provided energy during 53 of those hours (64% of the time) and produced a total energy of 1086 kWh. For 30 hours of the full desiccant cooling operation the solar irradiation was not sufficient to obtain the minimum temperature difference of 6 K. The mean collector efficiency during the operation hours was 48 %, which is a good performance value.

In Fig. 9.10, an example from 8th and 9th July of 2002 is shown for the temperature levels in the regeneration air flow after being heated with waste

heat from the production, the temperature after passing through the air collectors, the mixed temperature of the two volume flows and the temperature after passing through auxiliary heating. The operation hours of regeneration and regeneration with collector operation are also shown. A more in-depth look at the timing of the demanded full desiccant cooling operation shows that the temporal sequences and phase shifts between the desiccant cooling operation and the sufficient solar thermal energy contribution can be clearly seen.

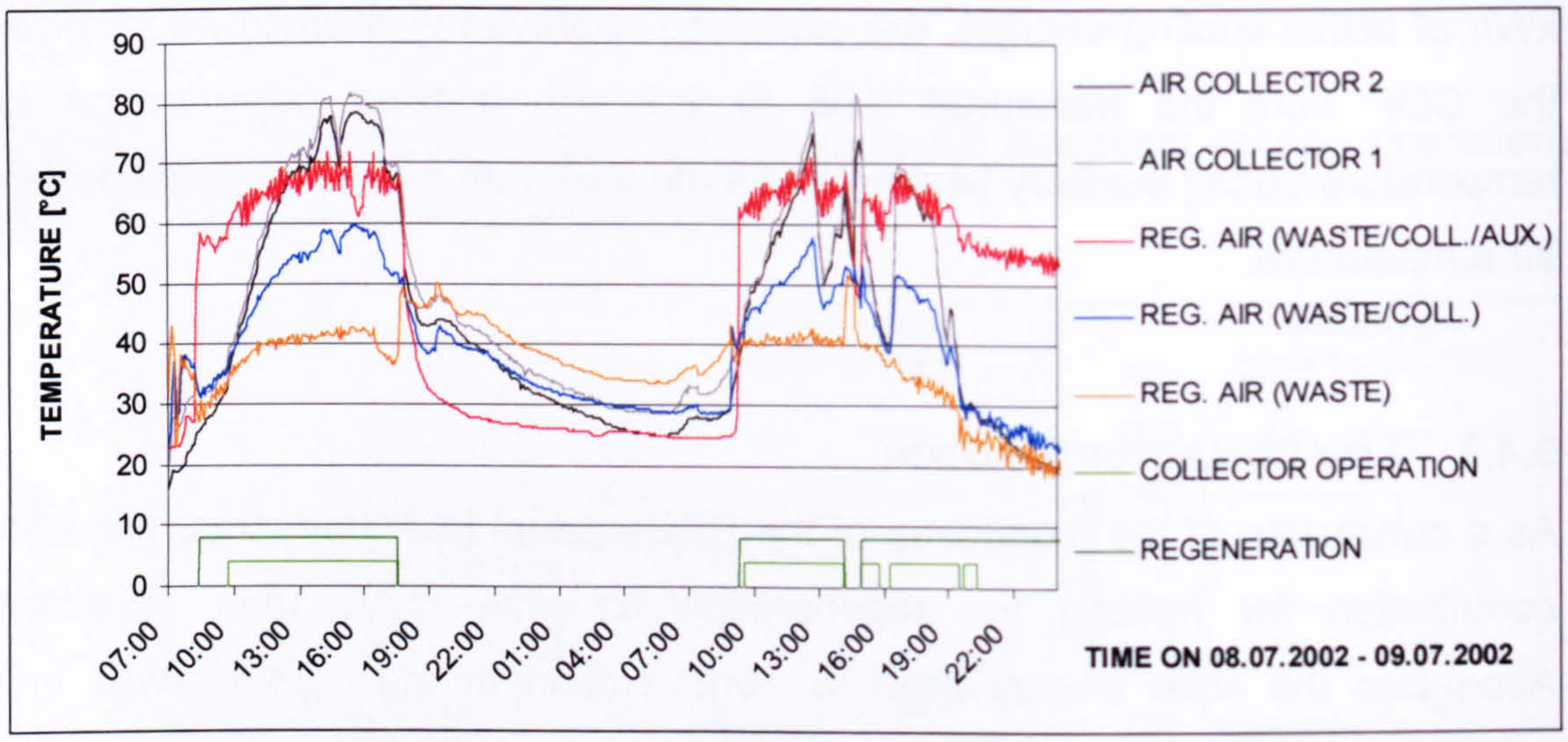

Fig. 9.10: *Regeneration air temperatures behind the different heating devices*

In the control strategy, during regeneration with auxiliary heating demand, the temperature levels of the regeneration air vary typically between 60 and 70°C. The two parallel connected air collector fields are capable of delivering this temperature level for nearly seven hours on a sunny day. As the air collector field only heats 55% of the total regeneration air flow due to its small size and the fact that the waste heat from the production only delivers air temperatures of 40°C, without auxiliary heating the temperature level of the complete regeneration volume flow of 11000 m³/h always remains under 60°C. Thus auxiliary heating is almost always required to reach the required regeneration air temperature of over 60°C.

The simulation with the improved control strategy shows that the simulated solar gain during full desiccant cooling operation (measured: 1086 kWh,

simulated: 745 kWh, see Fig. 9.9) does not decrease in the same rate as the corresponding collector operation times (measured: 53 hours, simulated: 28 hours).

Thus, only with the reduced times of full desiccant cooling operation due to the so far improved control strategy, the solar fraction on regeneration energy could have been increased from 18 % to about 40 % (control strategy with fixed regeneration air temperature) or even to about 51 % (control strategy with variable regeneration air temperature).

In addition, a further improvement of the amount of solar energy used for regeneration energy could be obtained if the solar air collector fields were enlarged. However, looking at the times with auxiliary heating demand, it can be seen that the solar irradiation is sometimes only minute during these times, thus an enlargement of the solar air collector fields would probably not improve the input from solar energy much. In Fig. 9.11 the time with auxiliary heating demand is shown simultaneously with the solar irradiation on the collector surface.

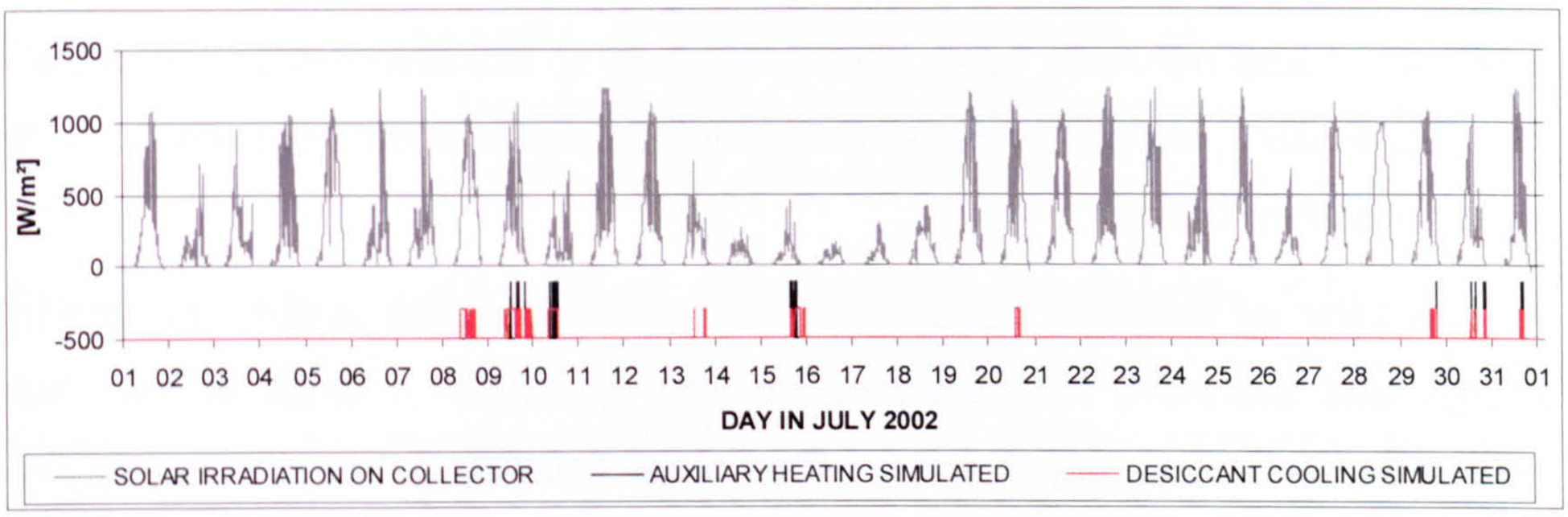

Fig. 9.11: *Solar irradiation and times with full desiccant cooling operation / auxiliary heating (simulated)*

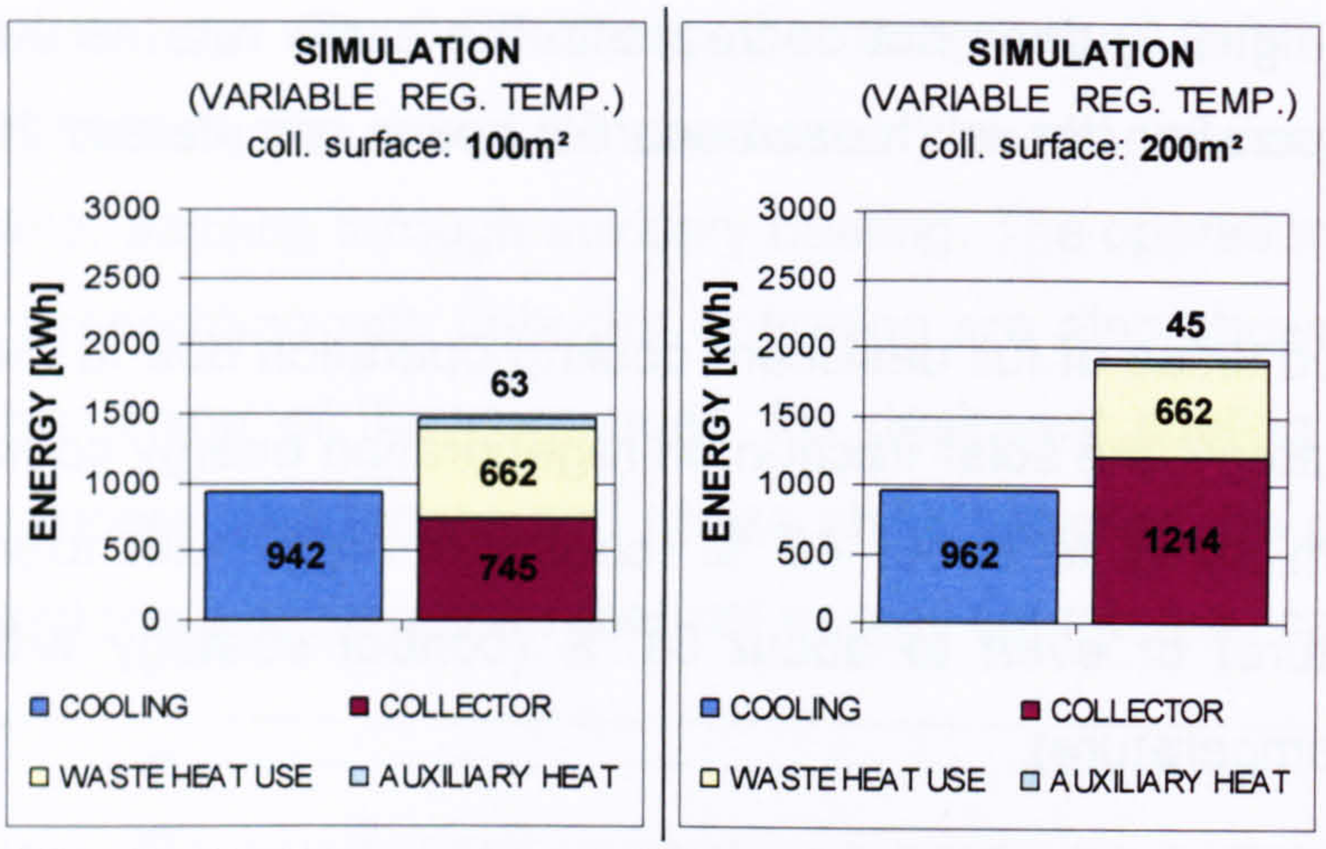

Fig. 9.12: *Comparison of air collector surface on provided cooling and required regeneration energy*

The simulation with twice the air collector surface (200m²) shows the expected results (Fig. 9.12).

The time with auxiliary heat demand could have been reduced from 6 hours to 4 hours, and the auxiliary energy from 63 kWh to 45 kWh. The solar energy gain could have been increased from 745 kWh to 1214 kWh. Of course, due to the higher regeneration air temperatures, the produced cooling energy would have also been slightly increased, but this effect is almost negligible (942 kWh compared to 962 kWh). Thus the amount of solar energy could have been clearly raised from 51% to 63%, but the COP related to desiccant cooling would have fallen from 0.64 to 0.50. Altogether the additional solar gain could not have been used effectively to improve the performance of the DEC-system, especially considering the additional investment costs and the higher pressure drops.

As with solar air collector based systems it is not possible to store the thermal energy and therefore full desiccant cooling operation in times without solar irradiation needs a supply of energy from other sources. An opportunity to avoid or at least to reduce such operating conditions could be to allow a temporary increase in the room humidity in the morning, meaning to allow cooling to be carried out by the humidifiers alone even if the indoor humidity is already higher than the setpoint. The high humidity could then be reduced when solar energy is available later on in the day. The use of solar energy for long operation hours until night would also only be possible if the storage mass of the building itself is used, meaning that in times with sufficient solar energy, full desiccant cooling

would be used to reduce the indoor humidity and the temperature level in order to have a higher humidification potential and a lower cooling demand for times without solar yield.

9.5 CONCLUSIONS

For the adequate control of a DEC-system, a step-by-step control strategy that takes the specific inertia of each individual components into consideration is required. Control steps e.g. from the heat recovery mode directly to full desiccant cooling operation as observed at the DEC-system in Althengstett must be prevented, especially at low ambient air temperatures when the efficiency of the DEC-system in full desiccant cooling mode is naturally low.

In addition, a control strategy that allows a variable auxiliary heating power can save high amounts of regeneration energy in contrast to a control strategy with a fixed regeneration temperature demand. Especially at low ambient air temperatures, full desiccant cooling operation with a fixed regeneration temperature needs high amounts of regeneration energy, but only achieves a small temperature decrease in the process air. Under such conditions (low cooling demand), an additional cooling system (e.g. compressor chiller, such as the one installed in the DEC-system in Mataró) could also be advantageous.

The enlargement of the solar air collector fields is only useful if full desiccant cooling operation is usually required during times in which solar irradiation is possible. If solar irradiation and full desiccant cooling operation are not in phase, this energy cannot be used due to the absence of the possibility of thermal storage with solar air collectors. In such cases, solar water collectors would be preferable due to their ability to store energy.

09 Optimisation Possibilities In Control Strategy And Design

CHAPTER 10

DESIGN GUIDELINES

10.1 INTRODUCTION

In this chapter the results and conclusions from this study will be summarized into general guidelines for both design and control strategies for DEC-systems. These guidelines are based on knowledge obtained through experience with the operation of two complete DEC-systems and provide detailed information about desiccant wheel operation. These guidelines are based on fundamental, proved knowledge and may be useful for planning and designing other DEC-systems, thus serving as a contribution that helps advance DEC technology by aiding planning engineers and by clarifying the still existing uncertainties about this forward-looking technology.

10.2 USE OF THE DEC-SYSTEM FOR AIR CONDITIONING

The profitable use of a DEC-system depends on the specific conditions in each single case. The most important criteria that are used to either support or oppose the use of the DEC-technology usually arise in the air-based principle of this technology. In contrast to the most other cooling systems that use a cooled liquid to provide cooling energy, the DEC-system supplies this cooling energy using a cooled airflow.

General conditions for which the use of the DEC-technology is recommended:

- large amount of fresh air required
- required temperatures are not under 16°C
- low grade thermal energy is already available or could be easily provided (waste heat, solar energy etc.)

- full air conditioning is required (heat recovery, cooling, air humidity handling).

These general conditions exist mostly in situations such as in public or factory buildings but can also be valid in office or even private buildings.

General situations for which the use of DEC-technology is not recommended include:

- a high cooling demand for a location at which high volume flows are not acceptable (e.g. due to limits on indoor flow velocities)
- only little space is available for the cooling system and tubing
- the required temperature is under 16°C.

10.3 GUIDELINES FOR DESIGN

10.3.1 DESIGN CONDITIONS

TEMPERATURES / HUMIDITIES

The design temperatures and humidities are determined by the climatic boundary conditions at the location and by the required indoor climate for the air-conditioned building. Usually the design conditions show the climatic "worst case scenario" under which the DEC-system is designed to still be able to achieve the required indoor temperatures.

VOLUME FLOWS

The supply air volume flow is determined by the cooling demand of the building in combination with the assumed temperatures and humidities. The maximum required supply air volume flow is usually calculated using the difference between the ambient air temperature and the lowest allowed supply air temperature and the cooling demand of the building under design conditions. The cooling demand is usually either calculated with a building simulation program or must be estimated via the given information about the building.

The evaluation of the measurements from the desiccant wheel test plant with different volume flow ratio shows that a ratio of 0.75 between the regeneration air and the process air results in the best performance. Thus the designed maximum regeneration airflow should be set to 75% of the supply air volume flow.

For both the process and the regeneration air volume flow, it should be possible to reduce the volume flow for partial load operation.

REGENERATION ENERGY

In order to estimate the maximum required regeneration energy, usually a COP that lies between 0.6 to 1.0 should be assumed for full desiccant cooling operation. Thus the available regeneration energy should be between 100% and 170% of the design cooling demand. The resulting regeneration air temperature is thereby usually between 50°C and 70°C at a volume flow ratio of 0.75.

10.3.2 COMPONENT CHOICE

DESICCANT WHEEL

The principle construction is almost the same for the available types of desiccant wheels. Only the materials that are used differ, especially the sorption materials. The sorption materials that are used are mainly silica gel, lithium chloride and molecular sieves. The pros and cons of the wheels that use these sorption materials are listed below. The choice of wheel should therefore be dependent on these pros and cons.

Silica gel: Pro:

- withstands high temperatures (120°C and higher)
- is inert, non toxic, stable and resistant to most chemicals
- is not water soluble (can be cleaned with water)

Con:

- relatively low maximum load (40% of dry weight) which requires higher rotation velocities and thus a higher heat transfer.

Lithium chloride: Pro:

- high maximum load (ten times its weight)
- prevents growth of bacteria
- is stable and resistant to many chemicals

Con:

- is water soluble (loads that are too large can cause damage)
- withstands only temperatures up to 70 °C.

Molecular sieve: Pro:

- very low achievable humidity levels
- withstands very high temperatures
- is highly stable and resistant to most chemicals

Con:

- relatively low maximum load (in contrast to lithium chloride) which requires higher rotation velocities and thus a higher heat transfer.

As the matrix rotates from regeneration airflow to the process airflow, it carries with it both small amounts of regeneration air and heat contained in the air and the matrix. This small carryover from the regeneration airflow to the process airflow is acceptable in most cases. In some cases however, this leakage is not acceptable and is thus to be prevented with the use of so-called purge sections. The principle of a purge section is shown in Fig. 10.1.

Situations in which leakage is not acceptable are, for example, applications for which very low dew points are required or the regeneration air is polluted with materials/gases that must not enter into the process air.

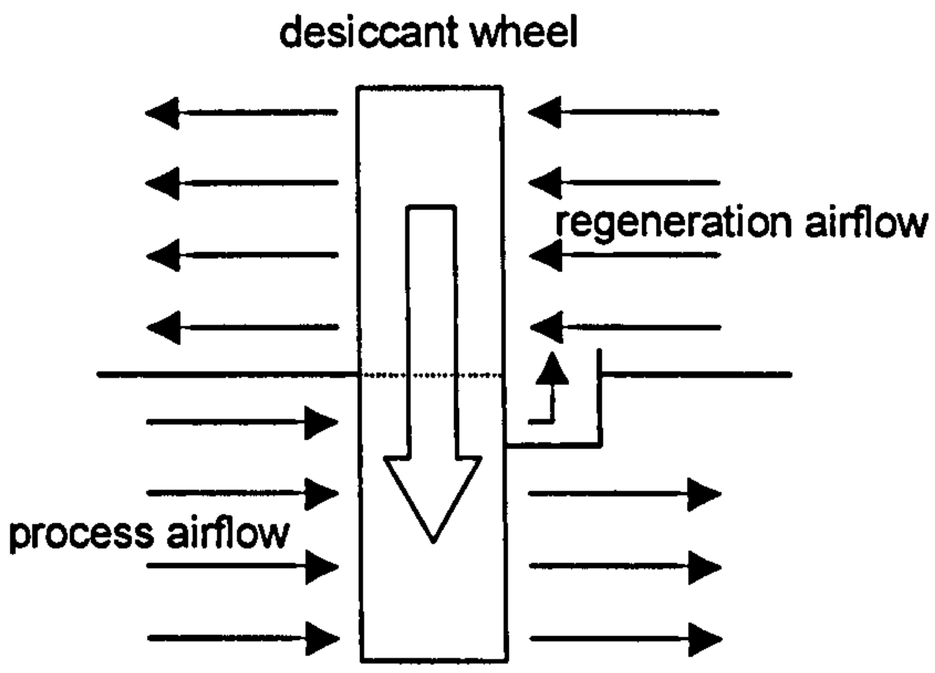

Fig. 10.1: *Principle of purge sections at desiccant wheels*

In low dew point applications, the purge is designed to pre-cool the matrix before it begins to condition the supply air. This is necessary because hot desiccant does not adsorb well. Without a purge section, the first several degrees of rotation dehumidify very little and thus allow untreated air into the process outlet. This is in addition to carryover from regeneration air that is trapped in the matrix by the wheel rotation.

Preventing carryover of air from the regeneration to the process side could be necessary if the regeneration air comes from an indoor source that may have high levels of volatile organic compounds (VOCs) or other pollutants.

HEAT EXCHANGER

Rotating heat exchangers (regenerators) have dominated on DEC-systems because of their high efficiencies which are given for example at about 0.7 to 0.8 by RECKNAGEL et. al., 1997. In addition the pressure drops are clearly lower with regenerators than with recuperators (e.g. plate heat exchangers). The disadvantage of rotating heat exchangers is that the air flows are not completely separated from each other, thus a mixing of air flows can not be completely avoided.

Only if a little admixture of one airflow to the other is not allowed, recuperators must be used. However it must be considered, that a mixture of the airflows is already possible with the desiccant wheel.

HUMIDIFIERS

For the DEC-system, usually all kinds of evaporative humidifiers are suitable that operate with liquid water (but not steam).

Evaporative humidifiers for DEC-systems are usually spray humidifiers or so-called contact or trickle humidifiers. On DEC-systems contact or trickle humidifiers have dominated because of the lower demand for maintenance and the lower space requirements. An additional advantage of these humidifiers is that almost no aerosols are generated.

If, however, the usually long response time of these humidifiers, especially at shut off, are problematic, e.g. because of a high demand on the steady supply air conditions, instead of the contact or trickle humidifiers, spray humidifiers should be used, even though they have the disadvantage of requiring higher maintenance and they often need water treatment (desalination).

SOLAR COLLECTORS

If the cooling demand is seasonally in phase with solar irradiation, the use of solar collectors for heating the regeneration air is advisable. If in addition the cooling demand is also in phase with the solar irradiation on a daily basis, solar air collectors are suitable, especially if solar irradiation contributes mainly to the cooling load.

An advantage of the use of solar air collectors is the ability to avoid an additional heat exchanger as the regeneration air is directly streamed through the collectors. An added advantage is the lower cost even compared with standard flat-plate collectors. The disadvantage of air collectors is that even short phase shifts between solar irradiation and energy demand cannot be bridged as no heat storage is possible.

10.3.3 SYSTEM CONSTRUCTION

CONSTRUCTION POSSIBILITIES

Of the variety of possible designs for DEC-systems, three main ones have been put into practise so far. These designs are:

- Closed cycle systems
- Open cycle systems
- Cascade systems.

These designs and their pros and cons will be described in the following section. In the literature, modified designs based on these systems are also presented, but most of them are only theoretical and have not been realised so far, most of them not even as a pilot plant.

CLOSED CYCLE SYSTEMS

In the closed cycle system as shown in Fig. 10.2, the room exhaust air is used as regeneration air.

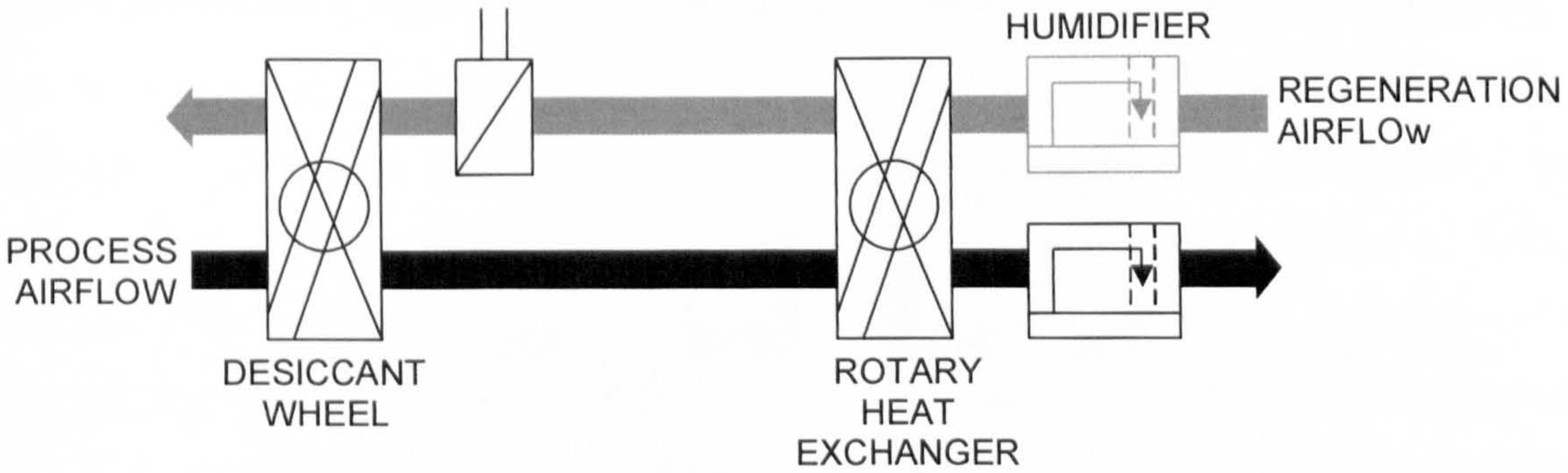

Fig. 10.2: *Closed cycle DEC-system*

An advantage of this system, is that the overall moved volume flow is lower than that of the open cycle systems, which saves high grade electricity that would otherwise be required for operation of the fan. However, the studies at the desiccant wheel test plant showed that the influence of the regeneration air humidity is also worth noting. Thus, e.g. the reduction of the relative humidity

within one series of experiments from 20% to 6% caused an increase of almost 100% in the dehumidification capacity. Due to this, the regeneration air should be as dry as possible in order to achieve good performance. Thus the humidification of the regeneration air must be rated as unfavourable. In addition, if there are pollutants in the exhaust air, they pass through the desiccant wheel and could damage the wheel or at least contaminate it and thus reduce the performance in the long run.

OPEN CYCLE SYSTEMS

Open cycle systems (as shown in Fig. 10.3) can be used e.g. if the room exhaust air is polluted and thus not suitable for regeneration. A disadvantage of the open cycle system is that in full desiccant cooling operation a higher total air volume flow must be moved than in a closed cycle system and thus more high grade electric energy is necessary for the fan operation. On the other hand, with less humidity in the regeneration air, the dehumidification performance is better and thus regeneration energy can be saved. An additional disadvantage is that the adsorption energy that is set free by dehumidification is not used to preheat the regeneration air.

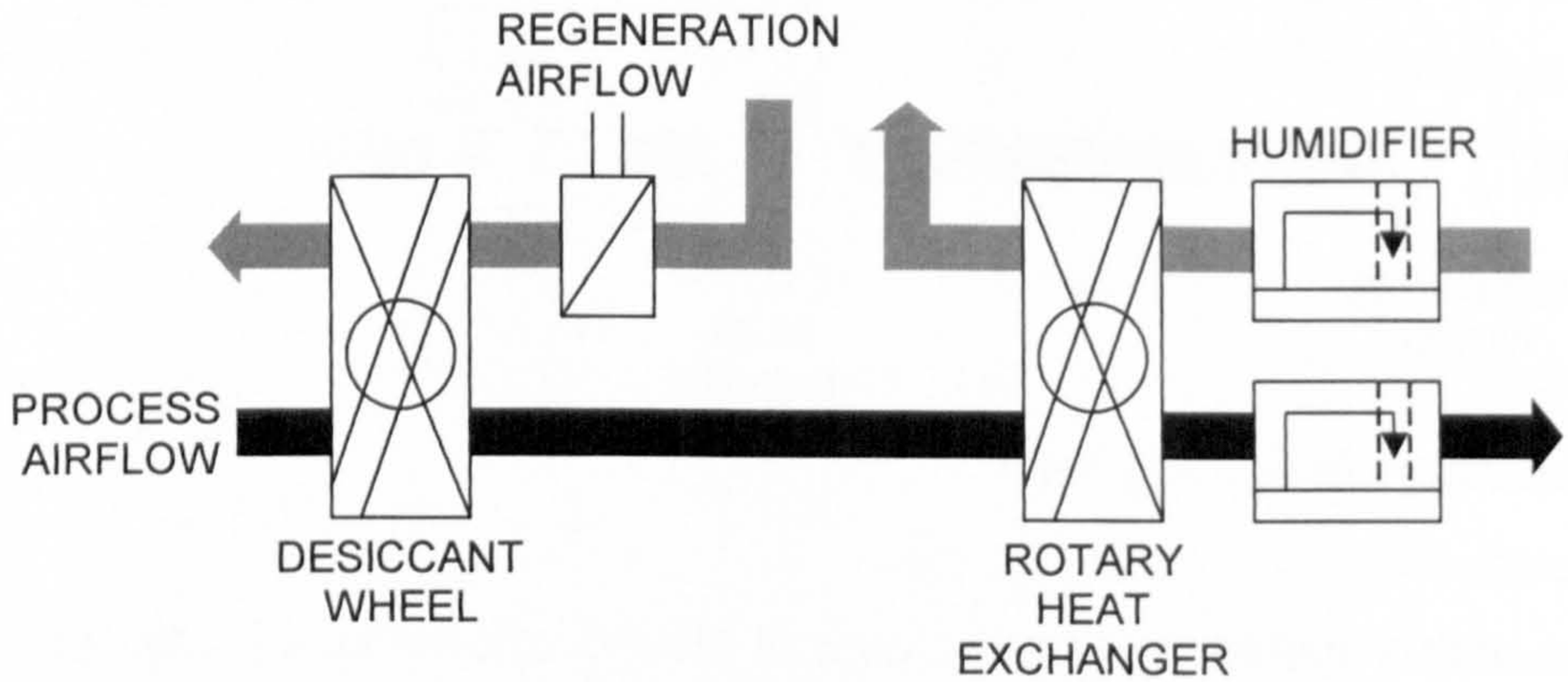

Fig. 10.3: *Open cycle DEC-system*

CASCADE SYSTEMS

Cascade systems (as shown in Fig. 10.4) are mostly modified versions of open cycle systems, but also closed cycle systems can be modified to cascade systems.

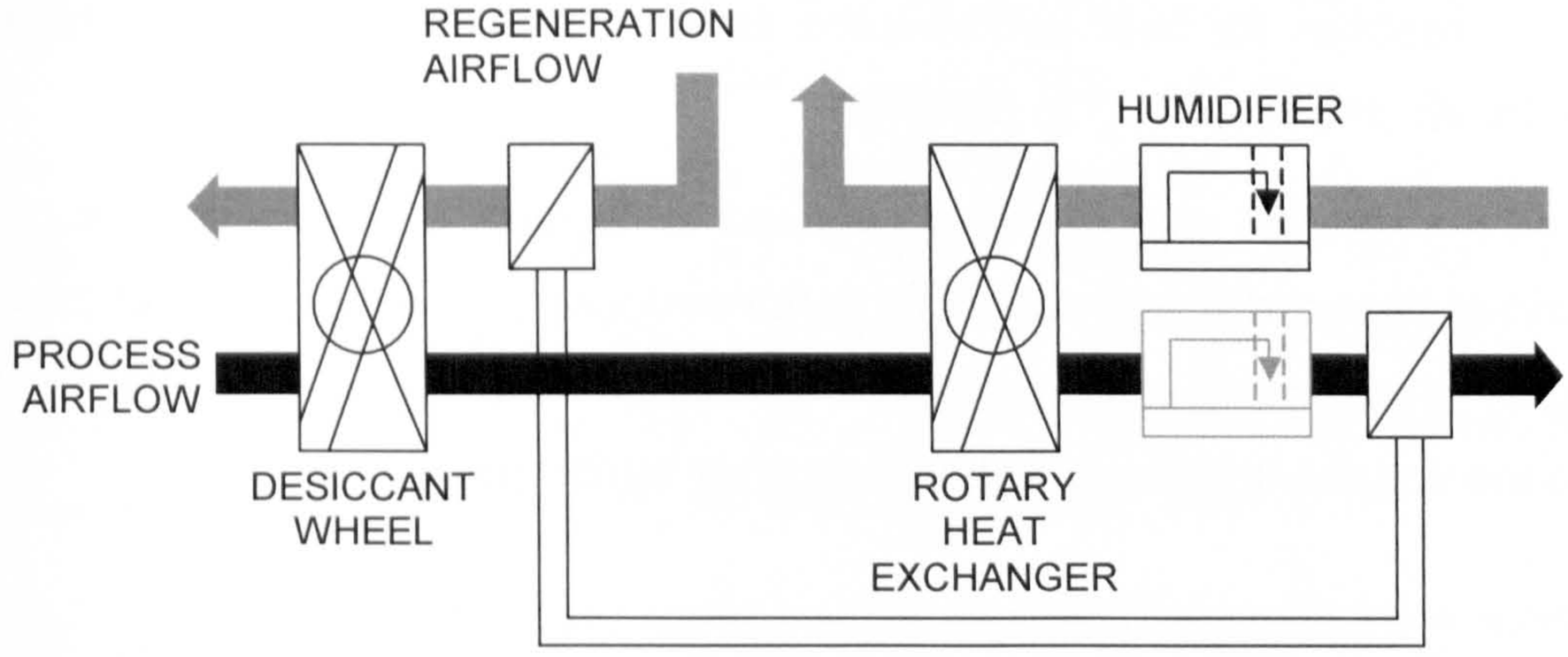

Fig. 10.4: *Open cycle, cascade DEC-system*

The main feature of cascade systems is the combination of DEC technology with conventional cooling technology (e.g. compressor chillers). This system is advantageous for situation in which full desiccant cooling is required but the cooling demand is low, which is usually the case with relatively low ambient air temperatures and a small humidification potential of the process air. For these operation conditions, the COP of a "standard" DEC-system is usually very low and a high amount of regeneration energy is required for only a small temperature decrease in the supply air. An additional advantage is that due to the sensible cooling possibility, dry and cool air can be provided if the supply air humidifier is not in use. The disadvantage of this system clearly is the use of the conventional cooling technology with all its disadvantages (harmful refrigerants, high grade electricity use etc.). However, in contrast to a conventional cooling system, the cascade system is much more environmentally friendly due to the much smaller power of the required conventional cooling device.

10.4 GUIDELINES FOR CONTROL STRATEGY

10.4.1 CONTROL OF DESICCANT WHEEL OPERATION

In this study the best rotation velocity was determined to be wheel specific and not decisively influenced by other operation parameters. The Hexcore wheel (silica gel) reaches its best performance at 85 to 100 RPH, the Klingenburg wheel (lithium chloride) at 20 to 30 RPH.

Naturally, the rotation velocity could be used to regulate a DEC-system, e.g. if the maximal dehumidification capacity is not necessary, however in most cases it would be much more energy efficient to change other operating parameters such as the volume flow or the regeneration air temperature.

10.4.2 VOLUME FLOW CONTROL

With a DEC-system, a large amount of electrical energy must be supplied for the fans. Thus the chosen volume flows should be as low as possible to save high grade electricity.

The lower limit of the supply air volume flow should usually set according to the minimum fresh air requirement for health and hygiene in the building. The maximal volume flow should be determined by the design volume flow that is calculated for the design conditions (see paragraph 10.3.1).

For the volume flow ratio between the regeneration air and the process air, the studies in chapter 05 (desiccant wheel test plant) showed, that a ratio of 0.75 results into the best performance. Using a higher volume flow for regeneration will usually not increase the performance, but sometimes even cause a decrease in the level of performance. With less demand on the dehumidification capacity, the regeneration air volume flow can be reduced even further, which would save energy twofold; first, less fan power is needed and secondly, the amount of energy required to heat the regeneration air is smaller.

10.4.3 CONTROL OF REGENERATION AIR TEMPERATURE

The experiments at the desiccant wheel test plant showed that a higher regeneration air temperature results principally in higher dehumidification capacities at almost equal dehumidification efficiencies. Due to the fact that for the regeneration air temperature, the enthalpy of the process air also rises due to the heat transferred by the matrix material, the regeneration air temperature should be set as low as possible. For the studied desiccant wheels, sensible dehumidification capacities were reached starting at about 50°C, but regeneration air temperatures over 70 °C did not usually result in a further improvement of the dehumidification capacity, however the enthalpy of the supply air did increase due to the rising heat transfer rate.

The evaluation of the DEC-system in Althengstett showed (see Chapters 08 and 09), that the use of a fixed regeneration air temperature is not adequate and results, especially with partial load operation, in very low COPs. If in addition the regeneration energy must then be supplied by auxiliary heating (powered by gas, oil or electricity), the operation of the DEC-system is generally not economical.

10 DESIGN GUIDELINES

CHAPTER 11

SUMMARY

11.1 MAIN CONCLUSIONS

11.1.1 EXPERIMENTAL INVESTIGATIONS ON A TEST PLANT

The evaluation of the measurements from a desiccant wheel test plant at the University of Applied Sciences in Stuttgart leads to new, detailed knowledge about the influence of the different operating parameters on the performance of the sorption wheels tested in this study.

The best rotation velocity was determined to be wheel specific.

The evaluation of the measurements with different volume flow ratios shows, that a ratio of 0.75 between the regeneration air and the process air leads to the best performance for the tested wheels. Using a higher volume flow for regeneration cannot increase the performance and for the most part lower volume flow ratios resulted in lower performance.

The investigation of the regeneration air conditions showed, that a higher regeneration air temperature leads principally to higher dehumidification potentials at almost equal dehumidification efficiencies. The energy efficiency (RSHI) worsened slightly as the regeneration temperatures rose. It is however to be considered, that along with the regeneration air temperature, the enthalpy of the process air also rises due to the heat transferred by the matrix material. The influence of the regeneration air humidity was also notable. Due to this, the regeneration air should be as dry as possible in order to achieve good performance.

Finally, the measurements show as a further matter of principle, that rising water content in the ambient air causes the dehumidification capacity to rise, whereby the dehumidification efficiency falls as a result of rising water content.

11.1.2 DESICCANT WHEEL SIMULATION MODEL

After the calibration of the desiccant wheel model was made, the results of the calculations were in good agreement with the measured values. The remaining small deviations in the results can be explained by processes that were not considered in the model, e.g. air leakage rates or heat losses/gains to/from the surroundings. Furthermore, the deviations could also be caused by measuring inaccuracies of the used devices.

For the calibration of the model, mainly two modifications were necessary. First, the mass of adsorption material given by the manufacturer had to be reduced to an "effective or operating" mass, which can be explained probably by the construction process. The second modification was the adjustment of the heat transfer from the air to the matrix material, which can in this case not be described by the heat transmission resistance alone, but is determined also by the internal heat transport in the wheel material (thermal conductivity).

Thus the use of the desiccant wheel simulation model for different wheels seems to need mainly the calibration by the "effective" mass of adsorption material and an "effective" value for the heat transfer coefficient.

11.1.3 MONITORING OF SOLAR POWERED DEC-SYSTEMS

Once a DEC-system in a public library in Mataró/Spain was monitored. The data monitored by sensors of the building management system confirm the planned/expected cooling power of the installed desiccant cooling plant. However, the attempt to evaluate single components (especially the humidifiers and the desiccant wheel) using this data failed. The measurement of the humidity seems to be especially difficult and susceptible to error, similar to experiences with the test plant for desiccant wheels in Stuttgart.

Further a DEC-system installed in a plastics processing factory in Althengstett/Germany was monitored. The monitoring on this plant was much more extensive than the monitoring on the above mentioned system in Spain.

For the evaluation of the comprehensive monitored data, it was mainly the inadequacy of the measuring devices that led to big problems. Further a comparison of two different evaluation procedures showed, in an impressive way, how different the outcomes can depend on the choice of sensors and evaluation criteria. Thus, the determined values must always be judged in relation to the evaluation procedures used.

If there is no cooling demand for the production hall, at this plant the regeneration energy (solar energy and waste heat) can be used to provide warm air for an air heating system that supplies an assembly hall and/or an older storage hall. The energy evaluation of this air heating system showed that about 59000 kWh of heating energy were supplied for heating demand but only 16 % of that energy was produced by solar collector operation and 84 % by waste heat use.

The evaluation of the solar air collector operation showed, that the gain from the solar air collectors was mainly used for the air heating system as the time with full desiccant cooling operation was short. The average efficiency of the air collectors was about 0.5, as expected.

For the operation of the DEC-System, the evaluation shows that altogether 78500 kWh of heat were supplied through heat recovery from the exhaust air to heat the new production hall at low ambient air temperatures. For cooling, only 11350 kWh were supplied. Thus despite the high thermal loads from production, the DEC-system acted more often as a heat recovery system (heating) than a cooling system.

The average COP associated with active cooling was 0.81, and associated with full desiccant cooling, it was only 0.32. While operating under design conditions however, the COP associated with full desiccant cooling reached values of between 0.8 and 1.1 as was assumed during planning. The low average COP was caused by full desiccant cooling operation at relative low ambient air temperatures, when high amounts of regeneration energy were used and only small temperature decreases could be achieved.

In summary the DEC-technology can be rated in principle as a forward looking, environmental friendly and also economically operating cooling system, if the cooling demand is in phase with available thermal energy (solar energy, waste heat etc.). There the system works much better in hot and dry climates than in climates with moderate temperatures and a high relative humidity.

In cases where the standard design conditions (usually: 32°C / 40 % r.h.) are rarely reached (moderate climate), the suitability of a DEC-system has to be checked in detail, because the manufacturer given cooling power or COP is only guilty for design conditions. With lower ambient air temperatures the cooling power and the efficiency strongly decreases.

11.1.4 OPTIMISATION POSSIBILITIES IN CONTROL STRATEGY AND DESIGN

For the adequate control of a DEC-system, a step-by-step control strategy that takes into consideration the specific inertia of each individual component is required. Control steps e.g. from the heat recovery mode directly to full desiccant cooling operation as observed at the DEC-system in Althengstett must be prevented, especially at low ambient air temperatures when the efficiency of the DEC-system in full desiccant cooling mode is naturally low.

In addition, a control strategy that allows a variable auxiliary heating power can save high amounts of regeneration energy in contrast to a control strategy with a fixed regeneration temperature demand. Especially at low ambient air temperatures, full desiccant cooling operation with a fixed regeneration temperature needs high amounts of regeneration energy, but only achieves a small temperature decrease in the process air. Under such conditions (low cooling demand), an additional cooling system (e.g. compressor chiller, such as the one installed in the DEC-system in Mataró) could also be advantageous.

The enlargement of the solar air collector fields is only useful if full desiccant cooling operation is usually required during times in which solar irradiation is possible. If solar irradiation and full desiccant cooling operation are not in

phase, this energy cannot be used due to the absence of the possibility of thermal storage with solar air collectors. In such cases, solar water collectors would be preferable due to their ability to store energy.

11.1.5 DESIGN GUIDELINES

In chapter 10 the results and conclusions from this study has been summarized into general guidelines for both design and control strategies for DEC-systems. These guidelines are based on knowledge obtained through experience with the operation of complete DEC-systems and provide detailed information about desiccant wheel operation. These guidelines are based on fundamental, proved knowledge and may be useful for planning and designing other DEC-systems, thus serving as a contribution that helps advance DEC technology by aiding planning engineers and by clarifying the still existing uncertainties about this forward-looking technology.

11.2 RECOMMENDATIONS FOR FURTHER WORK

For further work it seems to be meaningful to develop control strategies taking into account the gained knowledge and to investigate the suitability in practical use in real plants.

As a result of the rules and guidelines presented, an example of a step-by-step control strategy could be as follows:

For the example, the DEC-system is installed in a building with a minimum fresh air demand of V_{min}. The maximal cooling demand is determined for an ambient air temperature of 32°C. The allowed minimum supply air temperature is given as 17°C and a maximum allowed indoor air temperature is 26°C at design conditions (worst case scenario). The volume flow necessary to provide the maximal cooling demand under design conditions is V_{max}. The indoor temperature should be kept between 22°C and 26°C.

To realize a variable, economic and smooth volume flow control using low volume flows with a low cooling demand, the functional relationship between the indoor temperature and the demand on the supply air temperature level and supply air volume flow could be implemented in the control strategy e.g. as shown in Fig. 11.1.

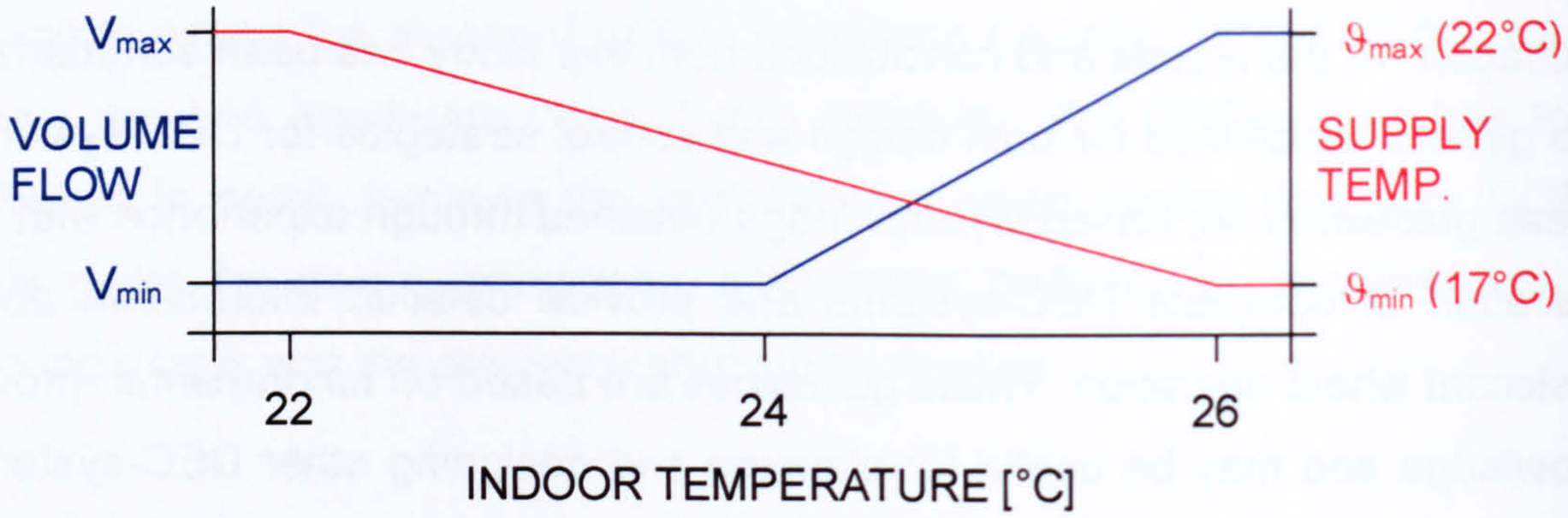

Fig. 11.1: *Functional relationship between indoor temperature and demand on supply air volume flow and temperature for a smooth control strategy (example)*

With this functional relationship, the cooling power rises due to the required supply air temperature as the indoor temperature increases but also the minimum volume flow is assured until the indoor temperature reaches 24 °C. The minimum supply air temperature is not required until the indoor temperature reaches its maximum temperature of 26°C. Please note however; the functional relationship that best meets the requirements in each single case can probably only be determined by a simulation of the DEC-system.

Additionally, the cooling power of a DEC-system can be divided into single stages in order to increase the active cooling power step-by-step. A sensible order of the single stages is shown in Tab. 11.1 (assuming the presence of a 3-stage supply air humidifier).

1.	Supply air humidifier (stage 1)
2.	Supply air humidifier (stage 2)
3.	Supply air humidifier (stage 3)
4.	Exhaust air humidifier and rotary heat exchanger
5.	Regeneration without auxiliary heating (only solar energy, waste heat etc.)
6.	Regeneration with auxiliary heating (oil, gas, electricity)
6.1	Regeneration air temperature: 50°C
6.2	Regeneration air temperature: 60°C
6.2	Regeneration air temperature: 70°C / ϑ_{max}

Tab. 11.1: *Order of stages for active cooling operation with DEC-systems*

To consider the possibility of a variable volume flow ratio (regeneration air to process air) between 0.5 and 0.75, a functional relationship between the regeneration temperature and volume flow ratio, shown in Fig. 11.2, could be implemented into the control strategy.

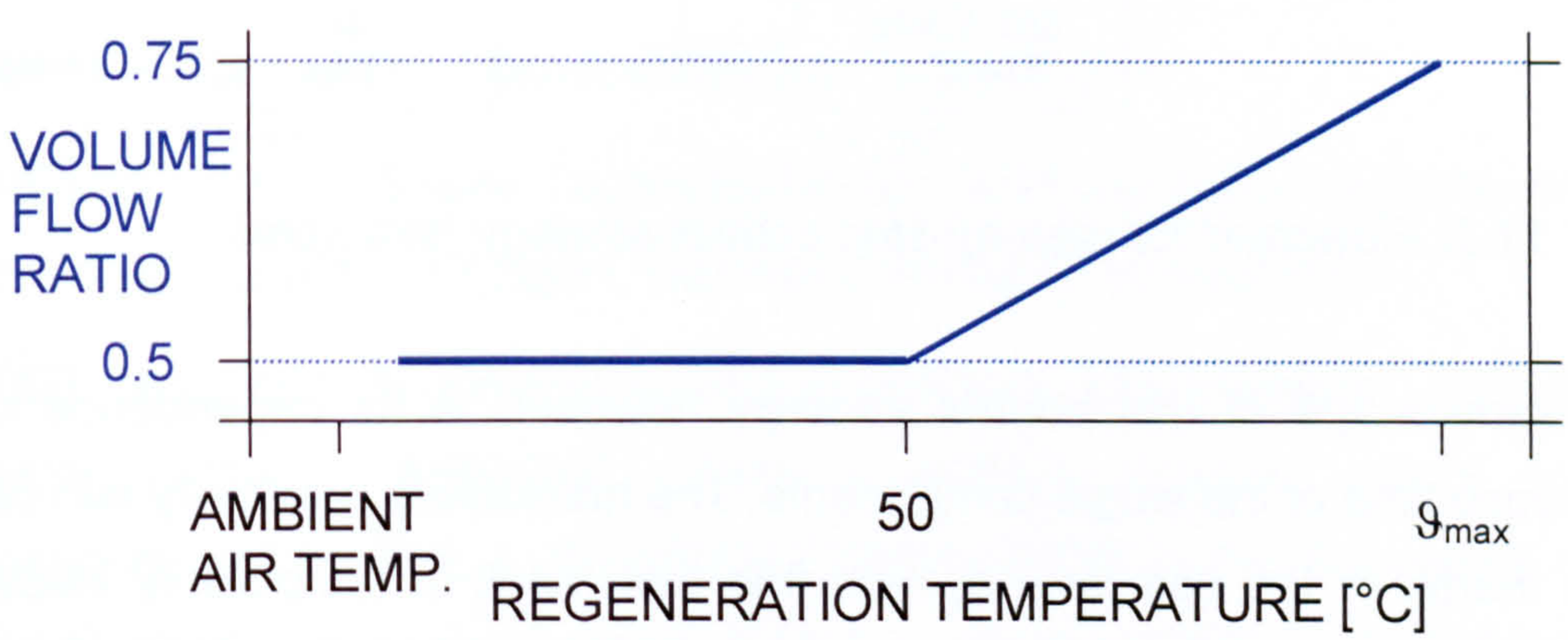

Fig. 11.2: *Functional relationship between regeneration air temperature and volume flow ratio (regeneration to process air)(example)*

As for the control of the supply air volume flow, also for the relationship shown in Fig. 11.2, the best variant could only be determined with a comprehensive simulation of the DEC-system.

A possible control strategy for the DEC-system could be realized as is shown in the flowchart (Fig. 11.3).

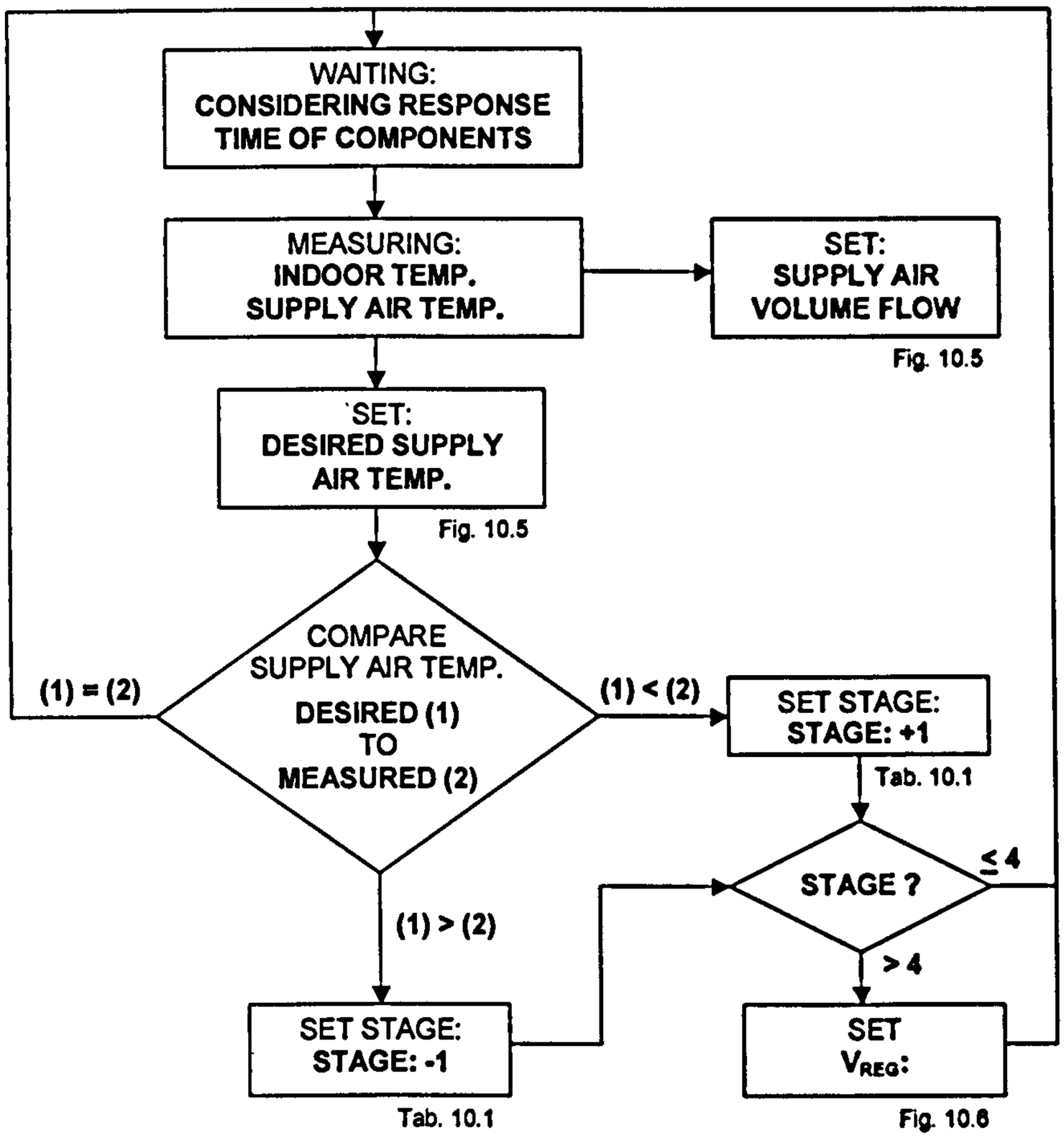

Fig. 11.3: *Flowchart for step-by-step control strategy (example)*

A disadvantage of this control strategy however, is its dependence on the response time of the single components. The humidifiers especially can cause a high inertia in the complete system that can result in temporarily inadequate operation of the DEC-system should a sudden change in the cooling demand occur.

A forward looking solution for this problem is a control strategy that is coupled to a simulation model of the DEC-system, so that the best operation mode can be calculated from the boundary conditions at every point in time and thus the inertia of the DEC-system can be mostly eliminated. The examination of such a control strategy could also be part of an additional study on DEC-systems in the future.

REFERENCES

AL-AMOURI, A. (1994). *Aufbau einer Wärmeübertragerdatei zur Charakterisierung und Auswahl von Wärmeübertragern* (Design of a heat exchanger data file for characterisation and choice of heat exchangers). Unpub. dissertation. Technische Universität Dresden, Germany.

BAUER, O. (1998). *Auslegung eines Sorptionsregenerators* (Dimensioning of a sorption regenerator). Unpub. paper. Technische Universität Hamburg-Harburg, Germany.

BRUNAUER, S., EMMETT, P. H. and TELLER, E. (1938). *Adsorption of gases in multimolecular layers.* Journal of the American Chemical Society. 60, 309-319.

DUBININ, M. M. (1960). Chemical Reviews. 60, 235-241.

EICKER, U. (2001). *Solare Technologien für Gebäude* (Solar technologies for buildings) (1st edit.). Stuttgart, Germany: Verlag B. G. Teubner.

EICKER, U. (2002). *Adsorption cooling of buildings with integrated PV/solar air heating facades - AIRCOOL -.* Final publishable progress report. (Project funded in part by THE EUROPEAN COMMISSION in the framework of the Non Nuclear Energy Programme JOULE III, Contract ERK6-CT1999-00010). Fachhochschule Stuttgart – Hochschule für Technik, Germany.

EICKER, U. and HUBER, M. and MAIER, C. (2002). *Pilotanlage zur Sorptionskühlung mit solaren Luftkollektoren.* (pilot plant for sorption cooling with solar air collectors). Final publishable progress report. (Project funded in part by DEUTSCHE BUNDESSTIFTUNG UMWELT, Ref.-No: 16661). Fachhochschule Stuttgart – Hochschule für Technik, Germany.

GAS RESEARCH INSTITUTE. (2001). *Desiccant systems tutorial.* Internet publication (www.gri.org/pub/solutions/desiccant/): Gas Research Institute, USA.

REFERENCES

GASSEL, A. (1998). *Programme extract* of TRNSYS Type 107

GLUECK, B. (1991). *Zustands- und Stoffwerte (Wasser, Dampf, Luft)* (State and material data (water, vapour, air)). Berlin, Germany: Verlag für Bauwesen.

GREGORIG, R. (1959). *Wärmetauscher Bd. 4. Berechnung – Konstruktion – Betrieb - Wirtschaftlichkeit* (heat exchanger Vol. 4. Calculation – construction – operation - economic efficiency). Aarau und Frankfurt a.M., Germany: Verlag H. R. Sauerländer & Co.

GUTERMUTH, W. (1980). *Untersuchung der gekoppelten Wärme- und Stoffübertragung in Sorptionsregeneratoren* (Investigation of coupled heat and mass transfer in sorption regenerators). Unpub. dissertation. Technische Universität Darmstadt, Germany.

HEINRICH, G. and FRANZKE, U. (1997). *Sorptionsgestützte Klimatisierung – Entfeuchtung und DEC in der Klima-Kälte-Technik* (Adsorption cooling systems – Dehumidification and DEC for air conditioning an refrigeration) (1st edit.). Heidelberg, Germany: C.F. Müller Verlag.

HERING, E. and MARTIN, R. and STOHRER, M. (1997). *Physik für Ingenieure* (Physics for engineers) (6th edit.). Berlin, Heidelberg, New York: Springer Verlag.

HOEFKER, G. (2001). *Desiccant cooling with solar energy.* Unpub. dissertation. Institute of Energy and Sustainable Development, De Montfort University Leicester, Great Britain and Department of Building Physics, University of Applied Sciences Stuttgart, Germany.

KAST, W. (1988). *Adsorption aus der Gasphase (*Adsorption from gas phase). Weinheim, Germany: VCH Verlagsgesellschaft mbH.

KRISCHER, O. and KAST, W. (1978). *Trocknungstechnik Bd.1. Die wissenschaftlichen Grundlagen der Trocknungstechnik (*Drying technology, Vol.1. The scientific fundamental principles of drying technology) (3rd edit.). Berlin, Heidelberg, New York: Springer-Verlag.

LANGMUIR, I. (1918). *The Adsorption of gases on plane surfaces of glass, mica and platinum.* Journal of the American Chemical Society. 40, 1361-1403.

LEUPOLD, W. et. al. (1991). *Lehr- und Übungsbuch Mathematik III* (Textbook and exercise book of mathematics, Vol. III) (21st edit.). Leipzig: Fachbuchverlag GmbH Leipzig.

MATHEMATICA 4.2 (2002). Software: Wolfram Research, Inc. Champaign, IL 61820 (USA).

MERTINS, M. (2000). *Entwicklung eines Modells für Desiccant and Evaporative Cooling (DEC) und Implementation in eine Simulationsumgebung* (Development of a model for desiccant and evaporative cooling (DEC) and implementation in a simulation platform). Unpub. diploma thesis. Technische Universität Karlsruhe, Germany.

MUNTERS CARGOCAIRE ENGINEERING CORP. (2001). *Dehumidification for all requirements.* Internet publication (www.muntersamerica.com/dh/htm/desiccant.htm): Munters Cargocaire Engineering Corp, USA.

OTTEN, W. (1989). *Simulationsverfahren für die nichtisotherme Ad- und Desorption im Festbett auf der Basis der Stoffdaten des Einzelkorns am Beispiel der Lösungsmitteladsorption.* (Simulation process of the not isotherm ad- and desorption in fixed beds basing on material data of the grain at sample of solvent adsorption). Fortschrittsberichte VDI. Reihe 3, Nr. 186. Düsseldorf, Germany: VDI Verlag.

POLANYI, M. (1914). *On the adsorption from the standpoint of the third law of thermodynamics.* Verhandlungen der Deutschen Physikalischen Gesellschaft. 16, 1012 ff.

RECKNAGEL and SPRENGER and SCHRAMEK. (1997). *Taschenbuch für Heizung und Klimatechnik (for Heating and Air)* (68th edit.). München, Germany: R. Oldenbourg Verlag.

SCHELLER, G. (2003). *Messunsicherheit einer Temperaturmesskette* (Inaccuracy of a temperature measurement arrangement) (1st edit.). Germany: M. K. Juchheim GmbH & Co. KG.

SLAYZAK, S. J. and PESARAN, A. A. and HANCOCK, C. E. (1999). *Experimental evaluation of commercial desiccant dehumidifier wheels.* Internet publication (www.nrel.gov/desiccantcool/wheels.htm): U.S. Department of Energy, National Renewable Energy Laboratory, Advanced Desiccant Cooling & Dehumidification Program.

SLAYZAK, S. J. and RYAN, J. P. (2000). *Desiccant Dehumidification Wheel Test Guide*. Technical report: National Renewable Energy Laboratory, U.S. Department of Energy laboratory, Colorado (USA)

WEBER, R. (2001). *Hochisolationsleitungen* (High insulation ducts). Final report of a preliminary study: EMPA, Department of Energy-Systems / Domestic Technique . Dübendorf, Swiss: EMPA ZEN.

APPENDIX

APPENDIX A

Overview and detailed outcomes of measurements from the desiccant wheel test facility at the University of Applied Sciences, Stuttgart

APPENDIX B

Comparison of measured values from the desiccant wheel test facility at the University of Applied Sciences, Stuttgart and calculated values by the desiccant wheel model

APPENDIX C

Overview of measurement points for the monitoring of the DEC-system in a plastics processing Factory in Althengstett, Germany

APPENDIX D

Evaluation of monitored data from the DEC-system in a plastics processing factory in Althengstett/Germany: COMPONENT OPERATION TIME

APPENDIX E

Evaluation of monitored data from the DEC-system in a plastics processing factory in Althengstett/Germany: OPERATION MODE OF DEC-SYSTEM (TIME)

APPENDIX F

Evaluation of air collector operation (DEC-system in a plastics processing factory in Althengstett/Germany): SOLAR IRRADIATION / COLLECTOR GAIN

COLLECTOR EFFICIENCY

OUTCOMES OF MEASUREMENTS FROM THE DESICCANT WHEEL TEST FACILITY

measurement series overview

Desiccant wheel: **Engelhard HexCore, LP / DES-H-Hexcore-DC15/N**

No:	process airflow (set values)			reg. airflow (set values)			Volume flow ratio
	θ [°C]	φ [%]	V [m³/h]	θ [°C]	φ [%]	V [m³/h]	$V_{reg}/V_{process}$ [-]
H1	32	40	2000	75	-	2000	1.0
H2	28	40	2000	60	-	1500	0.75
H3	36	60	2000	75	-	1500	0.75
H4	32	40	2000	60	-	1500	0.75
H5	32	40	2000	75	-	1500	0.75
H6	32	40	2000	75	-	1000	0.5
H7	36	50	2000	60	-	1500	0.75
H8	28	40	2000	75	-	1500	0.75
H9	32	40	2000	90	-	1500	0.75

Desiccant wheel: **Klingenburg, SECO 1000**

No:	process airflow (set values)			reg. airflow (set values)			Volume flow ratio
	θ [°C]	φ [%]	V [m³/h]	θ [°C]	φ [%]	V [m³/h]	$V_{reg}/V_{process}$ [-]
K1	32	40	2000	60	-	1500	0.75
K2	32	40	2000	60	10	2000	1.0
K3	32	40	2000	60	10	1000	0.5
K4	28	40	2000	60	10	1500	0.75
K5	36	50	2000	60	10	1500	0.75
K6	32	40	2000	70	10	1500	0.75
K7	32	40	2000	50	10	1500	0.75
K8	32	40	2000	45	10	1500	0.75
K9	32	40	2000	60	10	1500	0.75
K10	32	40	2000	60	20	1500	0.75
K11	32	60	2000	60	-	1500	0.75
K12	28	60	2000	60	-	1500	0.75
K13	32	60	1500	60	-	1125	0.75
K14	32	40	1500	60	-	1125	0.75

OUTCOMES OF MEASUREMENTS FROM THE DESICCANT WHEEL TEST FACILITY

measurement series H1

Desiccant wheel: **Engelhard HexCore, LP / DES-H-Hexcore-DC15/N**

Set values:

	temperature [°C]	rel humidity [%]	vol flow [m³/h]
process airflow	32	40	2000 $l_{20°C}$
reg airflow	75	-	2000 $l_{20°C}$

$V_{reg} : V_{process}$ 1

Measured values:

RPH	ambient air					supply air				
	θ [°C]	φ [%]	x [g/kg]	h [kJ/kg]	Vnorm [m³/h]	θ [°C]	φ [%]	x [g/kg]	h [kJ/kg]	Vnorm [m³/h]
25	31,98 ± 0,09	39,48 ± 0,24	11,78 ± 0,07	62,1 ± 0,2	2022 ± 13	42,44 ± 0,22	17,28 ± 0,74	9,07 ± 0,44	65,8 ± 1,3	2062 ± 6
40	32,00 ± 0,08	39,73 ± 0,21	11,87 ± 0,06	62,4 ± 0,2	2000 ± 12	41,35 ± 0,25	16,77 ± 0,92	8,30 ± 0,50	62,7 ± 1,4	2039 ± 8
55	31,96 ± 0,06	39,79 ± 0,31	11,86 ± 0,06	62,3 ± 0,2	1980 ± 11	46,82 ± 0,09	11,38 ± 0,54	7,46 ± 0,38	66,1 ± 1,1	2018 ± 6
70	31,96 ± 0,05	39,69 ± 0,58	11,83 ± 0,17	62,2 ± 0,5	1997 ± 12	54,75 ± 0,04	7,43 ± 0,29	7,19 ± 0,28	73,4 ± 0,7	2000 ± 7
85	31,94 ± 0,05	40,63 ± 0,56	12,10 ± 0,17	62,9 ± 0,4	1999 ± 12	56,11 ± 0,06	7,10 ± 0,23	7,33 ± 0,24	75,2 ± 0,6	2008 ± 8
100	31,98 ± 0,06	41,06 ± 0,59	12,26 ± 0,18	63,3 ± 0,5	1981 ± 9	57,37 ± 0,10	6,83 ± 0,22	7,48 ± 0,25	76,9 ± 0,7	1983 ± 8
150	31,95 ± 0,07	41,02 ± 0,57	12,22 ± 0,18	63,2 ± 0,5	1985 ± 9	59,07 ± 0,04	6,28 ± 0,18	7,45 ± 0,22	78,5 ± 0,6	1985 ± 7

RPH	regeneration air					waste air				
	θ [°C]	φ [%]	x [g/kg]	h [kJ/kg]	Vnorm [m³/h]	θ [°C]	φ [%]	x [g/kg]	h [kJ/kg]	Vnorm [m³/h]
25	74,72 ± 0,22	3,10 ± 0,04	7,81 ± 0,11	95,3 ± 0,4	2153 ± 30	60,42 ± 0,18	13,22 ± 0,22	16,95 ± 0,36	104,7 ± 1,1	2182 ± 8
40	75,05 ± 0,07	2,80 ± 0,01	7,14 ± 0,02	93,9 ± 0,1	1972 ± 16	48,14 ± 0,09	12,37 ± 0,21	8,67 ± 0,16	70,6 ± 0,5	2160 ± 7
55	75,03 ± 0,07	2,76 ± 0,02	7,04 ± 0,04	93,6 ± 0,1	1991 ± 13	45,37 ± 0,06	15,08 ± 0,23	9,21 ± 0,16	69,1 ± 0,4	2177 ± 7
70	75,11 ± 0,02	2,22 ± 0,00	5,67 ± 0,01	90,1 ± 0,0	2153 ± 29	50,52 ± 0,05	17,66 ± 0,17	14,09 ± 0,15	87,0 ± 0,4	2229 ± 7
85	75,15 ± 0,09	2,23 ± 0,01	5,70 ± 0,02	90,2 ± 0,1	2135 ± 18	49,13 ± 0,05	19,09 ± 0,18	14,20 ± 0,15	85,9 ± 0,4	2245 ± 7
100	75,14 ± 0,22	2,19 ± 0,02	5,60 ± 0,07	89,9 ± 0,3	2172 ± 37	48,47 ± 0,09	19,57 ± 0,19	14,08 ± 0,15	84,9 ± 0,4	2278 ± 7
150	75,28 ± 0,06	2,20 ± 0,01	5,64 ± 0,03	90,2 ± 0,2	2146 ± 24	46,58 ± 0,05	21,15 ± 0,10	13,83 ± 0,08	82,3 ± 0,2	2260 ± 6

Figures of merit:

RPH	$\Delta x_{emb-sup}$ [g/kg]	RSHI [kJ/g]	η_{dehum} [-]	$\Delta h_{sup-emb}$ [kJ/kg]
25	2,71	16,90	0,31	3,7
40	3,57	11,98	0,40	0,4
55	4,40	9,90	0,49	3,8
70	4,64	10,10	0,49	11,2
85	4,77	9,74	0,50	12,3
100	4,78	9,98	0,49	13,5
150	4,77	9,88	0,49	15,3

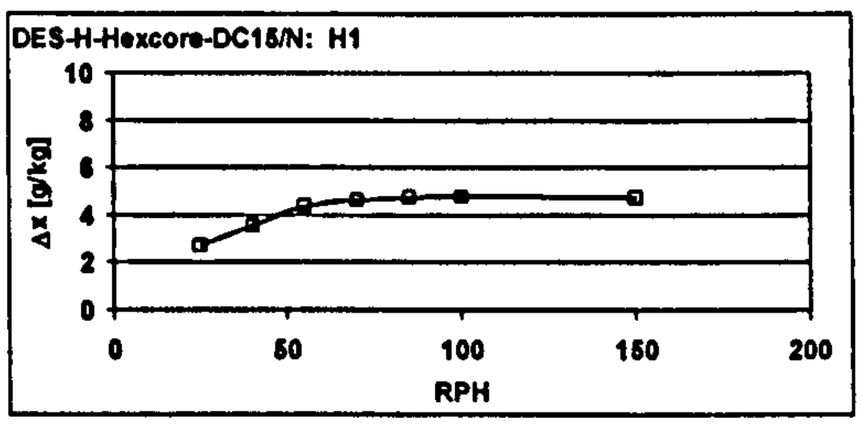

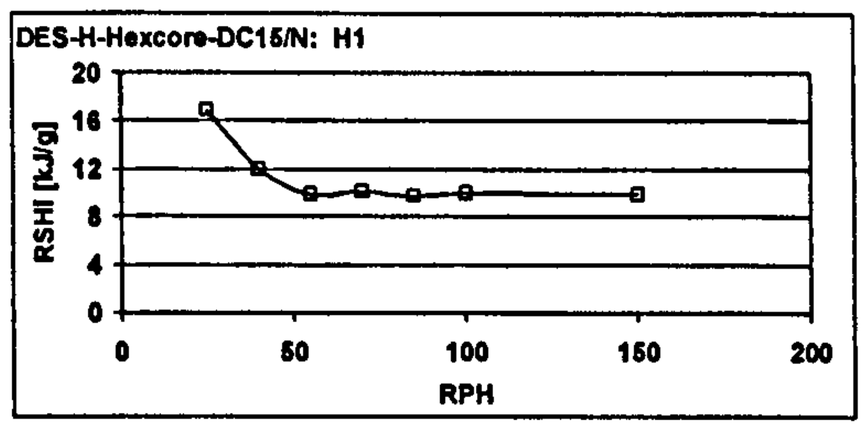

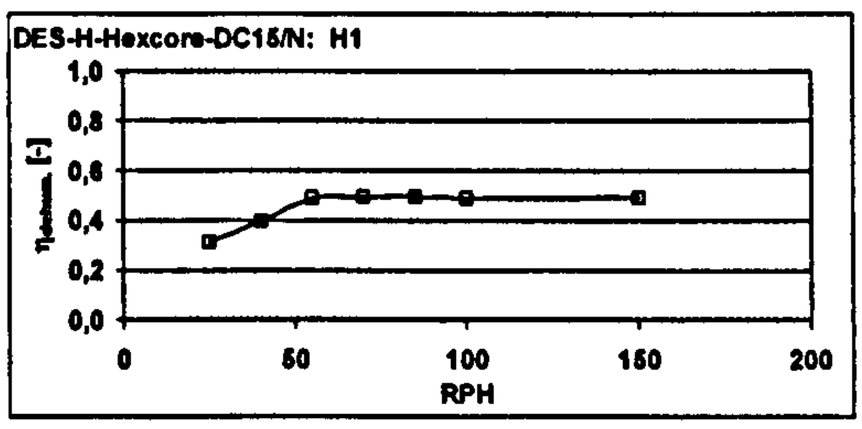

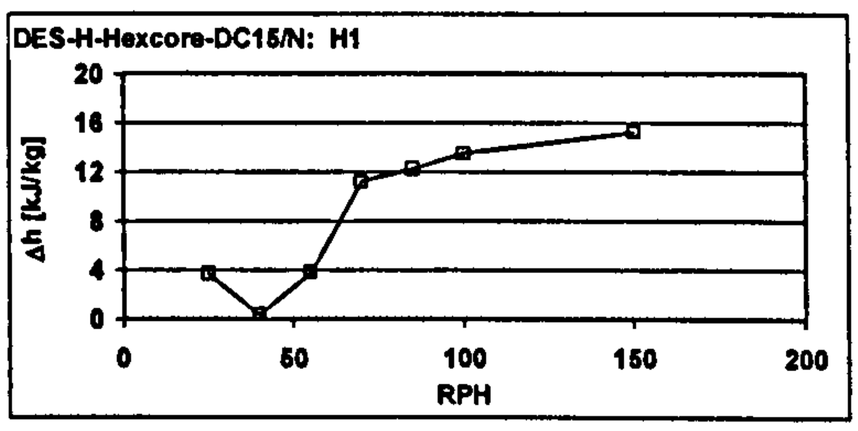

APPENDIX A

OUTCOMES OF MEASUREMENTS FROM THE DESICCANT WHEEL TEST FACILITY

measurement series H2

Desiccant wheel: **Engelhard HexCore, LP / DES-H-Hexcore-DC15/N**

Set values:

	temperature [°C]	rel. humidity [%]	vol. flow [m³/h]
process airflow	28	40	2000 $l_{20°C}$
reg. airflow	60	-	1500 $l_{20°C}$

$V_{reg} : V_{process}$ 0,75

Measured values:

RPH	ambient air					supply air				
	θ [°C]	*φ [%]*	*x [g/kg]*	*h [kJ/kg]*	*Vnorm [m³/h]*	*θ [°C]*	*φ [%]*	*x [g/kg]*	*h [kJ/kg]*	*Vnorm [m³/h]*
25	27,99 ± 0,06	40,03 ± 0,35	9,46 ± 0,08	52,1 ± 0,2	2008 ± 11	35,75 ± 0,15	21,08 ± 0,55	7,71 ± 0,25	55,5 ± 0,8	2066 ± 8
40	27,98 ± 0,05	39,82 ± 0,31	9,41 ± 0,08	52,0 ± 0,2	1997 ± 13	39,38 ± 0,07	15,72 ± 0,45	6,99 ± 0,22	57,4 ± 0,6	2046 ± 7
55	27,99 ± 0,05	39,96 ± 0,41	9,44 ± 0,10	52,1 ± 0,3	2010 ± 9	40,71 ± 0,06	14,23 ± 0,40	6,79 ± 0,20	58,2 ± 0,5	2069 ± 7
70	27,99 ± 0,05	39,74 ± 0,38	9,40 ± 0,09	52,0 ± 0,2	1991 ± 10	41,94 ± 0,01	13,07 ± 0,28	6,65 ± 0,15	59,1 ± 0,4	2040 ± 6
85	27,96 ± 0,06	39,50 ± 0,41	9,32 ± 0,09	51,7 ± 0,3	1996 ± 11	42,66 ± 0,05	12,25 ± 0,24	6,47 ± 0,13	59,4 ± 0,3	2043 ± 6
100	27,99 ± 0,05	39,80 ± 0,36	9,41 ± 0,08	52,0 ± 0,2	1988 ± 11	43,39 ± 0,05	11,92 ± 0,19	6,54 ± 0,10	60,3 ± 0,3	2040 ± 5
150	28,00 ± 0,05	39,60 ± 0,32	9,36 ± 0,08	51,9 ± 0,2	1978 ± 5	44,37 ± 0,07	11,53 ± 0,15	6,66 ± 0,08	61,5 ± 0,2	2032 ± 5

RPH	regeneration air					waste air				
	θ [°C]	*φ [%]*	*x [g/kg]*	*h [kJ/kg]*	*Vnorm [m³/h]*	*θ [°C]*	*φ [%]*	*x [g/kg]*	*h [kJ/kg]*	*Vnorm [m³/h]*
25	60,04 ± 0,06	4,55 ± 0,02	6,01 ± 0,03	75,7 ± 0,1	1579 ± 20	46,58 ± 0,09	18,67 ± 0,29	12,18 ± 0,21	78,1 ± 0,6	1631 ± 5
40	60,03 ± 0,06	4,44 ± 0,03	5,86 ± 0,03	75,3 ± 0,1	1592 ± 23	42,58 ± 0,07	23,18 ± 0,29	12,31 ± 0,17	74,3 ± 0,5	1638 ± 4
55	60,01 ± 0,03	4,44 ± 0,01	5,85 ± 0,00	75,3 ± 0,0	1618 ± 20	40,90 ± 0,04	25,25 ± 0,22	12,27 ± 0,12	72,5 ± 0,3	1634 ± 5
70	59,91 ± 0,03	4,33 ± 0,01	5,68 ± 0,02	74,7 ± 0,1	1598 ± 21	39,38 ± 0,02	27,26 ± 0,20	12,22 ± 0,10	70,8 ± 0,3	1655 ± 5
85	59,96 ± 0,05	4,27 ± 0,02	5,61 ± 0,02	74,6 ± 0,1	1613 ± 27	38,38 ± 0,03	28,54 ± 0,17	12,13 ± 0,08	69,6 ± 0,2	1661 ± 5
100	59,93 ± 0,03	4,34 ± 0,03	5,70 ± 0,03	74,8 ± 0,1	1608 ± 22	37,61 ± 0,04	29,81 ± 0,13	12,15 ± 0,06	68,8 ± 0,2	1663 ± 5
150	59,96 ± 0,09	4,59 ± 0,04	6,03 ± 0,04	75,7 ± 0,1	1631 ± 29	36,46 ± 0,04	31,79 ± 0,11	12,17 ± 0,05	67,7 ± 0,2	1666 ± 4

Figures of merit:

RPH	$\Delta x_{amb-sup}$ [g/kg]	RSHI [kJ/g]	η_{dehum} [-]	$\Delta h_{sup-amb}$ [kJ/kg]
25	1,75	14,53	0,26	3,4
40	2,42	10,65	0,36	5,4
55	2,65	9,78	0,40	6,1
70	2,75	9,39	0,41	7,1
85	2,85	9,15	0,43	7,6
100	2,86	9,09	0,43	8,3
150	2,71	9,80	0,41	9,7

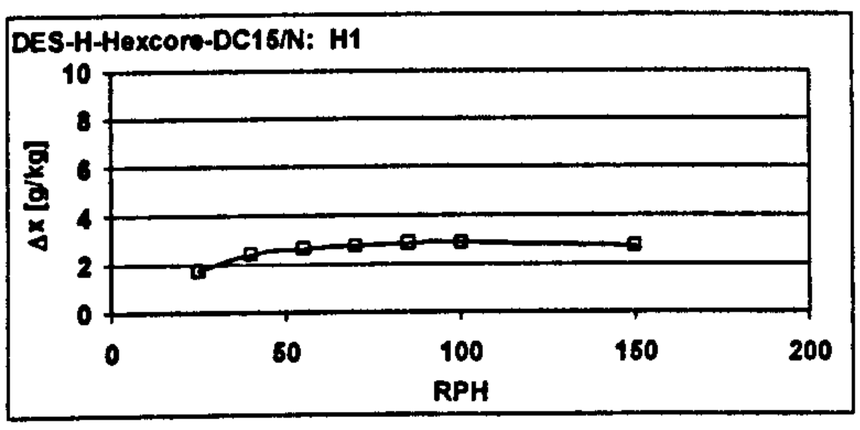

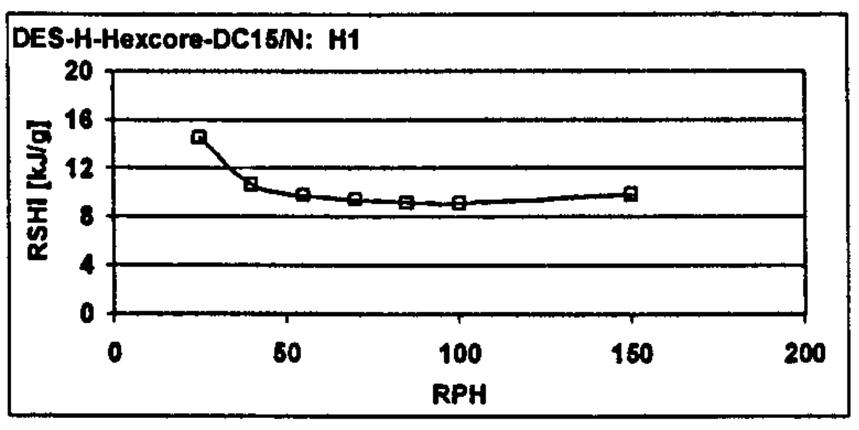

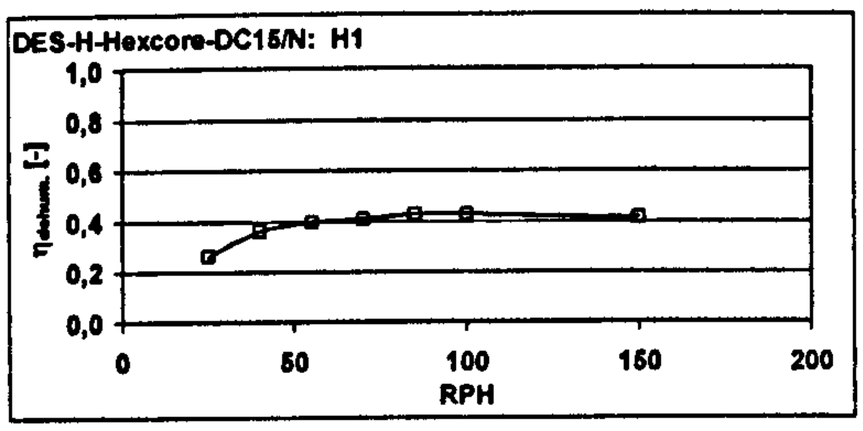

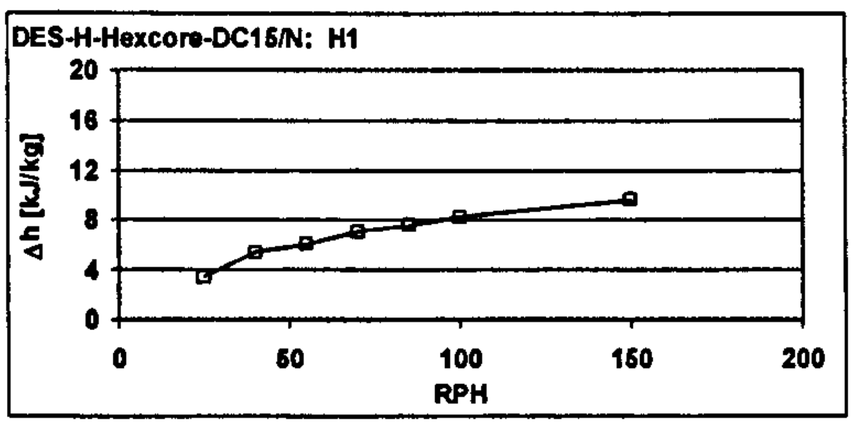

OUTCOMES OF MEASUREMENTS FROM THE DESICCANT WHEEL TEST FACILITY

measurement series H3

Desiccant wheel: **Engelhard HexCore, LP / DES-H-Hexcore-DC15/N**

Set values:

	temperature [°C]	rel. humidity [%]	vol. flow [m³/h]
process airflow	36	60	2000 $l_{20°C}$
reg. airflow	75	-	1500 $l_{20°C}$

$V_{reg} : V_{process}$ 0,75

Measured values:

RPH	ambient air					supply air				
	θ [°C]	φ [%]	x [g/kg]	h [kJ/kg]	Vnorm [m³/h]	θ [°C]	φ [%]	x [g/kg]	h [kJ/kg]	Vnorm [m³/h]
25	35,98 ± 0,07	59,68 ± 2,02	22,63 ± 0,80	94,0 ± 2,1	2012 ± 10	44,50 ± 0,27	29,42 ± 1,10	17,40 ± 0,74	89,4 ± 2,1	2090 ± 6
40	35,93 ± 0,06	59,65 ± 0,55	22,55 ± 0,26	93,8 ± 0,7	2001 ± 10	50,46 ± 0,13	20,37 ± 0,50	16,23 ± 0,48	92,5 ± 1,3	2065 ± 6
55	35,97 ± 0,09	59,58 ± 0,75	22,58 ± 0,33	93,9 ± 0,9	1995 ± 8	53,00 ± 0,08	17,49 ± 0,44	15,77 ± 0,43	93,9 ± 1,1	2061 ± 5
70	35,90 ± 0,08	59,35 ± 0,88	22,40 ± 0,34	93,4 ± 0,9	1994 ± 10	54,81 ± 0,08	15,63 ± 0,35	15,36 ± 0,35	94,7 ± 0,9	2052 ± 5
85	35,96 ± 0,07	59,89 ± 0,51	22,68 ± 0,21	94,2 ± 0,6	1983 ± 7	56,36 ± 0,05	14,74 ± 0,25	15,60 ± 0,27	97,0 ± 0,7	2026 ± 6
100	35,95 ± 0,06	59,76 ± 0,56	22,62 ± 0,22	94,0 ± 0,6	1980 ± 7	56,44 ± 0,05	14,72 ± 0,24	15,64 ± 0,26	97,1 ± 0,7	2023 ± 7
150	35,98 ± 0,07	59,72 ± 0,75	22,64 ± 0,30	94,1 ± 0,8	1973 ± 9	57,42 ± 0,05	14,14 ± 0,25	15,74 ± 0,28	98,4 ± 0,7	2018 ± 5

RPH	regeneration air					waste air				
	θ [°C]	φ [%]	x [g/kg]	h [kJ/kg]	Vnorm [m³/h]	θ [°C]	φ [%]	x [g/kg]	h [kJ/kg]	Vnorm [m³/h]
25	75,05 ± 0,11	3,70 ± 0,10	9,48 ± 0,26	100,0 ± 0,7	1506 ± 24	55,20 ± 0,16	16,22 ± 0,42	16,33 ± 0,45	102,9 ± 1,2	1523 ± 6
40	74,97 ± 0,04	3,77 ± 0,10	9,64 ± 0,25	100,4 ± 0,7	1525 ± 21	49,07 ± 0,07	25,08 ± 0,47	18,73 ± 0,37	97,6 ± 1,0	1545 ± 6
55	74,91 ± 0,06	4,08 ± 0,05	10,40 ± 0,11	102,3 ± 0,3	1671 ± 15	47,12 ± 0,06	30,55 ± 0,31	20,75 ± 0,24	100,8 ± 0,7	1616 ± 4
70	74,83 ± 0,09	3,92 ± 0,02	9,96 ± 0,02	101,1 ± 0,1	1674 ± 20	45,15 ± 0,06	33,23 ± 0,27	20,41 ± 0,18	97,9 ± 0,5	1636 ± 5
85	74,89 ± 0,05	4,19 ± 0,01	10,69 ± 0,02	103,1 ± 0,1	1634 ± 35	44,49 ± 0,05	35,97 ± 0,22	21,39 ± 0,15	99,7 ± 0,4	1678 ± 5
100	74,88 ± 0,11	4,22 ± 0,01	10,76 ± 0,04	103,3 ± 0,2	1556 ± 33	42,75 ± 0,09	39,73 ± 0,28	21,60 ± 0,14	98,4 ± 0,4	1593 ± 5
150	74,93 ± 0,10	4,19 ± 0,02	10,71 ± 0,05	103,2 ± 0,2	1597 ± 32	41,15 ± 0,05	42,89 ± 0,21	21,43 ± 0,10	96,3 ± 0,3	1576 ± 4

Figures of merit:

RPH	$\Delta x_{amb-sup}$ [g/kg]	RSHI [kJ/g]	η_{dehum} [-]	$\Delta h_{sup-amb}$ [kJ/kg]
25	5,23	5,63	0,37	-4,6
40	6,32	4,74	0,45	-1,3
55	6,81	4,82	0,50	0,0
70	7,04	4,68	0,51	1,4
85	7,09	4,56	0,52	2,8
100	6,98	4,42	0,51	3,2
150	6,91	4,60	0,51	4,3

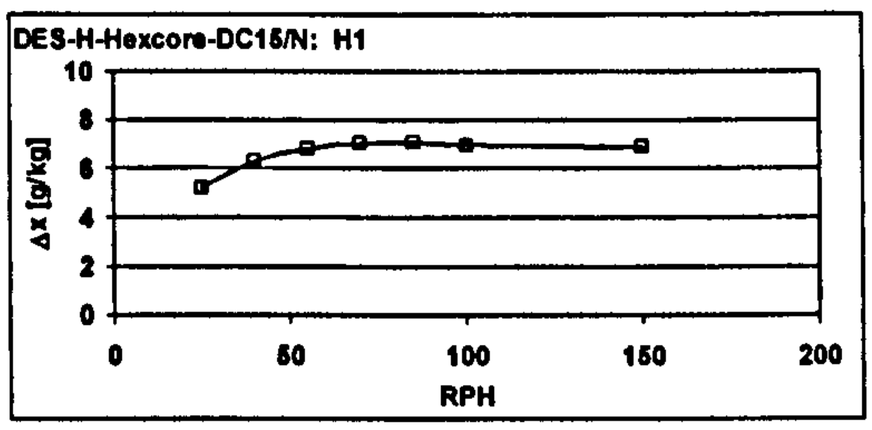

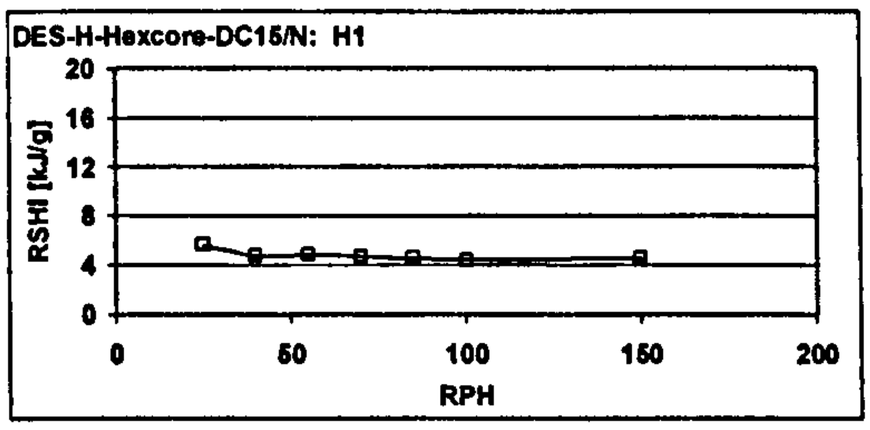

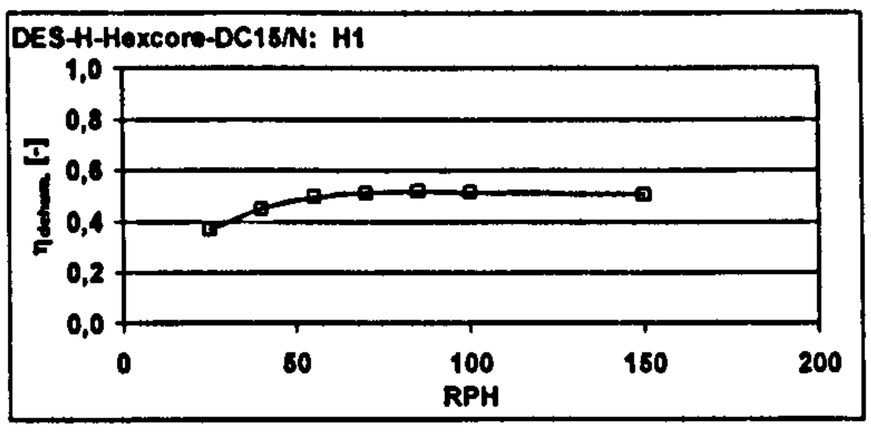

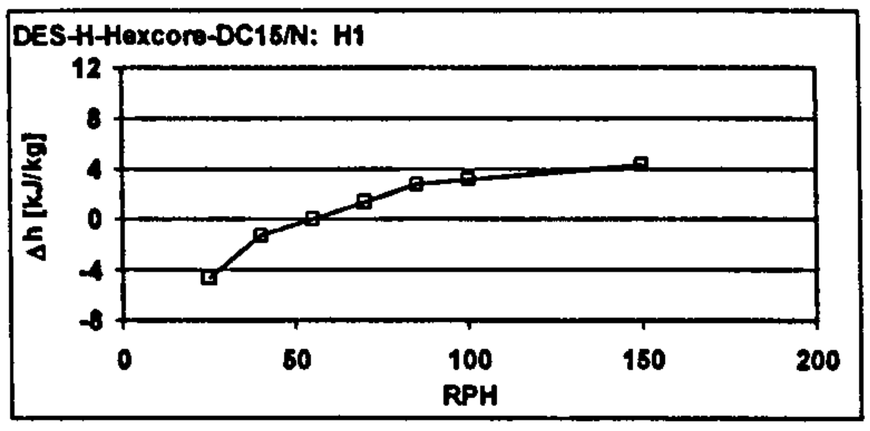

APPENDIX A

OUTCOMES OF MEASUREMENTS FROM THE DESICCANT WHEEL TEST FACILITY

measurement series H4

Desiccant wheel: **Engelhard HexCore, LP / DES-H-Hexcore-DC15/N**

Set values:

	temperature [°C]	rel. humidity [%]	vol. flow [m³/h]
process airflow	32	40	2000 $l_{20°C}$
reg. airflow	60	-	1500 $l_{20°C}$

$V_{reg} : V_{process}$ 0,75

Measured values:

RPH	ambient air					supply air				
	θ [°C]	φ [%]	x [g/kg]	h [kJ/kg]	Vnorm [m³/h]	θ [°C]	φ [%]	x [g/kg]	h [kJ/kg]	Vnorm [m³/h]
25	32,00 ± 0,05	39,21 ± 0,28	11,71 ± 0,08	62,0 ± 0,2	2009 ± 6	36 90 ± 0,14	22,50 ± 0,66	8,78 ± 0 29	59 4 ± 0,8	2110 ± 6
40	31,99 ± 0,06	39,61 ± 0,45	11,82 ± 0,14	62,2 ± 0,4	1988 ± 8	39,92 ± 0,06	18,01 ± 0,45	8,26 ± 0,23	61,2 ± 0,6	2136 ± 6
55	32,00 ± 0,05	40,12 ± 0,25	11,99 ± 0,09	62,7 ± 0,2	1995 ± 6	41,64 ± 0,05	16,29 ± 0,33	8,18 ± 0,17	62,7 ± 0,5	2093 ± 5
70	31,98 ± 0,06	39,79 ± 0,67	11,87 ± 0,21	62,4 ± 0,6	1993 ± 5	43,00 ± 0,07	14,69 ± 0,35	7,91 ± 0,19	63,4 ± 0,5	2089 ± 7
85	31,99 ± 0,05	39,62 ± 0,55	11,83 ± 0,18	62,3 ± 0,5	1992 ± 6	43,51 ± 0,05	14,15 ± 0,30	7,63 ± 0,17	63,7 ± 0 5	2091 ± 5
100	31,96 ± 0,06	39,75 ± 0,45	11,85 ± 0,15	62,3 ± 0,4	1991 ± 5	44,15 ± 0,04	13,71 ± 0,24	7,85 ± 0,13	64 4 ± 0,3	2086 ± 5
150	32 00 ± 0,07	39 84 ± 0,51	11 90 ± 0,15	62,5 ± 0 4	1986 ± 5	45 08 ± 0 03	13 26 ± 0 20	7 96 ± 0 12	65 6 ± 0 3	2082 ± 4

RPH	regeneration air					waste air				
	θ [°C]	φ [%]	x [g/kg]	h [kJ/kg]	Vnorm [m³/h]	θ [°C]	φ [%]	x [g/kg]	h [kJ/kg]	Vnorm [m³/h]
25	59,86 ± 0,04	5,59 ± 0,02	7,33 ± 0,01	79,0 ± 0,0	1585 ± 16	47,38 ± 0,10	20,59 ± 0 24	14,02 ± 0 19	83 6 ± 0,6	1644 ± 5
40	59 87 ± 0,05	5,36 ± 0,04	7,04 ± 0,06	78,2 ± 0,2	1585 ± 19	43,95 ± 0,07	24 02 ± 0,31	13,73 ± 0,19	79 4 ± 0 5	1677 ± 6
55	60,01 ± 0,04	5,39 ± 0,01	7,12 ± 0,01	78,6 ± 0,0	1607 ± 13	42,19 ± 0,05	26,84 ± 0,22	14,00 ± 0,13	78,3 ± 0,4	1661 ± 5
70	60,05 ± 0,06	5,25 ± 0,02	6,94 ± 0,03	78,2 ± 0,1	1577 ± 24	40,61 ± 0,01	29,00 ± 0,21	13,92 ± 0,10	76,4 ± 0,3	1649 ± 5
85	59,84 ± 0,00	5,27 ± 0,02	6,90 ± 0,02	77,8 ± 0,1	1581 ± 22	39,72 ± 0 03	30,13 ± 0,18	13,79 ± 0 09	75,2 ± 0,3	1653 ± 5
100	59,86 ± 0,04	5,28 ± 0,02	6,92 ± 0,03	77,9 ± 0,1	1576 ± 17	38,86 ± 0,05	31,41 ± 0,14	13,73 ± 0,06	74,2 ± 0,2	1644 ± 5
150	59 84 ± 0,02	5,30 ± 0,01	6,95 ± 0,02	78,0 ± 0,0	1579 ± 20	37,53 ± 0,05	33 13 ± 0 17	13 48 ± 0 06	72 2 ± 0 2	1627 ± 4

Figures of merit:

RPH	$\Delta x_{amb-sup}$ [g/kg]	RSHI [kJ/g]	η_{dehum} [-]	$\Delta h_{sup-amb}$ [kJ/kg]
25	2,93	7,54	0,41	-2,5
40	3,56	6,28	0,49	-1,1
55	3,80	5,97	0,51	0,1
70	3,96	5,65	0,53	1,0
85	4,00	5,56	0,54	1,4
100	4,00	5,56	0,54	2,1
150	3,94	5,66	0,53	3,2

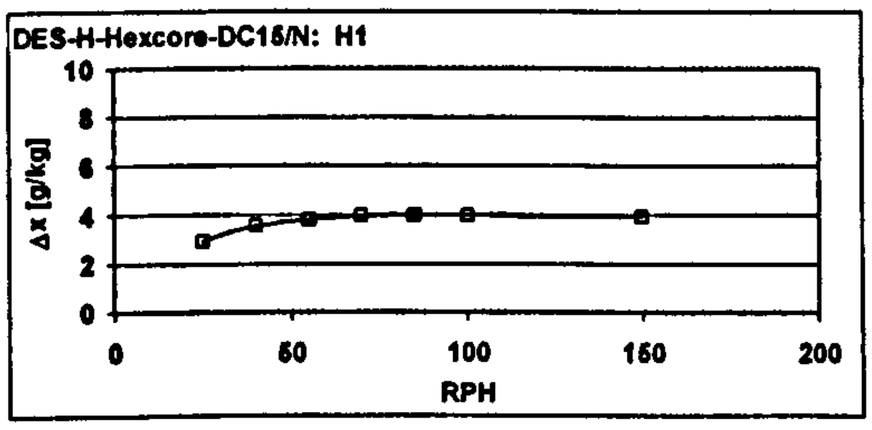

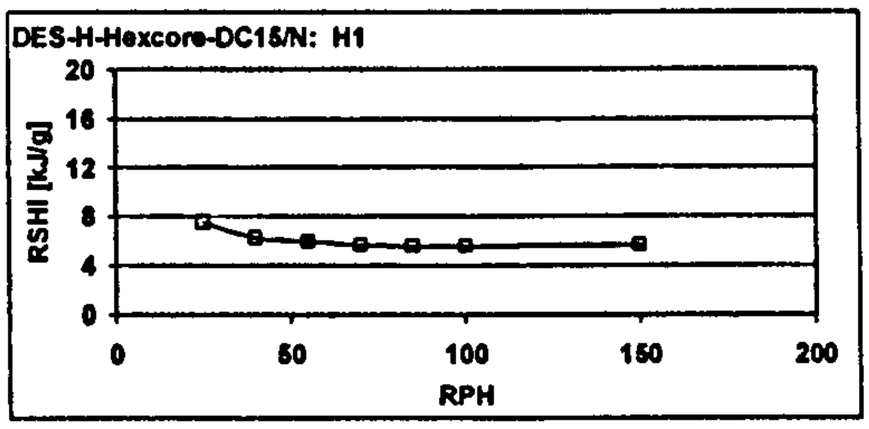

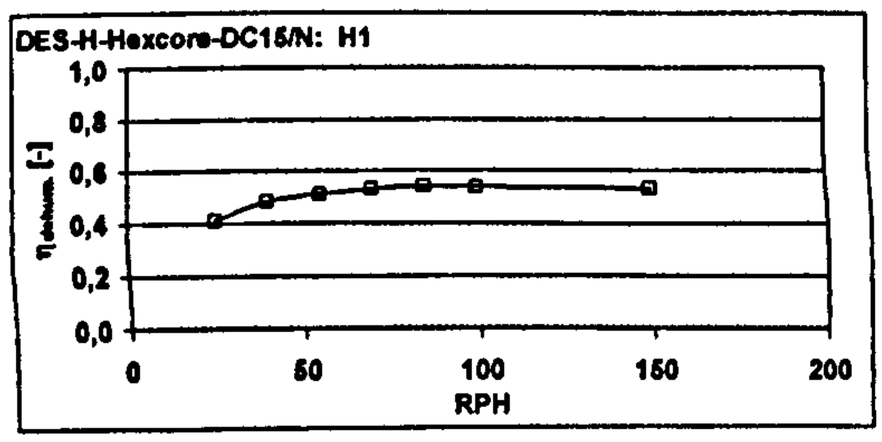

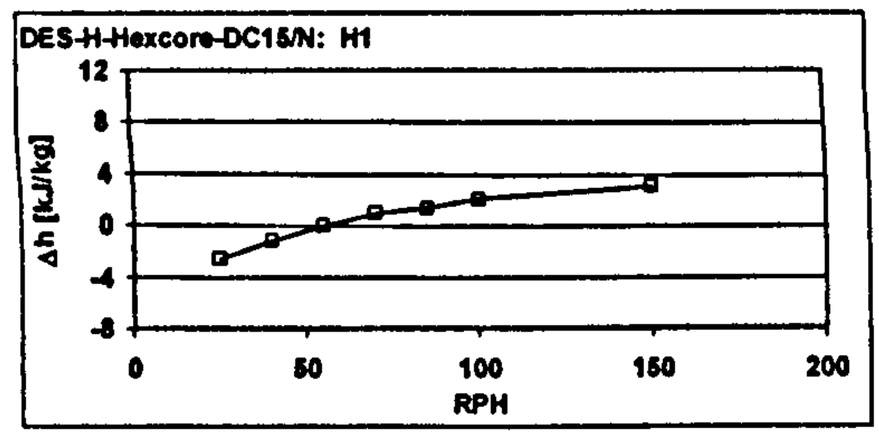

OUTCOMES OF MEASUREMENTS FROM THE DESICCANT WHEEL TEST FACILITY

measurement series H5

Desiccant wheel: **Engelhard HexCore, LP / DES-H-Hexcore-DC15/N**

Set values:

	temperature [°C]	rel. humidity [%]	vol. flow [m³/h]
process airflow	32	40	2000 $l_{20°C}$
reg. airflow	75	-	1500 $l_{20°C}$

$V_{reg} : V_{process}$ 0,75

Measured values:

RPH	ambient air					supply air				
	θ [°Y]	φ [%]	x [g/kg]	h [kJ/kg]	Vnorm [m³/h]	θ [°Y]	φ [%]	x [g/kg]	h [kJ/kg]	Vnorm [m³/h]
25	32,00 ± 0,12	39,80 ± 0,43	11,89 ± 0,12	62,4 ± 0,4	1997 ± 9	41,11 ± 0,24	16,85 ± 0,73	8,24 ± 0,41	62,3 ± 1,2	2107 ± 6
40	32,00 ± 0,09	40,10 ± 0,26	11,99 ± 0,09	62,7 ± 0,3	1992 ± 10	45,28 ± 0,12	12,37 ± 0,50	7,50 ± 0,33	64,7 ± 0,9	2080 ± 8
55	31,99 ± 0,06	39,75 ± 0,78	11,86 ± 0,23	62,3 ± 0,6	1986 ± 10	47,45 ± 0,07	10,40 ± 0,51	7,03 ± 0,36	65,6 ± 1,0	2082 ± 8
70	31,99 ± 0,07	39,80 ± 0,70	11,86 ± 0,21	62,4 ± 0,6	1980 ± 9	49,01 ± 0,16	9,35 ± 0,30	6,83 ± 0,25	66,7 ± 0,8	2073 ± 6
85	31,96 ± 0,05	39,84 ± 0,20	11,89 ± 0,07	62,4 ± 0,2	1985 ± 10	47,58 ± 0,13	9,94 ± 0,20	6,76 ± 0,15	65,1 ± 0,5	2086 ± 6
100	31,96 ± 0,05	39,83 ± 0,17	11,89 ± 0,05	62,4 ± 0,1	1990 ± 9	48,31 ± 0,08	9,56 ± 0,18	6,75 ± 0,12	65,8 ± 0,3	2095 ± 6
150	32,00 ± 0 05	40 03 ± 0 13	11 96 ± 0 05	62 6 ± 0,2	1985 ± 6	49,91 ± 0,05	9,12 ± 0,13	6 97 ± 0,10	66,0 ± 0,2	2092 ± 5

RPH	regeneration air					waste air				
	θ [°Y]	φ [%]	x [g/kg]	h [kJ/kg]	Vnorm [m³/h]	θ [°Y]	φ [%]	x [g/kg]	h [kJ/kg]	Vnorm [m³/h]
25	75,06 ± 0,13	2,95 ± 0,04	7,54 ± 0,07	94,9 ± 0 2	1488 ± 21	55 65 ± 0,17	15,74 ± 0,31	16,12 ± 0,35	97,6 ± 1,0	1509 ± 4
40	74,97 ± 0,06	2,87 ± 0 02	7,30 ± 0,03	94,2 ± 0,1	1485 ± 14	50,51 ± 0,09	20,13 ± 0,36	16,08 ± 0,32	92,2 ± 0,9	1531 ± 4
55	75,06 ± 0,07	2,90 ± 0,04	7,40 ± 0,11	94,6 ± 0,3	1502 ± 23	47,61 ± 0,09	23,28 ± 0,28	16,09 ± 0,21	89,2 ± 0,6	1542 ± 4
70	75,06 ± 0,17	2,88 ± 0,04	7,34 ± 0,06	94,4 ± 0,1	1524 ± 21	45,58 ± 0,11	25,91 ± 0,28	16,16 ± 0,18	87,3 ± 0,5	1551 ± 5
85	74,96 ± 0,14	2,96 ± 0,02	7,53 ± 0,02	94,8 ± 0,1	1482 ± 24	42 60 ± 0,05	32,67 ± 0,25	17,51 ± 0,15	87,7 ± 0,4	1452 ± 4
100	74,97 ± 0,05	2,96 ± 0,01	7,54 ± 0,02	94,8 ± 0,0	1487 ± 26	41,76 ± 0,12	33,52 ± 0,21	17,19 ± 0,10	86,0 ± 0,3	1453 ± 4
150	75 02 ± 0 07	3,01 ± 0 01	7 69 ± 0 02	95 3 ± 0,1	1518 ± 17	40,00 ± 0,05	35,55 ± 0,20	16,59 ± 0,09	82,7 ± 0,2	1459 ± 4

Figures of merit:

RPH	$\Delta x_{amb-sup}$ [g/kg]	RSHI [kJ/g]	η_{dehum} [-]	$\Delta h_{sup-amb}$ [kJ/kg]
25	3,65	8,84	0,41	-0,1
40	4,49	7,19	0,50	2,0
55	4,84	6,79	0,54	3,3
70	5,05	6,61	0,56	4,3
85	5,13	6,31	0,58	2,7
100	5,14	6,29	0,58	3,4
150	4,99	6,64	0,56	5,4

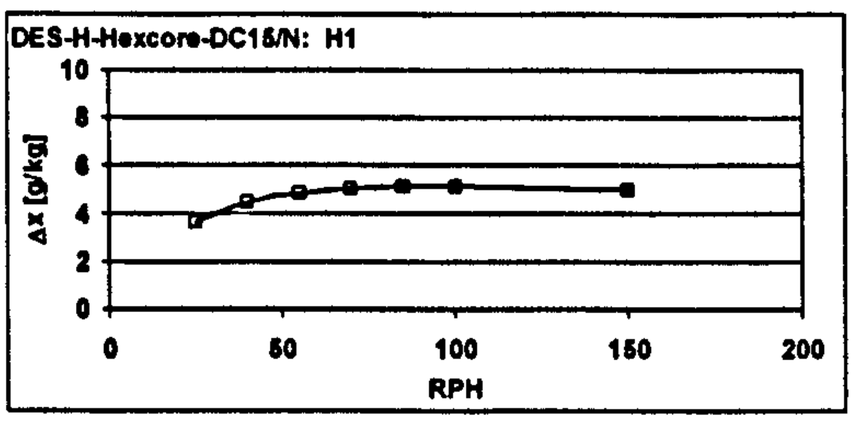

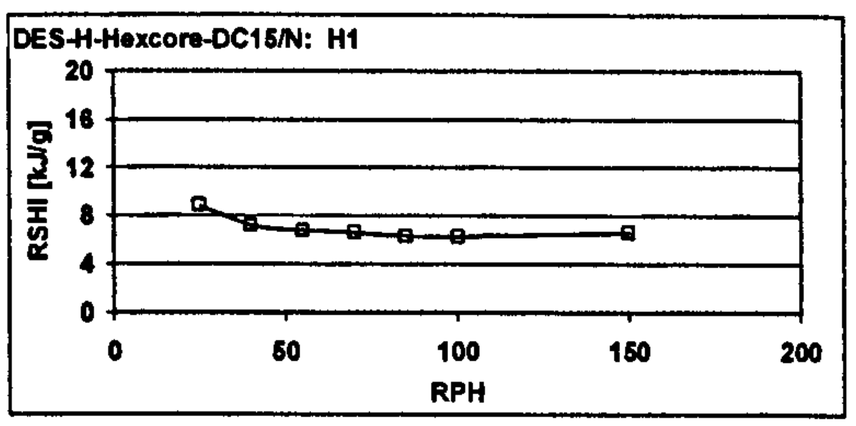

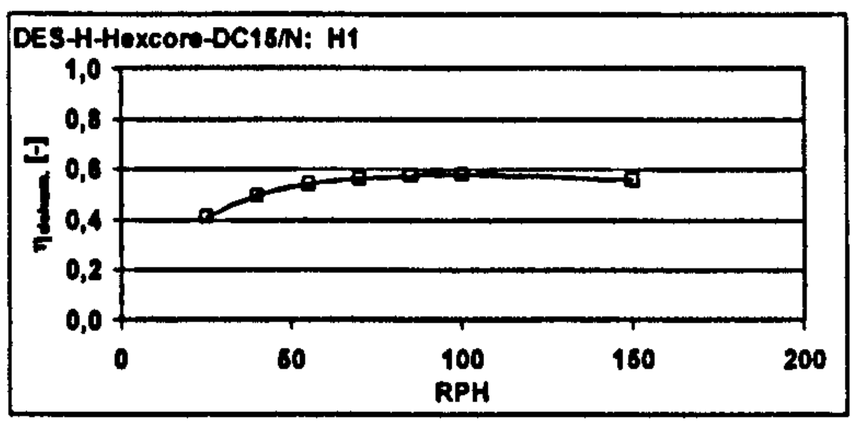

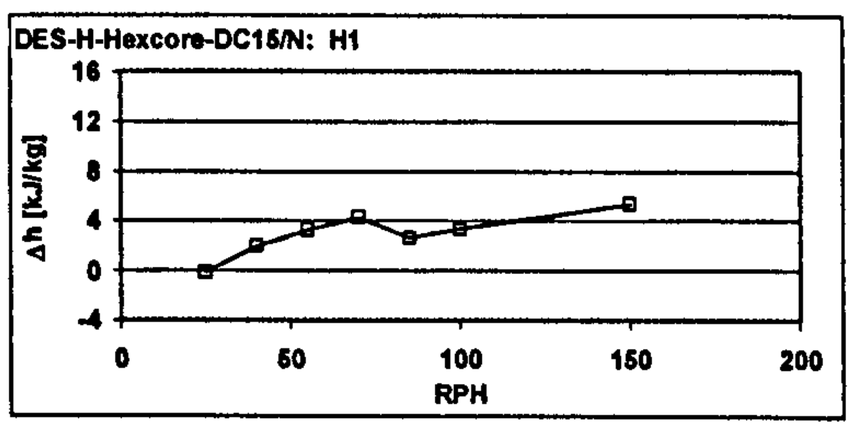

APPENDIX A

OUTCOMES OF MEASUREMENTS FROM THE DESICCANT WHEEL TEST FACILITY

measurement series H6

Desiccant wheel: **Engelhard HexCore, LP / DES-H-Hexcore-DC15/N**

Set values:

	temperature [°C]	rel. humidity [%]	vol. flow [m³/h]
process airflow	32	40	2000 $l_{20°C}$
reg. airflow	75	-	1000 $l_{20°C}$

$V_{reg} : V_{process}$ 0,5

Measured values:

RPH	ambient air					supply air				
	θ [°Y]	φ [%]	x [g/kg]	h [kJ/kg]	Vnorm [m³/h]	θ [°Y]	φ [%]	x [g/kg]	h [kJ/kg]	Vnorm [m³/h]
25	31,96 ± 0,07	39,81 ± 0,30	11,88 ± 0,10	62,4 ± 0,3	2022 ± 8	38,83 ± 0,23	20,64 ± 0,53	8,94 ± 0,27	61,8 ± 0,9	2161 ± 12
40	31,96 ± 0,07	39,81 ± 0,35	11,87 ± 0,11	62,3 ± 0,3	2008 ± 7	42,21 ± 0,10	16,27 ± 0,47	8,42 ± 0,27	63,9 ± 0,8	2148 ± 8
55	32,00 ± 0,06	40,06 ± 0,71	11,97 ± 0,21	62,6 ± 0,5	2002 ± 7	43,64 ± 0,06	14,79 ± 0,39	8,25 ± 0,24	64,9 ± 0,7	2139 ± 7
70	31,96 ± 0,06	39,97 ± 0,53	11,92 ± 0,18	62,5 ± 0,5	2005 ± 7	44,20 ± 0,11	14,14 ± 0,31	8,11 ± 0,20	65,1 ± 0,6	2155 ± 7
85	31,96 ± 0,05	39,72 ± 0,47	11,85 ± 0,15	62,3 ± 0,4	2000 ± 6	44,68 ± 0,06	13,71 ± 0,30	8,06 ± 0,20	65,5 ± 0,6	2147 ± 7
100	31,96 ± 0,05	40,09 ± 0,24	11,96 ± 0,07	62,6 ± 0,2	2006 ± 9	45,06 ± 0,06	13,60 ± 0,22	8,16 ± 0,14	66,1 ± 0,4	2146 ± 7
150	31,97 ± 0,05	40,00 ± 0,27	11,93 ± 0,10	62,5 ± 0,3	1999 ± 6	46,06 ± 0,06	13,18 ± 0,20	8,32 ± 0,13	67,6 ± 0,4	2144 ± 7

RPH	regeneration air					waste air				
	θ [°Y]	φ [%]	x [g/kg]	h [kJ/kg]	Vnorm [m³/h]	θ [°Y]	φ [%]	x [g/kg]	h [kJ/kg]	Vnorm [m³/h]
25	75,16 ± 0,33	2,94 ± 0,04	7,54 ± 0,01	95,0 ± 0,3	991 ± 14	48,54 ± 0,18	24,50 ± 0,74	17,79 ± 0,55	94,6 ± 1,5	940 ± 4
40	74,94 ± 0,33	2,89 ± 0,04	7,33 ± 0,02	94,3 ± 0,4	1014 ± 11	42,64 ± 0,07	33,16 ± 1,09	17,82 ± 0,58	88,6 ± 1,5	957 ± 5
55	75,16 ± 0,34	2,84 ± 0,04	7,29 ± 0,02	94,4 ± 0,3	1009 ± 13	40,03 ± 0,10	38,20 ± 1,28	17,89 ± 0,59	86,1 ± 1,5	967 ± 4
70	75,10 ± 0,30	3,14 ± 0,04	8,03 ± 0,03	96,3 ± 0,3	1023 ± 16	39,16 ± 0,09	41,07 ± 1,13	18,37 ± 0,49	86,4 ± 1,2	951 ± 4
85	75,02 ± 0,30	3,15 ± 0,04	8,04 ± 0,02	96,2 ± 0,3	1036 ± 10	38,05 ± 0,09	43,17 ± 1,04	18,19 ± 0,45	84,8 ± 1,2	955 ± 4
100	75,05 ± 0,29	3,15 ± 0,04	8,04 ± 0,02	96,3 ± 0,3	1015 ± 14	37,38 ± 0,05	43,89 ± 1,12	17,83 ± 0,46	83,2 ± 1,2	958 ± 4
150	75,01 ± 0,33	3,19 ± 0,05	8,14 ± 0,01	96,5 ± 0,3	1026 ± 12	35,98 ± 0,05	44,54 ± 1,11	16,73 ± 0,42	78,9 ± 1,1	974 ± 4

Figures of merit:

RPH	$\Delta x_{amb-sup}$ [g/kg]	RSHI [kJ/g]	η_{dehum} [-]	$\Delta h_{sup-amb}$ [kJ/kg]
25	2,94	7,25	0,33	-0,6
40	3,45	6,34	0,39	1,6
55	3,73	5,88	0,41	2,3
70	3,80	5,82	0,43	2,7
85	3,79	5,92	0,43	3,2
100	3,80	5,77	0,43	3,5
150	3,61	6,17	0,41	5,1

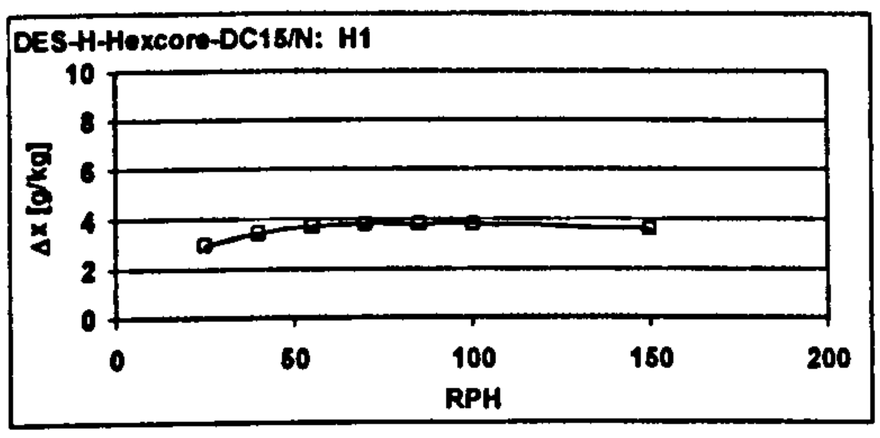

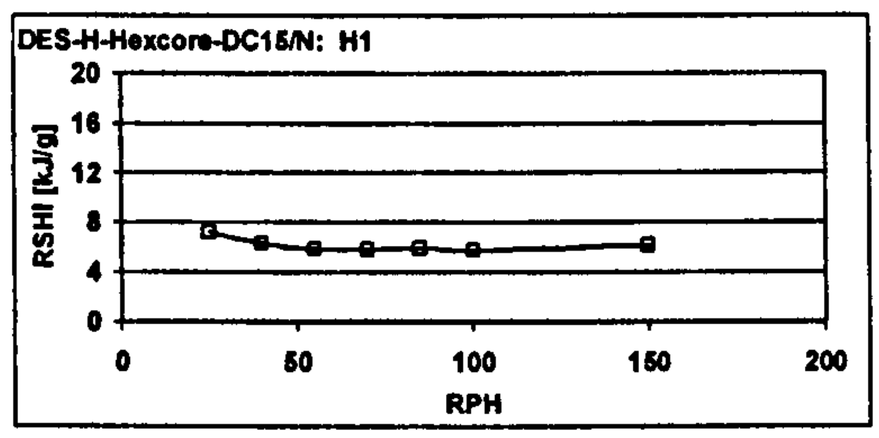

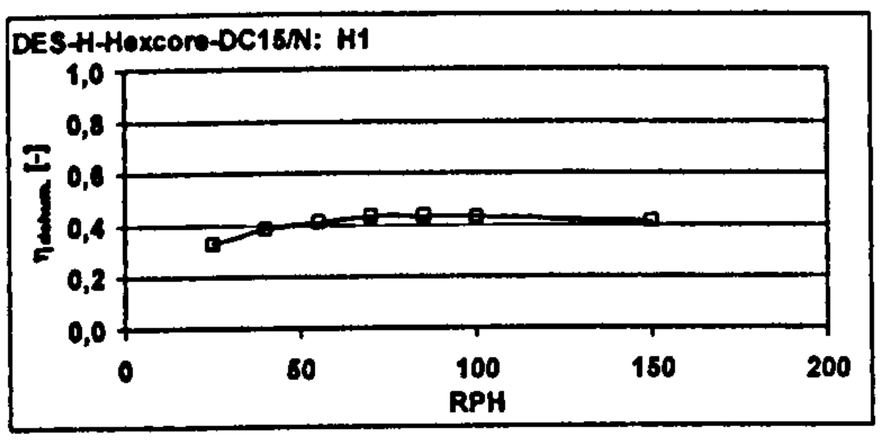

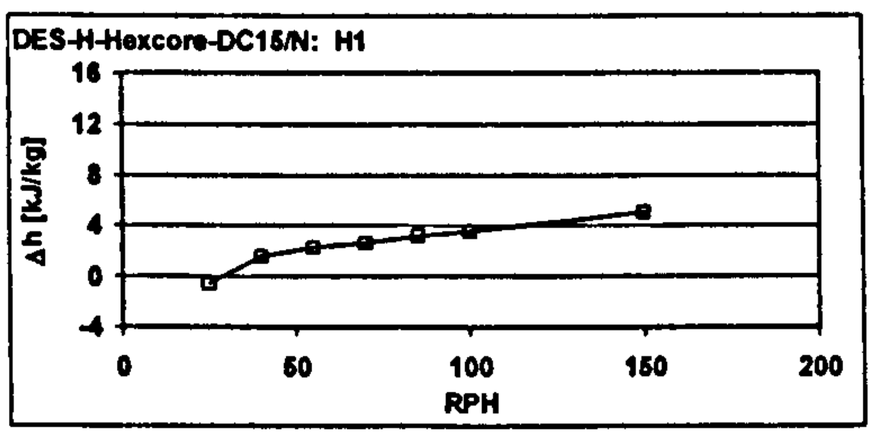

OUTCOMES OF MEASUREMENTS FROM THE DESICCANT WHEEL TEST FACILITY

measurement series H7

Desiccant wheel: **Engelhard HexCore, LP / DES-H-Hexcore-DC15/N**

Set values:

	temperature [°C]	rel. humidity [%]	vol. flow [m³/h]
process airflow	36	50	2000 $l_{20°C}$
reg. airflow	60	-	1500 $l_{20°C}$

$V_{reg} : V_{process}$ 0,75

Measured values:

RPH	ambient air					supply air				
	ϑ [°C]	φ [%]	x [g/kg]	h [kJ/kg]	Vnorm [m³/h]	ϑ [°C]	φ [%]	x [g/kg]	h [kJ/kg]	Vnorm [m³/h]
25	36,00 ± 0,05	50,07 ± 0,49	18,69 ± 0,20	84,5 ± 0,5	2003 ± 7	39,14 ± 0,14	34,22 ± 0,54	15,22 ± 0,27	78,3 ± 0,7	2068 ± 6
40	35,98 ± 0,06	49,76 ± 0,39	18,75 ± 0,16	84,1 ± 0,4	2001 ± 12	43,22 ± 0,06	26,35 ± 0,43	14,52 ± 0,28	80,7 ± 0,8	2081 ± 6
55	35,96 ± 0,04	49,87 ± 0,31	18,78 ± 0,13	84,1 ± 0,3	2005 ± 6	44,69 ± 0,06	23,99 ± 0,28	14,26 ± 0,18	81,5 ± 0,5	2082 ± 7
70	35,97 ± 0,10	49,53 ± 0,59	18,66 ± 0,29	83,8 ± 0,8	1987 ± 7	46,06 ± 0,06	21,77 ± 0,37	13,87 ± 0,25	81,9 ± 0,7	2039 ± 5
85	35,99 ± 0,05	49,73 ± 0,60	18,75 ± 0,23	84,1 ± 0,6	1982 ± 5	46,68 ± 0,05	21,05 ± 0,35	13,84 ± 0,23	82,5 ± 0,6	2037 ± 6
100	35,99 ± 0,05	49,61 ± 0,67	18,70 ± 0,24	84,0 ± 0,6	1983 ± 7	47,21 ± 0,05	20,28 ± 0,34	13,69 ± 0,23	82,6 ± 0,6	2036 ± 6
150	36,98 ± 0,05	49,79 ± 0,97	18,76 ± 0,39	84,1 ± 1,0	1978 ± 5	47,93 ± 0,11	19,59 ± 0,39	13,70 ± 0,30	83,4 ± 0,8	2033 ± 5

RPH	regeneration air					waste air				
	ϑ [°C]	φ [%]	x [g/kg]	h [kJ/kg]	Vnorm [m³/h]	ϑ [°C]	φ [%]	x [g/kg]	h [kJ/kg]	Vnorm [m³/h]
25	59,96 ± 0,05	7,79 ± 0,02	10,32 ± 0,02	86,9 ± 0,1	1586 ± 10	48,00 ± 0,10	24,66 ± 0,28	17,42 ± 0,22	93,1 ± 0,6	1554 ± 4
40	60,03 ± 0,09	7,07 ± 0,10	9,37 ± 0,14	84,5 ± 0,4	1478 ± 24	42,64 ± 0,05	30,45 ± 0,37	16,32 ± 0,22	84,7 ± 0,6	1468 ± 5
55	60,02 ± 0,16	7,13 ± 0,09	9,45 ± 0,12	84,7 ± 0,4	1524 ± 16	40,93 ± 0,04	33,59 ± 0,23	16,46 ± 0,13	83,3 ± 0,4	1461 ± 5
70	60,05 ± 0,05	7,43 ± 0,04	9,87 ± 0,04	85,8 ± 0,1	1604 ± 17	40,77 ± 0,07	35,69 ± 0,20	17,37 ± 0,14	85,5 ± 0,4	1566 ± 4
85	60,01 ± 0,00	7,44 ± 0,02	9,87 ± 0,02	85,8 ± 0,1	1609 ± 10	40,15 ± 0,05	37,16 ± 0,16	17,51 ± 0,06	85,2 ± 0,2	1568 ± 4
100	59,96 ± 0,05	7,36 ± 0,02	9,73 ± 0,03	85,3 ± 0,1	1604 ± 9	39,57 ± 0,04	38,21 ± 0,22	17,45 ± 0,09	84,5 ± 0,2	1569 ± 4
150	60,03 ± 0,04	7,35 ± 0,04	9,76 ± 0,05	85,5 ± 0,1	1593 ± 15	38,69 ± 0,11	40,10 ± 0,41	17,47 ± 0,11	83,6 ± 0,3	1560 ± 7

Figures of merit:

RPH	$\Delta x_{amb-sup}$ [g/kg]	RSHI [kJ/g]	η_{dehum} [-]	$\Delta h_{sup-amb}$ [kJ/kg]
25	3,67	5,20	0,40	-6,2
40	4,23	4,22	0,45	-3,4
55	4,52	4,07	0,48	-2,6
70	4,79	4,08	0,52	-2,0
85	4,92	3,99	0,53	-1,7
100	5,01	3,90	0,54	-1,4
150	5,08	3,86	0,54	-0,7

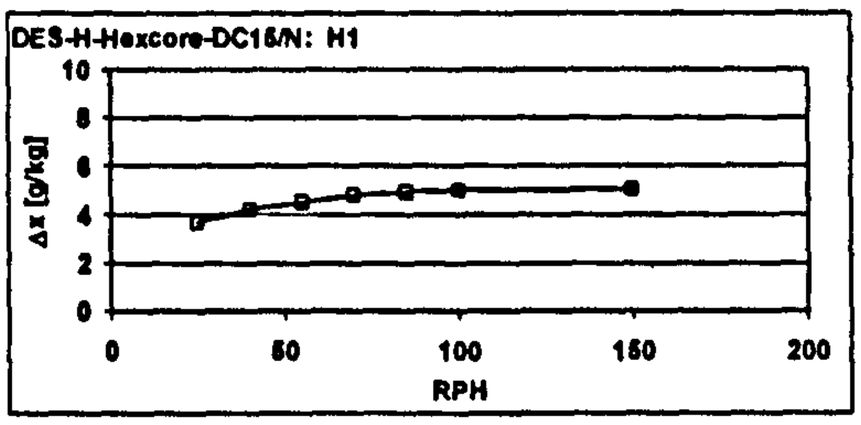

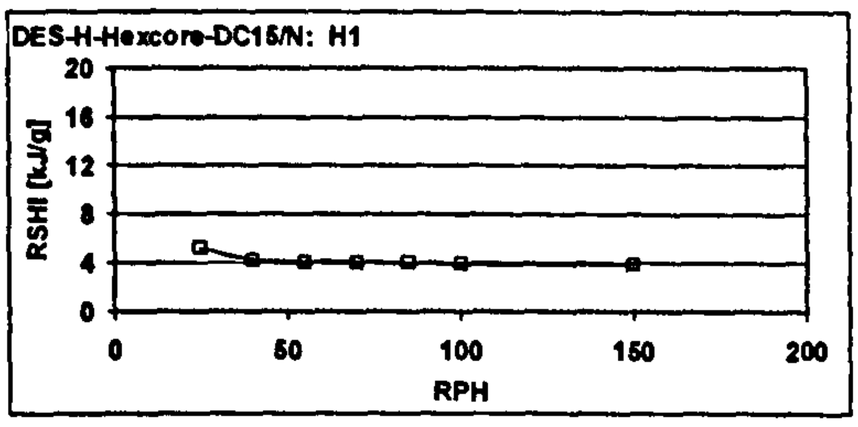

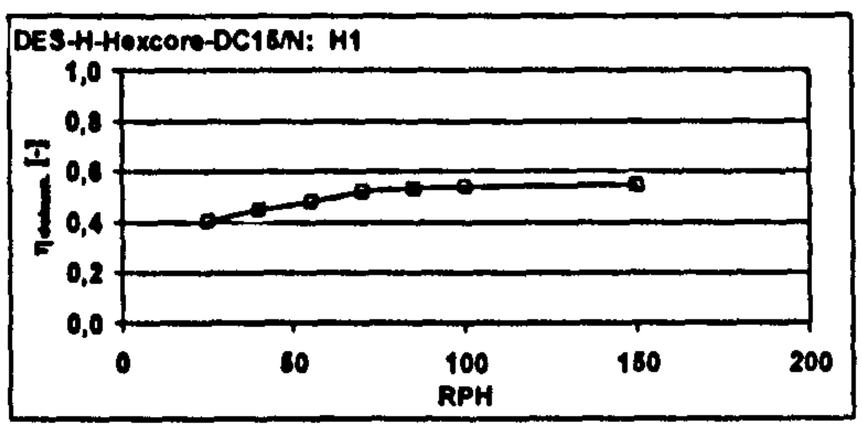

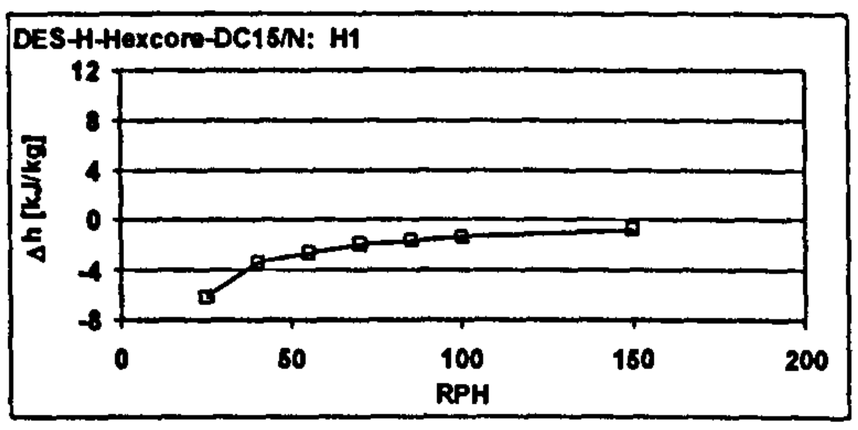

APPENDIX A

OUTCOMES OF MEASUREMENTS FROM THE DESICCANT WHEEL TEST FACILITY

measurement series H8

Desiccant wheel: **Engelhard HexCore, LP / DES-H-Hexcore-DC15/N**

Set values:

	temperature [°C]	rel humidity [%]	vol flow [m³/h]
process airflow	28	40	2000 $l_{20°C}$
reg airflow	75	-	1500 $l_{20°C}$

$V_{reg} : V_{process}$ 0,75

Measured values:

RPH	ambient air					supply air				
	θ [°Y]	φ [%]	x [g/kg]	h [kJ/kg]	Vnorm [m³/h]	θ [°\]	φ [%]	x [g/kg]	h [kJ/kg]	Vnorm [m³/h]
25	27,98 ± 0,05	39,80 ± 0,21	9,40 ± 0,05	52,0 ± 0,1	2014 ± 7	38,44 ± 0,21	14,27 ± 0,83	6,03 ± 0,39	53,9 ± 1,1	2092 ± 8
40	28,19 ± 0,17	39,79 ± 0,51	9,52 ± 0,05	52,5 ± 0,2	2019 ± 8	42,42 ± 0,06	10,42 ± 0,51	5,43 ± 0,29	56,4 ± 0,8	2095 ± 8
55	27,99 ± 0,05	39,95 ± 0,60	9,44 ± 0,15	52,1 ± 0,4	1990 ± 6	43,83 ± 0,11	9,24 ± 0,36	5,18 ± 0,22	57,2 ± 0,6	2098 ± 8
70	28,00 ± 0,06	39,71 ± 0,30	9,39 ± 0,06	52,0 ± 0,2	1983 ± 5	45,69 ± 0,05	7,88 ± 0,27	4,86 ± 0,17	58,2 ± 0,5	2082 ± 7
85	28,00 ± 0,05	40,01 ± 0,55	9,46 ± 0,13	52,1 ± 0,3	1988 ± 6	46,89 ± 0,11	7,54 ± 0,19	4,94 ± 0,14	59,7 ± 0,4	2070 ± 6
100	27,99 ± 0,05	39,86 ± 0,18	9,42 ± 0,04	52,0 ± 0,1	1986 ± 6	47,54 ± 0,04	7,29 ± 0,13	4,93 ± 0,09	60,3 ± 0,2	2067 ± 6
150	27,99 ± 0,05	39,84 ± 0,26	9,42 ± 0,06	52,0 ± 0,2	1983 ± 6	49,44 ± 0,03	7,20 ± 0,11	5,36 ± 0,08	63,3 ± 0,2	2066 ± 5

RPH	regeneration air					waste air				
	θ [°Y]	φ [%]	x [g/kg]	h [kJ/kg]	Vnorm [m³/h]	θ [°\]	φ [%]	x [g/kg]	h [kJ/kg]	Vnorm [m³/h]
25	75,00 ± 0,06	2,50 ± 0,02	6,36 ± 0,04	91,8 ± 0,1	1500 ± 26	54,23 ± 0,17	16,07 ± 0,41	15,37 ± 0,43	94,2 ± 1,2	1479 ± 4
40	74,97 ± 0,04	2,44 ± 0,02	6,20 ± 0,04	91,3 ± 0,1	1476 ± 26	47,68 ± 0,07	22,09 ± 0,37	15,46 ± 0,30	87,9 ± 0,8	1436 ± 4
55	75,02 ± 0,05	2,44 ± 0,01	6,21 ± 0,03	91,4 ± 0,1	1455 ± 24	45,43 ± 0,10	25,09 ± 0,36	15,51 ± 0,23	85,5 ± 0,6	1443 ± 5
70	74,98 ± 0,01	2,39 ± 0,02	6,08 ± 0,04	91,0 ± 0,1	1542 ± 20	43,81 ± 0,05	26,06 ± 0,31	14,82 ± 0,19	82,0 ± 0,5	1503 ± 3
85	75,12 ± 0,05	2,39 ± 0,02	6,12 ± 0,04	91,2 ± 0,1	1509 ± 21	41,71 ± 0,05	29,06 ± 0,25	14,80 ± 0,15	79,9 ± 0,4	1472 ± 4
100	74,90 ± 0,08	2,42 ± 0,02	6,13 ± 0,04	91,0 ± 0,1	1532 ± 19	40,74 ± 0,03	30,41 ± 0,20	14,72 ± 0,10	78,6 ± 0,3	1477 ± 4
150	75,13 ± 0,05	2,44 ± 0,01	6,23 ± 0,02	91,6 ± 0,1	1523 ± 13	38,01 ± 0,05	33,28 ± 0,29	13,90 ± 0,12	73,7 ± 0,3	1454 ± 3

Figures of merit:

RPH	$\Delta x_{amb-sup}$ [g/kg]	RSHI [kJ/g]	η_{dehum} [-]	$\Delta h_{sup-amb}$ [kJ/kg]
25	3,37	10,45	0,44	2,0
40	4,09	8,43	0,53	3,9
55	4,27	8,11	0,55	5,1
70	4,53	8,12	0,59	6,3
85	4,53	7,96	0,58	7,5
100	4,49	8,12	0,58	8,3
150	4,05	8,99	0,53	11,3

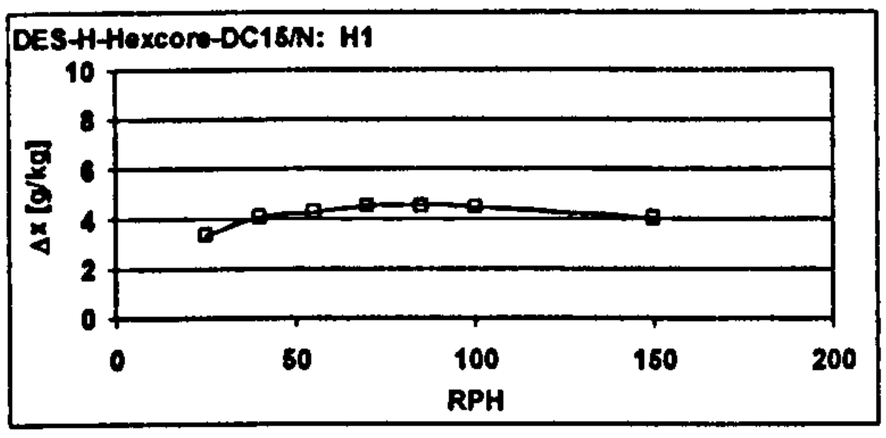

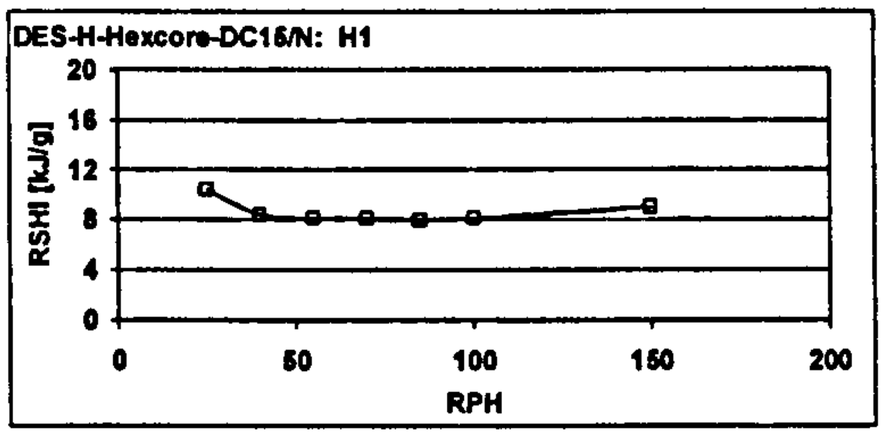

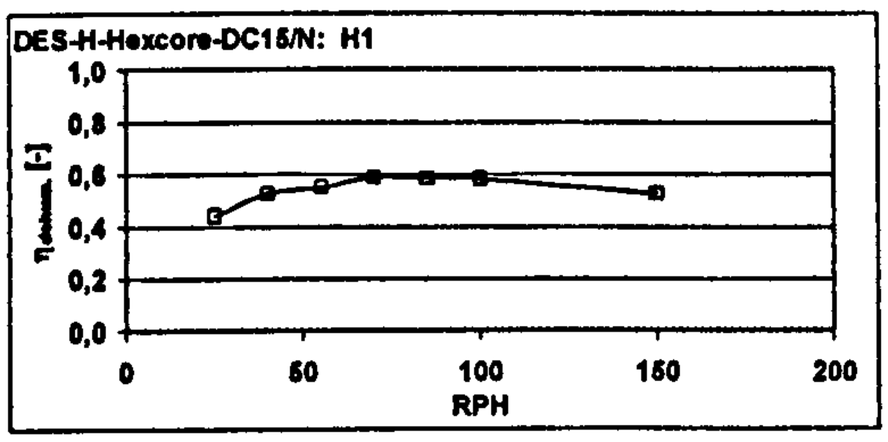

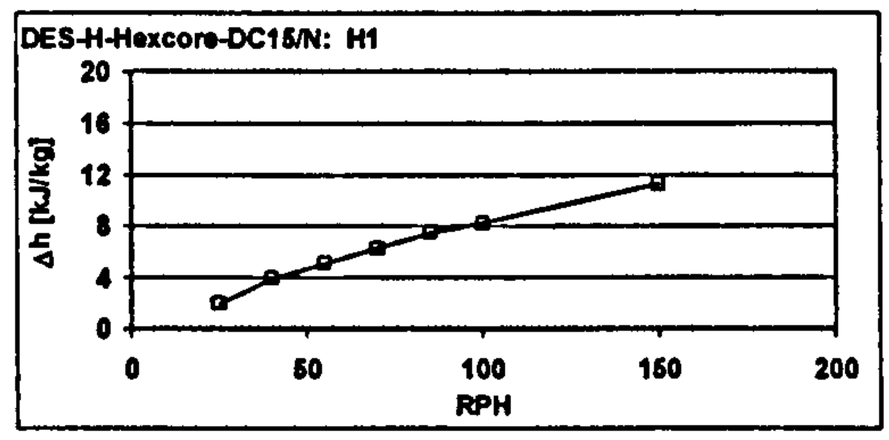

OUTCOMES OF MEASUREMENTS FROM THE DESICCANT WHEEL TEST FACILITY

measurement series H9

Desiccant wheel: **Engelhard HexCore, LP / DES-H-Hexcore-DC15/N**

Set values:

	temperature [°C]	rel. humidity [%]	vol. flow [m³/h]
process airflow	32	40	2000 $l_{20°C}$
reg. airflow	90	-	1500 $l_{20°C}$

$V_{reg} : V_{process}$ 0,75

Measured values:

RPH	ambient air					supply air				
	ϑ [°C]	φ [%]	x [g/kg]	h [kJ/kg]	Vnorm [m³/h]	ϑ [°C]	φ [%]	x [g/kg]	h [kJ/kg]	Vnorm [m³/h]
25	31,96 ± 0,06	40,00 ± 0,34	11,93 ± 0,11	62,5 ± 0,3	2004 ± 11	45,69 ± 0,32	13,03 ± 0,76	8,07 ± 0,55	66,5 ± 1,7	2137 ± 10
40	31,96 ± 0,06	39,71 ± 0,36	11,83 ± 0,11	62,2 ± 0,3	2004 ± 7	51,46 ± 0,10	8,19 ± 0,47	6,76 ± 0,41	69,0 ± 1,1	2132 ± 8
55	31,99 ± 0,05	39,84 ± 0,31	11,89 ± 0,11	62,4 ± 0,3	2005 ± 6	53,72 ± 0,07	7,03 ± 0,37	6,47 ± 0,35	70,5 ± 1,0	2129 ± 6
70	32,00 ± 0,09	40,33 ± 0,26	12,05 ± 0,09	62,8 ± 0,3	1996 ± 8	55,82 ± 0,05	6,24 ± 0,27	6,35 ± 0,26	72,3 ± 0,8	2111 ± 7
85	31,99 ± 0,05	40,26 ± 0,27	12,02 ± 0,08	62,7 ± 0,2	1994 ± 12	57,23 ± 0,04	5,82 ± 0,20	6,32 ± 0,22	73,7 ± 0,6	2098 ± 6
100	32,01 ± 0,06	39,69 ± 0,29	11,86 ± 0,09	62,4 ± 0,3	1981 ± 6	56,93 ± 0,04	5,42 ± 0,16	5,80 ± 0,18	72,0 ± 0,5	2081 ± 6
150	31,97 ± 0,07	39,73 ± 0,21	11,85 ± 0,08	62,3 ± 0,2	1986 ± 6	59,21 ± 0,05	5,27 ± 0,08	6,27 ± 0,10	75,6 ± 0,3	2067 ± 6
196	31,96 ± 0,06	40,13 ± 0,54	11,97 ± 0,17	62,6 ± 0,4	1989 ± 6	62,29 ± 0,06	5,23 ± 0,09	7,19 ± 0,14	81,1 ± 0,4	2107 ± 5

RPH	regeneration air					waste air				
	ϑ [°C]	φ [%]	x [g/kg]	h [kJ/kg]	Vnorm [m³/h]	ϑ [°C]	φ [%]	x [g/kg]	h [kJ/kg]	Vnorm [m³/h]
25	90,18 ± 0,00	1,49 ± 0,01	6,92 ± 0,06	108,6 ± 0,2	1489 ± 7	65,61 ± 0,23	12,11 ± 0,36	19,69 ± 0,72	117,2 ± 2,0	1406 ± 5
40	90,18 ± 0,00	1,37 ± 0,01	6,37 ± 0,06	107,1 ± 0,2	1512 ± 8	56,56 ± 0,16	17,61 ± 0,36	18,93 ± 0,45	105,9 ± 1,3	1439 ± 5
55	90,19 ± 0,00	1,37 ± 0,01	6,39 ± 0,05	107,2 ± 0,1	1523 ± 6	52,48 ± 0,06	21,13 ± 0,33	18,66 ± 0,34	100,9 ± 0,9	1457 ± 5
70	90,19 ± 0,00	1,40 ± 0,01	6,52 ± 0,04	107,8 ± 0,1	1525 ± 7	50,20 ± 0,09	23,96 ± 0,32	18,92 ± 0,29	99,2 ± 0,8	1466 ± 4
85	90,19 ± 0,00	1,40 ± 0,01	6,49 ± 0,04	107,5 ± 0,1	1526 ± 8	47,84 ± 0,05	26,41 ± 0,27	18,54 ± 0,20	95,8 ± 0,5	1473 ± 4
100	89,81 ± 0,05	1,40 ± 0,00	6,43 ± 0,02	106,9 ± 0,1	1485 ± 33	45,84 ± 0,04	28,44 ± 0,23	18,02 ± 0,16	92,4 ± 0,4	1438 ± 4
150	90,18 ± 0,00	1,46 ± 0,01	6,86 ± 0,06	108,5 ± 0,2	1528 ± 6	41,46 ± 0,03	31,12 ± 0,39	15,66 ± 0,20	81,8 ± 0,5	1458 ± 4
196	90,18 ± 0,00	1,46 ± 0,01	6,86 ± 0,06	108,5 ± 0,2	1528 ± 6	41,46 ± 0,03	31,12 ± 0,39	15,66 ± 0,20	81,8 ± 0,5	1458 ± 4

Figures of merit:

RPH	$\Delta x_{amb\ sup}$ [g/kg]	RSHI [kJ/g]	η_{dehum} [-]	$\Delta h_{sup-amb}$ [kJ/kg]
25	3,85	11,30	0,38	4,1
40	5,07	8,73	0,50	6,8
55	5,42	8,21	0,53	8,1
70	5,71	7,85	0,55	9,5
85	5,70	7,87	0,55	10,9
100	6,05	7,21	0,59	9,7
150	5,57	8,09	0,55	13,3
196	4,78	9,43	0,47	18,5

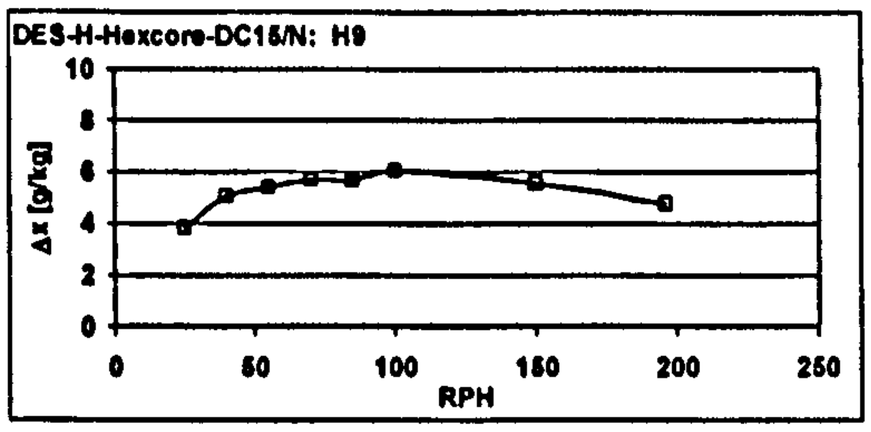

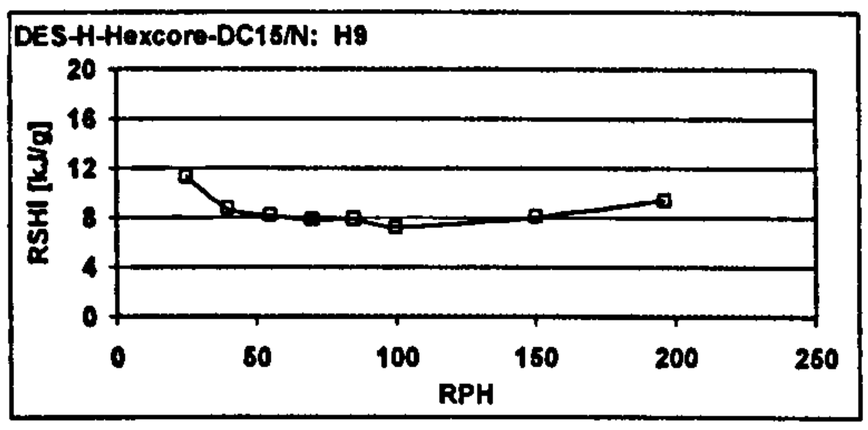

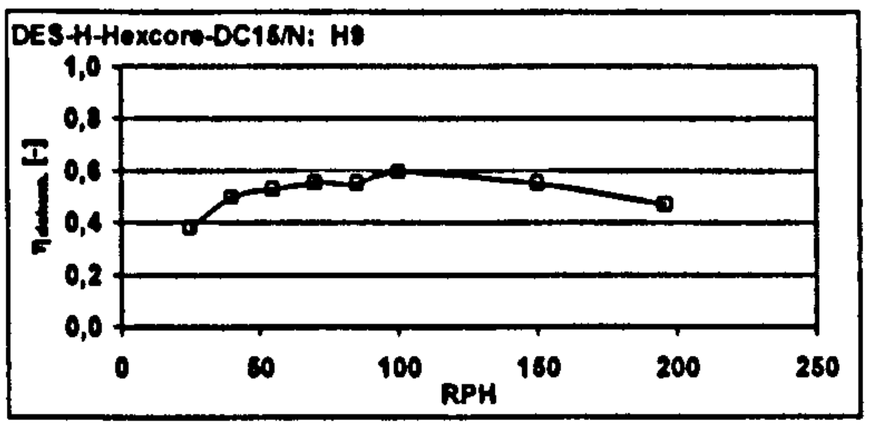

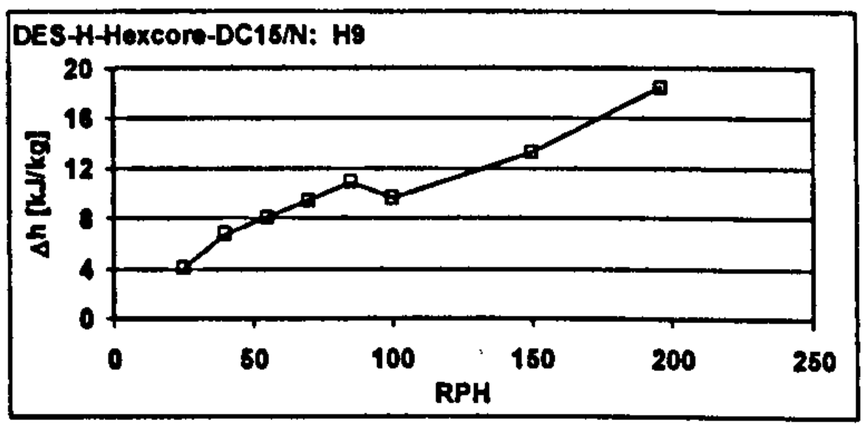

APPENDIX A

OUTCOMES OF MEASUREMENTS FROM THE DESICCANT WHEEL TEST FACILITY

measurement series K1

Desiccant wheel: **Klingenburg, SECO 1000**

Set values:

	temperature [°C]	rel. humidity [%]	vol. flow [m³/h]
process airflow	32	40	2000 $l_{20°C}$
reg. airflow	75	-	1500 $l_{20°C}$

$V_{reg} : V_{process}$ 0,75

Measured values:

RPH	ambient air					supply air				
	θ [°C]	φ [%]	x [g/kg]	h [kJ/kg]	Vnorm [m³/h]	θ [°C]	φ [%]	x [g/kg]	h [kJ/kg]	Vnorm [m³/h]
8	32,01 ± 0,06	40,19 ± 0,45	12,01 ± 0,15	62,7 ± 0,4	1986 ± 8	39,53 ± 0,06	19,27 ± 0,25	8,66 ± 0,11	61,6 ± 0,3	2015 ± 10
24	32,00 ± 0,06	39,80 ± 0,62	11,89 ± 0,20	62,4 ± 0,5	1986 ± 7	42,79 ± 0,02	14,57 ± 0,32	7,77 ± 0,17	62,8 ± 0,5	2021 ± 10
39	31,94 ± 0,07	39,79 ± 0,35	11,84 ± 0,12	62,2 ± 0,3	1984 ± 6	44,49 ± 0,03	13,33 ± 0,12	7,76 ± 0,07	64,5 ± 0,2	2021 ± 9
56	32,00 ± 0,05	39,72 ± 0,47	11,87 ± 0,15	62,4 ± 0,4	1987 ± 5	45,99 ± 0,02	12,62 ± 0,22	7,93 ± 0,14	66,5 ± 0,3	2025 ± 8
73	31,97 ± 0,05	39,61 ± 0,48	11,82 ± 0,13	62,2 ± 0,3	1981 ± 5	46,96 ± 0,04	12,27 ± 0,18	8,11 ± 0,12	68,0 ± 0,3	2021 ± 7
89	32,00 ± 0,05	39,63 ± 0,60	11,84 ± 0,19	62,3 ± 0,5	1986 ± 12	47,88 ± 0,00	12,13 ± 0,19	8,40 ± 0,13	69,6 ± 0,3	2017 ± 6
106	31,89 ± 0,06	39,71 ± 0,58	11,79 ± 0,18	62,1 ± 0,5	1983 ± 7	48,21 ± 0,04	12,02 ± 0,15	8,46 ± 0,10	70,1 ± 0,3	2017 ± 7
156	31,99 ± 0,05	39,71 ± 0,65	11,86 ± 0,20	62,3 ± 0,5	1990 ± 8	48,89 ± 0,00	11,94 ± 0,16	8,70 ± 0,12	71,4 ± 0,3	2023 ± 5
248	32,00 ± 0,05	39,74 ± 0,50	11,87 ± 0,18	62,4 ± 0,5	2002 ± 5	49,19 ± 0,01	11,75 ± 0,06	8,69 ± 0,05	71,7 ± 0,1	2018 ± 8

RPH	regeneration air					waste air				
	θ [°C]	φ [%]	x [g/kg]	h [kJ/kg]	Vnorm [m³/h]	θ [°C]	φ [%]	x [g/kg]	h [kJ/kg]	Vnorm [m³/h]
8	60,27 ± 0,05	3,31 ± 0,02	4,40 ± 0,02	71,8 ± 0,1	1519 ± 10	40,80 ± 0,07	26,05 ± 0,14	12,61 ± 0,06	73,3 ± 0,2	1551 ± 7
24	60,82 ± 0,06	3,13 ± 0,02	4,27 ± 0,02	72,0 ± 0,1	1526 ± 9	37,15 ± 0,07	31,96 ± 0,17	12,73 ± 0,11	69,8 ± 0,3	1563 ± 4
39	60,73 ± 0,03	3,10 ± 0,01	4,21 ± 0,01	71,7 ± 0,0	1519 ± 8	35,53 ± 0,05	32,94 ± 0,13	11,98 ± 0,05	66,3 ± 0,1	1551 ± 4
56	60,83 ± 0,01	3,15 ± 0,02	4,30 ± 0,03	72,0 ± 0,1	1524 ± 9	34,15 ± 0,05	33,99 ± 0,12	11,44 ± 0,06	63,5 ± 0,2	1550 ± 5
73	60,52 ± 0,00	3,21 ± 0,01	4,31 ± 0,02	71,8 ± 0,0	1528 ± 8	33,51 ± 0,02	34,00 ± 0,18	11,04 ± 0,06	61,8 ± 0,2	1551 ± 4
89	60,32 ± 0,02	3,32 ± 0,01	4,43 ± 0,02	71,9 ± 0,0	1519 ± 11	33,03 ± 0,04	34,51 ± 0,23	10,91 ± 0,07	61,0 ± 0,2	1535 ± 5
106	60,33 ± 0,04	3,26 ± 0,01	4,34 ± 0,02	71,7 ± 0,1	1512 ± 13	32,72 ± 0,04	34,71 ± 0,24	10,78 ± 0,07	60,3 ± 0,2	1537 ± 5
156	60,22 ± 0,01	3,34 ± 0,02	4,43 ± 0,02	71,8 ± 0,1	1529 ± 9	32,71 ± 0,02	35,17 ± 0,36	10,92 ± 0,11	60,7 ± 0,3	1551 ± 3
248	60,10 ± 0,02	3,32 ± 0,02	4,38 ± 0,02	71,5 ± 0,0	1537 ± 5	32,74 ± 0,05	35,85 ± 0,26	11,15 ± 0,09	61,3 ± 0,3	1549 ± 4

Figures of merit:

RPH	$\Delta x_{amb-sup}$ [g/kg]	RSHI [kJ/g]	η_{dehum} [-]	$\Delta h_{sup-amb}$ [kJ/kg]
8	3,35	6,50	0,38	-0,9
25	4,12	5,42	0,47	0,4
40	4,08	5,43	0,47	2,3
55	3,93	5,66	0,45	4,1
70	3,70	5,99	0,43	5,8
85	3,44	6,34	0,40	7,3
100	3,33	6,56	0,39	8,1
150	3,16	6,91	0,37	9,1
248	3,18	6,83	0,37	9,3

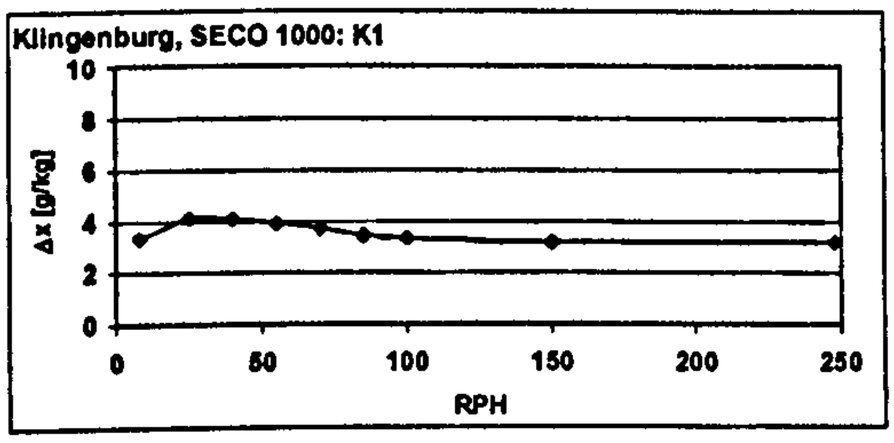

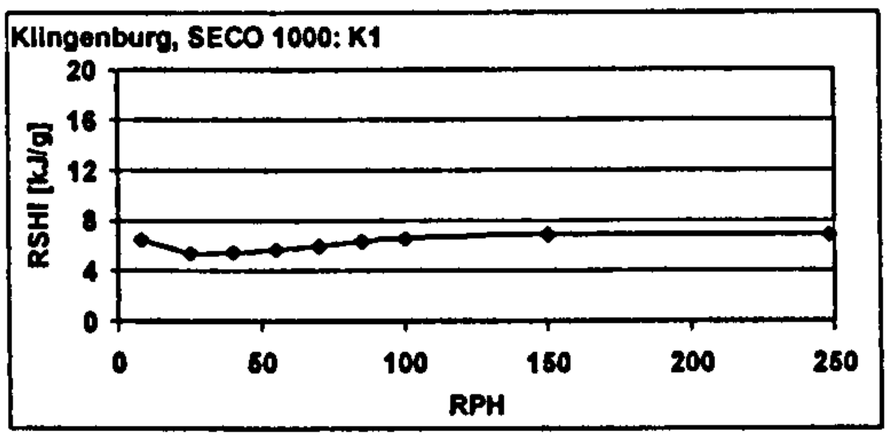

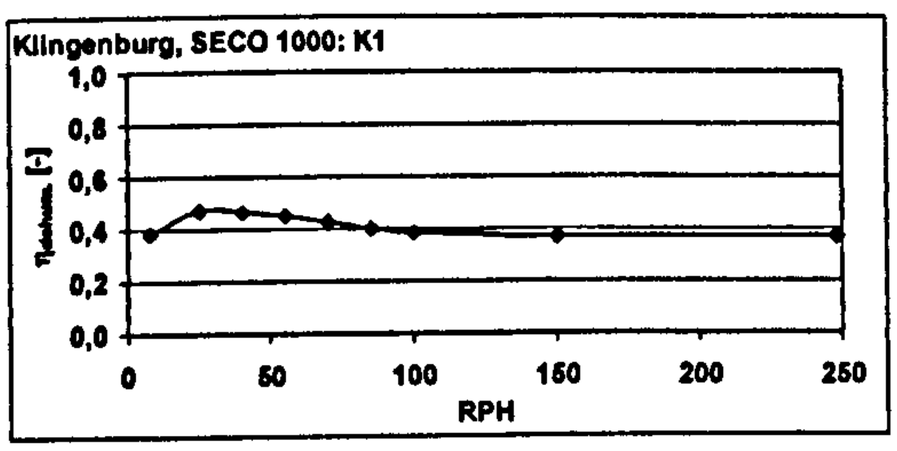

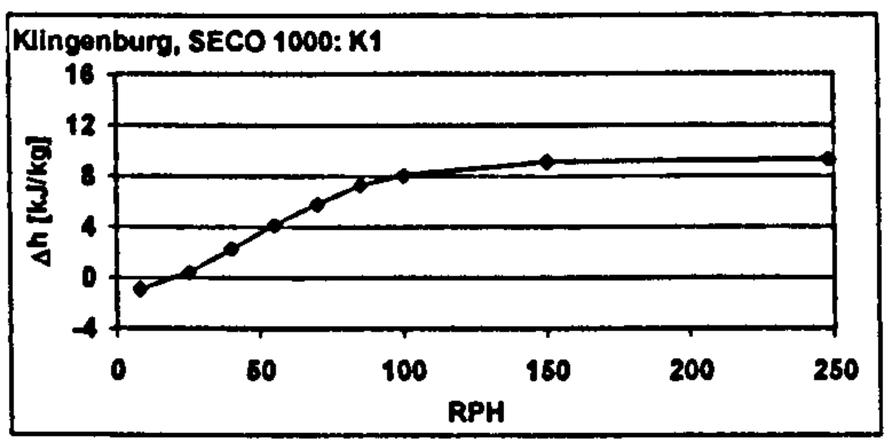

OUTCOMES OF MEASUREMENTS FROM THE DESICCANT WHEEL TEST FACILITY

measurement series K2

Desiccant wheel: **Klingenburg, SECO 1000**

Set values:

	temperature [°C]	rel. humidity [%]	vol. flow [m³/h]
process airflow	32	40	2000 $l_{20°C}$
reg. airflow	60	10	2000 $l_{20°C}$

$V_{reg} : V_{process}$ 1

Measured values:

RPH	ambient air					supply air				
	θ [°C]	φ [%]	x [g/kg]	h [kJ/kg]	Vnorm [m³/h]	θ [°C]	φ [%]	x [g/kg]	h [kJ/kg]	Vnorm [m³/h]
24	32,01 ± 0,07	39,61 ± 0,45	11,84 ± 0,17	62,3 ± 0,5	2003 ± 5	44,71 ± 0,06	15,53 ± 0,28	9,16 ± 0,16	68,4 ± 0,4	1620 ± 9
56	31,97 ± 0,05	39,70 ± 0,42	11,84 ± 0,14	62,3 ± 0,4	1992 ± 5	48,91 ± 0,00	13,03 ± 0,12	9,51 ± 0,09	73,5 ± 0,2	1800 ± 7
89	31,99 ± 0,05	39,89 ± 0,63	11,91 ± 0,22	62,5 ± 0,6	1986 ± 5	52,61 ± 0,04	11,98 ± 0,18	10,51 ± 0,17	79,9 ± 0,5	1799 ± 6
156	32,03 ± 0,06	40,27 ± 0,51	12,06 ± 0,16	62,9 ± 0,4	1999 ± 5	54,80 ± 0,00	12,95 ± 0,08	12,66 ± 0,06	87,7 ± 0,2	1823 ± 7

RPH	regeneration air					waste air				
	θ [°C]	φ [%]	x [g/kg]	h [kJ/kg]	Vnorm [m³/h]	θ [°C]	φ [%]	x [g/kg]	h [kJ/kg]	Vnorm [m³/h]
24	60,16 ± 0,27	11,26 ± 0,25	14,20 ± 0,29	97,2 ± 0,8	2003 ± 21	44,51 ± 0,06	30,70 ± 0,56	18,19 ± 0,33	91,5 ± 0,8	2293 ± 14
56	59,70 ± 0,21	11,39 ± 0,32	14,06 ± 0,46	96,4 ± 1,3	2029 ± 16	42,50 ± 0,05	32,96 ± 0,48	17,57 ± 0,27	87,8 ± 0,7	2313 ± 13
89	60,43 ± 0,14	11,16 ± 0,14	14,24 ± 0,22	97,6 ± 0,7	2018 ± 17	40,70 ± 0,04	34,33 ± 0,48	16,63 ± 0,22	83,5 ± 0,5	2301 ± 14
156	60,09 ± 0,05	11,60 ± 0,23	14,58 ± 0,29	98,1 ± 0,8	2017 ± 12	38,83 ± 0,10	34,33 ± 0,44	15,01 ± 0,16	77,4 ± 0,4	2261 ± 11

Figures of merit:

RPH	$\Delta x_{amb-sup}$ [g/kg]	RSHI [kJ/g]	η_{dehum} [-]	$\Delta h_{sup-amb}$ [kJ/kg]
24	2,68	10,56	0,54	6,0
56	2,32	12,23	0,47	11,3
89	1,40	20,79	0,28	17,4
156	-0,61			24,8

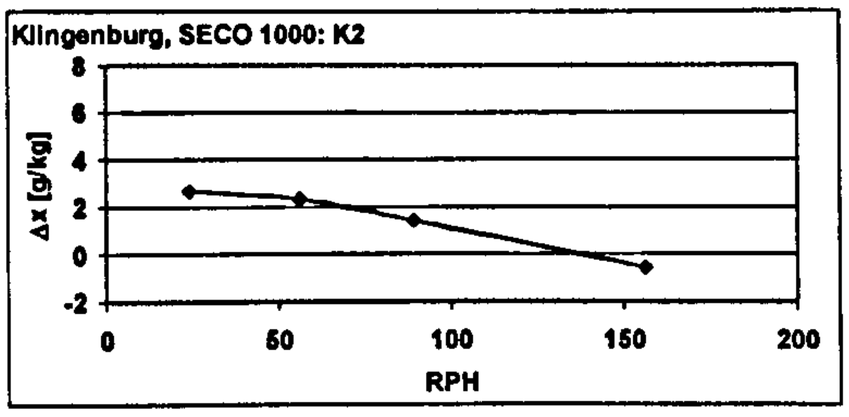

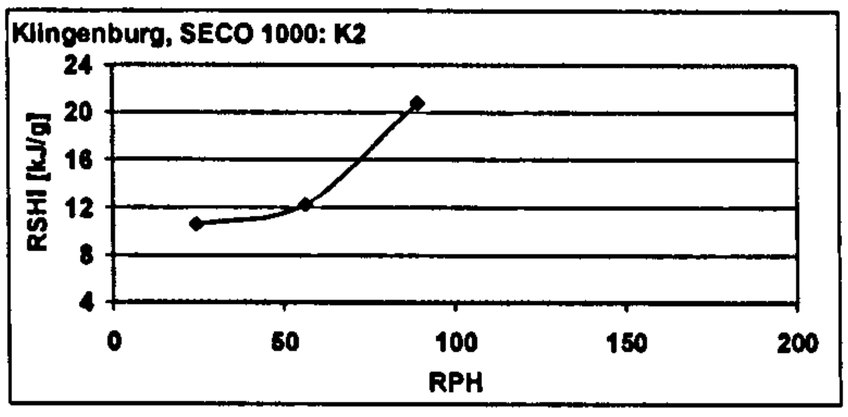

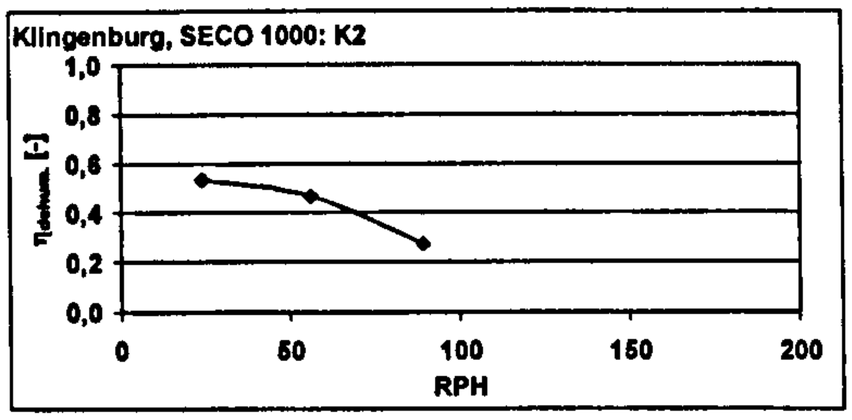

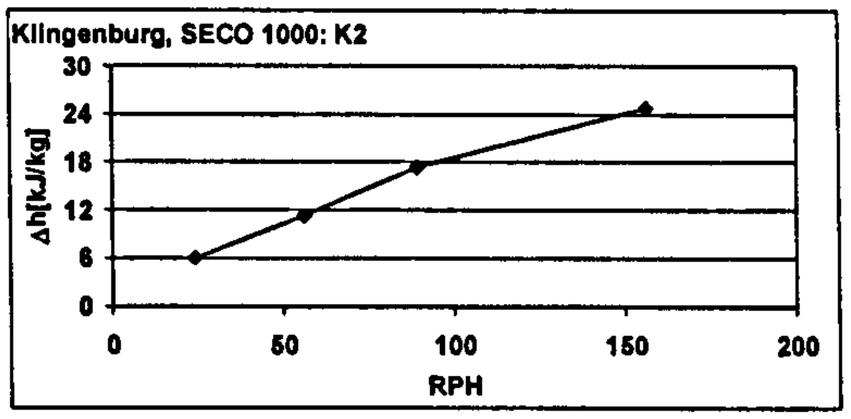

APPENDIX A

OUTCOMES OF MEASUREMENTS FROM THE DESICCANT WHEEL TEST FACILITY

measurement series K3

Desiccant wheel: **Klingenburg, SECO 1000**

Set values:

	temperature [°C]	rel humidity [%]	vol flow [m³/h]
process airflow	32	40	2000 $l_{20°C}$
reg airflow	60	10	1000 $l_{20°C}$

$V_{reg} : V_{process}$ 0,5

Measured values:

RPH	ambient air					supply air				
	θ [°C]	φ [%]	x [g/kg]	h [kJ/kg]	Vnorm [m³/h]	θ [°C]	φ [%]	x [g/kg]	h [kJ/kg]	Vnorm [m³/h]
24	32,00 ± 0,05	39,96 ± 0,24	11,94 ± 0,09	62,6 ± 0,3	1997 ± 6	39,62 ± 0,03	23 48 ± 0 17	10,75 ± 0 06	67,5 ± 0,2	2195 ± 8
56	32,00 ± 0,05	40,18 ± 0,45	12,00 ± 0,11	62,7 ± 0,3	1996 ± 4	41,04 ± 0,05	22,53 ± 0 31	11 02 ± 0,13	69 4 ± 0,3	2195 ± 9
89	31,96 ± 0,05	40,22 ± 0,37	12,00 ± 0,13	62,7 ± 0,4	1994 ± 5	42,15 ± 0 05	22,63 ± 0,17	11,74 ± 0,09	72 4 ± 0,2	2191 ± 7
156	31,95 ± 0,05	40,15 ± 0,58	11,96 ± 0,19	62,6 ± 0 5	1989 ± 5	44 03 ± 0 04	22 09 ± 0 25	12 65 ± 0 17	76 7 ± 0 5	2183 ± 6

RPH	regeneration air					waste air				
	θ [°C]	φ [%]	x [g/kg]	h [kJ/kg]	Vnorm [m³/h]	θ [°C]	φ [%]	x [g/kg]	h [kJ/kg]	Vnorm [m³/h]
24	60,24 ± 0,04	10,25 ± 0,17	12,94 ± 0,21	94,0 ± 0,5	1004 ± 8	39,33 ± 0,03	45 13 ± 0 43	20 44 ± 0 20	91 9 ± 0 5	818 ± 4
56	60,14 ± 0,05	11,61 ± 0,22	14,63 ± 0,31	96,3 ± 0,8	1001 ± 10	34,54 ± 0,15	45,76 ± 0 43	15 86 ± 0 26	75 2 ± 0 8	833 ± 4
89	59,94 ± 0,04	10,48 ± 0,07	13,06 ± 0,09	94,0 ± 0,3	1006 ± 8	33,12 ± 0,00	42,37 ± 0,17	13,51 ± 0,06	67,7 ± 0,1	833 ± 3
156	60 36 ± 0,05	11,43 ± 0,06	14,55 ± 0,10	96,3 ± 0 3	997 ± 10	32 81 ± 0 01	41,73 ± 0 56	13 07 ± 0 19	66 3 ± 0 5	831 ± 4

Figures of merit:

RPH	$\Delta x_{amb-sup}$ [g/kg]	RSHI [kJ/g]	η_{dehum} [-]	$\Delta h_{sup-amb}$ [kJ/kg]
24	1,19	12,00	0,22	4,9
56	0,99	14,37	0,20	6,7
89	0,27	53,58	0,05	9,7
156	-0,69			14,1

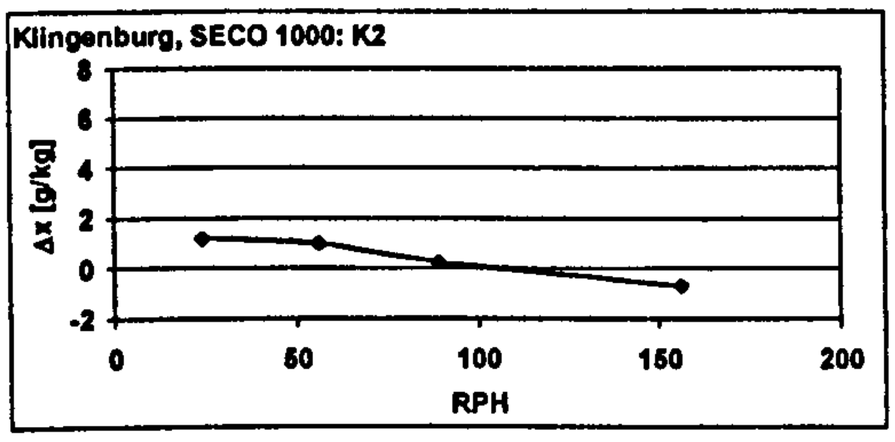

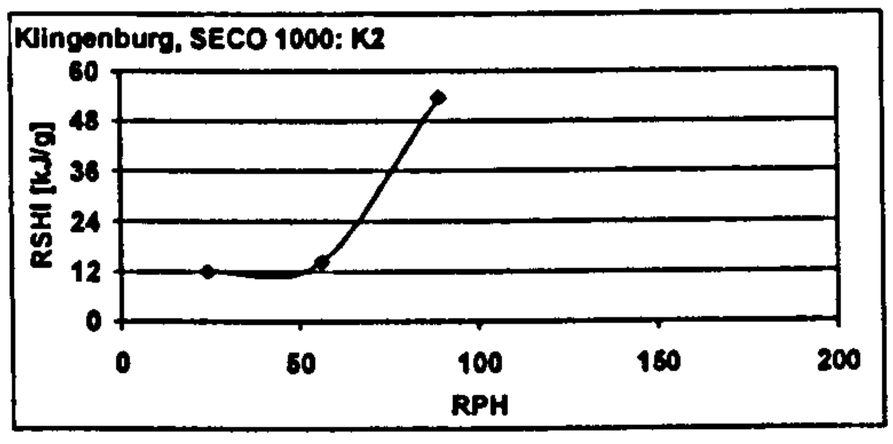

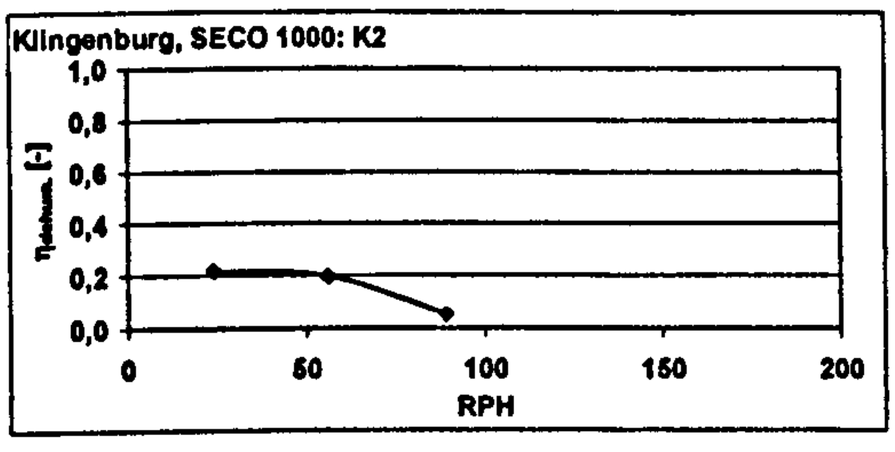

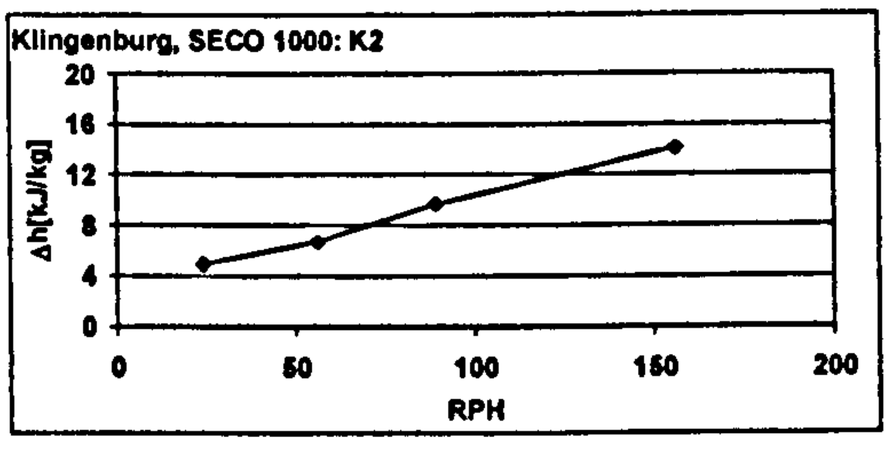

OUTCOMES OF MEASUREMENTS FROM THE DESICCANT WHEEL TEST FACILITY

measurement series K4

Desiccant wheel: **Klingenburg, SECO 1000**

Set values:

	temperature [°C]	rel humidity [%]	vol flow [m³/h]
process airflow	28	40	2000 $l_{20°C}$
reg airflow	60	10	1500 $l_{20°C}$

$V_{reg} : V_{process}$ 0,75

Measured values:

RPH	ambient air					supply air				
	θ [°Y]	φ [%]	x [g/kg]	h [kJ/kg]	Vnorm [m³/h]	θ [°Y]	φ [%]	x [g/kg]	h [kJ/kg]	Vnorm [m³/h]
24	27,99 ± 0,06	39,68 ± 0,58	9,38 ± 0,15	51,9 ± 0,4	1994 ± 8	39,59 ± 0,12	15,37 ± 0,23	6,91 ± 0,10	57,4 ± 0,3	2000 ± 10
56	28,00 ± 0,06	40,16 ± 0,35	9,50 ± 0,09	52,2 ± 0,2	1977 ± 9	43,87 ± 0,10	13,45 ± 0,16	7,58 ± 0,09	63,4 ± 0,3	1986 ± 8
89	28,01 ± 0,07	39,44 ± 0,68	9,33 ± 0,16	51,8 ± 0,4	1979 ± 8	46,86 ± 0,17	13,34 ± 0,24	8,79 ± 0,11	69,6 ± 0,3	2000 ± 7
156	27,99 ± 0,07	40,10 ± 0,29	9,48 ± 0,08	52,2 ± 0,2	1975 ± 12	49,60 ± 0,22	14,83 ± 0,24	11,24 ± 0,14	78,7 ± 0,4	1999 ± 10

RPH	regeneration air					waste air				
	θ [°Y]	φ [%]	x [g/kg]	h [kJ/kg]	Vnorm [m³/h]	θ [°Y]	φ [%]	x [g/kg]	h [kJ/kg]	Vnorm [m³/h]
24	59,97 ± 0,05	10,16 ± 0,23	12,67 ± 0,29	93,0 ± 0,8	1510 ± 29	41,53 ± 0,10	36,35 ± 0,39	18,45 ± 0,18	89,0 ± 0,5	1553 ± 5
56	59,77 ± 0,06	10,51 ± 0,29	13,00 ± 0,36	93,7 ± 0,9	1543 ± 15	37,17 ± 0,07	40,69 ± 0,56	16,30 ± 0,21	79,0 ± 0,5	1554 ± 4
89	59,93 ± 0,14	10,67 ± 0,25	13,29 ± 0,31	94,6 ± 0,8	1528 ± 21	33,76 ± 0,05	41,02 ± 0,47	13,56 ± 0,16	68,5 ± 0,4	1535 ± 4
156	59,83 ± 0,14	11,06 ± 0,30	13,73 ± 0,38	95,6 ± 1,0	1527 ± 16	31,35 ± 0,11	40,38 ± 0,45	11,62 ± 0,11	61,1 ± 0,3	1508 ± 4

Figures of merit:

RPH	$\Delta x_{amb-sup}$ [g/kg]	RSHI [kJ/g]	η_{dehum} [-]	$\Delta h_{sup-amb}$ [kJ/kg]
24	2,47	9,88	0,53	5,5
56	1,92	13,02	0,42	11,2
89	0,54	45,80	0,12	17,8
156	-1,76			26,5

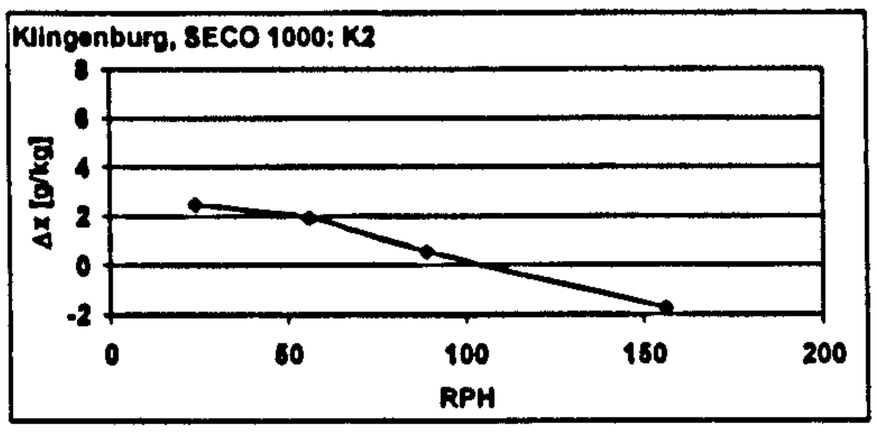

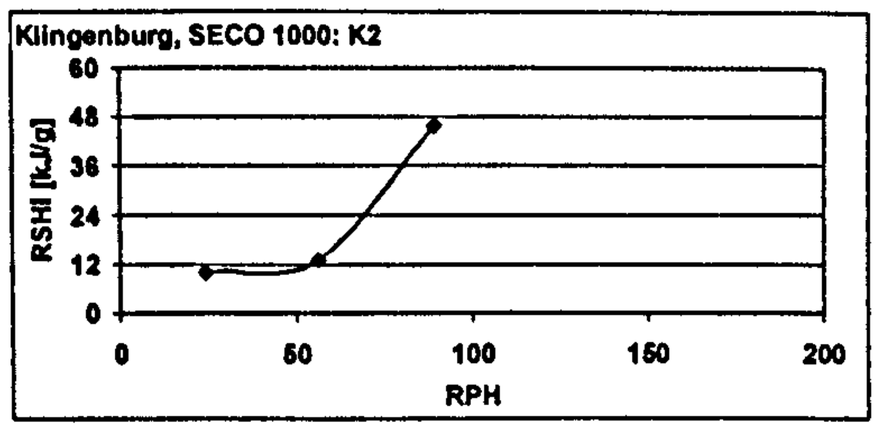

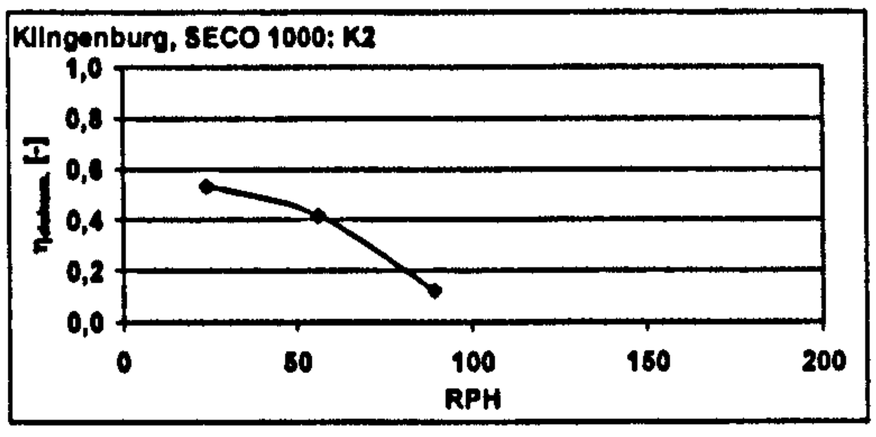

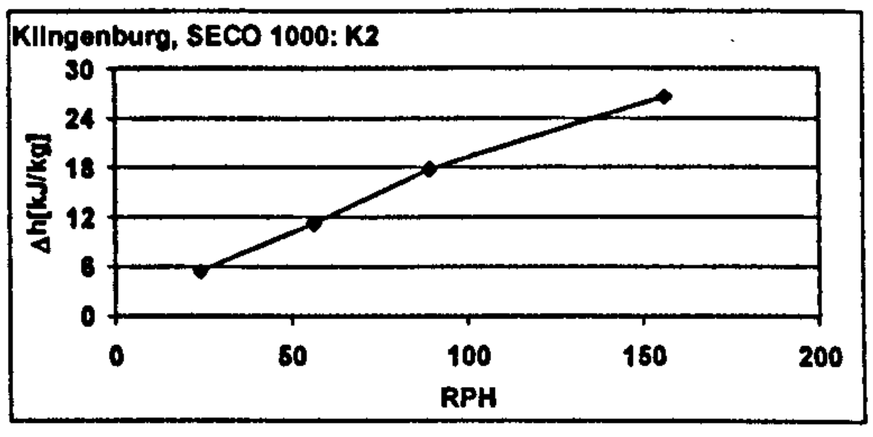

APPENDIX A

OUTCOMES OF MEASUREMENTS FROM THE DESICCANT WHEEL TEST FACILITY

measurement series K5

Desiccant wheel: **Klingenburg, SECO 1000**

Set values:

	temperature [°C]	rel. humidity [%]	vol. flow [m³/h]
process airflow	36	50	2000 $l_{20°C}$
reg. airflow	60	10	1500 $l_{20°C}$

$V_{reg} : V_{process}$ 0,75

Measured values:

RPH	ambient air					supply air				
	θ [°C]	φ [%]	x [g/kg]	h [kJ/kg]	Vnorm [m³/h]	θ [°C]	φ [%]	x [g/kg]	h [kJ/kg]	Vnorm [m³/h]
24	35,97 ± 0,09	49,63 ± 0,60	18,69 ± 0,25	83,9 ± 0,7	1988 ± 5	49,91 ± 0,10	19,88 ± 0,27	15,39 ± 0,21	89,8 ± 0,6	2070 ± 10
56	35,94 ± 0,05	49,89 ± 0,57	18,77 ± 0,23	84,1 ± 0,6	1995 ± 5	51,53 ± 0,05	18,26 ± 0,23	15,32 ± 0,19	91,3 ± 0,5	2075 ± 7
89	35,99 ± 0,06	49,85 ± 0,55	18,79 ± 0,22	84,2 ± 0,6	1991 ± 5	52,02 ± 0,06	18,26 ± 0,20	15,69 ± 0,19	92,7 ± 0,5	2073 ± 7
156	35,98 ± 0,06	49,75 ± 0,62	18,75 ± 0,25	84,1 ± 0,7	1978 ± 4	52,77 ± 0,14	18,31 ± 0,22	16,34 ± 0,16	95,2 ± 0,5	2054 ± 7

RPH	regeneration air					waste air				
	θ [°C]	φ [%]	x [g/kg]	h [kJ/kg]	Vnorm [m³/h]	θ [°C]	φ [%]	x [g/kg]	h [kJ/kg]	Vnorm [m³/h]
24	59,93 ± 0,07	10,64 ± 0,16	13,26 ± 0,21	94,5 ± 0,6	1490 ± 12	39,83 ± 0,10	46,68 ± 0,32	21,77 ± 0,18	95,6 ± 0,5	1451 ± 4
56	59,70 ± 0,03	9,22 ± 0,20	11,33 ± 0,26	89,2 ± 0,7	1508 ± 17	37,22 ± 0,03	47,49 ± 0,36	19,17 ± 0,18	86,4 ± 0,5	1474 ± 4
89	60,09 ± 0,01	10,19 ± 0,29	12,78 ± 0,37	93,4 ± 1,0	1505 ± 14	37,72 ± 0,09	47,14 ± 0,43	19,56 ± 0,19	88,0 ± 0,5	1472 ± 4
156	59,62 ± 0,05	10,76 ± 0,14	13,21 ± 0,17	94,1 ± 0,4	1493 ± 16	37,49 ± 0,11	47,46 ± 0,55	19,44 ± 0,19	87,4 ± 0,5	1460 ± 4

Figures of merit:

RPH	$\Delta x_{amb-sup}$ [g/kg]	RSHI [kJ/g]	η_{dehum} [-]	$\Delta h_{sup-amb}$ [kJ/kg]
24	3,29	5,49	0,43	5,9
56	3,45	5,24	0,42	7,2
89	3,10	5,92	0,40	8,5
156	2,41	7,46	0,32	11,1

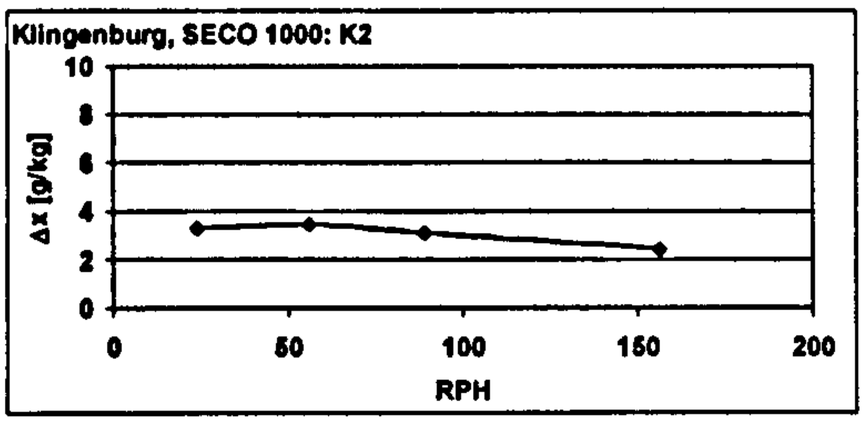

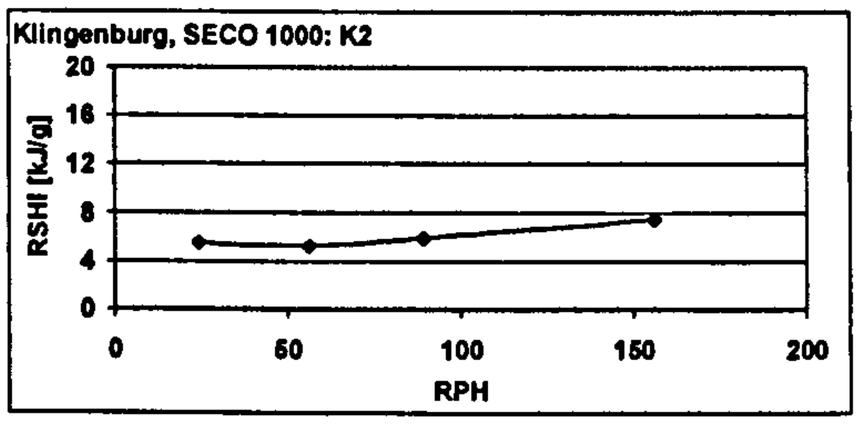

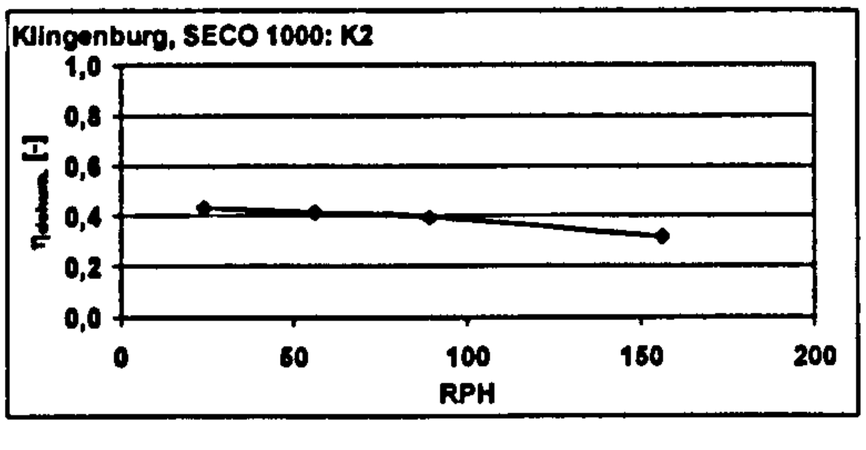

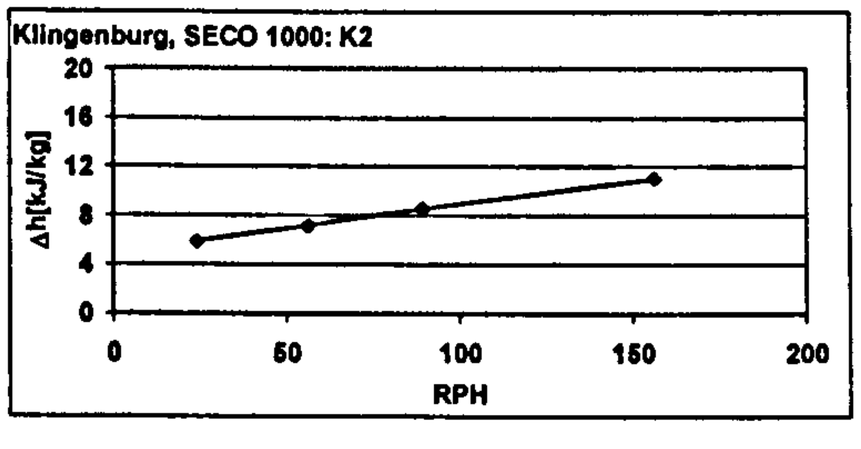

OUTCOMES OF MEASUREMENTS FROM THE DESICCANT WHEEL TEST FACILITY

measurement series K6

Desiccant wheel: **Klingenburg, SECO 1000**

Set values:

	temperature [°C]	rel. humidity [%]	vol. flow [m³/h]
process airflow	32	40	2000 $\|_{20°C}$
reg. airflow	70	10	1500 $\|_{20°C}$

$V_{reg} : V_{process}$ 0,75

Measured values:

RPH	ambient air					supply air				
	θ [°Y]	φ [%]	x [g/kg]	h [kJ/kg]	Vnorm [m³/h]	θ [°Y]	φ [%]	x [g/kg]	h [kJ/kg]	Vnorm [m³/h]
24	31,98 ± 0,06	39,56 ± 0,37	11,80 ± 0,12	62,2 ± 0,3	2003 ± 5	45,36 ± 0,12	14,87 ± 0,19	9,07 ± 0,11	68,8 ± 0,3	2087 ± 10
56	31,97 ± 0,07	39,65 ± 0,50	11,82 ± 0,16	62,2 ± 0,4	1998 ± 6	49,23 ± 0,17	12,94 ± 0,25	9,60 ± 0,16	74,1 ± 0,4	2084 ± 7
89	31,97 ± 0,06	39,82 ± 0,43	11,88 ± 0,14	62,4 ± 0,4	1987 ± 5	52,53 ± 0,09	12,80 ± 0,20	11,20 ± 0,15	81,6 ± 0,4	2069 ± 8
156	31,98 ± 0,06	40,24 ± 0,47	12,01 ± 0,15	62,7 ± 0,4	1987 ± 4	56,44 ± 0,13	14,07 ± 0,15	14,93 ± 0,16	95,3 ± 0,5	2060 ± 7

RPH	regeneration air					waste air				
	θ [°Y]	φ [%]	x [g/kg]	h [kJ/kg]	Vnorm [m³/h]	θ [°Y]	φ [%]	x [g/kg]	h [kJ/kg]	Vnorm [m³/h]
24	69,94 ± 0,12	9,81 ± 0,14	19,26 ± 0,26	120,5 ± 0,7	1497 ± 15	47,28 ± 0,05	38,46 ± 0,46	26,58 ± 0,30	116,0 ± 0,8	1476 ± 4
56	69,96 ± 0,01	9,98 ± 0,17	19,64 ± 0,35	121,6 ± 0,9	1508 ± 16	43,67 ± 0,18	41,98 ± 0,64	24,03 ± 0,31	105,7 ± 0,8	1490 ± 4
89	69,96 ± 0,04	10,28 ± 0,17	20,25 ± 0,35	123,2 ± 0,9	1520 ± 15	39,67 ± 0,08	43,73 ± 0,46	20,17 ± 0,25	91,6 ± 0,7	1505 ± 4
156	70,06 ± 0,07	10,52 ± 0,17	20,83 ± 0,36	124,8 ± 1,0	1539 ± 14	36,05 ± 0,11	42,42 ± 0,45	15,98 ± 0,17	77,0 ± 0,5	1518 ± 4

Figures of merit:

RPH	$\Delta x_{amb-sup}$ [g/kg]	RSHI [kJ/g]	η_{dehum} [-]	$\Delta h_{sup-amb}$ [kJ/kg]
24	2,73	10,46	0,50	6,6
56	2,22	12,99	0,41	11,9
89	0,68	43,22	0,13	19,2
156	-2,92			32,6

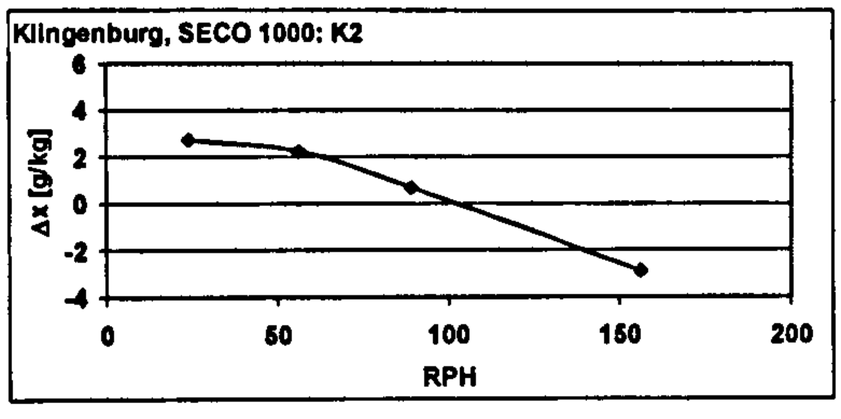

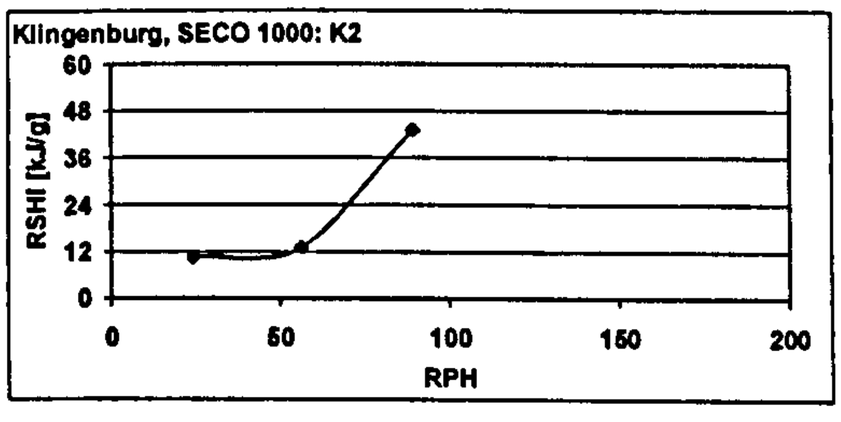

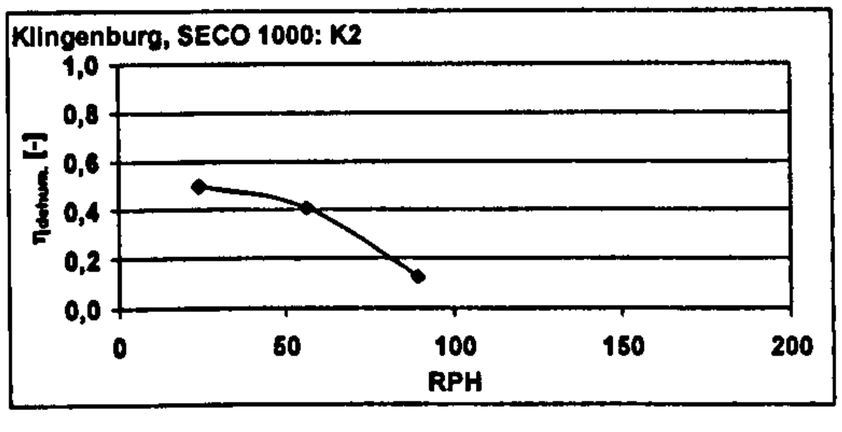

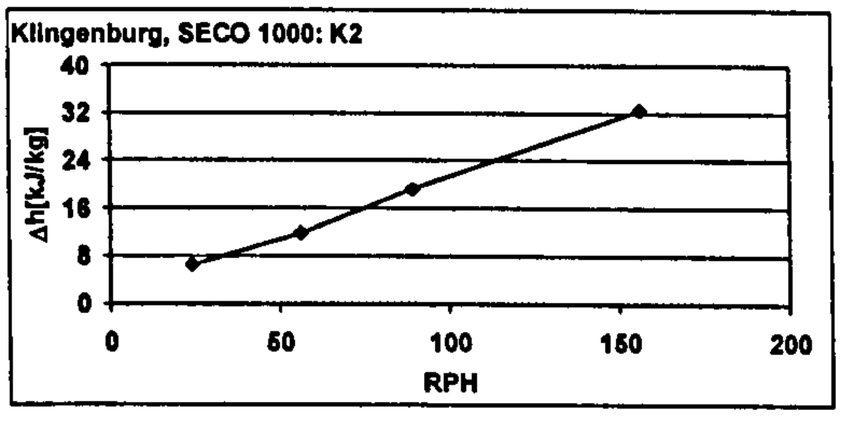

APPENDIX A

OUTCOMES OF MEASUREMENTS FROM THE DESICCANT WHEEL TEST FACILITY

measurement series K7

Desiccant wheel: **Klingenburg, SECO 1000**

Set values:

	temperature [°C]	rel. humidity [%]	vol. flow [m³/h]
process airflow	32	40	2000 $l_{20°C}$
reg. airflow	50	10	1500 $l_{20°C}$

$V_{reg} : V_{process}$ 0,75

Measured values:

RPH	ambient air					supply air				
	θ [°C]	φ [%]	x [g/kg]	h [kJ/kg]	Vnorm [m³/h]	θ [°C]	φ [%]	x [g/kg]	h [kJ/kg]	Vnorm [m³/h]
24	31,99 ± 0,09	40,13 ± 0,51	11,98 ± 0,16	62,6 ± 0,4	1997 ± 6	42,35 ± 0,06	18,83 ± 0,39	9,84 ± 0,19	67,7 ± 0,5	2058 ± 12
56	31,97 ± 0,11	39,96 ± 0,47	11,92 ± 0,16	62,5 ± 0,5	2004 ± 6	43,50 ± 0,12	17,85 ± 0,32	9,91 ± 0,18	69,1 ± 0,5	2062 ± 10
89	31,99 ± 0,09	39,97 ± 0,61	11,23 ± 2,83	60,7 ± 7,2	2002 ± 7	44,03 ± 0,05	17,81 ± 0,30	9,58 ± 2,41	68,7 ± 6,2	2061 ± 9
156	32,01 ± 0,09	39,83 ± 0,50	9,61 ± 4,73	56,6 ± 12,1	2001 ± 8	44,72 ± 0,05	17,38 ± 0,15	8,29 ± 4,08	66,1 ± 10,5	2060 ± 8

RPH	regeneration air					waste air				
	θ [°C]	φ [%]	x [g/kg]	h [kJ/kg]	Vnorm [m³/h]	θ [°C]	φ [%]	x [g/kg]	h [kJ/kg]	Vnorm [m³/h]
24	50,06 ± 0,05	10,52 ± 0,09	6,12 ± 0,07	71,1 ± 0,2	1480 ± 9	35,60 ± 0,05	38,12 ± 0,25	13,96 ± 0,10	71,4 ± 0,3	1449 ± 5
56	50,06 ± 0,05	10,53 ± 0,14	6,12 ± 0,11	71,1 ± 0,3	1493 ± 13	34,17 ± 0,16	38,48 ± 0,29	13,00 ± 0,10	67,5 ± 0,4	1469 ± 7
89	50,07 ± 0,06	10,51 ± 0,16	7,65 ± 1,93	69,9 ± 5,0	1506 ± 7	33,48 ± 0,10	39,06 ± 0,32	11,94 ± 3,00	64,1 ± 7,7	1469 ± 6
156	50,04 ± 0,14	10,24 ± 0,12	6,36 ± 3,13	66,5 ± 8,1	1509 ± 10	33,23 ± 0,06	39,14 ± 0,36	10,12 ± 4,98	59,1 ± 12,8	1471 ± 6

Figures of merit:

RPH	$\Delta x_{amb-sup}$ [g/kg]	RSHI [kJ/g]	η_{dehum} [-]	$\Delta h_{sup-amb}$ [kJ/kg]
24	2,14	6,31	0,40	5,1
56	2,01	6,74	0,38	6,6
89	1,66	8,26	0,33	8,0
156	1,32	10,37	0,30	9,5

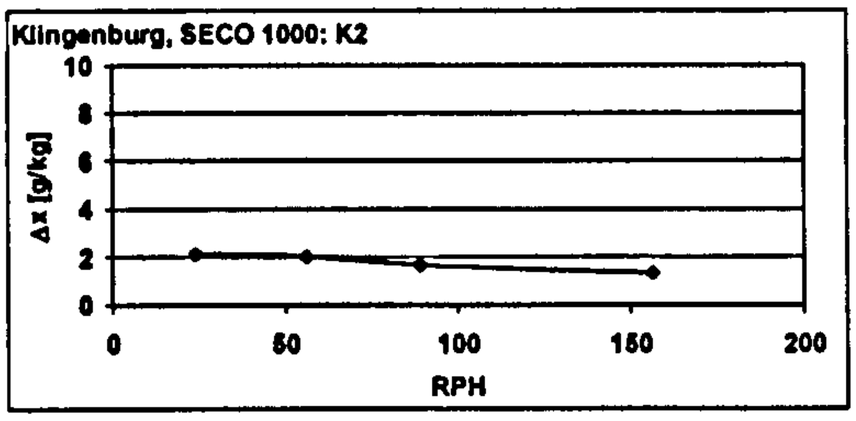

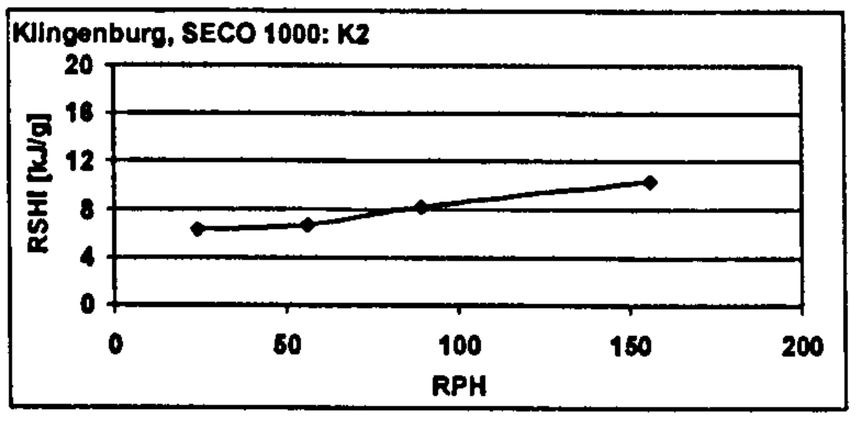

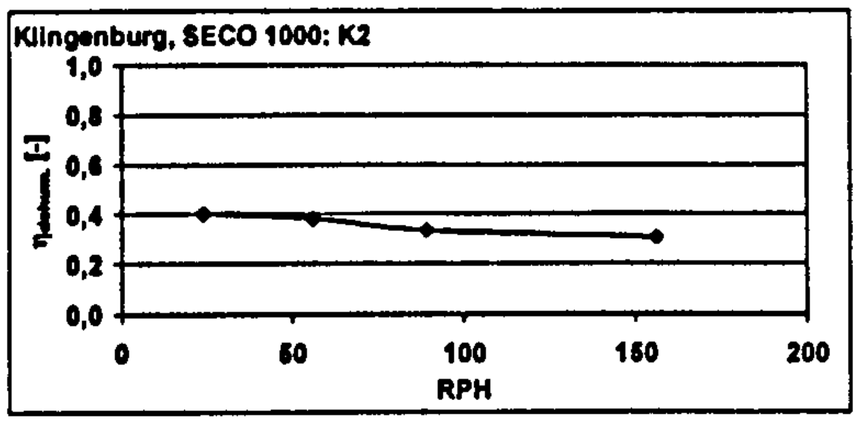

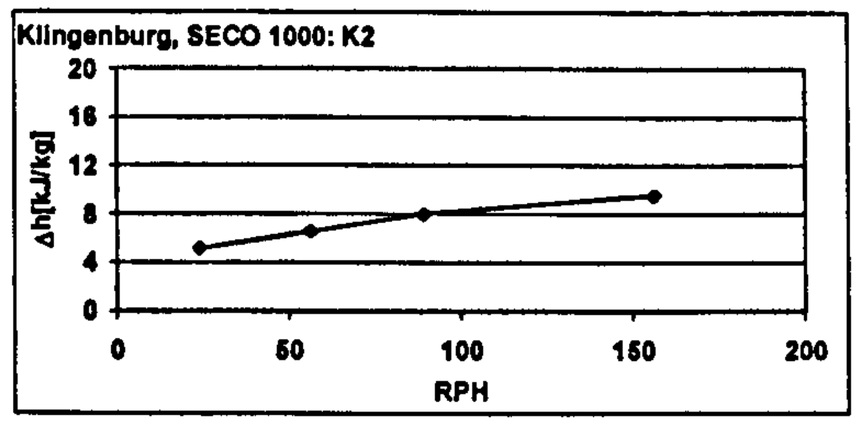

OUTCOMES OF MEASUREMENTS FROM THE DESICCANT WHEEL TEST FACILITY

measurement series K8

Desiccant wheel: **Klingenburg, SECO 1000**

Set values:

	temperature [°C]	rel humidity [%]	vol flow [m³/h]
process airflow	32	40	2000 $l_{20°C}$
reg airflow	45	10	1500 $l_{20°C}$

$V_{reg} : V_{process}$ 0,75

Measured values:

RPH	ambient air					supply air				
	θ [°Y]	φ [%]	x [g/kg]	h [kJ/kg]	Vnorm [m³/h]	θ [°Y]	φ [%]	x [g/kg]	h [kJ/kg]	Vnorm [m³/h]
24	31,97 ± 0,05	39,74 ± 0,69	11,85 ± 0,21	62,3 ± 0,5	1991 ± 12	40,95 ± 0,05	20,34 ± 0,35	9 88 ± 0,17	66,4 ± 0,5	2070 ± 15
56	31,94 ± 0,06	39,92 ± 0,61	11,89 ± 0,20	62,4 ± 0,5	2001 ± 12	41,47 ± 0,05	20,00 ± 0,34	9,98 ± 0,17	67,2 ± 0,5	2078 ± 12
89	31,96 ± 0,05	39,51 ± 0,63	11,77 ± 0,19	62,1 ± 0,5	2008 ± 7	41,70 ± 0,03	19,57 ± 0,25	9,89 ± 0,12	67,2 ± 0,3	2086 ± 7
156	32 04 ± 0 06	39,57 ± 0 60	11,84 ± 0 18	62 3 ± 0,5	1998 ± 8	42,00 ± 0,01	19,07 ± 0,15	9,79 ± 0,08	67,2 ± 0,2	2075 ± 9

RPH	regeneration air					waste air				
	θ [°Y]	φ [%]	x [g/kg]	h [kJ/kg]	Vnorm [m³/h]	θ [°Y]	φ [%]	x [g/kg]	h [kJ/kg]	Vnorm [m³/h]
24	45,45 ± 0,05	11,76 ± 0,06	7,18 ± 0 04	64,0 ± 0,1	1509 ± 9	33,76 ± 0,05	36 89 ± 0,09	12,17 ± 0 04	64,9 ± 0,2	1506 ± 5
56	45,43 ± 0,03	12,14 ± 0,14	7,41 ± 0,09	64,6 ± 0,3	1501 ± 11	33,02 ± 0,03	38,15 ± 0,21	12,07 ± 0,07	63,9 ± 0,2	1514 ± 6
89	45,52 ± 0,02	12,11 ± 0,07	7,43 ± 0,04	64,7 ± 0,1	1501 ± 9	32,89 ± 0,05	38,07 ± 0,23	11,96 ± 0,08	63,5 ± 0,2	1514 ± 4
156	45,44 ± 0,04	11,87 ± 0,07	7,25 ± 0,04	64 2 ± 0,1	1505 ± 9	33,16 ± 0,05	37,97 ± 0,36	12,11 ± 0,12	64,2 ± 0,3	1511 ± 4

Figures of merit:

RPH	$\Delta x_{amb-sup}$ [g/kg]	RSHI [kJ/g]	η_{dehum} [-]	$\Delta h_{sup-amb}$ [kJ/kg]
24	1,97	5,22	0,41	4,1
56	1,90	5,35	0,40	4,8
89	1,89	5,41	0,40	5,1
156	2,06	4,94	0,43	4,9

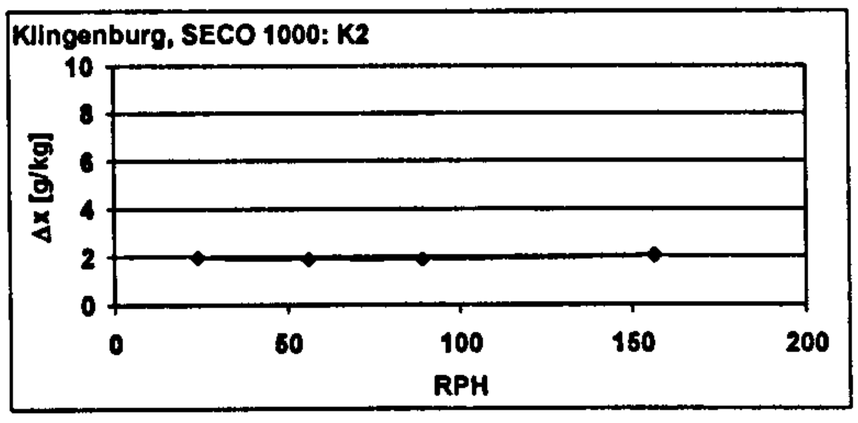

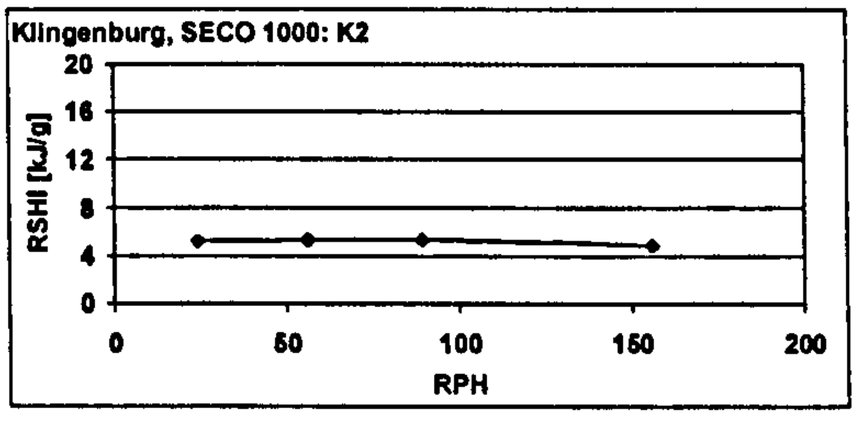

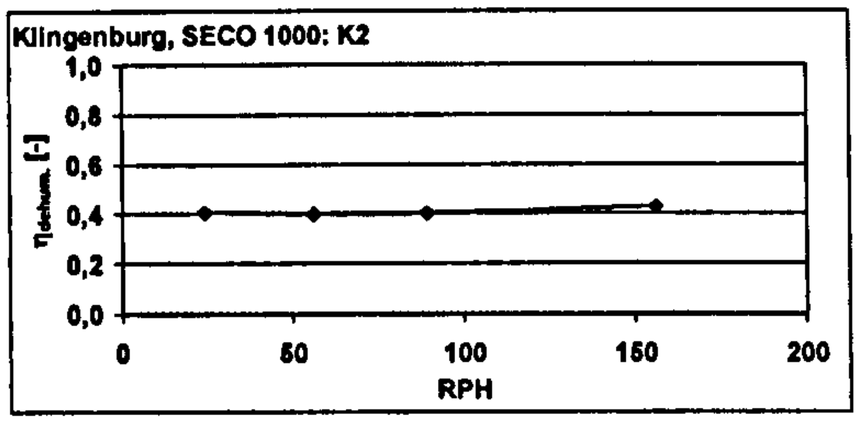

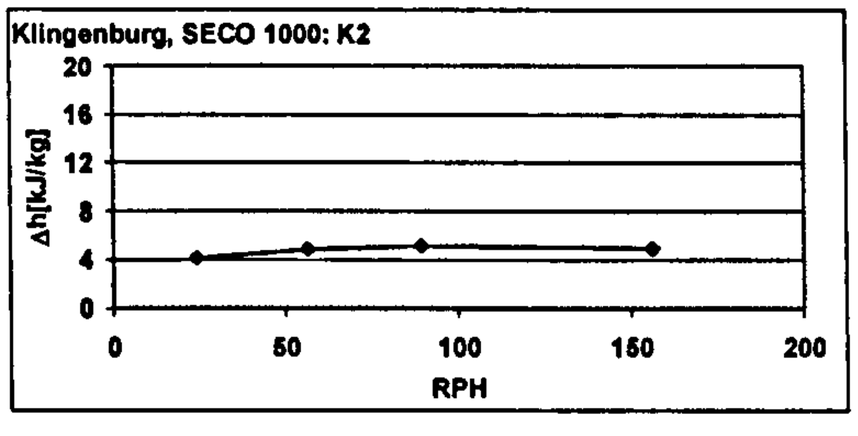

APPENDIX A

OUTCOMES OF MEASUREMENTS FROM THE DESICCANT WHEEL TEST FACILITY

measurement series K9

Desiccant wheel: **Klingenburg, SECO 1000**

Set values:

	temperature [°C]	rel humidity [%]	vol flow [m³/h]
process airflow	32	40	2000 $\|_{20°C}$
reg airflow	60	10	1500 $\|_{20°C}$

$V_{reg} : V_{process}$ 0,75

Measured values:

RPH	ambient air					supply air				
	θ [°X]	φ [%]	x [g/kg]	h [kJ/kg]	Vnorm [m³/h]	θ [°X]	φ [%]	x [g/kg]	h [kJ/kg]	Vnorm [m³/h]
24	32,00 ± 0,05	39,67 ± 0,35	11,85 ± 0,11	62,3 ± 0,3	2001 ± 4	43,59 ± 0,06	16,48 ± 0,15	9,18 ± 0 09	67,3 ± 0,3	2031 ± 8
56	32,02 ± 0,07	39,74 ± 0,49	11,88 ± 0,16	62,4 ± 0,4	1991 ± 4	46,61 ± 0,03	14,72 ± 0,27	9,58 ± 0,17	71,4 ± 0,5	2011 ± 11
89	31,98 ± 0,10	39,90 ± 0,50	11,91 ± 0,21	62,5 ± 0,6	1983 ± 4	49,53 ± 0,05	14,04 ± 0,19	10,59 ± 0,15	77,0 ± 0,4	2000 ± 6
156	31,94 ± 0,05	39,40 ± 0,45	11,73 ± 0,13	62 0 ± 0,3	1986 ± 5	51,29 ± 0,00	15 12 ± 0,12	12,46 ± 0,10	83,7 ± 0 3	2011 ± 6

RPH	regeneration air					waste air				
	θ [°X]	φ [%]	x [g/kg]	h [kJ/kg]	Vnorm [m³/h]	θ [°X]	φ [%]	x [g/kg]	h [kJ/kg]	Vnorm [m³/h]
24	60,33 ± 0,01	10,29 ± 0,21	13,06 ± 0,27	94,4 ± 0,7	1491 ± 22	41,14 ± 0,11	39,19 ± 0,35	19,52 ± 0,15	91,4 ± 0,4	1529 ± 4
56	60,24 ± 0,01	10,42 ± 0,31	13,17 ± 0,40	94,6 ± 1,0	1514 ± 15	38,30 ± 0,07	40,14 ± 0,56	17,12 ± 0,23	82,3 ± 0,6	1548 ± 4
89	60,15 ± 0,05	10,64 ± 0,24	13,40 ± 0,32	95,1 ± 0,8	1521 ± 12	36,50 ± 0,10	39,08 ± 0,46	15,07 ± 0,17	75,2 ± 0,5	1548 ± 5
156	60,32 ± 0,01	10 81 ± 0 18	13,72 ± 0,24	96,1 ± 0 6	1511 ± 8	34,01 ± 0,00	39 83 ± 0,30	13,35 ± 0,10	68 2 ± 0,3	1532 ± 4

Figures of merit:

RPH	$\Delta x_{amb-sup}$ [g/kg]	RSHI [kJ/g]	η_{dehum} [-]	$\Delta h_{sup-amb}$ [kJ/kg]
24	2,67	7,95	0,50	4,9
56	2,31	9,38	0,44	8,9
89	1,32	16,45	0,25	14,5
156	-0,75			21,7

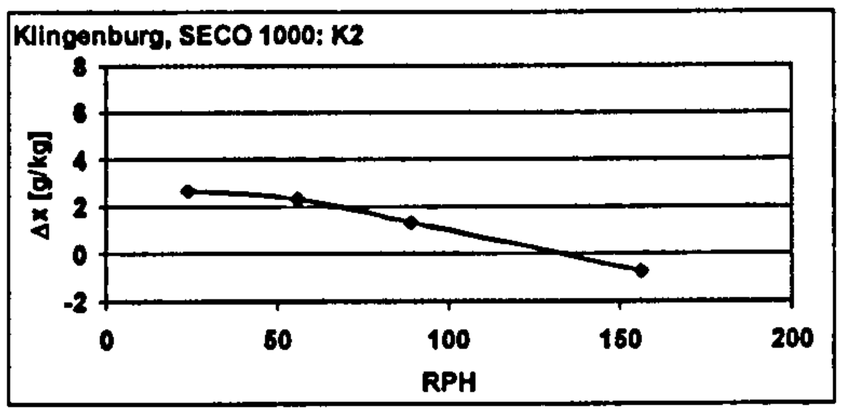

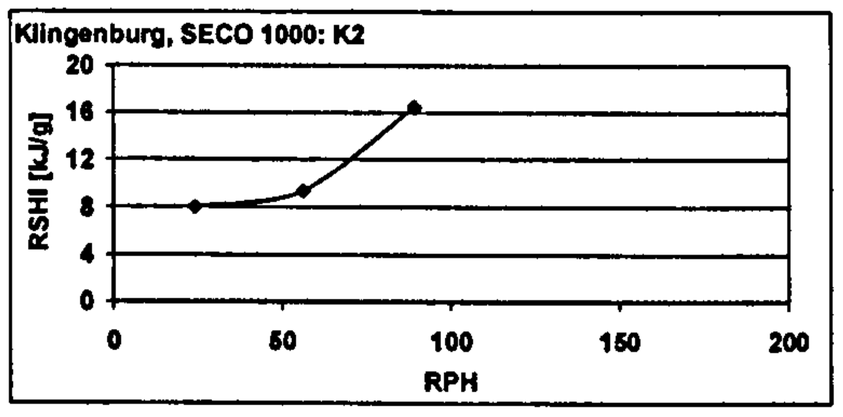

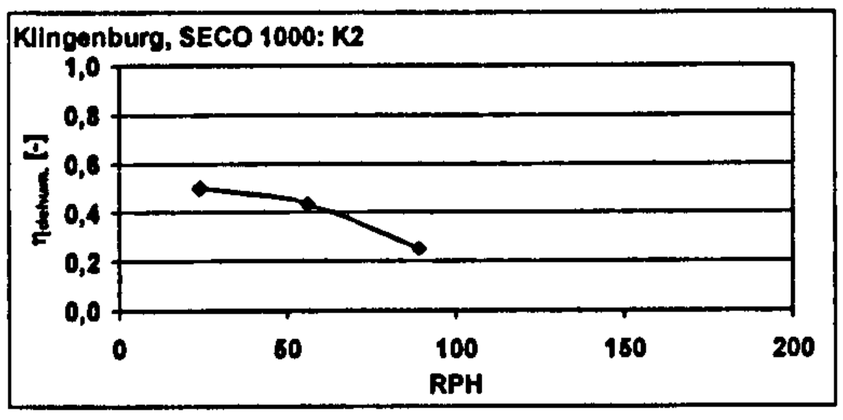

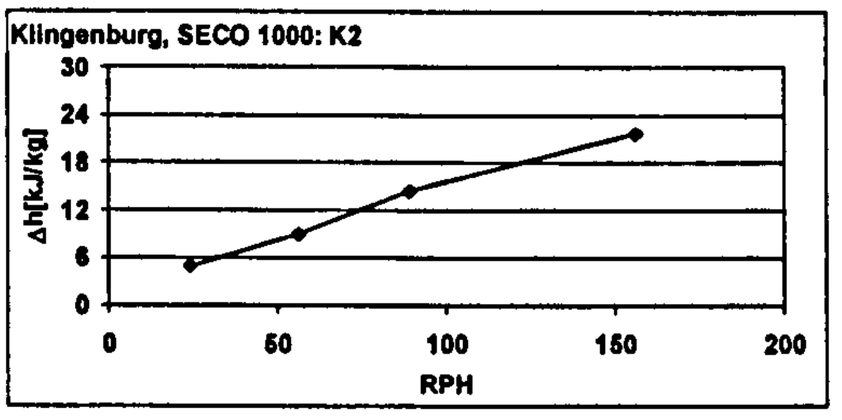

OUTCOMES OF MEASUREMENTS FROM THE DESICCANT WHEEL TEST FACILITY

measurement series K10

Desiccant wheel: **Klingenburg, SECO 1000**

Set values:

	temperature [°C]	rel humidity [%]	vol flow [m³/h]
process airflow	32	40	2000 $l_{20°C}$
reg. airflow	60	20	1500 $l_{20°C}$

$V_{reg} : V_{process}$ 0,75

Measured values:

RPH	ambient air				
	θ [°Y]	φ [%]	x [g/kg]	h [kJ/kg]	Vnorm [m³/h]
24	31,95 ± 0,03	39,32 ± 0,50	11,71 ± 0,17	61,9 ± 0,4	2021 ± 7
56	32,04 ± 0,06	39,62 ± 0,48	11,86 ± 0,14	62,4 ± 0,3	2004 ± 4
89	32,00 ± 0,10	39,84 ± 0,63	11,90 ± 0,24	62,4 ± 0,7	1992 ± 9
156	32,02 ± 0,05	39,94 ± 0,41	11,95 ± 0,14	62,6 ± 0,4	1973 ± 5

RPH	supply air				
	θ [°Y]	φ [%]	x [g/kg]	h [kJ/kg]	Vnorm [m³/h]
24	38,17 ± 0,04	22,41 ± 0,36	9 38 ± 0,14	62,3 ± 0,4	2101 ± 9
56	41,44 ± 0,05	20,27 ± 0,27	10,10 ± 0,12	67,5 ± 0,3	2088 ± 7
89	44,12 ± 0,05	21,87 ± 0,35	12,59 ± 0,20	76,6 ± 0,5	2073 ± 6
156	49,40 ± 0,04	23 30 ± 0,16	17,66 ± 0,14	95,1 ± 0,4	2035 ± 6

RPH	regeneration air				
	θ [°Y]	φ [%]	x [g/kg]	h [kJ/kg]	Vnorm [m³/h]
24	59 83 ± 0,07	19,35 ± 0,20	24,42 ± 0,26	123,5 ± 0,7	1469 ± 9
56	60,37 ± 0,05	19,11 ± 0,18	24,72 ± 0,24	124,9 ± 0,6	1498 ± 9
89	60,04 ± 0,01	20,15 ± 0,23	25,72 ± 0,31	127,2 ± 0,8	1506 ± 8
156	60 05 ± 0,00	20,26 ± 0,23	25 88 ± 0,30	127,6 ± 0 8	1522 ± 7

RPH	waste air				
	θ [°Y]	φ [°₀]	x [g/kg]	h [kJ/kg]	Vnorm [m³/h]
24	46,38 ± 0,05	45,94 ± 0,57	30,52 ± 0,39	125,3 ± 1,0	1473 ± 3
56	43,27 ± 0,07	48,77 ± 0,68	27,49 ± 0,39	114,2 ± 1,0	1484 ± 3
89	38,90 ± 0,05	49,39 ± 0,82	21,91 ± 0,36	95,2 ± 0,9	1503 ± 4
156	34,39 ± 0,04	45,23 ± 0,38	15,54 ± 0,15	74,2 ± 0 4	1528 ± 4

Figures of merit:

RPH	$\Delta x_{amb-sup}$ [g/kg]	RSHI [kJ/g]	η_{dehum} [-]	$\Delta h_{sup-amb}$ [kJ/kg]
24	2,33	8,87	0,80	0,4
56	1,76	12,15	0,58	5,1
89	-0,69			14,2
156	-5,71			32,5

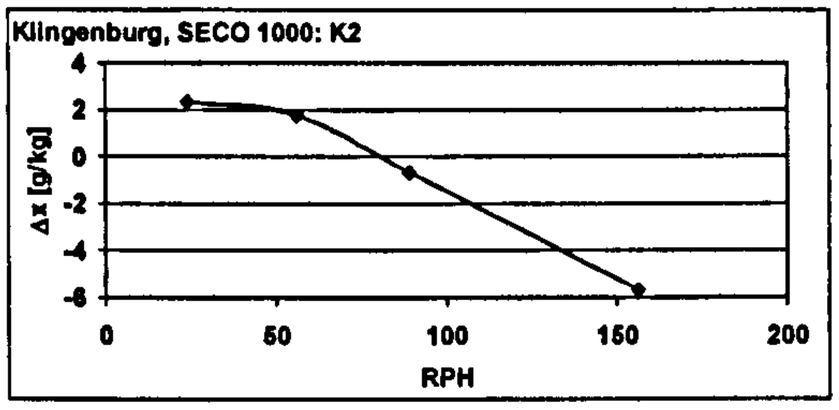

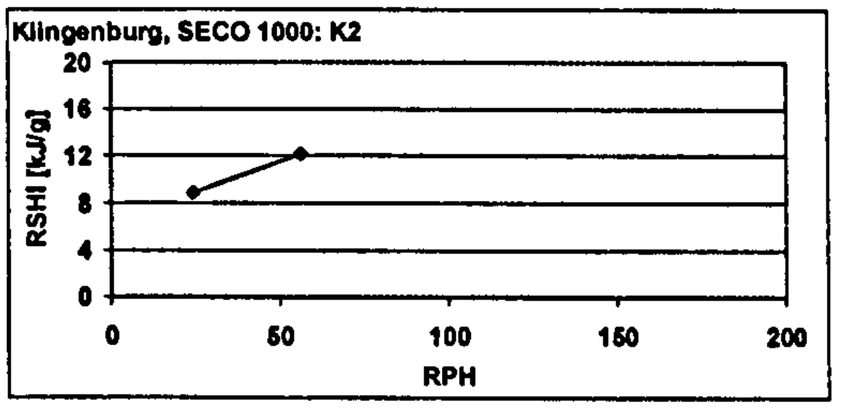

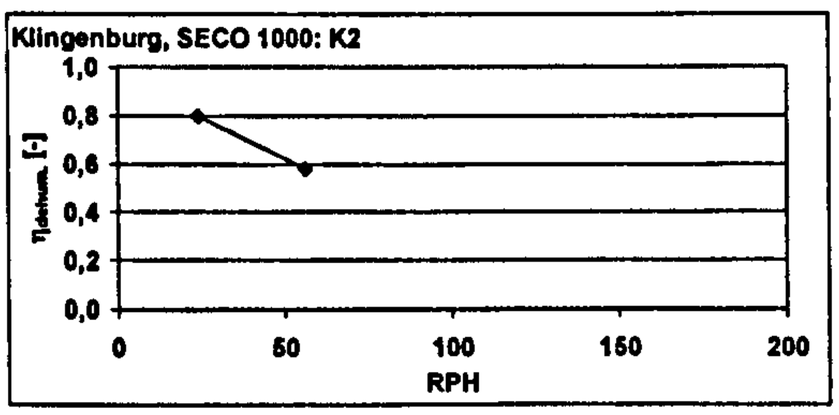

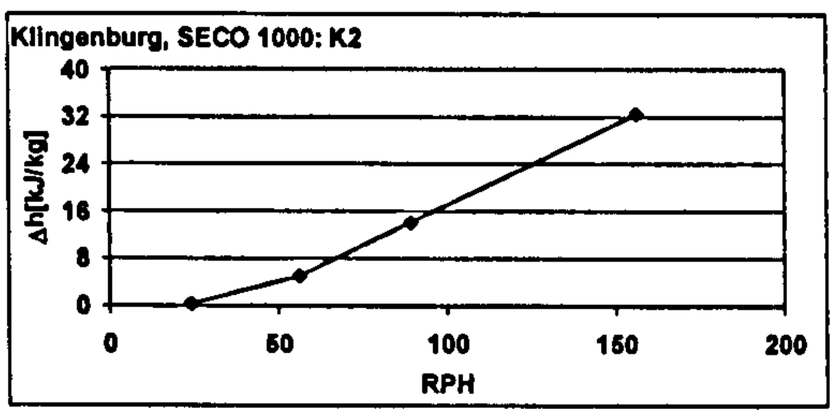

APPENDIX A

OUTCOMES OF MEASUREMENTS FROM THE DESICCANT WHEEL TEST FACILITY

measurement series K11

Desiccant wheel: **Klingenburg, SECO 1000**

Set values:

	temperature [°C]	rel humidity [%]	vol flow [m³/h]
process airflow	32	60	2000 $l_{20°C}$
reg airflow	60	-	1500 $l_{20°C}$

$V_{reg} : V_{process}$ 0,75

Measured values:

RPH	ambient air					supply air				
	θ [°K]	φ [%]	x [g/kg]	h [kJ/kg]	Vnorm [m³/h]	θ [°K]	φ [%]	x [g/kg]	h [kJ/kg]	Vnorm [m³/h]
24	32,00 ± 0,08	59,65 ± 0,63	17,99 ± 0,19	78,0 ± 0,5	2012 ± 5	48,07 ± 0,07	20,36 ± 0,37	14,38 ± 0,26	85,3 ± 0,7	2096 ± 11
56	31,97 ± 0,09	59,78 ± 0,55	18,01 ± 0,20	78,0 ± 0,6	2001 ± 6	49,74 ± 0,06	18,84 ± 0,28	14,44 ± 0,22	87,2 ± 0,6	2067 ± 11
89	32,02 ± 0,07	59,72 ± 0,47	18,03 ± 0,17	78,2 ± 0,5	1991 ± 7	50,23 ± 0,04	19,03 ± 0,21	14,97 ± 0,16	89,0 ± 0,4	2084 ± 9
156	32,06 ± 0,06	60,19 ± 0,54	18,22 ± 0,15	78,7 ± 0,4	1992 ± 5	51,61 ± 0,00	17,98 ± 0,17	15,13 ± 0,15	90,9 ± 0,4	2079 ± 8

RPH	regeneration air					waste air				
	θ [°K]	φ [%]	x [g/kg]	h [kJ/kg]	Vnorm [m³/h]	θ [°K]	φ [%]	x [g/kg]	h [kJ/kg]	Vnorm [m³/h]
24	60,09 ± 0,01	7,26 ± 0,02	9,66 ± 0,03	85,3 ± 0,1	1505 ± 12	36,94 ± 0,06	54,43 ± 0,26	21,72 ± 0,08	92,7 ± 0,2	1522 ± 4
56	60,03 ± 0,05	7,35 ± 0,03	9,76 ± 0,02	85,5 ± 0,1	1498 ± 12	35,73 ± 0,00	55,23 ± 0,14	20,58 ± 0,05	88,5 ± 0,1	1527 ± 3
89	60,34 ± 0,03	7,18 ± 0,03	9,66 ± 0,04	85,6 ± 0,1	1465 ± 12	34,35 ± 0,04	56,87 ± 0,29	19,62 ± 0,11	84,6 ± 0,3	1482 ± 5
156	59,73 ± 0,00	6,88 ± 0,01	9,00 ± 0,02	83,2 ± 0,0	1482 ± 13	34,33 ± 0,01	55,42 ± 0,41	19,08 ± 0,15	83,2 ± 0,4	1492 ± 3

Figures of merit:

RPH	$\Delta x_{amb-sup}$ [g/kg]	RSHI [kJ/g]	η_{dehum} [-]	$\Delta h_{sup-amb}$ [kJ/kg]
24	3,61	5,86	0,37	7,3
56	3,56	5,94	0,37	9,1
89	3,07	6,84	0,31	10,9
156	3,09	6,71	0,31	12,2

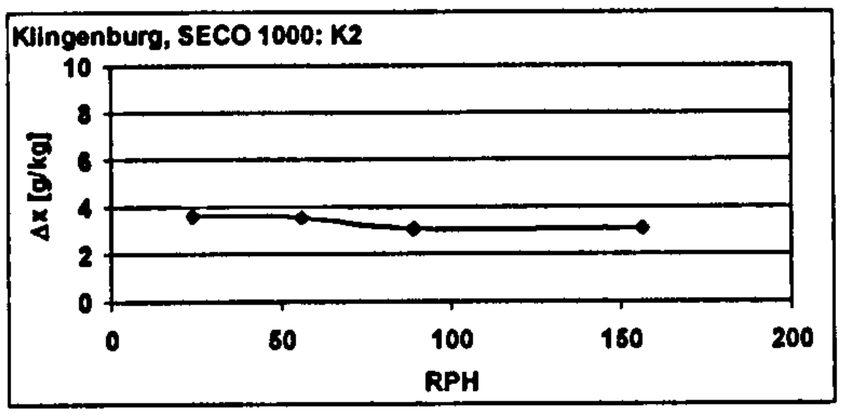

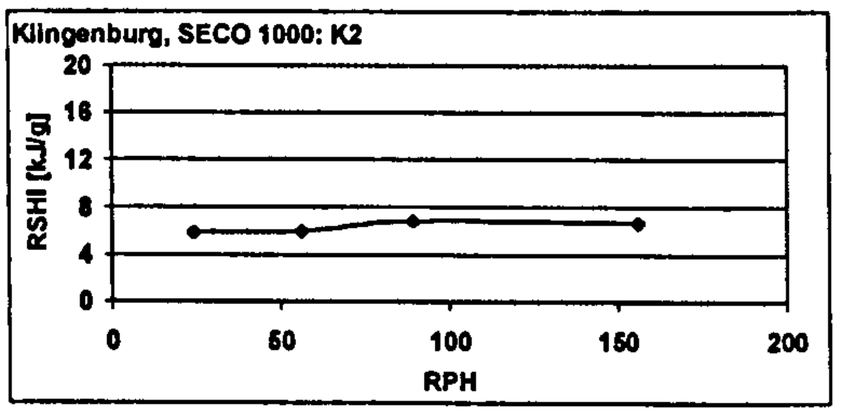

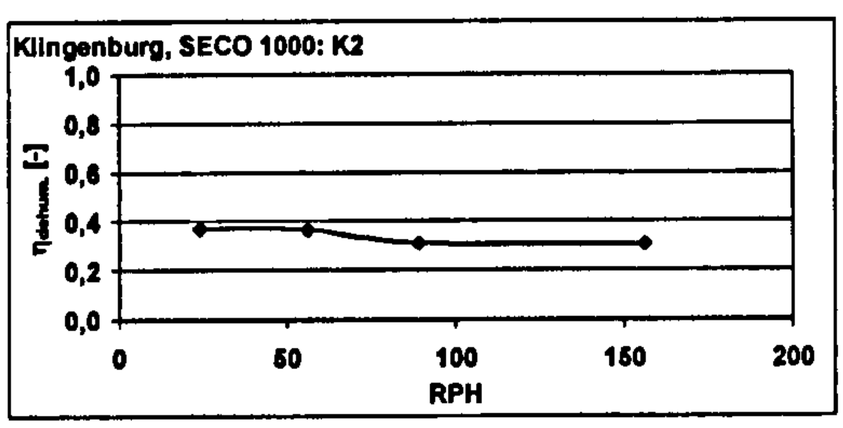

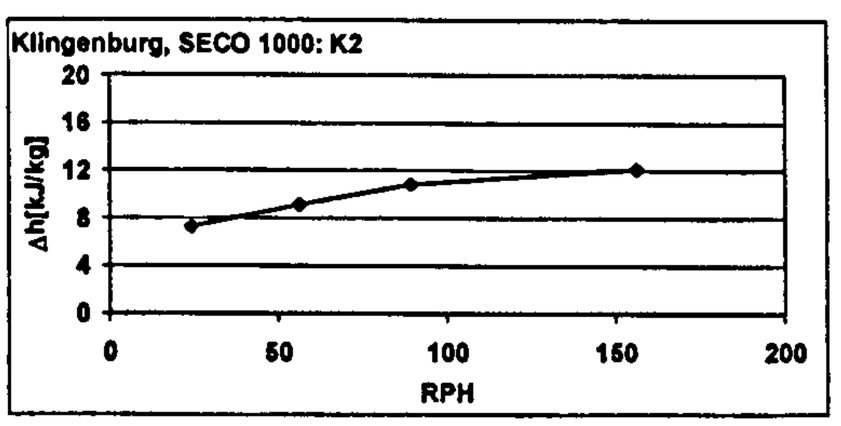

OUTCOMES OF MEASUREMENTS FROM THE DESICCANT WHEEL TEST FACILITY

measurement series K12

Desiccant wheel: **Klingenburg, SECO 1000**

Set values:

	temperature [°C]	rel humidity [%]	vol flow [m³/h]
process airflow	28	60	2000 $l_{20°C}$
reg airflow	60	-	1500 $l_{20°C}$

$V_{reg} : V_{process}$ 0,75

Measured values:

RPH	ambient air					supply air				
	θ [°Y]	*φ [%]*	*x [g/kg]*	*h [kJ/kg]*	*Vnorm [m³/h]*	*θ [°Y]*	*φ [%]*	*x [g/kg]*	*h [kJ/kg]*	*Vnorm [m³/h]*
24	28,07 ± 0,06	59,59 ± 0,70	14,26 ± 0,20	64,5 ± 0,5	2030 ± 6	43,95 ± 0,08	16,49 ± 0,31	10,51 ± 0,16	71,1 ± 0,4	2131 ± 12
56	28,00 ± 0,07	59,71 ± 0,51	14,23 ± 0,13	64,3 ± 0,4	2018 ± 7	46,12 ± 0,09	16,69 ± 0,27	10,74 ± 0,16	73,9 ± 0,4	2117 ± 8
89	28,00 ± 0,06	59,47 ± 0,60	14,17 ± 0,14	64,1 ± 0,4	2017 ± 6	48,15 ± 0,05	16,15 ± 0,19	11,39 ± 0,14	77,6 ± 0,4	2109 ± 8
156	27,95 ± 0,12	59,55 ± 0,61	14,15 ± 0,15	64,0 ± 0,4	2013 ± 6	50,12 ± 0,03	16,33 ± 0,18	12,72 ± 0,14	83,1 ± 0,4	2095 ± 7

RPH	regeneration air					waste air				
	θ [°Y]	*φ [%]*	*x [g/kg]*	*h [kJ/kg]*	*Vnorm [m³/h]*	*θ [°Y]*	*φ [%]*	*x [g/kg]*	*h [kJ/kg]*	*Vnorm [m³/h]*
24	60,08 ± 0,02	6,30 ± 0,02	8,36 ± 0,03	81,9 ± 0,1	1513 ± 11	36,06 ± 0,06	52,82 ± 0,37	20,03 ± 0,09	87,5 ± 0,2	1524 ± 4
56	60,06 ± 0,03	6,52 ± 0,02	8,66 ± 0,02	82,6 ± 0,1	1509 ± 14	33,72 ± 0,03	55,29 ± 0,25	18,38 ± 0,06	80,6 ± 0,2	1534 ± 5
89	59,88 ± 0,00	6,77 ± 0,01	8,91 ± 0,02	83,1 ± 0,0	1519 ± 14	32,19 ± 0,05	54,68 ± 0,32	16,63 ± 0,09	74,7 ± 0,2	1541 ± 5
156	59,79 ± 0,01	7,05 ± 0,02	9,24 ± 0,02	83,9 ± 0,1	1519 ± 10	31,29 ± 0,05	53,89 ± 0,58	15,55 ± 0,18	71,1 ± 0,5	1550 ± 4

Figures of merit:

RPH	$\Delta x_{amb-sup}$ [g/kg]	RSHI [kJ/g]	η_{dehum} [-]	$\Delta h_{sup-amb}$ [kJ/kg]
24	3,75	6,40	0,42	6,6
56	3,49	6,91	0,40	9,6
89	2,78	8,71	0,32	13,5
156	1,43	16,93	0,17	19,0

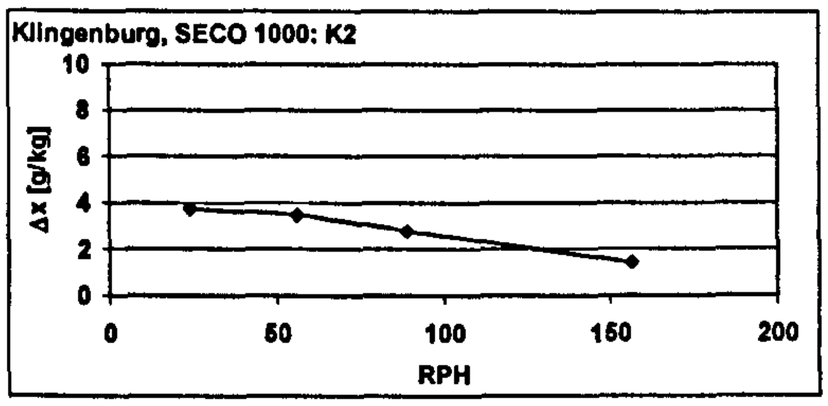

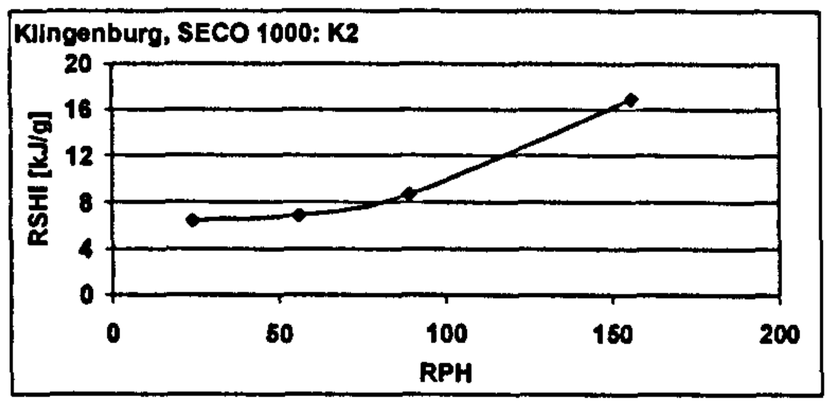

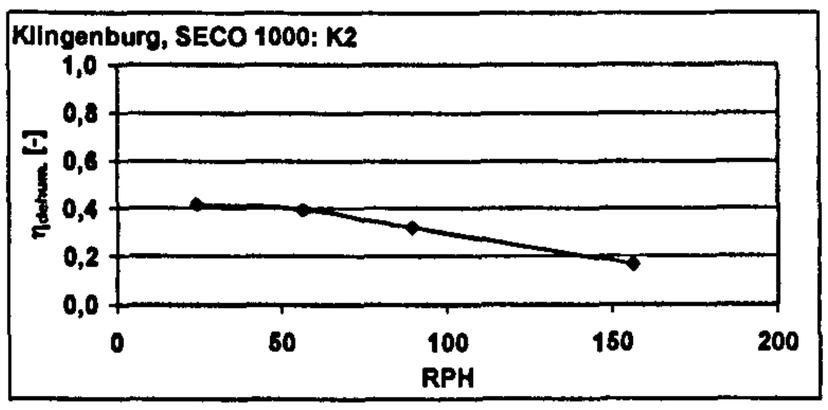

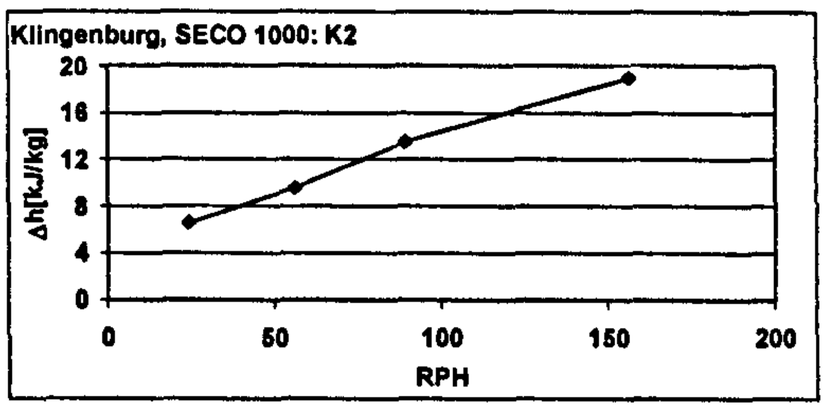

APPENDIX A

OUTCOMES OF MEASUREMENTS FROM THE DESICCANT WHEEL TEST FACILITY

measurement series K13

Desiccant wheel: **Klingenburg, SECO 1000**

Set values:

	temperature [°C]	rel. humidity [%]	vol. flow [m³/h]
process airflow	32	60	1500 $l_{20°C}$
reg. airflow	60	-	1125 $l_{20°C}$

$V_{reg} : V_{process}$ 0,75

Measured values:

RPH	ambient air					supply air				
	θ [°Y]	φ [%]	x [g/kg]	h [kJ/kg]	Vnorm [m³/h]	θ [°Y]	φ [%]	x [g/kg]	h [kJ/kg]	Vnorm [m³/h]
24	32,06 ± 0,04	59,70 ± 0,42	18,07 ± 0,14	78,3 ± 0,4	1534 ± 6	48,64 ± 0,07	20,24 ± 0,15	14,70 ± 0,14	66,7 ± 0,4	1624 ± 10
56	31,98 ± 0,07	59,57 ± 0,82	17,95 ± 0,24	77,9 ± 0,6	1526 ± 10	50,09 ± 0,04	18,97 ± 0,33	14,82 ± 0,25	68,5 ± 0,6	1610 ± 10
89	32,04 ± 0,05	60,06 ± 0,69	18,17 ± 0,21	78,5 ± 0,5	1519 ± 6	51,11 ± 0,02	18,64 ± 0,21	15,31 ± 0,17	90,8 ± 0,4	1600 ± 8
156	31,96 ± 0,08	59,90 ± 0,55	18,03 ± 0,17	78,1 ± 0,5	1527 ± 6	52,01 ± 0,06	17,84 ± 0,08	15,31 ± 0,07	91,8 ± 0,2	1599 ± 9

RPH	regeneration air					waste air				
	θ [°Y]	φ [%]	x [g/kg]	h [kJ/kg]	Vnorm [m³/h]	θ [°Y]	φ [%]	x [g/kg]	h [kJ/kg]	Vnorm [m³/h]
24	60,19 ± 0,03	7,16 ± 0,01	9,56 ± 0,01	85,1 ± 0,1	1128 ± 15	35,78 ± 0,05	59,41 ± 0,18	22,26 ± 0,09	92,9 ± 0,3	1102 ± 4
56	60,00 ± 0,00	7,28 ± 0,03	9,64 ± 0,04	85,2 ± 0,1	1130 ± 11	34,54 ± 0,04	58,64 ± 0,30	20,47 ± 0,12	87,0 ± 0,3	1110 ± 4
89	60,02 ± 0,02	7,24 ± 0,03	9,60 ± 0,04	85,1 ± 0,1	1125 ± 15	34,21 ± 0,00	58,67 ± 0,39	20,10 ± 0,14	85,7 ± 0,4	1114 ± 4
156	60,02 ± 0,00	7,09 ± 0,02	9,40 ± 0,02	84,6 ± 0,1	1126 ± 10	34,33 ± 0,05	58,07 ± 0,46	20,02 ± 0,15	85,6 ± 0,4	1119 ± 3

Figures of merit:

RPH	$\Delta x_{amb-sup}$ [g/kg]	RSHI [kJ/g]	η_{dehum} [-]	$\Delta h_{sup-amb}$ [kJ/kg]
24	3,37	6,19	0,34	8,4
56	3,13	6,67	0,32	10,6
89	2,85	7,31	0,29	12,3
156	2,72	7,68	0,27	13,7

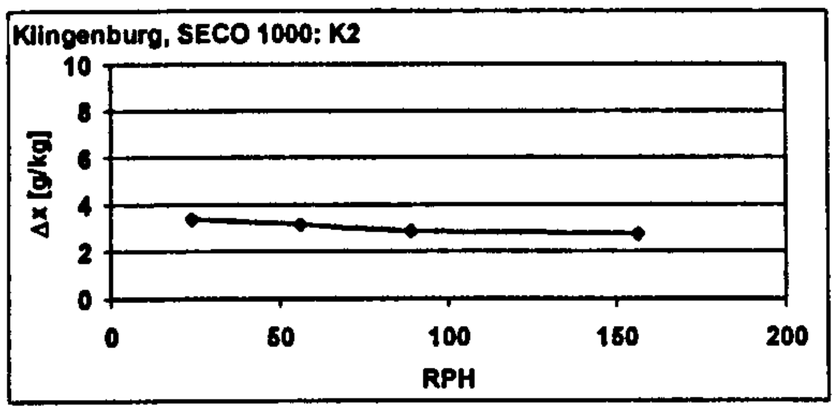

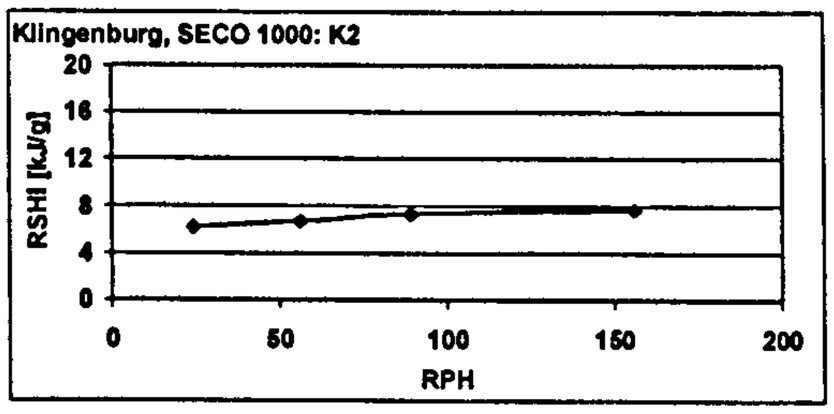

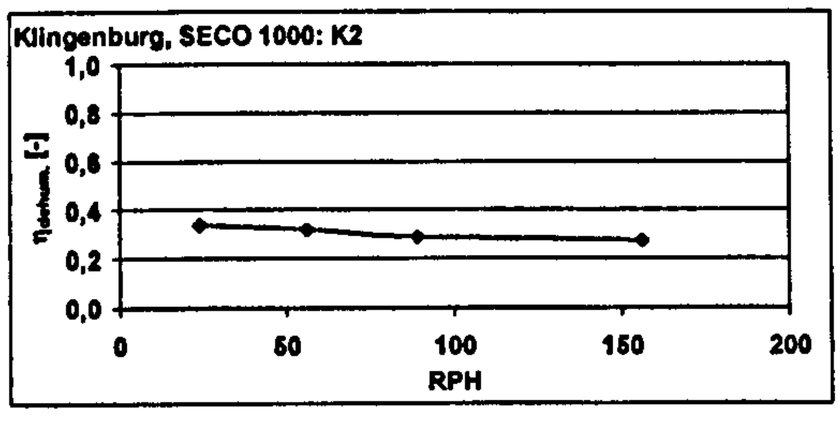

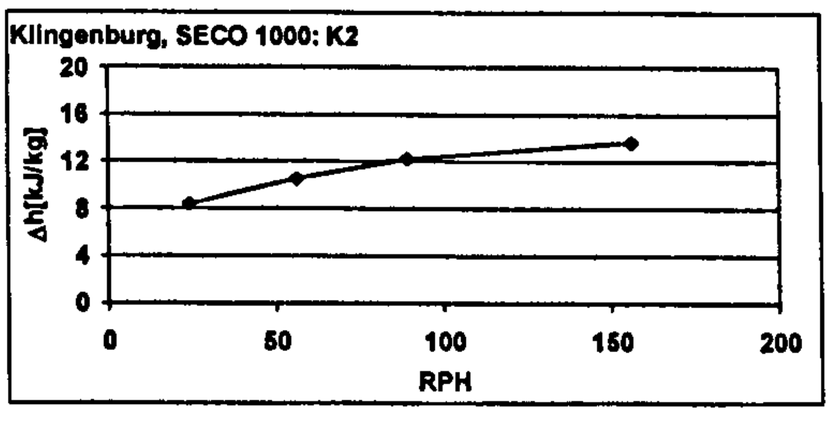

OUTCOMES OF MEASUREMENTS FROM THE DESICCANT WHEEL TEST FACILITY

measurement series K14

Desiccant wheel: **Klingenburg, SECO 1000**

Set values:

	temperature [°C]	rel humidity [%]	vol flow [m³/h]
process airflow	32	40	1500 $l_{20°C}$
reg airflow	60	-	1125 $l_{20°C}$

$V_{reg} : V_{process}$ 0,75

Measured values:

RPH	ambient air					supply air				
	θ [°X]	*φ [%]*	*x [g/kg]*	*h [kJ/kg]*	*Vnorm [m³/h]*	*θ [°X]*	*φ [%]*	*x [g/kg]*	*h [kJ/kg]*	*Vnorm [m³/h]*
24	31,94 ± 0,07	39,93 ± 0,25	11,89 ± 0,07	62,3 ± 0,2	1553 ± 5	45,24 ± 0,04	15,81 ± 0,12	9,59 ± 0,09	70,0 ± 0,2	1650 ± 12
56	31,98 ± 0,07	40,05 ± 0,54	11,95 ± 0,16	62,6 ± 0,4	1541 ± 8	48,07 ± 0,05	14,42 ± 0,21	10,11 ± 0,15	74,2 ± 0,4	1634 ± 10
89	32,00 ± 0,09	40,47 ± 0,30	12,09 ± 0,12	62,9 ± 0,4	1538 ± 6	49,85 ± 0,05	14,52 ± 0,15	11,14 ± 0,11	78,7 ± 0,3	1627 ± 8
156	31,99 ± 0,09	39,56 ± 0,35	11,81 ± 0,13	62,2 ± 0,4	1529 ± 11	50,85 ± 0,07	15,06 ± 0,13	12,15 ± 0,09	82,4 ± 0,2	1615 ± 11

RPH	regeneration air					waste air				
	θ [°X]	*φ [%]*	*x [g/kg]*	*h [kJ/kg]*	*Vnorm [m³/h]*	*θ [°X]*	*φ [%]*	*x [g/kg]*	*h [kJ/kg]*	*Vnorm [m³/h]*
24	59,79 ± 0,02	6,00 ± 0,02	7,85 ± 0,02	80,3 ± 0,1	1124 ± 9	38,43 ± 0,00	40,97 ± 0,28	17,60 ± 0,12	83,7 ± 0,3	1095 ± 3
56	59,88 ± 0,02	6,21 ± 0,01	8,17 ± 0,01	81,2 ± 0,0	1130 ± 7	35,92 ± 0,01	40,98 ± 0,23	15,31 ± 0,09	75,2 ± 0,2	1104 ± 4
89	60,06 ± 0,00	6,42 ± 0,02	8,53 ± 0,02	82,3 ± 0,1	1130 ± 5	34,68 ± 0,05	41,13 ± 0,40	14,33 ± 0,15	71,4 ± 0,4	1110 ± 3
156	59,98 ± 0,01	6,68 ± 0,02	8,83 ± 0,03	83,0 ± 0,1	1144 ± 12	34,16 ± 0,05	40,99 ± 0,45	13,87 ± 0,15	69,7 ± 0,4	1112 ± 4

Figures of merit:

RPH	$\Delta x_{amb-sup}$ [g/kg]	RSHI [kJ/g]	η_{dehum} [-]	$\Delta h_{sup-amb}$ [kJ/kg]
24	2,29	8,86	0,32	7,7
56	1,84	11,18	0,26	11,7
89	0,96	21,74	0,14	15,8
156	-0,34			20,1

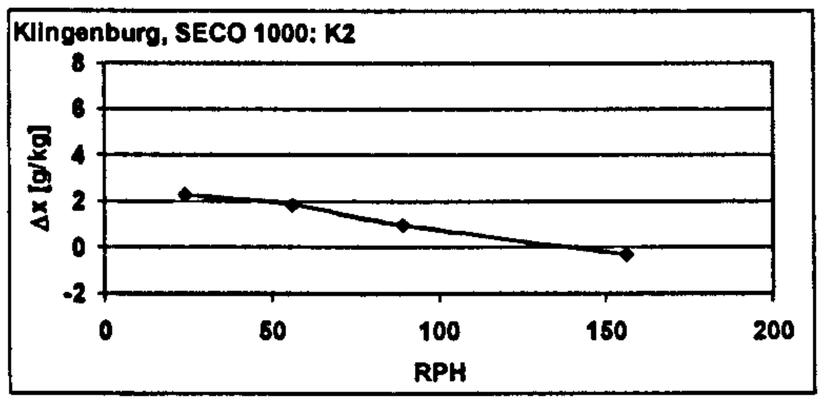

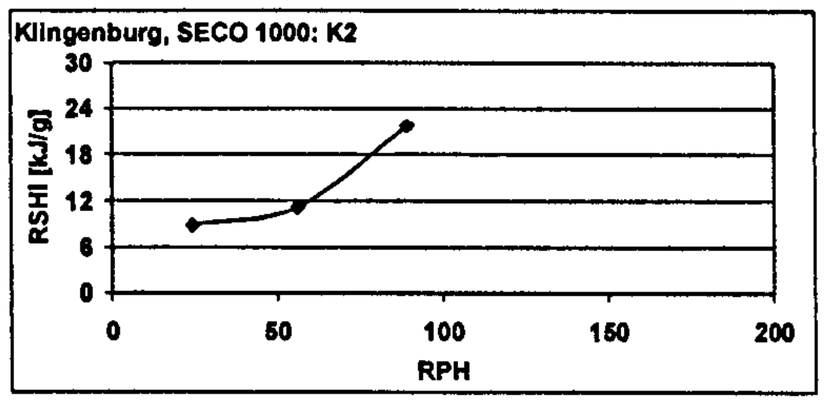

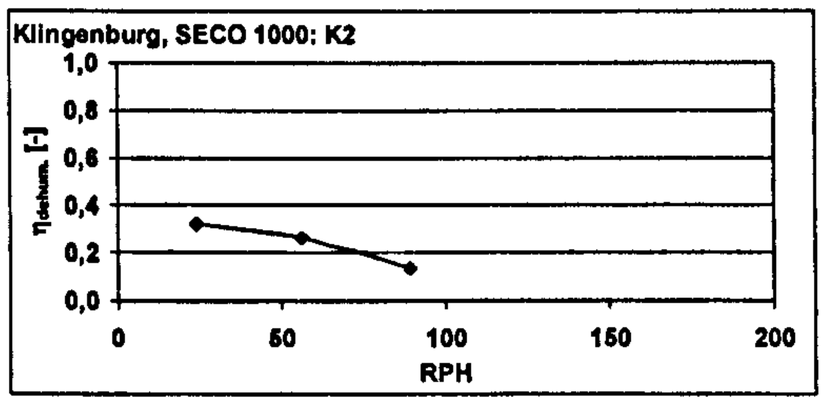

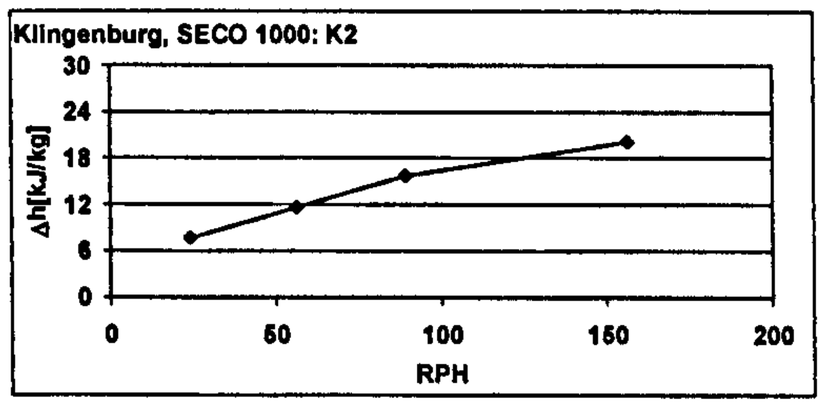

APPENDIX B

COMPARISON MEASUREMENTS / CALCULATION

Comparison of measured values (measurement series H1 to H9, see also Appendix A) from the desiccant wheel test facility at the University of Applied Sciences in Stuttgart and calculated values by the desiccant wheel model.

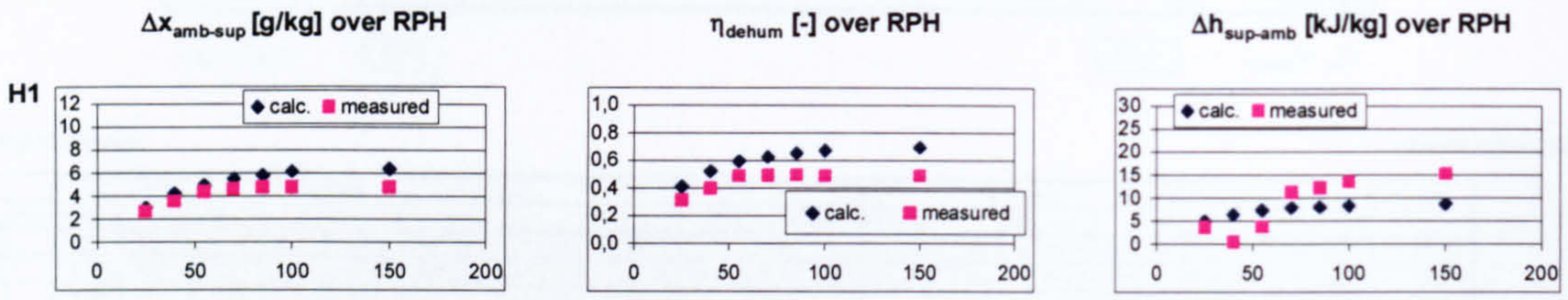

$\Delta x_{amb\text{-}sup}$ [g/kg] over RPH

η_{dehum} [-] over RPH

$\Delta h_{sup\text{-}amb}$ [kJ/kg] over RPH

H7

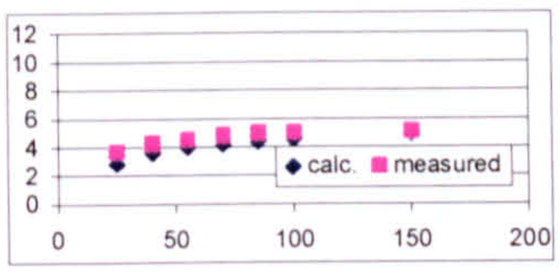

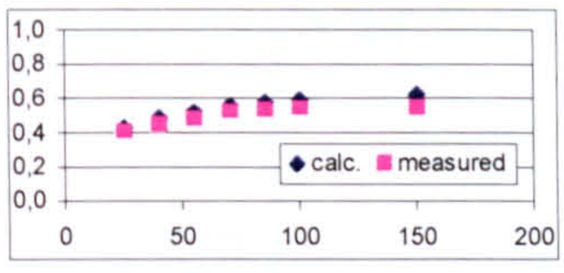

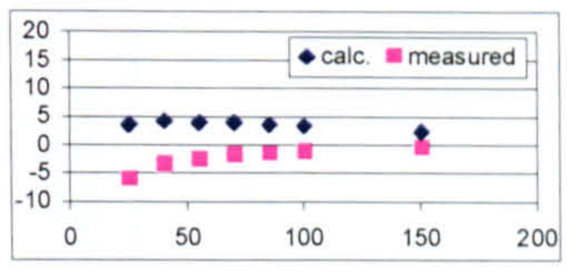

H8

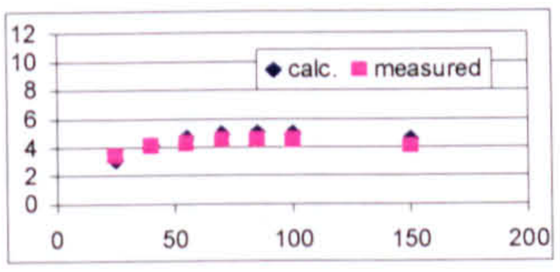

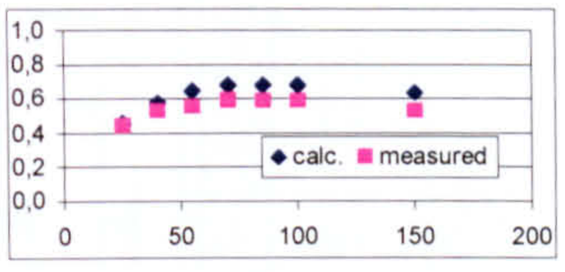

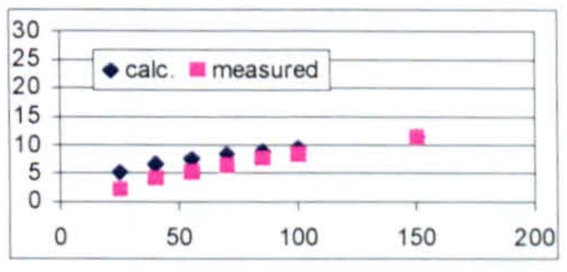

H9

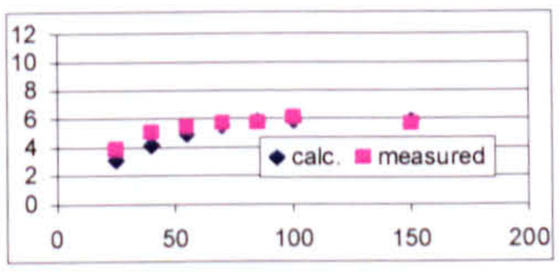

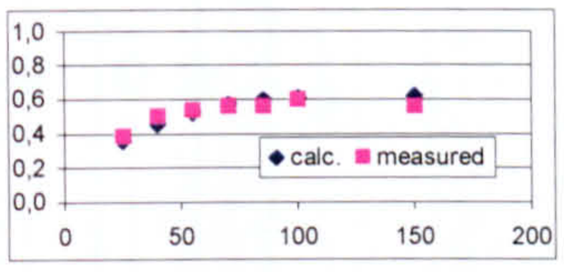

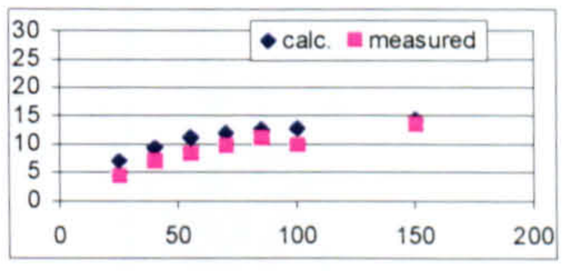

APPENDIX C

MEASUREMENT POINTS AT THE DEC-SYSTEM IN ALTHENGSTETT, GERMANY

Temperature:

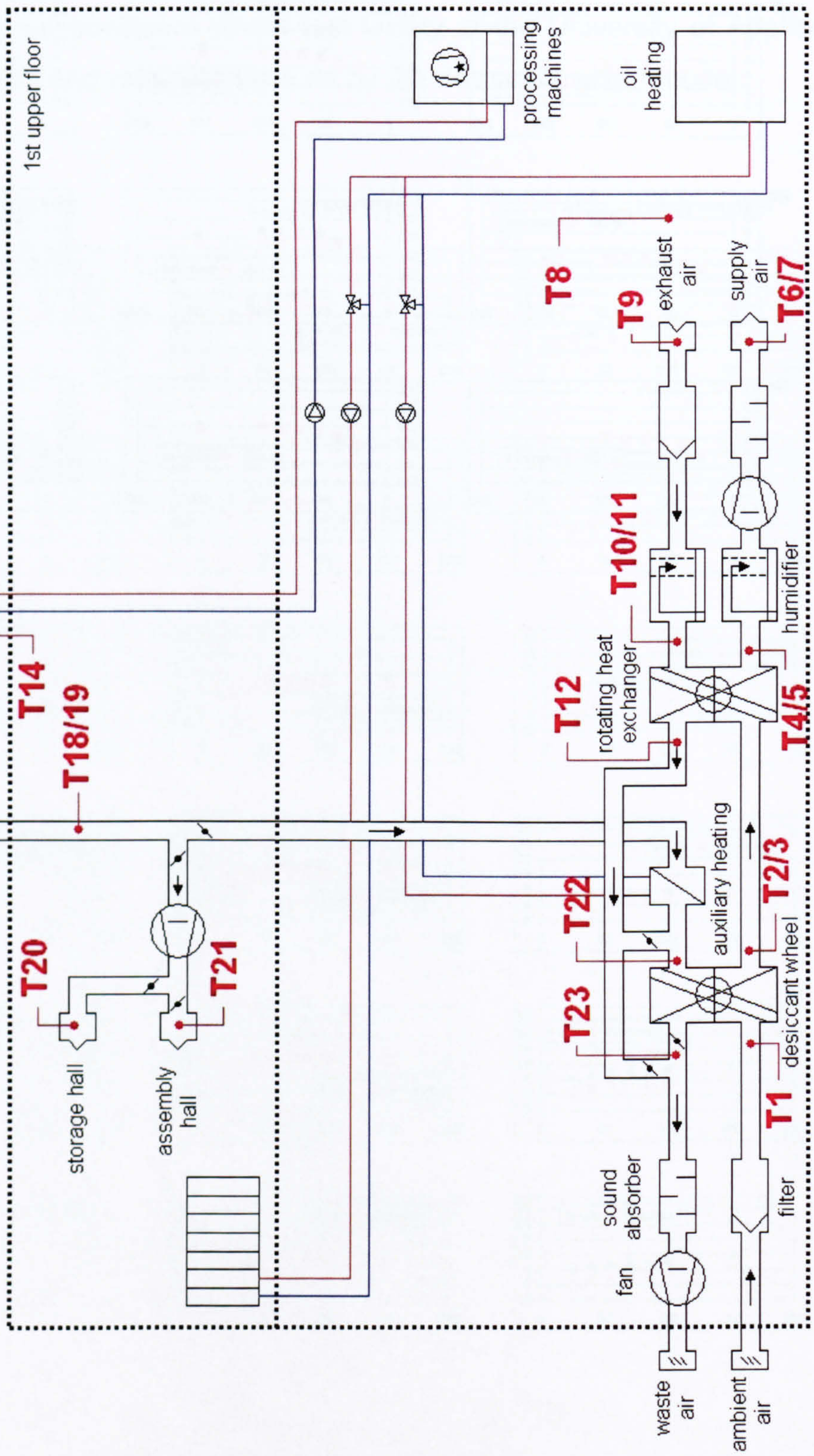

MEASUREMENT POINTS AT THE DEC-SYSTEM IN ALTHENGSTETT, GERMANY

Relative humidity:

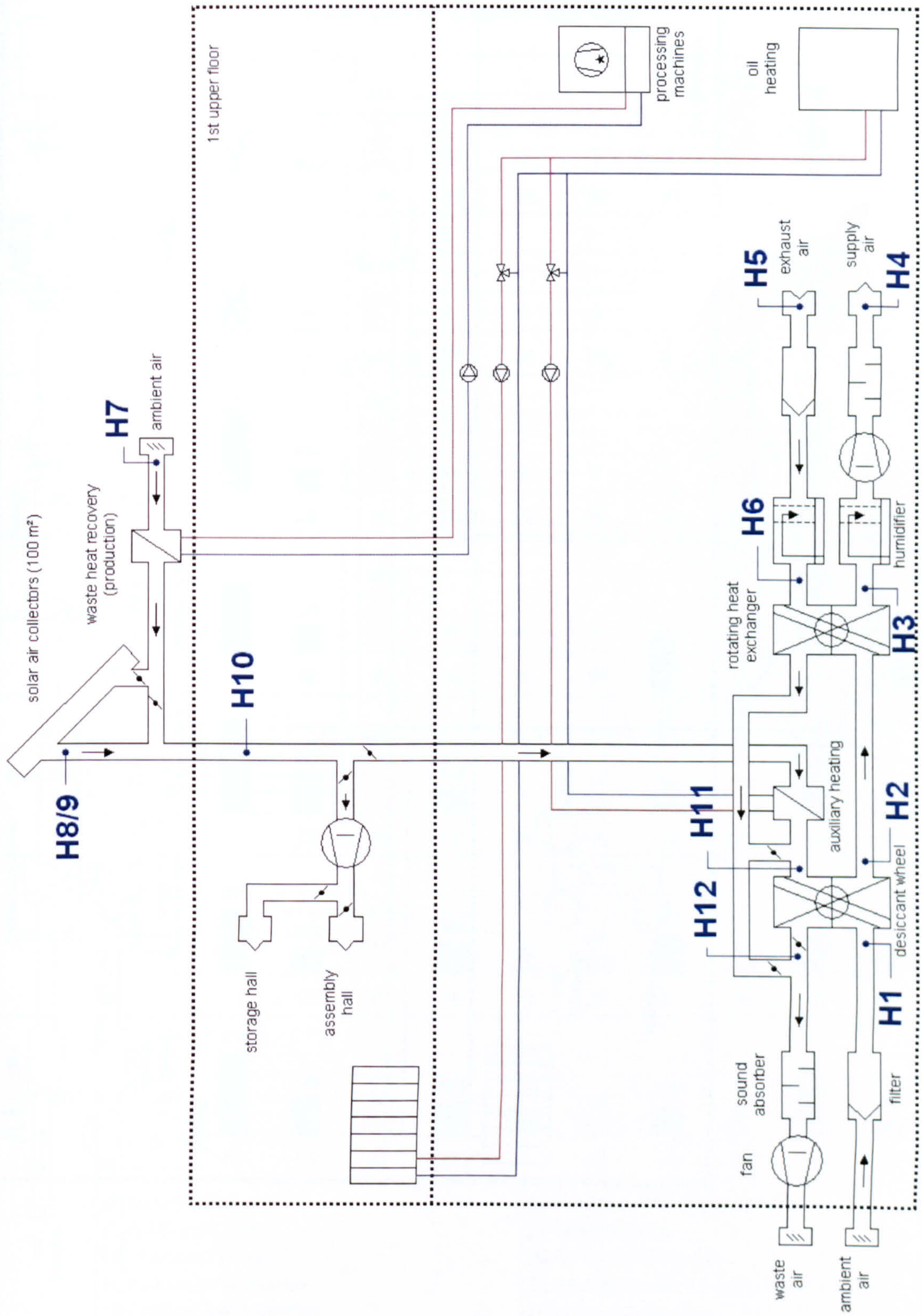

APPENDIX C

MEASUREMENT POINTS AT THE DEC-SYSTEM IN ALTHENGSTETT, GERMANY

Volume flow:

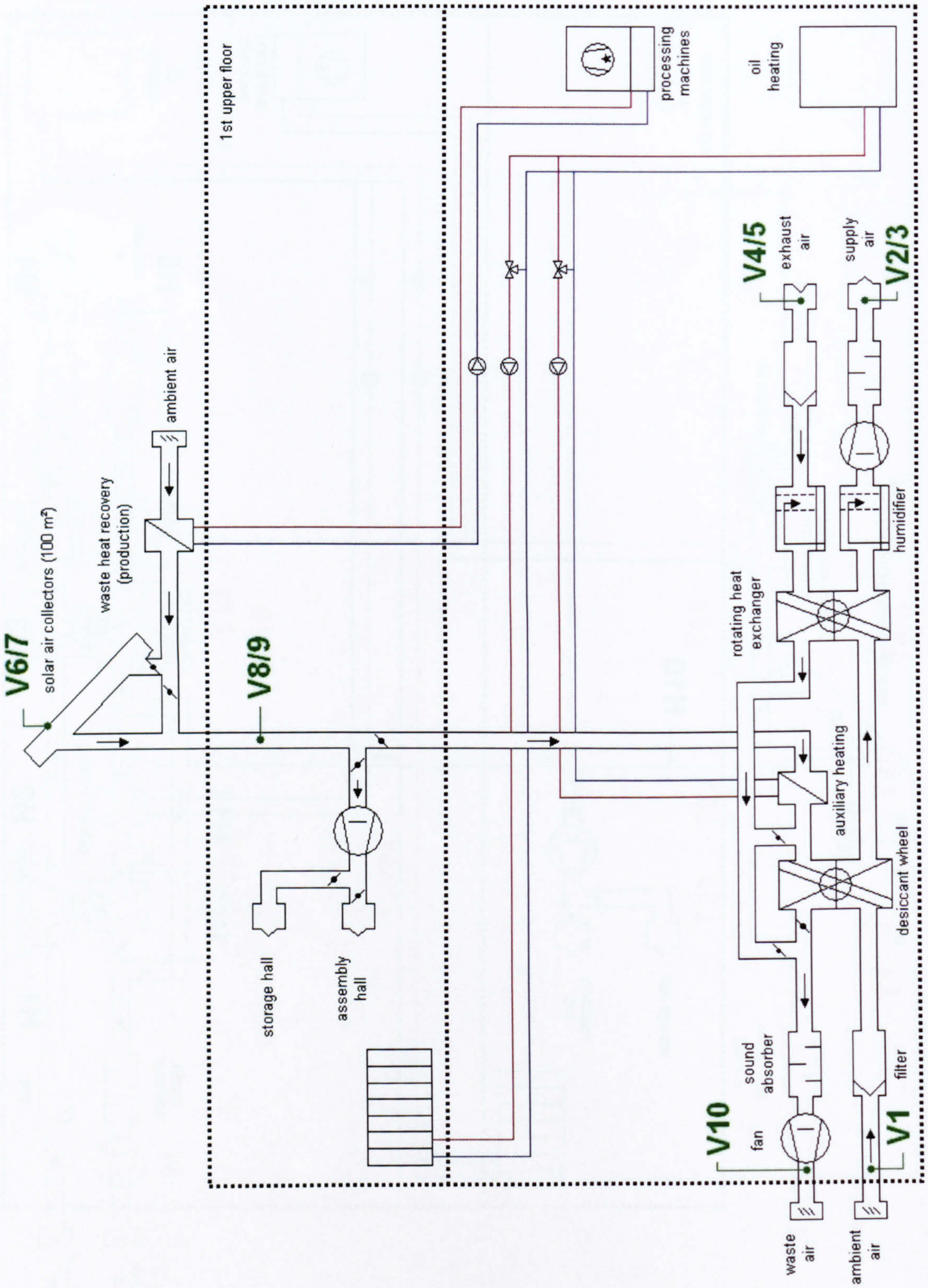

EVALUATION OF MONITORED DATA FROM THE DEC-SYSTEM IN A PLASTICS FACTORY IN ALTHENGSTETT/GERMANY

COMPONENT OPERATION TIME

JANUARY 2002	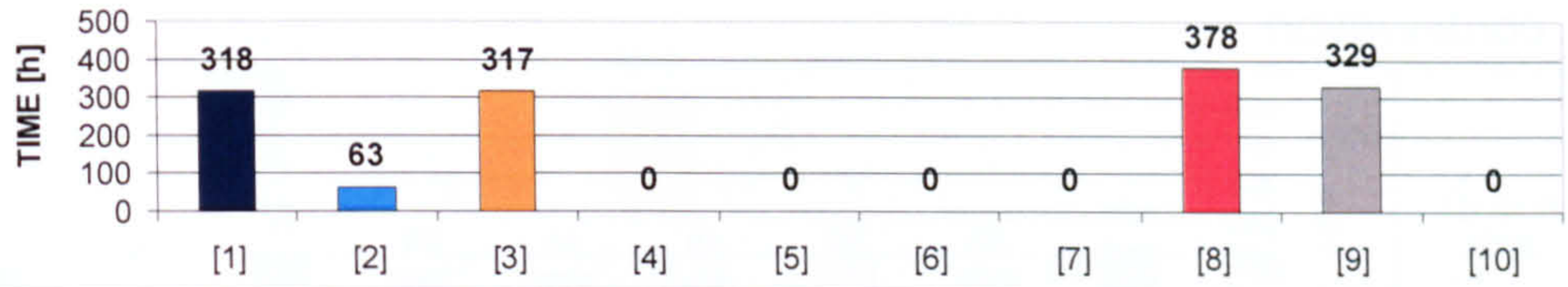
FEBRUARY 2002	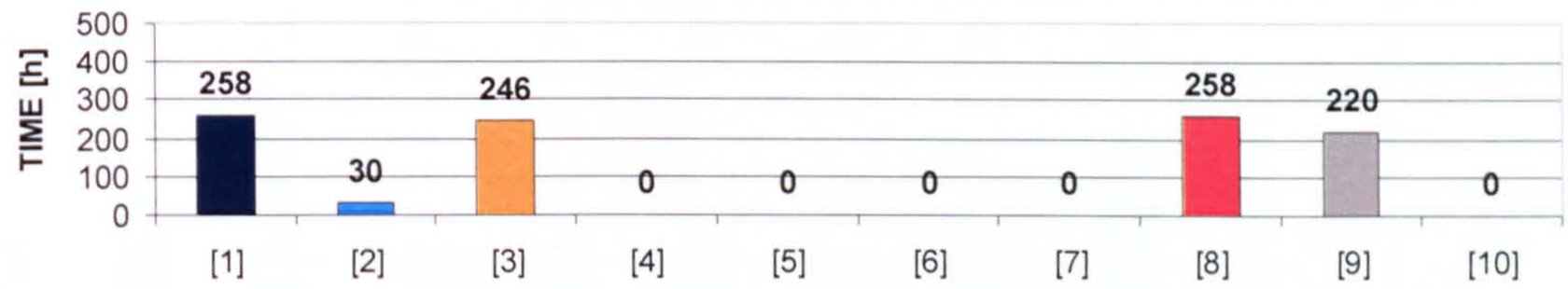
MARCH 2002	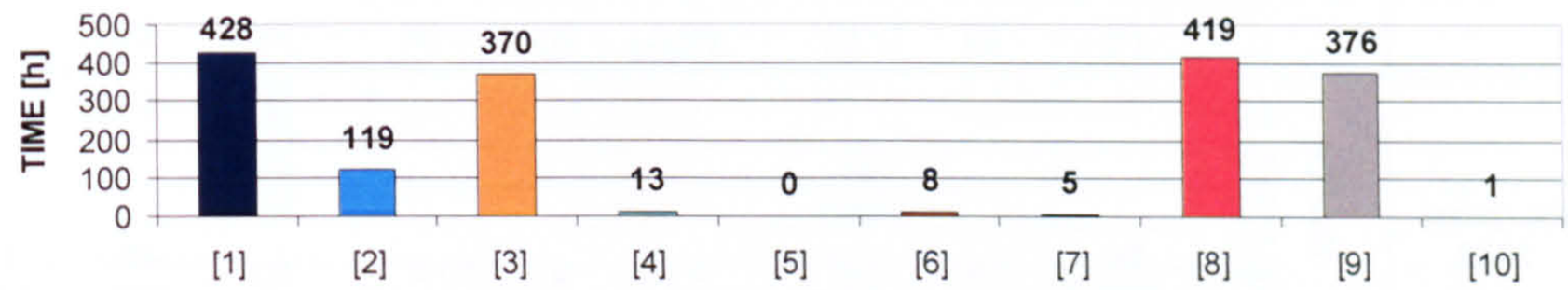
APRIL 2002	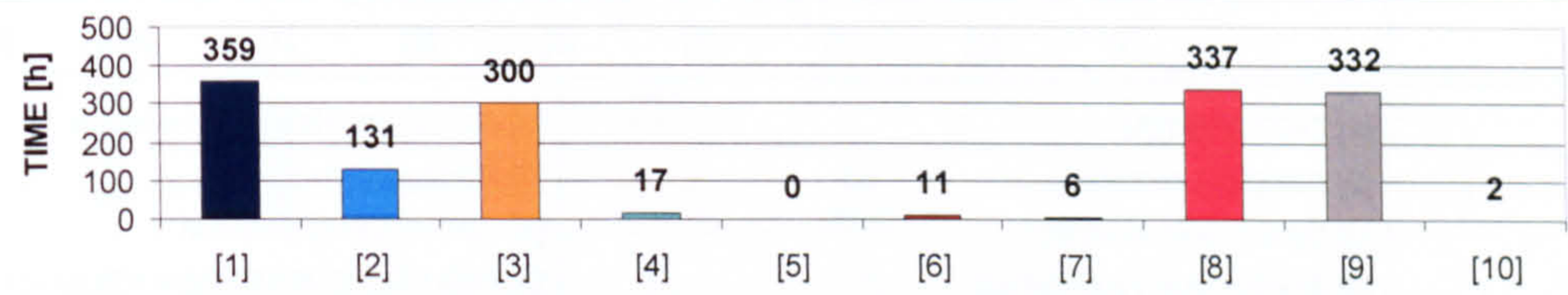
MAY 2002	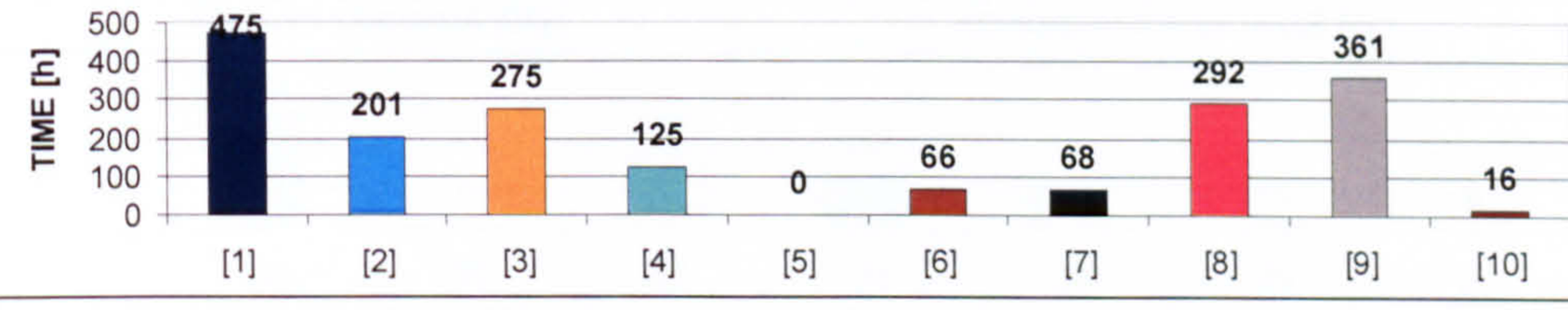
JUNE 2002	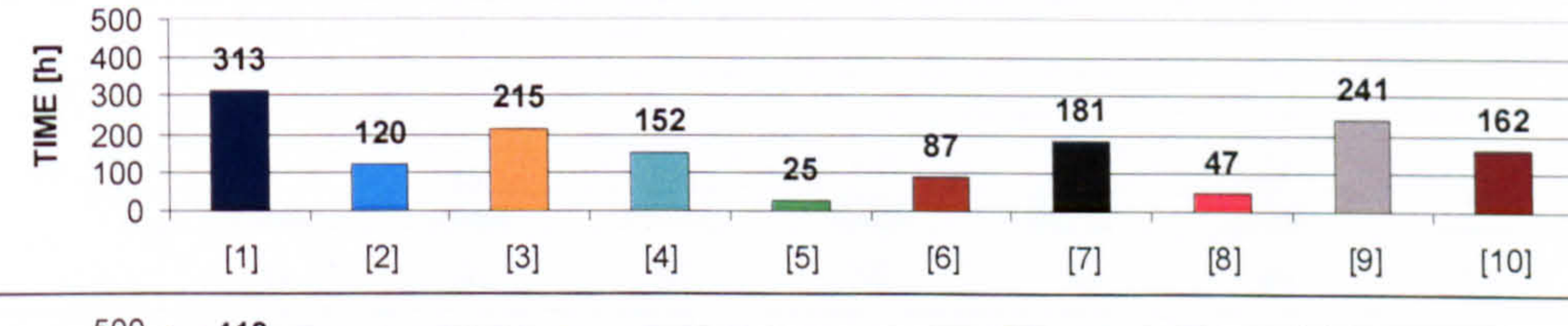
JULY 2002	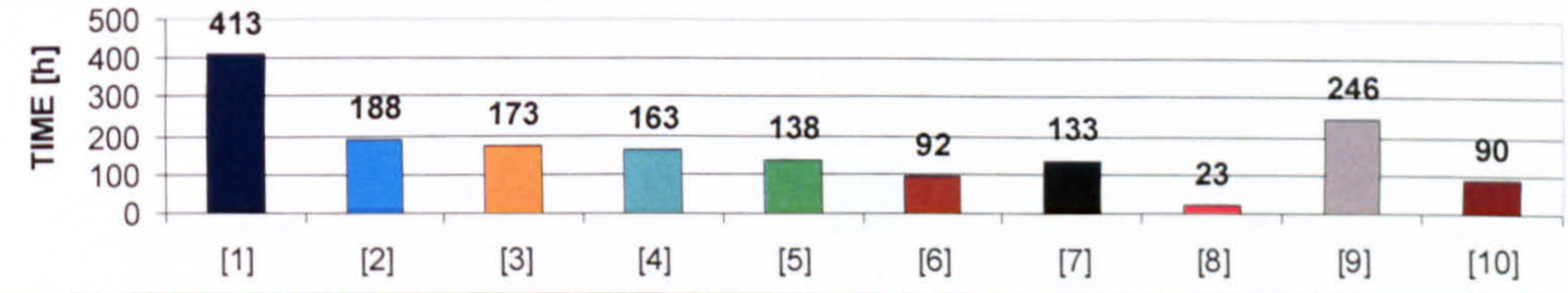

[1] DEC-SYSTEM	[6] ROTATING HEAT EXCHANGER
[2] AIR COLLECTORS	[7] REGENERATION
[3] DESICCANT WHEEL	[8] AIR HEATING SYSTEM
[4] SUPPLY AIR HUMIDIFIER	[9] HEAT RECOVERY FROM PRODUCTION
[5] EXHAUST AIR HUMIDIFIER	[10] AUXILIARY HEATING

APPENDIX D

EVALUATION OF MONITORED DATA FROM THE DEC-SYSTEM IN A PLASTICS FACTORY IN ALTHENGSTETT/GERMANY

COMPONENT OPERATION TIME

...continuation

AUGUST 2002	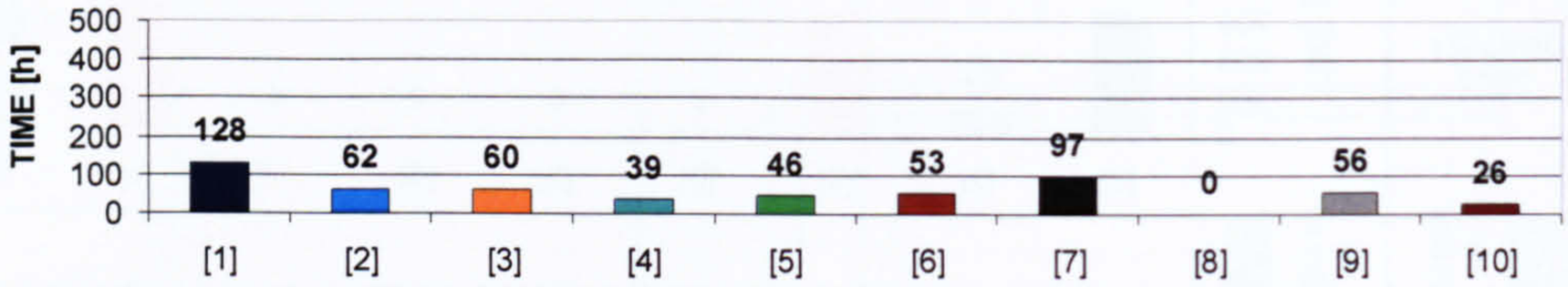
SEPTEMBER 2002	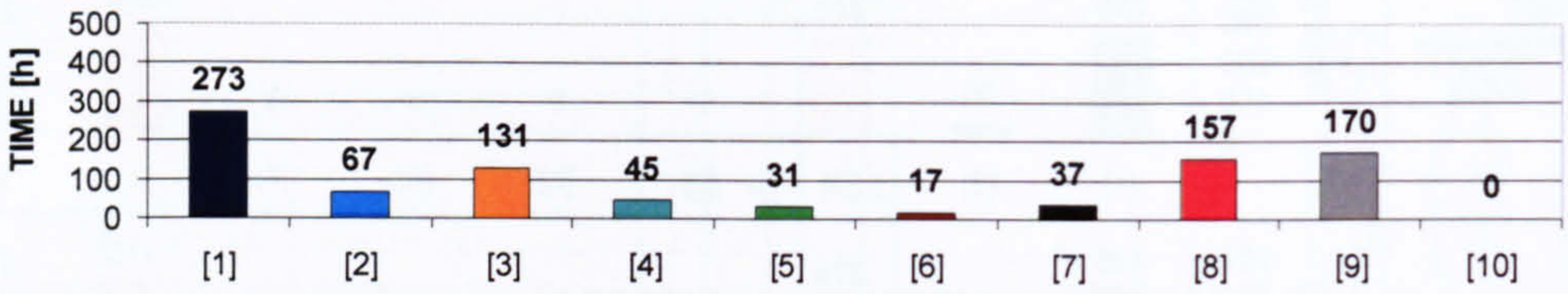
OCTOBER 2002	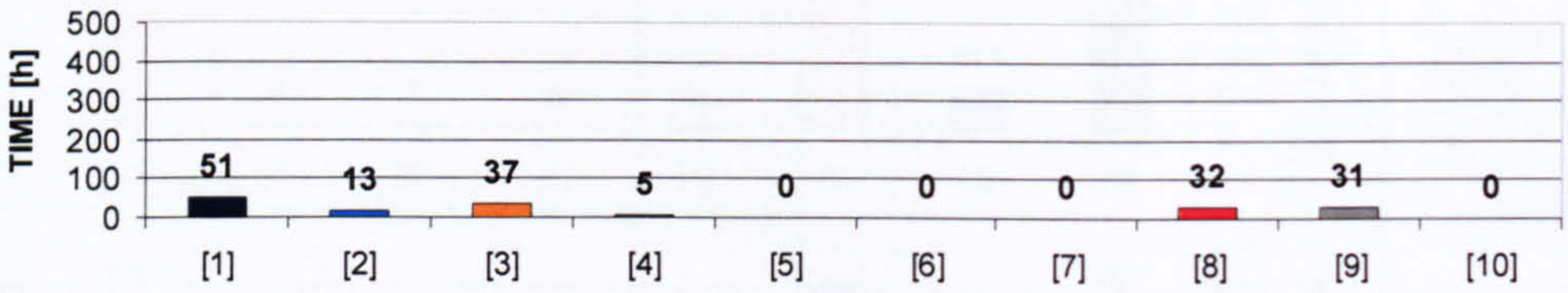

[1] DEC-SYSTEM	[6] ROTATING HEAT EXCHANGER
[2] AIR COLLECTORS	[7] REGENERATION
[3] DESICCANT WHEEL	[8] AIR HEATING SYSTEM
[4] SUPPLY AIR HUMIDIFIER	[9] HEAT RECOVERY FROM PRODUCTION
[5] EXHAUST AIR HUMIDIFIER	[10] AUXILIARY HEATING

EVALUATION OF MONITORED DATA FROM THE DEC-SYSTEM IN A PLASTICS FACTORY IN ALTHENGSTETT/GERMANY

OPERATION MODE OF DEC-SYSTEM (TIME)

JANUARY 2002	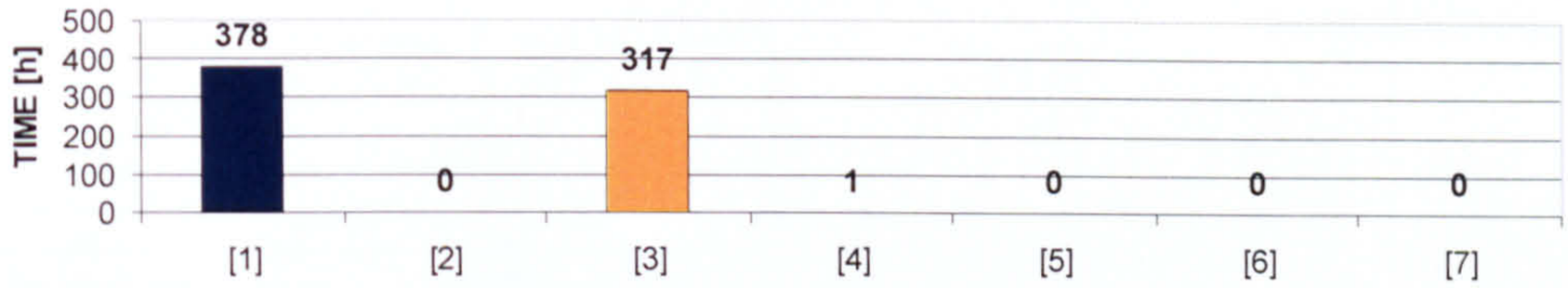
FEBRUARY 2002	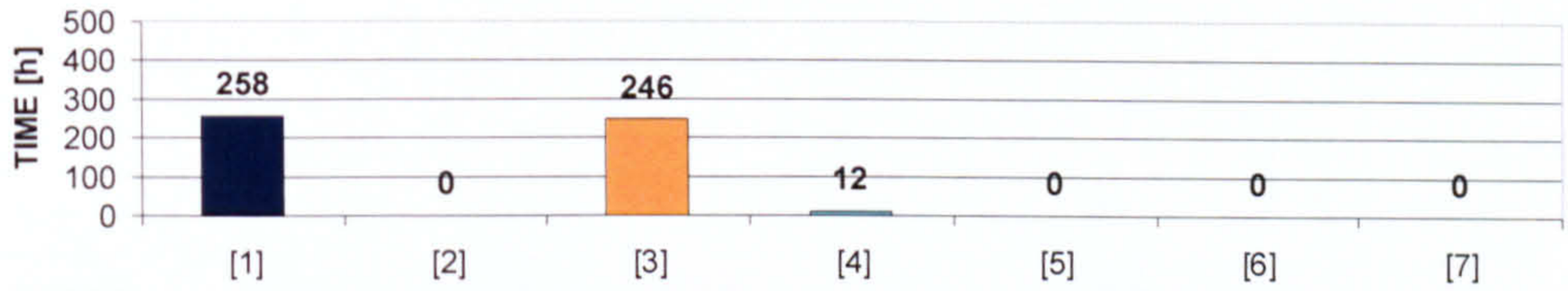
MARCH 2002	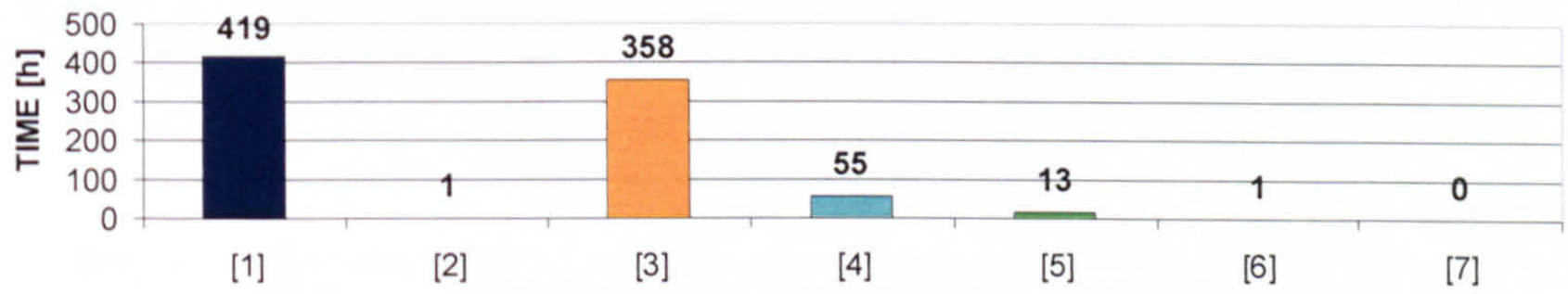
APRIL 2002	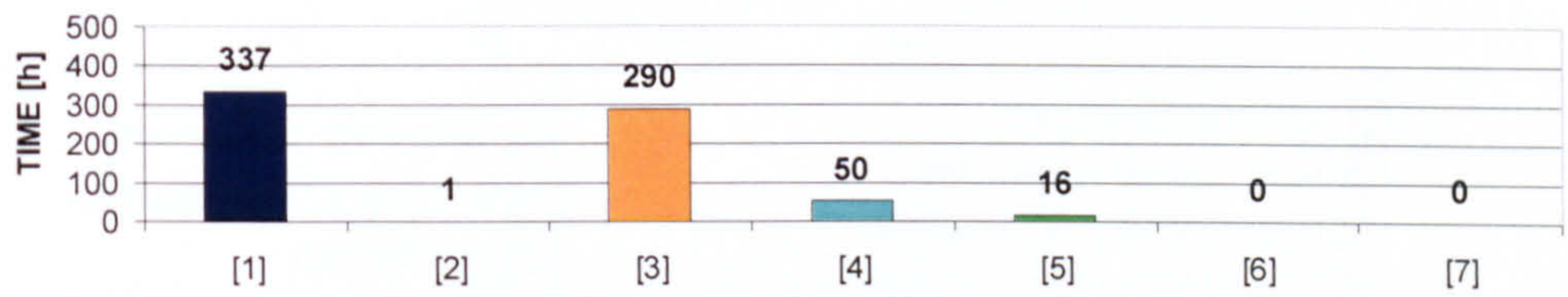
MAY 2002	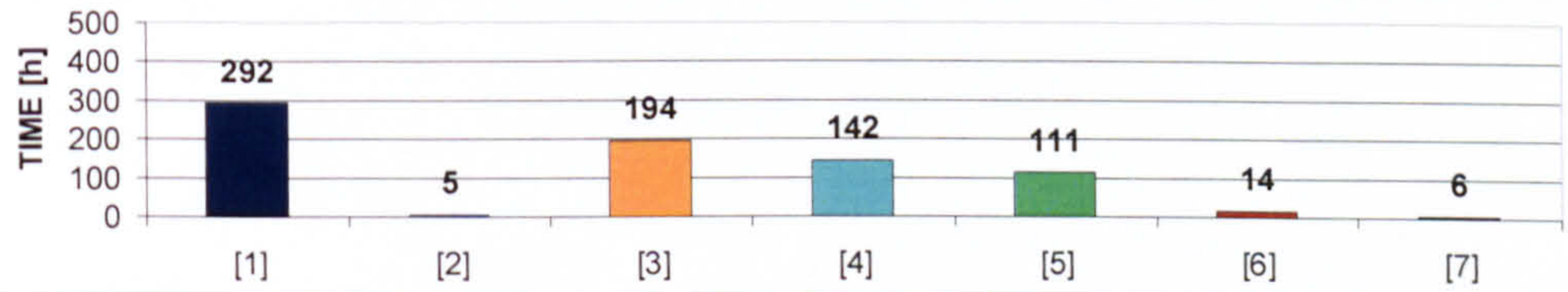
JUNE 2002	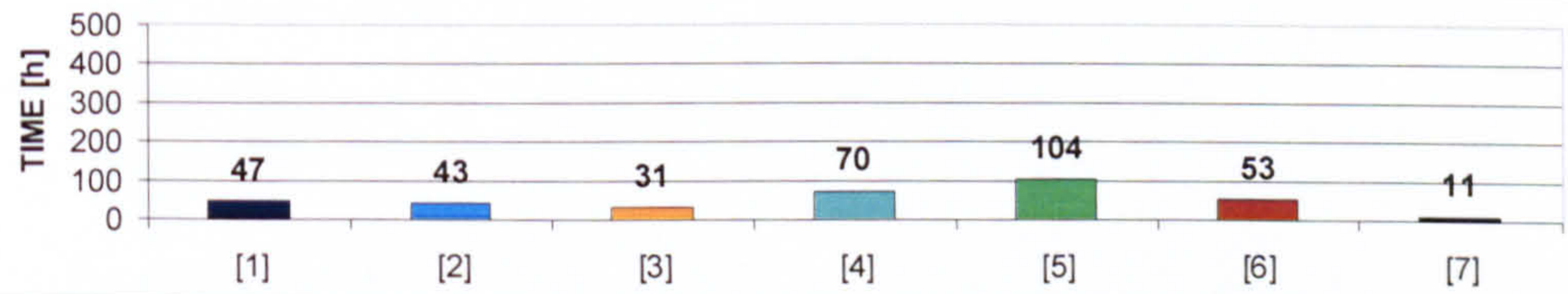
JULY 2002	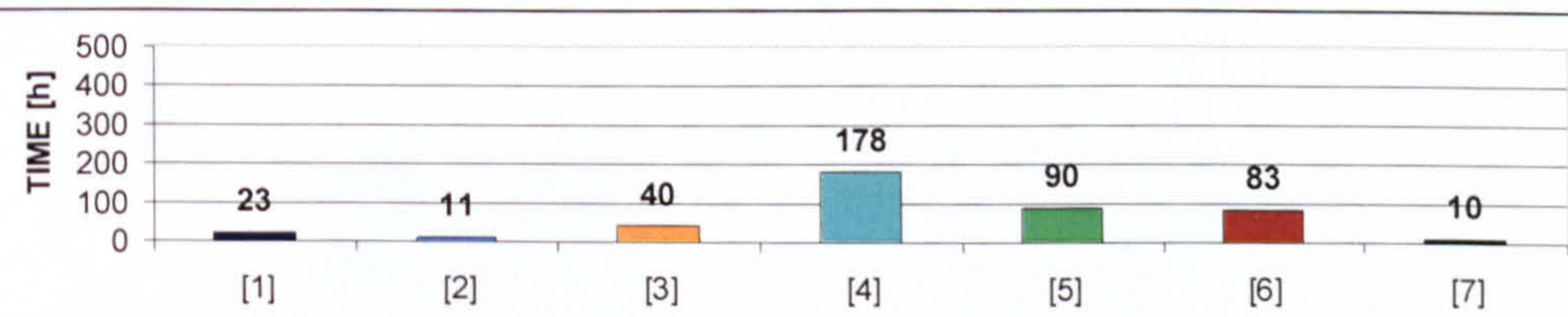
	[1] AIR HEATING SYSTEM [2] HEAT RECOVERY REG. AIR [3] HEAT RECOVERY EXHAUST. AIR [4] FREE VENTILATION [5] COOLING BY HUMIDIFIERS [6] COOLING BY REGENERATION [7] NOT DEFINED

EVALUATION OF MONITORED DATA FROM THE DEC-SYSTEM IN A PLASTICS FACTORY IN ALTHENGSTETT/GERMANY

OPERATION MODE OF DEC-SYSTEM (TIME)

...continuation

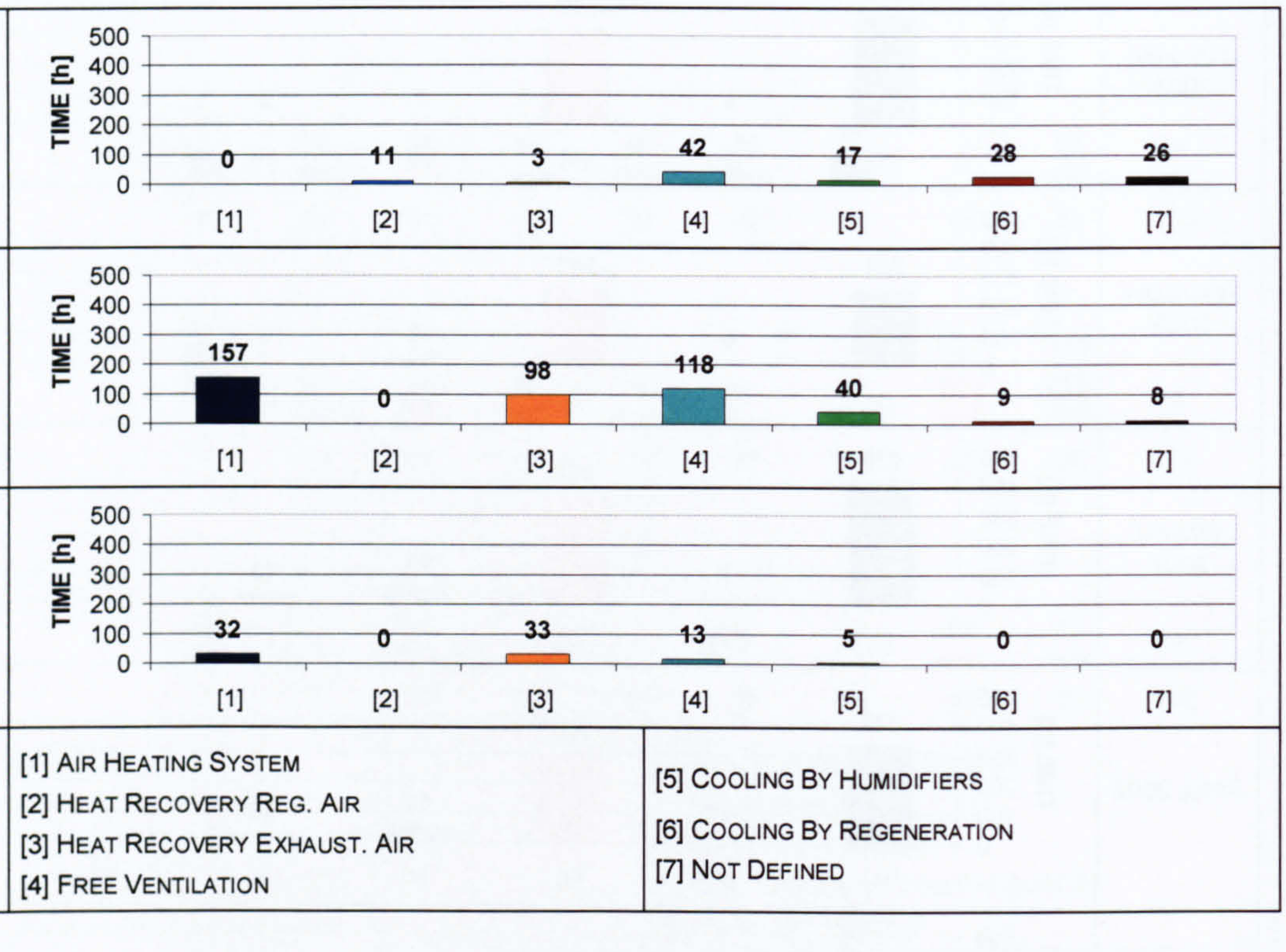

EVALUATION OF AIR COLLECTOR OPERATION (ALTHENGSTETT/GERMANY)

SOLAR IRRADIATION / COLLECTOR GAIN

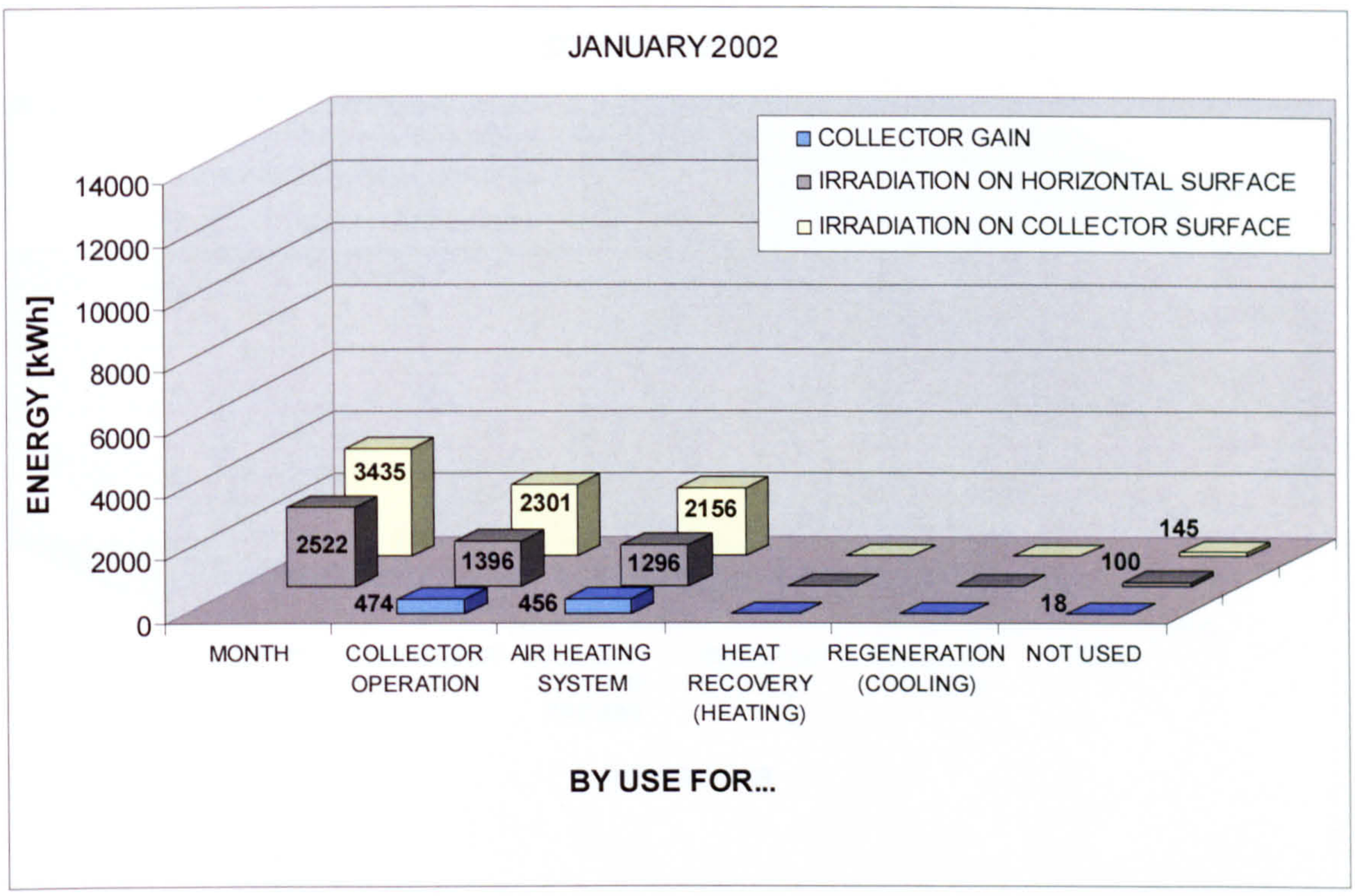

COLLECTOR EFFICIENCY

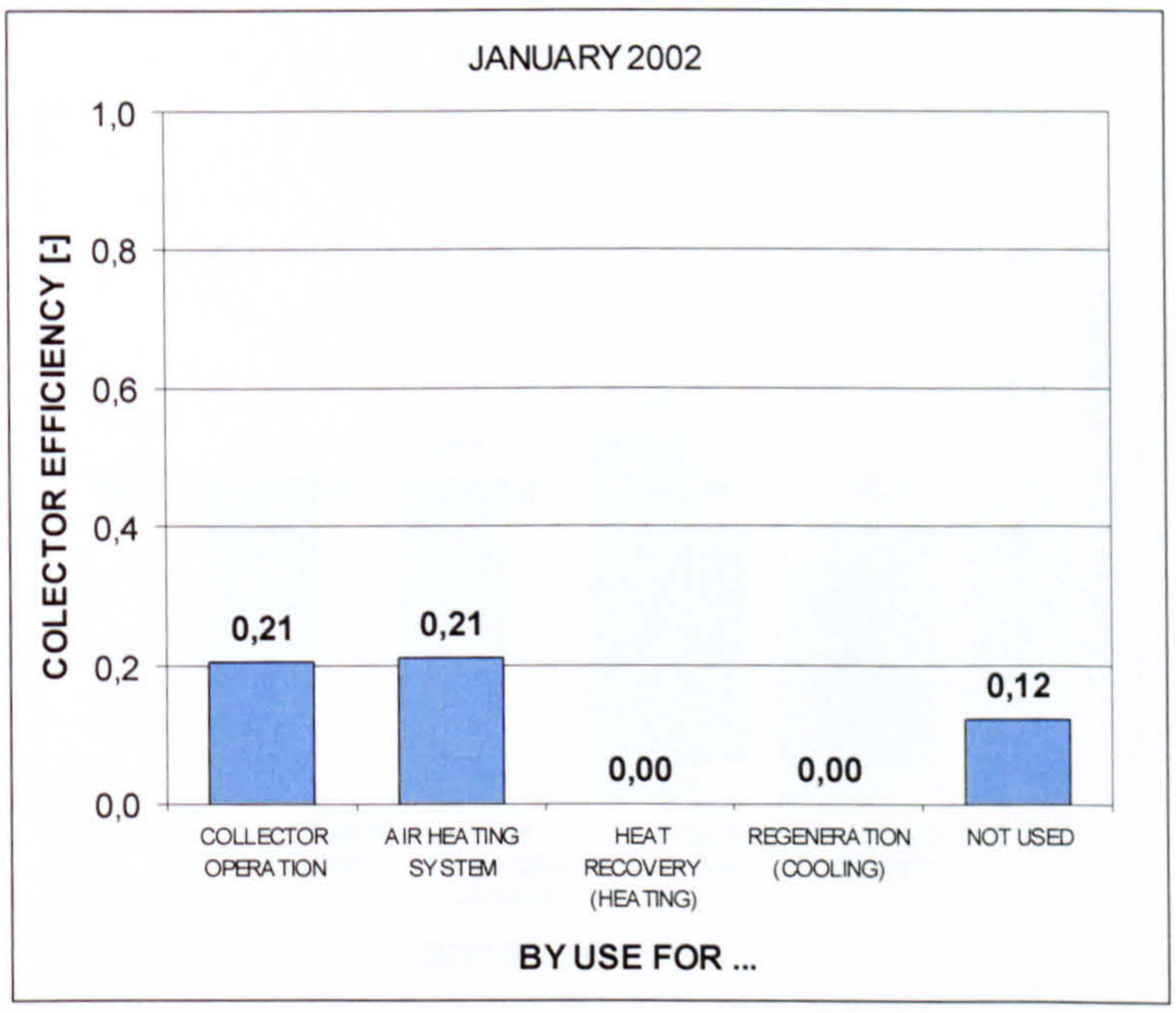

APPENDIX F

EVALUATION OF AIR COLLECTOR OPERATION (ALTHENGSTETT/GERMANY)

SOLAR IRRADIATION / COLLECTOR GAIN

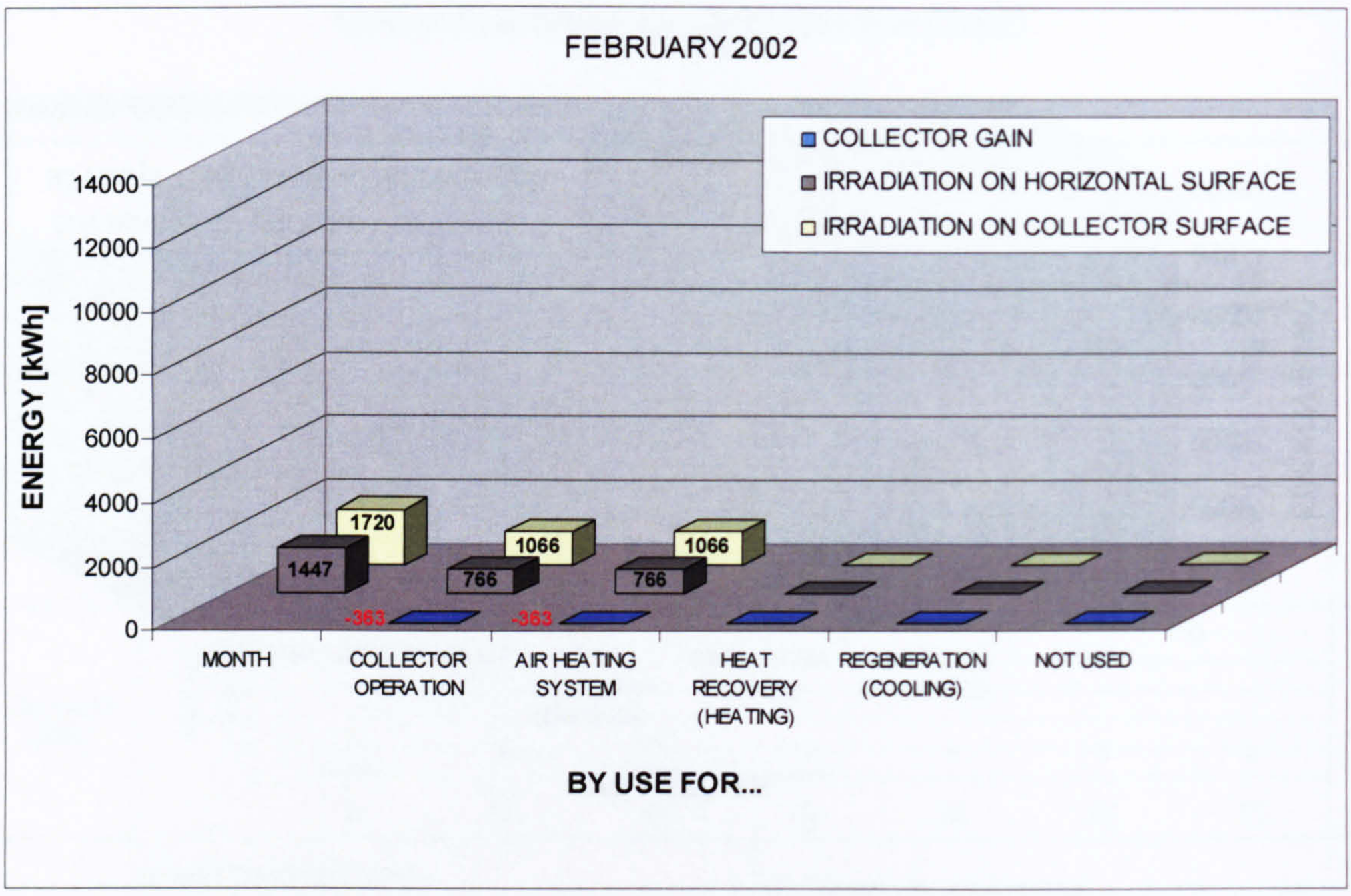

COLLECTOR EFFICIENCY

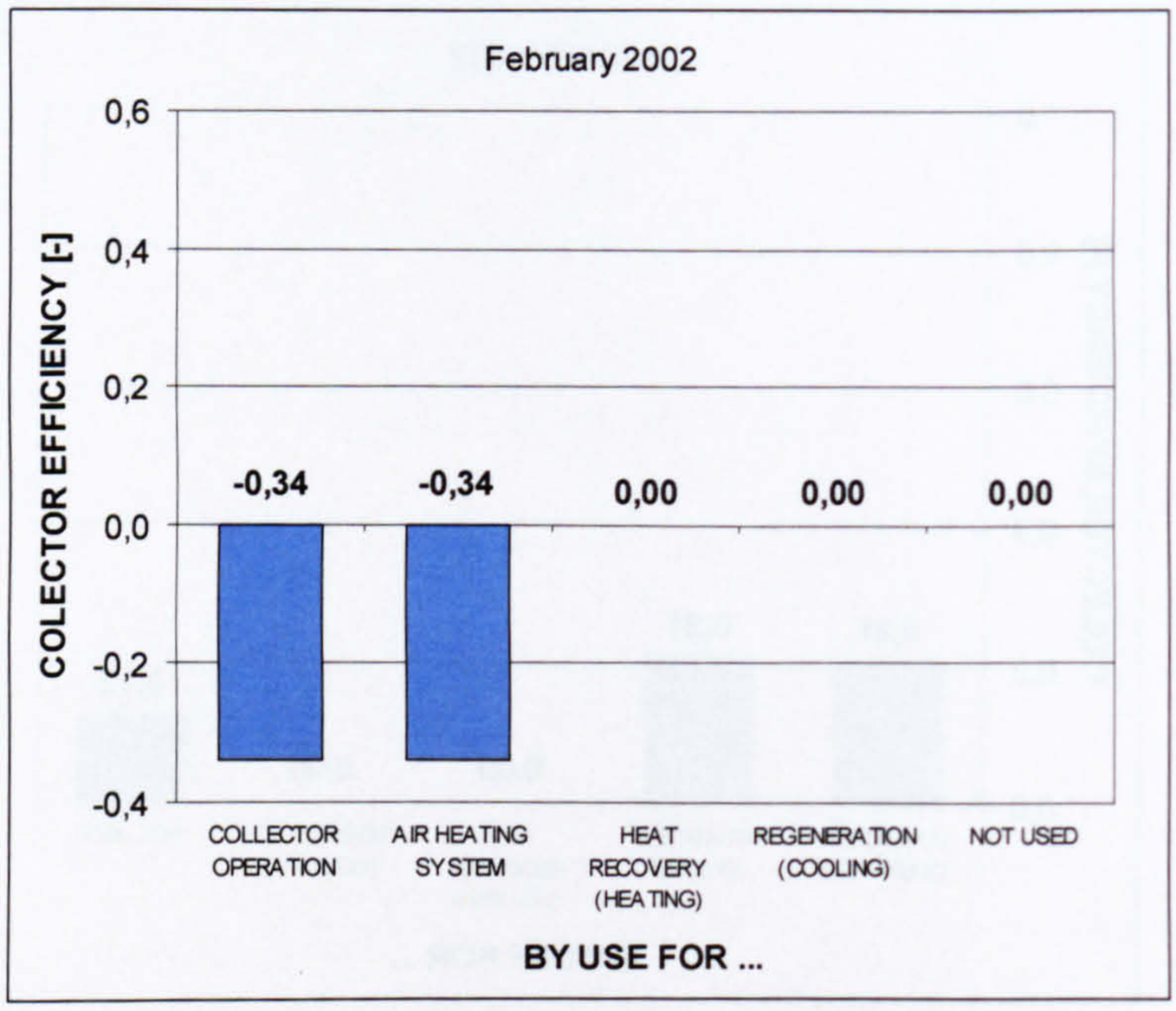

EVALUATION OF AIR COLLECTOR OPERATION (ALTHENGSTETT/GERMANY)

SOLAR IRRADIATION / COLLECTOR GAIN

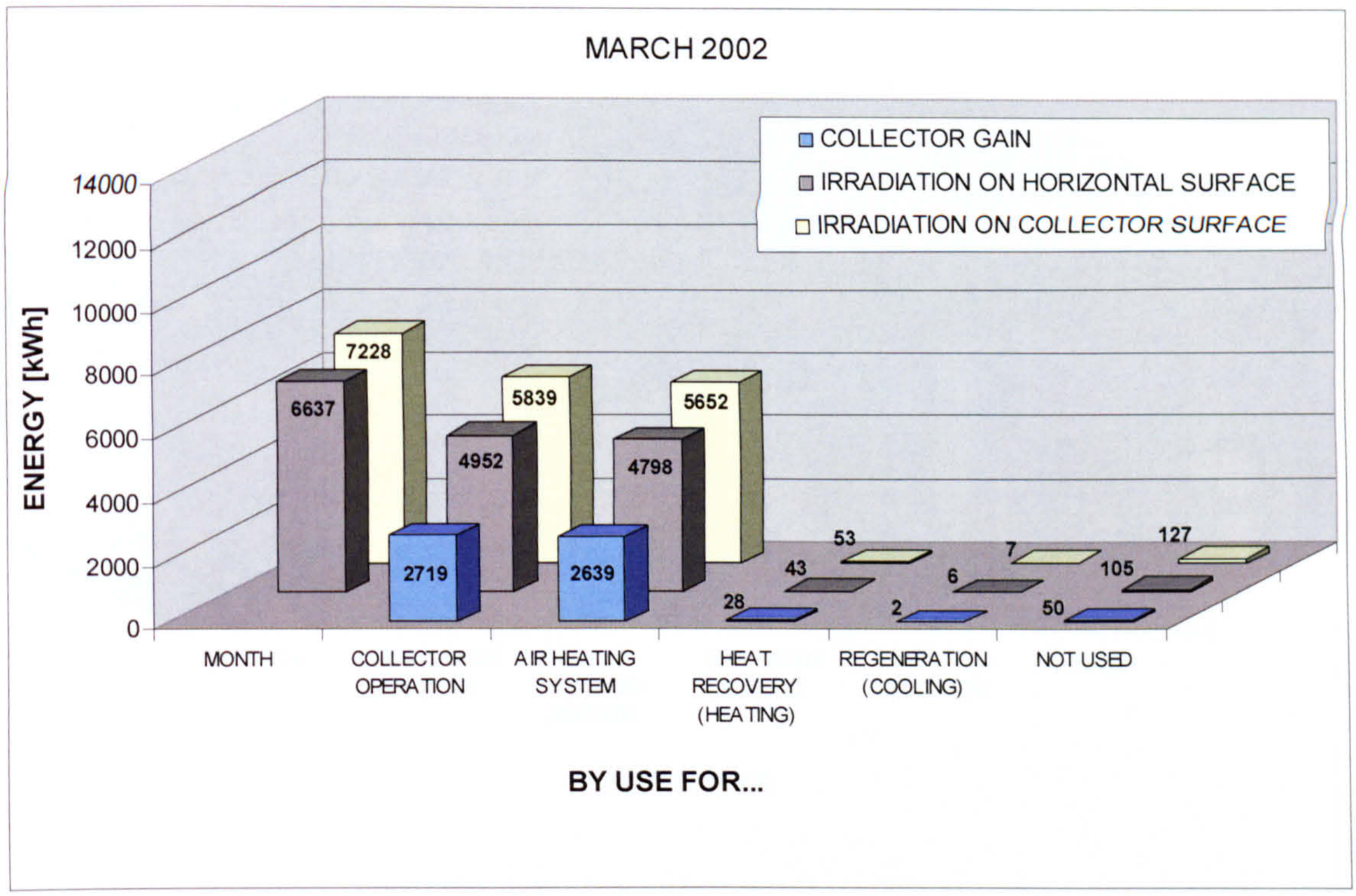

COLLECTOR EFFICIENCY

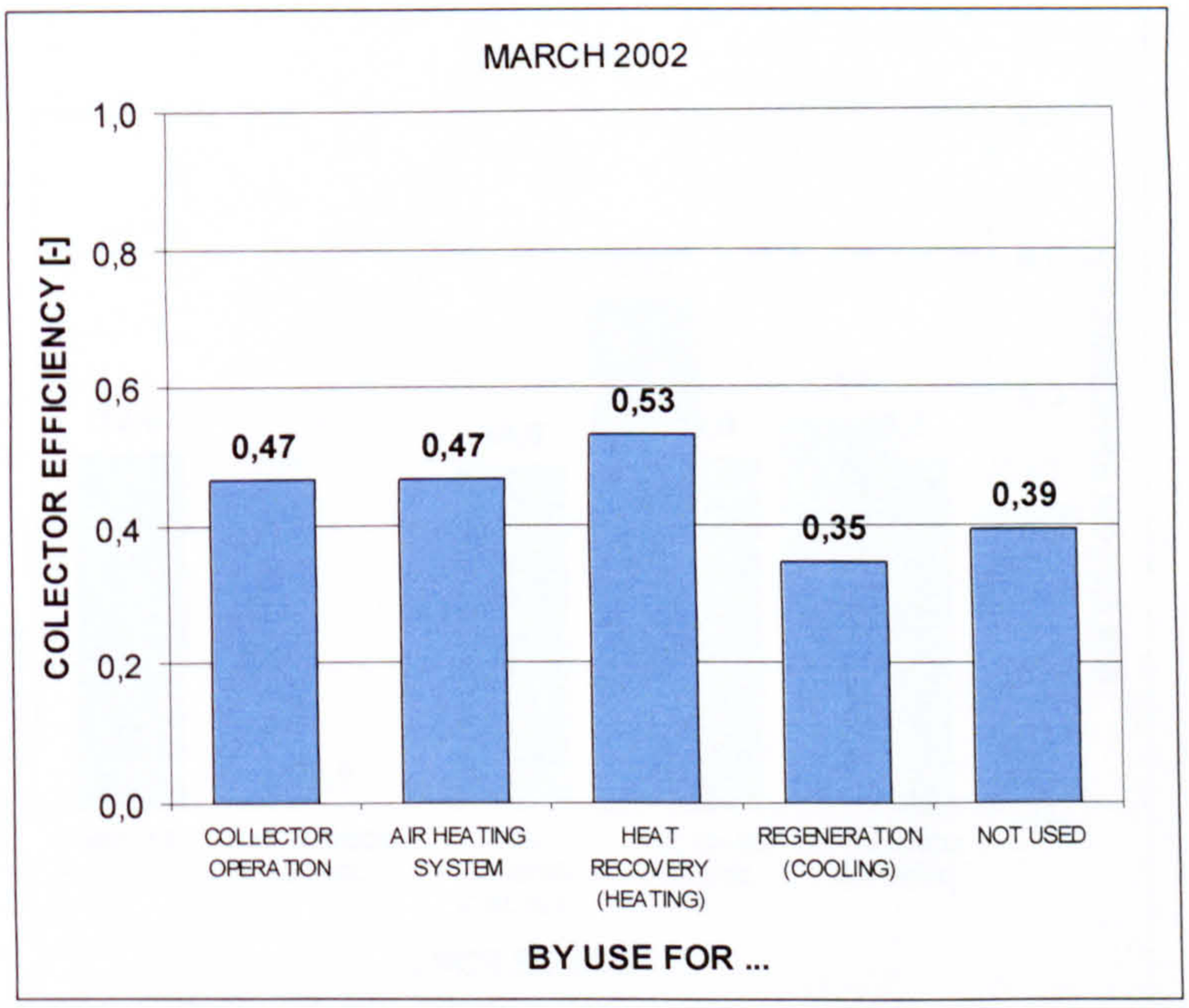

APPENDIX F

EVALUATION OF AIR COLLECTOR OPERATION (ALTHENGSTETT/GERMANY)

SOLAR IRRADIATION / COLLECTOR GAIN

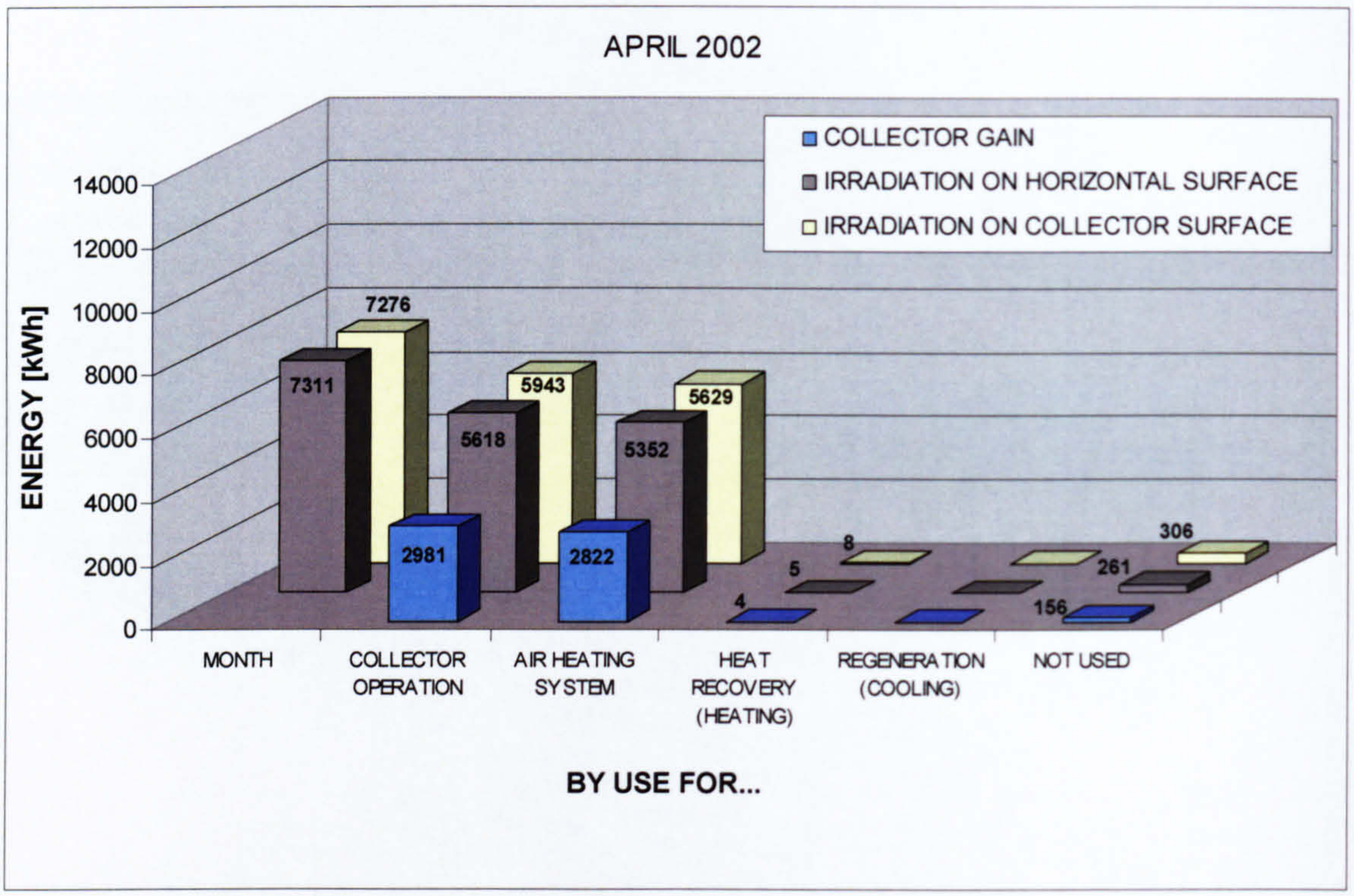

COLLECTOR EFFICIENCY

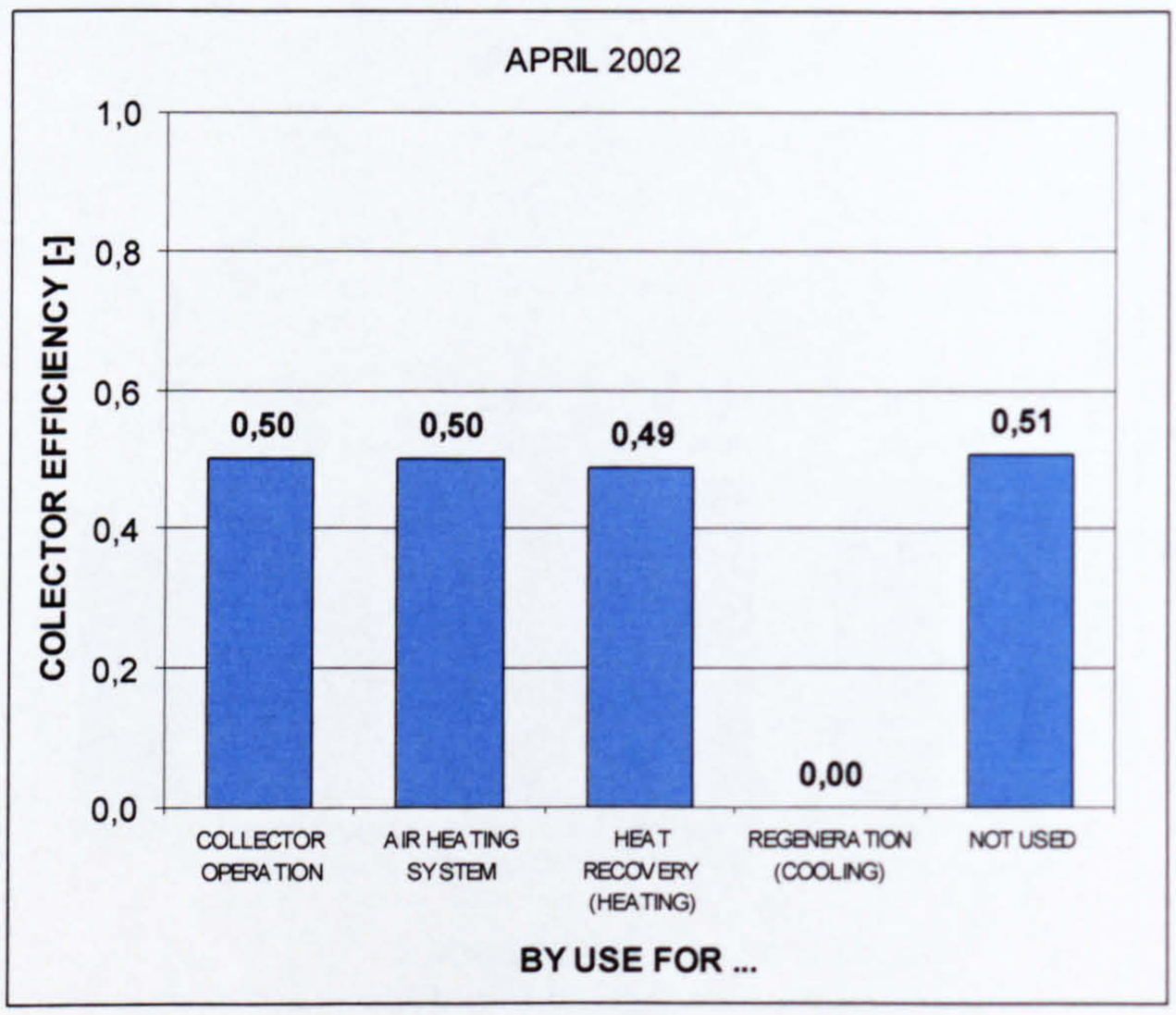

EVALUATION OF AIR COLLECTOR OPERATION (ALTHENGSTETT/GERMANY)

SOLAR IRRADIATION / COLLECTOR GAIN

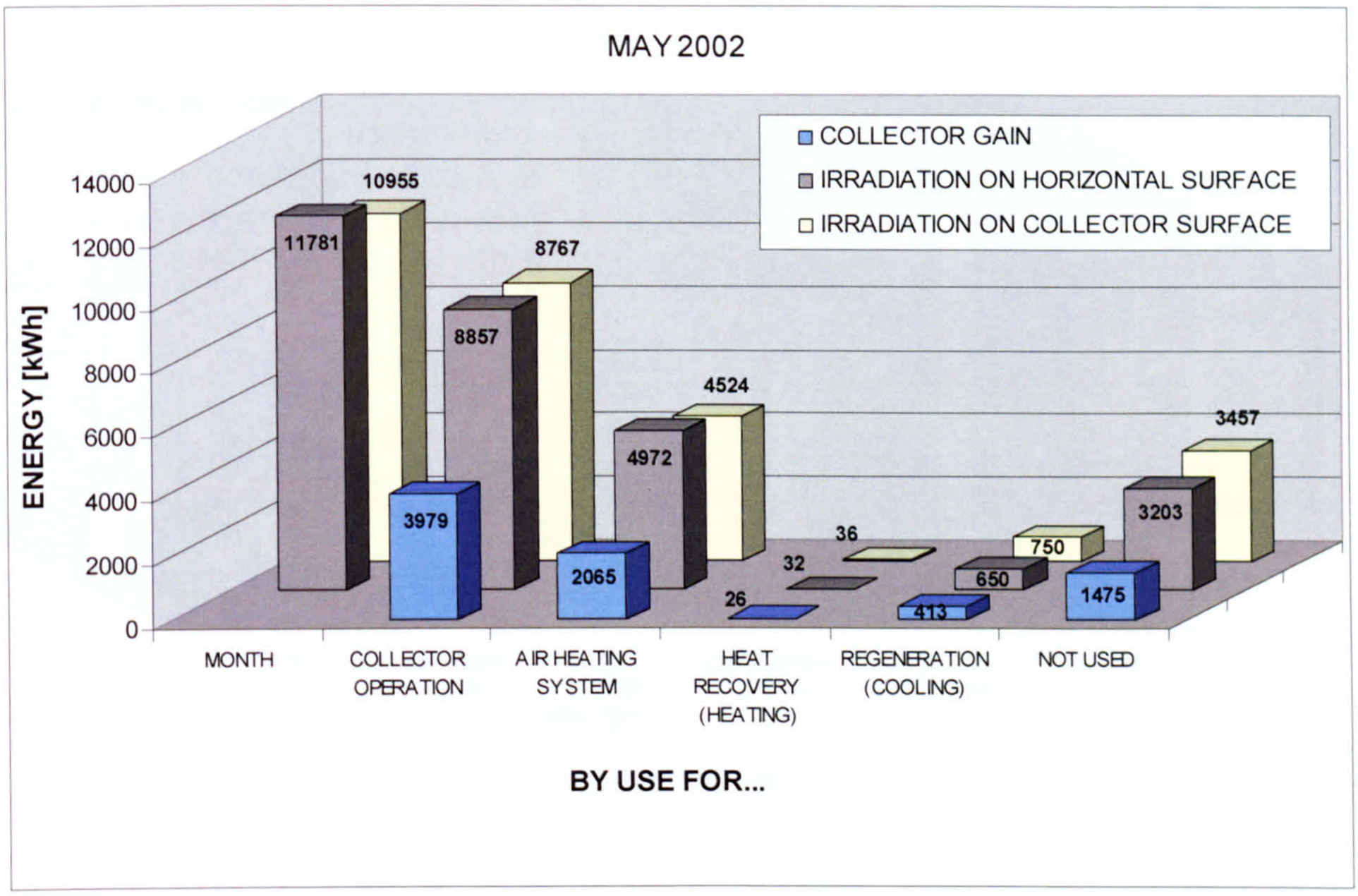

COLLECTOR EFFICIENCY

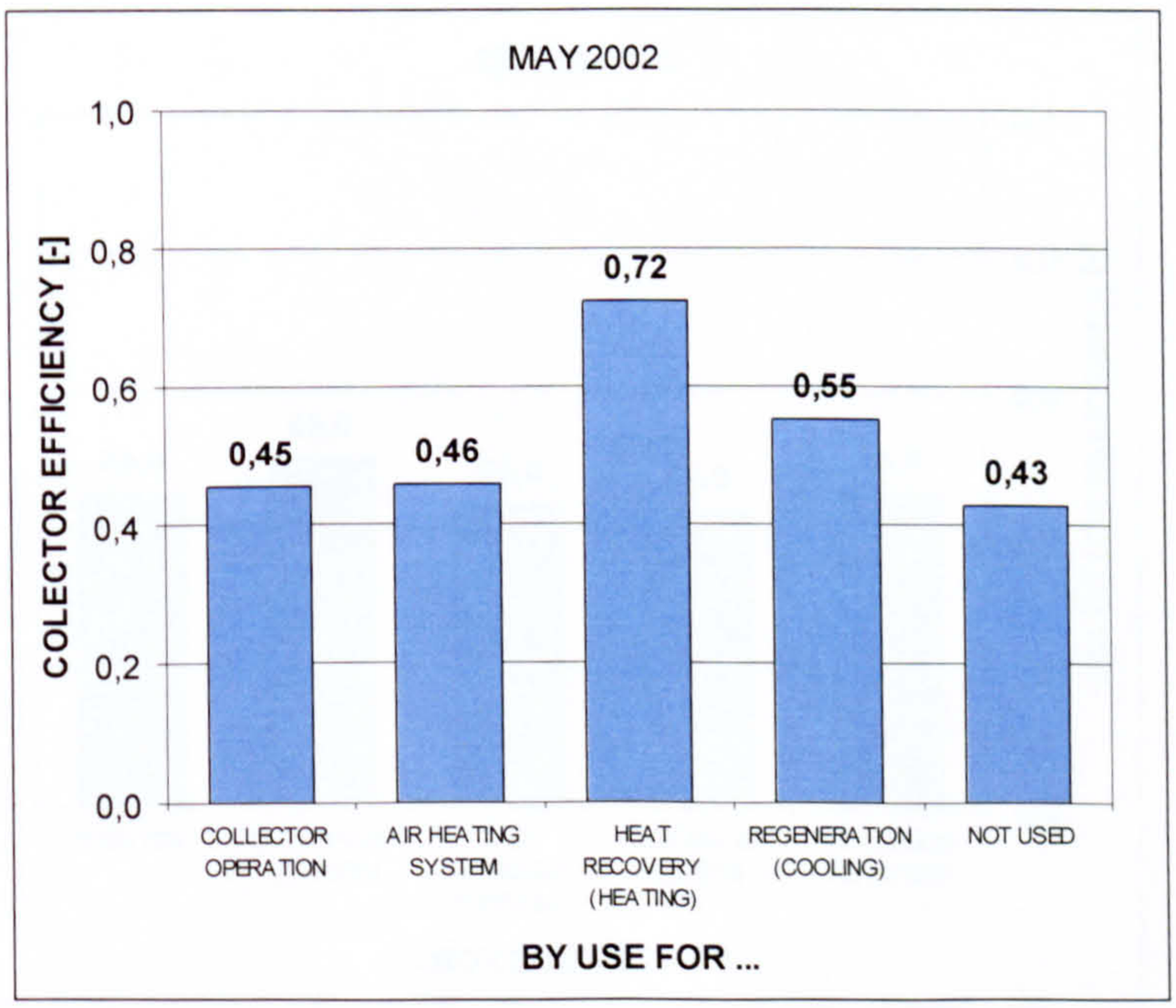

APPENDIX F

EVALUATION OF AIR COLLECTOR OPERATION (ALTHENGSTETT/GERMANY)

SOLAR IRRADIATION / COLLECTOR GAIN

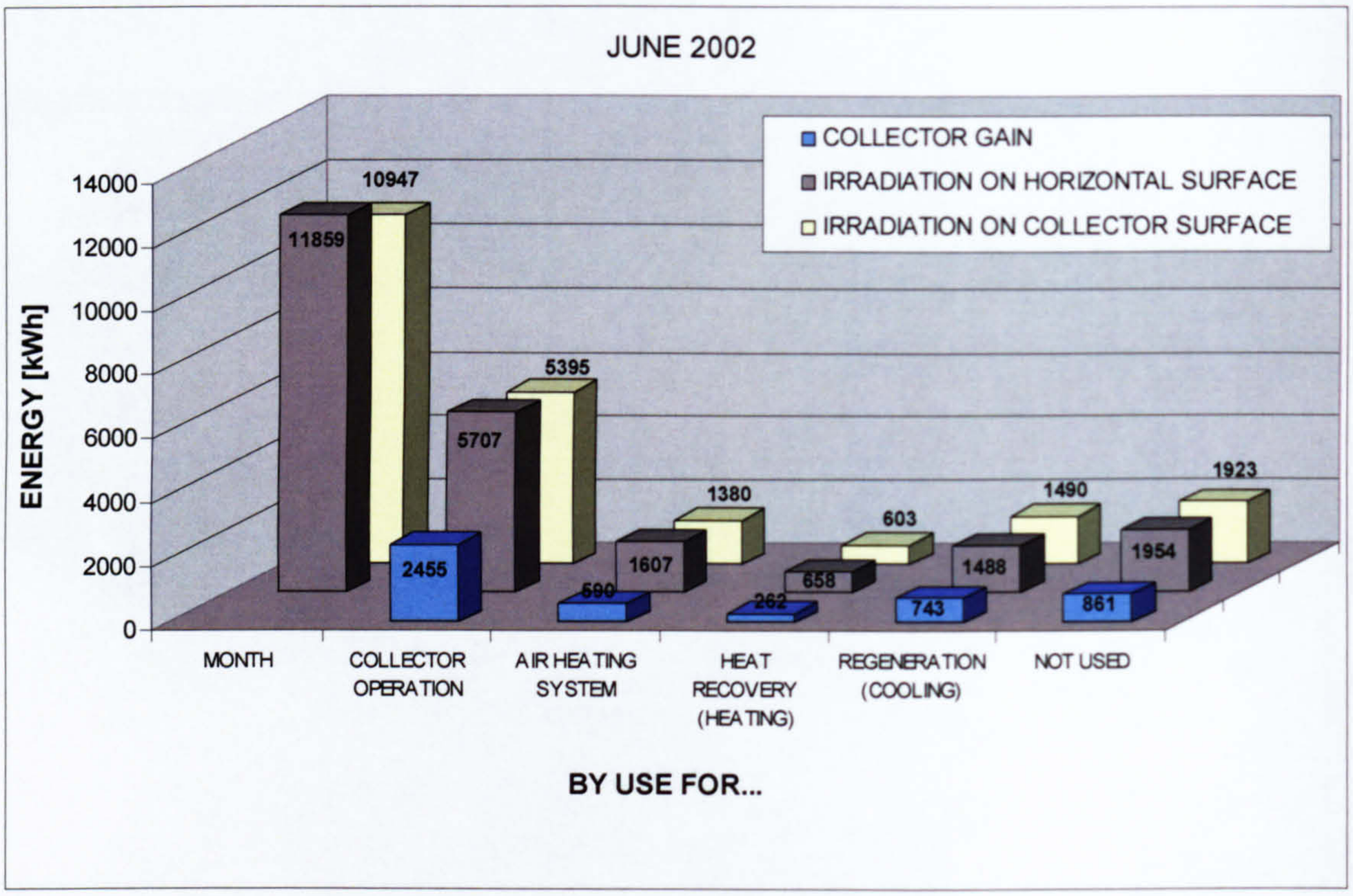

COLLECTOR EFFICIENCY

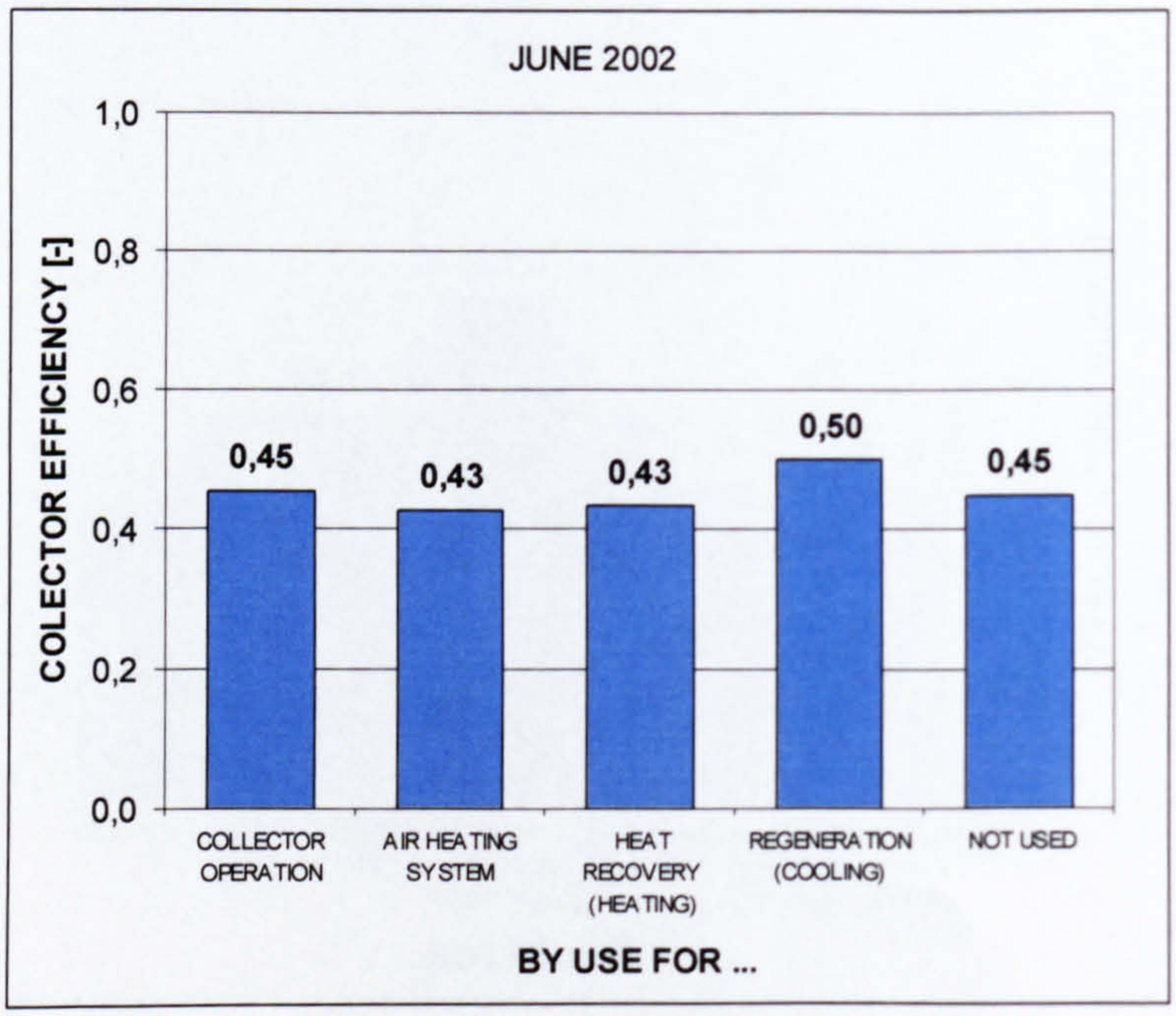

EVALUATION OF AIR COLLECTOR OPERATION (ALTHENGSTETT/GERMANY)

SOLAR IRRADIATION / COLLECTOR GAIN

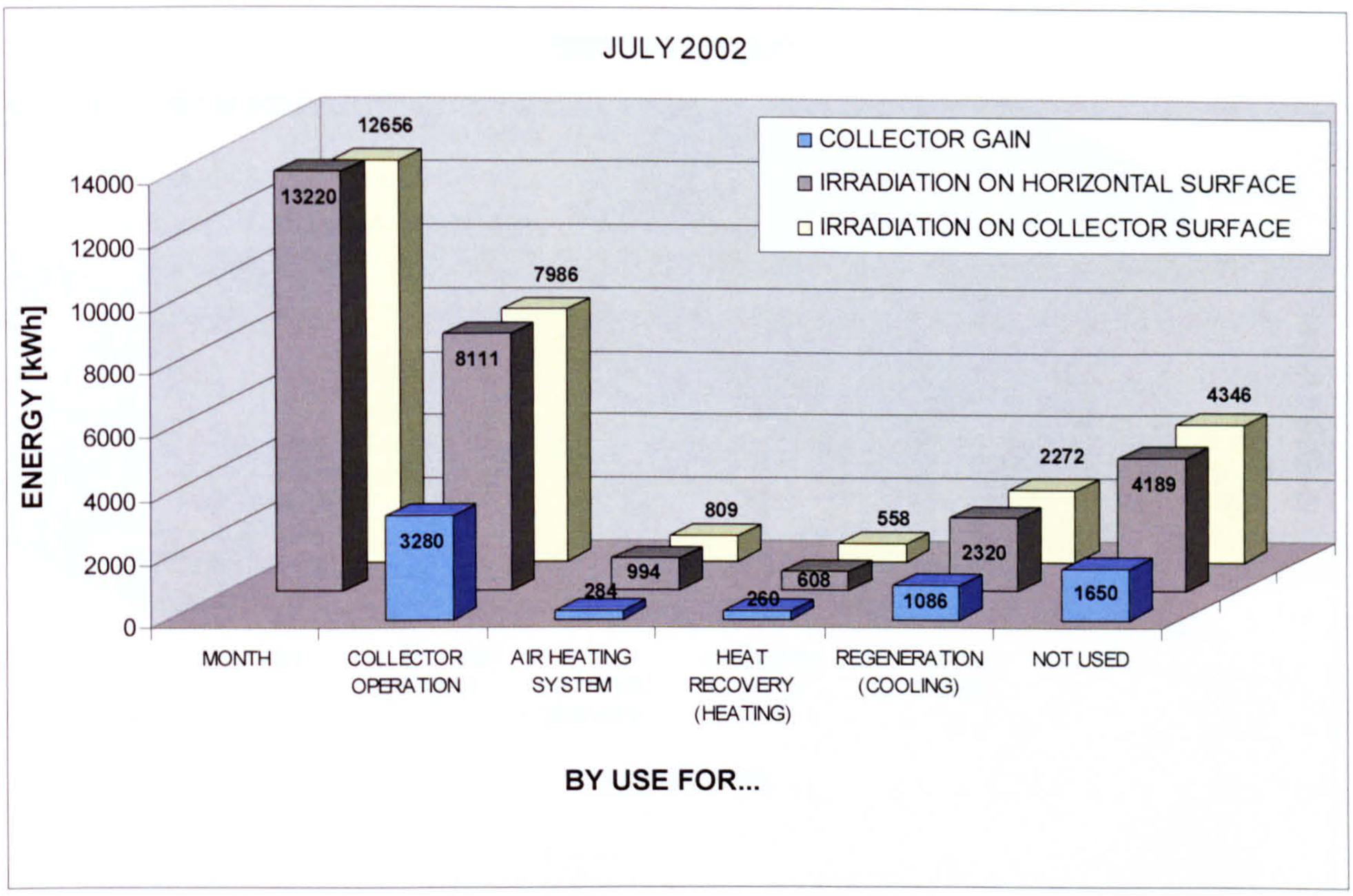

COLLECTOR EFFICIENCY

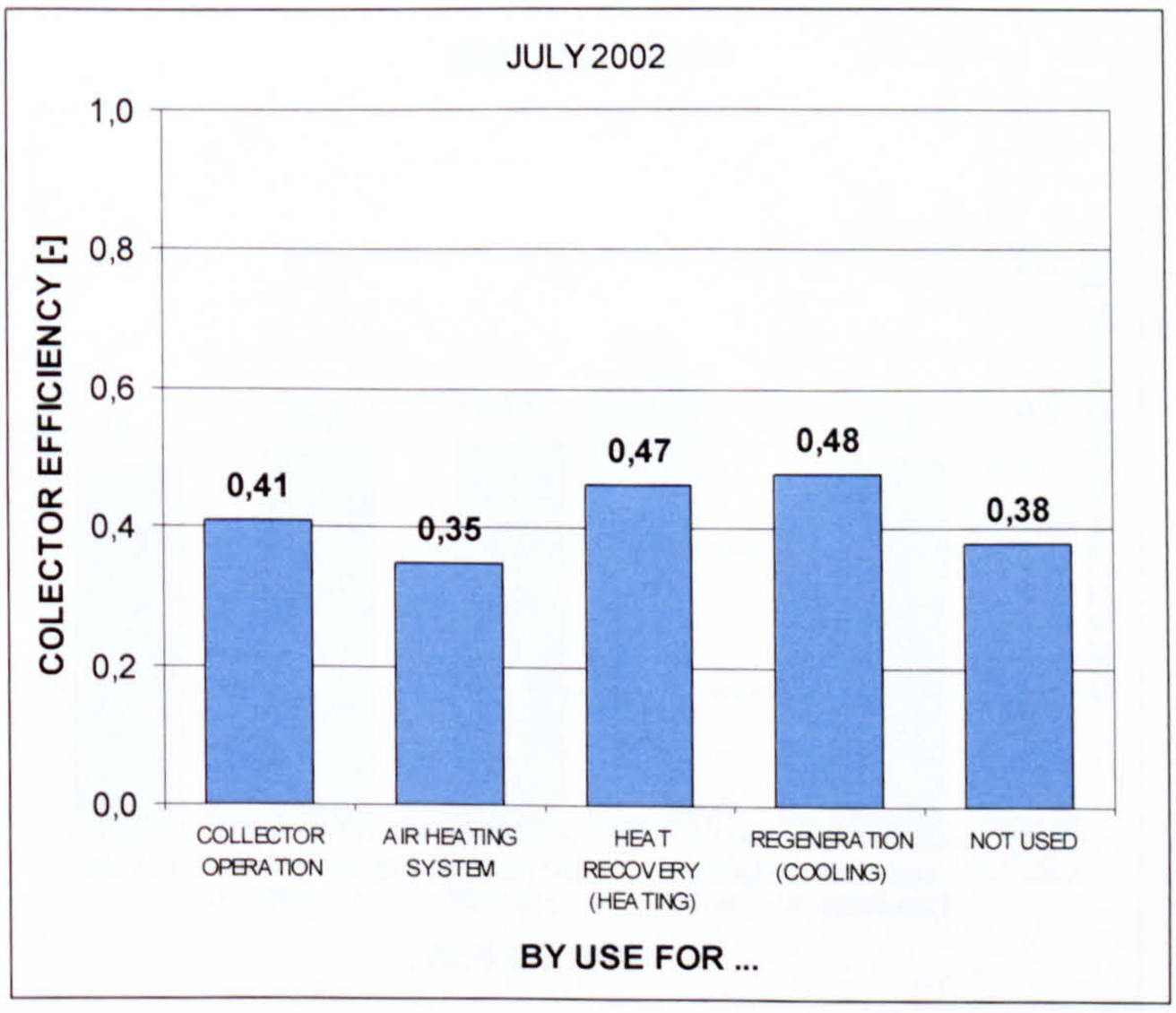

APPENDIX F

EVALUATION OF AIR COLLECTOR OPERATION (ALTHENGSTETT/GERMANY)

SOLAR IRRADIATION / COLLECTOR GAIN

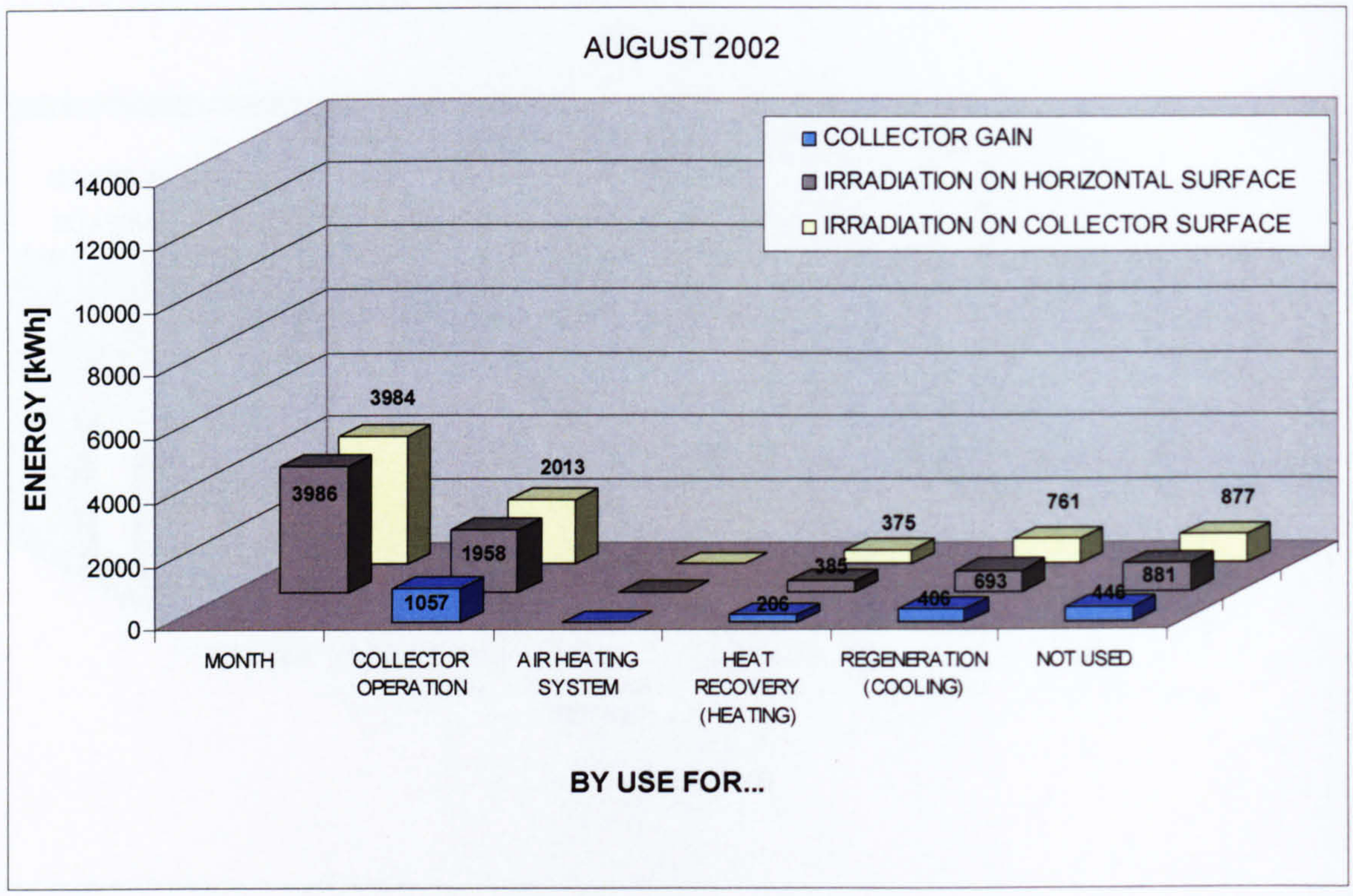

COLLECTOR EFFICIENCY

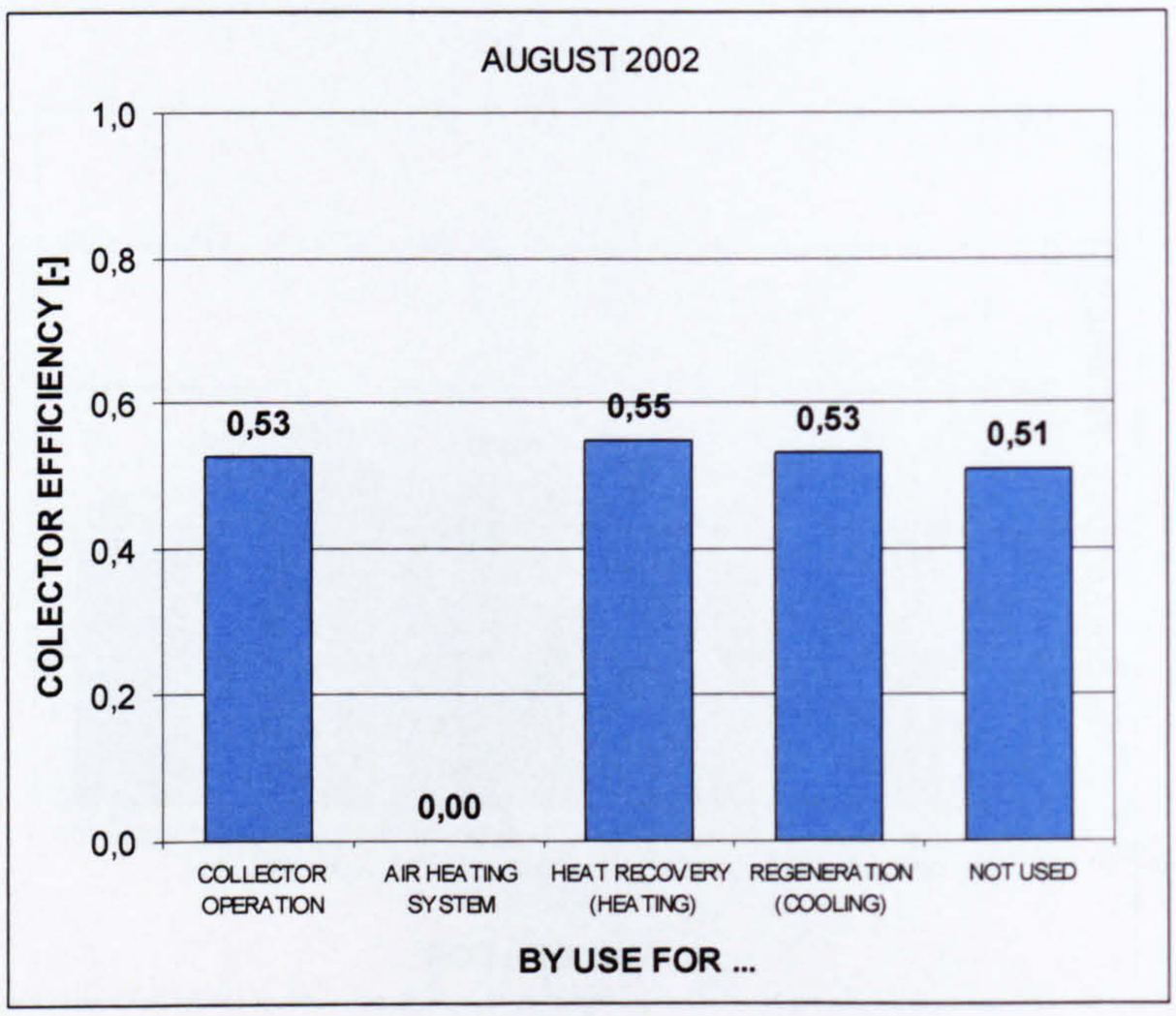

EVALUATION OF AIR COLLECTOR OPERATION (ALTHENGSTETT/GERMANY)

SOLAR IRRADIATION / COLLECTOR GAIN

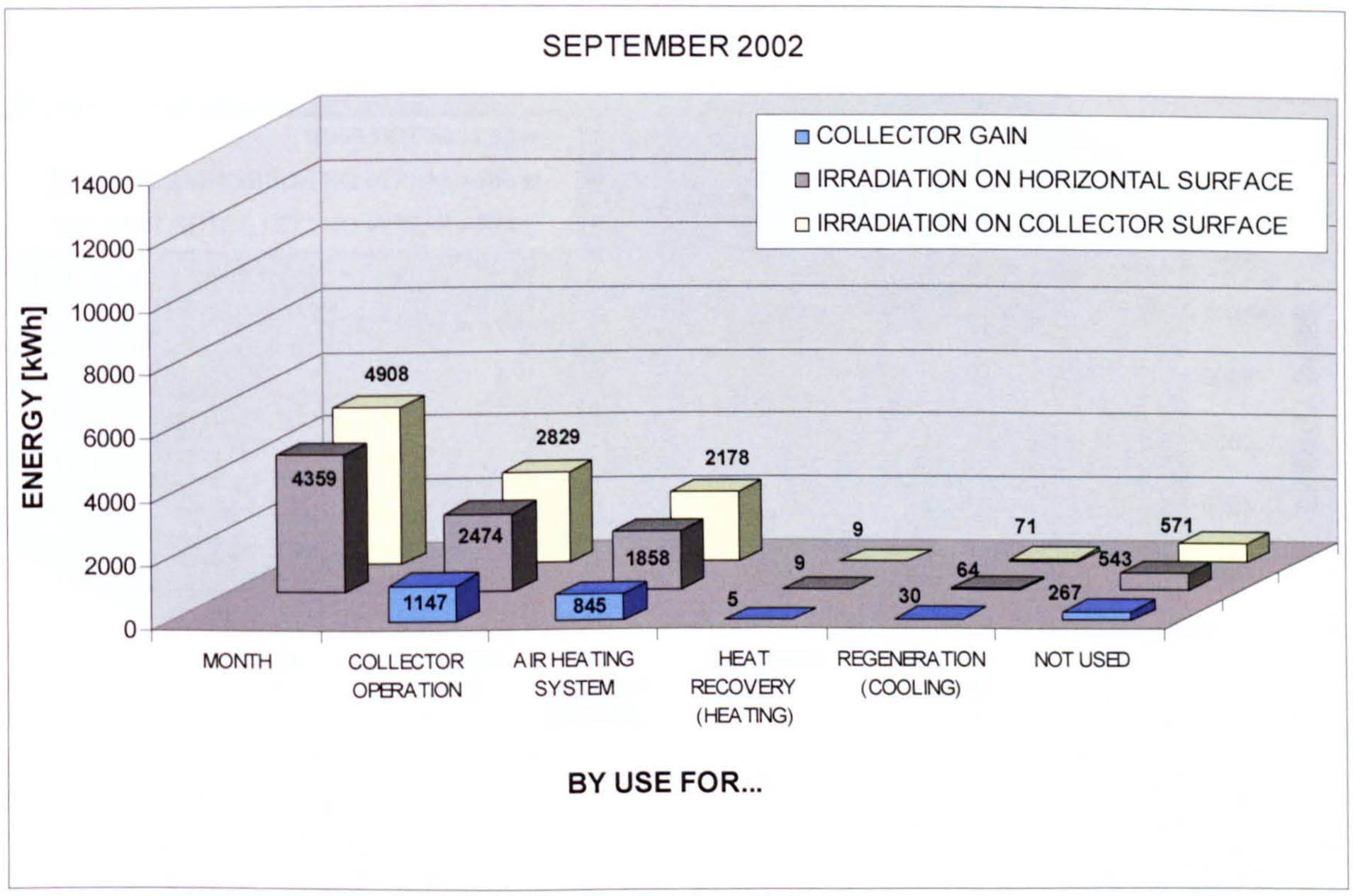

COLLECTOR EFFICIENCY

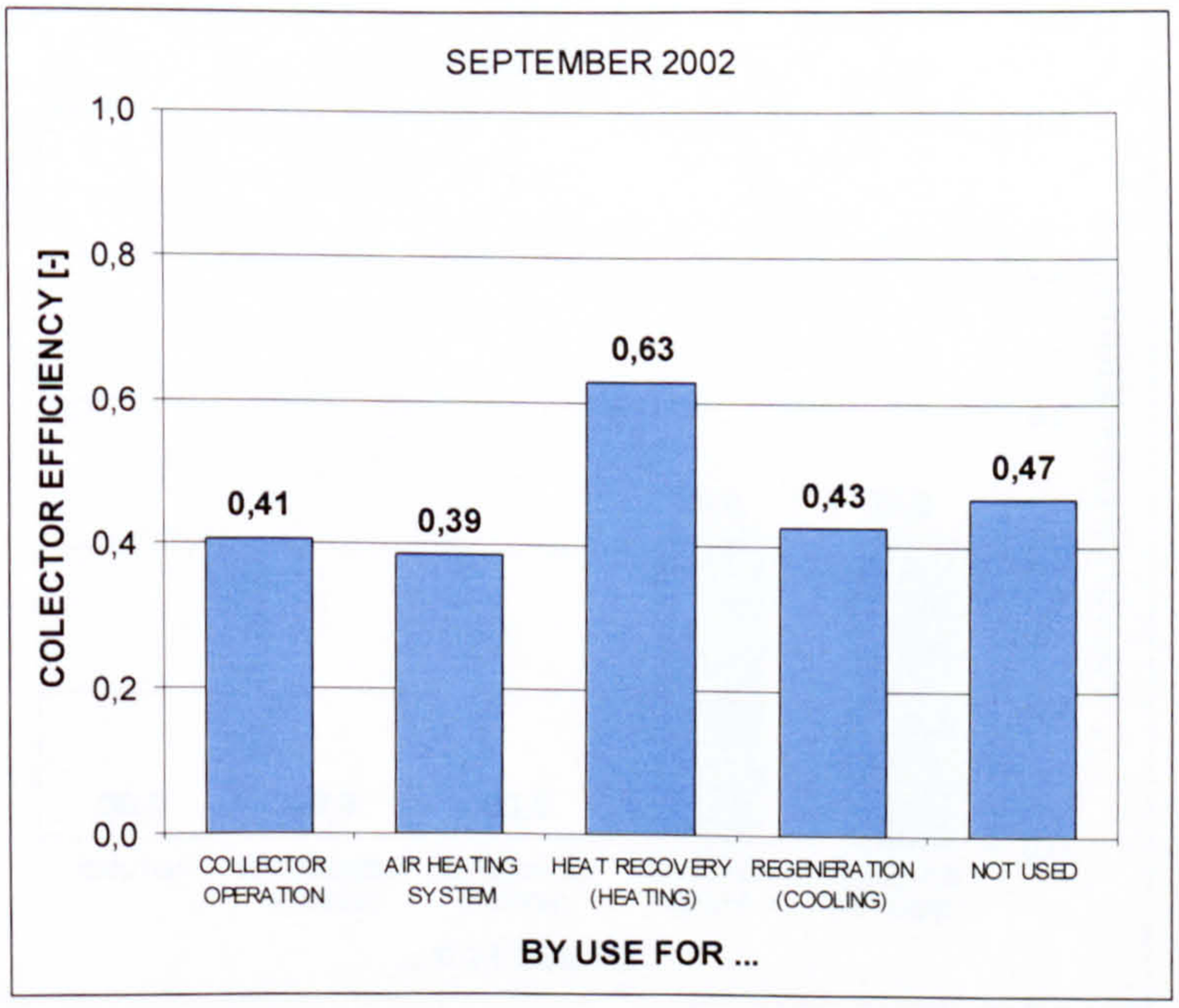

APPENDIX F

EVALUATION OF AIR COLLECTOR OPERATION (ALTHENGSTETT/GERMANY)

SOLAR IRRADIATION / COLLECTOR GAIN

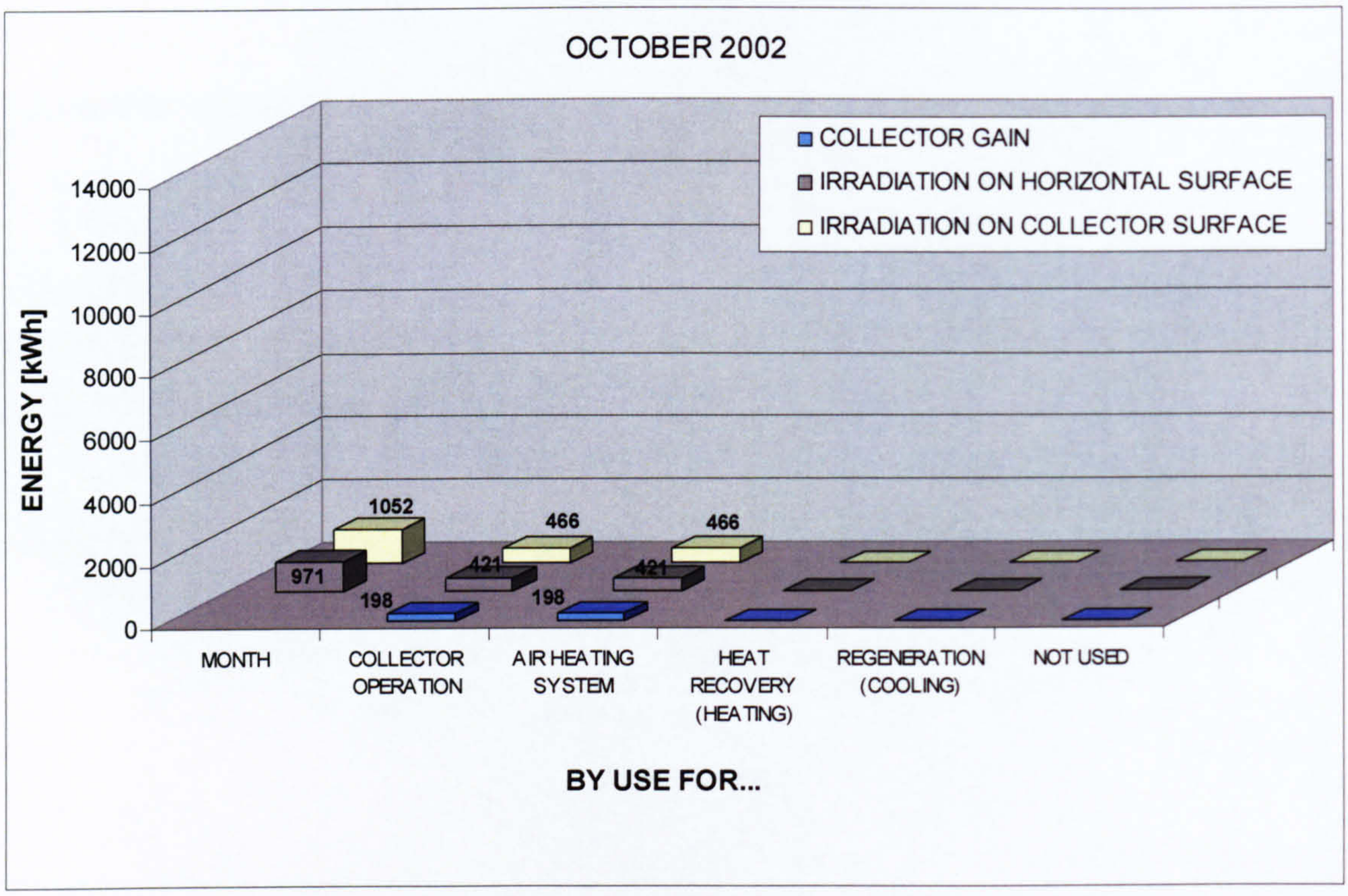

COLLECTOR EFFICIENCY